DISSERTATION

ADVANCING THE UTILITY OF ORGANIC SUPERBASES IN SYNTHETIC METHODOLOGY

Submitted by

Stephen J. Sujansky

Department of Chemistry

In partial fulfillment of the requirements

For the Degree of Doctor of Philosophy

Colorado State University

Fort Collins, Colorado

Summer 2023

Doctoral Committee:

Advisor: Jeffrey Bandar

Garret Miyake
Justin Sambur
Robert Cohen

ABSTRACT

ADVANCING THE UTILITY OF ORGANIC SUPERBASES IN SYNTHETIC METHODOLOGY

Deprotonation is one of the most fundamental and important modes of molecular activation, making Brønsted bases a critical part of a synthetic chemist's toolbox. An exceptional class of Brønsted bases are organic superbases, which are finding increased use in modern synthetic methods due to their unique properties. This thesis describes the use of these unique properties to advance the synthetic utility of superbases in two ways; 1) improving superbase-catalyzed alkene hydrofunctionalization reactions; and 2) developing air-stable and convenient organic superbase prereagents.

Chapter One describes organic superbases in detail to provide background and context for Chapters Two and Three. Within Chapter One, various classes of superbases are presented, as well as their unique properties, syntheses, and example applications. Finally, the limitations and challenges associated with the use of superbases are discussed.

Chapter Two describes the Bandar Group's superbase-catalyzed alkene hydrofunctionalization methodology. Within this chapter mechanistic studies as well as computational modeling, done as part of a collaboration with the Paton Group, are presented. These mechanistic studies provided insight into the factors controlling the reaction equilibrium. This insight was then used to logically address the limitations associated with the original conditions reported by the Bandar Group in 2018. The results of this work help to improve reaction efficiency and to expanded substrate scope. This understanding also led to the development of a

catalytic anti-Markovnikov aryl alkene hydration method that allows convenient access to β-aryl alcohols.

Chapter Three describes the development of air-stable organic superbase precatalysts and prereagents. Superbase salts that decarboxylate were developed as a first strategy method to generate the neutral superbase in solution. This initial salt system then led to the discovery of stable superbase carboxylate salts that react with and open epoxide additives *in situ* to neutralize the superbase conjugate acid. This ring strain release strategy is shown to be effective at promoting a range of reactions including Michael-type addition, ester amidation, deoxyfluorination, S_NAr and Pd-catalyzed cross coupling reactions. These superbase precatalysts and prereagents provide a means to access the unique properties of organic superbases from air-stable and easy-to-handle salts.

Overall, Chapters Two and Three represent significant progress in advancing the utility of organic superbases in synthetic methodology. My work in Chapter Two, along with the Bandar's and Paton Group's efforts, meaningfully expanded the scope and usefulness of superbase-catalyzed alcohol addition reactions. Our new mechanistic understanding proved to be fundamental to a range of addition reactions and pushed the boundary of possible nucleophilic addition reactions. My efforts in Chapter Three, along with Garrett's significant contributions, have made organic superbase much more convenient to use, synthesize and store. This greater convenience and potentially lower cost can be expected to improve access to superbase chemistry and serve as the foundation for future discoveries. Additionally, the ability to control the concentration of superbase in solution will have many benefits in expanding substrate scopes and modulating reaction profiles where a strong base is required but is also detrimental to the overall process.

ACKNOWLEDGEMENTS

There are many people I would like to thank for their help and support during my time in the Bandar Group. I would like to start with the people I worked with every day in the Bandar Group. Thank you for challenging me, pushing me to be better, and for all the great and insightful conversations. When I joined the Bandar Group in 2018, it was small with only 3 graduate students, Tom, Shawn and Spencer and 2 post-doctoral researchers Chaosheng and Zisong. It has been a real pleasure to grow and establish the group with the five of you and I am very grateful for all that you have taught me. This research group would not be what it is today without the original core group of scientists, and I am very proud to be a part of that. Tom, I would like to thank you specifically as you were not only a good mentor and model graduate student, but also a great friend outside of lab. It was truly a joy to work with you and go for beers after long days in lab.

To the group members that have joined since the start, thank you. You have kept the group going strong and I am confident this will continue long into the future. I would like to specifically thank two post-doctoral research Mike and Tyler as your experience, advice and knowhow have been invaluable. I would also like to specifically thank Garrett; it has been a true pleasure to be your mentor and build a new project area with you. Your efforts and talents have been indispensable over the past couple of years.

To my advisor, Professor Jeff Bandar, it is not possible to thank you for everything you have done for me over the last five years. Thank you for all the guidance you have provided and for the countless hours of editing, critiquing and feedback on reports and presentations of mine. Your time and effort have been instrumental in advancing my career and learning how to be a proper scientist. You have been and still are a great mentor and boss to not only me but the group

too. This is reflected in what the group has become. I am really looking forward to watching what the group will accomplish in the future.

I would also like to thank the McNally and Paton Groups as well. I am very grateful for the Paton Group's computational contributions to our mechanistic studies on superbase-catalyzed alcohol addition. It was a great opportunity for me to learn how computational calculations can be combined with experimental results to create a deeper understanding of the chemistry. This experience has made me a better scientist. I am also very grateful to the McNally Group for their experience and willingness to help us in the Bandar Group when we were first starting. Additionally, without access to your large chemical inventory things would have been much slower at the start and we would have missed many important results, so thank you. Hopefully, we have returned the many favors and this close relationship will continue.

I would now like to thank everyone who has supported me from outside of CSU. To start, I want to thank my Mom and Dad. Without your love and support, I would not have been able to move to Colorado and succeed in grad school. You taught me a strong work ethic and instilled a never quit attitude. You are the reason I am where I am today. I would next like to thank my siblings, Sam, Simon and Sadie, your support is greatly appreciated. I would also like to thank my grandparents; you have been extremely influential and a big part of my life.

To the brew crew, Cam, Jeremy, and Anthony, thank you for all the fun times and memories trying to make a good beer. It was always a good break from lab work, and maybe one day we will succeed in this endeavor. I would also like to thank two of my best friends from Lock Haven University, Scott and Alex, your friendship is a huge part of me being here today. I also want to thank my best friends from Somerset, Pennsylvania; Braiden, Sam, and Zach thank you for all of the good memories. I lastly need to specifically thank Anthony, the first and best friend I made in

Colorado. From me emailing the first random name on the list of people looking for roommates to the shenanigans of the COVID lockdown to all the camping and skiing trips, you helped make grad school a truly awesome time.

I would like to end these acknowledgements with the most important person in my life over the past five years, my girlfriend Kaitlyn. Despite graduating high school and even being in the same homeroom together, it took moving to Colorado at the same time and my Aunt Mandy giving you my number (thanks Aunt Mandy) for us to go on a first date. Your support over the past five years has been the thing I have relied on the most. You have made the hard times much easier and the good times that much better, even in the years where you were 1500 miles away in Pennsylvania. Thank you for all of the support and fun memories on all of our Colorado adventures. I should also mention our furry and not-so-little dog, Opal. Opal has been a much-needed source of stress release, fun and cuteness over the past year. She is by far the best surprise to have come home to after a long interview on the other side of the country. I cannot wait to see what Boston holds for us.

TABLE OF CONTENTS

CHAPTER ONE

ORGANIC SUPERBASES IN MODERN SYNTHETIC CHEMISTRY

1.1 Chapter Overview

Deprotonation is one of the most fundamental and important modes of molecular activation, making Brønsted bases critical components in a synthetic chemist's toolbox.[1-4] The identity of the base and its properties often govern the outcome of a given reaction, which makes the base an important variable in reaction optimization.[5] Organic superbases are an exceptional class of Brønsted base at the cutting-edge of synthetic chemistry due to their unique properties.[6,7] I, along with my coworkers Dr. Tom Puleo and Dr. Shawn Wright, recently authored a review highlighting these features of organic superbases and their application in modern synthetic methods.[7] This chapter will describe the background and current state of organic superbase chemistry, based in part on our superbase review, and outline why they are an important class of reagents worthy of continued research and improvement. Organic superbases were essential at the start of the Bandar Group in 2017 and still play a pivotal role in the group today. The role superbases played at the start of the group and how they were used to discover new areas of research are highlighted in this chapter. Chapter One is intended to be the foundation of this thesis and convey the importance of continual improvements within superbase chemistry.

1.2 Organic Superbase Definition and Structural Features

Organic superbases have been defined in several ways, but these definitions can be summarized as neutral organic compounds with a basicity greater than that of Proton Sponge® (pK_a, = 18.6, MeCN).[6-10] Figure 1-1a and b show examples of various classes of organic

superbases.[9,10] A number of organic structures can be classified as superbases and all derive this property from the ability to delocalize the positive charged developed upon protonation.[10-14] The degree to which they can distribute this positive charge determines the base's strength.[14] In general, appending superbasic functional group units such as guanidines, cyclopropenimines, and P_1 phosphazenes to a central superbasic unit leads to greater basicity, these are called higher order superbases.[12-15] Two examples of this feature include the combination of three guanidine units with one central phosphazene units to make a PG_3 superbase[15] and the combination of three P_1 phosphazene units with one central iminophosphorane to make P_4-*t*-Bu (Figure 1-1b).[11, 16-18] The later, P_4-*t*-Bu, is the strongest commercially available superbase and it plays a key role in the Bandar Group, as will be discussed in Section 1.6 and Chapter Two.

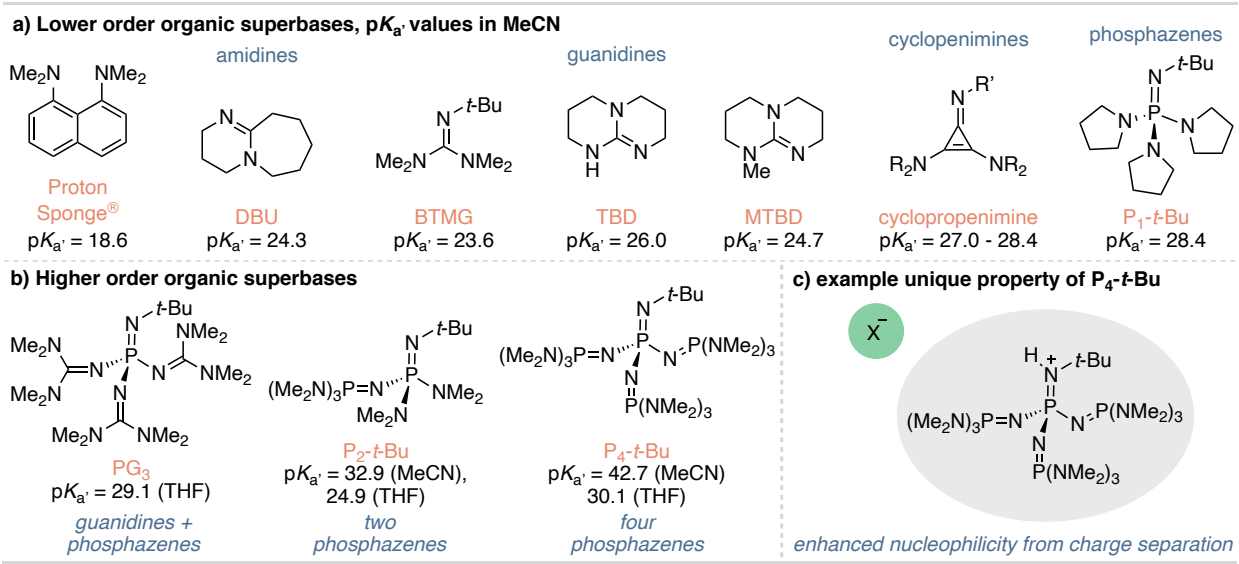

Figure 1-1: Overview of common organic superbases.

The neutral charge of organic superbases gives rise to many unique and desirable properties compared to inorganic Brønsted bases. These properties include excellent solubility in nonpolar solvents,[11] low nucleophilicity,[19] unique hydrogen bonding abilities,[20] distinct ion-pairing characteristics (i.e., they become cationic upon protonation), and their large cation size[21] can lead to more nucleophilic anion (Figure 1-1c). These unique properties lead to their use in modern base-

promoted chemistry,[7] and Section 1.5 will describe several representative examples. Sections 1.3 and 1.4 will describe specific superbase classes in more detail to provide more context for this thesis.

1.3 Amidines, Guanidines and Cyclopropenimines

Amidines[22, 23] and guanidines[24, 25] are the two most common classes of organic superbase, but generally have lower basicity than phosphazenes (Figure 1-1a).[7] Despite this, they still possess many of the attractive properties of other superbases such as excellent solubility and unique hydrogen bonding abilities and are relatively inexpensive, thus they are broadly useful bases. It is also notable that they can function as nucleophilic catalysts unlike other larger superbases that are mostly used as Bronsted bases and find utility in reactions such as ester amidation due to this property.[26] Cyclopropenimines, a more recently invented class of organic superbases, are less common but generally possess higher basicity.[12, 27-29] Cyclopropenimines are unique among organic superbases in that their high basicity originates from the formation of an aromatic cyclopropenium cation when protonated.[12] Cyclopropenimines are most notable for their chiral derivatives used for catalytic, asymmetric Michael addition reactions.[28]

Amidines, guanidines and cyclopropenimine are straightforward to synthesize as shown in Figure 1-2. Amidines, such as DBU, are prepared from ε-caprolactam, beginning with an aza-Michael addition with acrylonitrile, followed by reduction of the nitrile and condensation of the amine to produce the amidine base.[22] Guanidines are similarly simple to prepare through a condensation reactions.[24, 25] BTMG is prepared from tetramethylurea and *tert*-butyl amine, while bicyclic guanidines, like TBD, are prepared from triamine **1-1** and dimethyl carbonate.[30] Cyclopropenimines are readily prepare by treating pentachlorocyclopropane or tetrachlorocyclopropene with a secondary amine, followed by treatment with a primary amine to

generate the cyclopropeniminium HCl salt.[29] This section provides details and context for other common organic superbases as a point of comparison to the phosphazene class, which will be discussed in the next section. Other classes of organic superbases have been developed, such as phosphazenyl phosphines,[31] phosphatranes,[32, 33] phosphorous ylides,[34] carbodiphosphoranes,[35] and proton sponge variants[10, 36] but are not as relevant to this thesis. Phosphazene superbases are the central part of my research in the Bandar Group and the main focus of this thesis.

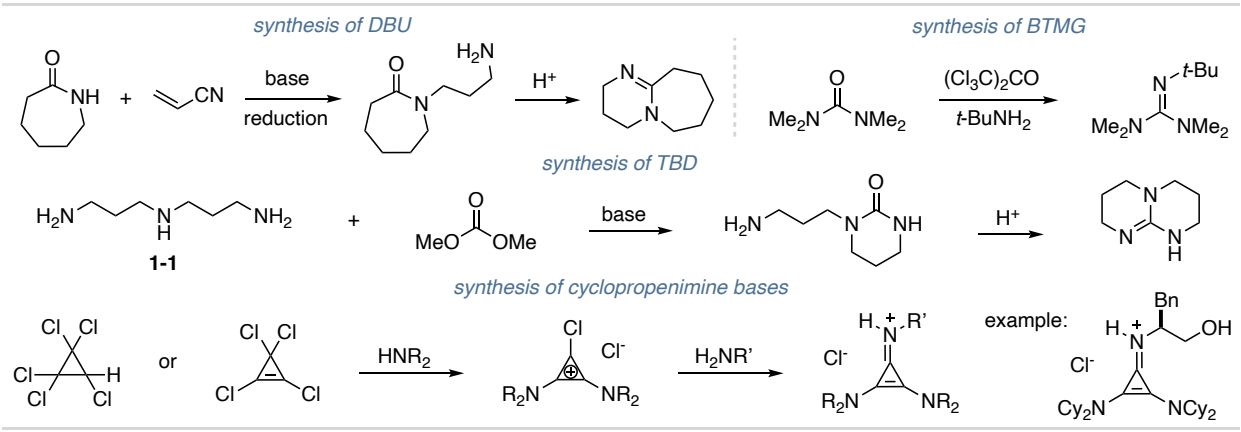

Figure 1-2: Synthesis of amidines, guanidines and cyclopropenimines.

1.4 Phosphazene Superbase Discovery and Synthesis

Phosphazenes are of particular interest to the Bandar Group and me as they are the strongest of the commercially available organic superbases. They derive this high basicity from their ability to delocalize positive charge to the peripheral hydrogen atoms (Figure 1-1).[11] Phosphazenes were first reported in the late 1980s[16, 17] and early 1990s[18] by Schwesinger but saw relatively limited use in the synthetic methodology until the mid-2000s. They are particularly non-nucleophilic due to the *tert*-butyl group on the basic nitrogen; however, this group is modular can be altered to change the properties of the base.[11] This modularity is pronounced for higher order phosphazene superbases as the individual superbasic units can be exchanged for others as was previously noted for PG_3 and P_4-*t*-Bu (Figure 1-1b).[9]

Protonated phosphazene superbase salts are straightforward to prepare from inexpensive starting materials available in bulk quantities (Figure 1-3).[11, 18, 37] In general, phosphorus pentachloride (PCl_5) is first treated with *tert*-butyl amine to access iminophosphorous trichloride **1-2**. Then iminophosphorous trichloride **1-2** is treated with an excess of the desired secondary amine, usually dimethylamine or pyrrolidine, to access the HCl salt (Figure 1-3a, left). Alternatively, PCl_5 can be treated with the desired secondary amine to generate intermediate **1-3**, which is then treated with primary amine (R' must be smaller than *tert*-butyl) to access the phosphazene•HCl salt (Figure 1-3a, right). The synthesis of P_4-*t*-Bu requires both approaches and is shown in Figure 1-3b. To neutralize the phosphazene•HCl salt, treatment with either hydroxide or alkoxide can be done, followed by distillation for lower order bases like P_1-*t*-Bu or P_2-*t*-Bu.[11] The stronger P_4-*t*-Bu superbase, however, must be neutralized with an even stronger base, such as potassium amide (KNH_2) generated *in situ* from potassium metal and ammonia (Figure 1-3b).[11, 37] Section 1.7 will provide more details on these final synthetic steps.

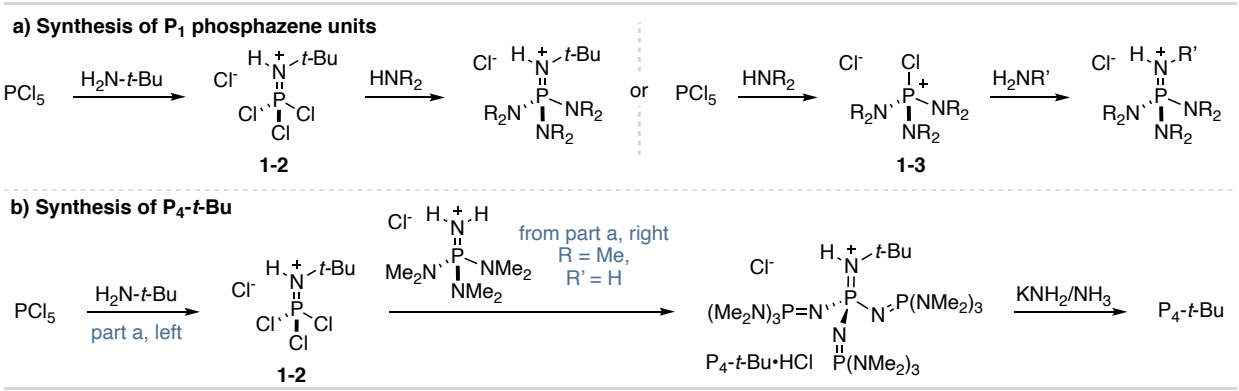

Figure 1-3: Synthesis of phosphazene superbases.

1.5 Selected Examples of Superbases in Modern Synthesis

To highlight the current synthetic utility of organic superbases, I have selected four applications (out of many options) to discuss in this section and, where possible, the unique properties of the superbase that enable the reaction will be noted. The first application is a TBD-

catalyzed isomerization of allylic alcohols to ketones and stereospecific isomerization of allylic ethers to vinyl ethers developed by Martín-Matute (Figure 1-4).[20] This reaction is made possible due to the unique hydrogen bonding and ion-pairing abilities of TBD (Figure 1-4, right). Other inorganic bases and organic bases were capable of promoting the reaction but to a much smaller extent, indicating that the ability of TBD to act as both a hydrogen-bond donor and acceptor is essential for this reaction to result in high yields.

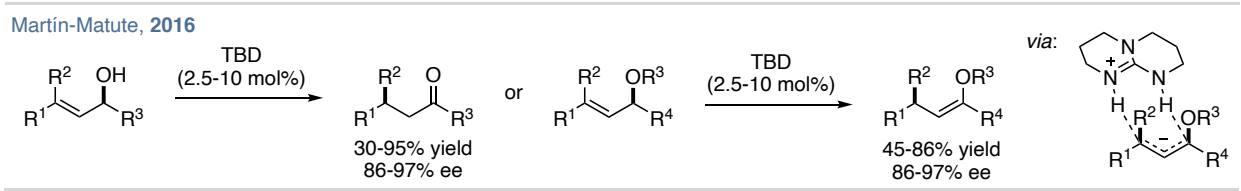

Figure 1-4: Example application of the unique hydrogen bonding properties of TBD.[20]

In 2003, Kondo reported the use of a stoichiometric amounts of P_4-*t*-Bu to deprotonate mildly acid aromatic C–H bonds with alternate selectivity to metal-containing inorganic bases, such as lithium diisopropylamide (Figure 1-5).[38] This switch in selectivity is due to the unique ion-pairing properties of P_4-*t*-Bu, as there is no metal cation present and lone pair repulsion between the superbase and heteroatom. In traditional aromatic C–H deprotonation, the selectivity is often driven by coordination to a metal cation of the base contact ion-pair with either a directing group or heteroatom of a heteroarene (Figure 1-5, right). Thus *ortho*-selectivity is most common when using a strong inorganic base. Without a metal present, the P_4-*t*-Bu superbase can deprotonate the most acidic position even in the presence of a directing group, overriding its selectivity. Additionally, the low nucleophilicity of P_4-*t*-Bu allows for a variety of electrophiles to be present during aromatic deprotonation.

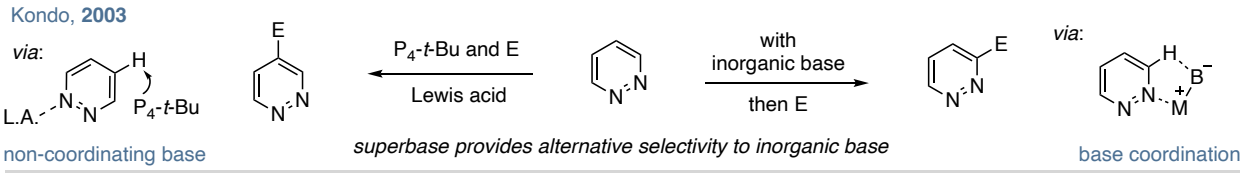

Figure 1-5: The unique ion-pairing properties of P_4-*t*-Bu provide alternative selectivity to inorganic bases.[38]

Recently, the Doyle Group reported the use of multiple superbases to effect alcohol deoxyfluorination with sulfonyl fluorides as both a fluoride source and alcohol activating agent (Figure 1-6).[39-41] This reaction is prone to multiple side reactions including elimination, alcohol dimerization, and base sulfonylation and alkylation.[42] Superbases were found to be uniquely effective in obtaining high yields and minimizing side reactions since they are non-nucleophilic yet strongly basic.[39-42] Since the reaction mechanism can differ between substrates, the optimal superbase varies for different substrates.[38] This results in a large number of parameters to optimize for each substrate (e.g., base identity, sulfonyl fluoride reagent, reaction time, etc.). To develop a modern solution to this complexity, the authors took advantage of the homogeneous reaction conditions enabled by organic superbases and employed robotic high-throughput experimentation (HTE). This generated a large dataset that was combined with substrate descriptors to build a powerful predictive model with random forest machine learning that could accurately identify the optimal reaction conditions on an individual substrate basis.[39, 40] This application of superbases highlights their compatibility in complex and potentially base-sensitive reaction mechanisms and their ability to enable modern technologies, such as HTE and machine learning.[41]

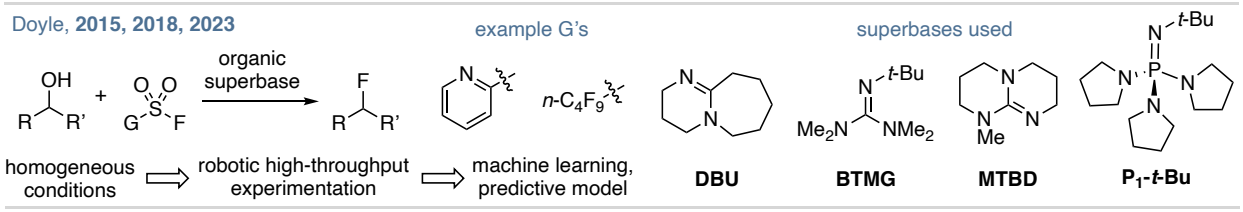

Figure 1-6: The Doyle Group's alcohol deoxyfluorination reaction with sulfonyl fluorides and organic superbases, combined with HTE and machine learning.[38-41]

A fourth application of organic superbases is their use as mild, soluble bases the aid in cutting-edge reaction methods. This is exemplified by metallaphotoredox catalysis pioneered by

the MacMillan Group.[43] Guanidine bases are the most commonly used superbase in this chemistry, as shown in Figure 1-7, left, where aliphatic carboxylic acids are converted to trifluoromethylalkanes with an Ir(III) photocatalyst and Cu(I) catalyst.[44] Other metallaphotoredox-catalyzed reactions that use guanidine superbases include decarboxylative hydroalkylation of alkynes,[45] decarboxylative amination with azodicarboxylates,[46] decarboxylative arylation of α -fluorocarboxylic acids,[47] and sulfonamidation of aryl bromides.[48] One particularly impressive reaction developed by the MacMillan Group featuring P_1-*t*-Bu or TMG as the base is shown in Figure 1-7, right.[49] Here, carboxylic acids, alkyl bromides or other radical precursors are combined with [1.1.1]-propellane and amines in a three-component coupling reaction to access 1,3-disubstituted [1.1.1]-bicyclopentanes. These described examples showcase the utility of organic superbases in both transition metal and photoredox catalysis broadly.

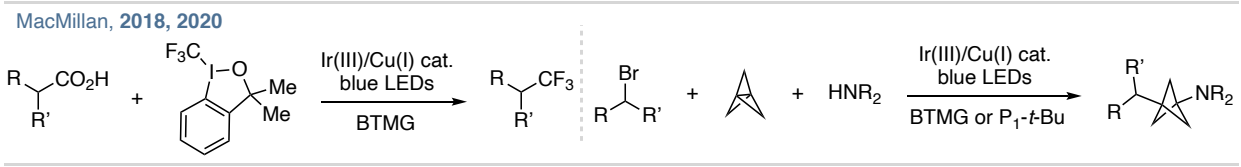

Figure 1-7: Examples of metallaphotoredox-catalyzed reaction that use organic superbases.[44, 49]

1.6 The Role of Superbases in the Bandar Research Group

The Bandar Group began at Colorado State University in 2017 with the goal of exploiting the unique properties of organic superbases to discover new strong Brønsted base-promoted reactions. This central objective has led to a productive research group with four active areas of chemistry, all initially discovered with or focused on the use of organic superbases. The first area of research developed in the Bandar Group is organic superbase-catalyzed alkene hydrofunctionalization reactions. This project was first reported in 2018 in the *Journal of the American Chemical Society* (*JACS*) shortly before I joined the group in 2018.[50] In this initial communication, the unique properties of P_4-*t*-Bu enabled catalytic anti-Markovnikov alcohol

addition to styrene derivatives. The guiding hypothesis was that the high basicity of P_4-*t*-Bu ($pK_{a'}$ = 30.2 in DMSO), which has similar basicity to alkoxides ($pK_{a'}$ = 28-32 in DMSO), and its large size would lead to full deprotonation of the alcohol and a more naked and nucleophilic ion-pair (Figure 1-8a). As shown in Figure 1-8a this method tolerates a broad scope of electron-deficient styrene derivatives and alcohol substrates.[50, 51] Shortly after this first publication a former graduate student, Dr. Tom Puleo, exploited the reversibility and unfavorable reaction equilibrium in DMSO to develop the first α-selectivity styrene deuteration method (Figure 1-8b).[52] The discovery of this method was originally made with P_4-*t*-Bu; however, it was found that inorganic bases were equally capable of catalyzing hydrogen isotope exchange in the α-position of styrenes. Chapter Two will discuss this area of research in more detail and outline my contributions to the project.

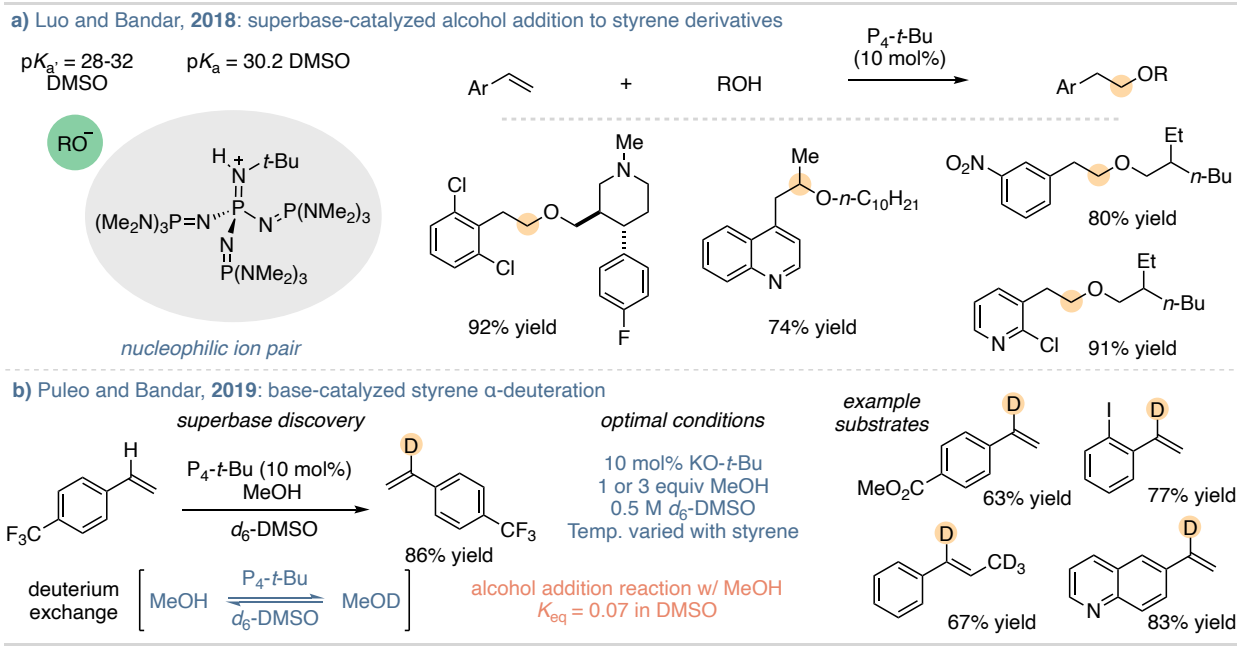

Figure 1-8: The Bandar Group's initial use of P_4-*t*-Bu to functionalize styrene derivatives.[50-52]

In addition to the work done with alkene hydrofunctionalization reactions, the Bandar Group has also discovered two more areas of base-promoted chemistry with P_4-*t*-Bu. The first of these research areas is the defluorofunctionalization of trifluoromethylarenes (Figure 1-9, left). A former post-doctoral researcher in the group, Dr. Choasheng Luo, observed that P_4-*t*-Bu functions

as a Lewis-base with allyltrimethylsilane to promote defluoroallylation of di- and trifluoromethylarenes.[53] The original intent of this experiment was to deprotonate a difluoromethylarene with P$_4$-*t*-Bu and use the resulting carbanion in a challenging nucleophilic addition reaction. Dr. Luo found that simple Lewis basic salts such as cesium fluoride are more efficient at promoting the reaction. These findings have led to a thriving area of research in the Bandar Group that was discovered with P$_4$-*t*-Bu and diligent chemical research.[53-55] The second research area discovered using P$_4$-*t*-Bu was made by Dr. Tom Puleo in an attempt to promote a S$_N$Ar reaction on 3-bromopyridine with alcohols (Figure 1-9, right). He observed 4-selective functionalization of 3-bromopyridine through an intermolecular "halogen dance" mechanism.[56] Through continual reaction development and discovery this initial observation turned into a completely new approach to C–H bond functionalization, an area we term as base-catalyzed halogen transfer chemistry.[57]

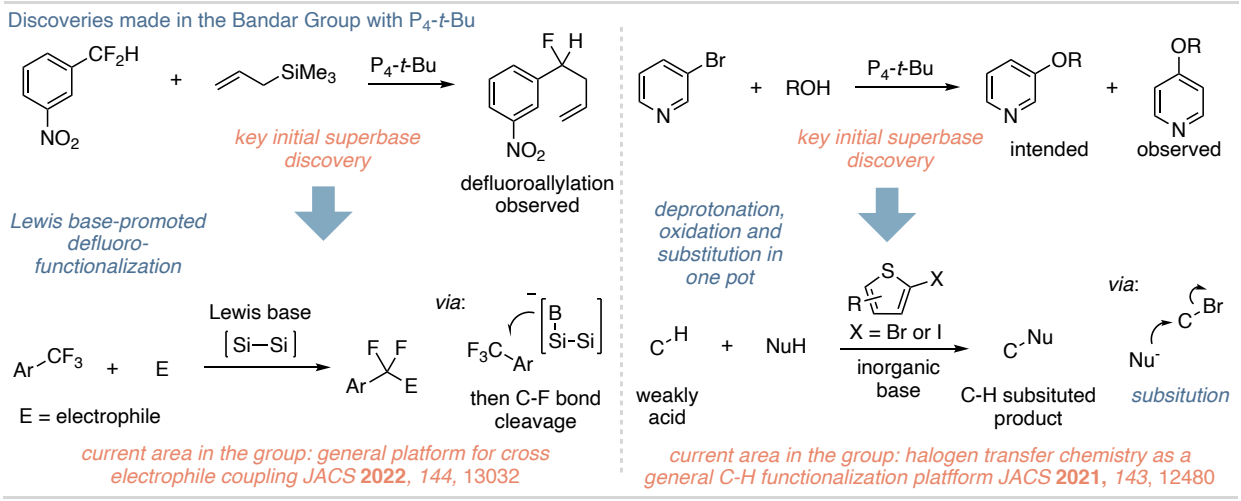

Figure 1-9: The Bandar Group's use of P$_4$-*t*-Bu in reaction discovery, the development of two new areas of research.[53-57]

This section highlights the value of organic superbases in the discovery of new concepts and reactions in synthetic chemistry. Three of the four areas of research within the Bandar group were discovered using organic superbases. The fourth area is a central part of our research program

and supports all of the other areas by making superbases more user friendly through prereagent design and is described in Chapter Three. The next section discusses the major limitations and practical concerns associated with organic superbases. These limitations are the inspiration for the design of new superbasic reagents.

1.7 Limitations and Restrictions of Organic Superbases

1.7.1 Practical Concerns of Amidine, Guanidine and Cyclopropenimine Superbases

The previous two sections outline cutting-edge reaction applications of superbases and their use in discovery settings. These applications make use of superbases despite significant practical concerns limiting their widespread use. These limitations include includes high cost, difficult synthesis, and instability to air and moisture.

Amidines and guanidines are the most practical classes of superbases as they are relatively inexpensive (DBU $0.41/g, TMG $0.42/g, and BTMG $34.80/mL from Millipore Sigma) and straightforward to synthesize (as outlined in Figure 1-2).[22, 24, 25, 30] Due to their low basicity, the neutralization step in their synthesis is safe and procedurally simple. However, they are prone to hydrolysis under basic aqueous conditions (Figure 1-10a).[58] This decomposition pathway results in products that are able to engage side pathways under certain reaction conditions.

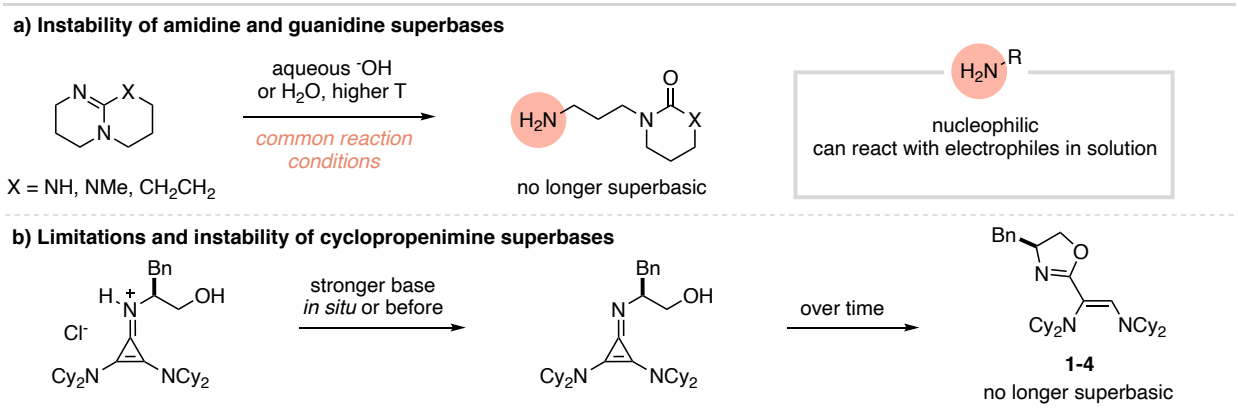

Figure 1-10: Stability issues of amidine, guanidine and cyclopropenimine superbases.

Cyclopropenimines are more basic than amidines and guanidines and are stored as HCl salts. Several cyclopropenimine superbases are commercially available and they can also be easily synthesized from readily available starting materials, as discussed in Section 1.3 and shown in Figure 1-2.[29] The biggest challenges and barriers to cyclopropenimine use are that neutralized just prior to use or *in situ* (Figure 1-10b).[27, 59] If the head group has an alcohol, the neutral cyclopropenimine is not stable over time and will isomerize to the dihydrooxazole, **1-4**.[59] These factors hinder the practicality of cyclopropenimines and thus they have limited use as compared to other superbase classes discussed herein.

1.7.2 Practical Concerns and Limitations of the Phosphazene Class of Organic Superbases

Phosphazenes are the most widely used class of strong neutral base. As mentioned in Section 1.4, phosphazene HCl salts are prepared from inexpensive and readily available commodity chemicals, PCl_5 and simple secondary and primary amines.[11, 16-18] However, phosphazenes are prohibitively expensive in many settings as P_1-*t*-Bu costs \$27.00/g (\$8,414/mol, sold neat 25 mL/\$690.00), P_2-*t*-Bu costs \$95.26/g (\$35,000/mol, sold as 2.0 M solution in THF 25 mL/\$1,750) and P_4-*t*-Bu costs \$110.50/g (\$70,000/mol, sold as 0.8 M solution in hexane 25 mL/\$1,400) from Millipore Sigma. To note, there are other commercially available phosphazene superbases and they all have similar properties, this includes P_4-*t*-Oct, P_2-Et and BEMP, of most interest to this thesis are P_1-*t*-Bu, P_2-*t*-Bu, and P_4-*t*-Bu.[11] Therefore, discussions about phosphazene bases will be in reference to these bases unless otherwise noted.

The high cost of phosphazene bases is in part due to challenging and/or dangerous synthetic steps.[11, 37] The first challenging step is the isolation of the iminophophorous trichloride **1-1** or intermediate **1-2** (Figure 1-3), as these intermediates are highly moisture sensitive and thus this step must be carried out air-free. Further complicating this step is the amine•HCl salt byproduct

that is a very fine precipitate. The next major challenge in their synthesis are the final neutralization and purification steps (Figure 1-11). P_1-*t*-Bu•HCl can be neutralized with a potassium hydroxide wash; however, the neutral and nonvolatile superbase must be distilled under air-free conditions. This distillation step required very low pressure and high temperature, which if not monitored closely, can lead to base decomposition. P_2-*t*-Bu•HCl is neutralized and purified in a similar way but with potassium methoxide instead of potassium hydroxide. P_4-*t*-Bu•HCl was reported by Schwesinger to be neutralized with potassium amide in liquid ammonia, which is a pyrophoric reagent that makes this method very hazardous. To note, Hoge reported in 2019 that HP_4-*t*-Bu•OH could be neutralized by heating under vacuum for extended periods of time, this removes hydroxide as water.[37] This method to neutralize P_4-*t*-Bu salts is inconvenient since it requires multiple passes through an anion exchange column to generate HP_4-*t*-Bu•OH and extended time under high vacuum (0.01 mbar) and elevated temperatures.

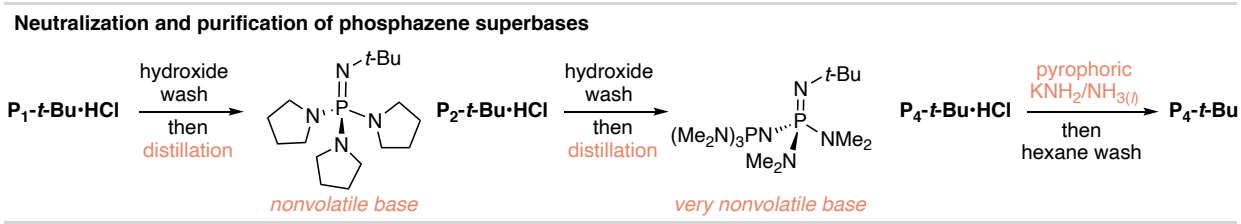

Figure 1-11: The neutralization and purification steps of phosphazene superbase synthesis.

Phosphazenes are further limited by instability towards ambient air. Unlike the weaker superbases discussed in Section 1.7.1 phosphazenes are not prone to hydrolysis and are stable to water. However, they do react with carbon dioxide in ambient air to form phosphoramides and *tert*-butyl isocyanate (Figure 1-12, left).[60] Phosphazenes are also highly hygroscopic and will absorb water even from dry air (Figure 1-12, right). Even though they are stable to water, it can be difficult to dry phosphazene•hydrates, as indicated by the conditions developed by Hoge.[37]

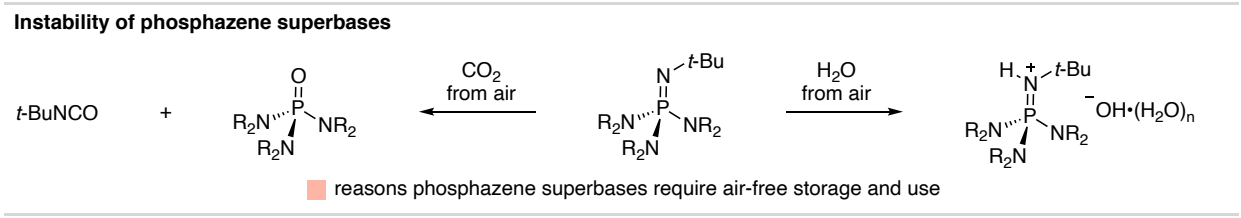

Figure 1-12: The air instability of phosphazene superbases.

1.8 Conclusion

The chemistry described in Chapter One is intended to provide background and context for the continual development of organic superbase chemistry. Organic superbases have a range of unique properties that lead to their use in modern chemical methods and technologies, many of which would not be possible without the use of superbases. A key application is in reaction discovery as evidenced by the Bandar Group's own work with organic superbases. For these reasons it is essential to continue to study organic superbases in hypothesis-driven research and to develop more convenient ways to access and exploit their unique properties. Chapter Two will describe my work in further developing superbase-catalyzed alkene hydrofunctionalization reactions and Chapter Three will detail my efforts to address the instability and practicality issues of superbases by developing air-stable superbase prereagents.

REFERENCES

[1] Rathman, T. L.; Schwindeman, J. A. Preparation, Properties, and Safe Handling of Commercial Organolithiums: Alkyllithiums, Lithium sec-Organoamides, and Lithium Alkoxides *Org. Process Res. Dev*. **2014**, *18*, 1192–1210.

[2] Collum, D. B.; McNeil, A. J.; Ramirez, A. Lithium Diisopropylamide: Solution Kinetics and Implications for Organic Synthesis *Angew. Chem. Int. Ed*. **2007**, *46*, 3002 – 3017.

[3] Haag, B.; Mosrin, M.; Ila, H.; Malakhov, V.; Knochel, P. Regio- and Chemoselective Metalation of Arenes and Heteroarenes Using Hindered Metal Amide Bases *Angew. Chem. Int. Ed.* **2011**, *50*, 9794 – 9824.

[4] Pearson, D. E.; Buehler, C. A. Potassium tert-butoxide in synthesis *Chem. Rev*. **1974**, *74*, 45–86.

[5] Henderson, R. K.; Hill, A. P.; Redman, A. M.; Sneddon, H. F. Development of GSK's acid and base selection guides *Green Chem*. **2015**, *17*, 945 – 949.

[6] *Superbases for Organic Synthesis: Guanidines, Amidines, Phosphazenes and Related Organocatalysts* (Ed.: T. Ishikawa), Wiley, Chichester, **2009**.

[7] Puleo, T. R.; Sujansky, S. J.; Wright, S. E.; Bandar, J. Organic Superbases in Recent Synthetic Methodology Research. *Chem. – Eur. J*. **2020**, *27,* 4216 – 4229.

[8] Busca, G. Bases and Basic Materials in Chemical and Environmental Processes. Liquid versus Solid Basicity. *Chem. Rev*. **2010**, *110*, 2217−2249.

[9] Kaljurand, I.; Saame, J.; Rodima, T.; Koppel, I.; Koppel, I. A.; Kögel, J. F.; Sundermeyer, J.; Köhn, U.; Coles, M. P.; Leito, I. Experimental Basicities of Phosphazene, Guanidinophosphazene, and Proton Sponge Superbases in the Gas Phase and Solution. *J. Phys. Chem. A* **2016**, *120*, 2591−2604.

[10] Vazdar, K.; Margetić, D.; Kovačević, B.; Sundermeyer, J.; Leito, I.; Jahn, U. Design of Novel Uncharged Organic Superbases: Merging Basicity and Functionality *Acc. Chem. Res.* **2021**, *54*, 3108−3123.

[11] Schwesinger, R.; Schlemper, H.; Hasenfratz, C.; Willaredt, J.; Dambacher, T.; Breuer, T.; Ottaway, C.; Fletschinger, M.; Boele, J.; Fritz, H.; Putzas, D.; Rotter, H. W.; Bordwell, F. G.; Satish, A. V.; Ji, G.-Z.; Peters, E.-M.; Peters, K.; von Schnering, H. G.; Walz, L. Extremely Strong, Uncharged Auxiliary Bases; Monomeric and Polymer-Supported Polyaminophosphazenes (P2- P5)* *Liebigs Ann*. **1996**, 1055 – 1081.

[12] Nacsa, E. D.; Lambert, T. H. Higher-Order Cyclopropenimine Superbases: Direct Neutral Brønsted Base Catalyzed Michael Reactions with α-Aryl Esters *J. Am. Chem. Soc*. **2015**, *137*, 10246−10253.

[13] Vazdar, K.; Kunetskiy, R.; Saame, J.; Kaupmees, K.; Leito, I.; Jahn U. Very Strong Organosuperbases Formed by Combining Imidazole and Guanidine Bases: Synthesis, Structure, and Basicity *Angew. Chem. Int. Ed.* **2014**, *53*, 1435 – 1438.

[14] Leito, I.; Koppel, I. A.; Koppel, I.; Kaupmees, K.; Tshepelevitsh, S.; Saame J. Basicity Limits of Neutral Organic Superbases *Angew. Chem. Int. Ed*. **2015**, *127*, 9394 –9397.

[15] Kolomeitsev, A. A.; Koppel, I. A.; Rodima, T.; Barten, J.; Lork, E.; Röschenthaler, G.-V.; Kaljurand, I.; Agnes Kütt, A.; Koppel, I.; Mäemets, V.; Leito, I. Guanidinophosphazenes: Design, Synthesis, and Basicity in THF and in the Gas Phase *J. Am. Chem. Soc*. **2005**, *127*, 17656-17666.

[16] Schwesinger, R. Chimia **1985**, *39*, 269 – 272.
[17] Schwesinger, R.; Schlemper, H. Peralkylated Polyaminophosphazenes- Extremely Strong, Neutral Nitrogen Bases *Angew. Chem. Int. Ed. Engl*. **1987**, *26*, 1167 – 1169.
[18] Schwesinger, R.; Willaredt, J.; Schlemper, H.; Keller, M.; Schmitt, D.; Fritz, H. Novel, Very Strong, Uncharged Auxiliary Bases; Design and Synthesis of Monomeric and Polymer-Bound TriaminoiminophosphoraneBases of Broadly Varied Steric Demand *Chem. Ber*. **1994**, *127*, 2435 – 2454.
[19] Gholamipour-Shirazi, A.; Rolando, C. Kinetics screening of the N-alkylation of organic superbases using a continuous flow microfluidic device: basicity versus nucleophilicity *Org. Biomol. Chem***. 2012**, *10*, 8059–8063.
[20] Martinez-Erro. S.; Sanz-Marco, A.; Gómez, A.; Vázquez-Romero, A.; Ahlquist, M. A. G.; Martín-Matute, B. Base-Catalyzed Stereospecific Isomerization of Electron-Deficient Allylic Alcohols and Ethers through Ion-Pairing *J. Am. Chem. Soc*. **2016**, *138,* 13408−13414.
[21] Mamdaniand, H. T.; Hartley, R. C. Phosphazene bases and the anionic oxy-Cope rearrangement *Tetrahedron Lett*. **2000**, *41*, 747–749.
[22] Oediger, H.; Möller, F.; Eiter, K. Bicyclic Amidines as Reagents in Organic Syntheses *Synthesis* **1972**, *11*, 591 – 598.
[23] Oediger, H.; Möller, F.; 1,5-Diazabicyclo[5.4.0]undec-5-ene, a New Hydrogen Halide Acceptor *Angew. Chem. Int. Ed. Engl*. **1967**, *6*, 76.
[24] Barton, D. H. R.; Elliott, J. D.; Géro, S. D. Synthesis and properties of a series of sterically hindered guanidine bases *J. Chem. Soc. Perkin Trans. 1* **1982**, 2085–2090.
[25] Ishikawa, T.; Kumamoto, T. Guanidines in Organic Synthesis *Synthesis* **2006**, 5, 737–752.
[26] Kiesewetter, M. K.; Scholten, M. D.; Kirn, N.; Weber, R. L.; Hedrick, J. L.; Waymouth, R. M. Cyclic Guanidine Organic Catalysts: What Is Magic About Triazabicyclodecene? *J. Org. Chem.* **2009**, *74*, 9490–9496.
[27] Bandar, J. S.; Barthelme, A.; Mazori, A. Y.; Lambert, T. H. Structure–activity relationship studies of cyclopropenimines as enantioselective Brønsted base catalysts *Chem. Sci*., **2015**, *6*, 1537–1547.
[28] Bandar, J. S.; Lambert, T. H. Cyclopropenimine-Catalyzed Enantioselective Mannich Reactions of tert-Butyl Glycinates with N-Boc-Imines *J. Am. Chem. Soc*. **2013**, *135*, 11799−11802.
[29] Bandar, J. S.; Lambert, T. H. Aminocyclopropenium Ions: Synthesis, Properties, and Applications *Synthesis* **2013**, *45*, 2485–2498.
[30] Boyd, D. W.; Eswarakrishnan, V.; Hickenboth, C. R.; Karabin, R. F.; McCollum, G. J.; Minch, B. A.; Moriarity, T. C.; Zawacky, S. R. Method for producing bicyclic guanidines by use of a cyclic urea Patten Number US20090281314 date **2009**-11-12
[31] Ullrich, S.; Kovačević, B.; Xie, X.; Sundermeyer, J. Phosphazenyl Phosphines: The Most Electron-Rich Uncharged Phosphorus Brønsted and Lewis Bases. *Angew. Chem. Int. Ed*. **2019**, *58*, 10335−10339.
[32] Kisanga, P. B.; Verkade, J. G.; Schwesinger, R. PK_a Measurements of $P(RNCH_2CH_3)_3N$. *J. Org. Chem*. **2000**, *65*, 5431−5432.
[33] Lensink, C.; Xi, S. K.; Daniels, L. M.; Verkade, J. G. The Unusually Robust Phosphorus-Hydrogen Bond in the Novel Cation [Cyclic] $HP(NMeCH_2CH_2)_3N^+$. *J. Am. Chem. Soc*. **1989**, *111*, 3478− 3479.

[34] Saame, J.; Rodima, T.; Tshepelevitsh, S.; Kütt, A.; Kaljurand, I.; Haljasorg, T.; Koppel, I. A.; Leito, I. Experimental Basicities of Superbasic Phosphonium Ylides and Phosphazenes. *J. Org. Chem.* **2016**, *81*, 7349−7361.

[35] Ullrich, S.; Kovačević, B.; Koch, B.; Harms, K.; Sundermeyer, J. Design of Non-Ionic Carbon Superbases: Second Generation Carbodiphosphoranes. *Chem. Sci*. **2019**, *10*, 9483−9492.

[36] Kögel, J. F.; Margetić, D.; Xie, X.; Finger, L. H.; Sundermeyer, J. A Phosphorus Bisylide: Exploring a New Class of Superbases with Two Interacting Carbon Atoms as Basicity Centers. *Angew. Chem., Int. Ed*. **2017**, *56*, 3090−3093.

[37] Weitkamp, R. F.; Neumann, B.; Stammler, H. G.; Hoge, B Generation and Applications of the Hydroxide Trihydrate Anion, $[OH(OH_2)_3]^-$, Stabilized by a Weakly Coordinating Cation *Angew. Chem. Int. Ed*. **2019**, *58*, 14633 –14638.

[38] Imahori, T.; Kondo, Y.; A New Strategy for Deprotonative Functionalization of Aromatics: Transformations with Excellent Chemoselectivity and Unique Regioselectivities Using t-Bu-P4 Base *J. Am. Chem. Soc*. **2003**, *125*, 8082–8083.

[39] Nielsen, M. K.; Ugaz, C. R.; Li, W.; Doyle, A. G. PyFluor: A Low-Cost, Stable, and Selective Deoxyfluorination Reagent *J. Am. Chem. Soc*. **2015**, *137*, 9571−9574.

[40] Nielsen, M. K.; Ahneman, D. T.; Riera, O.; Doyle, A. G. Deoxyfluorination with Sulfonyl Fluorides: Navigating Reaction Space with Machine Learning *J. Am. Chem. Soc*. **2018**, *140*, 5004−5008.

[41] Żurański, A. M.; Gandhi, S. S.; Doyle, A. G. A Machine Learning Approach to Model Interaction Effects: Development and Application to Alcohol Deoxyfluorination *J. Am. Chem. Soc.* **2023**, *145*, 7898–7909.

[42] Pirnot, M,; Stone, K.; Wright, T. J.; Lamberto, D. J.; Schoell, J.; Lam, Y.; Zawatzky, K.; Wang, X.; Dalby, S. M.; Fine, A. J. McMullen, J. P. Manufacturing Process Development for Belzutifan, Part 6: Ensuring Scalability for a Deoxyfluorination Reaction *Org. Process Res. Dev.* **2022**, *26*, 551–559.

[43] Twilton, J.; Le, C.; Zhang, P.; Shaw, M. H.; Evans, R. W.; MacMillan, D. W. C. The merger of transition metal and photocatalysis *Nat. Rev. Chem*. **2017**, *1*, 0052.

[44] Kautzky, J. A.; Wang, T.; Evans, R. W.; MacMillan, D. W. C. Decarboxylative Trifluoromethylation of Aliphatic Carboxylic Acids *J. Am. Chem. Soc*. **2018**, *140*, 6522 – 6526.

[45] Till, N. A.; Smith, R. T.; MacMillan, D. W. C. Decarboxylative Hydroalkylation of Alkynes *J. Am. Chem. Soc*. **2018**, *140*, 5701–5705.

[46] Lang, S. B.; Cartwright, K. C.; Welter, R. S.; Locascio, T. M.; Tunge, J. A. Photocatalytic Aminodecarboxylation of Carboxylic Acid *Eur. J. Org. Chem*. **2016**, 3331–3334.

[47] Wang, H.; Liu, C.-F.; Song, Z.; Yuan, M.; Ho, Y. A.; Gutierrez, O.; Koh, M. J. Engaging α-Fluorocarboxylic Acids Directly in Decarboxylative C–C Bond Formation *ACS Catal*. **2020**, *10*, 4451 – 4459.

[48] Kim, T.; McCarver, S. J.; Lee, C.; MacMillan, D. W. C. Sulfonamidation of Aryl and Heteroaryl Halides through Photosensitized Nickel Catalysis *Angew. Chem. Int. Ed*. **2018**, *57*, 3488–3492.

[49] Zhang, X.; Smith, R. T.; Le, C.; McCarver, S. J.; Shireman, B. T.; Carruthers, N. I.; MacMillan, D. W. C. Copper-mediated synthesis of drug-like bicyclopentanes *Nature* **2020**, *580*, 220–226.

[50] Luo, C.; Bandar, J. S. Superbase-Catalyzed anti-Markovnikov Alcohol Addition Reactions to Aryl Alkenes *J. Am. Chem. Soc*. **2018**, *140*, 3547−3550.
[51] Luo, C.; Bandar, J. S. Synthesis of β-Phenethyl Ethers by Base-Catalyzed Alcohol Addition Reactions to Aryl Alkenes *Synlett* **2018**, *29*, 2218–2224.
[52] Puleo, T. R.; Strong, A. J.; Bandar, J. S. Catalytic α-Selective Deuteration of Styrene Derivatives *J. Am. Chem. Soc*. **2019**, *141*, 1467–1472.
[53] Luo, C.; Bandar, J. S. Selective Defluoroallylation of Trifluoromethylarenes *J. Am. Chem. Soc*. **2019**, *141*, 14120–14125.
[54] Wright, S. E.; Bandar, J. S. A Base-Promoted Reductive Coupling Platform for the Divergent Defluorofunctionalization of Trifluoromethylarenes *J. Am. Chem. Soc*. **2022**, *144*, 13032–13038.
[55] Reidl, T. W.; Bandar, J. S. Lewis Basic Salt-Promoted Organosilane Coupling Reactions with Aromatic Electrophiles *J. Am. Chem. Soc*. **2021**, *143*, 11939–11945.
[56] Puleo, T. R.; Bandar, J. S. Base-Catalyzed Aryl Halide Isomerization Enables the 4-Selective Substitution of 3-Bromopyridines *Chem. Sci*., **2020**,*11*, 10517-0522.
[57] Puleo, T. R.; Klaus, D. R.; Bandar, J. S. Nucleophilic C−H Etherification of Heteroarenes Enabled by Base- Catalyzed Halogen Transfer *J. Am. Chem. Soc*. **2021**, *143*, 12480–12486.
[58] Hyde, A. M.; Calabria, R.; Arvary, R.; Wang, X.; Klapars, A. Investigating the Underappreciated Hydrolytic Instability of 1,8-Diazabicyclo[5.4.0]undec-7-ene and Related Unsaturated Nitrogenous Bases *Org. Process Res. Dev*. **2019**, *23*, 1860−1871.
[59] Bandar, J. S.; Lambert, T. H. Enantioselective Brønsted Base Catalysis with Chiral Cyclopropenimines *J. Am. Chem. Soc*. **2012**, *134*, 5552−5555.
[60] Courtemanche, M.-A.; Légaré, M.-A.; Rochette, É.; Fontaine, F.-G. Phosphazenes: efficient organocatalysts for the catalytic hydrosilylation of carbon dioxide *Chem. Commun.*, **2015**, *51*, 6858–6861.

CHAPTER TWO

ORGANIC SUPERBASE-CATALYZED ALCOHOL ADDITION TO ARYL ALKENES; EXPANDING THE SCOPE OF NUCLEOPHILIC ADDITION REACTIONS

2.1 Chapter Overview

The Michael addition, first reported over a century ago, is among the most prevalent strategies to construct C_{sp3}-C_{sp3} bonds.[1] It is also one of the first reactions taught to undergraduate students.[2] While the Michael addition is ubiquitous across synthetic chemistry, it still has key limitations.[3, 4] These limitations are discussed in this chapter along with how modern research has been applied to solve these challenges. Heteroatom Michael-type additions are a means to achieve anti-Markovnikov alkene functionalization. Markovnikov and anti-Markovnikov describe alkene hydrofunctionalization selectivity. Markovnikov selectivity is the addition of hydrogen to the least substituted side of an alkene, while anti-Markovnikov refers to the opposite selectivity, addition of a hydrogen to the most substituted side.[5] Chapter Two describes the Bandar Group's and my own work in expanding the scope of Michael-type additions using the superbase P_4-*t*-Bu as a uniquely effective catalyst.

First, the value of β-aryl ethers and alcohols as well as traditional methods and an ideal way to access them are discussed. Next, the state of this ideal route, Michael-type additions, in particular oxa-Michael additions are discussed. Then, the Bandar Group's initial work on superbase-catalyzed hydroetherification of aryl alkenes is presented in detail. Then, I discus our mechanistic studies on this reaction. These mechanistic studies were conducted by a team of researchers through an experimental-computational collaboration with the Paton Group at

Colorado State University. Findings obtained by other researchers are presented throughout and are indicated as such. Their results were critical to this work and essential to fully understand the reaction mechanism and energetics. Finally, improvements to and expansion of superbase-catalyzed hydroetherification methodology made possible by our mechanistic insight are presented. This includes more efficient reaction conditions, expanded substrate scopes, more practical catalytic systems, and anti-Markovnikov aryl alkene hydration.

2.2 β-Aryl Ethers and Alcohols

2.2.1 Importance of β-Aryl Ethers and Alcohols

β-Aryl ethers and alcohols are important structural motifs as they are found in a wide range of chemicals, including biologically active compounds,[6] pharmaceuticals,[7-9] agrochemicals,[10] natural products[11] (Figure 2-1a). β-Aryl ethers and alcohols are also highly versatile synthetic intermediates, especially β-aryl alcohols as they can be further functionalized to a wide range of β-aryl functional groups (Figure 2-1b).[12,13] Catalytic access to this motif from alcohols and aryl alkenes is the most direct synthetic route from readily available starting materials in a single synesthetic step.[14-17] Section 2.2.2 discusses traditional synthetic routes and their limitations.

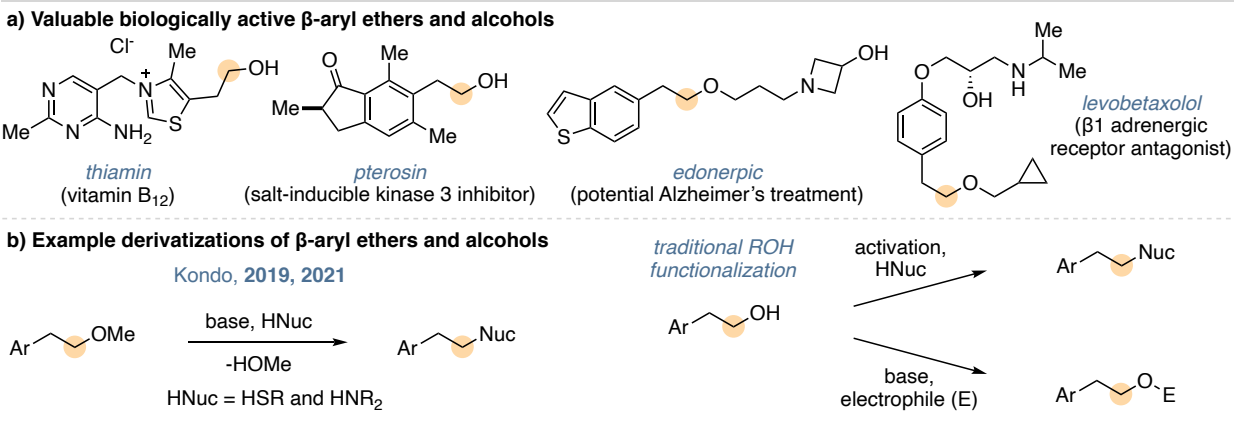

Figure 2-1: The value of β-aryl ethers and alcohols.

2.2.2 Hydroboration/Oxidation/Substitution and Alternative Approaches to β-Aryl Ethers and Alcohols

Hydroboration/oxidation, sometimes called the Brown oxidation, is the most common way to access β-aryl alcohols from aryl alkenes.[18-21] Access to β-aryl ethers then requires an additional substitution process that requires stoichiometric activating reagents (Figure 2-6a). Hydroboration is usually highly regioselective for anti-Markovnikov functionalization, a fact driven by both steric and electronic effects.[20] Common boranes used are BH_3•THF complex and 9-BBN and oxidation is usually accomplished with sodium hydroxide and hydrogen peroxide (Figure 2-2a). Transition metal-catalyzed hydroboration has been developed that improves or alter the inherent selectivity of the alkene, but this overall process is still limited by oxidation and substitution to access β-aryl ethers and alcohols.[22, 23] More broadly, this methodology is usually reliable for most substrate classes including aryl alkenes. However, there are significant limitations to this methodology.[21]

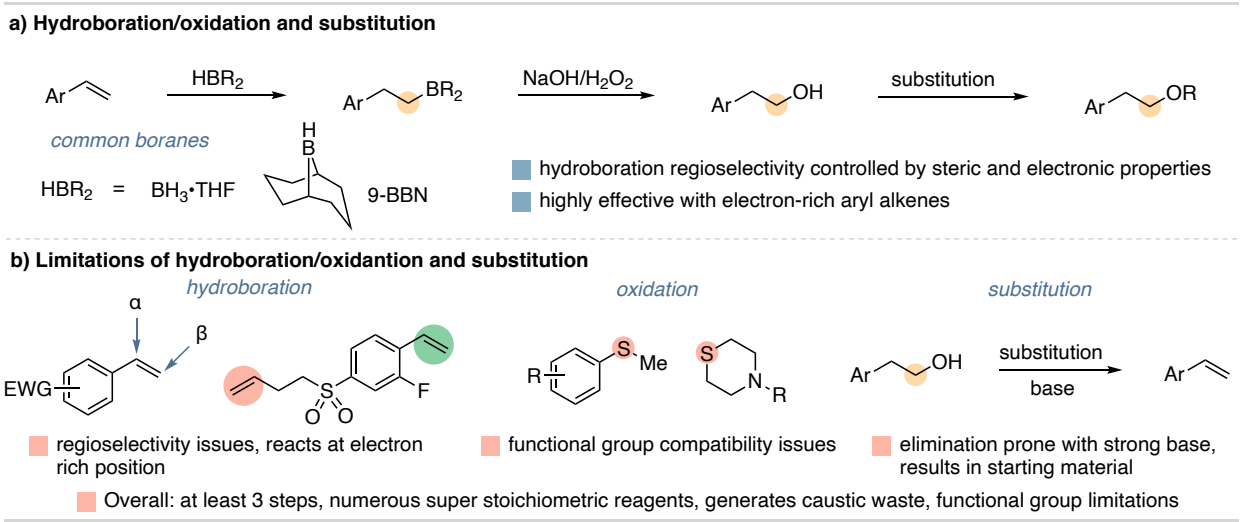

Figure 2-2: Overview of traditional method to access β-aryl ethers and alcohols.

Hydroboration can have regioselectivity issues with electron-deficient aryl alkenes due to the inverted polarity of the alkene (Figure 2-2b). This will result in a mixture of β- and α-aryl alcohol products. Another issue in regioselective hydroboration is the presence of electron-rich

alkenes, as hydroboration will selectively react with the most electron-rich alkene (Figure 2-2b).[20, 21] Additionally, hydroboration can be sensitive to heterocycles as the nucleophilic heteroatom can coordinate to the borane and shutdown the reaction.[21] Meanwhile, the oxidation step has limitations as well. For example, oxidation prone functional groups such as thioethers or other alkenes can undergo undesired oxidation. Once the β-aryl alcohol is accessed substitution must be done to generate the β-aryl ether.[14-17] Substitution reactions with alcohols generally require strong base, but when exposed to strong base β-aryl ethers and activated alcohols are prone to elimination, which would result in the starting aryl alkene (Figure 2-2b, right). This problem is particularly pronounced with electron-deficient arenes. Overall, this synthetic route requires numerous super stoichiometric reagents and generates a caustic waste stream, further highlighting its limitations.

An alternative approach to β-aryl ethers and alcohols is aryl acetic acid/ester reduction, followed by substitution to access the β-aryl ether (Figure 2-3).[24-26] While this approach would avoid the limitations of hydroboration, this process is still be limited by the substitution step, and reduction of esters and carboxylic acids can have functional group limitations such as ketones. Additionally, if the aryl acetic acid derivative is not commercially available it will need to be prepared either through α-arylation or through carboxylation of a methyl arene.

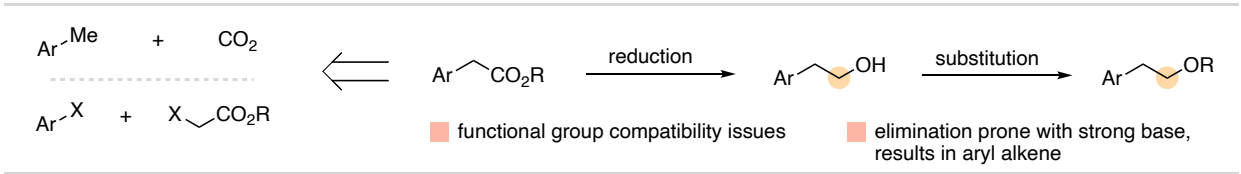

Figure 2-3: Alternative synthetic route to β-aryl ethers and alcohols.

The value of β-aryl ethers and alcohols necessitates efficient preparation from readily available starting materials such as alcohols and aryl alkenes. Currently, hydroboration/oxidation/substitution and aryl acetic acid/ester reduction then substitution have major drawbacks that limit access to β-aryl ethers and alcohols. Base-catalyzed alcohol addition

to aryl alkenes in an oxa-Michael type reaction represents an ideal approach to this valuable motif. Section 2.3 discuss the current state of oxa-Michael type additions and modern approaches to this transformation.

2.3 Nucleophilic Addition Reactions to Alkene Electrophiles

2.3.1 Overview of Well-Developed Pronucleophile Addition to Alkene Electrophiles

A Michael addition or Michael reaction is the nucleophilic addition of a stabilized carbanion to a 1,4-activated π-system (Figure 2-4a).[1] Heteroatom pronucleophiles such as alcohols and amines can also function in Michael-type additions.[3,4] Common electronic activating groups on the alkene include aldehydes, ketones, esters, nitriles and nitro groups. Common pronucleophiles include the acidic α-position of carbonyl derivatives and nitro groups, as well as amines in an aza-Michael addition. The Michael addition reaction becomes more difficult as the alkene acceptor becomes less polarized and more substituted (Figure 2-4b, left).[27] Heteroatom pronucleophiles, such as alcohols are notorious for being reversible and having unfavorable thermodynamics.[3,4,28] Electron-deficient aryl alkenes appear similar to common Michael acceptors and have been used in such reaction with some pronucleophile classes such as amines.[29,30] However, prior to the Bandar Group's work, alkoxides or alcohol pronucleophiles, were considered very poor nucleophiles for aryl alkene electrophiles (Figure 2-4b, right).[31] The Combination of alcohol pronucleophiles and aryl alkene electrophiles will be discussed in the follow subsections.

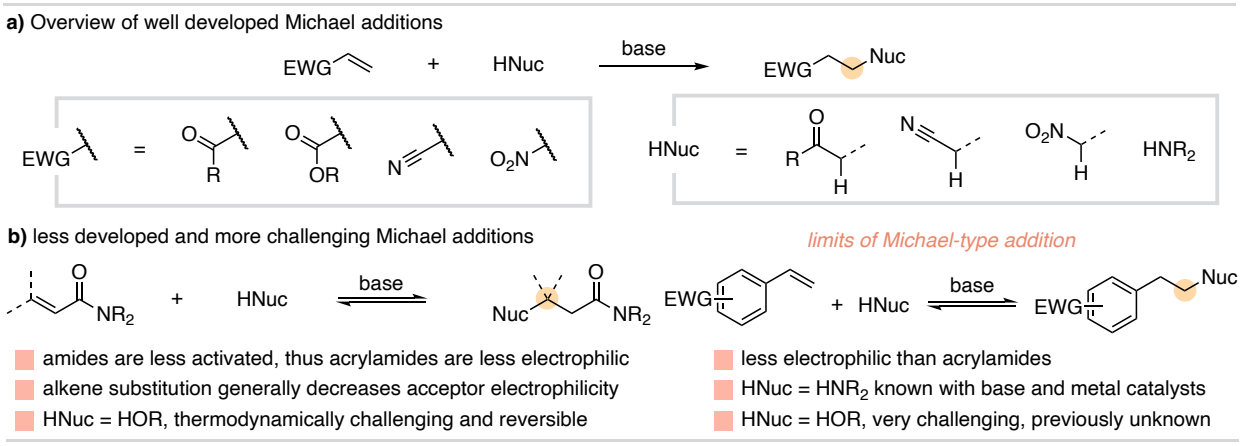

Figure 2-4: Overview of the Michael addition and its limits.

Despite oxa-Michael-type additions being challenging, they have found utility in total synthesis to construct saturated *O*-heterocycles, an example of which is shown in Figure 2-5a.[4,28,32] Very few examples of oxa-Michael-type additions have been reported to effect anti-Markovnikov hydroetherification of aryl alkenes. Two examples were disclosed as part of medicinal chemistry campaigns to access β-aryl ethers (Figure 2-5b and c)[33,34] and one example was developed in which chromium styrene complexes undergo alcohol addition (Figure 2-5d).[35] This last example was the most general base-catalyzed approach; however, the scope was still limited to three alcohols and three styrene derivatives even with chromium activation of the aryl alkene.

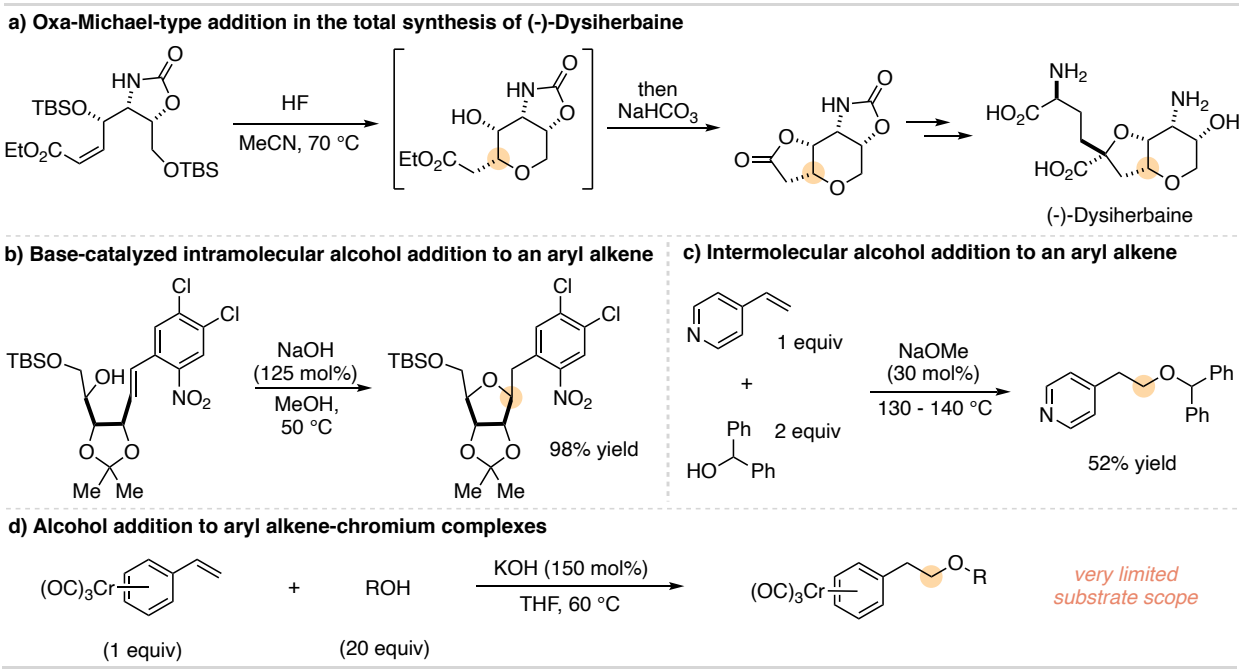

Figure 2-5: Oxa-Michael-type addition reaction examples and precedent for oxa-Michael-type additions to effect anti-Markovnikov hydroetherification.

2.3.2 First Report of Alcohol Addition to Aryl Alkenes

The hitherto accepted mismatch of alkoxide nucleophiles and aryl alkene electrophiles dates back to 1956 and Miller's work.[31] Miller reported that styrene is a much poorer electrophile to a methoxide nucleophile than phenylacetylene. He observed very little anti-Markovnikov addition to styrene even after 20 days of heating styrene, methanol, and sodium methoxide in a sealed ampule at 150 °C (Figure 2-6). From this it was determined that alkoxides were poor nucleophiles for styrene electrophiles. No widely general advancements have been made in base-promoted oxa-Michael-type additions to aryl alkene acceptors since this report. The few examples presented in the previous section are highly specific and not widely applicable. The next advancement in the ability to add alcohols to aryl alkene electrophiles came through the strategic application of photoredox catalysis, this will be discussed in Section 2.3.3.

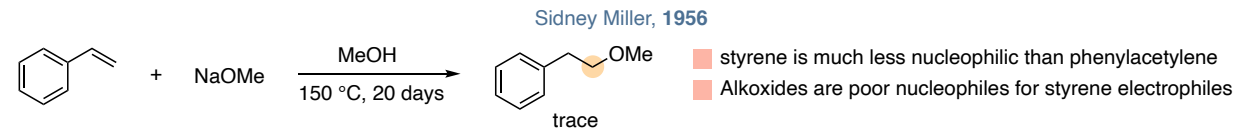

Figure 2-6: Miller's work from 1956. The conclusion from this study was that alkoxides are poor nucleophiles for a styrene electrophile.[31]

2.3.3 Modern Photoredox Approaches to anti-Markovnikov Alcohol Addition into Alkenes

In 2012, the Nicewicz Group reported the first general way to achieve anti-Markovnikov alkene hydroetherification (Figure 2-7).[36] In this method alkenols undergo intramolecular cyclization promoted by a photocatalyst (Figure 2-7). Nicewicz reported only one example of an intermolecular anti-Markovnikov hydroetherification reaction between **2-1** and 10 equiv of methanol (Figure 2-7, bottom right). This reaction proceeds first through excitation of the organic photocatalyst that then oxidizes the alkene to a radical cation. The alcohol then adds into the radical cation in an anti-Markovnikov fashion to generate the more substituted and stable radical. Hydrogen atom (H-atom) transfer from an H-atom donor generates the product and electron transfer between the reduced photocatalyst and H-atom donor closes the catalytic cycle. Figure 2-7, top right shows the key intermediate in this process, the alkene radical cation.

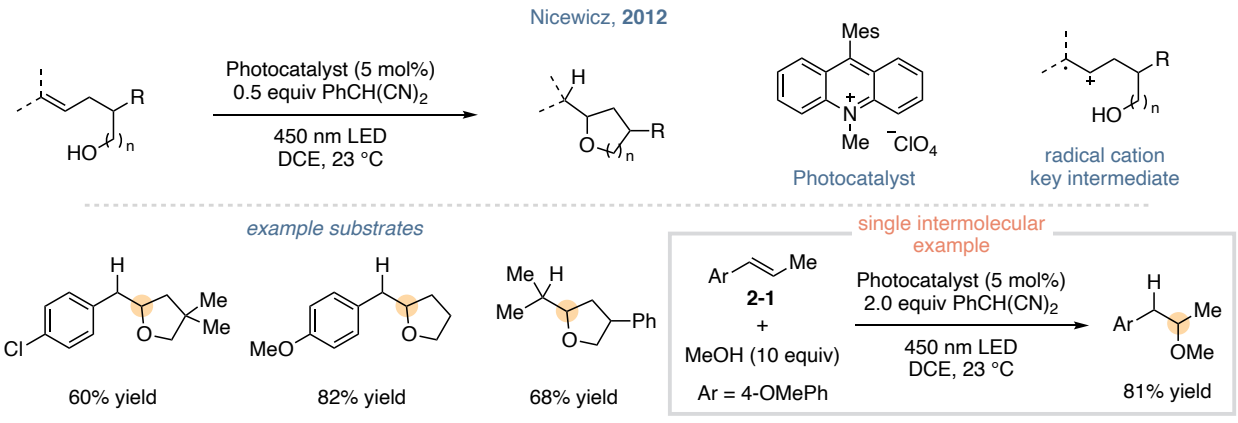

Figure 2-7: Nicewicz's work published in 2012, the first general anti-Markovnikov hydroetherification reaction on unactivated alkenes.[36]

More recently, the Knowles Group developed a related photoredox approach to anti-Markovnikov hydroetherification (Figure 2-8).[37] In this method, a photocatalyst is excited with a phosphate base to enable proton-coupled electron transfer (PCET) to access an *O*-centered radical that undergoes intramolecular cyclization with an alkene. H-atom transfer generates the product. Figure 2-8 shows the key intermediate in this reaction, an alkoxy radical. This method has a broad scope of alkenol substrates; however, no intermolecular versions were reported, most likely due to the instability and thus short lifetime of an *O*-centered radical in solution. The work discussed in this section represents the most direct approach to access β-aryl ethers even though the work was not exclusively focused on accessing this valuable motif. The next section presents the importance of this type of functionality and traditional ways this structural unit would be synthesized.

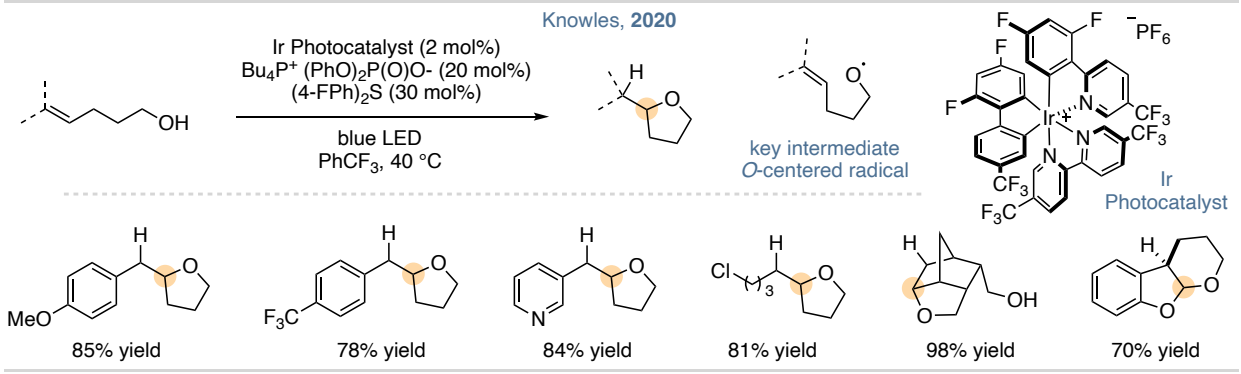

Figure 2-8: Knowles's PCET approach to anti-Markovnikov hydroetherification.[37]

2.4 Superbase-Catalyzed anti-Markovnikov Alcohol Addition to Aryl Alkenes, Bandar 2018[38]

2.4.1 Review of The Bandar Group's First Publication

A direct and complementary approach to the chemistry outlined in Section 2.3.2 would be a base-catalyzed addition of alcohols to aryl alkenes. Nucleophilic alcohol addition to aryl alkenes is expected to be anti-Markovnikov selective, due to the inherent polarity of the alkene and generation of a stabilized-benzylic carbanion. This would be most favorable with electron-

deficient aryl alkenes, the substrate class most limited with hydroboration. As discussed in Section 1.6, the Bandar Group, specifically Dr. Choasheng Luo, developed the first general method to add alcohols to electron-deficient aryl alkenes in 2018 (Figure 1-8).[38,39] The proposed Mechanism is shown in Figure 2-9. The reaction starts with alcohol deprotonation by the P$_4$-*t*-Bu catalyst to generate a nucleophilic ion-pair. The alkoxide anion then adds into the aryl alkene electrophile in an anti-Markovnikov fashion resulting in a benzylic anion. This carbanion is rapidly protonated by the cationic conjugate acid of P$_4$-*t*-Bu to close the cycle. This mechanism was envisioned based on the unique properties of P$_4$-*t*-Bu and its conjugate acid, namely its large size leading to a more nucleophilic alkoxide and the cationic nature of the conjugate acid that would undergo rapid proton transfer to the benzylic anion and thus prevent the elimination reaction.

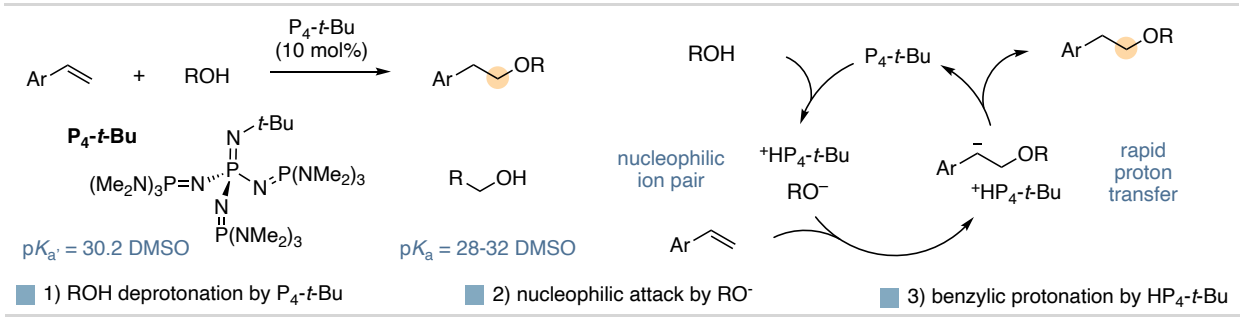

Figure 2-9: Proposed catalytic cycle of P$_4$-*t*-Bu-catalyzed alcohol addition to aryl alkenes.[38,39]

2.4.2 Reaction Conditions, Scope, and Limitation

The group's initial publication of superbase-catalyzed alcohol addition to aryl alkenes as mentioned above discloses the first general way to effect anti-Markovnikov hydroetherification on aryl alkenes. This transformation is accomplished by using an excess of the alcohol pronucleophile, 10 mol% of the P$_4$-*t*-Bu catalyst, *m*-xylene and generally high temperatures (Figure 2-10, top). Dr. Luo found this reaction to have a broad scope of electron-deficient aryl alkenes and alcohols, more examples are shown in Figure 2-10, bottom. 2-ethyl-1-hexanol was used with a range of aryl alkenes to access a variety of different electron-deficient β-aryl ether (**2-**

2 – **2-7** and **2-10**). β-Methyl aryl alkenes **2-9** and **2-12** provided good yields and functionalized alcohols also provided good to excellent yields (**2-8**, **2-11**, **2-13**, **2-14**).[38]

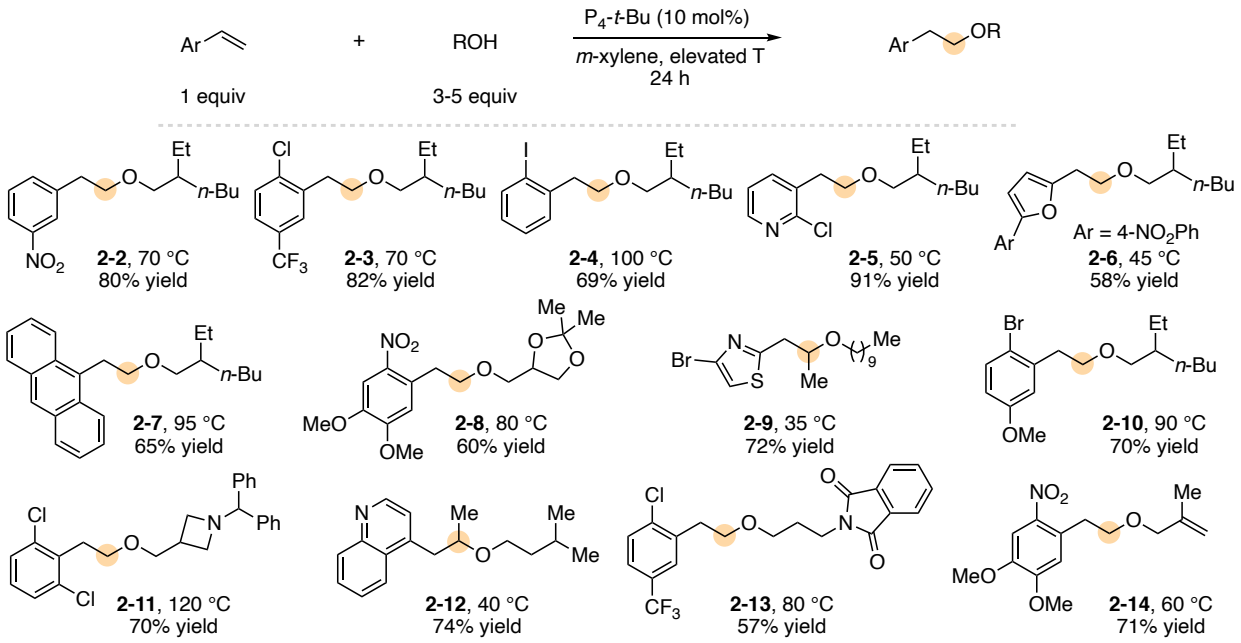

Figure 2-10: Examples of substrates from the Bandar Group's 2018 alcohol addition method.[38]

This reaction does have a few limitations that may prevent its widespread adoption and implementation on larger scales. There are three limitations that I, as a member of the Bandar Group identified in this regard:

(1) The first is the requirement of a large excess of alcohol (3-5 equiv) to obtain high yields. This may not be an issue on smaller scales and with readily available alcohols; however, on larger scale syntheses and with more complex, less available alcohols this can restrict the efficiency and increase the cost; an example of this is **2-19** (Figure 2-11).

(2) The next limitation is the requirement of high reaction temperatures as it can promote undesired side reactions such as competing hydroamination with substrate **2-18**.

(3) The final limitation is that the reaction requires an electron-deficient aryl alkene. Substrates **2-15** and **2-16** illustrate this restriction. While electron-neutral and electron-rich

aryl alkenes can be converted to β-aryl ethers using traditional hydroboration/oxidation/substitution reliably, a direct catalytic approach is still more practical and efficient.[38]

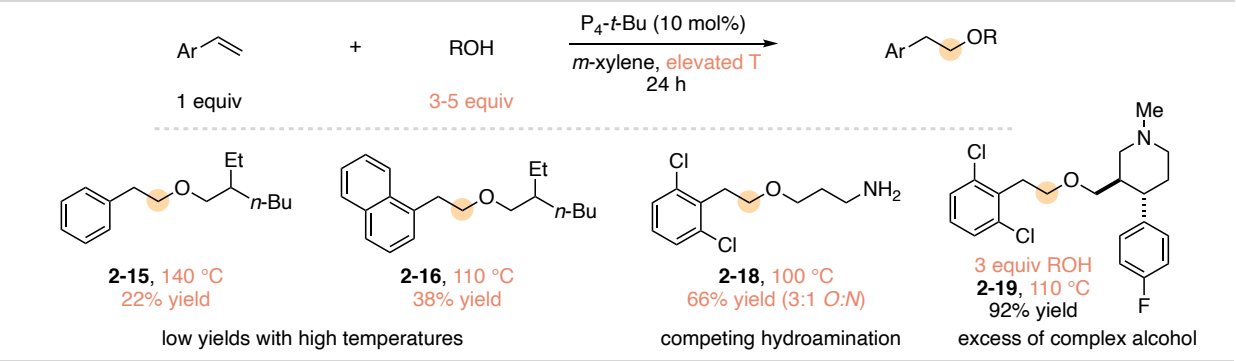

Figure 2-11: Example substrates that highlight limitations of P4-*t*-Bu-catalyzed alcohol addition. Isolated yields are reported.[38]

I joined the Bandar Group shortly after the initial work was published in 2018 and became part of a team of chemists from the Bandar Group and Paton Group working to address these limitations and make this method a practical way to access β-aryl ethers. The results of this collaboration and my contributions are highlighted in Sections 2.5 to 2.10.

2.5 Mechanistic Studies on Superbase-Catalyzed anti-Markovnikov Alcohol Addition[40]

2.5.1 Mechanistic Studies Overview

The Bandar and Paton Groups conducted mechanistic studies from several different approaches. The Paton Group used computational modeling to gain insight into intermediates, transition states, arene electronic impacts, and solvent property effects on the reaction outcome. The Bandar group and I used thermodynamic and kinetic experiments to probe the reaction energetics and factors that control the reaction rate. In the Paton Group a former post-doctoral research, Dr. Juan V. Alegre-Requena and graduate student Liliana Gallegos worked on modeling these reactions. From the Bandar Group, Dr. Chaosheng Luo and a former graduate student, Spencer Pajk worked on the thermodynamic studies, while I preformed the kinetic studies. We set

out to determine what factors control the reaction thermodynamics and mechanism, and especially the reaction kinetics. We reasoned with this insight we would be able to rationally improve and address the aforementioned limitations.

2.5.2 Thermodynamic Studies Summary

The reason for investigating the thermodynamic parameters of superbase-catalyzed anti-Markovnikov alcohol addition is Dr. Luo's observation that the reaction is reversible and under thermodynamic equilibrium control (Figure 2-12). Thermodynamic measurements therefore provide insight into the factors controlling the equilibrium position of the reaction.[38,40]

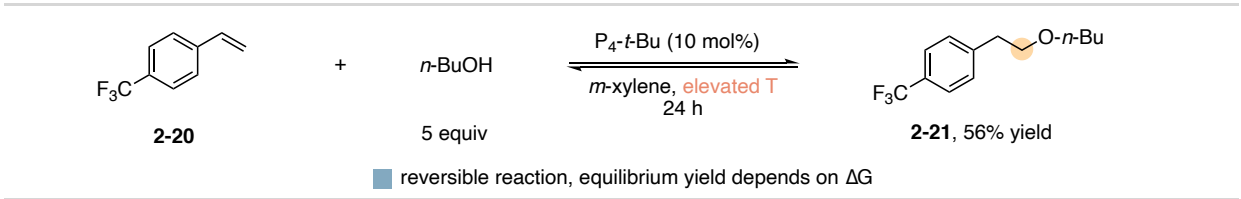

Figure 2-12: The reversibility of P4-*t*-Bu-catalyzed alcohol addition reaction, and the model reaction used in most mechanistic studies.

The model reaction shown in Figure 2-12 between **2-20** and *n*-butanol (*n*-BuOH) was chosen to investigate in depth because a moderate yield of 56% was observed at 80 °C with 5 equiv of *n*-BuOH. We reasoned this would allow for easy observation of a change in equilibrium position. First, Spencer Pajk and Dr. Luo measured the equilibrium position of the model reaction with 3 equiv of *n*-BuOH in twenty different solvents and determined K_{eq} and ΔG values (Table 2-1). It was found that nonpolar aromatic solvents generally provide the most favorable K_{eq} and ΔG values. This is in agreement with optimization studies from the initial report.[38,40]

Table 2-1: Equilibrium studies in different solvents. Reactions run in both directions at 80 °C for 24 h, forward: 1 equiv **2-20**, 0 equiv product, 3 equiv *n*-BuOH, reverse: 0 equiv **2-20**, 1 equiv product, 2 equiv *n*-BuOH at the start of the reaction. ^{1}H NMR analysis used to determin reaction outcomes.[40]

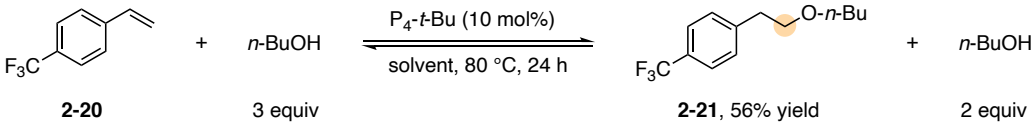

Solvent	K_{eq}	ΔG (kcal/mol)
PhMe	0.96	0.03
m-xylene	0.72	0.24
mesitylene	0.27	0.98
dodecane	0.13	1.46
cyclohexane	1.09	-0.06
N,N-dimethylformamide	0.15	1.46
quinoline	0.16	1.30
N-methyl-2-pyrrolidone	0.17	1.24
anisole	0.17	1.24
benzonitrile	0.25	0.97
pyridine	0.30	0.85
tetralin	0.31	086
dioxane	0.35	0.75
THF	0.45	0.56
1,2-dichlorobenzene	0.52	0.46
dibutyl ether	0.62	0.33
chlorobenzene	0.70	0.25
acetonitrile	0.38	0.67
dimethyl sulfoxide	0.11	1.56
nitrobenzene	0.31	0.82
1,2-dimethyloxyethane	0.35	0.73
ethyl orthoformate	0.39	0.65
cyclopentyl methyl ether	0.52	0.46
1,4-bis(trifluoromethyl)benzene	0.53	0.45
α,α,α-trifluorotoluene	0.91	0.06

Quantitative Model Built by Multivariate Linear Regression: To gain better insight into how the properties of the solvent effect the free energy of the addition, the Paton Group performed multivariate linear regression analysis on the K_{eq} and ΔG data from twelve of the twenty solvents and several solvent descriptors (Figure 2-13).[41] A quantitative model was obtained to predict ΔG with a mean absolute error of 0.22 kcal/mol for the training set of twelve solvents and a mean absolute error of 0.19 kcal/mol for the remaining eight solvents that were not included in the training set. Two solvent descriptors were found to be statistically significant, the second COSMO σ-moment (*Sig*2)[42,43] and McGowan molar volume (V).[44] Both descriptors are computationally determined; the first, *Sig*2 is an overall measure of the solvent's electrostatic polarity; the second,

V is a measure of a solvent molecule's size. V is needed to explain the difference in K_{eq} and ΔG between solvents like mesitylene, *m*-xylene and PhMe or dodecane and cyclohexane. We rationalized this finding as smaller solvent molecules would be better able to disrupt P_4-*t*-Bu – alcohol interactions, see Section 2.5.3 for more details about this interaction. This would slightly increase ΔG when using smaller solvent molecule over a very similar but larger solvent molecule.[40]

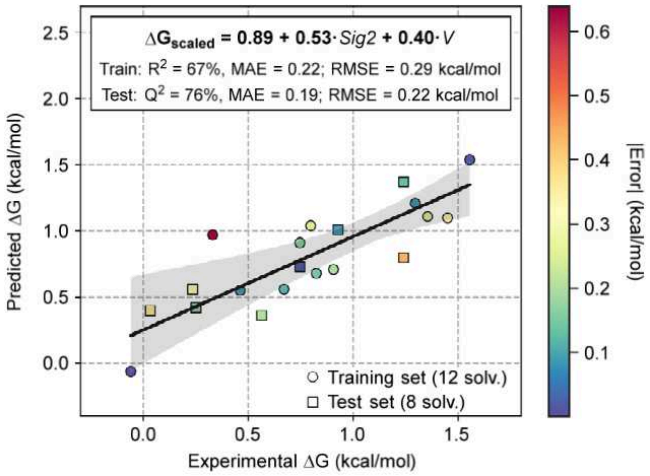

Figure 2-13: Multivariate linear regression analysis using solvent K_{eq} data to relate solvent properties to ΔG.[40]

Next, Spencer and Dr. Luo measured the equilibrium concentrations of the model reaction components at various temperatures and prepared van't Hoff plots to determine the change in enthalpy (ΔH) and entropy (ΔS) (Figure 2-14). This was done in PhMe and DMSO. They found the reaction is slightly exothermic (-ΔH) in both PhMe and DMSO, but most exothermic in PhMe. However, they also found the model reaction is entropically disfavored (-ΔS) in both solvents to a similar degree. The van't Hoff plot analysis suggest that careful optimization of reaction temperature is needed to minimize the entropic penalty and maximize the free energy (ΔG) of the addition reaction (ΔG=ΔH-**T**ΔS).[40]

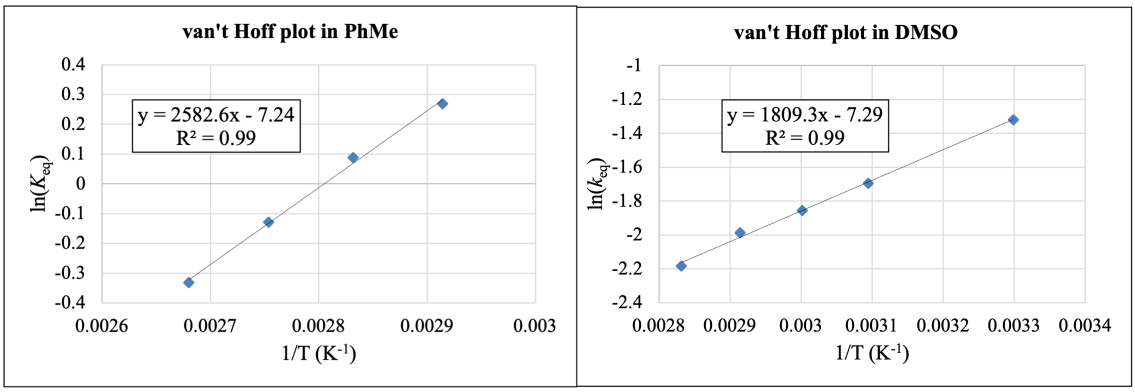

Figure 2-14: van't Hoff plots for the model reaction in PhMe (left) and DMSO (right). PhMe: ΔH = -5.1 kcal/mol, ΔS = -14.4 e.u. DMSO: ΔH = -3.6 kcal/mol, ΔS = -14.5 e.u. ^{1}H NMR analysis used to determin reaction outcomes.[40]

The final thermodynamic study Dr. Luo and Spencer conducted was an investigation into aryl alkene electronic linear free energy relationship (Figure 2-15). A positive, linear relationship was observed in a Hammett plot between the $\sigma_{p/m}$ of the substituent on the arene ring and log(K_{eq}).[45,46] This suggests that the requirement for an electron-deficient aryl alkene is thermodynamic in nature and not solely due to a higher kinetic barrier. This electronic effect on ΔG is likely due to an unfavorable and greater loss of conjugation with more electron-rich aryl alkenes. This was supported computational by isodesmic reaction calculations on aryl alkene hydroetherification, aryl alkene hydrogenation, and ethyl arene C-H etherification (Figure 2-16). The ΔΔG of a series of increasingly electron-rich arenes for each reaction was calculated. Aryl alkene hydroetherification and aryl alkene hydrogenation were observed to have the same trend. Both reactions have a loss of conjugation as the main similarity, suggesting the ΔΔG trend is due to this feature.[40]

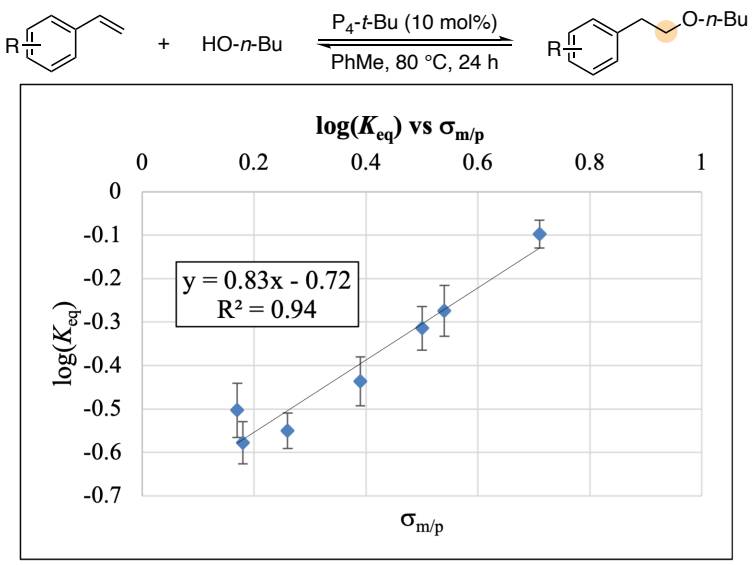

Figure 2-15: Hammett plot showing arene electronic effects on reaction equilibrium. ^{1}H NMR analysis used to determin reaction outcomes.[40,45,46]

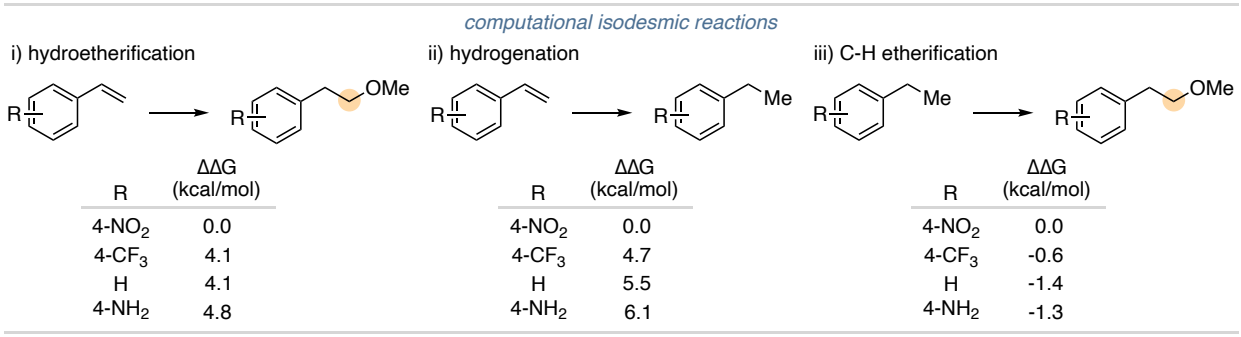

R	ΔΔG (kcal/mol)
4-NO_2	0.0
4-CF_3	4.1
H	4.1
4-NH_2	4.8

R	ΔΔG (kcal/mol)
4-NO_2	0.0
4-CF_3	4.7
H	5.5
4-NH_2	6.1

R	ΔΔG (kcal/mol)
4-NO_2	0.0
4-CF_3	-0.6
H	-1.4
4-NH_2	-1.3

Figure 2-16: Isodesmic reaction calculations to elucidate arene electronic effect on ΔG and K_{eq}.[40]

2.5.3 *Kinetic Studies*

My role within this collaboration and mechanistic investigation was to probe the factors that govern the reaction kinetics. I used the method of initial rates to measure the rate orders of each reactant of the model reaction (Figure 2.17). As expected based on our proposed catalytic cycle (Figure 2-9), I observed first order dependance on **2-20** concentration. Unexpectedly, I observed -4.6 order dependance on *n*-BuOH concentration and 2.6 order dependance on P_4-*t*-Bu concentration. We reasoned the observation of large nonlinear rate orders in *n*-BuOH and P_4-*t*-Bu concentrations could be due to the formation of "off-cycle" hydrogen bonding (H-bonding) aggregates (Figure 2-18). This is similar to the known use of alkoxide bases in alcohol solvents

wherein extensive H-bonding decreases basicity and nucleophilicity.[47,48] Additionally, similar behavior has been observed in crystal structures of P_4-*t*-Bu•alcohol salts, in which the ion-pair co-crystalizes with 3-4 excess equivalents of alcohol.[49-52] Section 2.6 explores this observation and hypothesis in more detail with computational modeling and more kinetic studies.[40]

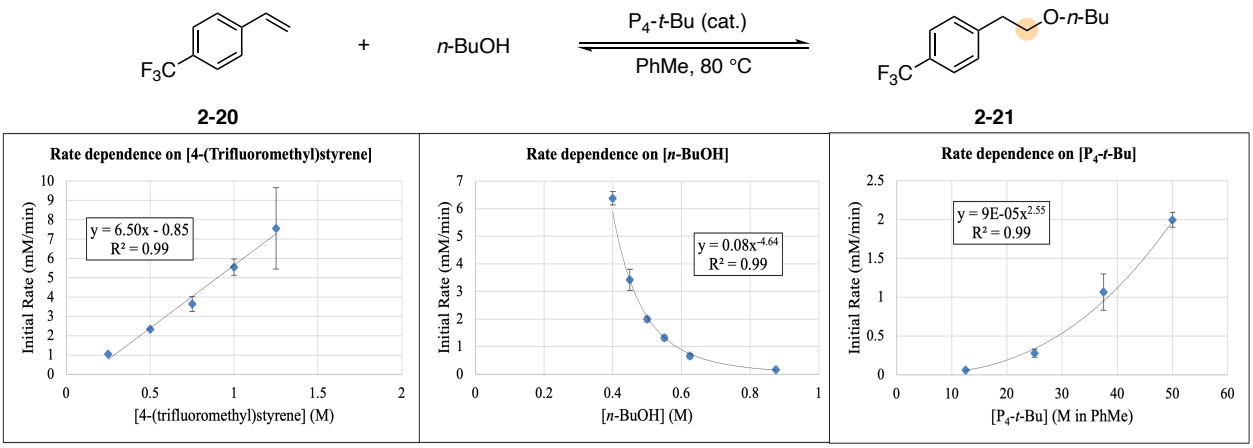

Figure 2-17: Kinetic studies of the model reaction in PhMe, observed rate orders; **2-20**: 1st, *n*-BuOH: -4.6, P_4-*t*-Bu: 2.6. GC analysis using dodecane as an internal standard used to determine reaction progression.[40]

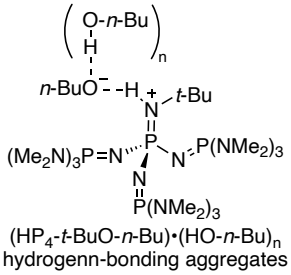

Figure 2-18: H-bonding aggregate between P_4-*t*-Bu and excess *n*-BuOH.

2.6 Ion-Pairing Studies on P_4-*t*-Bu•HOR

Based on the kinetic studies described in Section 2.5 and the hypothesis derived from my observations, I reasoned that the solvent properties would have a large effect on the H-bonding aggregates of P_4-*t*-Bu and alcohol. The specific solvent parameter that should have the largest impact on the kinetic profile of the reaction is the ability of a solvent to accept an H-bond. The greater a solvent's ability to accept an H-bond the more easily HP_4-*t*-Bu•OR and excess alcohol should dissociate as the solvent will more strongly interact with the alcohol (Figure 2-19).

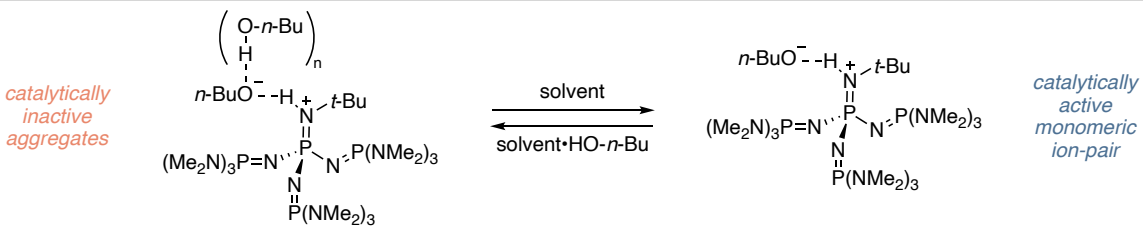

Figure 2-19: Solvent disruption of the H-bonding aggregates, formation of catalytically active monomeric ion-pair.

To test this proposal, I again measured the observed rated orders with the method of initial rate for each reactant, but this time in solvents that had varied β values. A β value is a measure of a solvent's ability to accept an H-bond, with larger β values indicating a stronger H-bond acceptor. For reference, cyclohexane, a very weak H-bond acceptor has a β value of 0, while HMPA, a very strong hydrogen bond acceptor, has a β value of 1.05.[55] β values correlate well to a solvent's general polarity. To measure rate orders in polar solvents, I found that a new model reaction was needed with an aryl alkene (**2-21**) that has a higher K_{eq} value in polar solvents (Figure 2-20, top). The results of this study are shown in Figure 2-20 with the solvents being PhMe, *n*-Bu_2O and DMSO that have β values of 0.14, 0.45 and 0.88, respectively.[55] For comparison, the dielectric constants (ε) of each solvent are shown; ε are considered to be a general measure of a solvent's polarity. I observed similar rate orders for this new model reaction as to the previous in PhMe, indicating similar behavior in the new system. However, the observed rate orders of *n*-BuOH and P_4-*t*-Bu concentrations became more linear as the β value of the solvent increased. For example, the observed rate orders of *n*-BuOH and P_4-*t*-Bu concentrations in DMSO are -2.0 and 1.5, respectively. This indicates that the catalytic system becomes more active in more polar solvents or more active as the solvent is better able to accept a H-bond. This is also evidenced by the fact that I had to measure the rate orders in DMSO at 40 °C instead of 80 °C, as was the case for PhMe and *n*-Bu_2O, since the reaction in DMSO was too fast to measure at 80 °C. This increased activity

is due to the solvent disrupting the H-bonding aggregates and increasing the concentration of active monomeric ion-pairs.[40]

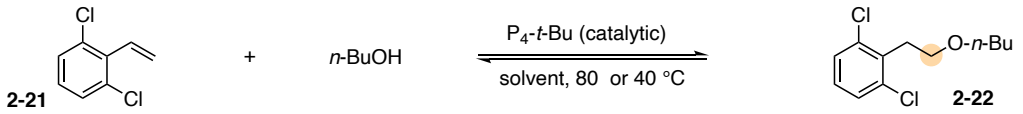

solvent	ε dielectric constant	β values	observed rate orders	
PhMe, 80 °C	2.37	0.14	aryl alkene	1.0
			n-BuOH	-4.1
			P_4-*t*-Bu	2.7
n-Bu_2O, 80 °C	3.05	0.45	aryl alkene	1.0
			n-BuOH	-3.1
			P_4-*t*-Bu	2.3
DMSO, 40 °C	46.8	0.88	aryl alkene	1.0
			n-BuOH	-2.0
			P_4-*t*-Bu	1.5

Figure 2-20: Kinetic studies in varied solvents, indicates polar solvents help break up H-bonding aggregates. GC analysis using dodecane as an internal standard used to determine reaction progression.[40]

2.7 Computational Reaction Modeling

We next worked side-by-side with members of the Paton Group to study the alcohol addition reaction computationally. Specifically, our experimental data was used to guide this work for understanding solvent effects and to develop proposals for the reaction profile. Here, I summarize some of their key findings as it relates to my hypotheses derived from reaction kinetic studies. These computational models proved critical in gaining a complete picture of the mechanism of alcohol addition to aryl alkenes.

2.7.1 Computational Modeling of P_4-t-Bu

Further insight into the ion-pairing properties of P_4-*t*-Bu were gained through computational modeling of the neutral base and its cationic conjugate acid by the Paton Group. Using ωB97X-D/6-31+G(d) level of theory, the gas phase protonation reaction of P_4-*t*-Bu was modeled and electrostatic potential (ESP) mapping and natural charge analysis were performed

(Figure 2-21). First, the optimized geometries were found to be in good agreement with reported crystal structures of P_4-*t*-Bu. Second, the ESP maps highlight the origins of P_4-*t*-Bu's high basicity as the positive charge is distributed to the peripheral methyl hydrogen (green to blue Figure 2-21). Natural charge analysis shows more than half of the charge is delocalized from the introduced H^+, which has a charge of +0.43, whereas the peripheral methyl hydrogen collectively has a charge of +0.40.[40] Additionally, this computational analysis on P_4-*t*-Bu was used as a starting point for further reaction modeling that will be discussed in Section 2.7.2.

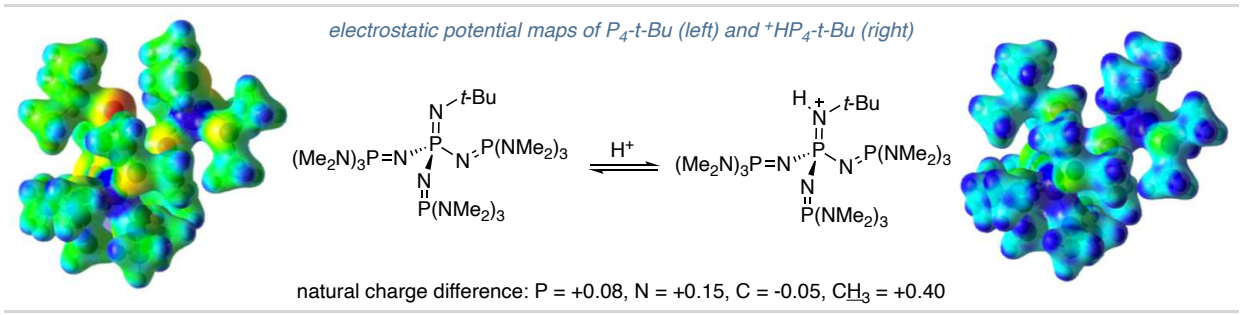

Figure 2-21: electrostatic potential maps and natural charge analysis on P_4-*t*-Bu and $^+HP_4$-*t*-Bu.[40]

2.7.2 Computed Free Energy Reaction Profile

To further probe the reaction mechanism and support experimental findings, the Paton Group calculated the free energy profile of the model reaction between **2-20** and MeOH with varied amounts of MeOH (Figure 2-22). Both density functional theory and coupled-cluster theory was used with DLPNO-CCSD(T)/cc-pV(DT)Z//ωB97X-D/6-31+G(d), (SMD = PhMe, 80 °C) level of theory. The black line shows the reaction profile with one molecule of MeOH, while the red line shows the reaction profile with three molecules of MeOH. Both profiles show small barriers for MeOH deprotonation; however, deprotonation with excess MeOH present is more favorable than with one alcohol molecule present (Int-II, n=0 vs. n=2). The difference in energy between one and three MeOH molecules is about 4 kcal/mol. This indicates that the HP_4-*t*-Bu•OR

and excess alcohol aggregates are likely the resting state of the catalytic system, which is in agreement with my kinetic studies.[40]

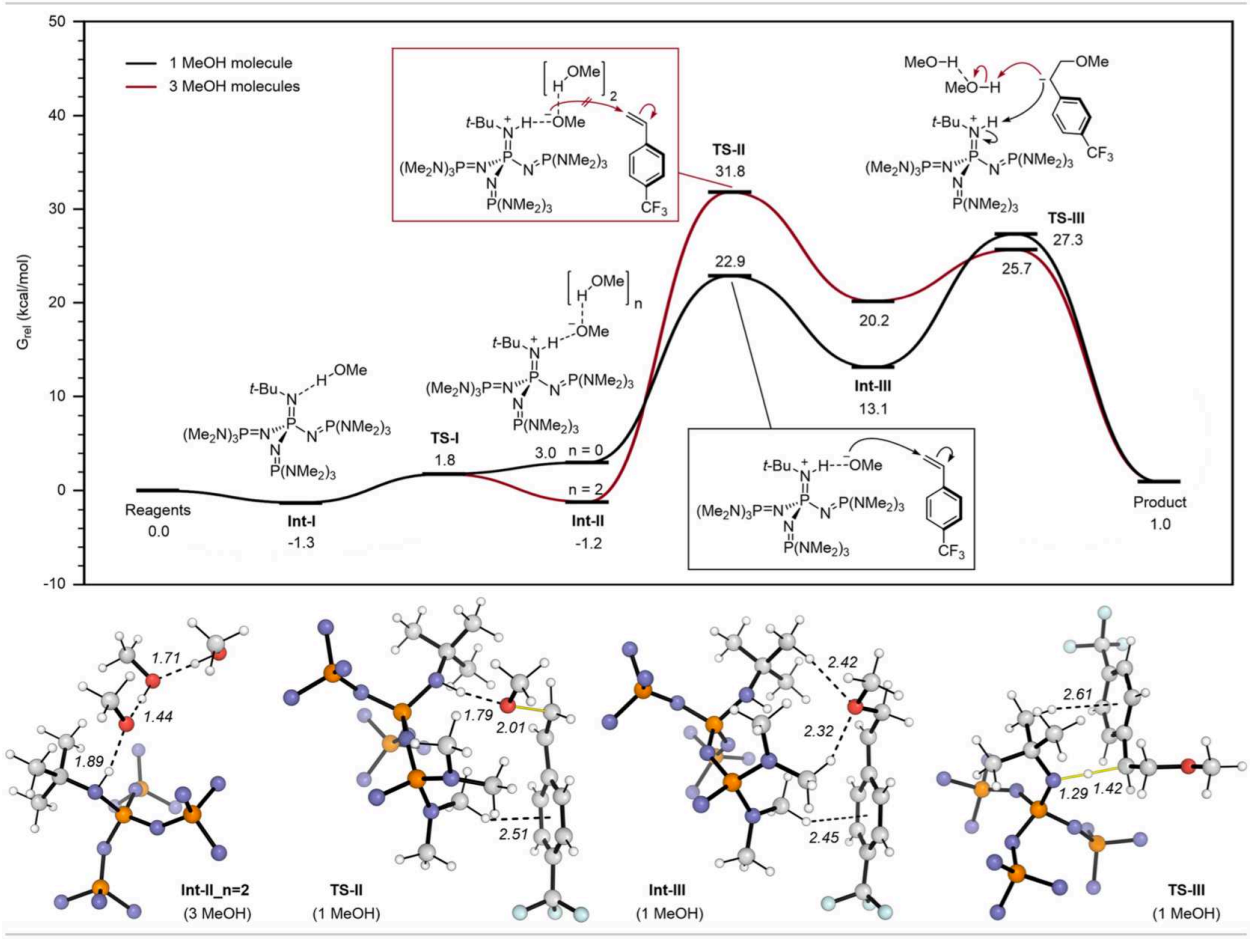

Figure 2-22: Computed free energy profile for the addition of MeOH to **2-20**. Black line calculated with 1 equiv of MeOH, red line calculated with 3 equiv of MeOH.[40]

Next, there is a significant difference between $\Delta G^{\ddagger}$ of Ts-II, n=0 and TS-II, n=2 as Ts-II, n=0 is about 8.9 kcal/mol lower in energy. This indicates that the monomeric ion-pair is significantly more nucleophilic than higher order aggregates. Based on this, lower order aggregates are likely the active catalytic species. This is again in agreement with the observed rate orders of -4.6 for alcohol and 2.6 for P_4-*t*-Bu. In practice, as more alcohol is added the aggregation behavior is magnified and the kinetic barrier, TS-II increases, slowing down the reaction. As more P_4-*t*-Bu is added the concentration of monomeric ion-pairs or lower order aggregates increases and the TS-

II barrier decreases, thus the reaction rate increases. Lastly, we were unable to find a concerted alcohol addition and benzylic protonation pathway, but instead found a distinct carbanion intermediate, Int-III, that is protonated through TS-III to generate the final product.[40]

2.7.3 Investigation into Electronic Variation and Reaction Rate

The last remaining mechanistic feature we sought to investigate is the variation in reaction rate with respect to the electron property of the aryl alkene. This was done experimentally and computationally. However, the forward reaction with electron-rich aryl alkenes establishes an equilibrium that heavily favors the starting material. This posed a significant problem, as I was seeking to experimentally measure the rates of the reaction with electron-rich aryl alkenes. To circumvent this challenge, we reasoned we could simply study the reverse reaction (Figure 2-23). Calculations showed the $\Delta G^{\ddagger}$ for benzylic deprotonation, the first step in the reverse reaction, increased as the aryl alkene became more electron rich for a series of methyl β-aryl ethers. I then measured the elimination rate for the same series of methyl β-aryl ethers and found that the 4-trifluoromethyl substituted arene, the most electron-deficient, reacted the fastest and the 4-methoxy substituted arene, the most electron-rich, reacted the slowest. These results are in agreement with the computed trend in activation energy. To note, for the 4-methoxy substituted arene to have a measurable elimination rate the reaction had to be done at 120 °C in *m*-xylene. This is far above the boiling point of MeOH. To verify our results and experimental setup, I measure the elimination rates of the corresponding *n*-butyl β-aryl ethers and observed the same trend (Figure 2-23, bottom).[40] The next section details how we used our new mechanistic understanding to rationally improve the addition reaction and address the limitations highlighted earlier in this chapter.

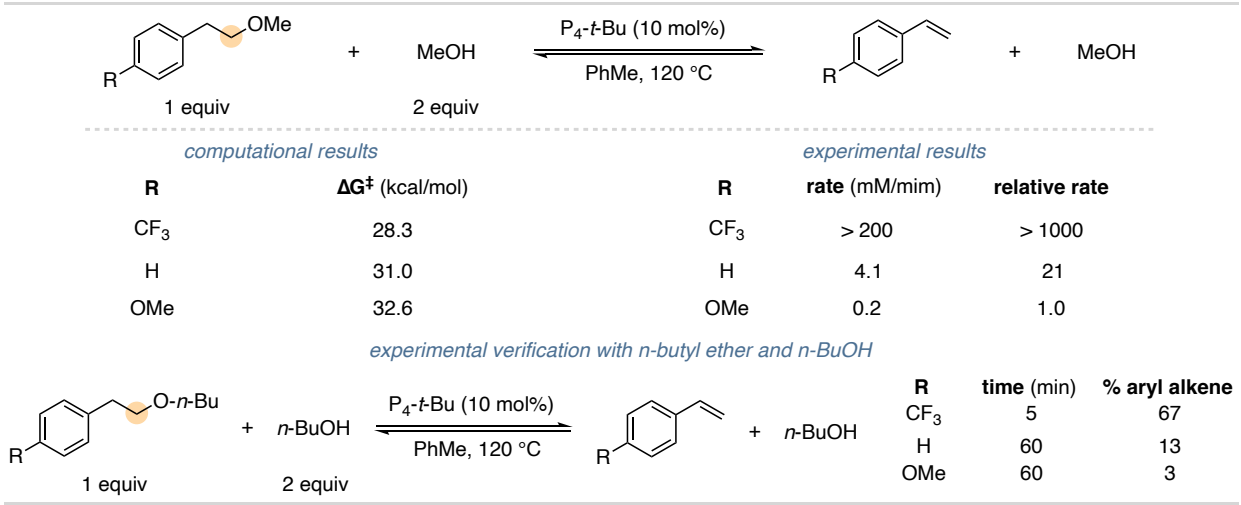

Figure 2-23: Rate dependance of alcohol elimination on arene electronic properties. ^{1}H NMR analysis used to determin reaction outcomes. $\Delta G^{\ddagger}$ predicted for rate determining step, benzylic deprotonation.[40]

2.8 Improvements to Superbase-Catalyzed anti-Markovnikov Alcohol Addition Reactions

2.8.1 Development of Efficient Reaction Conditions

The above mechanistic studies provided clarity regarding the limitations of the reaction published in 2018. The limitations are the requirement of a large excess of alcohol (3-5 equiv), the need for generally high reaction temperatures and the requirement for the aryl alkene to be highly electron deficient. The first key mechanistic finding is that the reaction is most exothermic in nonpolar aromatic solvents like PhMe but that the reaction is entropically disfavored (Figure 2-13). This ultimately means the high reaction temperatures were shifting the equilibrium to favor the reactants by magnifying the entropic penalty ($\Delta G = \Delta H - T\Delta S$). The next key finding is that the reaction is much faster with less alcohol, as I observed -4.6 order dependance on alcohol concentration. The reason for this large negative rate ordering being HP_4-*t*-Bu•OR(HOR)$_n$ aggregation, which is more prevalent in nonpolar solvents such as PhMe. This means a fine balance of temperature and alcohol equivalents is needed for a high equilibrium yield. The final key observation is with more electron-rich aryl alkenes the reaction is less thermodynamically favored,

due to an increased loss of conjugation, and the reaction is much slower, requiring even higher temperatures to reach equilibrium.[40]

The solution to solving the first two limitations is counterintuitive without the mechanistic studies. The solution is to use less alcohol and lower temperatures (Figure 2-24) to shift the reaction energetics to favor the products. By using few equivalents of alcohol, the HP_4-*t*-Bu•$OR(HOR)_n$ aggregation will be minimized, thus increasing the concentration of active monomeric ion-pairs. This results in a more catalytically active system and enables lower reaction temperatures. Lower reaction temperatures shift the equilibrium to favor the products and counterbalance the loss caused by Le Chatelier's principle, thus increasing the yields. Conveniently, this addresses the first two limitations, requiring excess alcohol and high reaction temperatures. A demonstration of these improvements is highlighted in the next section. The third limitation, requirement of electron-deficient aryl alkenes, is addressed in Section 2.8.3.

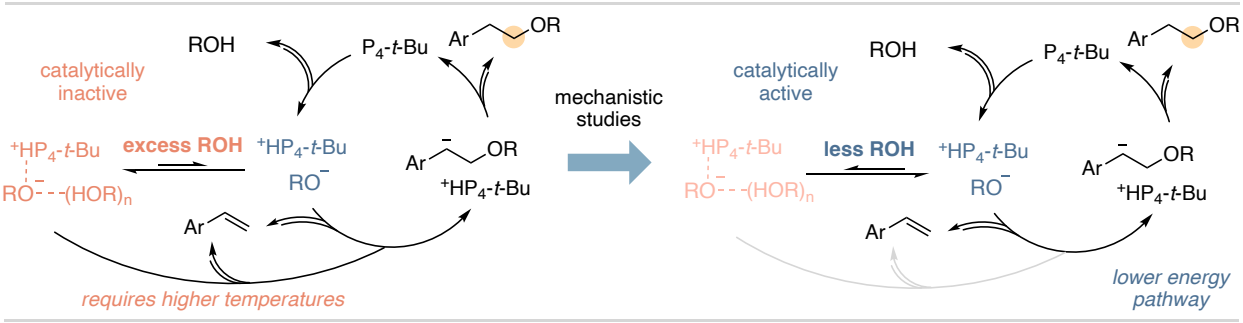

Figure 2-24: Mechanistic understanding of reaction limitations and counterintuitive solutions to address these limitations.[40]

2.8.2 Expanded Scope of Alcohols

Based on the hypothesis that using less alcohol and lower temperatures would enable a high yielding reaction, Dr. Luo identified that 1.2 equiv of alcohol and temperatures generally below 60 °C leads to an equilibrium that favors product formation (Figure 2-25, top). Substrate **2-19** provides a good example of this improvement; this substrate was previously prepared using 3

equiv of alcohol at 110 °C in a 92% yield, under the new conditions a 90% yield is obtained with only 1.2 equiv of alcohol at 60 °C. Next, Dr. Luo developed a scope of substrates with more complex alcohols to highlight the practicality of these new conditions (Figure 2-25, bottom). Pharmaceutical derived **2-23** and steroid derivative **2-24** are obtained in good equilibrium yields. Secondary alcohols (**2-25** to **2-27**) undergo β-addition smoothly to give good yields. More densely functionalized alcohols (**2-29** and **2-30**) result in moderate to good yields of anti-Markovnikov addition product as well. These new conditions and mechanistic understanding also led to an improvement in chemoselectivity with aminoalcohols, as at room temperature competing hydroamination is completely suppressed, **2-31**.[40]

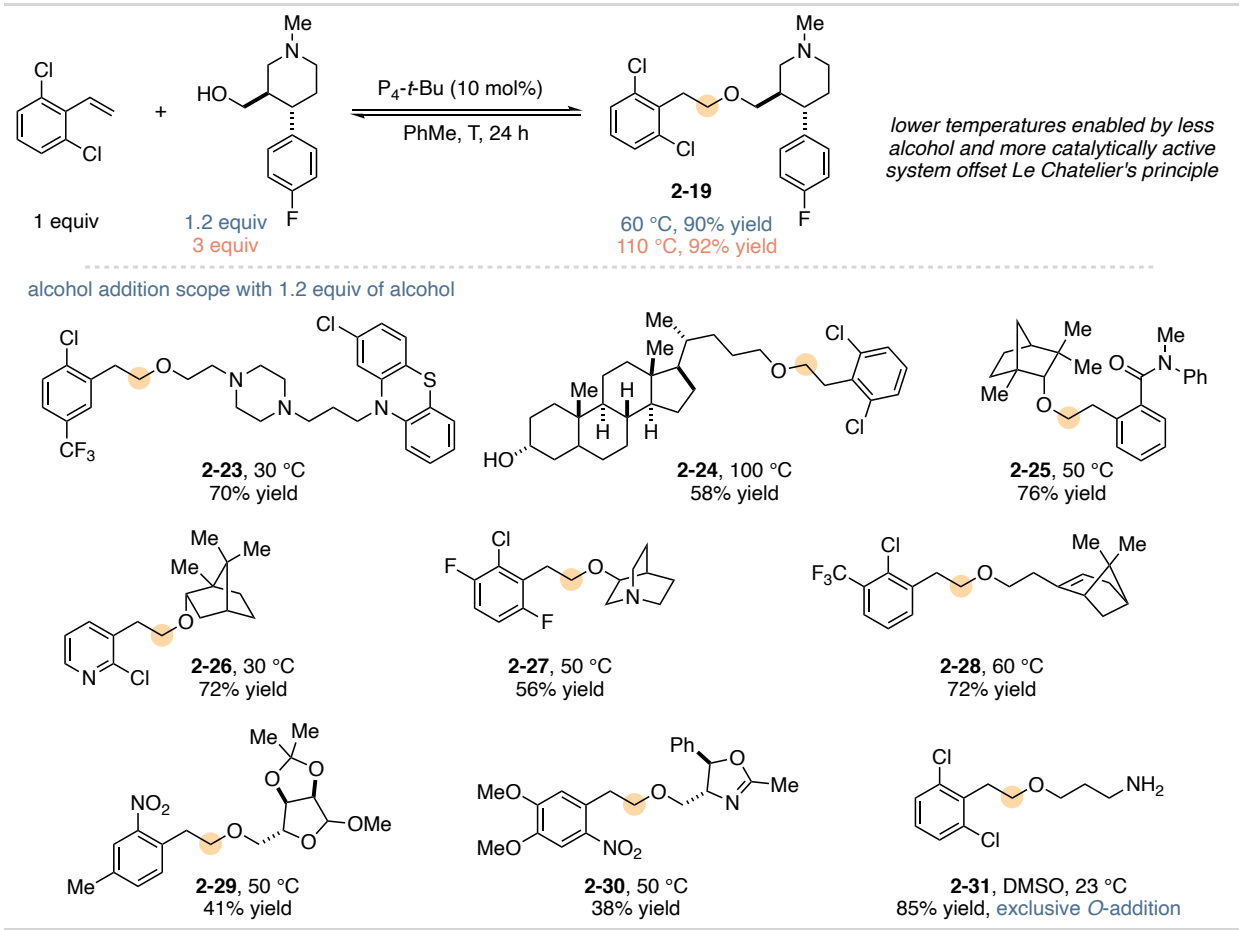

Figure 2-25: Alcohol scope improvements, use of 1.2 equiv makes more complex alcohols more practical and enables lower temperatures. Isolated yields are reported.[40]

2.8.3 Expanded Scope of Styrene Derivatives

Section 2.8.2 addressed two of the three limitations; this section describes my efforts to address the third major limitation, requirement of an electron-deficient aryl alkene. As revealed by computational modeling and experimental studies in Section 2.5.2, with the arene becoming more electron-rich the reaction becomes less favorable. However, the experiments in Section 2.7.3 show that alcohol addition and alcohol elimination are possible with electron-rich aryl alkenes. I reasoned kinetically favorable conditions could be identified under which alcohol addition occurs to more electron-neutral aryl alkenes and the equilibrium favors the addition product. My approach was to invert the stoichiometry of alcohol and aryl alkene to use an excess of the aryl alkene. While this is not the most atom-economical solution, it is relatively cost effective for scenarios where the aryl alkene is inexpensive and readily available. H-bonding aggregation under these conditions would be minimal and the excess aryl alkene should shift the equilibrium to favor addition according to Le Chatelier's principle. Figure 2-26 demonstrates this with the addition of *n*-BuOH to **2-20**; using 5 equiv of **2-20** a good 76% yield of the addition product is obtained. The bottom of Figure 2-26 shows a small scope using these conditions to access the β-aryl ethers of less-activated aryl alkenes with complex alcohol partners.[40]

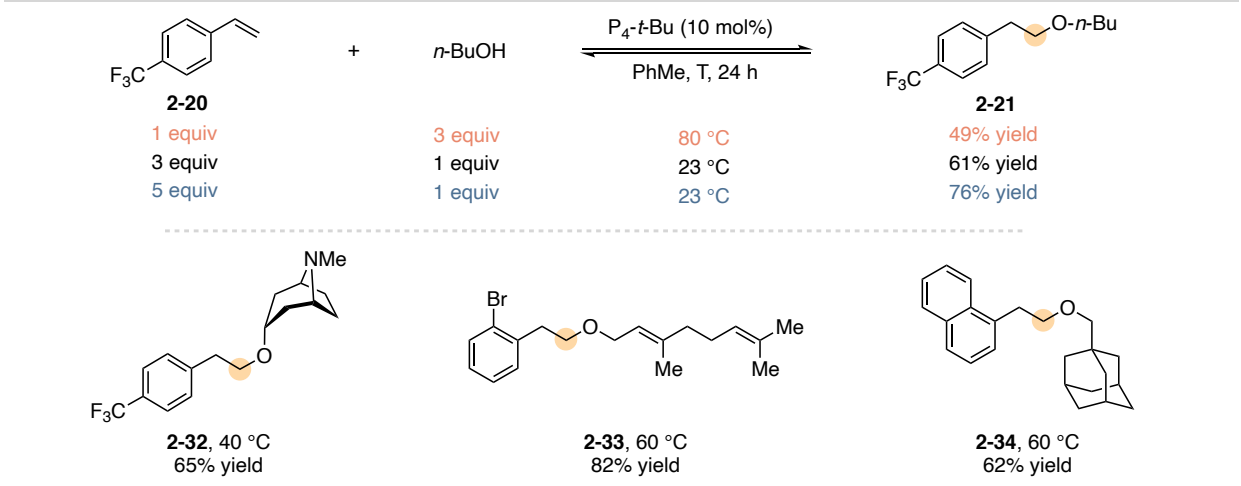

Figure 2-26: New conditions developed to enable less electronically activated aryl alkenes. Isolated yields are reported.[40]

2.8.4 Expansion of Addition Methodology to New Classes of Alkenes

The main limiting factor of alcohol addition to electron-rich aryl alkenes is the entropic penalty which is magnified by the high temperatures needed to overcome high barriers for nucleophilic addition. Given this, I reasoned intramolecular alcohol addition to electron-rich aryl alkenes would be possible since the entropic penalty is decreased. The realization of this proposal is shown with substrates **2-35** and **3-37** in Figure 2-27. This base-catalyzed approach to 2-substituted tetrahydrofuran derivatives completements the photoredox-catalyzed methods developed by the Nicewicz[36] and Knowles Groups[37] well (Section 2.3.3). Figure 2-27ii shows an example process that I developed that could only be promoted *via* a base pathway, wherein an alkene first undergoes base-catalyzed isomerization to the aryl alkene followed by base-catalyzed alcohol addition. The P_4-*t*-Bu catalyst also enables access to 2-substituted 1,4-dioxane heterocycles (Figure 2-27iii). In this application I found DMF was needed to avoid isomerization to the undesired vinyl ether. Beyond aryl alkenes, I was able to expand our insight to enable another unprecedented addition reaction, an oxa-Michael addition to a β-substituted acrylamide (Figure 2-27iv). This addition reaction represents the first reported example of its kind.[40]

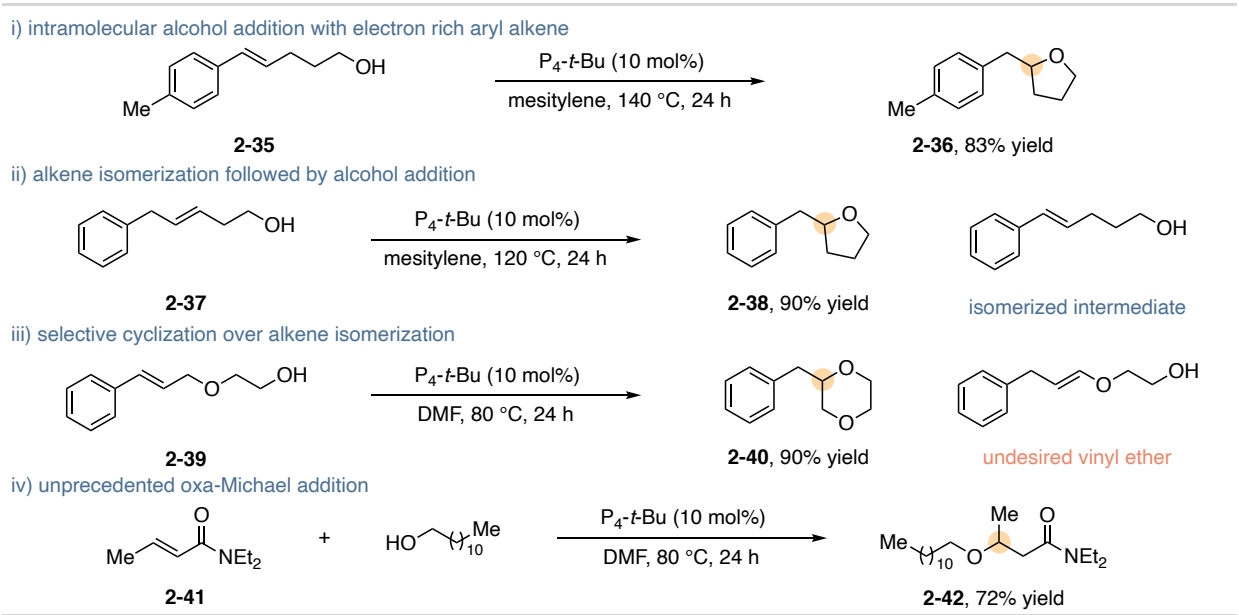

Figure 2-27: Expansion of alcohol addition methodology intramolecular cyclization and oxa-Michael additions. Isolated yields are reported.[40]

2.8.5 Development of Practical Catalytic Conditions

One limitation of P_4-*t*-Bu-catalyzed alcohol addition that is yet to be addressed in this chapter is that P_4-*t*-Bu is a very expensive superbase (see Chapter One Section 1.7.2). Given that alcohol addition to aryl alkenes is slightly exothermic, myself and Dr. Luo reasoned we could identify practical conditions using an inexpensive inorganic catalyst. In the Bandar Group's original work in 2018, many inorganic base and solvent combinations were tried. Dr. Luo and I used this as a starting point and ultimately found that 18-crown-6 ligated KO-*t*-Bu in DME enables moderate to good equilibrium yields of β-aryl ethers. Figure 2-28 shows a substrate scope and comparison of the inorganic catalytic system to the P_4-*t*-Bu catalyst. The organic superbase consistently outperforms the inorganic catalytic system; however, useful synthetic yields can be obtained with the inexpensive metal alkoxide catalyst. The difference in yield is presumably due to a difference in solvent equilibrium effects, as PhMe was found to be the most favorable solvent in Section 2.5.2. Notably, the inorganic base is not active in PhMe.[40]

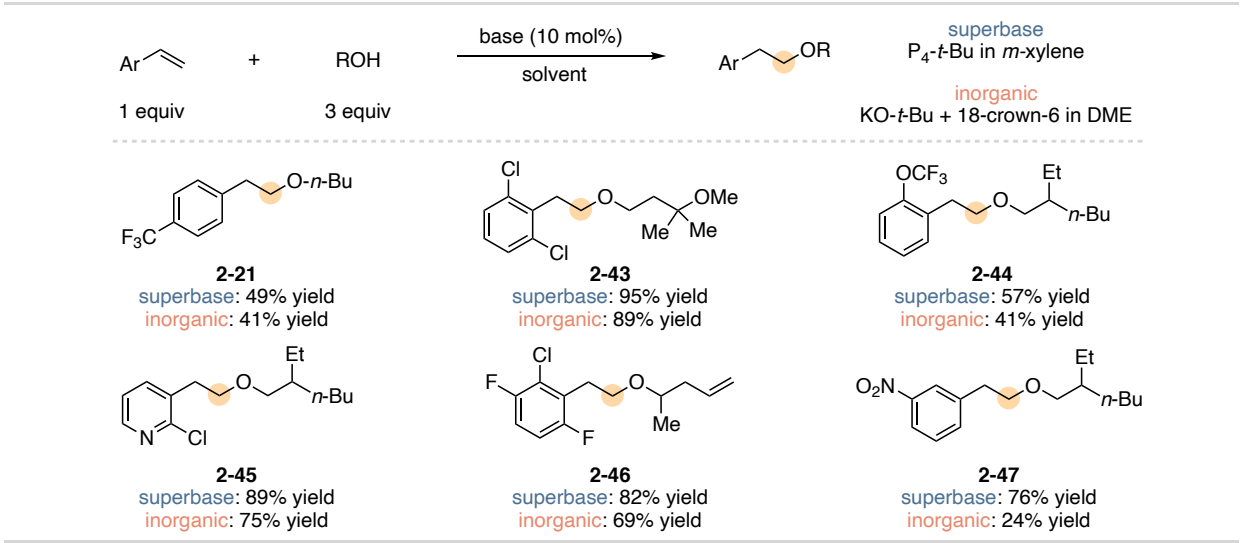

Figure 2-28: Inorganic and superbase catalyst comparison. Isolated yields are reported.[40]

Finally, to further address the high cost of P$_4$-*t*-Bu and to develop a high yielding practical catalytic system, Dr. Luo and I reasoned we could recover P$_4$-*t*-Bu from reaction mixtures as a salt and reuse it with *in situ* deprotonation. We found that P$_4$-*t*-Bu can be easily recovered from spent reactions through a series of washes as the P$_4$-*t*-Bu•HCl salt. The P$_4$-*t*-Bu•HCl salt could be purified and converted to the P$_4$-*t*-Bu•HBF$_4$ salt for long term storage as it is an air-stable solid. Furthermore, stirring the P$_4$-*t*-Bu•HBF$_4$ salt in THF with KO-*t*-Bu, followed by filtration leads to a P$_4$-*t*-Bu solution that can be used in anti-Markovnikov alcohol addition reactions. Figure 2-29 shows this development on substrate **2-47**, which the superbase-catalyst outperformed the inorganic catalyst by 52%. This organic superbase salt can be viewed as a convenient way to recycle and reduce the long-term cost of P$_4$-*t*-Bu.[40]

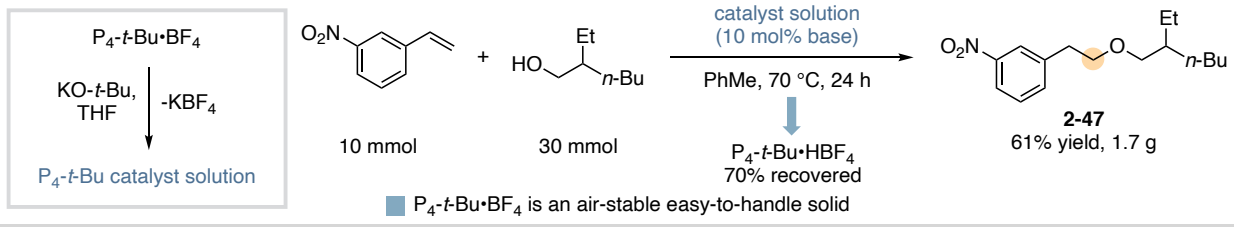

Figure 2-29: Use of HP$_4$-*t*-Bu•BF$_4$ as a practical precatalyst for alcohol addition and recovery of HP$_4$-*t*-Bu•BF$_4$. Isolated yields are reported.[40]

2.9 Anti-Markovnikov Aryl Alkene Hydration

2.9.1 Catalytic anti-Markovnikov Styrene Hydration as a Standing Synthetic Challenge

β-Aryl alcohols are valuable synthetic targets as discussed in Section 2.3.1, and usually prepared in route to β-aryl ethers. This means that their synthesis is limited in many of the same ways as β-aryl ethers. Catalytic anti-Markovnikov hydration of aryl alkenes has been a desired synthetic goal as a sustainable and complementary approach to hydroboration/oxidation. To this end several sophisticated strategies have been developed. The first was published in 2011 by the Grubbs Group, in which triple relay catalysis was used (Figure 2-30).[56] In this reaction, a Pd catalyst oxidizes the aryl alkene to the aldehyde in a Wacker-type oxidation and a ruthenium catalyst (Shvo's catalyst) reduces the aldehyde to the primary alcohol with a copper co-catalyst. 1,4-Benzoquinone (BQ) is used as a terminal oxidant and as a hydrogen acceptor, while 2-propanol (*i*-PrOH) is used as a reductant. This impressive catalytic system does have a few limitations; the first being the over reduced ethyl benzene, ketone and secondary alcohol are common side products of the reaction. The second drawback is that this requires three catalysts, including precious metals. And the third drawback is that this method was only demonstrated on only simple aryl alkenes, although several alkyl-substituted alkenes underwent hydration but with poor yields and selectivity.

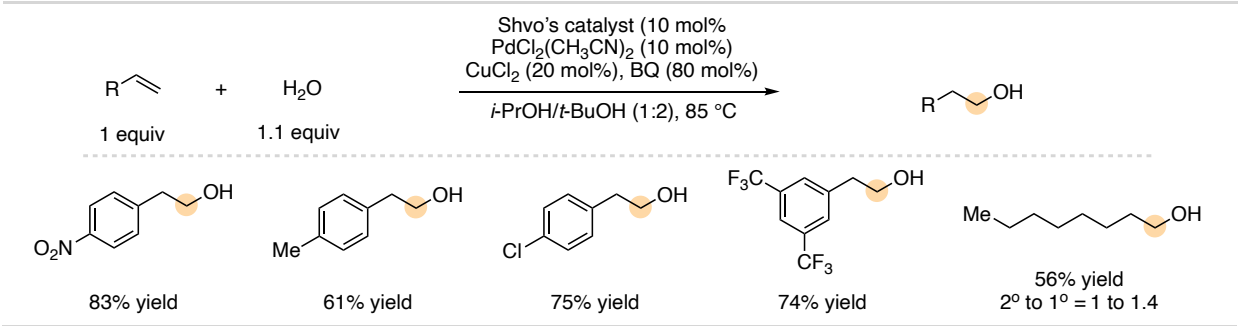

Figure 2-30: Anti-Markovnikov aryl alkene hydration method developed by the Grubbs Group.[56]

In 2017 The Arnold Group used metal-oxo-mediated enzyme catalysis to affect anti-Markovnikov hydration on aryl alkenes. A cytochrome P450 enzyme (aMOx) was engineered to catalyze the anti-Markovnikov oxidation. This engineered enzyme was combined with an alcohol dehydrogenase, *i*-PrOH and $NADP^+$ to enable net anti-Markovnikov hydration (Figure 2-31, left).[57] This system was shown to be effective with a range of simple aryl alkene substrates. Also in 2017, Li showed that engineered *E. coli* cells could convert aryl alkenes into β-aryl alcohols or amines depending on the cell variant used (Figure 2-31, right).[58] In both of these biocatalytic approaches only simple mono-substituted aryl alkenes were demonstrated and heteroaryl alkenes were not shown.

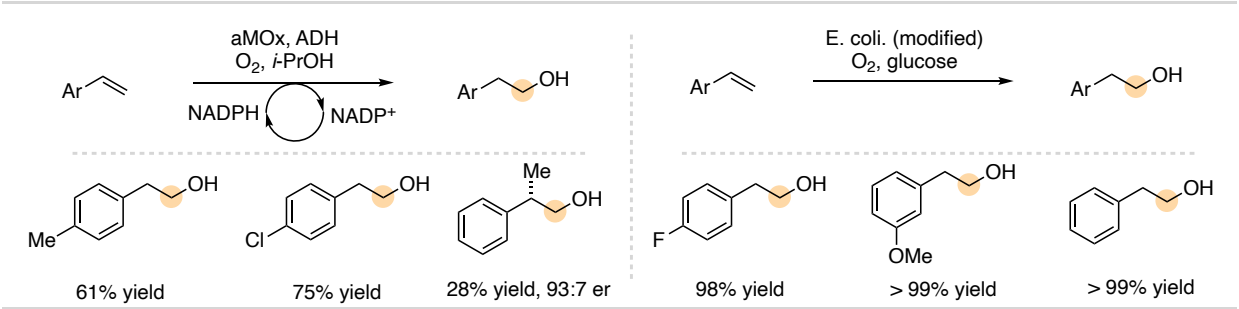

Figure 2-31: Biocatalytic approaches to aryl alkene anti-Markovnikov hydration.[57,58]

A photoredox catalytic approach was developed in 2017 by Lei, shown in Figure 2-32.[59] This reaction works through oxidation of the alkene substrate by the photoexcited catalyst to generate the alkene radical cation (Figure 2-32, right). Water then adds into the radical cation to generate a stabilized radical that abstracts a hydrogen atom from thiophenol to generate the product. Thiophenol is generated from reduction of diphenyl sulfide by the reduced photocatalyst, followed by thiolate protonation to close the catalytic cycle. A range of alkenes work well with different substitution patterns, examples are shown in Figure 2-32. This method is best suited for electron-rich alkenes, electron-deficient variants and heteroaryl alkenes were not shown.[59]

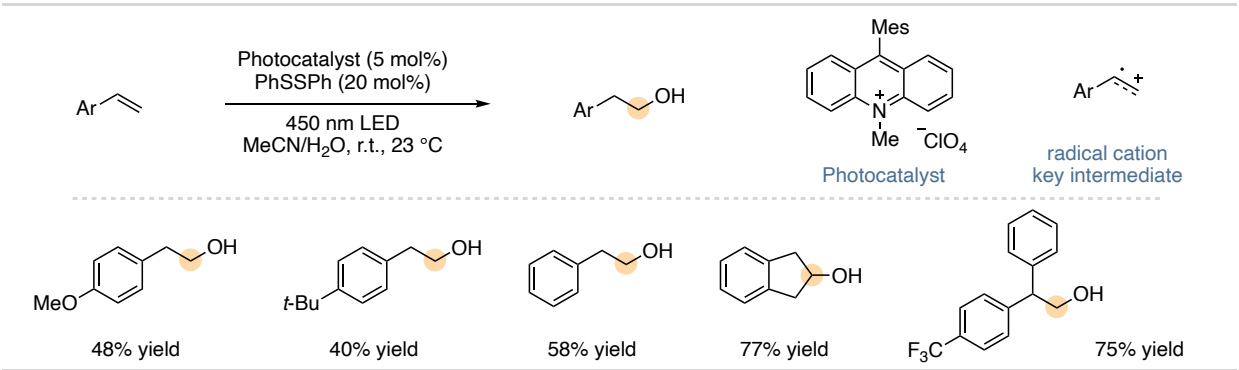

Figure 2-32: Photoredox catalytic approach to aryl alkene anti-Markovnikov hydrate.[59]

2.9.2 The Bandar Group's Superbase-Catalyzed anti-Markovnikov Aryl Alkene Hydration[60]

The Bandar Group reasoned we could develop a complementary approach to aryl alkene anti-Markovnikov hydration using superbase catalysis. However, water does not participate in P_4-*t*-Bu-catalyzed alcohol addition. A former graduate student in the Bandar Group, Spencer Pajk, identified 1-cyclopropylethanol (**2-48**) as a nucleophilic water surrogate after screening a range of alcohols with potential protecting groups.[60] The resulting cyclopropylmethyl ether of **2-48** addition is an uncommon protecting group developed for use in carbohydrate chemistry. The cyclopropylmethyl ether can be easily cleaved with an acidic work up, presumably through a cyclopropyl-stabilized carbocation formed *via* ether protonation (Figure 2-33). A former post-doctoral researcher in the Bandar Group, Dr. Zisong Qi, and Spencer developed a broad scope of aryl alkene substrates, shown in Figure 2-33, bottom. This scope includes di- and tri-substituted aryl alkenes (all but **2-50** and **2-54**), heterocycles (**2-57** – **2-60**) and a ketone (**2-54**). This scope complements traditional hydroboration/oxidation and the anti-Markovnikov methods discussed above well.[60]

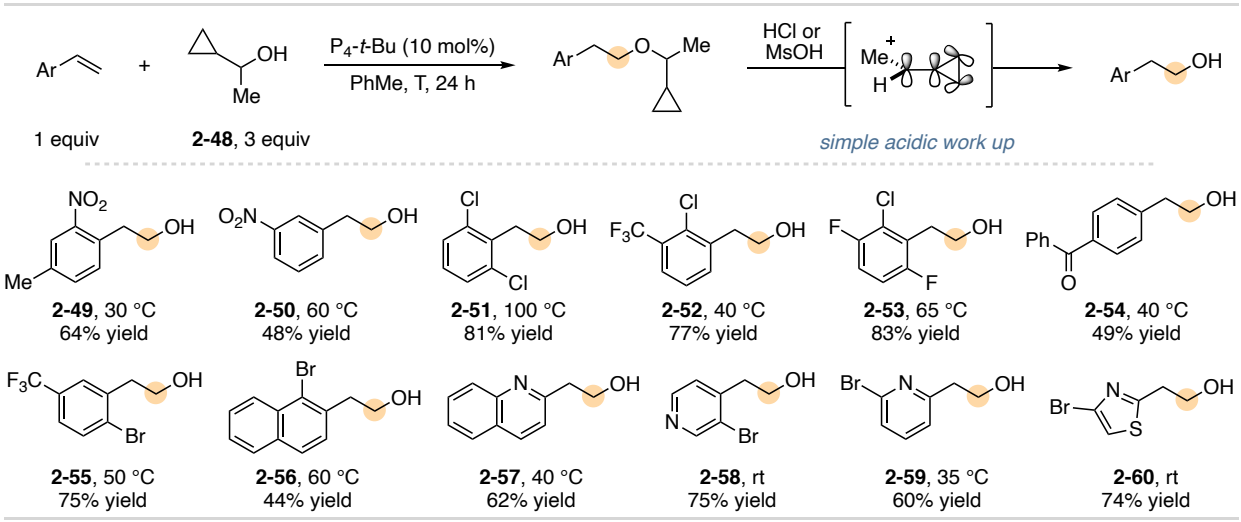

Figure 2-33: Superbase-catalyzed aryl alkene anti-Markovnikov hydration substrate scope.[60]

2.10 Utility of New anti-Markovnikov Hydration Method, My Contributions

2.10.1 Practical Inorganic Catalytic Conditions

My role in this project was to demonstrate the utility of this new aryl alkene hydration method as both Spencer and Dr. Qi left the Bandar Group before the work was completed. My first contribution was to apply the practical inorganic catalytic conditions Dr. Luo and I developed for anti-Markovnikov hydroetherification to catalytic hydration. The results are shown in Figure 2-34. Here, again, the superbase catalyst outperformed the inorganic catalyst; however, in this application 18-crown-6 ligated KO-*t*-Bu worked almost as well in PhMe as in DME. With alcohol **2-48**, DME was found to provide only slightly better yields for some substrates, so it was selected as the solvent for the inorganic catalytic conditions.[60]

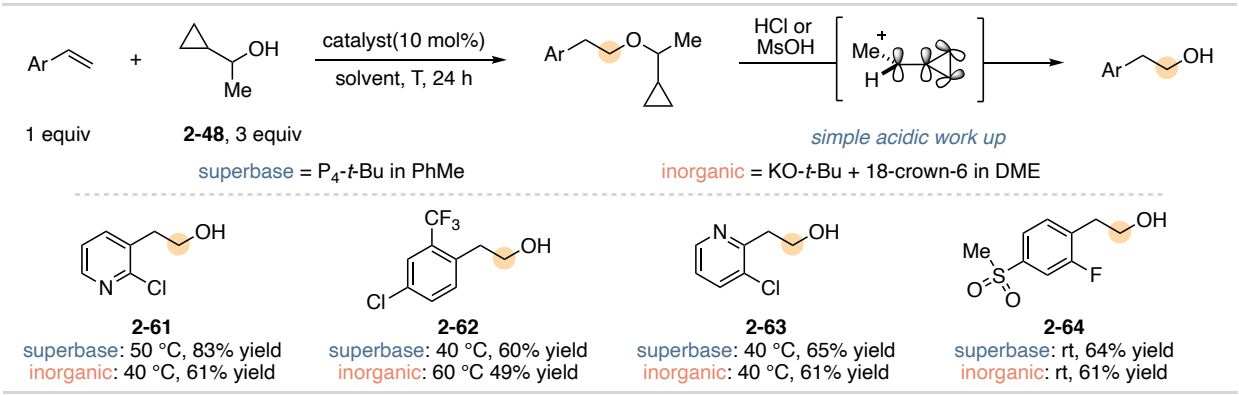

Figure 2-34: Anti-Markovnikov hydration with a practical inorganic catalytic system. Isolated yields are reported.[60]

2.10.2 Comparison to Hydroboration/Oxidation

To highlight the complementarity of P_4-*t*-Bu-catalyzed anti-Markovnikov hydration to traditional hydroboration/oxidation, I demonstrated common hydroboration/oxidation conditions on substrates **2-65**, **2-66** and **2-67**, Figure 2-35a. Aryl alkene **2-65** provided a mixture of β- and α-aryl alcohols with both BH_3•THF and 9-BBN, while P_4-*t*-Bu-catalyzed hydration results in 81% yield of exclusive β-aryl alcohol. Hydroboration/oxidation with both borane reagents on **2-66** provided low yields of only β-aryl alcohol, while P_4-*t*-Bu-catalyzed hydration gave a much higher yield of 64%. Heteroaryl alkene **2-67** failed to provide any yield of alcohol in hydroboration/oxidation; however, superbase-catalysis results in a good 75% yield of exclusive β-aryl alcohol. Shown in Figure 2-35b are substrates with functional groups that are not tolerated in hydroboration/oxidation; **2-68** and **2-69** contain thioethers that would be oxidized during oxidation and **2-70** contains an alkyl-substituted alkene that would preferentially react during hydroboration but remains unreacted during superbase-catalyzed hydration; Dr. Qi completed this portion of the scope before leaving the Bandar Group. These results showcase the utility of base-catalyzed aryl alkene hydration on electron-deficient aryl and heteroaryl alkenes.[60]

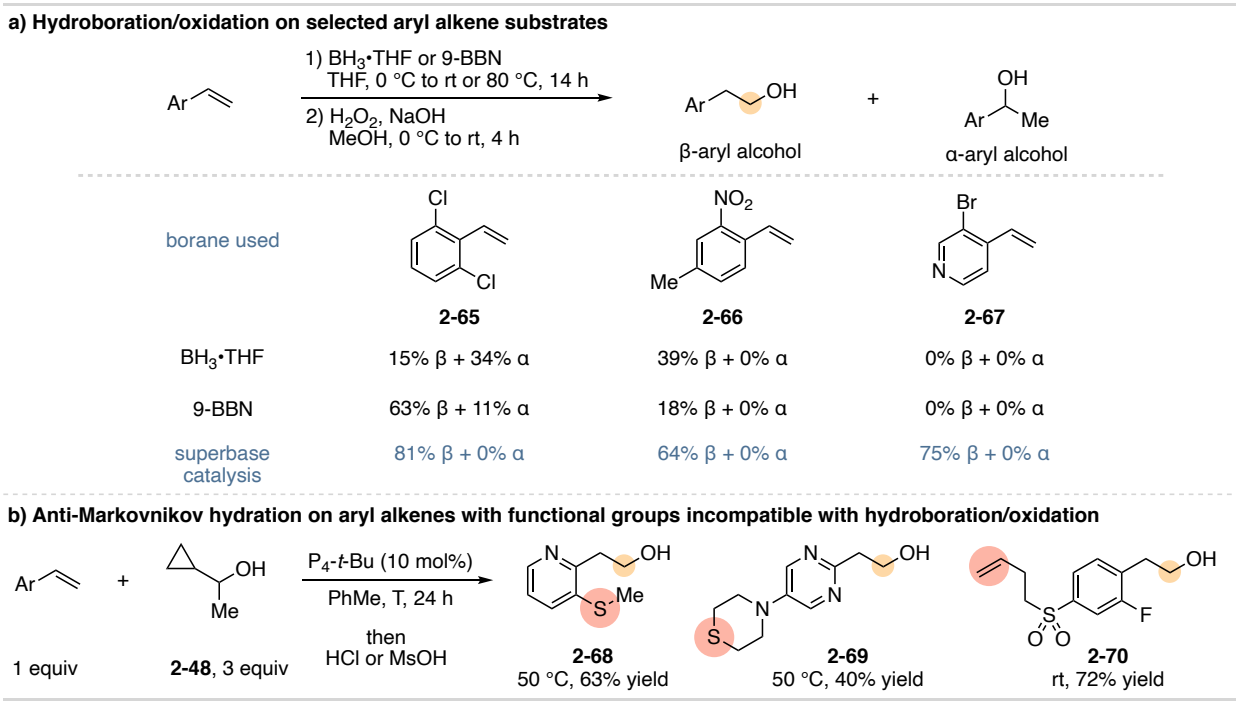

Figure 2-35: Hydroboration/oxidation comparison to superbase-catalyzed hydration.[60]

2.10.3 β-Aryl Alcohol Derivatization

Superbase-catalyzed alcohol addition is effective in achieving anti-Markovnikov hydration on aryl alkenes not compatible in traditional hydroboration/oxidation and other modern catalytic approaches outlined in Section 2.9.1. Given this, we wanted to further leverage the utility of this method by derivatizing these newly accessible β-aryl alcohols into compounds that would be challenging to prepare *via* other synthetic routes. Dr. Qi and I subjected several *ortho*-halo β-aryl alcohol products to cyclization conditions to obtain valuable dihydrobenzofuran heterocycles (Figure 2-36). Dr. Qi prepared products **2-71** with copper-catalyzed cyclization and dihydrobenzofuran **2-72** *via* intramolecular S_NAr. I prepared **2-73** to **2-75** *via* intramolecular palladium-catalyzed etherification.[60]

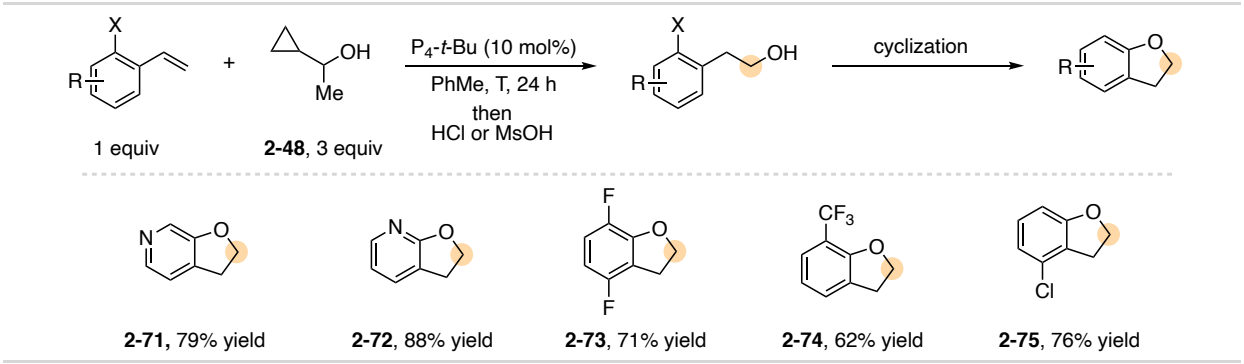

Figure 2-36: Derivatization of β-aryl alcohol products to dihydrobenzofuran products.[60]

2.11 Conclusion

The mechanistic studies on and improvements to superbase-catalyzed hydroetherification of aryl alkenes was published in the *Journal of the American Chemical Society* in 2022 and superbase-catalyzed hydration of aryl alkenes was published in *Chemical Science* in 2022. The methods represent the state-of-the-art in anti-Markovnikov aryl alkene hydroetherification and hydration and they were developed with the use of an organic superbase, supported through detailed mechanistic studies. More broadly, this work expands the oxa-Michael addition reactions to alkene acceptors and pronucleophiles traditionally thought of as incompatible. While the simplicity of the superbasic catalytic system is attractive it, suffers from practicality concerns. Initial steps were taken to address this issue through the use of an inorganic catalytic system and use of P_4-*t*-B•BF_4 as a precatalyst salt; however, these developments were not as effective as the neutral superbase. My efforts to further address this practicality concern for superbases in general is described in Chapter Three.

REFERENCES

[1] Kürti, L., Czakó, B., Corey, E. J., & Nicolaou, K. C., *Strategic applications of named reactions in organic synthesis: Background and detailed mechanisms* Elsevier. **2005**, Chapter VII. pp. 286–287.

[2] Bruice, Paula, Yurkanis, *Organic Chemistry* 6th Ed. Prentice Hall. **2011**, Chapter 19. pp. 848–850.

[3] Nising, C. F.; Bräse, S. Recent developments in the field of oxa-Michael reactions *Chem. Soc. Rev.*, **2012**, *41*, 988–999.

[4] Nising, C. F.; Bräse, S. The oxa-Michael reaction: from recent developments to applications in natural product synthesis Chem. Soc. Rev., **2008**, 37, 1218–1228.

[5] Bruice, Paula, Yurkanis, *Organic Chemistry* 6th Ed., Prentice Hall. **2011**, Chapter 4. pp. 161 - 174.

[6] Kitamori, N,; Maeno, M.; Izuhara, S. Granules of thiamine salt and the production thereof U.S. Patent US4702919, issued July, **1974**.

[7] Yamashita, D.; Shiotani, A.; Kanzaki, S.; Nakagawa, M.; Ogawa, K. Neuroprotective effects of T-817MA against noise-induced hearing loss *Neurosci Res*. **2008**, *61*, 38–42.

[8] Yahara, Y.; Takemori, H.; Okada, M.; Kosai, A.; Yamashita, A.; Kobayashi, T.; Fujita, K.; Itoh, Y.; Nakamura, M.; Fuchino, H.; Kawahara, N.; Fukui, N. Watanabe, A.; Kimura, T.; Tsumaki, N. Pterosin B prevents chondrocyte hypertrophy and osteoarthritis in mice by inhibiting Sik3 *Nat. Commun*., **2016**, *7*, 10959.

[9] Goodman, L. Sanford, Brunton, L. L. Chabner, Bruce. Knollman, Bjorn C. (**2011**). *Goodman and Gilman's the pharmacological basis of therapeutics, Pharmacological basis of therapeutics* (12th ed.). New York: McGraw-Hill.

[10] Sparks, T. C.; DeAmicis, C. V. *In Modern Crop Protection Compounds; 3 Vo. l* Krämer, W.; Schirmer, U., Eds.; Wiley-VCH: Weinheim, **2007**, 895.

[11] de Silva, E. D.; Williams, D. E.; Anderson, R. J.; Klix, H.; Holmes, C. F. B.; Allen, T. M. Motuporin, A Potent Protein Phosphatase Inhibitor Isolated from the Papua New Guinea Sponge Theonella swinhoei Gray *Tetrahedron Lett*. **1992**, *33*, 1561–1564.

[12] Shigeno, M.; Hayashi, K.; Nozawa-Kumada, K.; Kondo, Y. Organic Superbase t-Bu-P4 Catalyzes Amination of Methoxy(hetero)arenes *Org. Lett*. **2019**, *21*, 5505–5508.

[13] Shigeno, M.; Shishido, Y.; Hayashi, K.; Nozawa-Kumada, K.; Kondo, Y. KO-t-Bu Catalyzed Thiolation of β-(Hetero)aryl ethyl Ethers via MeOH Elimination/hydrothiolation *Eur. J. Org. Chem*. **2021**, 3932–3935.

[14] Smith, M. B. *March's Advanced Organic Chemistry*, 7th ed.; Wiley: New York, **2013**; pp 367−475 and 859−1066.

[15] Mitsunobu, O. *In Comprehensive Organic Synthesis*; Trost, B. M., Fleming, I., Winterfeldt, E., Eds.; Pergamon Press: Oxford, **1991**; Vol. 6, pp 22−31.

[16] Brewster, J. H. *In Comprehensive Organic Synthesis*; Trost, B. M., Fleming, I., Eds.; Pergamon Press: Oxford, **1991**; Vol. 8, pp 211−234.

[17] Barrett, A. G. M. *In Comprehensive Organic Synthesis*; Trost, B. M., Fleming, I., Eds.; Pergamon Press: Oxford, **1991**; Vol. 8, pp 235−257.

[18] Brown, H. C.; Sharp, R. L. Hydroboration. XXIV. Directive Effects in the Hydroboration of Some Substituted Styrenes *J. Am. Chem. Soc*. **1966**, *88*, 5851–5854.

[19] Brown, H. C. *Hydroboration*; W. A. Benjamin: New York, 1962.
[20] Vishwakarma, L. C.; Fry, A. Relative Rates and Regioselectivity in the Hydroboration of Substituted Styrenes with 9-Borabicyclo[3.3.1]nonane in Tetrahydrofuran J. *Org. Chem*., **1980**, *45*, 5306–5308.
[21] Brown, H. C.; Vara Prasad, J. V. N.; Zee, S.-H. Hydroboration. 75. Directive Effects in the Hydroboration of Vinyl and Propenyl Heterocycles with Representative Hydroborating Agents *J. Org. Chem*. **1986**, *51*, 439-445.
[22] Dhillon, R. S. *Hydroboration and Organic Synthesis*; Springer: Berlin, Germany, 2007
[23] Semba, K.; Fujihara, T.; Terao, J.; Tsuji, Y. Copper-catalyzed borylative transformations of non-polar carbon− carbon unsaturated compounds employing borylcopper as an active catalyst species. *Tetrahedron* **2015**, *71*, 2183−2197.
[24] M. B. Smith, *March's Advanced Organic Chemistry*, 7th ed., Wiley, New York, **2013**, pp. 1497–1519.
[25] Werkmeister, S.; Junge, K.; Beller, M. Catalytic Hydrogenation of Carboxylic Acid Esters, Amides, and Nitriles with Homogeneous Catalysts *Org. Process Res. Dev*. **2014**, *18*, 289–302.
[26] Pritchard, J.; Filonenko, G. A.; van Putten, R.; Hensen, E. J. M.; Pidko, E. Heterogeneous and homogeneous catalysis for the hydrogenation of carboxylic acid derivatives: history, advances and future directions A. *Chem. Soc. Rev*., 2**015**, *44*, 3808–3833.
[27] Allgäuer, D. S.; Jangra, H.; Asahara, H.; Li, Z.; Chen, Q.; Zipse, H.; Ofial, A. R.; Mayr, H. Quantification and Theoretical Analysis of the Electrophilicities of Michael Acceptors *J. Am. Chem. Soc.* **2017**, *139*, 13318–13329.
[28] Hu, J.; Bian, M.; Ding, H. Recent application of oxa-Michael reaction in complex natural product synthesis *Tetrahedron Lett*. **2016**, *57*, 5519–5539.
[29] Seayad, J.; Tillack, A.; Hartung, C. G.; Beller, M. Base-Catalyzed Hydroamination of Olefins: An Environmentally Friendly Route to Amines *Adv. Synth. Catal*. **2002**, *344*, 795–813.
[30] Müller, T. E.; Hultzsch, K. C.; Yus, M.; Foubelo, F.; Tada, M. Hydroamination: Direct Addition of Amines to Alkenes and Alkynes *Chem. Rev*. **2008**, *108*, 3795–3892.
[31] Miller, S. I. Notes - A Comparison of the Electrophilic Reactivity of Styrene and Phenylacetylene *J. Org. Chem*. **1956**, *21*, 247–248.
[32] Masaki, H.; Maeyama, J.; Kamada, K.; Esumi, T.; Iwabuchi, Y.; Hatakeyama, S. Total Synthesis of (−)-Dysiherbaine *J. Am. Chem. Soc*. **2000**, *122*, 5216–5217.
[33] Chen, J. J.; Drach, J. C.; Townsend, L. B. Convergent Synthesis of Polyhalogenated Quinoline C-Nucleosides as Potential Antiviral Agents *J. Org. Chem*. **2003**, *68*, 4170–4178.
[34] Kharkar, P. S.; Batman, A. M.; Zhen, J.; Beardsley, P. M.; Reith, M. E. A.; Dutta, A. K. Synthesis and Biological Characterization of (3R,4R)-4-(2-(Benzhydryloxy)ethyl)-1-((R)-2-hydroxy-2-phenylethyl)-piperidin-3-ol and Its Stereoisomers for Activity towardMonoamine Transporters *ChemMedChem* **2009**, *4*, 1075–1085.
[35] Otsuka, M.; Endo, K.; Shibata, T. Regioselective Addition of Various Heteronucleophiles to (Styrene)$Cr(CO)_3$ Complexes *Organometallics* **2011**, *30*, 3683–3685.
[36] Hamilton, D. S.; Nicewicz, D. A. Direct Catalytic Anti-Markovnikov Hydroetherification of Alkenols *J. Am. Chem. Soc*. **2012**, *134*, 45, 18577–18580.

[37] Tsui, E.; Metrano, A. J.; Tsuchiya, Y.; Knowles, R. R. Catalytic Hydroetherification of Unactivated Alkenes Enabled by Proton-Coupled Electron Transfer *Angew. Chem. Int. Ed*. **2020**, *59*, 11845 –11849.
[38] Luo, C.; Bandar, J. S. Superbase-Catalyzed anti-Markovnikov Alcohol Addition Reactions to Aryl Alkenes *J. Am. Chem. Soc*. **2018**, *140*, 3547−3550.
[39] Luo, C.; Bandar, J. S. Synthesis of β-Phenethyl Ethers by Base-Catalyzed Alcohol Addition Reactions to Aryl Alkenes *Synlett* **2018**, *29*, 2218–2224.
[40] Luo, C.; Alegre-Requena, J. V.; Sujansky, S. J.; Pajk, S. P.; Gallegos, L. C.; Paton, R. S.; Bandar, J. S. Mechanistic Studies Yield Improved Protocols for Base-Catalyzed Anti-Markovnikov Alcohol Addition Reactions *J. Am. Chem. Soc*. **2022**, *144*, 9586−9596.
[41] Borhani, T. N.; García-Muñoz, S.; Luciani, C. V.; Galindo, A.; Adjiman, C. S. Hybrid QSPR models for the prediction of the free energy of solvation of organic solute/solvent pairs. *Phys. Chem. Chem. Phys*. **2019**, *21*, 13706−13720.
[42] Klamt, A. Conductor-like Screening Model for Real Solvents: A New Approach to the Quantitative Calculation of Solvation Phenomena. *J. Phys. Chem*. **1995**, *99*, 2224−2235.
[43] Klamt, A.; Eckert, F.; Diedenhofen, M. Prediction of Soil Sorption Coefficients with COSMO-RS. *Environ. Toxicol. Chem*. **2002**, *21*, 2562−2566.
[44] McGowan, J. C. Molecular volumes and structural chemistry. *Recueil Trav. Chim. Pays-Bas* **1956**, *75*, 193−208.
[45] Chang, R.; Thoman, J. W., Jr. *Physical Chemistry for the Chemical Sciences*; University Science Books: Canada, **2014**; pp. 323− 326.
[46] Stoner, C. D. Inquiries into the Nature of Free Energy and Entropy in Respect to Biochemical Thermodynamics. *Entropy* **2000**, *2,* 106−141.
[47] Msayib, K. J.; Watt, C. I. F. Ion Pairing and Reactivity of Alkali Metal Alkoxides *Chem. Soc. Rev.* **1992**, *21*, 237−243.
[48] Exner, J. H.; Steiner, E. C. Solvation and Ion Pairing of Alkali-Metal Alkoxides in Dimethyl Sulfoxide. Conductometric Studies. *J. Am. Chem. Soc*. **1974**, *96*, 1782−1787.
[49] Weitkamp, R. F.; Neumann, B.; Stammler, H.-G.; Hoge, B. Generation and Applications of the Hydroxide Trihydrate Anion, $[OH(OH_2)_3]^-$, Stabilized by a Weakly Coordinating Cation. *Angew. Chem., Int. Ed*. **2019**, *58*, 14633−14638.
[50] Weitkamp, R. F.; Neumann, B.; Stammler, H.-G.; Hoge, B. Synthesis and Reactivity of the First Isolated Hydrogen-Bridged Silanol−Silanolate Anions. *Angew. Chem., Int. Ed*. **2020**, *59*, 5494−5499.
[51] Weitkamp, R. F.; Neumann, B.; Stammler, H.-G.; Hoge, B. Phosphorus-Containing Superbases: Recent Progress in the Chemistry of Electron-Abundant Phosphines and Phosphazenes. *Chem. Eur. J***. 2021**, *27*, 10807−10825.
[52] Kolonko, K. J.; Reich, H. J. Stabilization of Ketone and Aldehyde Enols by Formation of Hydrogen Bonds to Phosphazene Enolates and Their Aldol Products. *J. Am. Chem. Soc*. **2008**, *130*, 9668−9669.
[53] Msayib, K. J.; Watt, C. I. F. Ion Pairing and Reactivity of Alkali Metal Alkoxides *Chem. Soc. Rev.* **1992**, *21*, 237−243.
[54] Exner, J. H.; Steiner, E. C. Solvation and Ion Pairing of Alkali-Metal Alkoxides in Dimethyl Sulfoxide. Conductometric Studies. *J. Am. Chem. Soc*. **1974**, *96*, 1782−1787.
[55] Kamlet, M. J.; Abboud, J.-L. M.; Abraham, M. H.; Taft, R. W. Linear Solvation Energy Relationships. 23. A Comprehensive Collection of the Solvatochromic Parameters, π*, α,

and β, and Some Methods for Simplifying the Generalized Solvatochromic Equation *J. Org. Chem.* **1983**, *48*, 2877-2887.

[56] Dong, G.; Teo, P.; Wickens Z. K.; Grubbs, R. H. Primary Alcohols from Terminal Olefins: Formal Anti-Markovnikov Hydration via Triple Relay Catalysis *Science*, **2011**, *333*, 1609–1612.

[57] Hammer, S. C.; Kubik, G.; Watkins, E.; Huang, S.; Minges H.; Arnold, F. H, Anti-Markovnikov alkene oxidation by metal-oxo–mediated enzyme catalysis *Science*, **2017**, *358*, 215–218.

[58] Wu, S.; Liu J.; Li, Z. Biocatalytic Formal Anti-Markovnikov Hydroamination and Hydration of Aryl Alkenes *ACS Catal*., **2017**, *7*, 5225–5233.

[59] Hu, X.; Zhang, G.; Bu F.; Lei, A. Visible-Light-Mediated Anti-Markovnikov Hydration of Olefins *ACS Catal*., **2017**, *7*, 1432–1437.

[60] Pajk, S. P.; Qi, Z.; Sujansky, S. J.; Bandar, J. S. A base-catalyzed approach for the anti-Markovnikov hydration of styrene derivatives *Chem. Sci*., **2022**, *13*, 11427-11432.

CHAPTER THREE

CONTROLLABLE GENERATION OF ORGANIC SUPERBASES FROM PRECATALYST SALTS

3.1 Chapter Overview

This chapter describes my efforts to establish the fourth area of research in the Bandar Group. As the sole member of the second class of students in the Bandar Group, I had the opportunity to start working on a completely untested idea: the development of superbase precatalyst, which are air-stable but inactive superbase salts that spontaneously generate the active superbase when added to solution. This led to the initial development of superbase•carboxylate salts that decarboxylate to activate the superbase, with limited success. However, this semi-failed system led to me discovering a new strategy that does not involve the loss of CO_2 but instead relies on epoxide ring strain release to drive superbase activation. This later strategy evolved into system that is highly effective at promoting a range of reactions and enables unique reaction features that will expand substrate scopes and improve safety.

During my second year in the Bandar Group, Garrett Hoteling joined and started working on superbase precatalyst salt development. I served as his mentor within this project area and his contributions to this project proved vital for success. We focused our efforts on developing precatalyst systems for P_1-*t*-Bu and P_2-*t*-Bu. While a precatalyst system for P_4-*t*-Bu is the Bandar Group's end goal, P_1-*t*-Bu and P_2-*t*-Bu were selected as the starting point for this project as they suffer from the same limitations and drawbacks as P_4-*t*-Bu but are less basic and easier to deprotonate. After I identified solid and stable phosphazene salts, Garrett took the lead in

developing efficient activation and applications for the P_2-*t*-Bu salt, while I further developed efficient and controllable activation as well as applications for the P_1-*t*-Bu salt. The principles and ideas laid out in this chapter are currently being applied to the development of a P_4-*t*-Bu precatalyst system. To being this discussion Section 3.2 describes what a precatalyst is and our motivation and hypothesis for the development of superbase precatalyst.

3.2 Concept of a Precatalyst and Motivation

A precatalyst is a chemical compound that is converted to the active catalyst in the reaction solution.[1] Precatalysts are commonly used to access an unstable catalyst from a stable, easy-to-handle reagent. The intent here is to make the chemistry enabled by the unstable catalyst more convenient. This is exemplified by the Buchwald Pd precatalyst (Figure 3-1, left).[2-4] In this example, the active catalyst is Pd^0-*t*-BuXPhos, but Pd^0 is not stable to ambient conditions; however, Pd^{2+} oxidative addition complexes are stable and converted to Pd^0 through reductive elimination.[4] I reasoned this concepted could be used to develop user-friendly superbase reagents. Superbases, in particular phosphazenes, are not air-stable, but their conjugate acids are, as discussed in Section 1.7.2. Their conjugate acid stability originates from a proton occupying the highly basic and reactive lone pair on the central N atom. HP_4-t-BuBF_4 highlights this stability as this salt has been stored on our benchtop open-to-air for over four years, and it is still a free-flowing pure powder. The superbase conjugate acid's stability and ionic nature present an opportunity to develop a precatalyst, so long as a "turn-on" mechanism can be developed to neutralize the superbase *in situ* and generate a weakly acidic HX species (Figure 3-1, right).

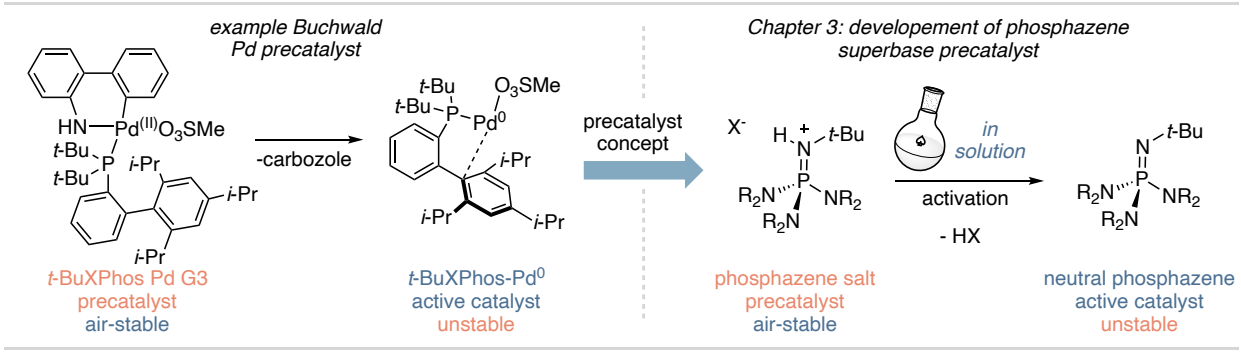

Figure 3-1: The concept of a precatalyst in Palladium catalysis and application to phosphazene superbases.

The development of a superbase precatalyst would be highly impactful for several reasons. First, the main practicality concern with superbase use is that they are not air stable and must be stored under an inert atmosphere. An air-stable superbase precatalyst could simply be stored on any benchtop for more convenient use and access. Second, a protonated superbase salt could be engineered to be a free-flowing powder and thus would be very easy to handle compared to a viscous oil (P_1-*t*-Bu) or solution that changes concentration over time (P_2-*t*-Bu and P_4-*t*-Bu). Third, in the case of phosphazene superbases, the use of a protonated salt would eliminate the hazardous and costly neutralization step in their synthesis.[5] Phosphazenes are prepared as HCl salts, which could be converted to the precatalyst salt without the need for neutralization.[5] Additionally, recrystallization or washing procedures could be used for purification in place of distillation. Overall, the outcome of the development of superbase precatalysts would be more convenient access to superbase chemistry, potentially at a lower cost, as they can be more easily prepared, purified, and handled.

For the superbase salt precatalyst to be practical, a stronger base cannot be used to generate the active superbase. This would be shifting the burden of instability from the organic superbases to another other strong bases and the system in total would not be air stable. In this regard, the unique ion-pairing property of superbases can provide an alternative approach, as the conjugate

acid of a superbase is cationic and has a counter anion (Figure 3-2, middle), unlike inorganic bases which are neutral in charge once protonated (Figure 3-2, left). The Bandar Group and I reasoned that we could exploit the counter anion of a superbase conjugate acid salt and use it as a chemical handle to deprotonate the superbase conjugate acid and generate an inert byproduct (Figure 3-2, right). To enable this deprotonative activation strategy, a driving force is needed as the superbase conjugate acid is lower in energy than the neutral and active superbase. The first attempt at the development of a superbase precatalyst salt is described in the next section using decarboxylation as a driving force.

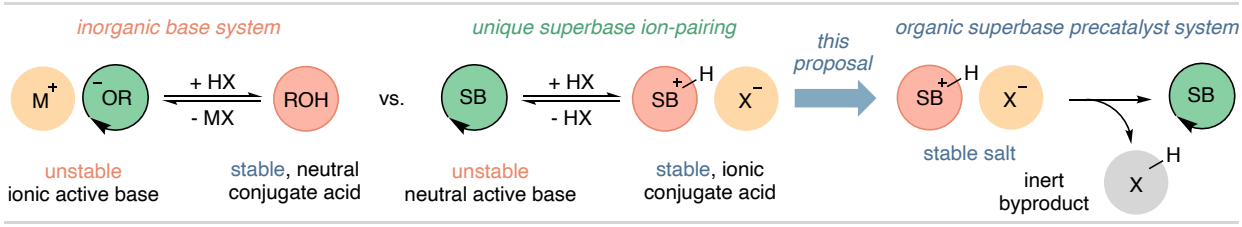

Figure 3-2: Comparison of inorganic base and superbase ion-pairing and idea to use the counter anion of superbase conjugate acid salt to develop a precatalyst. SB = superbase.

3.3 Discovery of Decarboxylation-Active Superbase Salts; First Superbase Precatalyst Salt

In 2001, Schroeder reported a study on the decarboxylation of polyfluorobenzoic acids in the presence of organic superbases (Figure 3-3a).[6] The authors observed that the rate of decarboxylation decreases with the strength of the superbase. The product of this process is carbon dioxide (CO_2), polyfluorobenzene and neutral superbase. The polyfluorobenzene results from proton transfer between the protonated superbase (P_2-Et pK_a = 21.2 in DMSO)[5] and polyfluoroaryl anion (predicted pK_a, = 29.0 (R = F) and 23.1 (R = H) in DMSO)[7] generated from decarboxylation, which results in the active superbase. Based on these results, I prepared salts **3-1** – **3-4** shown in Figure 3-3b. Our hypothesis was that the loss of CO_2 would drive deprotonation of the phosphazene conjugate acid and lead to efficient generation of freebase in solution and not in the solid state. Of the first four salts I prepared, salts **3-1** and **3-2** are not solid and were not investigated

further while salts **3-3** and **3-4** are free-flowing crystalline powders. To study the decarboxylation of salts **3-3** and **3-4**, I dissolved them in deuterated solvent and used nuclear magnetic resonance (NMR) spectroscopy to monitor changes. Although I observed rapid decarboxylation, only phosphoramide was observed by ^{31}P NMR spectroscopy (Figure 3-3c). As mentioned in Section 1.7.2, phosphazene superbases react with CO_2 to form phosphoramide, therefore for a decarboxylation process to be a viable means for precatalyst activation CO_2 must be removed from the system as it is generated.

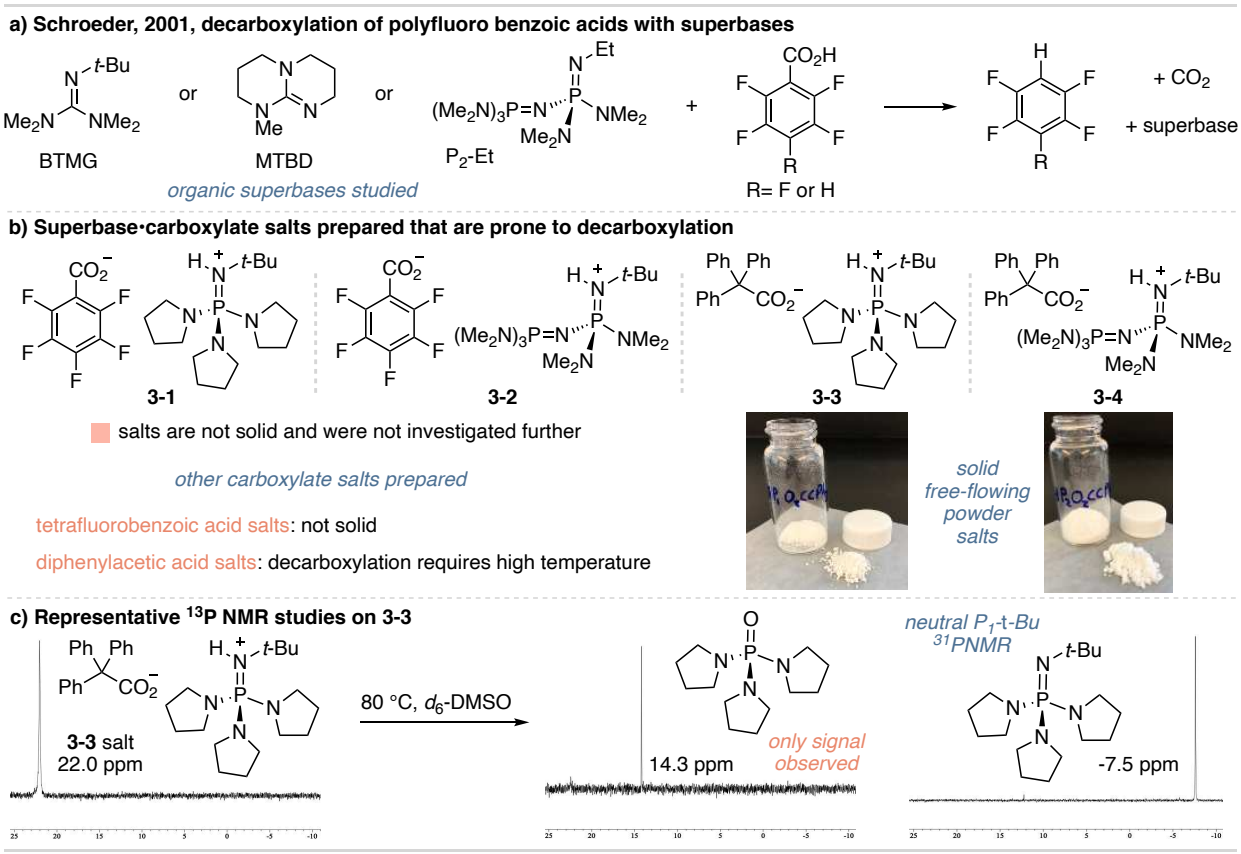

Figure 3-3: Superbase•carboxylate salt decarboxylation and ^{31}PNMR studies to neutralize superbase conjugate acid.

One strategy to effectively remove CO_2 from solution would be to chemically sequester it without deactivating the superbase. Shortly before I joined the Bandar Group in 2018, Kleij reported the use of DBU and TBD superbases to catalyze a cyclization reaction between CO_2 and

epoxy alcohols (Figure 3-4a).[8] Inspired by this report, I added glycidol (**3-5**) to precatalyst salt decarboxylation studies and observed >90% conversion to the neutral phosphazenes by ^{31}P NMR and formation of cyclic carbonate **3-6** by ^{1}H NMR (Figure 3-4b). The epoxy alcohol additive proved to be effective at removing CO_2 in NMR studies under multiple conditions. I next use catalytic amounts of salts **3-3** and **3-4** and epoxy alcohol **3-5** in simple test reactions shown in Figure 3-4c. Good yields were obtained for both test reactions indicating the potential for this system to be an effective precatalyst.

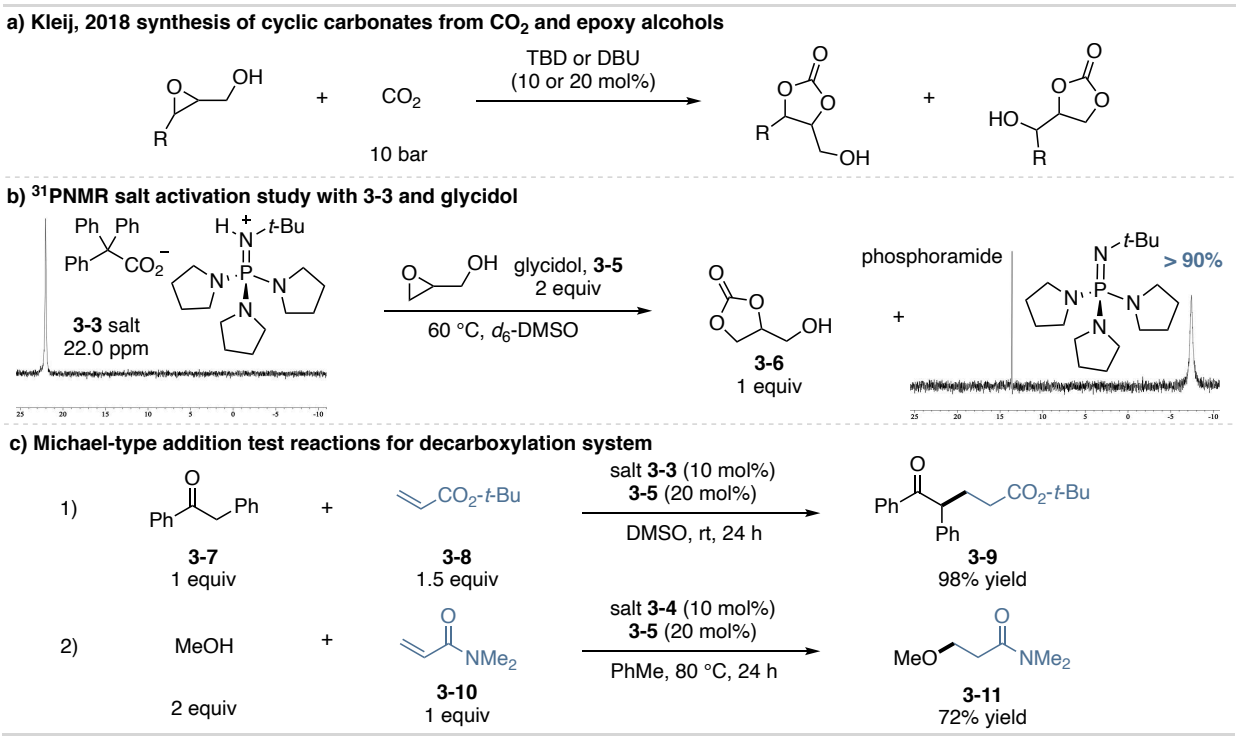

Figure 3-4: Strategy to sequester CO_2 and enable clean generation of superbase and use in test reactions. ^{1}H and ^{31}P NMR spectroscopy used to determine yields.

With encouraging results for a decarboxylative precatalyst system, I next investigated the stability of the salts, because to be an effective precatalyst, the salt must be more stable than the neutral superbase. Salts **3-3** and **3-4** were stored under ambient conditions (exposed to air and at room temperature) on the benchtop and after a week, both **3-3** and **3-4** became sticky yellow masses (Figure 3-5). ^{1}H and ^{31}P NMR analysis indicated that decarboxylation was occurring in the

solid state to form triphenyl methane and phosphoramide. To note, salts **3-3** and **3-4** are stable for short amounts of time at room temperature, less than a week, but indefinitely stable stored in a freezer at -30 °C. Furthermore, beyond the two simple test reactions shown in Figure 3-4, salts **3-3** and **3-4** and epoxy alcohol **3-5** are not effective at promoting other known reactions with superbases. These further studies indicated that a decarboxylative approach to a superbase precatalyst is likely not viable as the salts are not stable at room temperature and the system is not capable of promoting a broad range of reactions. Section 3.4 discusses how these shortcomings have been addressed in a second generation of a superbase precatalyst.

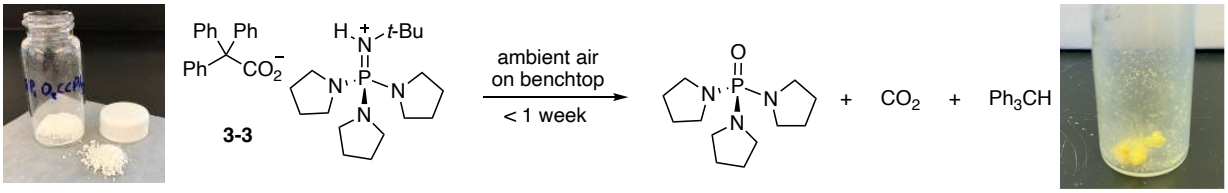

Figure 3-5: Representative example of the instability of superbase•triphenylacetate salts at room temperature.

3.4 Discovery of a Nondecarboxylative Salt System

3.4.1 Inspiration for New Precatalyst System

The reason the dual decarboxylative/epoxide cyclization system above could generate the neutral superbase is due to superbase-catalyzed cyclization between CO_2 and the epoxy alcohol additive, which proceeds through the mechanism shown in Figure 3-6, top.[8] A superbase carbonate salt, **3-12** opens the adjacent epoxide to form a cyclic carbonate and alkoxide in a Payne-type rearrangement. In effect, this decarboxylative system has two distinct driving forces leading to base deprotonation; the first is decarboxylation and the second is release of epoxide ring strain that generates an alkoxide (pK_a = 28 to 32 in DMSO).[9] I reasoned the first driving force, decarboxylation is not necessary given the generated alkoxide basicity and if the epoxide opening step could be made intermolecular by using a carboxylate superbase salt and epoxide additive

(Figure 3-6, bottom). This new strategy of using only the release of epoxide ring strain (about 27 kcal/mol)[10] as a driving force would allow for a more inert carboxylic acid to be used in the superbase salt and resolve the instability issues of the decarboxylative salts. Furthermore, the resulting ester byproduct may be more stable than the cyclic carbonate byproduct produced in the first system. The next section details the initial results and discovery of a nondecarboxylative superbase precatalyst system.

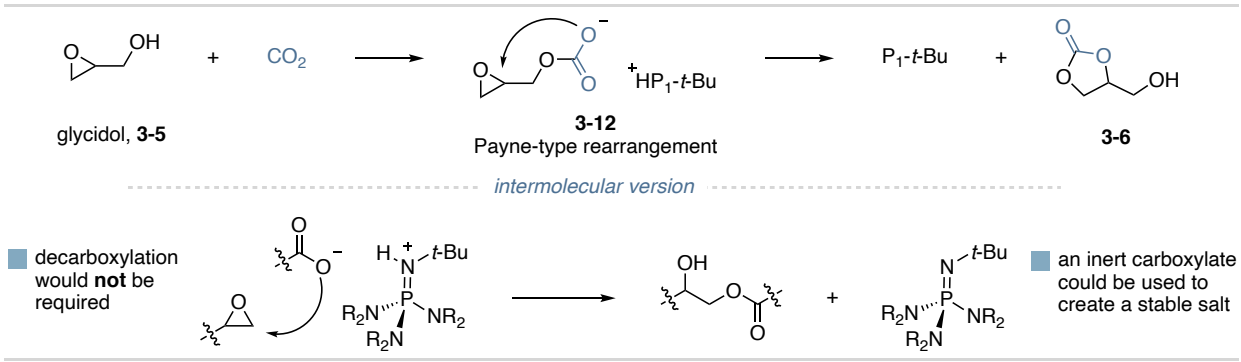

Figure 3-6: Mechanism of CO_2 trapping by epoxy alcohol **3-5** and hypothesis to develop an intermolecular version.

3.4.2 Preliminary Results

With the hypothesis outline in the previous section, I treated phenyl acetic acid with an equal molar amount of P_1-*t*-Bu in d_6-DMSO, then added styrene oxide and heated the reaction mixture at 80 °C for 2 h (Figure 3-7). ^{1}H and ^{31}P NMR analysis of the reaction mixture revealed two ester-containing byproducts, **3-13** and **3-14**, with a total conversion of 61%. Neutral P_1-*t*-Bu was observed in 50% by ^{31}P NMR spectroscopy, which indicated the intermolecular opening of an epoxide by a carboxylate can deprotonate a superbase conjugate acid. Alkyl substituted epoxides, such as 1-hexeneoxide, were not effective activators. Varied alkyl substituents on the carboxylate did not alter the reactivity of the system; however, benzoic acid derivatives were less effective as less byproduct was observed by ^{1}H NMR spectroscopy. Next, I prepared and isolated phenyl acetate salts of P_1-*t*-Bu and P_2-*t*-Bu, which are not easy-to-handle solids. For a precatalyst to be

practical, it must be convenient and easy to handle. The next section outlines Garrett's and my efforts in designing a practical, easy-to-handle superbase salt system.

Figure 3-7: The initial discovery of an intermolecular epoxide opening to activate superbase salts. ^{1}H and ^{31}P NMR spectroscopy used to determine yields.

3.5 Precatalyst Design and Identification of Controllable Features

3.5.1 Carboxylate Salts with P_1-t-Bu and P_2-t-Bu

With initial results demonstrating the neutral base can be generated from superbase•carboxylate salts, the next step in precatalyst development is the identification of an easy-to-handle salt for both P_1-*t*-Bu and P_2-*t*-Bu. After screening several different acid structures, I identified **3-15** and **3-16** as solid free-flowing powders that are easy to handle (Figure 3-8). One of the design elements I considered in searching for easy-to-handle salts was the stability of the resulting epoxide-opened byproducts. Since the byproduct of activation is an ester, α-protons present on the carboxylic acid would be acidified (ethyl phenylacetate pK_a = 22.7 in DMSO) and could interfere with subsequent base-promoted chemistry. Therefore, tertiary carboxylic acids were prioritized for the investigation. I next tested the stability of **3-15** and **3-16** under ambient conditions. After more than three years of storage in a benchtop desiccator, no changes have been observed to their physically appearance or to their NMR spectra. While **3-15** and **3-16** do not decompose when stored in air, they do absorbed water as they are hygroscopic, although not as hygroscopic as the neutral superbases. The next section details Garrett's efforts in identifying non-hygroscopic salts and my efforts in the development of a procedure to dry **3-15** and **3-16** after they absorb water.

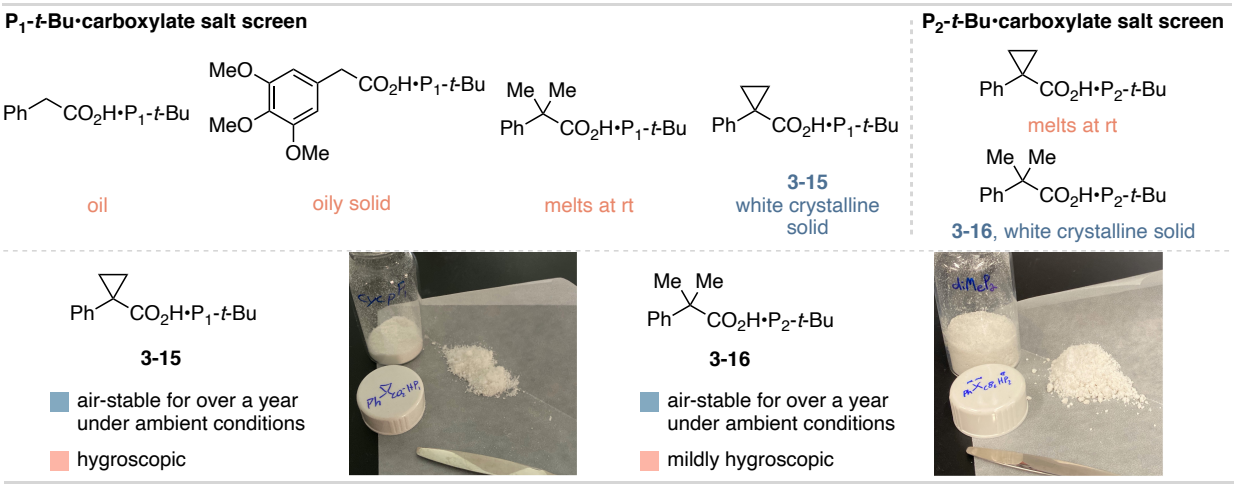

Figure 3-8: Identification of solid and air-stable phosphazene•carboxylate salts.

3.5.2 Nonhygroscopic Superbase Salts and Regeneration

After observing **3-15** and **3-16** to be hygroscopic in humid environments, I started to develop simple drying procedures to remove the absorbed water. Many drying procedures were found to be effective. The first procedure attempted was solubilizing **3-15** and **3-16** in ethyl acetate and adding common drying agents such as sodium sulfate or magnesium sulfate followed by filtration and removal of solvent *in vacuo*, which effectively removed the water. Another procedure that was effective to dry **3-15** was simple exposure to high vacuum for 24 h; however, this was not effective for **3-16**. The final but most effective method is to use an azeotrope between PhMe and the absorbed water. Simply adding PhMe to the wet superbase salt and removing the solvent *in vacuo* gives a dry ready-to-use precatalyst salts for both **3-15** and **3-16**.

To further address and minimize the hygroscopic nature of superbase precatalyst salts, Garrett identified salts **3-17** and **3-18** (Figure 3-9) as nonhygroscopic free-flowing powders. To test the hygroscopic properties of these superbase salts, sealed glass chambers containing moisture packets to mimic humid environments were set up giving environments of about 70% and 85% humidity. Salt **3-15** turns into an oily material within 10 minutes of exposure to 70% humidity. Salt **3-16** turns to an oily material after 20 min at 85% humidity. In contrast, the less hygroscopic

salts Garrett identified, **3-17** and **3-18**, did not turn into oily materials after more than 8 h at 85% humidity (Figure 3-9). These solutions practically address a limitation of the superbase•carboxylate salt precatalyst.

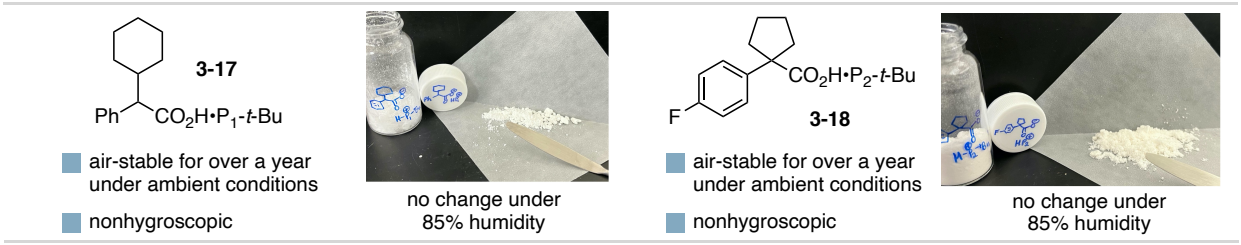

Figure 3-9: Identification of nonhygroscopic and air-stable phosphazene•carboxylate salts.

3.5.3 Epoxide Structure Design for Precatalyst Salt Activation

While the work above was going on to optimize the superbase•carboxylate structure, Garrett and I were also developing epoxide activators for the salts. As mentioned in Section 3.4.2, two byproducts were observed (**3-13** and **3-14**, Figure 3-7) when styrene oxide was used as the activator with the P_1-*t*-Bu system, and no byproducts were observed with alkyl substituted epoxides under the same conditions. We reasoned the primary and secondary alcohols in the byproducts would not be completely inert and would pose compatibility issues in some reaction applications. To address this issue, we prepared epoxide **3-19** that has a methyl group geminal to the aryl ring, which we reasoned would lead to a single byproduct with a tertiary alcohol. In activation studies with salt **3-15** only one byproduct in 73% yield, **3-20** and 80% neutral P_1-*t*-Bu were observed (Figure 3-10a). However, in activation studies with salt **3-16**, only 50% of byproduct **3-20** and 50% neutral P_2-*t*-Bu was observed. After further investigation, we found that salt **3-16** and aryl substituted epoxide **3-19** reach equilibrium at 50% neutral P_2-*t*-Bu and byproduct **3-20** with 50% salt **3-16** and epoxide **3-19** (Figure 3-10b). After further optimization of the epoxide additive, Garrett found that spirocyclic epoxide **3-21** generates 90% neutral P_2-*t*-Bu and a single byproduct **3-22** in 87% yield after 3 h at 80 °C in a range of solvents (Figure 3-10c). This activation

was found to be irreversible as when **3-22** is treated with commercial P_2-*t*-Bu no reaction occurs. While this dialkyl substituted epoxide requires higher temperatures to activate, this additive is effective at fully "turning-on" P_2-*t*-Bu from salt **3-16**.

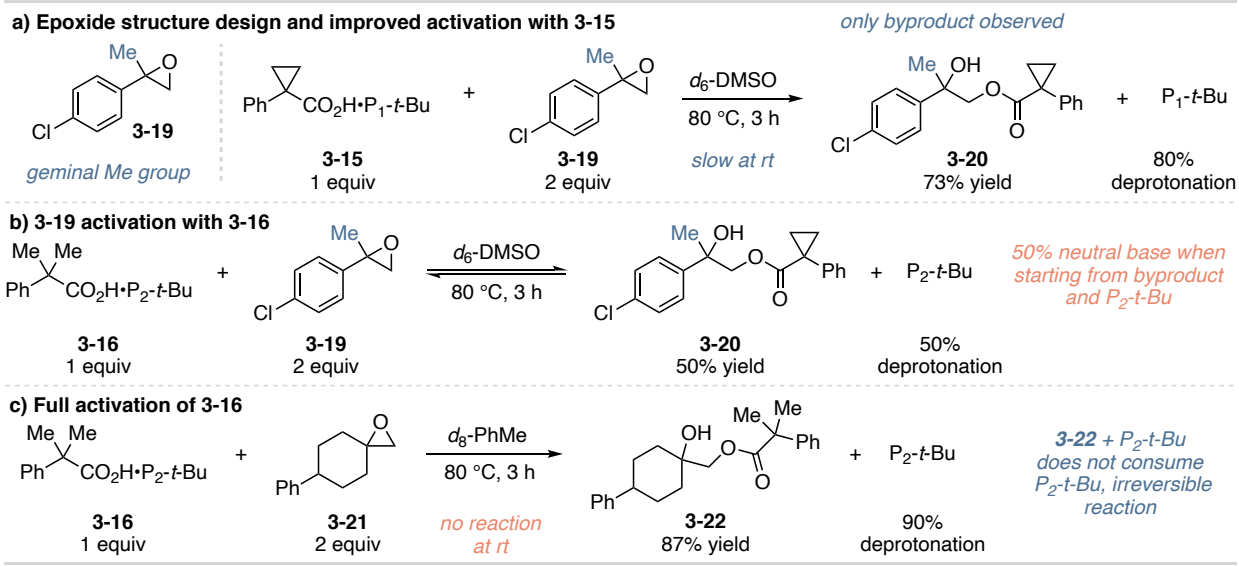

Figure 3-10: Improvements to epoxide activator, generation of a tertiary alcohol byproduct and complete activation for salt **3-16**. ^{1}H and ^{31}P spectroscopy used to determine yields.

3.5.4 Electronic Property Variation of Aryl Epoxide, Control of Activation Rate

During the course of the epoxide structure optimization, I noted the aryl groups electronic properties effect the rate of salt activation. To investigate this further, I prepared a series of epoxides, shown in Figure 3-11, and measured their activation curves under the same conditions, 40 °C in DMSO. I found that highly electron-deficient aryl epoxide **3-23** "turns-on" salt **3-15** rapidly, while electron-neutral epoxides **3-19** and **3-25** activated salt **3-15** more slowly under the same conditions. This discovery presents the opportunity to control the rate that a strong base is introduced into a reaction, simply by selecting the epoxide additive at the start. Currently, the only way to control the rate a base is introduced into a reaction is with manual slow addition either with a syringe pump or manually. The Utility of this feature is exploited later in this chapter (see Section 3.9.4 and 3.9.5).

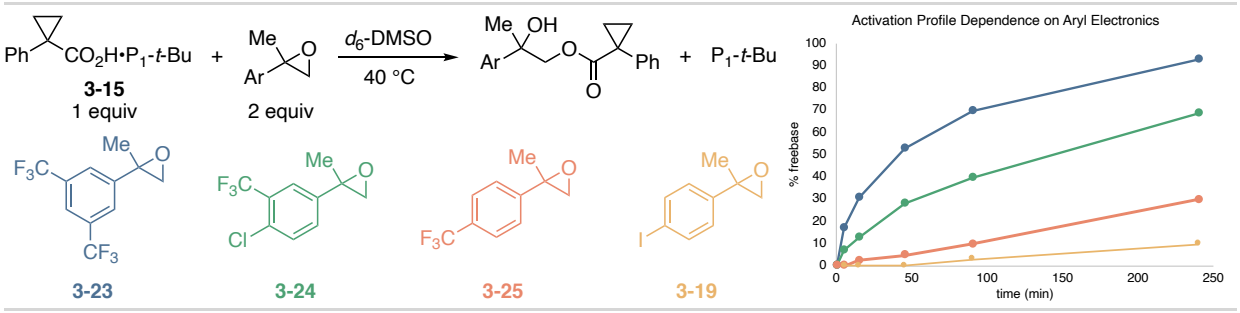

Figure 3-11: The activation rate dependence on the electronic properties of the aryl group of the epoxide activator. ^{1}H and ^{31}P spectroscopy used to determine yields.

3.5.5 Condition Variation as a Means to Control Activation Rate

Another method of controlling the activation rate was quickly realized during these studies as the solvent and temperature have a large impact on the rate a carboxylate opens an epoxide. In polar solvents such as DMSO and THF activation of salt **3-15** by epoxide **3-23** is rapid, whereas activation in PhMe is slower (Figure 3-12, left). Surprisingly, acetonitrile, a polar solvent, activates salt **3-15** more slowly than PhMe and does not completely "turn-on" the superbase salt. Temperature has a more profound impact on activation rate as shown in Figure 3-12, right. Activation at room temperature, 25 °C, occurs at a moderate rate with epoxide **3-23**; however, at 80 °C activation using epoxide **3-23** is complete within 5 minutes. This temperature control provides a way to generate a superbasic solution within minutes from an air stable and easy-to-handle salt. The utility of extremely rapid activation is used later in this chapter, see Section 3.7.3 and 3.8.1.

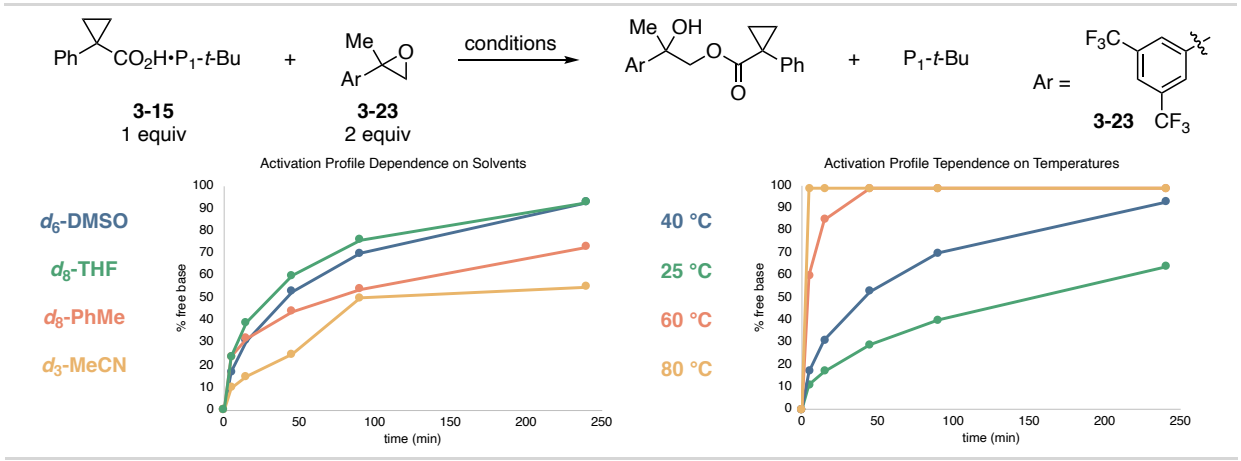

Figure 3-12: The activation rate dependence on solvent and temperature using epoxide **3-23**. ^{1}H and ^{31}P NMR spectroscopy used to determine yields.

3.5.6 System Design Conclusion and Outcomes

The above sections describe Garrett's and my efforts to design a new superbase salt precatalyst system based on my initial discovery. Our findings are summarized in Figure 3-13. I initially identified two solid and stable superbases salts, one for P_1-*t*-Bu (**3-15**) and one for P_2-*t*-Bu (**3-16**) with relatively inexpensive carboxylic acids. Garrett found nonhygroscopic P_1-*t*-Bu (**3-17**) and P_2-*t*-Bu (**3-18**) carboxylate salts. While these nonhygroscopic carboxylate salts are very easy to handle, they are more expensive. For this reason, the salts we primarily used in applications and further development are **3-15** and **3-16**. It should be noted that salts **3-15** and **3-16** are just as easy to handle as salts **3-17** and **3-18** in environments with low humidity. Next, I found a series of aryl substituted epoxides that allow for the rate of activation to be precisely controlled. Garrett identified an effective epoxide additive to fully "turn-on" P_2-*t*-Bu salts **3-16** and **3-18**. Taken all together, we have developed a modular system to controllably "turn-on" superbases in solution and access superbase reactivity from inert salts (Figure 3-13).

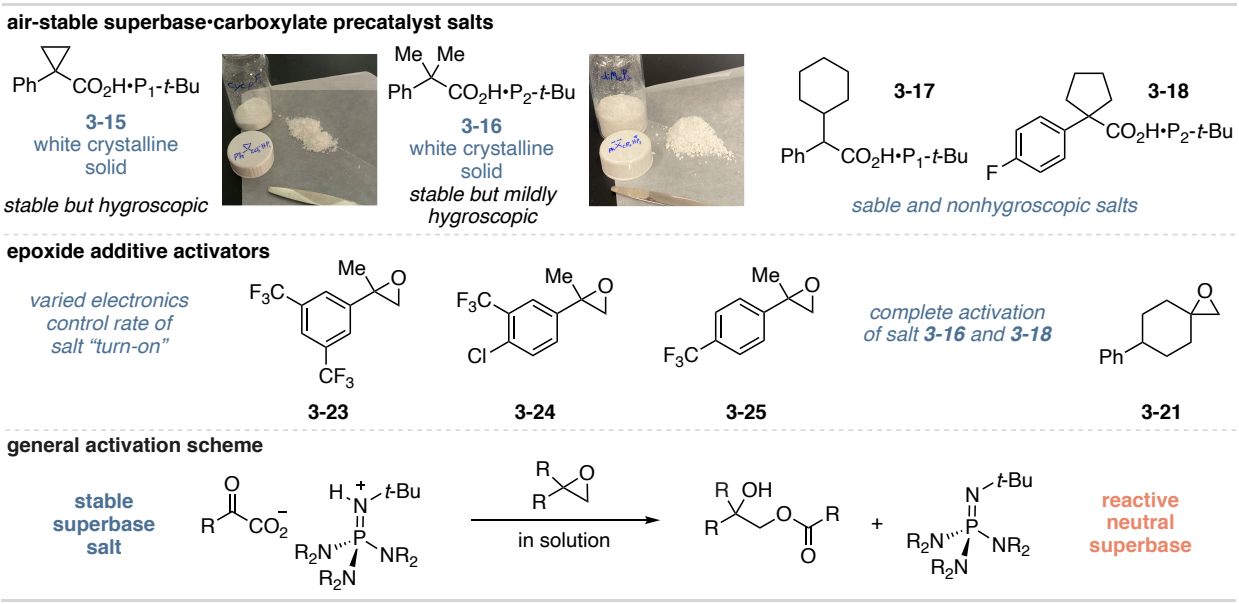

Figure 3-13: Summary of precatalyst system.

3.6 Improved Synthesis of Superbases *via* Salt 3-15

3.6.1 Published Method to Prepare P_1-t-Bu

Another major benefit of accessing superbase chemistry from a superbase precatalyst salt is that the phosphazene base does not need to be neutralized and distilled during its synthesis. This is exemplified in the synthesis of P_1-*t*-Bu, which was discussed in Chapter One and is shown in Figure 3-14. To be specific, PCl_5 is treated with *tert*-butyl amine in *n*-pentane under inert atmosphere at 0 °C. The solution is then refluxed for 1.5 h, followed by stirring at room temperature overnight. Following this, the solution is filtered to remove the solid HN-*t*-BuCl salt under nitrogen. *n*-Pentane is then removed *in vacuo*. Here, care must be taken as **1-2** is highly moisture sensitive and must be kept under inert atmosphere, additionally **1-2** is volatile and can be unintentionally removed *in vacuo* with the solvent. Following the removal of solvent, **1-2** is purified by distillation.[5,11] Next, under inert atmosphere pyrrolidine is cooled to -78 °C and **1-2** is added dropwise.[5] Then the solution is refluxed for 2 h and stirred at room temperature overnight and then a 50 wt.% KOH solution is added, and the organic layer is separated. The aqueous layer

is extracted with pyrrolidine three times. The combined organic layers are then distilled over Na_2O or BaO. Pyrrolidine is removed at atmospheric pressure; however, P_1-*t*-Bu requires high temperatures and high vacuum to be distilled.[5] Careful monitoring is required as P_1-*t*-Bu can decompose at high temperatures. Additionally, a 50 wt.% KOH solution can be dangerous to handle and requires caution. These synthetic features are major contributing factors to the high cost of phosphazene superbases.

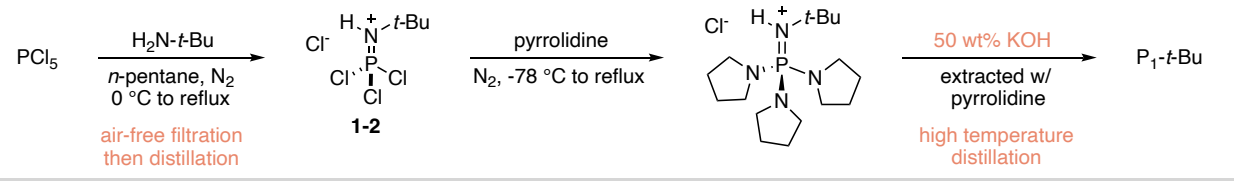

Figure 3-14: Published synthetic route to P_1-*t*-Bu.

*3.6.2 Improved Synthesis of P_1-t-Bu via Salt **3-15***

To develop an improved synthesis of P_1-*t*-Bu *via* salt **3-15**, I prepared the salt from the same starting materials as the neutral base, but with significant modifications to the procedure (Figure 3-15). I found that 25 g of PCl_5 can be suspended in *n*-hexane under nitrogen gas followed by slow addition of *tert*-butyl amine at 0 °C, then refluxing for 2 h. This is similar to the above procedure; however, I found stirring overnight is not necessary nor is the filtration step and distillation of **1-2**. Simply cooling the *n*-hexane solution to 0 °C, followed by slow addition of pyrrolidine and refluxing for 2 h provides complete conversion to HP_1-*t*-BuCl within hours of starting, as opposed to the multiday synthesis for the neutral superbase. The HP_1-*t*-BuCl salt can be isolated *via* addition of water to the crude reaction solution and extraction with DCM (3x), followed by drying with brine and magnesium sulfate. Removal of the solvent *in vacuo* results in HP_1-*t*-BuCl as an orange-brown oil that is >99% pure by ^1H and ^{31}P NMR spectroscopy. The HP_1-*t*-BuCl does not need to be neutralized or further purified and can be converted to the active precatalyst salt *via* simple anion metathesis. To accomplish this, the crude HP_1-*t*-BuCl is

solubilized in MeOH with stirring and a MeOH solution of potassium carboxylate **3-26** is added. Potassium chloride precipitates out of solution and, after removal of MeOH *in vacuo,* filtration with EtOAc results in a solution of salt **3-15**. The salt can be collected by removing EtOAc so that salt **3-15** crystalizes. This material is further purified with recrystallized from a minimal amount of hot EtOAc to give an overall yield of 61%.

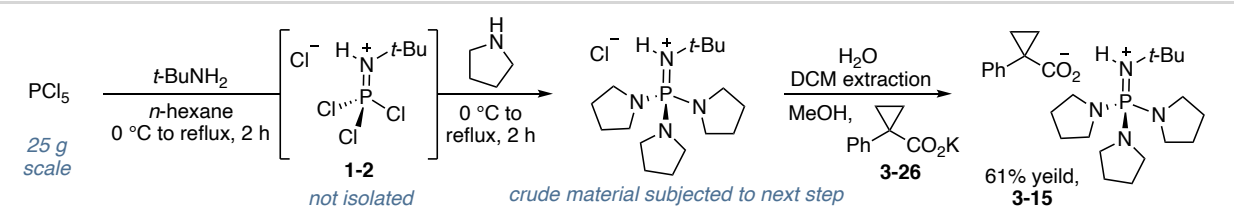

Figure 3-15: Improved synthesis of phosphazene superbase *via* anion metathesis to access the precatalyst.

3.6.3 Outlook of Improved Phosphazene Synthesis

Section 3.6.2 highlights the ease of phosphazene synthesis since highly reactive intermediate, **1-2** does not need to be isolated and the crude reaction solution can be easily telescoped into the second amine substitution step. The synthesis of salt **3-15** is easily scalable and safe with minimal handling of highly reactive or dangerous reagents. This improved synthetic protocol streamlines access to phosphazene•HCl salts. Furthermore, by not having to neutralize the HCl salt a simple anion metathesis procedure can be used to prepare the phosphazene precatalyst salt **3-15** in good yield. These general improvement strategies can be expected to expand access to other phosphazene superbases in their precatalyst form as well.

3.7 Application of P_1-*t*-Bu and P_2-*t*-Bu Carboxylate Salts in Catalytic Reactions

*3.7.1 Catalysis of Michael Additions with Salt **3-15** and Epoxide **3-23***

With a system developed to release neutral superbases from stable precatalyst salts *in situ*, we next tested this system in reactions. The Michael addition between deoxybenzoin (**3-7**) and *tert*-butyl acrylate (**3-8**) was selected as a model reaction to test salt **3-15** and epoxide **3-23** (Figure

3-16a). At room temperature, I found the precatalyst system gave complete conversion, which matched the performance of commercial P_1-*t*-Bu. Control reactions with varied basic systems strongly suggest the active catalyst is P_1-*t*-Bu generated from the opening of the epoxide activator by the carboxylate (Figure 3-16a, left). Reaction profiles of the model substrates with epoxides **3-23** and **3-24** show induction periods of differing lengths depending on the epoxide electronics (Figure 3-16a, right). These induction periods and their varied length are indicative of controllable precatalyst activation. A proposed catalytic cycle for this model reaction is shown in Figure 3-16b. First, the precatalyst salt is activated by the epoxide to release P_1-*t*-Bu. The base can then deprotonate **3-7** and facilitate conjugate addition. Proton transfer from the P_1-t-Bu conjugate acid generates product **3-9**. I next tested other pronucleophiles and Michael acceptors with the P_1-*t*-Bu precatalyst system (Figure 3-17). A glycine derived Schiff base pronucleophile and acrylamide acceptor provide an excellent 97% yield (**3-27**). Acrylate Michael acceptors provide complete conversion with both α-aryl ketone and ester pronucleophiles (**3-28** and **3-29**). Garrett found that the P_1-*t*-Bu precatalyst system is also effective in promoting aldol reactions with phenyl ketones and benzaldehyde derivatives (**3-30**). He also found Mannich reactions with α-aryl esters and aldimines (**3-31**), and Mannich-type elimination reactions (**3-32**) work well with the P_1-*t*-Bu precatalyst system (Figure 3-17).

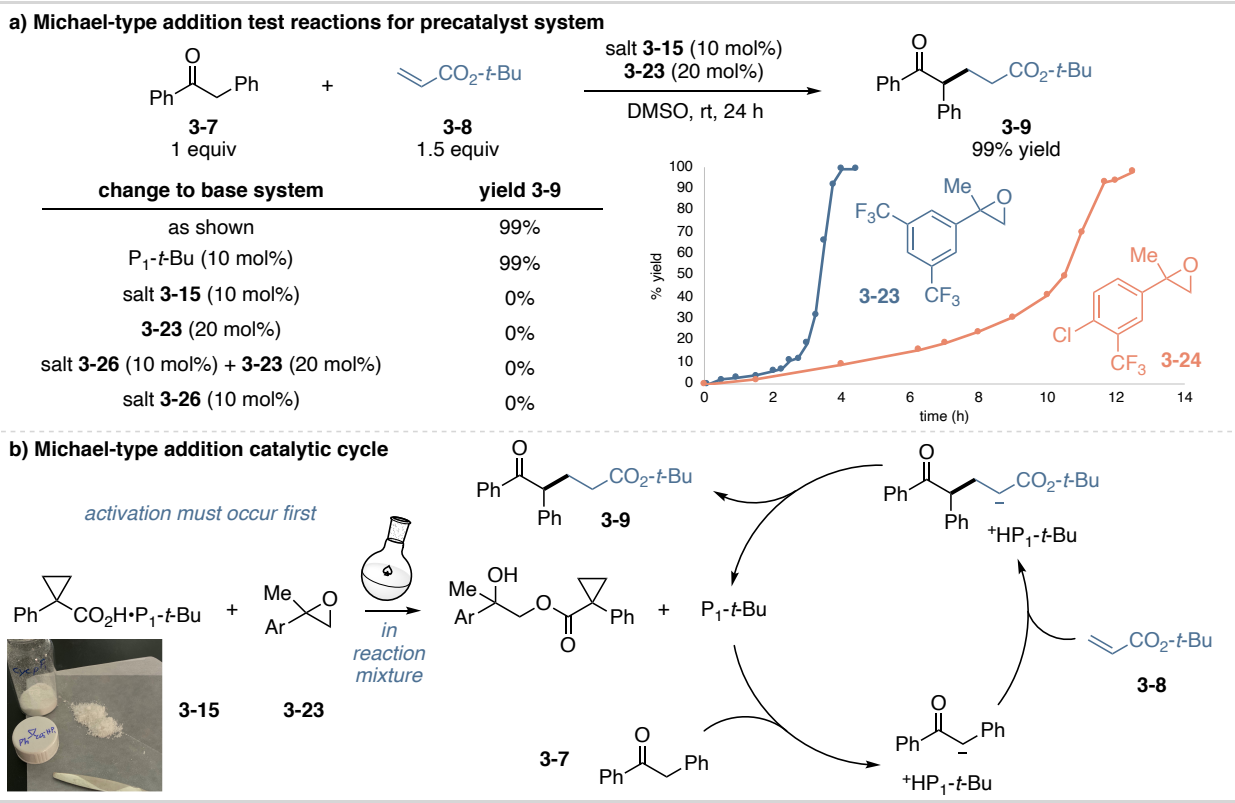

Figure 3-16: Test Michael addition, control reaction, reaction profile and catalytic cycle. Reaction profiles collected at 40 °C. ^{1}H NMR spectroscopy used to determine yields.

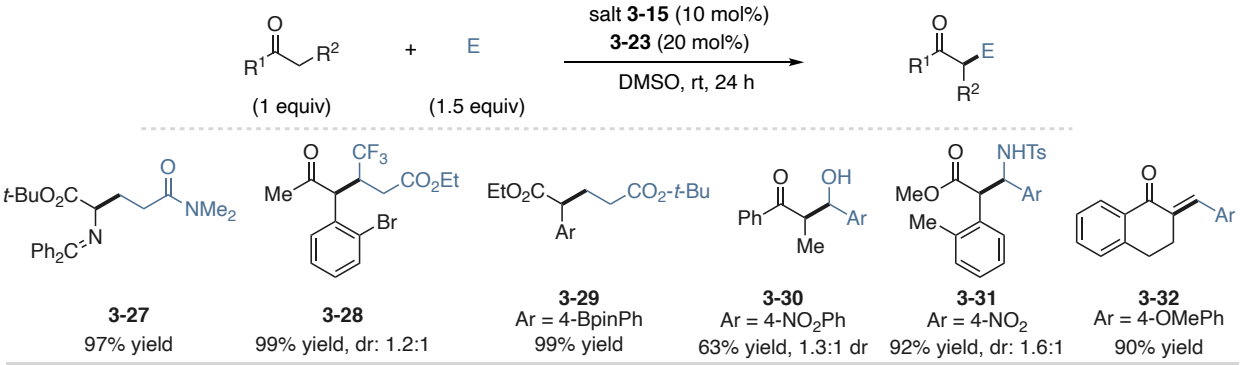

Figure 3-17: Substrate scope of Michael-type additions and aldol-type reactions using salt **3-15** and epoxide **3-23**. ^{1}H NMR spectroscopy used to determine yields.

*3.7.2 Catalysis of Oxa- and Aza-Michael Additions with Salt **3-16** and Epoxide Additive*

Given the importance of oxa-Michael additions in total synthesis and medicinal chemistry programs as discussed in Chapter Two, we reason it would be impactful to develop the use of salt **3-16** to enable these transformations.[12-14] We selected the oxa-Michael addition between MeOH

and *N,N*-dimethylacrylamide as the model reaction. Using 10 mol% salt **3-16** and 20 mol% epoxide **3-21**, Garrett observed complete conversion to the addition product **3-11**, this matches the yield obtained with the commercial P_2-*t*-Bu superbase (Figure 3-18a). As before, control reactions were conducted that strongly support the active catalyst as P_2-*t*-Bu generated from salt activation. To note, aryl substituted epoxides such as **3-23** are effective at activating salt **3-16** *in situ* for reaction promotion. Epoxide **3-21** was selected for further use in catalytic applications as it was shown to release the maximum amount of superbase catalyst. Next, Garrett employed the P_2-*t*-Bu precatalyst system in other oxa-michael additions with 1-adamantanemethanol, and an alkynol (**3-34** and **3-35**, Figure 3-18b). Garrett also found that the precatalyst system was effective in promoting aza-Michael additions with pyrazoles (**3-36**) and indoles with aryl alkene acceptors (**3-37**).

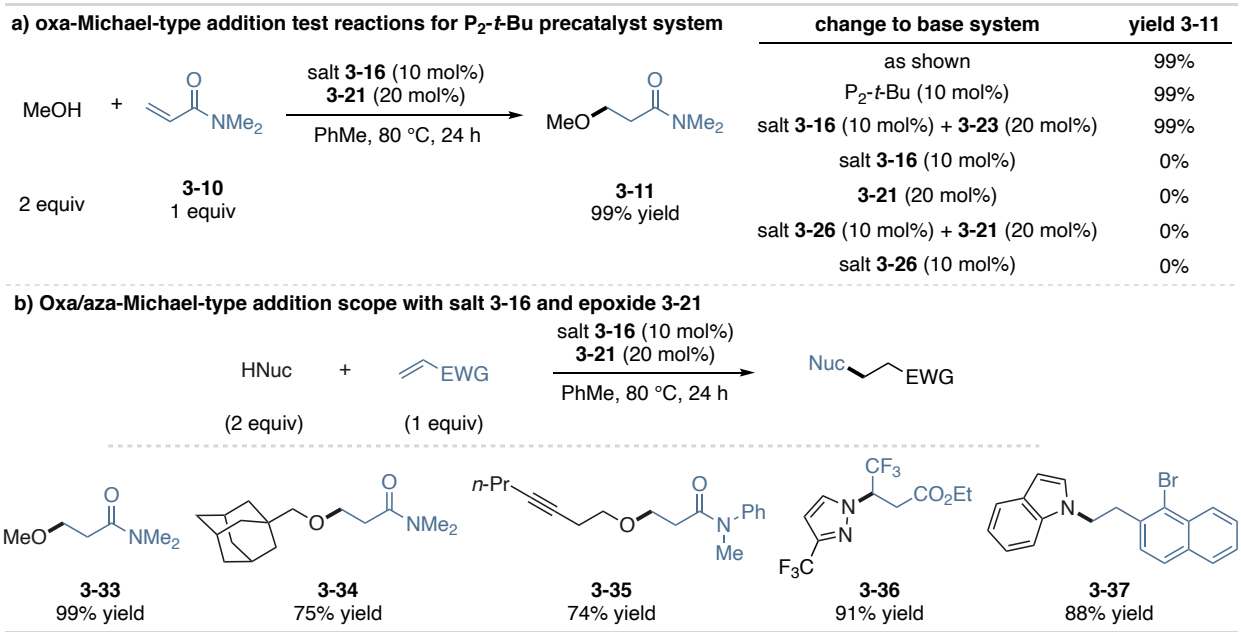

Figure 3-18: Catalytic application of salt **3-16** and epoxide **3-21** in oxa/aza-Michael-type addition reactions. ^{1}H NMR spectroscopy used to determine yields.

*3.7.3 Catalysis of Ester Amidation with Aminoalcohols Using Salt **3-15***

The next catalytic application I developed using our precatalyst system is ester amidation with amino alcohols since amidation is one of the most common reactions in medicinal and amino alcohol-based functionality is highly prevent in pharmaceuticals.[15] (Figure 3-19). In 2013, P_1 phosphazene superbases were reported to catalyze the amidation of esters with aminoalcohols.[16] Furthermore, P_1 phosphazene bases at room temperature were found to provide higher yields than common inorganic bases such as KO-*t*-Bu and Cs_2CO_3 at higher temperatures.[16] Based on this report, I applied our P_1-*t*-Bu precatalyst system using the reported optimal conditions; however, unlike previous applications no product was observed (Figure 3-19a). After further investigation, I found that the aminoalcohol substrate was inhibiting precatalyst activation. To resolve this challenge, a pre-activation procedure was developed exploiting the significantly enhanced precatalyst activation rate at elevated temperature. This procedure involves simply heating salt **3-15** and epoxide **3-23** at 80 °C for 5 min in THF. Within this time salt **3-15** is fully activated and the solution can be directly transferred to a solution of starting materials, identical to the use of the commercial superbase. Use of this procedure results in excellent conversion to amide **3-40**. Control reactions again suggest the active catalyst is P_1-*t*-Bu. I found the P_1-*t*-Bu precatalyst system and pre-activation procedure provides excellent yields on many of the same substrates reported in 2013 (**3-40** to **3-44**, Figure 3-19b).

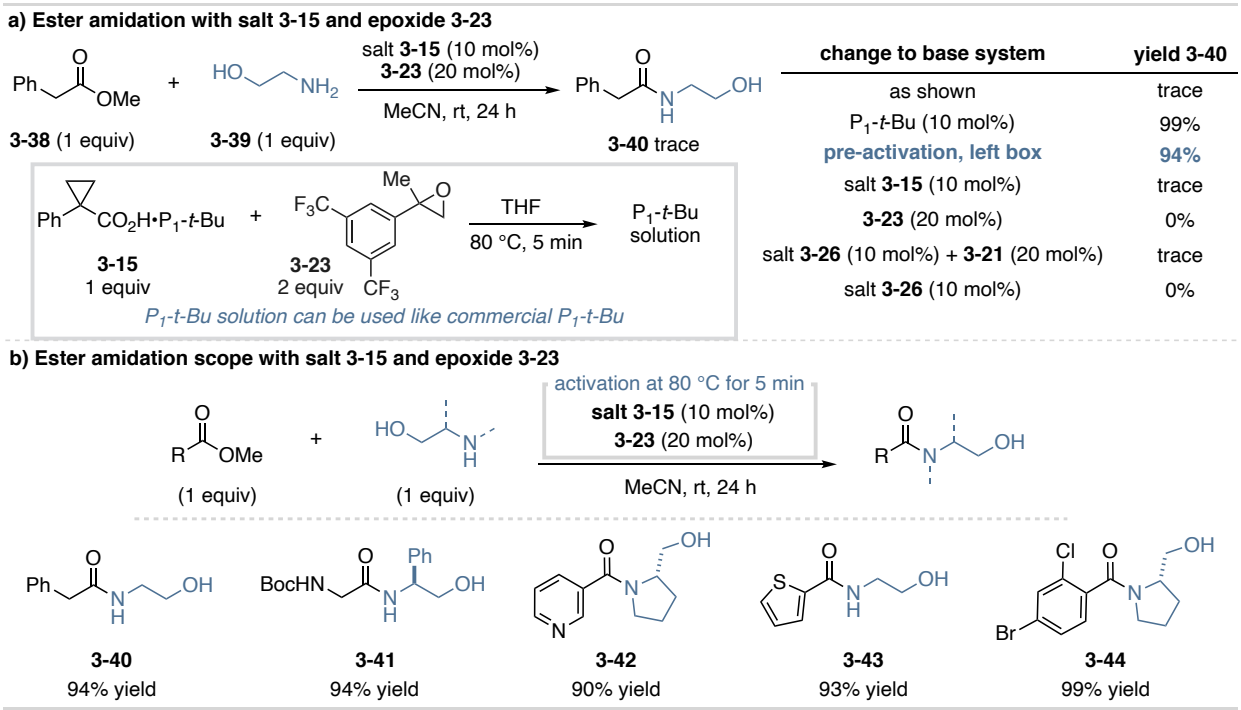

Figure 3-19: Ester amidation using salt **3-15** and epoxide **3-23**, pre-activation of salt system required for this application. ^{1}H NMR spectroscopy used to determine yields.

3.8 Application of P_1-*t*-Bu and P_2-*t*-Bu Carboxylate Salts in Reactions Requiring Stoichiometric Base

*3.8.1 Promotion of Alcohol Deoxyfluorination Using Salt **3-15***

Many applications of organic superbases typically require their use in stoichiometric quantities.[17] Given the success of the phosphazene precatalyst systems in catalytic applications, we reasoned they would be effective in stoichiometric settings as prereagents. The first reaction I targeted was alcohol deoxyfluorination developed by the Doyle Group.[18-21] Alcohol deoxyfluorination using sulfonyl fluorides is prone to side reactions, as discussed in Chapter One, and the authors found that superbases were critical for high yielding reactions. This reaction was selected as it should challenge our salt activation system. Should another basic component of our prereagent system be responsible for promoting the reaction, many side reactions would be expected. Additionally, the sulfonyl fluoride reagent could react unfavorably with the epoxide

additive, carboxylate, and/or the byproduct (**3-47**) of salt activation in undesired deoxyfluorination (Figure 3-20a). With these challenges, it is not surprising that initial attempts to promote the model reaction shown in Figure 3-20a failed to provide any product. Further studies indicated that the carboxylate was reacting with the sulfonyl fluoride to prevent the activation of salt **3-15**, thus consuming the alcohol activator and fluoride source in the process (Figure 3-20a, right). This issue was resolved with a similar pre-activation procedure as before but with a longer activation period of twenty minutes, to ensure all carboxylate is consumed. Control reactions again strongly indicate the active promotor is P_1-*t*-Bu (Figure 3-20b, left). A range of alcohols can be converted to the alkyl fluoride using the pre-activation procedure; however, slightly lower yields are obtained when compared to use of commercial P_1-*t*-Bu (Figure 3-20b, right, **3-46**, **3-49 to 3-52**). In general, this is a practical way to rapidly access alkyl fluorides from stable and readily available starting materials.

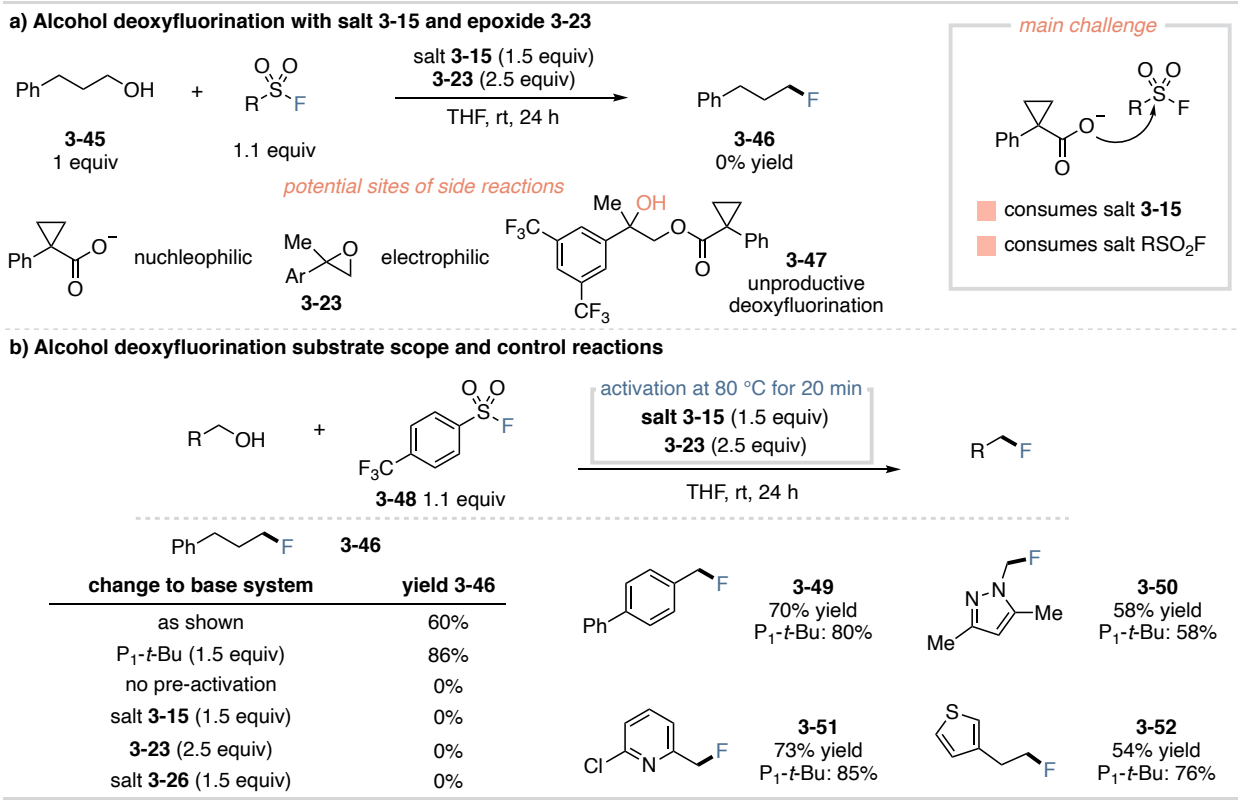

Figure 3-20: Alcohol deoxyfluorination with stoichiometric salt **3-15** and epoxide **3-23**, pre-activation was required: salt **3-15** and epoxide **3-23** in THF at 80 °C for 20 min. ^{1}H NMR spectroscopy used to determine yields.

*3.8.2 Promotion of Nucleophilic Aromatic Substitution Using Salt **3-16***

The next stoichiometric application we targeted is one of the most common reactions used in the pharmaceutical industry, nucleophilic aromatic substitution (S_NAr).[15] P_2-Phosphazenes have been shown to promote this transformation with a variety of complex nucleophiles and aryl halide electrophiles.[22] To test the effectiveness of the P_2-*t*-Bu prereagent system, Garrett selected methanol and 2-bromoquinoline (**3-53**) as a model reaction (Figure 3-21, top). He found that an equimolar amount of salt **3-16** and epoxide **3-21** (1.5 equiv) was highly effective at promoting S_NAr in similar yields to the commercial P_2-*t*-Bu. Alcohols (**3-54**, **3-55**), amines (**3-56** – **3-58**) and C–H (**3-59**) pronucleophiles were found to provide good to excellent yields. Of note is **3-55** as the S_NAr reaction was found to be regioselective and tolerant to the complex functionality on the aryl bromide. Control reactions support the active promotor being P_2-*t*-Bu.

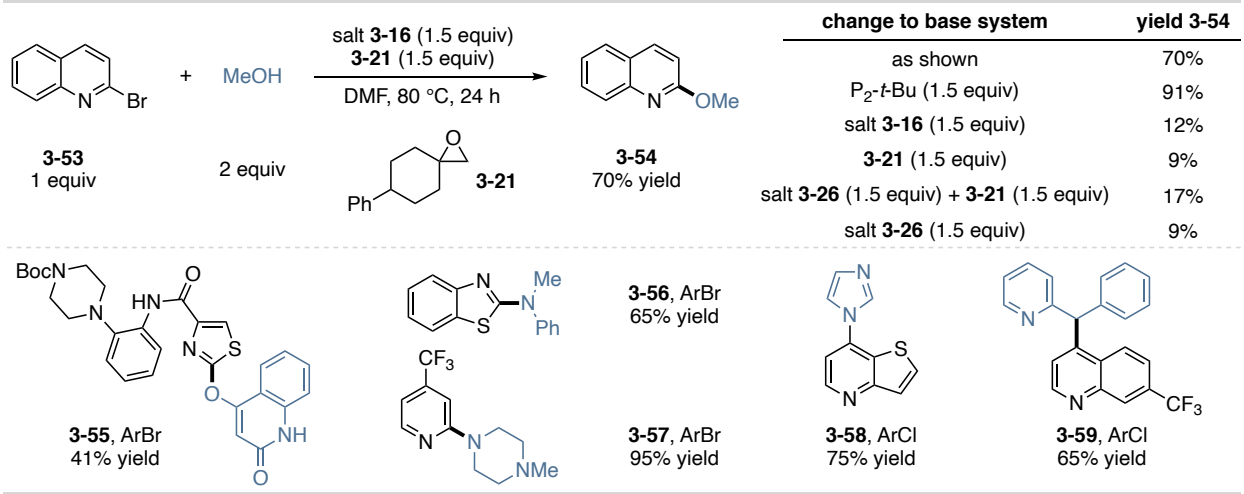

Figure 3-21: Stoichiometric application of salt **3-16** and epoxide **3-21** in S_NAr reactions, conditions for substrate scope shown in top scheme. ^{1}H NMR spectroscopy used to determine yields.

3.9 Application of Superbase Carboxylate Salt Systems in Palladium-Catalyzed Cross-Coupling Reactions

3.9.1 Superbases in Pd Catalysis Enabling Mild Conditions and Base-Sensitive Substrates

Pd-catalyzed cross-coupling reactions are among the most use reactions in the pharmaceutical industry.[15] In particular, Pd-catalyzed amination reactions are very prevalent and allow for the construction of *N*-aryl bonds on a wide range of substrate classes.[15] This leads advancements in this area of chemistry to be highly impactful and desired. Scientists at Merck in 2015 pioneered the use of organic superbases in palladium-catalyzed cross-coupling reactions.[23,24] They found that the use of organic superbases enabled mild and homogeneous conditions that were amendable to robotic high-throughput experimentation (HTE) (Figure 3-22). HTE was used to screen a broad range of reaction space that lead to the discovery of optimal conditions (5 mol% *t*-BuXPhos Pd G3, 2 equiv P_2-Et, 0.2 M DMSO, room temperature) for the coupling of a broad range of substrates, including highly complex aryl halides and amines.[24] Pd-catalyzed amination reactions typically require strong bases such as NaO-*t*-Bu or metal silyl amide base salts at room temperatures or carbonate and phosphate bases at elevated temperatures.[2] These inorganic bases lead to heterogeneous reaction conditions that often have reproducibility issues at larger scales due to different rates of stirring and/or insoluble-base particle size.[25,26] These conditions can also complications flow reactions and hinder the use of robotic dosing or HTE techniques.[27,28] Additionally, the need for high temperatures with week inorganic bases or the presences of a strong alkoxide base can lead to functional group compatibility issues.[24] Whereas the use of soluble organic superbases alleviates most of these concerns and allows for the coupling of complex, medicinally relevant and drug-like molecules more routinely.[22-24,29] This work by Merck scientists

represents the first general use of organic superbases in Pd catalysis and a remarkable advancement in reaction miniaturization and automation, technologies of high importance to modern chemistry.

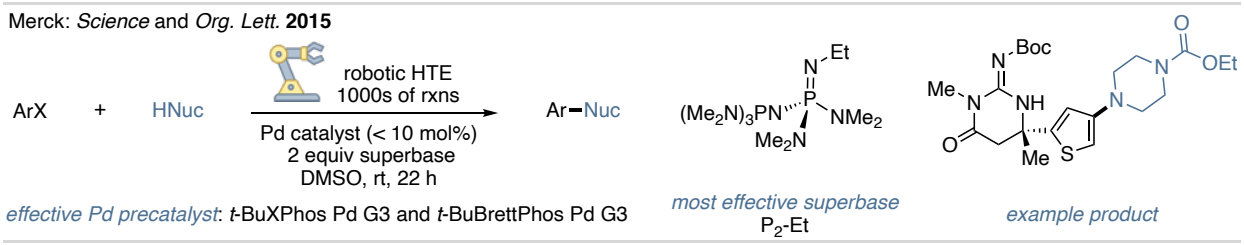

Figure 3-22: Superbases in Pd catalysis and use of robotic high-throughput experimentation to rapidly run thousands of reactions.

Shortly after Merck's pinioning work, the Buchwald Group disclosed the use of DBU, a weaker superbase, for the coupling of (hetero)aryl halides and triflates with anilines, amides and primary alkyl amines (Figure 3-23).[27,30] Key to the success of this reaction is the use of the AlPhos ligand, as the bulky adamantly groups on the phosphorous center decrease electron donation to the Pd-center.[27] This makes the Pd-center more electropositive, acidifying the protons on the bound amine, allowing for deprotonation by the weak superbase (Figure 3-23, right).[27] In a follow up mechanistic study, DBU was observed to have a negative rate order due to competitive binding between amine substrate and superbase with the Pd catalyst.[30] The substrate scope was improved with the slow addition of DBU with a syringe pump, as well as through the use of MTBD, a more sterically hindered superbase. Both slow addition and use of a more sterically blocked superbase helps to limit competitive binding with the Pd catalyst and lead to more catalytically active conditions.[30] The idea to slowly introduce base into a coupling reaction is interesting as it not only limits competitive binding, but it should allow for the coupling of base-sensitive substrates since no excess base would be present in the reaction solution. This idea will be further discussed and exploited in Section 3.9.5.

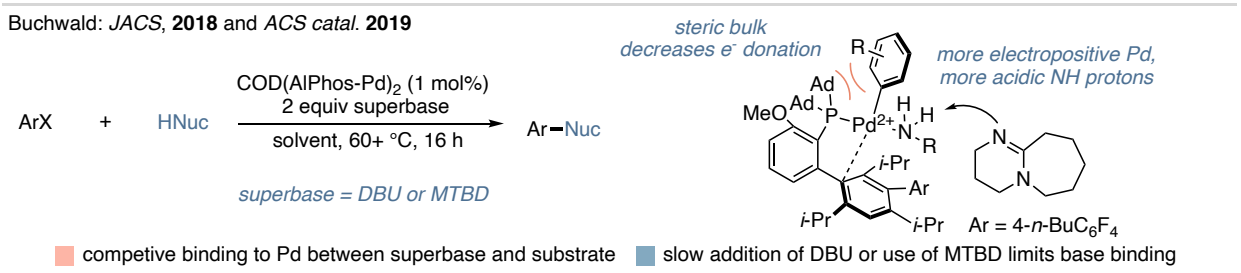

Figure 3-23: Use of weaker superbases in Pd catalysis, possible due to increased acidity of NH protons from ligand steric bulk in Pd oxidative addition complex.[27,30]

3.9.2 Scope of Superbase Prereagent Systems in Pd Catalysis

Based on the benefits of superbases in Pd catalysis and the importance of this reaction paradigm to modern chemistry, I reasoned it would be impactful to develop the use of superbase prereagent salts as a means to practically access superbases for Pd catalysis. Starting with the optimal conditions identified by Merck scientists and using the model reaction of **3-60** and **3-61** coupling to **3-62**, I found that 2 equiv of salt **3-16** and 3 equiv of epoxide **3-23** gives moderate yields (Figure 3-24a).[23,24] A simple solvent switch to THF results in excellent yield of the coupling product. THF proved to be a more general solvent when using the superbase prereagent system; however, other solvents such as DMSO and *tert*-amyl alcohol can provide good to excellent yields, depending on the substrates. *t*-BuBrettPhos Pd G3 was found to be a highly effective Pd precatalyst, but *t*-BuXPhos Pd G3 was selected as the standard Pd precatalyst due to its lower cost and while maintaining high performance. Control reactions indicate that P_2-*t*-Bu generated from salt activation is the active base in the system. Figure 3-24b shows the substrate scope I developed for Pd-catalyzed amination reactions using salt **3-16** and epoxide **3-23** as a prereagent system. To note, aryl substituted epoxides can be used for salt **3-16** in stoichiometric applications even though in activation studies only 50% neutral base is observed due to equilibrium control. These epoxides are effective because they lead to rapid activation and, in this reaction, the P_2-*t*-Bu base is consumed as it is generated, therefore shifting the equilibrium towards complete generation of P_2-

t-Bu. Use of epoxide **3-23** allows for the easy coupling of 3-chloro (**3-63 and 3-70**) and 3-bromopyridines (**3-64** and **3-65**) with various amines. Vinyl groups are tolerated under these conditions to provide good to excellent coupling yields (**3-66** to **3-68** and **3-72**). Cyclic, primary, and secondary alkyl amines (**3-62** to **3-69**) provide good to excellent yields of the *N*-aryl product. More acidic amine nucleophiles such as benzamide (**3-70**) and aniline derivatives (**3-71** to **3-73**) provide good yields as well. The use of salt **3-16** and epoxide **3-23** proved to be quite general in Pd-catalyzed aminations and enable very convenient procedures. Conveniently, all starting reagents in these coupling reactions are air-stable and can be weighted out open-to-air then placed under a N_2 atmosphere for the reaction.

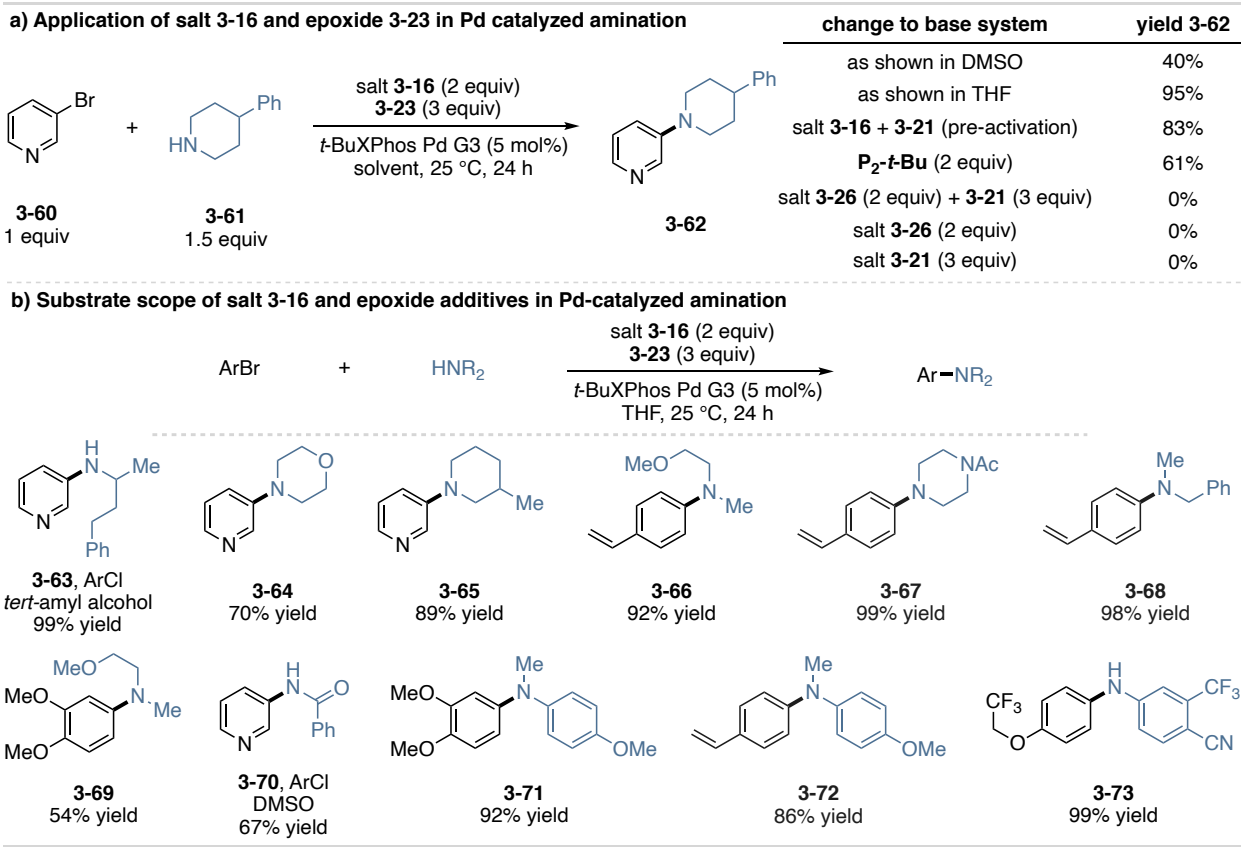

Figure 3-24: Application of prereagent system in Pd-catalyzed amination reactions. ^{1}H NMR spectroscopy used to determine yields.

Amination was not the only type of Pd-catalyzed cross-coupling reaction reported by scientists at Merck; etherification, hydration, α-arylation, and Suzuki cross-couplings were also shown.[24] Using identical conditions as shown in Figure 3-24 α-arylation of diethyl malonate with 3-chloropyridine was achieved in good yield of **3-74** (Figure 3-25, left). However, cross-coupling with water, alcohols and boronic esters using the superbase prereagent system did not provide product above 20% yield. Further investigation revealed the ROH pronucleophiles (water added in Suzuki coupling) were reacting with both the epoxide and byproduct **3-47** to give diol and transesterified side products. This inhibited salt activation as well as consumed the neutral superbase and reactant. This incompatibility was resolved using a pre-activation procedure with epoxide **3-21**, which reaches complete activation with an equimolar amount of salt **3-16**. Salt **3-16** and epoxide **3-21** are heated at 80 °C for 3 h in THF or PhMe then added to a solution of other reagents. This results in significantly improved yields for **3-75**, **3-76** and **3-77** (Figure 3-73).

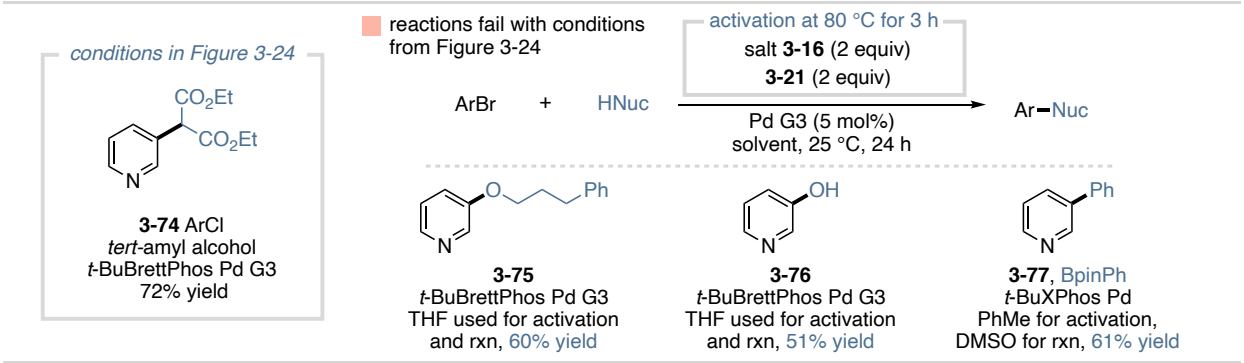

Figure 3-25: Pd-catalyzed α-arylation, etherification, hydration, and Suzuki cross-coupling using salt **3-16** and epoxide **3-21**. ^{1}H NMR spectroscopy used to determine yields.

Notably, P_1 phosphazene superbases are underexplored in the literature on superbase use in Pd catalysis. While not as basic as P_2 phosphazenes, P_1 phosphazenes (P_1-*t*-Bu p$K_{a'}$ = 28.4 in MeCN)[5] are several p$K_{a'}$ unites more basic than the most basic guanidine superbase (TBD p$K_{a'}$ = 26.0 in MeCN)[31] and far less expensive than P_2 phosphazenes (see Chapter One; P_1-*t*-Bu: \$27/g vs. P_2-*t*-Bu: \$95/g). Given this and the practicality of the P_1-*t*-Bu prereagent system, I wanted to

explore the reaction space of P_1-*t*-Bu in Pd catalysis. Using the general conditions from Figure 3-24, I found that salt **3-15** and epoxide **3-23** provide good to excellent yields for a variety of coupling product (Figure 3-26). Aryl triflates (**3-78** and **3-79**) and aryl halides (**3-73** and **3-80**) work well with more acid amine pronucleophiles such as aniline derivatives and fluoroalkyl amines. The successful application of salts **3-15** and **3-16** with epoxide additives leads to a much more convenient and potentially cost-effective way to enable Pd catalysis, especially the use of salt **3-15** and P_1-phosphazenes more generally.

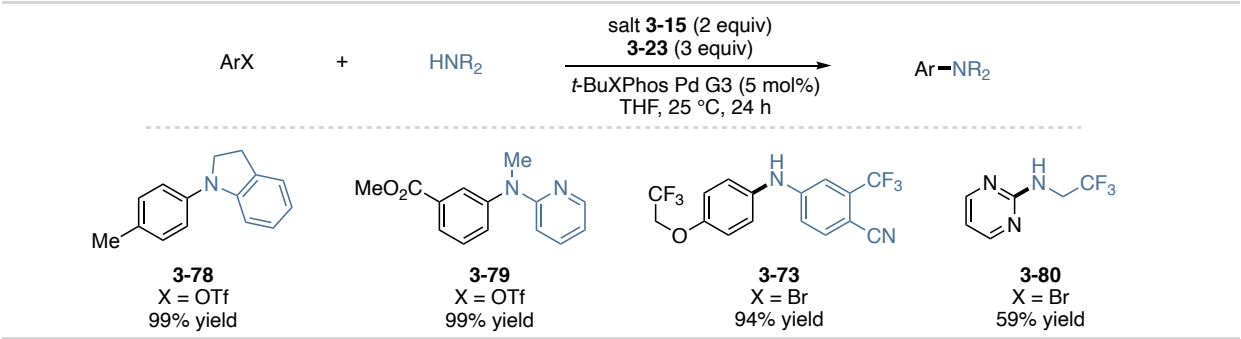

Figure 3-26: Pd catalysis using salt **3-15** and epoxide **3-23**. ^{1}H NMR spectroscopy used to determine yields.

3.9.3 Improved Economics of Superbases in Pd Catalysis

Application of superbases in Pd catalysis can be economically challenging for larger scale use given the super-stoichiometric quantities needed and the high cost of superbases. I reasoned the superbase prereagent could be easily recycled from these types of applications since the final neutralization step to the strong superbase is not required in prereagent synthesis. I found that through a series of aqueous HCl washes, HP_2-*t*-BuCl can be cleaning recovered from a reaction mixture (Figure 3-27). Treating the aqueous solution of HP_2-*t*-BuCl with activated carbon was found to be essential to remove trace organics that can interfere with crystallization of salt **3-16**. After HP_2-*t*-BuCl is recovered it can be smoothly converted to salt **3-16** *via* anion metathesis in a very similar procedure as was done in Section 3.6.2. Subsequent reuse of this recycled P_2-*t*-Bu salt

3-16 provides equally high yields as the freshly synthesized salt. This development is particularly advantageous on larger scales or when large amounts of material are being used in reaction screening as numerous reactions containing P_2-*t*-Bu can be combined and recycled.

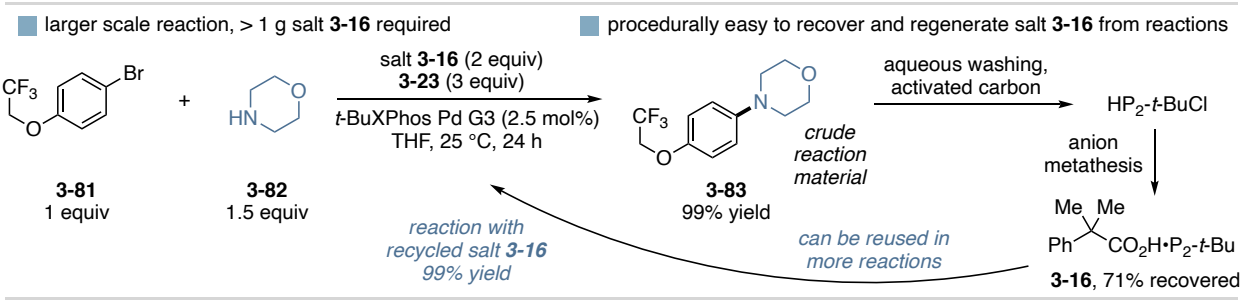

Figure 3-27: Larger scale reaction, 1 mmol, with salt **3-16** and epoxide **3-23**. Salt **3-16** was recovered and reused in the same reaction ^{1}HNMR spectroscopy used to determine yields.

3.9.4 Controlling the Rate of Pd Catalysis and Potential Benefits

As discussed in Section 3.5.4 and 3.7.1, the identity of the epoxide and its electronic properties can govern the rate at which the base is "turned-on", and thus the rate of a given reaction. This could have several benefits in Pd catalysis: first, the controllable rate could be used to mitigate an exotherm present in some amination reactions, and second, it could be used to expand the scope of base-sensitive substrates in coupling reaction (see next Section, 3.9.5). To investigate I measured the reaction profile of the coupling of bromobenzene (**3-84**) and morpholine (**3-82**) (Figure 3-28, left) under a variety of reaction conditions. Unsurprisingly, P_2-*t*-Bu reached full conversion first since no activation is required. Epoxide **3-23** closely matched the rate of P_2-*t*-Bu as this epoxide activates salt **3-16** very rapidly. Epoxide **3-24** reached full conversion at 2 h and epoxide **3-25** eventually reached 86% yield at 24 h.

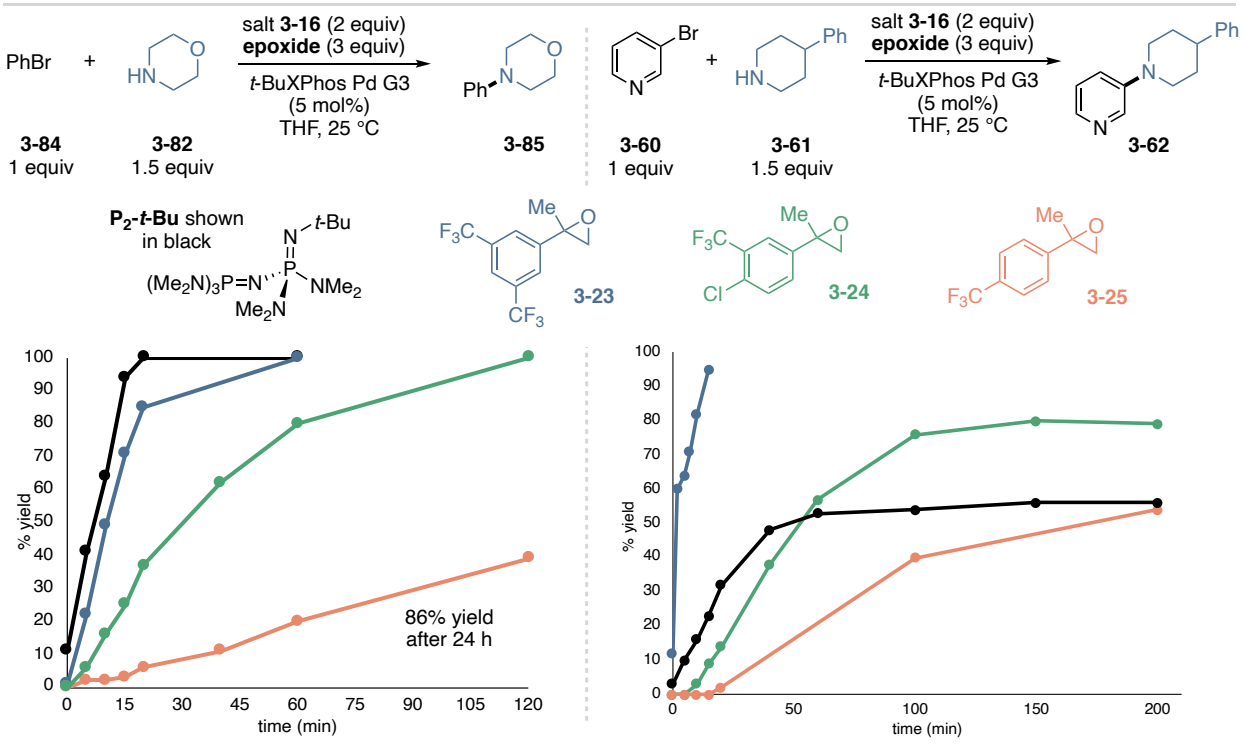

Figure 3-28: Reaction profiles of Pd-catalyzed amination reactions, reaction rate and outcome controlled by epoxide additive. ^{1}H NMR spectroscopy used to determine yields.

I next measured the reaction profile for the model reaction in Section 3.9.2, the coupling of 3-bromopyridine (**3-60**) with 4-phenylpiperidine (**3-61**) (Figure 3-28, right). In this reaction, induction periods are observed for epoxides **3-24** and **3-25**, which is indicative of a slower rate of base "turn-on". The use of salt **3-16** and epoxide **3-23** results in complete conversion within 15 min and a 60% yield after only 2 min. This is a much faster reaction than what was observed when commercial P$_2$-*t*-Bu. This could potentially be due to the lack of competitive binding between the superbase and substrate when the P$_2$-*t*-Bu prereagent system is used, as other superbases were shown to have a negative rate order dependances in Pd-catalyzed amination reactions for that reason. Overall, these reaction profiles demonstrate that the electronic properties of the epoxide additive can be used to control the rate of a given reaction and limit excess strong base in solution. This could potentially serve as a means to mitigate uncontrolled exotherms in Pd catalysis by slowing the reaction down.[32]

3.9.5 Pushing the Limits of Base-Sensitive Substrate Coupling

As previously discussed in Section 3.9.1, Buchwald and coworkers demonstrated that slow addition of superbase can improve yields in Pd-catalyzed coupling reactions.[33] Given this and the control over superbase "turn-on" demonstrated in the previous section, I reasoned the superbase prereagent system could be used to expand the scope of base-sensitive coupling partners based on the epoxide used. More recently, the Buchwald Group demonstrated that GPhos Pd G6 with NaOTMS as the base is a highly effective system at coupling base-sensitive 5-membered heterocycles. One of the published reactions is between **3-86** and **3-87** to give **3-88** (Figure 3-29). I found that this same reaction with commercial P_2-*t*-Bu and *t*-BuXPhos Pd G3 provides 8% yield and that there is very little **3-86** remaining. Epoxides **3-23** and **3-24** result in 11% and 24% yield, respectively, again with poor mass balance of **3-86**. However, epoxide **3-25** results in complete conversion to the product. This result suggest that the epoxide electronics can be used to match the rate of base "turn-on" *in situ* to the rate of coupling, thus preventing any buildup of base in solution and enabling the coupling of highly base sensitive substrates. Control reactions show that both **3-86** and **3-87** lose mass balance when treated with neutral P_2-*t*-Bu. The loss of mass balance is greater when **3-86** and **3-87** are treated with neutral P_2-*t*-Bu in the same solution, indicating that both reagents are base-sensitive, and this base-sensitivity is magnified under reaction conditions.

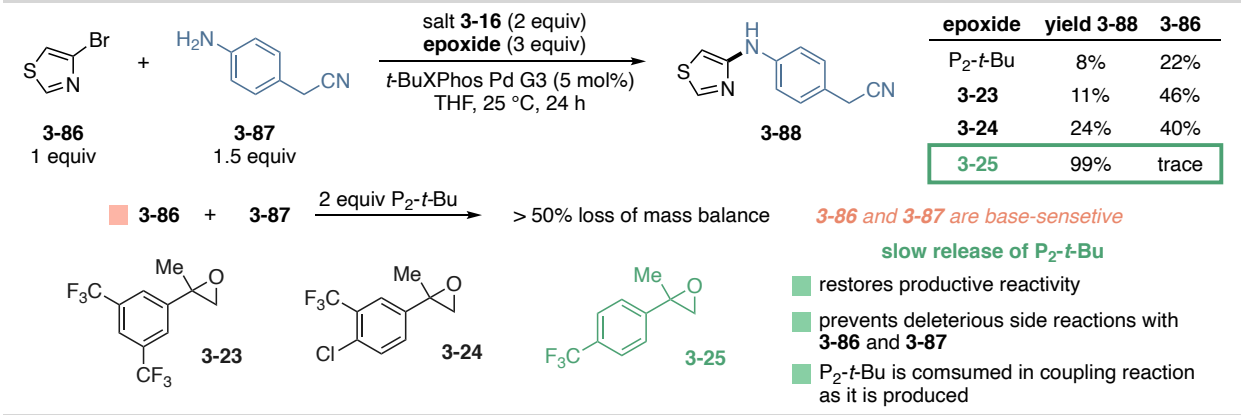

Figure 3-29: Use of prereagent system and slow-release mechanism to couple a base-sensitive substrate. ^{1}H NMR spectroscopy used to determine yields.

3.10 Conclusion and Outlook

Chapter Three describes the fourth area of research in the Bandar Group, the area of chemistry I established after joining the group in 2018. I first used decarboxylation as a driving force to effect superbase salt activation; however, this strategy only saw limited success as decarboxylative superbase salts are not stable under ambient conditions. Additionally, the cyclic carbonate byproduct from CO_2 trapping was not compatible in a broad range of reactions. The method used to prevent CO_2 from reacting with the neutral phosphazene ultimately led to the use of epoxide ring strain to drive the superbase activation. Within this new precatalyst system Garrett and I developed highly stable superbase•carboxylate salts that, when coupled with a range of epoxide additives, can controllably "turn-on" the superbase in solution. The byproduct from this "turn-on" process proved to be compatible in a variety of different application in which the prereagent or precatalyst system provided good to excellent yields. These applications include classic Michael additions and Mannich reactions as well as alcohol deoxyfluorination and some of the most common reactions in organic synthesis: amidations, S_NAr and Pd-catalyzed cross-coupling reactions. The development of organic superbase precatalyst salts is being prepared for publication now.

Overall, these superbase precatalyst/prereagent systems provide convenient access to the unique chemistry of organic superbases and make the synthesis of phosphazene superbases more practical and safer. The improved synthesis of phosphazenes stands to decreases the cost of these superbases dramatically and could potentially lead to the preparation of more derivatives, thus expanding the unique chemistry of superbases. Additionally, these superbase salts will improve the economics of superbase use as they can be easily recycled from reactions and reused. The

improved access to superbase chemistry also stands to increase superbase use in discovery chemistry settings. This can be expected to accelerate the discovery of new reactions as evidenced by the Bandar Group's own use of superbases to establish three other active areas of research (see Chapter One). Furthermore, the controllable release of superbase has the potential to improve the scope of base-sensitive substrates in base-promoted chemistry, as in the case of Pd catalysis discussed in Section 3.9.5.

This is still an active area of research in the Bandar Group as younger group members are further exploring the application of controllable base release with base-sensitive substrates in Pd catalysis and the group is also working to develop a precatalyst system for P_4-*t*-Bu. Currently, the release of epoxide ring strain is not sufficient to drive the deprotonation of P_4-*t*-Bu; however other driving forces are being explored, like the generation of hydrogen (H_2) gas. In the end, the groundwork myself and Garrett have laid in the development of stable organic superbases will serve as the foundation for further discovery within the Bandar Group and in base-promoted-chemistry more broadly.

REFERENCES

[1] "precatalysts" – WordSense Online Dictionary (12th June, 2023) URL: https://www.wordsense.eu/precatalysts/

[2] Ingoglia, B. T.; Wagen, C. C.; Buchwald, S. L. Biaryl monophosphine ligands in palladium-catalyzed C–N coupling: An updated User's guide *Tetrahedron* **2019**, *75*, 4199 – 4211.

[3] Bruneau, A.; Roche, M.; Alami, M.; Messaoudi, S. 2-Aminobiphenyl Palladacycles: The "Most Powerful" Precatalysts in C−C and C−Heteroatom Cross-Couplings *ACS Catal*. **2015**, *5*, 1386−1396.

[4] Bruno, N.C.; Tudge, M.T.; Buchwald, S. L. Design and preparation of new palladium precatalysts for C–C and C–N cross-coupling reactions *Chem. Sci*., **2013**, *4*, 916-920.

[5] Schwesinger, R.; Schlemper, H.; Hasenfratz, C.; Willaredt, J.; Dambacher, T.; Breuer, T.; Ottaway, C.; Fletschinger, M.; Boele, J.; Fritz, H.; Putzas, D.; Rotter, H. W.; Bordwell, F. G.; Satish, A. V.; Ji, G.-Z.; Peters, E.-M.; Peters, K.; von Schnering, H. G.; Walz, L. Extremely Strong, Uncharged Auxiliary Bases; Monomeric and Polymer-Supported Polyaminophosphazenes (P2- P5)* *Liebigs Ann*. **1996**, 1055 – 1081.

[6] Gierczyk, B.; Wojciechowski, G.; Brzezinski, B.; Grech, E.; Schroeder, G. Study of the decarboxylation mechanism of fluorobenzoic acids by strong N-bases *J. Phys. Org. Chem*. **2001**, *14*, 691–696.

[7] Shen, K.; Fu, Y.; Li, J.-N.; Liu, L.; Guo, Q.-X. What are the pKa values of C–H bonds in aromatic heterocyclic compounds in DMSO? *Tetrahedron* **2007**, *63*, 1568–1576.

[8] Sopeña, S.; Cozzolino, M.; Maquilón, C.; Escudero-Adun, E. C.; Belmonte, M. M.; Kleij, A. W. Organocatalyzed Domino [3+2] Cycloaddition/Payne-Type Rearrangement using Carbon Dioxide and Epoxy Alcohols *Angew. Chem. Int. Ed*. **2018**, *57*, 11203 –11207.

[9] Olmstead, W. N.; Margolin, Z.; Bordwell, F. G. *J. Org. Chem*. **1980**, *45*, 3295–3299.

[10] Morgan, K. M.; Ellis, J. A.; Lee, J.; Fulton, A.; Wilson, S. L.; Dupart, P. S.; Dastoori, R. Thermochemical Studies of Epoxides and Related Compounds *J. Org. Chem*. **2013**, *78*, 4303−4311,

[11] Weitkamp, R. F.; Neumann, B.; Stammler, H. G.; Hoge, B Generation and Applications of the Hydroxide Trihydrate Anion, $[OH(OH_2)_3]^-$, Stabilized by a Weakly Coordinating Cation *Angew. Chem. Int. Ed*. **2019**, *58*, 14633 –14638.

[12] Nising, C. F.; Bräse, S. Recent developments in the field of oxa-Michael reactions *Chem. Soc. Rev.*, **2012**, *41*, 988–999.

[13] Nising, C. F.; Bräse, S. The oxa-Michael reaction: from recent developments to applications in natural product synthesis Chem. Soc. Rev., **2008**, 37, 1218–1228.

[14] Hu, J.; Bian, M.; Ding, H. Recent application of oxa-Michael reaction in complex natural product synthesis *Tetrahedron Lett*. **2016**, *57*, 5519–5539.

[15] Brown, D. G.; Boström, J. Analysis of Past and Present Synthetic Methodologies on Medicinal Chemistry: Where Have All the New Reactions Gone? *J. Med. Chem*. **2016**, *59*, 4443−4458.

[16] Cladwell, N.; Jamieson, C.; Simpson, I.; Tuttle, T. Organobase-Catalyzed Amidation of Esters with Amino Alcohols *Org. Lett*., **2013**, *15*, 2506–2509.

[17] Puleo, T. R.; Sujansky, S. J.; Wright, S. E.; Bandar, J. Organic Superbases in Recent Synthetic Methodology Research. *Chem. – Eur. J*. **2020**, *27,* 4216 – 4229.
[18] Nielsen, M. K.; Ugaz, C. R.; Li, W.; Doyle, A. G. PyFluor: A Low-Cost, Stable, and Selective Deoxyfluorination Reagent *J. Am. Chem. Soc*. **2015**, *137*, 9571−9574.
[19] Nielsen, M. K.; Ahneman, D. T.; Riera, O.; Doyle, A. G. Deoxyfluorination with Sulfonyl Fluorides: Navigating Reaction Space with Machine Learning *J. Am. Chem. Soc*. **2018**, *140*, 5004−5008.
[20] Żurański, A. M.; Gandhi, S. S.; Doyle, A. G. A Machine Learning Approach to Model Interaction Effects: Development and Application to Alcohol Deoxyfluorination *J. Am. Chem. Soc.* **2023**, *145*, 7898–7909.
[21] Pirnot, M.; Stone, K.; Wright, T. J.; Lamberto, D. J.; Schoell, J.; Lam, Y.; Zawatzky, K.; Wang, X.; Dalby, S. M.; Fine, A. J. McMullen, J. P. Manufacturing Process Development for Belzutifan, Part 6: Ensuring Scalability for a Deoxyfluorination Reaction *Org. Process Res. Dev.* **2022**, *26*, 551–559.
[22] Gesmundo, N. J.; Sauvagnat, B.; Curran, P. J.; Richards, M. P.; Andrews, C. L.; Dandliker, P. J.; Cernak, T. Nanoscale synthesis and affinity ranking *Nature*, **2018**, *557*, 228–232.
[23] Santanilla, A. B.; Regalado, E. L.; Pereira, T.; Shevlin, M.; Bateman, K.; Campeau, L.-C.; Schneeweis, J.; Berritt, S.; Shi, Z.-C.; Nantermet, P.; Liu, Y.; Helmy, R.; Welch, C. J.; Vachal, P.; Davies, I. W.; Cernak, T.; Dreher, S. D. Nanomole-scale high-throughput chemistry for the synthesis of complex molecules *Science* **2015**, *347,* 49 - 53.
[24] Santanilla, A. B.; Christensen, M.; Campeau, L.-C.; Davies, I. W.; Dreher, S. D. P_2Et Phosphazene: A Mild, Functional Group Tolerant Base for Soluble, Room Temperature Pd-Catalyzed C−N, C−O, and C−C Cross- Coupling Reactions *Org. Lett*. **2015**, *17*, 3370−3373.
[25] Meyers, C.; Maes, B. U. W.; Loones, K. T. J.; Bal, G.; Lemière, G. L. F.; Dommisse, R. A. Study of a New Rate Increasing "Base Effect" in the Palladium-Catalyzed Amination of Aryl Iodides *J. Org. Chem*. **2004**, *69*, 6010−6017.
[26] Kuethe, J. T.; Childers, K. G.; Humphrey, G. R.; Journet, M.; Peng, Z. A Rapid, Large-Scale Synthesis of a Potent Cholecystokinin (CCK) 1R Receptor Agonist *Org. Process Res. Dev*. **2008**, *12*, 1201−1208.
[27] Dennis, J. M.; White, N. A.; Liu, R. Y.; Buchwald, S. L. Breaking the Base Barrier: An Electron-Deficient Palladium Catalyst Enables the Use of a Common Soluble Base in C−N Coupling *J. Am. Chem. Soc*. **2018**, *140*, 4721–4725.
[28] Yang, J. C.; Niu, D.; Karsten, B. P.; Lima, F.; Buchwald, S. L. Use of a "Catalytic" Cosolvent, *N,N*-Dimethyl Octanamide, Allows the Flow Synthesis of Imatinib with no Solvent Switch *Angew. Chem., Int. Ed*. **2016**, *55*, 2531−2535.
[29] Uehling, M. R.; King, R. P.; Krska, S. W.; Cernak, T.; Buchwald, S. L. Pharmaceutical diversification via palladium oxidative addition complexes *Science*, **2019**, *363*, 405–408.
[30] Dennis, J. M.; White, N. A.; Liu, R. Y.; Buchwald, S. L. Pd-Catalyzed C−N Coupling Reactions Facilitated by Organic Bases: Mechanistic Investigation Leads to Enhanced Reactivity in the Arylation of Weakly Binding Amines *ACS Catal*. **2019**, *9*, 3822−3830.
[31] Kolomeitsev, A. A.; Koppel, I. A.; Rodima, T.; Barten, J.; Lork, E.; Röschenthaler, G.-V.; Kaljurand, I.; Agnes Kütt, A.; Koppel, I.; Mäemets, V.; Leito, I. Guanidinophosphazenes: Design, Synthesis, and Basicity in THF and in the Gas Phase *J. Am. Chem. Soc*. **2005**, *127*, 17656-17666.

[32] Yang, Q.; Babij, N. R.; Good, S. Potential Safety Hazards Associated with Pd-Catalyzed Cross-Coupling Reactions *Org. Process Res. Dev.* **2019**, *23*, 2608–2626.
[33] Reichert, E. C.; Feng, K.; Sather, A. C.; Buchwald, S. L. Pd-Catalyzed Amination of Base-Sensitive Five-Membered Heteroaryl Halides with Aliphatic Amines *J. Am. Chem. Soc.* **2023**, *145*, 3323−3329.

APPENDIX ONE

MECHANISTIC STUDIES YIELD IMPROVED PROTOCOLS FOR BASE-CATALYZED ANTI-MARKOVNIKOV ALCOHOL ADDITION REACTIONS: EXPERIMENTAL

A1.1 General Information

This appendix is adapted from "Mechanistic Studies Yield Improved Protocols for Base-Catalyzed anti-Markovnikov Alcohol Addition Reactions" *J. Am. Chem. Soc*. **2022**, *144*, 9586−9596. It is intended to provide experimental details for my contributions to this work and for the experimental work that was critical to improving the overall method. Refer to the supporting information of the above publication for computational details and coordinates.

General Reagent Information: 1-*tert*-Butyl-4,4,4-tris(dimethylamino)-2,2-bis[tris(dimethylamino)phosphoranylidenamino]-2λ^5,4λ^5-catenadi(phosphazene) (P_4-*t*-Bu) was purchased from Millipore Sigma as a 0.8 M solution in hexanes (product #79421) and was stored in a -30 °C freezer inside a nitrogen-filled glovebox. Before use, the P_4-*t*-Bu solution was allowed to warm to room temperature and homogenize if any solid was evident. Tetrahydrofuran and toluene were deoxygenated and dried by passage over packed columns of neutral alumina and copper (II) oxide under positive pressure of nitrogen. Potassium *tert*-butoxide (KO-*t*-Bu) from Chem-Impex (product number #27317) was used as purchased and stored inside a nitrogen-filled glovebox. 18-Crown-6 (1,4,7,10,13,16-hexaoxacyclooctadecane) was purchased from Chem-Impex (product #03901) and used as received. Sodium hydride (NaH) was purchased from Acros as a 60% dispersion in mineral oil (product #189862500) and was stored in a desiccator with $CaSO_4$ as the desiccant. Methyltriphenylphosphonium bromide was purchased from Combi-

Blocks (product #QA-8732) and used as received. *n*-Butanol was purchased from Millipore Sigma (#B7906) and stored over activated molecular sieves in a nitrogen-filled glovebox. The following solvents were purchased anhydrous from Millipore Sigma and used as received: dimethyl sulfoxide (#276855), dibutyl ether (#271454), dodecane (#297879), *N*,*N*-dimethylformamide (#227056), *N*-methyl-2-pyrrolidone (#328634), anisole (#296295), benzonitrile (#294098), tetralin (#522651), 1,4-dioxane (#296309), 1,2-dimethoxyethane (#259527), triethyl orthoformate (#304050), 1,2-dichlorobenzene (#240664), cyclopentyl methyl ether (#791962), chlorobenzene (#284513), α,α,α-trifluorotoluene (#547948), cyclohexane (#227048). All other reagents were purchased from Millipore Sigma, Combi-Blocks, TCI, Acros Organics, Matrix, or Alfa Aesar and used as received unless otherwise noted. Flash Chromatography was performed on 40-63 μm silica gel (SiliaFlash® F60 from Silicycle).

General Analytical Information: All new compounds were characterized by ^{1}H, ^{13}C, ^{19}F and ^{31}P (as appropriate) NMR spectroscopy, FTIR spectroscopy, mass spectrometry, melting point analysis (if solid) and specific rotation analysis (if chiral). ^{1}H NMR, ^{13}C NMR, ^{19}F NMR, and ^{31}P NMR spectra were obtained on a Bruker Advanced NEO or Varian Inova 400 MHz spectrometer. ^{1}H NMR data is reported as follows: chemical shift (δ ppm), multiplicity (s = singlet, d = doublet, t = triplet, q = quartet, dd = doublet of doublets, td = triplet of doublets, m = multiplet), coupling constant (Hz), and integration. ^{13}C NMR data is reported as follows: chemical shift (δ ppm), multiplicity (if applicable, q = quartet, T = 1:1:1 multiplicity). All ^{1}H NMR signals are reported as chemical shifts (δ ppm) relative to residual $CHCl_3$ at 7.26 ppm and ^{13}C NMR signals are reported as chemical shifts (δ ppm) relative to $CDCl_3$ at 77.16 ppm. All ^{19}F NMR signals are reported as chemical shifts (δ ppm) relative to *α,α,α*-trifluorotoluene (δ -63.72 ppm) that was added as an internal standard. Gas chromatography (GC) analyses were performed on an Agilent Technologies

7890B GC system with an FID detector using a J&W HP-5 column (30 m, 0.320 mm D). A general GC method was used for all studies with an injection volume of 1 μL, initial temperature of 100 °C, rate of 30 °C/min, maximum temperature of 300 °C and a run time of 6 min. High resolution mass spectra (HRMS) were recorded on an Agilent 6210 TOF interfaced to a DART 100 or APCI source provided by Colorado State University's Materials and Molecular Analysis Center. If the substrate would not ionize using alternative methods, a GC-MS method was used on an Agilent 5977A GC/MSD system. Infrared spectra were recorded using a Thermo Scientific Nicolet iS-50 FTIR Spectrometer and reported as frequency of absorption (cm^{-1}). Melting point analyses were conducted using a Mel-Temp capillary melting point apparatus. Thin-layer chromatography analysis was performed on silica gel 60Å F_{254} plates (250 μm, SiliaPlate from Silicycle, #TLG-R10014B-323) and interpreted using UV light (254 nm) or $KMnO_4$ stain.

Note on nomenclature: The names provided for the structures below were obtained from ChemDraw Professional 16.0.

A1.2 Experimental Thermodynamic Studies

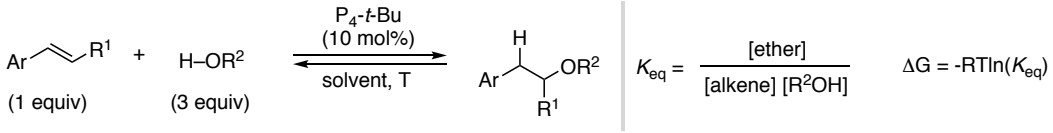

General description. The alcohol addition reaction is reversible. The forward and backward reactions were run at a given temperature and concentration until they converged as judged by ^1H NMR integration of ether and styrene signals of a reaction aliquot. The concentration of each component was then determined (calculated as the molar quantity of each component divided by the estimated overall volume of solution) and K_{eq} was calculated. Average K_{eq} values are shown and standard deviation error bars are included for the plots shown below. The experimental procedures are described below for the different types of thermodynamic studies.

General procedure for forward reaction. In a nitrogen-filled glovebox, aryl alkene (0.15 mmol, 1.0 equiv), *n*-butanol (41 μL, 0.45 mmol, 3.0 equiv) and solvent (0.3 mL) were added to an oven-dried 4 mL reaction vial (Thermo Scientific B7990-2) containing a magnetic stir bar. P_4-*t*-Bu (0.8 M in hexane, 19 μL, 0.015 mmol, 0.1 equiv) was then added to the reaction solution. The reaction vial was capped (Thermo Scientific C4015-1A with 10/50 septa), removed from the glovebox, and placed in a preheated oil bath at the indicated temperature. After stirring for 24 h, the reaction vial was removed from the oil bath and then cooled to room temperature (rt). To the reaction mixture was added dibenzyl ether (14.3 μL, 0.075 mmol, 0.5 equiv). An aliquot (approximately 50 μL) of the reaction solution was directly transferred to an NMR tube with $CDCl_3$ (0.6 mL). The amounts of aryl alkene, *β*-phenethyl ether, and alcohol were calculated by comparison of respective integrations to the dibenzyl ether internal standard. In cases where *n*-butanol signals overlapped with others, the amount was assumed to be 0.45 mmol minus the mmol of the formed *β*-phenethyl ether.

General procedure for reverse reaction. In a nitrogen-filled glovebox, *β*-phenethyl ether (0.15 mmol, 1.0 equiv), *n*-butanol (28 μL, 0.30 mmol, 2.0 equiv) and solvent (0.3 mL) were added to an oven-dried 4 mL reaction vial (Thermo Scientific B7990-2) containing a magnetic stir bar. P_4-*t*-Bu (0.8 M in hexane, 19 μL, 0.015 mmol, 0.1 equiv) was then added to the reaction solution. The reaction vial was capped (Thermo Scientific C4015-1A with 10/50 septa), removed from the glovebox, and placed in a preheated oil bath at the indicated temperature. After stirring for 24 h, the reaction vial was removed from the oil bath and then cooled to rt. To the reaction mixture was added dibenzyl ether (14.3 μL, 0.075 mmol, 0.5 equiv). An aliquot (approximately 50 μL) of the reaction solution was directly transferred to an NMR tube with $CDCl_3$ (0.6 mL). The amounts of aryl alkene, *β*-phenethyl ether, and alcohol were calculated by comparison of respective

integrations to the dibenzyl ether internal standard. In cases where *n*-butanol signals overlapped with others, the amount was assumed to be 0.30 mmol plus the mmol of the formed aryl alkene. In the following sections (a - c), K_{eq} and ΔG were calculated separately with concentrations obtained from the forward and reverse reactions, then averaged. The standard deviation was calculated with the K_{eq} and ΔG values from the forward and reverse reactions.

A1.2.1 Solvent Effects on the Addition of n-Butanol to 4-(Trifluoromethyl)styrene.

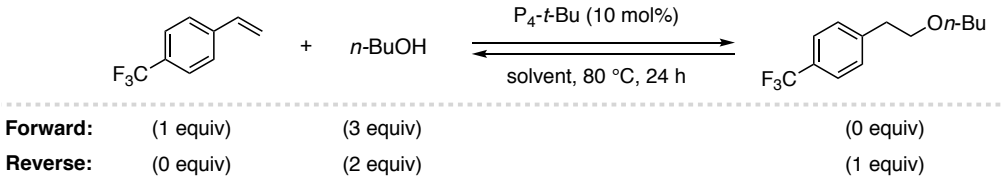

The above general procedures for the forward and reverse reactions were performed in the following solvents at 80 °C. All solvents were purchased as anhydrous or were stored over molecular sieves before use. For these reactions, the total volume of solution was estimated to be 0.382 mL resulting in the initial concentration for the styrene or ether to be 0.39 M. Tetrahydrofuran and acetonitrile were only run in the reverse direction and stopped once the reaction reached equilibrium and standard deviations were not calculated for these solvents (this was done due to the low boiling point of these solvents and the fact that the reverse reaction proceeds significantly faster than the forward reaction).

Table A1-1. Solvent effects on equilibrium position with calculated K_{eq} and ΔG values.

Solvent	**[ether]** (M)	**[styrene]** (M)	**[*n*-BuOH]** (M)	K_{eq}	K_{eq} std. dev.	ΔG kcal/mol	ΔG std. dev.
dodecane	0.05	0.34	1.13	0.13	0.03	1.46	0.14
N,*N*-dimethylformamide	0.05	0.34	1.12	0.15	0	1.36	0
quinoline	0.06	0.33	1.12	0.16	0.02	1.30	0.08
N-methyl-2-pyrrolidone	0.06	0.33	1.11	0.17	0.04	1.24	0.16
anisole	0.06	0.33	1.11	0.17	0	1.24	0
benzonitrile	0.08	0.31	1.09	0.25	0.01	0.97	0.03
pyridine	0.10	0.30	1.08	0.30	0.06	0.85	0.14

tetralin	0.10	0.30	1.08	0.31	0.11	0.86	0.26
dioxane	0.11	0.29	1.07	0.35	0	0.75	0
tetrahydrofuran	0.13	0.27	1.05	0.45	-	0.56	-
1,2-dichlorobenzene	0.14	0.26	1.04	0.52	0	0.46	0
dibutyl ether	0.15	0.24	1.02	0.62	0	0.33	0
chlorobenzene	0.16	0.23	1.01	0.70	0.07	0.25	0.07
m-xylene	0.16	0.23	1.01	0.72	0.05	0.24	0.05
toluene	0.19	0.20	0.99	0.96	0.15	0.03	0.11
cyclohexane	0.20	0.19	0.98	1.09	0.03	-0.06	0.02
acetonitrile	0.11	0.28	1.06	0.38	-	0.67	-
dimethyl sulfoxide	0.04	0.35	1.13	0.11	0	1.56	0
mesitylene	0.07	0.32	1.11	0.27	0.18	0.98	0.33
nitrobenzene	0.10	0.29	1.08	0.31	0	0.82	0
1,2-dimethoxyethane	0.11	0.28	1.07	0.35	0.01	0.73	0.03
ethyl orthoformate	0.12	0.28	1.06	0.39	0.01	0.65	0.03
cyclopentyl methyl ether	0.14	0.26	1.04	0.52	0	0.46	0
1,4-bis(trifuoromethyl)benzene	0.14	0.25	1.04	0.53	0.09	0.45	0.12
α,α,α-trifluorotoluene	0.19	0.21	0.99	0.91	0.03	0.06	0.02

A1.2.2 van't Hoff Plots for the Addition of n-Butanol to 4-(Trifluoromethyl)styrene.

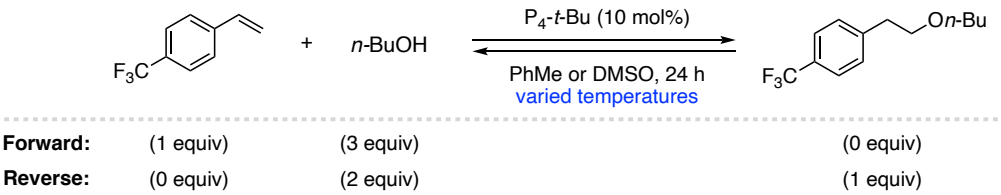

The above general procedures for the forward and reverse reactions were followed in PhMe and DMSO at the indicated temperatures. The observed equilibrium data is recorded below; for these reactions, the total volume of solution was estimated to be 0.382 mL. Equilibrium constant (K_{eq}) values at each temperature were then used to plot the van't Hoff equation. The ΔH and ΔS parameters were determined by the slope and intercept, respectively.

$$\ln K_{eq} = -\frac{\Delta H}{R}\left(\frac{1}{T}\right) + \frac{\Delta S}{R}$$

Table A1-2. Equilibrium data collected in DMSO at various temperatures.

DMSO								
T (°C)	1/T (K^{-1})	[styrene] (M)	[ether] (M)	[*n*-BuOH] (M)	K_{eq}	K_{eq} std. dev.	ln(K_{eq})	ln(K_{eq}) std. dev.
30	0.0033	0.30	0.09	1.09	0.26	0.000	-1.33	0.001
50	0.0031	0.33	0.06	1.11	0.18	0.006	-1.73	0.033
60	0.0030	0.34	0.06	1.12	0.15	0.005	-1.89	0.033
70	0.0029	0.34	0.05	1.13	0.13	0.002	-2.03	0.019
80	0.0028	0.35	0.04	1.14	0.11	0.001	-2.25	0.009

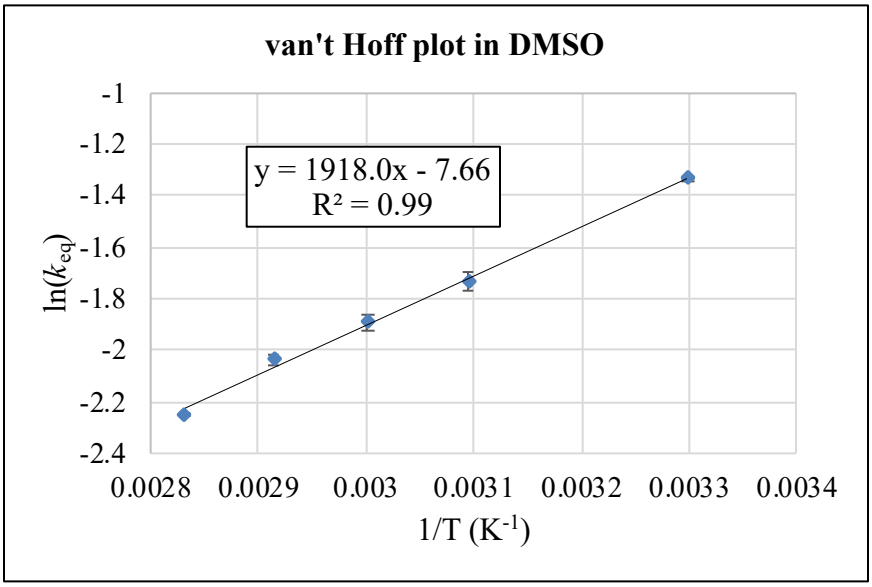

Figure A1-1. van't Hoff plot in DMSO; $\Delta H = -3.8 \pm 0.1$ kcal/mol, $\Delta S = -15.2 \pm 0.4$ e.u.

Table A1-3. Equilibrium data collected in PhMe at various temperatures.

In PhMe								
T (°C)	1/T (K^{-1})	[styrene] (M)	[ether] (M)	[n-BuOH] (M)	K_{eq}	K_{eq} std. dev.	ln(K_{eq})	ln(K_{eq}) std. dev.
70	0.0029	0.18	0.21	0.96	1.25	0.115	0.22	0.092
80	0.0028	0.19	0.20	0.98	1.08	0.016	0.07	0.015
90	0.0028	0.22	0.18	1.00	0.82	0.003	-0.20	0.004
100	0.0027	0.24	0.16	1.02	0.65	0.020	-0.44	0.031

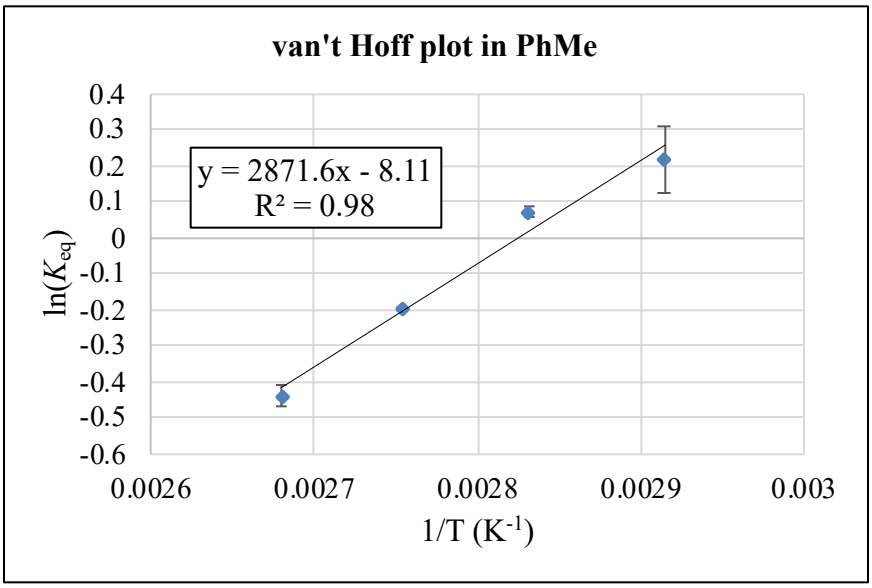

Figure A1-2. van't Hoff plot in toluene; ΔH = -5.7 ± 0.5 kcal/mol, ΔS = -16.1 ± 1.5 e.u.

A1.2.3 Alkene and Alcohol Structure Effects on Thermodynamic Parameters.

A variety of alkene and alcohol substrates were examined to assess structural effects on the equilibrium constant for the alcohol addition reaction. The general procedures for the forward and reverse reactions were followed for each substrate. The average ^{1}H NMR yields of equilibrated reactions, calculated K_{eq} values and standard deviations are provided below. A Hammett plot is also provided that shows a linear free energy relationship between log(K_{eq}) and the styrene electronic character (Hammett substituent constants). The preparation and characterization of the styrenes and ether products are described in Section A1.7.

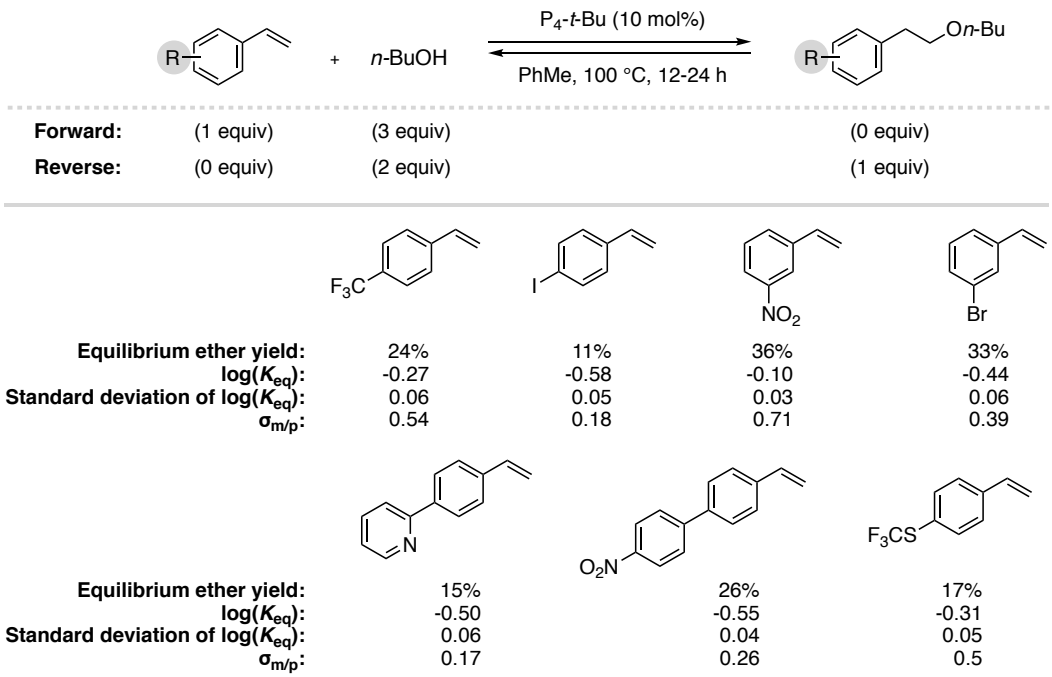

Figure A1-3. Styrene derivatives used to study styrene electronic effects on K_{eq}.

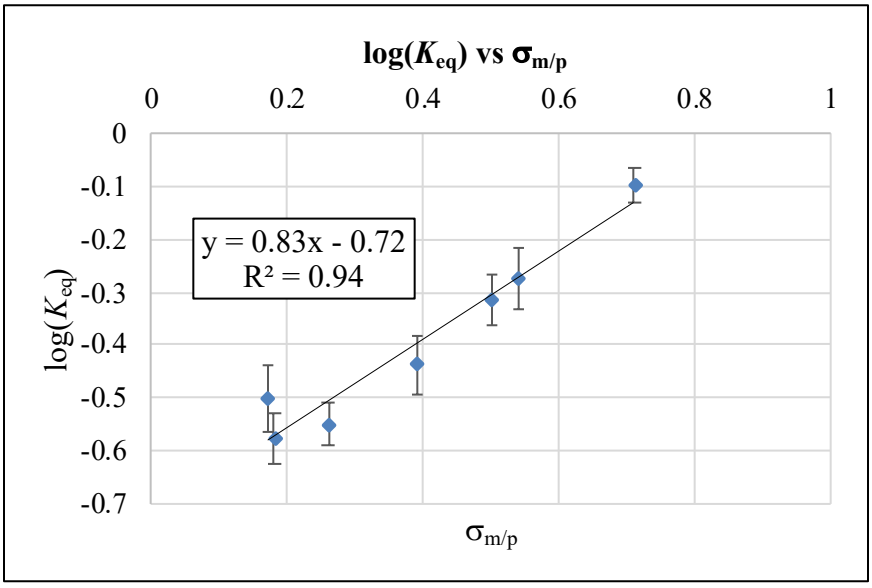

Figure A1-4. Hammett plot constructed from the equilibrium data in Figure A1-3.

The effect of alkene and alcohol substitution patterns was also examined according to the general procedures for the forward and reverse directions. The results are shown below for substrates for which K_{eq} could be determined:

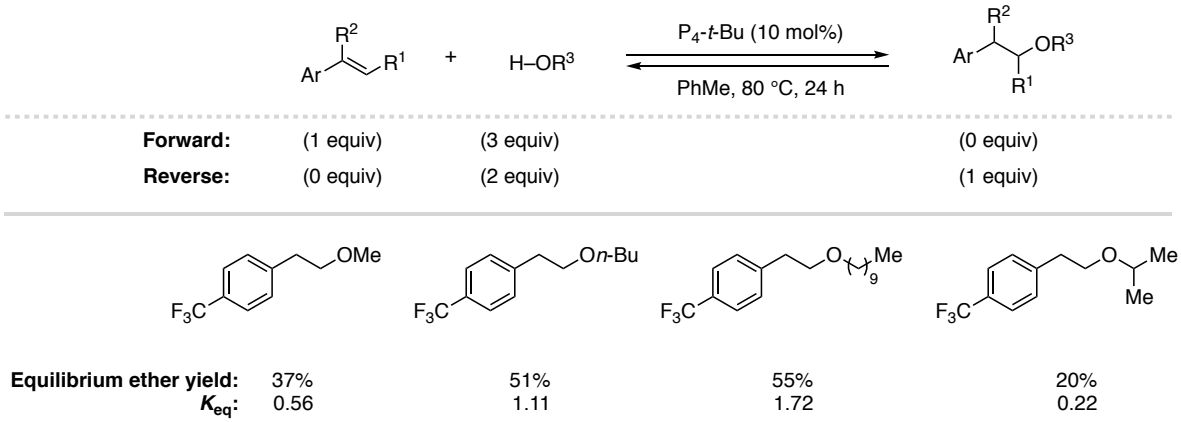

Figure A1-5. Alcohol structure effect on K_{eq}.

Note on alkene substitution: For α- and β-methyl derivatives of 4-trifluoromethylstyrene, K_{eq} was not able to be accurately determined. For α-methyl 4-trifluoromethylstyrene, the forward reaction yielded no ether product and the reverse reaction yielded α-methyl 4-trifluoromethylstyrene as the major product with other unidentified side products. For β-methyl 4-trifluoromethylstyrene, the forward and reverse reactions both led to less than 10% ether product and thus K_{eq} is less than 0.1. These results are consistent with our previous observations of lower ether yields for substituted styrene substrates.

A1.3 Experimental Kinetic Studies

General description. Reaction profile and kinetic studies were initially performed using the addition of *n*-butanol to 4-(trifluoromethyl)styrene in PhMe as a model reaction system. Subsequently, the addition of *n*-butanol to 2,6-dichlorostyrene was studied to examine solvent effects on reactant rate orders; this was necessary because this addition reaction proceeds to a greater extent in polar solvents than does addition to 4-(trifluoromethyl)styrene.

GC analysis method description. Gas chromatography (GC) analyses were performed on an Agilent Technologies 7890B GC system with an FID detector using a J&W HP-5 column (30 m, 0.320 mm D). A general GC method was used for all studies with an injection volume of 1 μL,

initial temperature of 100 °C, rate of 30 °C/min, maximum temperature of 300 °C and a run time of 6 min. Reaction progress was determined by integration of product signals compared to dodecane internal standard using a response factor that was determined for each ether product.

A1.3.1 Reaction Profile for the Addition of n-Butanol to 4-(Trifluoromethyl)styrene in PhMe.

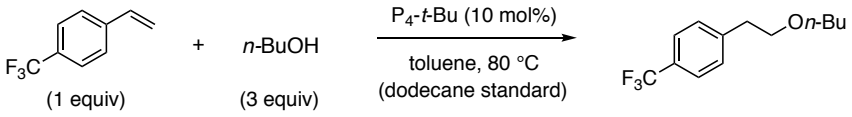

Procedure. In a nitrogen-filled glovebox, 4-trifluoromethylstyrene (86 mg, 0.5 mmol, 1.0 equiv), *n*-butanol (111 mg, 1.5 mmol, 3.0 equiv) and toluene (1 mL) were added to an oven-dried 4 mL reaction vial (Thermo Scientific B7990-2) containing a magnetic stir bar. P_4-*t*-Bu (0.8 M in hexane, 62.5 µL, 0.05 mmol, 0.1 equiv) was then added to the reaction solution, and dodecane (23.3 mg, 0.125 mmol, 0.25 equiv) was added as an internal standard. The reaction vial was capped (Thermo Scientific C4015-1A with 10/50 septa), removed from the glovebox, and placed in a preheated oil bath at 80 °C with stirring. Aliquots (approximately 20 µL) were taken using a nitrogen-filled syringe for GC analysis at the indicated time intervals. The reaction progress is tabulated and plotted below.

Table A1-4. Reaction time point data.

Time (min)	yield (%)	[ether](M)
10	2.1	0.0082
20	4.0	0.0157
30	6.2	0.0243
45	9.4	0.0367
75	15.2	0.0595
120	23.1	0.0907
180	31.7	0.1244
240	38.6	0.1515
300	43.4	0.1701
360	46.5	0.1825
420	48.4	0.1900
480	49.7	0.1951
600	50.2	0.1969

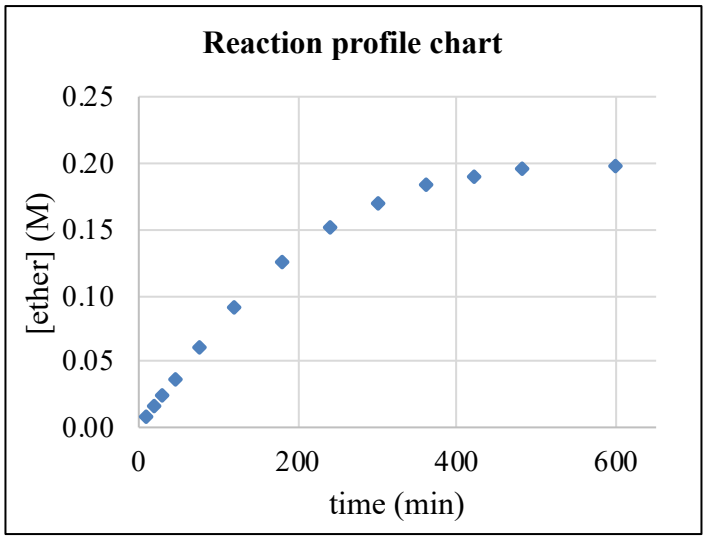

Figure A1-6. Reaction profile over time.

A1.3.2 Rate Dependence Studies for the Addition of n-BuOH to 4-(Trifluoromethyl)styrene in PhMe.

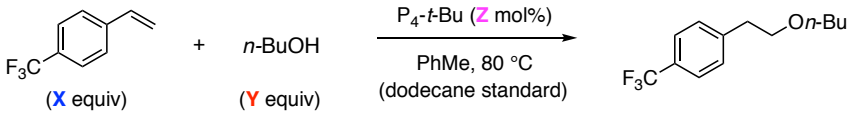

General overview of steps used for kinetic experiments. To estimate the rate orders of the alkene, alcohol and catalyst, the method of initial rates was used. The sequence of steps used for these experiments is described below in Steps 1-8. The experimental reaction setup is described in the procedure below. In Section A1.3, a detailed description and pictures of an individual experiment is provided for further illustration.

Step 1: The necessary stock solutions of reagents were prepared in a nitrogen-filled glovebox.

Step 2: The reagent being varied was added to reaction vials followed by the stock solution containing the remaining reagents, except for P4-*t*-Bu catalyst.

Step 3: The vials were capped, removed from the glovebox and inserted into a preheated oil bath at the indicated temperature.

Step 4: The required amount of P_4-*t*-Bu catalyst solution was transferred from the glovebox and injected into the reaction vials. The reaction timer was then started.

Step 5: Aliquots for GC analysis of ether concentration were taken at indicated time points.

Step 6: The ether concentration over time was plotted to determine the reaction initial rate (in mM/min) from the linear portion of the plot (typically 10 to 20% conversion).

Step 7: Steps 1-6 were repeated for each indicated concentration to obtain an average initial rate.

Step 8: The average initial rates versus concentrations were plotted and a power trendline fit was used to approximate rate order of the varied reagent. Linear trendline plots are also provided for any substrates that showed less than a 1.5 rate order.

Experimental procedure. In a nitrogen-filled glovebox, a stock solution of dodecane (0.25 equiv), toluene and other reactants not being varied (4-(trifluoromethyl)styrene and/or *n*-butanol, see table descriptions below for amounts of reactants added) was prepared in an oven-dried 8 mL reaction vial (Fisherbrand 14-955-328); P_4-*t*-Bu was never included in the stock solution. Reactions were carried out on a 0.25 mmol scale, the reactant of which the rate order was being determined (except P_4-*t*-Bu) was massed into 4 mL reaction vials (ThermoFisher, C4015-1) containing oven-dried stir bars. The stock solution (0.5 mL) was then added to each vial. The vial was capped (Thermo Scientific C4015-1A with Teflon-lined rubber 10/50 septa), removed from the glovebox, connected to a nitrogen-filled balloon, and inserted into an 80 °C preheated oil bath with stirring. In the glovebox, a solution of P_4-*t*-Bu (0.8 M in hexanes) was drawn into an airtight microsyringe and capped with a rubber septum. The syringe was removed from the glovebox, the

P_4-*t*-Bu solution was immediately injected into the preheated reaction solution, and a timer was started. Aliquots of approximately 25 µL were taken at given time intervals with a nitrogen-flushed hypodermic needle, added to a plug of silica gel (SiliaFlash® F60) in a glass pipette, and the silica plug was flushed with diethyl ether (about 1 mL) directly into a GC vial. The aliquot solution was subjected to GC analysis and product concentration was calculated by comparison of ether product integration to dodecane internal standard integration. All trials were repeated in duplicate and the average rates are shown. See Section A1.3.3 for detailed example of reaction setup and overall process, GC time points/yields, and graph of initial ether product concertation versus time. **Note:** all concentrations (reagents, catalyst and product) were calculated with respect to toluene.

Table A1-5. Reactions done at 80 °C in toluene, 0.50 M is equal to 1 equiv, 50 mM is equivalent to 10 mol%.

Reactant Varied	**[Styrene], (X eq)**	**[*n*-BuOH], (Y eq)**	**[P_4-*t*-Bu], (Z mol%)**	**Ave Rate (mM/min)**	**Standard Deviation**
P_4-*t*-Bu	0.50 M	0.50 M	12.5 mM, (2.5)	0.06	0.01
	0.50 M	0.50 M	25 mM, (5.0)	0.28	0.05
	0.50 M	0.50 M	37.5 mM, (7.5)	1.07	0.23
	0.50 M	0.50 M	50 mM, (10)	1.99	0.10
n-BuOH	0.50 M	0.40 M, (0.8)	50 mM	6.38	0.24
	0.50 M	0.45 M, (0.9)	50 mM	3.42	0.39
	0.50 M	0.50 M, (1.0)	50 mM	1.99	0.10
	0.50 M	0.55 M, (1.1)	50 mM	1.33	0.10
	0.50 M	0.625 M, (1.25)	50 mM	0.66	0.10
	0.50 M	0.875 M, (1.75)	50 mM	0.17	0.04
Styrene	0.25 M, (0.5)	0.50 M	50 mM	1.04	0.04
	0.50 M, (1.0)	0.50 M	50 mM	2.34	0.05
	0.75 M, (1.5)	0.50 M	50 mM	3.65	0.39
	1.0 M, (2.0)	0.50 M	50 mM	5.55	0.42
	1.25 M, (2.5)	0.50 M	50 mM	7.56	2.11

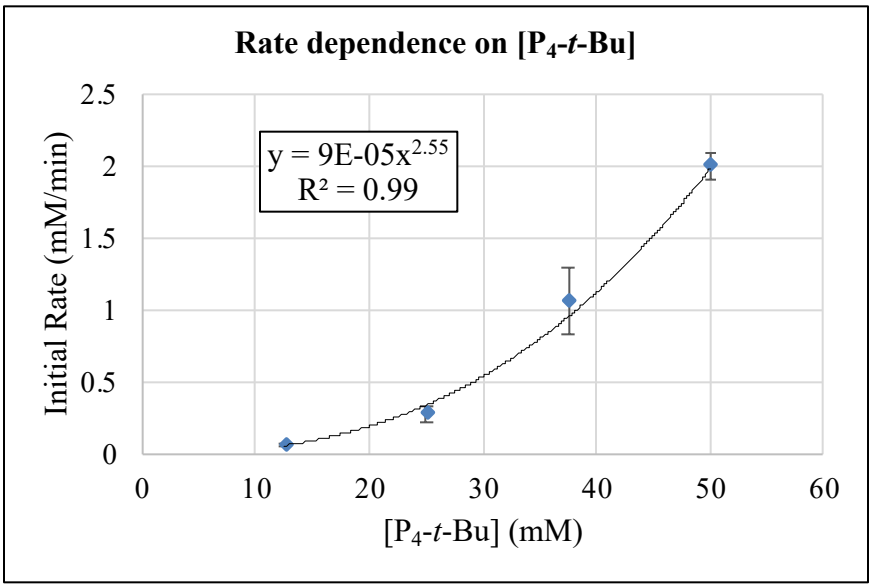

Figure A1-7. Initial rate dependence on [P_4-*t*-Bu] using 1 equiv *n*-BuOH and 1 equiv 4-(trifluoromethyl)styrene.

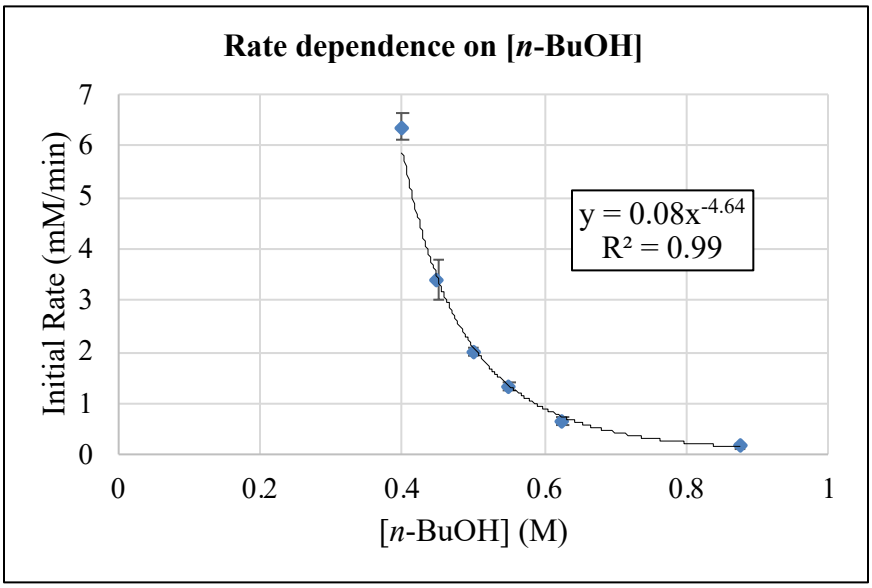

Figure A1-8. Initial rate dependence on [*n*-BuOH] using 10 mol% P_4-*t*-Bu and 1 equiv 4-(trifluoromethyl)styrene.

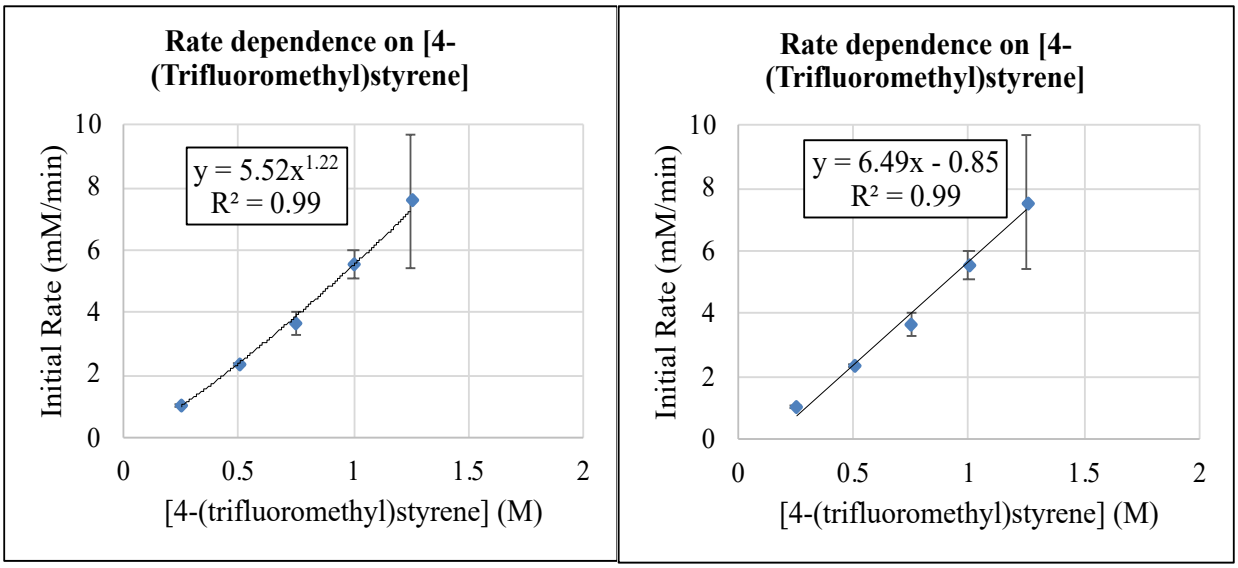

Figure A1-9. Initial rate dependence on [4-(trifluoromethyl)styrene] using 10 mol% P_4-*t*-Bu and 1 equiv *n*-BuOH. Graphs with power and linear trendline fits are provided.

A1.3.3 Rate Order Studies for the Addition of n-Butanol to 2,6-Dichlorostyrene in Various Solvents.

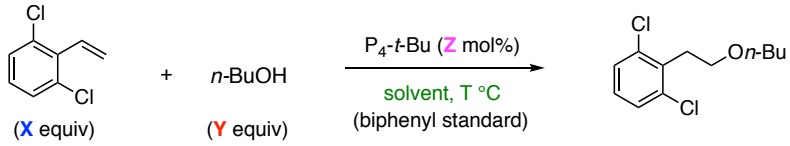

General description. An identical procedure as described above (Section A1.3.2.) was used to determine the initial reaction rate versus initial concentration for the addition of *n*-butanol to 2,6-dichlorostyrene (biphenyl, 0.25 equiv used in place of dodecane for the internal standard). The temperature was varied for the solvent as necessary so that initial linear conversion could be determined; for example, the reaction rate was substantially faster in DMSO and a lower temperature was required for accurate rate measurements. The initial reaction rates versus reactant concentrations are tabulated below (Tables A1-7-9). The assembled plots that were used to determine approximate rate orders are also provided. **Note:** all concentrations (reagents, catalyst and product) were calculated with respect to the amount of solvent used.

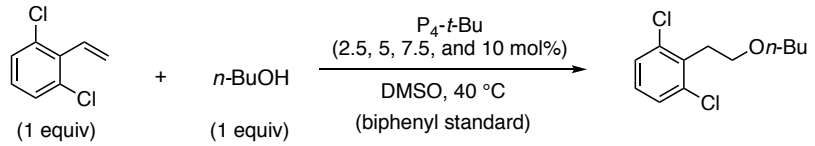

Detailed prototypical example procedure. As an example, an experiment to measure the initial rate dependence on [P_4-*t*-Bu] in DMSO is described here. In a nitrogen-filled glovebox, a stock solution containing *n*-butanol (4.5 equiv, 1.125 mmol, 83.4 mg, 103.0 μL; equal to 1 equiv, 0.25 mmol per reaction), 2,6-dichlorostyrene (4.5 equiv, 1.125 mmol, 194.7 mg; equal to 1 equiv, 0.25 mmol per reaction), biphenyl (1.125 equiv, 0.281 mmol, 60.7 mg; equal to 0.25 equiv, 0.0625 mmol per reaction) in DMSO (2.25 mL total; 0.5 mL per reaction) was prepared in an oven-dried 8 mL reaction vial (Fisherbrand 14-955-328). To four oven-dried 4 mL reaction vials (ThermoFisher, C4015-1) containing magnetic stir bars, stock solution was added (0.5 mL per vial). The vials were capped (Thermo Scientific C4015-1A with 10/50 septa), removed from the glovebox, connected to a nitrogen-filled balloon, and inserted into a preheated 40 °C oil bath with stirring. In the glovebox, commercial 0.8 M hexanes solution of P_4-*t*-Bu (7.8 μL, 2.5 mol%; 15.6 μL, 5 mol%; 23.4 μL, 7.5 mol%; 31.25 μL, 10 mol%) were drawn into airtight microsyringes that were capped with a rubber septum. The microsyringes containing P_4-*t*-Bu were removed from the glovebox and the solutions were injected in the four separate reaction vials. Aliquots (approximately 25 μL) were taken at given time intervals with a nitrogen-flushed hypodermic needle. An initial aliquot was taken at 30 seconds for each reaction. For reactions with 2.5 and 5 mol% P_4-*t*-Bu, aliquots were then taken every 15 min for 45 min, and for reactions with 7.5 and 10 mol% P_4-*t*-Bu, aliquots were taken every 5 min for 15 min. Aliquots were added to a plug of silica gel (SiliaFlash® F60) in a glass pipette, and the silica plug was flushed with diethyl ether (about 1 mL) directly into a GC vial. Shown below (Table A1-6) is an example of GC data using 2.5 mol% P_4-*t*-Bu set up in accordance with the described procedure.

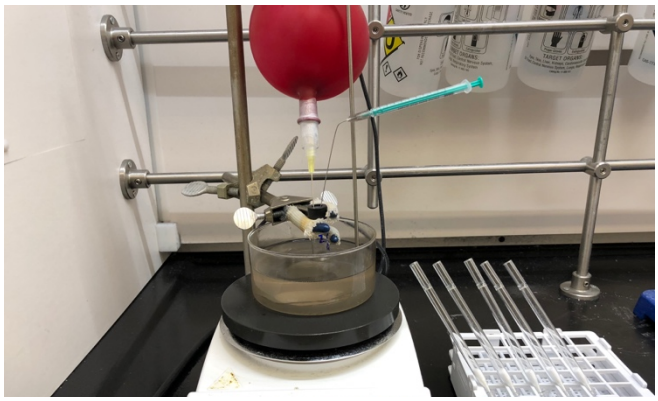

Figure A1-10. Image of reaction set up with nitrogen-filled balloon and hypodermic needle used to take aliquots. To the right, plugs of silica gel in glass pipettes used to prepare aliquots for GC analysis.

Table A1-6. Example data set using 2.5 mol% P_4-*t*-Bu at 40 °C in DMSO; mmol of ether determined by GC with comparison to an internal standard (biphenyl); concentration calculated using volume of stock solution used (0.5 mL).

time (min)	mmol ether	[ether] (mM)
0.5	0.0010	1.90
15	0.0115	23.0
30	0.0221	44.2
45	0.0317	63.5

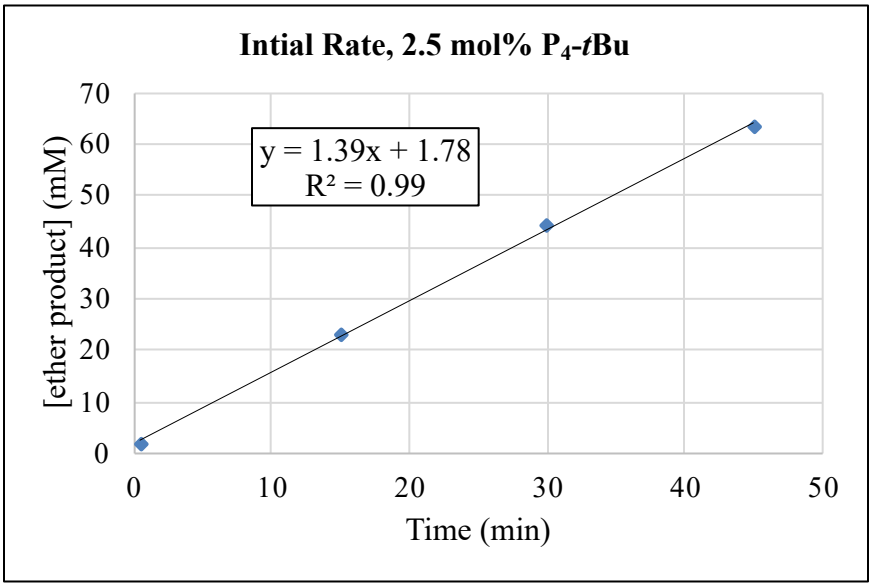

Figure A1-11. Graph of [ether] over time used to find initial reaction rate using 2.5 mol% P_4-*t*-Bu at 40 °C in DMSO.

Table A1-7. Reactions done at 40 °C in DMSO; 0.50 M is equal to 1 equiv and 50 mM is equivalent to 10 mol%.

DMSO, 40 °C					
Reactant Varied	**[Styrene], (X equiv)**	**[*n*-BuOH], (Y equiv)**	**[P$_4$-*t*-Bu], (Z mol%)**	**Ave Rate (mM/min)**	**Standard Deviation**
P$_4$-*t*-Bu	0.50 M	0.50 M	12.5 mM, (2.5)	1.33	0.20
	0.50 M	0.50 M	25 mM, (5.0)	3.56	0.23
	0.50 M	0.50 M	37.5 mM, (7.5)	6.60	0.07
	0.50 M	0.50 M	50 mM, (10.0)	10.06	0.28
n-BuOH	0.50 M	0.30 M, (0.6)	50 mM	19.48	1.62
	0.50 M	0.40 M, (0.8)	50 mM	15.25	0.23
	0.50 M	0.45 M, (0.9)	50 mM	12.03	0.34
	0.50 M	0.50 M, (1.0)	50 mM	10.06	0.28
	0.50 M	0.55 M, (1.1)	50 mM	7.56	0.04
	0.50 M	0.625 M, (1.25)	50 mM	5.60	0.28
	0.50 M	1.0 M, (2.0)	50 mM	1.87	0.17
Styrene	0.25 M, (0.5)	0.50 M	50 mM	5.70	0.48
	0.50 M, (1.0)	0.50 M	50 mM	11.82	1.06
	0.75 M, (1.5)	0.50 M	50 mM	16.50	0.24
	1.0 M, (2.0)	0.50 M	50 mM	20.64	5.23
	1.25 M, (2.5)	0.50 M	50 mM	27.90	2.39
	1.5 M, (3.0)	0.50 M	50 mM	34.79	4.79

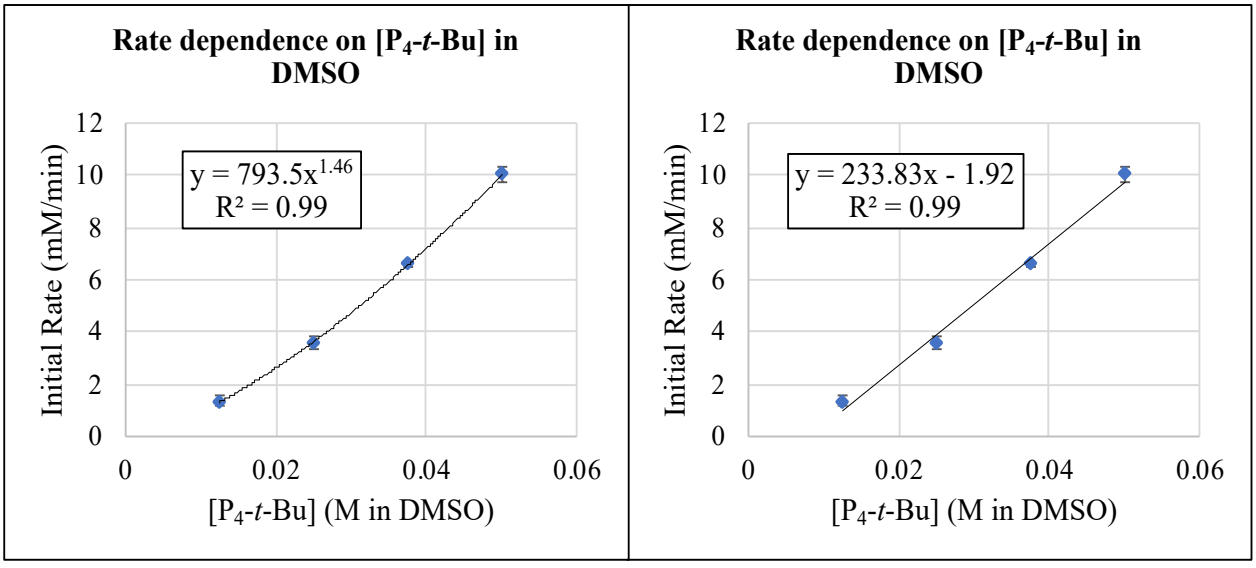

Figure A1-12. Initial rate dependence on [P$_4$-*t*-Bu] using 1 equiv *n*-BuOH and 1 equiv 2,6-dichlorostyrene in DMSO. Graphs with power and linear trendline fits are provided.

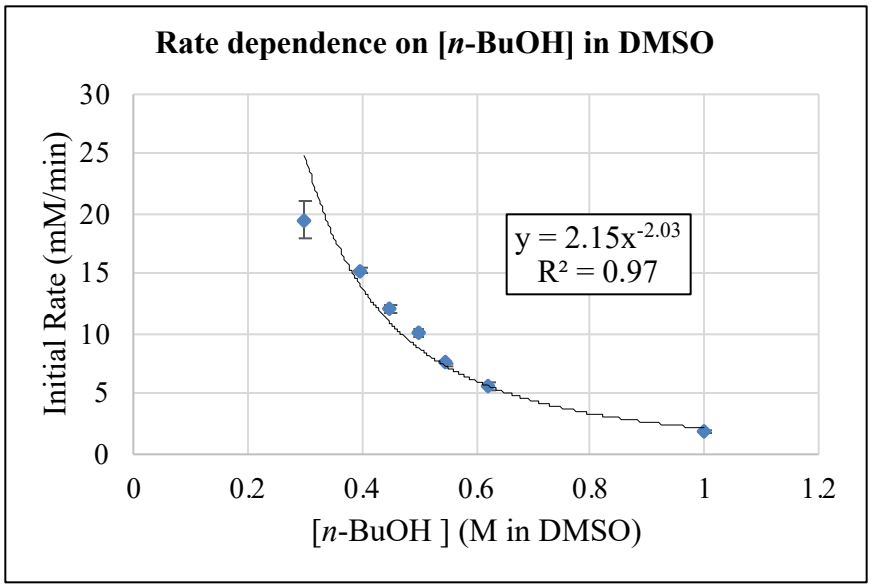

Figure A1-13. Initial rate dependence on [*n*-BuOH] using 10 mol% P_4-*t*-Bu and 1 equiv 2,6-dichlorostyrene in DMSO.

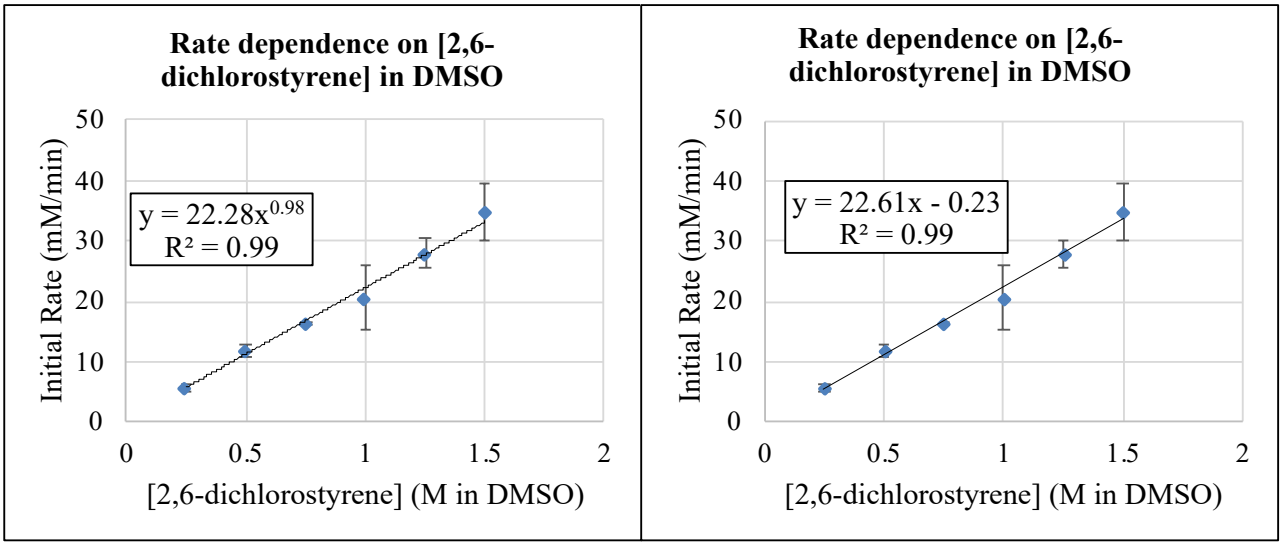

Figure A1-14. Initial rate dependence on [2,6-dichlorostyrene] using 10 mol% P_4-*t*-Bu and 1 equiv *n*-BuOH in DMSO. Graphs with power and linear trendline fits are provided.

Table A1-8. Reactions done at 80 °C in toluene; 0.50 M is equal to 1 equiv and 50 mM is equivalent to 10 mol%.

Toluene, 80 °C					
Reactant Varied	**[Styrene], (X equiv)**	**[*n*-BuOH], (Y equiv)**	**[P_4-*t*-Bu], (Z mol%)**	**Ave Rate (mM/min)**	**Standard Deviation**
P_4-*t*-Bu	0.50 M	0.50 M	12.5 mM, (2.5)	0.41	0.01
	0.50 M	0.50 M	25 mM, (5.0)	1.65	0.09
	0.50 M	0.50 M	37.5 mM, (7.5)	6.40	0.75

	0.50 M	0.50 M	50 mM, (10.0)	18.44	0.23
n-BuOH	0.50 M	0.30 M, (0.6)	50 mM	45.75	4.30
	0.50 M	0.40 M, (0.8)	50 mM	19.22	6.92
	0.50 M	0.45 M, (0.9)	50 mM	10.94	2.94
	0.50 M	0.50 M, (1.0)	50 mM	5.71	2.34
	0.50 M	0.55 M, (1.1)	50 mM	2.78	0.07
	0.50 M	0.625 M, (1.25)	50 mM	2.17	1.11
	0.50 M	1.0 M, (2.0)	50 mM	0.41	0.06
Styrene	0.25 M, (0.5)	0.50 M	50 mM	1.60	0.45
	0.50 M, (1.0)	0.50 M	50 mM	3.38	0.22
	0.75 M, (1.5)	0.50 M	50 mM	4.01	0.37
	1.0 M, (2.0)	0.50 M	50 mM	4.43	0.49
	1.25 M, (2.5)	0.50 M	50 mM	6.81	1.00
	1.5 M, (3.0)	0.50 M	50 mM	8.67	1.13

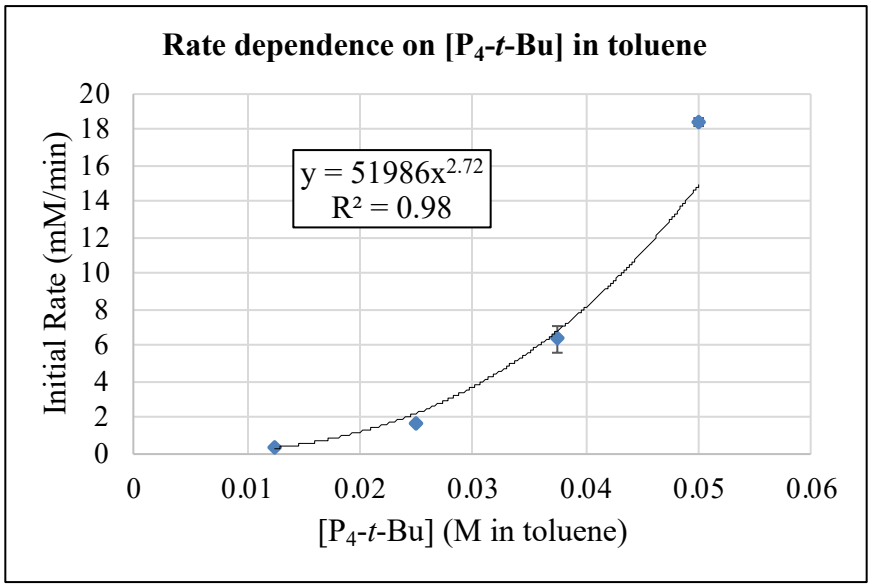

Figure A1-15. Initial rate dependence on [P_4-*t*-Bu] using 1 equiv *n*-BuOH and 1 equiv 2,6-dichlorostyrene in toluene.

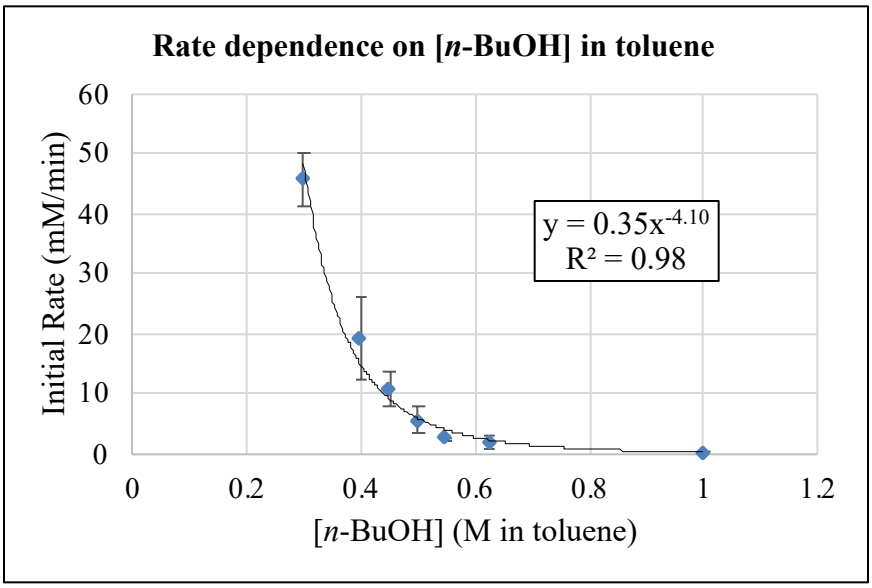

Figure A1-16. Initial rate dependence on [*n*-BuOH] using 10 mol% P$_4$-*t*-Bu and 1 equiv 2,6-dichlorostyrene in toluene.

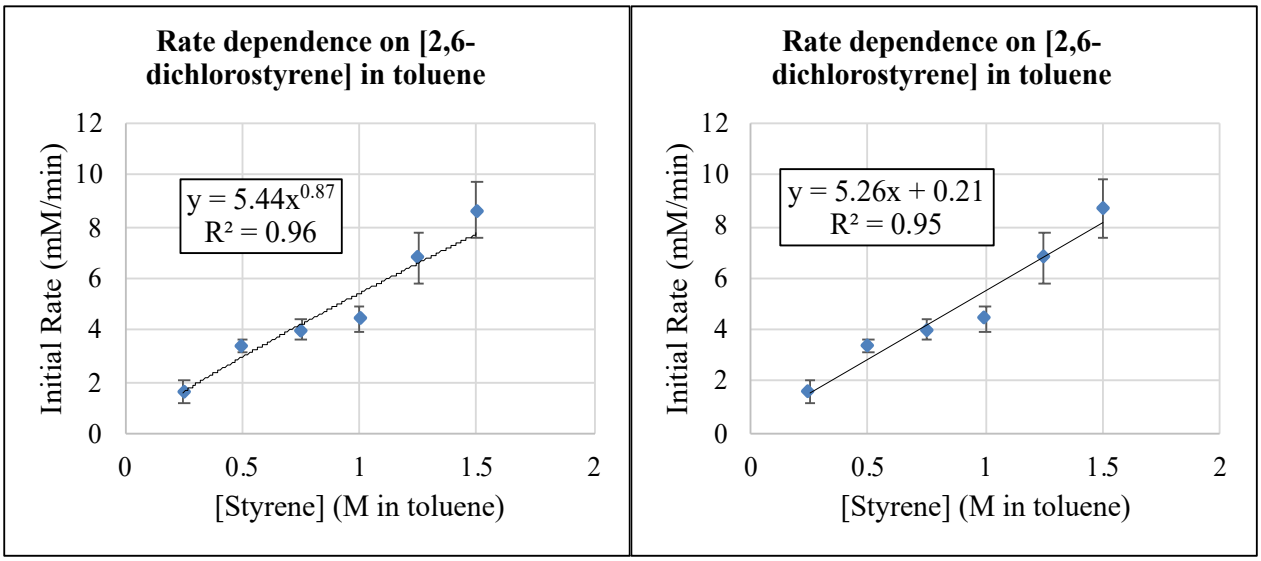

Figure A1-17. Initial rate dependence on [2,6-dichlorostyrene] using 10 mol% P$_4$-*t*-Bu and 1 equiv *n*-BuOH in toluene. Graphs with power and linear trendline fits are provided.

Table A1-9. Reactions done at 80 °C in *n*-Bu$_2$O; 0.50 M is equal to 1 equiv and 50 mM is equivalent to 10 mol%.

Dibutyl ether, 80 °C					
Reactant Varied	**[Styrene], (X equiv)**	**[*n*-BuOH], (Y equiv)**	**[P$_4$-*t*-Bu], (Z mol%)**	**Ave Rate (mM/min)**	**Standard Deviation**
P$_4$-*t*-Bu	0.50 M	0.50 M	12.5 m, (2.5)	0.33	0.05
	0.50 M	0.50 M	25 m, (5.0)	1.28	0.15
	0.50 M	0.50 M	37.5 m, (7.5)	3.68	0.33

	0.50 M	0.50 M	50 m, (10.0)	8.62	0.06
n-BuOH	0.50 M	0.375 M, (0.75)	50 mM	5.21	0.66
	0.50 M	0.45 M, (0.9)	50 mM	2.57	0.25
	0.50 M	0.50 M, (1.0)	50 mM	1.81	0.07
	0.50 M	0.55 M, (1.1)	50 mM	1.49	0.07
	0.50 M	0.625 M, (1.25)	50 mM	1.05	0.05
Styrene	0.25 M, (0.5)	0.50 M	50 mM	2.68	0.25
	0.50 M, (1.0)	0.50 M	50 mM	5.64	0.13
	0.75 M, (1.5)	0.50 M	50 mM	8.20	1.55
	1.0 M, (2.0)	0.50 M	50 mM	11.10	2.20

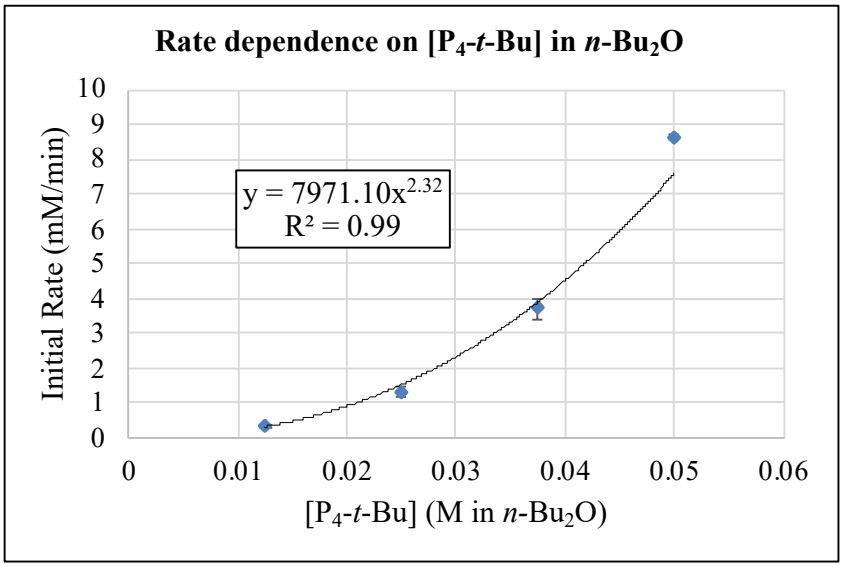

Figure A1-18. Initial rate dependence on [P_4-*t*-Bu] using 1 equiv *n*-BuOH and 1 equiv 2,6-dichlorostyrene in *n*-Bu_2O.

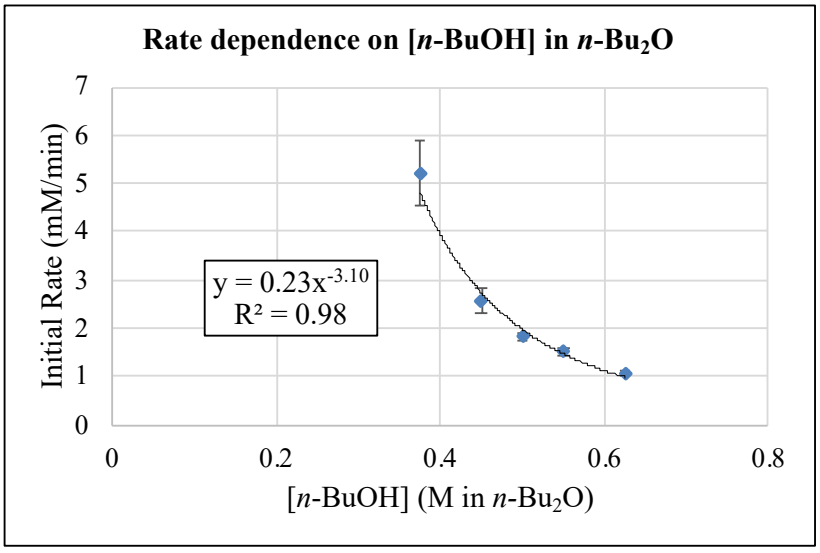

Figure A1-19. Initial rate dependence on [*n*-BuOH] using 10 mol% P_4-*t*-Bu and 1 equiv 2,6-dichlorostyrene in *n*-Bu_2O.

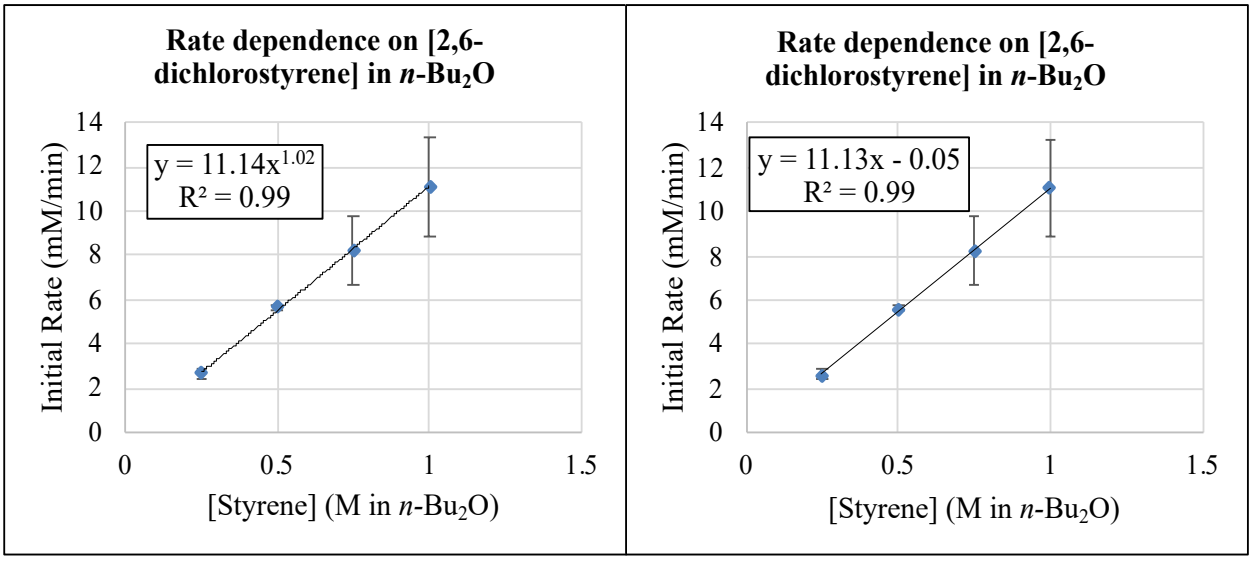

Figure A1-20. Initial rate dependence on [2,6-dichlorostyrene] using 10 mol% P_4-*t*-Bu and 1 equiv *n*-BuOH in *n*-Bu_2O. Graphs with power and linear trendline fits are provided.

A1.3.4 Electronic Effects on the Rate of Alcohol Elimination of Various β-Phenethyl Ether Adducts.

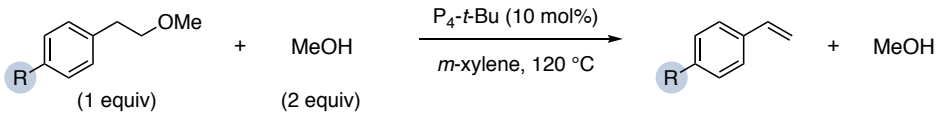

General description. To assess the relationship between styrene electronic properties and the rate of alcohol addition, we examined the relative rate of elimination from three methyl ether products. The three substrates (R = OMe, H and CF_3) were chosen so that a comparison could be made to computed relative energies for addition. Instead of the rate of addition, the rate of elimination was measured because these styrenes (especially R = OMe and H) do not provide significant ether yields such that rate measurement of the addition reaction would be very difficult. These reactions were run in *m*-xylene due to the higher temperature required for the 4-methoxy-substituted substrate to react.

Procedure. In a nitrogen-filled glovebox, methyl *β*-phenethyl ether (0.1 mmol, 1 equiv), methanol (0.2 mmol, 2 equiv, 6.4 mg, 8.1 μL), *m*-xylene (200 μL), and P_4-*t*-Bu (10 mol%, 12.5

μL of a 0.8 M solution in hexanes) were added to an oven-dried 4 mL reaction vial (Thermo Scientific B7990-2) containing a magnetic stir bar and capped (Thermo Scientific C4015-1A with 10/50 septa). Once capped, the vials were immediately removed from the glovebox, placed in an aluminum reaction block preheated to 120 °C with stirring and a timer was started. Reactions were stopped at the times indicated via the addition of $CDCl_3$ (approximately 1 mL). The elimination yields were determined by percent conversion with ^1H NMR spectroscopy; >95% mass balance was observed when an NMR standard was used. One reaction vial was prepared per time point taken; this protocol was followed so that septa were not pierced throughout the course of a reaction. This procedure was repeated in duplicate and the average conversions of each time point for each substrate is provided below.

Table A1-10. Elimination rates determined by ^1H NMR spectroscopy.

R group	Time (min)	Average conversion (%)	Estimated rate (mM/min)
CF_3	0.5	43	>200
	2	88	
	5	86	
	10	88	
H	5	3	4.1
	15	23	
	30	27	
	60	46	
	120	55	
OMe	10	1	0.2
	60	5	
	180	7	
	300	11	
	540	17	

The elimination reaction performed above in Table A1-10 required reaction temperatures significantly higher than the boiling point of methanol. Reproducible results were consistently obtained; however, to confirm the observed trend in the methyl β-phenethyl ether adducts, the

following experiment was performed with the corresponding *n*-butyl *β*-phenethyl ethers (the boiling point of *n*-BuOH is 116-118 °C).

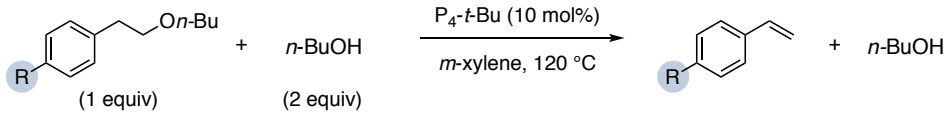

Procedure. In a nitrogen-filled glovebox, *n*-butyl *β*-phenethyl ether (0.1 mmol, 1 equiv), *n*-butanol (0.2 mmol, 2 equiv, 14.8 mg, 18.3 μL), *m*-xylene (200 μL), and P_4-*t*-Bu (10 mol%, 12.5 μL of a 0.8 M solution in hexanes) were added to an oven-dried 4 mL reaction vial (Thermo Scientific B7990-2) containing a stir bar and capped (Thermo Scientific C4015-1A with 10/50 septa). Once capped, the vials were removed from the glovebox, placed in an aluminum heating block preheated to 120 °C with stirring and a timer was started. Reactions were stopped at the times indicated via the addition of $CDCl_3$ (approximately 1 mL). The elimination yields were determined by percent conversion with ^{1}H NMR spectroscopy. One reaction vial was prepared per time point taken; this protocol was followed so that septa were not pierced throughout the course of a reaction. This procedure was repeated in duplicate and the average conversions of each time point for each substrate is provided below.

Table A1-11. Observed effect of styrene 4-substitution on elimination reaction yields for various *n*-butyl *β*-phenethyl ether adducts.

R group	Time (min)	Ave. Styrene Yield (%)	Ave. Mass Balance (%)
CF_3	5	67	90
H	60	13	90
OMe	60	3	96

A1.4. Inorganic Base Studies and Comparisons

A1.4.1 Inorganic Base and Additive Screening for the Addition of n-Butanol to 4-(Trifluoromethyl)styrene.

In our previous report of P_4-*t*-Bu-catalyzed alcohol addition reactions, extensive comparisons to inorganic bases under various reaction conditions were made.[1] Those screening attempts showed

that several inorganic bases in various solvents could provide appreciable product. Several of these reaction conditions were then compared to P_4-*t*-Bu and were found not to be general. Based on our new understanding of factors that control the reaction yield, especially solvent effects, we reexamined inorganic bases with solvents that provide the greatest ether equilibrium values (determined in Section A1.2.1). Screening efforts in this regard are described here.

General screening procedure. In a nitrogen-filled glovebox, the inorganic base (0.025 mmol, 0.1 equiv) and the ligating additive (0.03 mmol, 0.12 equiv) were added to an oven-dried 4 mL reaction vial (Thermo Scientific B7990-2) containing a magnetic stir bar followed by addition of anhydrous solvent (0.25 mL). To the solvent mixture was added alcohol (0.75 mmol, 3 equiv) and styrene (0.25 mmol, 1 equiv). The reaction vial was capped (Thermo Scientific C4015-1A with 10/50 septa), removed from the glovebox, and placed in a preheated aluminum reaction block at the indicated temperature with stirring for 24 h. The reaction solution was then cooled to rt. To the reaction mixture was added dibenzyl ether (23.8 μL, 0.125 mmol, 0.5 equiv) as internal standard, and an aliquot was subjected to ^{1}H NMR analysis.

Identification of possible inorganic catalysts. Using the above general procedure, we examined a variety of inorganic bases, additives and solvents for the addition of *n*-BuOH to 4-(trifluoromethyl)styrene. The goal of this screen was to identify the most active inorganic catalyst conditions to further optimize; yields close to 30% were considered active catalyst conditions as this yield is similar to the equilibrium yields for DME and THF solvents (determined in Section A1.2.1). First, we examined KO-*t*-Bu/18-crown-6 in a variety of solvents. The top yielding two solvents were then further screened with other inorganic bases and ligating additives.

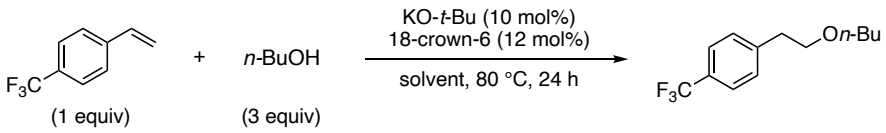

Table A1-12. Solvent screen with KO-*t*-Bu/18-crown-6; yields greater than 30% are highlighted in green.

Solvent	Styrene (%)	Ether (%)
toluene	95	5
xylene	95	5
α,α,α-trifluorotoluene	95	5
benzonitrile	67	33
tetrahydrofuran	61	39
cyclopentyl methyl ether	86	14
1,2-dimethoxyethane	65	35
diglyme	-	27
n-butyl ether	92	8
dimethyl sulfoxide	93	7
dimethylformamide	86	14
cyclohexane	97	3

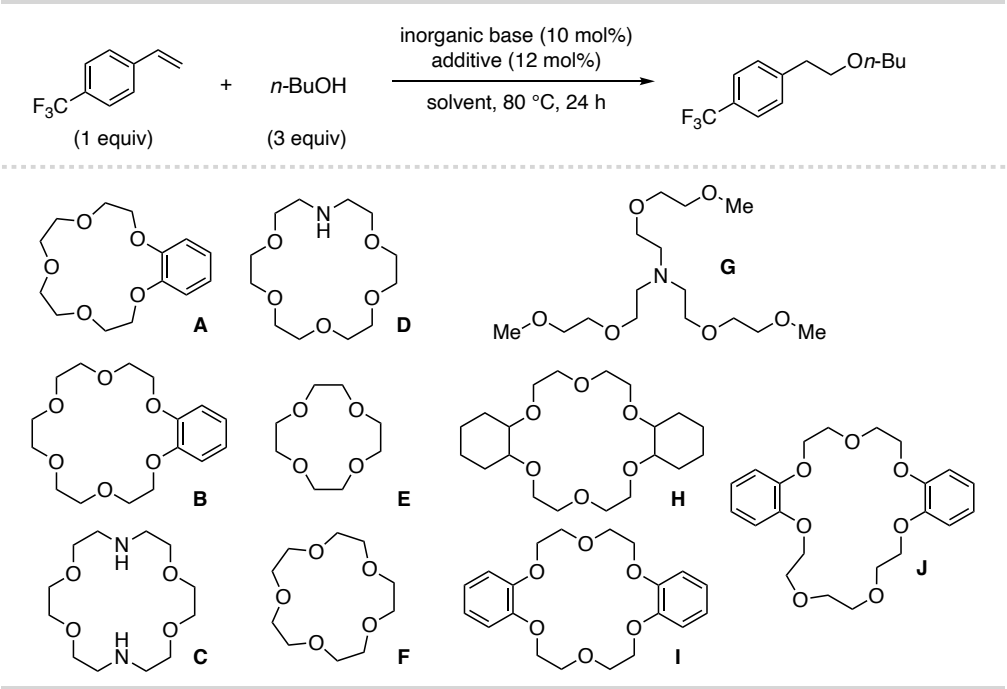

Figure A1-21. Additives screened in inorganic condition optimization.

Table A1-13 Inorganic base and additive screen in DME and THF; yields greater than 30% are highlighted in green.

Base	Additive	Solvent	Styrene (%)	Ether (%)
NaO-*t*-Bu	A	DME	88	12
KO-*t*-Bu	B	DME	68	32
KO-*t*-Bu	C	DME	81	19

KO-*t*-Bu	D	DME	75	25
LiO-*t*-Bu	E	DME	94	6
$CsOH•H_2O$	J	DME	76	24
KO-*t*-Bu	J	DME	68	32
$CsOH•H_2O$	G	DME	89	11
KO-*t*-Bu	G	DME	87	13
NaO-*t*-Bu	G	DME	90	10
LiO-*t*-Bu	G	DME	100	0
NaO-*t*-Bu	F	DME	73	27
KO-*t*-Bu	F	DME	66	34
$CsOH•H_2O$	I	DME	71	29
KO-*t*-Bu	I	DME	71	29
KO-*t*-Bu	H	DME	66	34
NaO-*t*-Bu	A	THF	85	15
KO-*t*-Bu	B	THF	65	35
KO-*t*-Bu	C	THF	72	28
KO-*t*-Bu	D	THF	67	33
LiO-*t*-Bu	E	THF	94	6
$CsOH•H_2O$	J	THF	67	33
KO-*t*-Bu	J	THF	66	34
$CsOH•H_2O$	G	THF	93	7
KO-*t*-Bu	G	THF	89	11
NaO-*t*-Bu	G	THF	95	5
LiO-*t*-Bu	G	THF	100	0
NaO-*t*-Bu	F	THF	77	23
KO-*t*-Bu	F	THF	66	34
$CsOH•H_2O$	I	THF	73	27
KO-*t*-Bu	I	THF	68	32
KO-*t*-Bu	H	THF	64	36

Further condition optimization and procedure. To optimize the inorganic conditions further, we identified potassium bases with 18-crown-6 from the above screening conditions to examine additional solvent effects. Alcohol addition to 2,6-dichlorostyrene was used in this section since this is a thermodynamically favored addition reaction. In a nitrogen-filled glovebox, 2,6-dichlorostyrene (43 mg, 0.25 mmol, 1.0 equiv), 3-methoxy-3-methylbutan-1-ol (96 μL, 0.75 mmol, 3.0 equiv) and solvent (0.25 mL) was added to an oven-dried 4 mL reaction vial (Thermo Scientific B7990-2) containing a magnetic stir bar. To the vial was added 18-crown-6 (8 mg, 0.03

mmol, 0.12 equiv) and the indicated base (0.25 mmol, 0.1 equiv). The reaction vial was capped (Thermo Scientific C4015-1A with 10/50 septa), removed from the glovebox, and placed in a preheated aluminum reaction block at 95 °C with stirring for 24 h. The reaction solution was then cooled to rt. To the reaction mixture was added dibenzyl ether (23.8 μL, 0.125 mmol, 0.5 equiv) as internal standard, and an aliquot was subjected to ^{1}H NMR analysis. **Note:** 95 °C was used as this is the optimal temperature for obtaining high ether yield using the superbase catalyst (P_4-*t*-Bu); at higher temperatures, the yield decreases due to entropic effects.**Error! Bookmark not defined.**

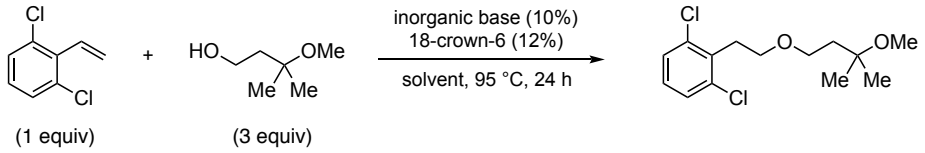

Table A1-14. Yields of above reaction with inorganic bases in different solvents.

	Yield in examples of solvents examined (%)					
Base	***m*-xylene**	**DME**	**CH_3NO_2**	**1,4-dioxane**	**CH_3CN**	**chlorobenzene**
KOH	20	73	-	50	78	25
KO-*t*-Bu	25	79	-	65	76	25
KO-Me	16	54	-	45	50	18

A1.4.2 Comparison of Inorganic Base Conditions to Superbase Conditions.

As shown above, our screening efforts suggested the combination of KO-*t*-Bu and 18-crown-6 in 1,2-dimethoxyethane may be a viable alternative to P_4-*t*-Bu. To examine this, we compared the inorganic conditions to the superbase conditions for various substrates. The ^{1}H NMR addition yields are provided below. These experiments show that the inorganic conditions can provide comparable yields for certain substrates, although P_4-*t*-Bu in aromatic solvents is an overall more general and active catalyst system.

Inorganic procedure. In a nitrogen-filled glovebox, aryl alkene (0.25 mmol, 1.0 equiv), alcohol (0.75 mmol, 3.0 equiv) and 1,2-dimethoxyethane (0.25 mL) were added to an oven-dried 4 mL reaction vial (Thermo Scientific B7990-2) containing a magnetic stir bar. To the solution was

added potassium *tert*-butoxide (2.8 mg, 0.025 mmol, 0.1 equiv), 18-crown-6 (8 mg, 0.03 mmol, 0.12 equiv). The reaction vial was capped (Thermo Scientific C4015-1A with 10/50 septa), removed from the glovebox, and placed in a preheated aluminum reaction block at the indicated temperature with stirring for 24 h. The reaction solution was then cooled to rt. To the reaction mixture was added dibenzyl ether (23.8 µL, 0.125 mmol, 0.5 equiv) as internal standard, and an aliquot was subjected to ^{1}H NMR analysis. For substrates **2-21** and **2-43 to 2-45** and **2-47** full characterization is provided in reference 1. **Note:** under these reaction conditions the inorganic base is fully soluble in 1,2-dimethoxyethane.

Superbase procedure. Alongside the inorganic procedure above, reactions were also setup using P_4-*t*-Bu (31 µL, 0.025 mmol, 0.1 equiv) and *m*-xylene (0.25 mL) for a direct ^{1}H NMR yield comparison at the indicated temperature. The ^{1}H NMR yield comparisons are shown in the figure below; isolation and characterization is also described for the new product **2-46**.

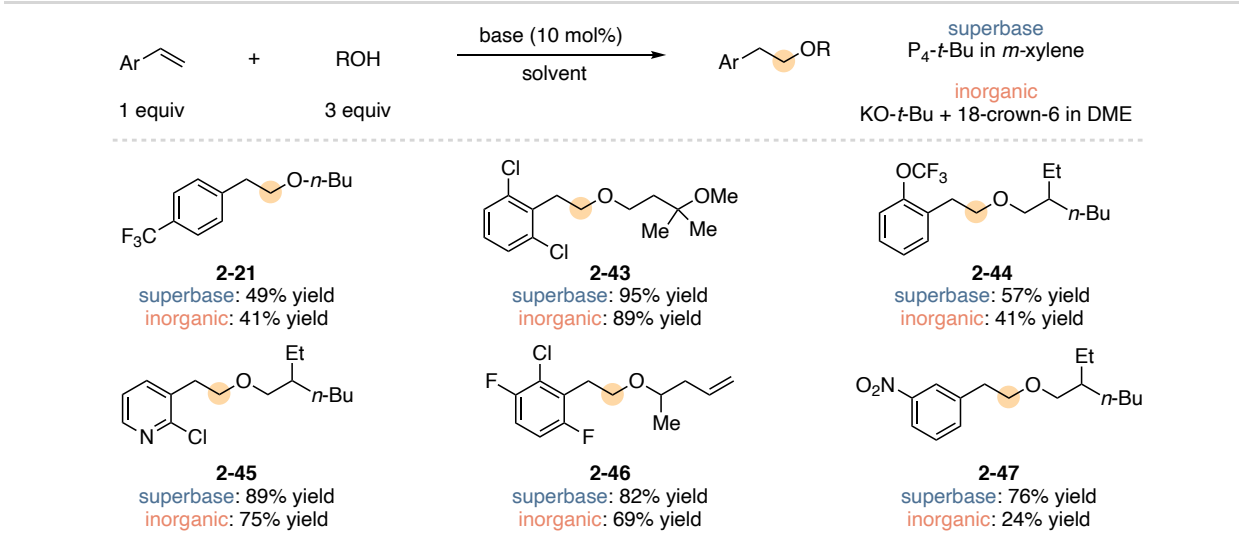

Figure A1-22. Inorganic and superbase yield comparisons for alcohol addition reaction.

2-chloro-1,4-difluoro-3-(2-(pent-4-en-2-yloxy)ethyl)benzene (2-46)

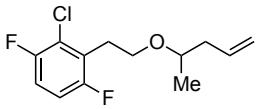

To isolate and characterize the title product, the above superbase procedure was followed using 2-chloro-1,4-difluoro-3-vinylbenzene (88 mg, 0.5 mmol, 1.0 equiv), 4-penten-2-ol (126 μL, 1.5 mmol, 3.0 equiv), *m*-xylene (0.5 mL) and P_4-*t*-Bu (31 μL, 0.025 mmol, 0.1 equiv). The reaction mixture was stirred at 60 °C for 24 h. The product was isolated by direct subjection of the crude reaction material to flash column chromatography (diethyl ether:hexane = 3:100) and obtained as a colorless oil (98 mg, 0.38 mmol, 75% yield). **^{1}H NMR** (400 MHz, CDCl3) δ 6.90 – 7.02 (m, 2H), 5.71 – 5.81 (m, 1H), 4.99 – 5.06 (m, 2H), 3.54 – 3.68 (m, 2H), 3.44 – 3.49 (sextet, J = 6.1 Hz, 1H), 3.05 – 3.10 (m, 2H), 2.25 – 2.32 (m, 1H), 2.11 – 2.19 (m, 1H), 1.12 (d, J = 6.2 Hz, 3H). **^{13}C NMR** (101 MHz, CDCl3) δ 157.5 (d, J = 242.1 Hz), 154.9 (dd, J = 246.6, 5.6 Hz), 135.0, 126.8 (d, J = 20.6 Hz), 122.5 (dd, J = 19.1, 6.9 Hz), 116.9, 114.5 (dd, J = 23.9, 9.5 Hz), 114.1 (dd, J = 25.8, 7.8 Hz), 75.4, 66.2, 41.0, 27.9, 19.6. **^{19}F NMR** (376 MHz, CDCl3) δ -118.55, -118.89. **LCMS** [M+H]$^+$ calcd. for $[C_{12}H_{16}OClF_2]^+$ 261.1, 261.1 found. **IR** (neat): 1474.2, 1232.2, 1092.1, 1059.0, 808.6 cm^{-1}.

A1.5 Improved Superbase-Catalyzed Addition Protocols

A1.5.1 P_4-t-Bu-Catalyzed Addition Reactions Using 1.2 Equivalents of Alcohol.

In our initial report, 3-5 equivalents of alcohol were required to achieve synthetically useful ether equilibrium yields.[Error! Bookmark not defined.] To address this issue, we developed a protocol using 1.2 equivalents of alcohol that reaches high equilibrium yield at lower reaction temperatures.

General procedure. In a nitrogen-filled glovebox, aryl alkene (1.0 mmol, 1.0 equiv), alcohol (1.2 mmol, 1.2 equiv) and toluene (1 mL) were added to an oven-dried 1-dram reaction vial (Thermo Scientific B7990-2) containing a magnetic stir bar. P_4-*t*-Bu (0.8 M in hexane, 125 μL, 0.1 mmol, 0.1 equiv) was then added to the reaction solution. The reaction vial was capped (Thermo Scientific

C4015-1A with 10/50 septa), removed from the glovebox, and placed in a preheated aluminum reaction block at the indicated temperature. After stirring for 24 h, the reaction vial was cooled to rt. The reaction mixture was directly loaded for flash column chromatography using the given eluent conditions.

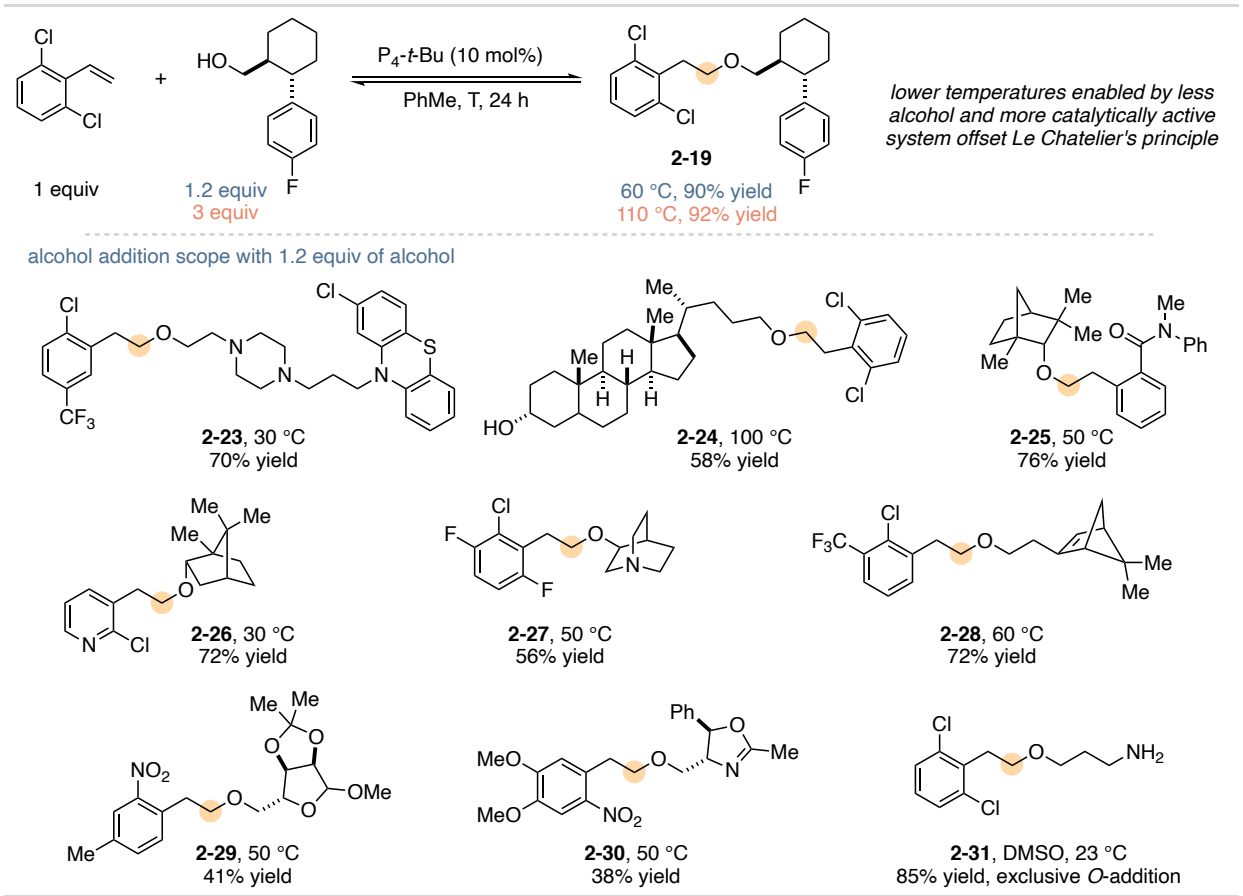

Figure A1-23. Scope of alcohol addition reaction using 1.2 equivalents of alcohol.

(3*S*,4*R*)-3-((2,6-dichlorophenethoxy)methyl)-4-(4-fluorophenyl)-1-methylpiperidine (2-19)

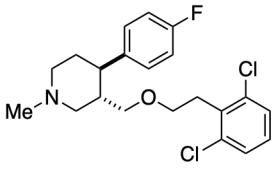

The general procedure was followed using 2,6-dichlorostyrene (173 mg, 1 mmol, 1 equiv), ((3*S*,4*R*)-4-(4-fluorophenyl)-1-methylpiperidin-3-yl)methanol (268 mg, 1.2 mmol, 1 equiv) and P$_4$-*t*-Bu (0.8 M in hexane, 125 µL, 0.1 mmol, 0.1 equiv). The reaction solution was stirred at 80 °C for 24 h. The product was isolated by flash column chromatography (methanol:dichloromethane from 5:100 to 10:100) as a

light yellow oil (348 mg, 0.88 mmol, 88% yield). This procedure was done to obtain an isolated yield, the ^{1}H NMR yield at 60 °C is 90% yield. The spectroscopic data matches our previous report.[1]

2-chloro-10-(3-(4-(2-(2-chloro-5-(trifluoromethyl)phenethoxy)ethyl)piperazin-1-yl)propyl)-10H-phenothiazine (2-23)

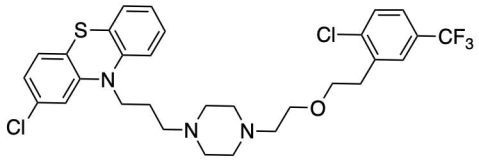

A slight modification to the general procedure was made as this substrate was not run on a 1 mmol scale, although the stoichiometry, concentrations and experimental operations remained the same. The general procedure was followed using 1-chloro-4-(trifluoromethyl)-2-vinylbenzene (62 mg, 0.3 mmol, 1 equiv), perphenazine (146 mg, 0.36 mmol, 1.2 equiv), P_4-*t*-Bu (0.8 M in hexane, 38 μL, 0.03 mmol, 0.1 equiv) and PhMe (0.3 mL). The reaction solution was stirred at 30 °C for 24 h. The product was isolated by flash column chromatography (methanol:dichloromethane = 4:100) as a yellow resin-like solid (129 mg, 0.21 mmol, 70% yield). **^{1}H NMR** (400 MHz, CDCl3) δ 7.53 (m, 1H), 7.45 – 7.40 (m, 2H), 7.09 – 7.16 (m, 2H), 7.00 (d, J = 8.1 Hz, 1H), 6.84 – 6.94 (m, 4H), 3.88 (t, J = 6.8 Hz, 2H), 3.68 (t, J = 6.7 Hz, 2H), 3.56 (t, J = 5.7 Hz, 2H), 3.05 (t, J = 6.7 Hz, 2H), 2.55 (t, J = 5.7 Hz, 2H), 2.42 – 2.46 (m, 10H), 1.89 – 1.96 (p, J = 7.0 Hz, 2H). **^{13}C NMR** (101 MHz, CDCl3) δ 146.8, 144.8, 138.1, 138.1, 133.4, 130.1, 129.3 (q, J = 32.6 Hz), 128.2 (q, J = 3.7 Hz), 128.1, 127.7, 127.7, 124.9, 124.6 (q, J = 3.7 Hz), 124.0 (q, J = 272.4 Hz), 123.7, 123.1, 122.4, 116.1, 116.1, 69.8, 69.2, 58.0, 55.8, 53.9, 53.4, 45.7, 34.1, 24.5. **^{19}F NMR** (376 MHz, CDCl3) δ -62.43. **HRMS [ESI]** $[M+H]^+$ calcd. for $[C_{30}H_{33}F_3N_3Cl_2OS]^+$ 610.1668, 610.1689 found. **IR** (neat): 1457.5, 1323.5, 1276.4, 1165.4, 1120.6, 1081.7 cm^{-1}.

***N*-methyl-*N*-phenyl-2-(2-(((1*S*,2*R*,4*S*)-1,3,3-trimethylbicyclo[2.2.1]heptan-2-yl)oxy)ethyl)benzamide (2-25)**

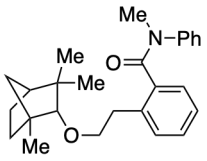

The general procedure was followed using *N*-methyl-*N*-phenyl-2-vinylbenzamide (237 mg, 1 mmol, 1 equiv), (1*R*)-endo-(+)-fenchyl alcohol (185 mg, 1.2 mmol, 1.2 equiv) and P_4-*t*-Bu (0.8 M in hexane, 125 µL, 0.1 mmol, 0.1 equiv). The reaction solution was stirred at 50 °C for 24 h. The product was isolated by flash column chromatography (diethyl ether:hexane = 2.5:100) as a colorless oil (297 mg, 0.76 mmol, 76% yield). **^{1}H NMR** (400 MHz, $CDCl_3$) δ 7.96 (dd, J = 7.7, 1.5 Hz, 1H), 7.43 (td, J = 7.5, 1.5 Hz, 1H), 7.23 – 7.31 (m, 4H), 6.79 (d, J = 7.8 Hz, 2H), 6.69 (m, 1H), 4.63 (d, J = 2.0 Hz, 1H), 3.60 – 3.64 (m, 2H), 3.20 – 3.29 (m, 2H), 2.92 (s, 3H), 1.86 – 1.92 (m, 1H), 1.74 – 1.79 (m, 2H), 1.69 (m, 1H), 1.47 – 1.54 (m, 1H), 1.18 – 1.28 (m, 5H), 1.15 (s, 3H), 0.89 (s, 3H). **^{13}C NMR** (101 MHz, $CDCl_3$) δ 167.6, 149.1, 142.0, 132.1, 132.0, 130.6, 130.3, 129.3, 126.4, 116.0, 112.2, 86.9, 54.3, 48.7, 48.6, 41.6, 40.0, 38.3, 31.9, 29.0, 27.1, 26.1, 20.7, 19.8. **HRMS [ESI]** $M+H^+$ calcd. for $[C_{26}H_{34}NO_2]^+$ 392.2584, 392.2602 found. **IR** (neat): 2957.7, 2932.3, 1709.6, 1506.6, 1260.7, 1108.7, 1075.1 cm^{-1}. **Specific rotation** $[\alpha]_D^{24}$= -35.0 (c = 1.0 in CH_2Cl_2).

(3*R*,5*R*,8*R*,10*S*,13*R*)-17-((*R*)-5-(2,6-dichlorophenethoxy)pentan-2-yl)-10,13-dimethylhexadecahydro-1H-cyclopenta[a]phenanthren-3-ol (2-24)

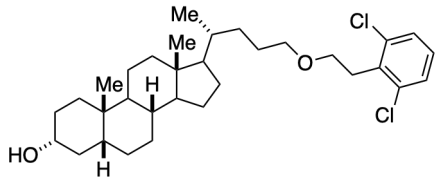

The general procedure was followed using 2,6-dichlorostyrene (173 mg, 1 mmol, 1 equiv), lithocholic alcohol[2] (432 mg, 1.2 mmol, 1.2 equiv) and P_4-*t*-Bu (0.8 M in hexane, 125 µL, 0.1 mmol, 0.1 equiv). The reaction solution was stirred at 100 °C for 24 h. The product was isolated by flash column (ethyl acetate:hexane = 1:3.5) as a white viscous solid (310

mg, 0.58 mmol, 58% yield). **Note on regioselectivity:** The addition product was obtained as an approximate 4:1 ratio of primary alcohol addition to secondary alcohol addition. The selectivity for primary alcohol addition is consistent with our previously reported studies on diol hydroetherification.[1] ^{1}H and ^{13}C NMR spectra in $CDCl_3$ and benzene-d_6 are provided in the NMR spectra section below where the two regioisomeric products can be distinguished; comparison of the major product's ^{13}C NMR chemical shifts to the starting diol's ^{13}C NMR spectrum[2] indicates the secondary alcohol (71.9 ppm in the starting diol) did not undergo hydroetherification. Provided here is the characterization data for the major isomer. **^{1}H NMR** (400 MHz, CDCl3) δ 7.24 (d, J = 8.0 Hz, 2H), 7.03 – 7.07 (m, 1H), 3.55 – 3.62 (m, 3H), 3.40 – 3.45 (m, 2H), 3.21 – 3.25 (m, 2H), 0.88 – 1.95 (multiple m, 35 H), 0.62 (s, 3H). **^{13}C NMR** (101 MHz, CDCl3) δ 135.9, 134.6, 128.2, 128.0, 71.8, 71.5, 68.0, 56.6, 56.2, 42.7, 42.2, 40.5, 40.2, 36.5, 35.9, 35.6, 35.5, 34.6, 32.1, 31.8, 30.6, 28.3, 27.3, 26.5, 26.3, 24.3, 23.5, 20.9, 18.7, 12.1. **Melting point:** 55 – 57 °C. **HRMS [ESI]** $[M+H]^+$ calcd. for $[C_{32}H_{49}Cl_2O_2]^+$ 535.3110, 569.2705 found of a chlorinated adduct of the product, calcd. for $[C_{32}H_{48}Cl_3O_2]^+$ 569.2714. **IR** (neat): 2926.5, 2861.3, 1435.1, 1102.7, 1037.1, 774.3 cm^{-1}. **Specific rotation** $[\alpha]_D^{24}$= +35.0 (c = 2.6 in CH_2Cl_2).

2-chloro-3-(2-(((1*S*,2*R*,4*S*)-1,7,7-trimethylbicyclo[2.2.1]heptan-2-yl)oxy)ethyl)pyridine (2-26)

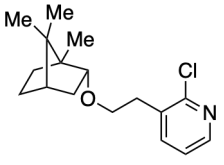

The general procedure was followed using 2-chloro-3-vinylpyridine (140 mg, 1.0 mmol, 1 equiv), (-)-borneol (154 mg, 1.2 mmol, 1.2 equiv) and P_4-*t*-Bu (0.8 M in hexane, 125 μL, 0.1 mmol, 0.1 equiv). The reaction solution was stirred at 30 °C for 24 h. The product was isolated by flash column chromatography (ethyl acetate:hexane = 1:15) as a colorless oil (213 mg, 0.72 mmol, 72% yield). **^{1}H NMR** (400 MHz, CDCl3) δ 8.25

(dd, J = 4.7, 2.0 Hz, 1H), 7.65 (dd, J = 7.5, 2.0 Hz, 1H), 7.16 (dd, J = 7.5, 4.7 Hz, 1H), 3.70 (dt, J = 9.4, 6.4 Hz, 1H), 3.60 (dt, J = 9.4, 6.2 Hz, 1H), 3.51 – 3.54 (m, 1H), 2.97 (t, J = 6.3 Hz, 2H), 2.02 – 2.09 (m, 1H), 1.86 – 1.92 (m, 1H), 1.63 – 1.69 (m, 1H), 1.57 – 1.60 (m, 1H), 1.06 – 1.19 (m, 2H), 0.87 (dd, J = 13.0, 3.3 Hz, 1H), 0.81 (s, 3H), 0.80 (s, 3H), 0.78 (s, 3H). **^{13}C NMR** (101 MHz, CDCl3) δ 151.4, 147.5, 140.2, 134.2, 122.4, 85.0, 68.0, 49.3, 47.9, 45.1, 36.2, 34.0, 28.3, 26.8, 19.9, 18.9, 14.1. **HRMS [ESI]** $[M+H]^+$ calcd. for $[C_{17}H_{25}ClNO]^+$ 294.1619, 294.1627 found. **IR** (neat): 2948.1, 1563.0, 1408.0, 1117.7, 1095.5, 1078.7, 795.1 cm^{-1}. **Specific rotation** $[\alpha]_D^{24}$= -11.4 (c = 3.7 in CH_2Cl_2).

(1*R*,5*S*)-2-(2-(2-chloro-3-(trifluoromethyl)phenethoxy)ethyl)-6,6-dimethylbicyclo[3.1.1]hept-2-ene (2-28)

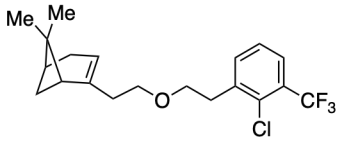

The general procedure was followed using 2-chloro-3-trifluoromethylstyrene (207 mg, 1 mmol, 1 equiv), (1*R*)-(–)-nopol (200 mg, 1.2 mmol, 1.2 equiv) and P_4-*t*-Bu (0.8 M in hexane, 125 µL, 0.1 mmol, 0.1 equiv). The reaction solution was stirred at 60 °C for 24 h. The product was isolated by flash column chromatography (100% hexanes) as a colorless oil (268 mg, 0.72 mmol, 72% yield). **^{1}H NMR** (400 MHz, CDCl3) δ 7.57 (dd, J = 7.8, 1.7 Hz, 1H), 7.48 (dd, J = 7.8, 1.7 Hz, 1H), 7.27 (t, J = 8.1 Hz, 1H), 5.22 (m, 1H), 3.65 (t, J = 6.8 Hz, 2H), 3.40 – 3.49 (m, 2H), 3.09 (t, J = 6.8 Hz, 2H), 2.33 (dt, J = 8.5, 5.6 Hz, 1H), 2.10 – 2.25 (m, 4H), 1.95 – 2.05 (m, 2H), 1.25 (s, 3H), 1.11 (d, J = 8.5 Hz, 1H), 0.79 (s, 3H). **^{13}C NMR** (101 MHz, CDCl3) δ 145.2, 139.5, 134.8, 132.1, 129.1 (q, J = 30.3 Hz) 126.4, 126.0 (q, J = 5.5 Hz), 123.3 (q, J = 273.0 Hz), 118.1, 69.5, 69.2, 46.0, 40.9, 38.1, 37.2, 34.3, 31.8, 31.5, 26.5, 21.2. **^{19}F NMR** (376 MHz, CDCl3) δ -62.39. **HRMS [DART]**

$[M+H]^+$ calcd. For $[C_{20}H_{25}ClF_3O]^+$ 373.1541, 373.1561 found. **IR** (neat): 2914.3, 1433.8, 1314.8, 1136.2, 110 9.5 cm^{-1}. **Specific rotation** $[\alpha]_D^{24}$= -19.6 (*c* = 2.6 in CH_2Cl_2).

(1*S*,4*S*)-3-(2-chloro-3,6-difluorophenethoxy)quinuclidine (2-27)

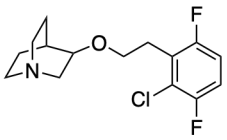

A slight modification to the general procedure was made as this substrate was not run on a 1 mmol scale, although the stoichiometry, concentrations and experimental operations remained the same. The general procedure was followed using 2-chloro-1,4-difluoro-3-vinylbenzene (53 mg, 0.3 mmol, 1 equiv), 3-quinuclidinol (46 mg, 0.36 mmol, 1.2 equiv), P_4-*t*-Bu (0.8 M in hexane, 38 µL, 0.03 mmol, 0.1 equiv) and PhMe (0.3 mL). The reaction solution was stirred at 50 °C for 24 h. The product was isolated by preparative thin layer chromatography (methanol:dichloromethane = 12:100) as a yellow oil (51 mg, 0.17 mmol, 56% yield). **^{1}H NMR** (400 MHz, CDCl3) δ 6.90 – 7.02 (m, 2H), 3.60 – 3.66 (m, 1H), 3.51 – 3.57 (m, 1H), 3.44 – 3.48 (m, 1H), 3.01 – 3.11 (m, 3H), 2.70 – 2.81 (m, 3H), 2.59 – 2.69 (m, 2H), 1.95 – 1.97 (m, 1H), 1.62 – 1.74 (m, 2H), 1.37 – 1.43 (m, 1H), 1.25 – 1.30 (m, 1H). **^{13}C NMR** (101 MHz, CDCl3) δ 157.6 (dd, *J* = 242.8, 1.4 Hz), 154.9 (dt, *J* = 243.8, 8.1 Hz), 126.9 (d, *J* = 20.8 Hz), 122.5 (dd, *J* = 19.0, 6.6 Hz), 114.6 (dd, *J* = 23.9, 9.5 Hz), 114.1 (dd, *J* = 25.8, 7.7 Hz), 75.6, 66.0, 56.1, 47.6, 46.9, 27.7 (t, *J* = 1.6 Hz), 24.7, 24.5, 19.3. **^{19}F NMR** (376 MHz, CDCl3) δ -118.46 (d, *J* = 15.8 Hz), -118.86 (d, *J* = 15.8 Hz). **HRMS [ESI]** $[M+H]^+$ calcd. for $[C15H19ClF_2NO]^+$ 302.1118, 302.1140 found. **IR** (neat): 2938.9, 2864.0, 1473.8, 1232.3, 1090.1, 1057.4 cm^{-1}. **Specific rotation** $[\alpha]_D^{24}$= -1.1 (*c* = 3.8 in CH_2Cl_2).

(3a*R*,4*R*,6*R*,6a*R*)-4-methoxy-2,2-dimethyl-6-((4-methyl-2-nitrophenethoxy)methyl)tetrahydrofuro[3,4-d][1,3]dioxole (2-29)

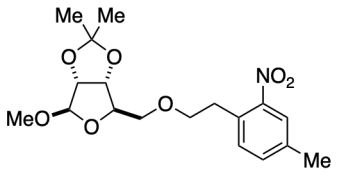

The general procedure was followed using 4-methyl-2-nitro-1-vinylbenzene (163 mg, 1 mmol, 1 equiv), methyl 2,3-O-isopropylidene-β-D-ribofuranoside (245 mg, 1.2 mmol, 1.2 equiv) and P_4-*t*-Bu (0.8 M in hexane, 125 µL, 0.1 mmol, 0.1 equiv). The reaction solution was stirred at 50 °C for 24 h. The product was isolated by flash column chromatography (ethyl acetate:hexane = 1:6.5) as a yellow oil (151 mg, 0.41 mmol, 41% yield). **^{1}H NMR** (400 MHz, $CDCl_3$) δ 7.68 (s, 1H), 7.24 – 7.30 (m, 2H), 4.90 (s, 1H), 4.55 (d, J = 6.0 Hz, 1H), 4.50 (d, J = 6.0 Hz, 1H), 4.24 (m, 1H), 3.65 – 3.71 (m, 2H), 3.36 – 3.45 (m, 2H), 3.23 (s, 3H), 3.09 (t, J = 6.5 Hz, 2H), 2.35 (s, 3H), 1.44 (s, 3H), 1.27 (s, 3H). **^{13}C NMR** (101 MHz, $CDCl_3$) δ 149.5, 137.8, 133.7, 132.8, 130.9, 125.0, 112.4, 109.3, 85.2, 85.0, 82.2, 71.9, 71.0, 54.8, 33.1, 26.5, 25.0, 20.8. **HRMS [ESI]** $[M+NH_4]^+$ calcd. for $[C_{18}H_{29}N_2O_7]^+$ 385.1969, 385.1995 found. **IR** (neat): 2936.2, 1527.5, 1346.3, 1088.1, 1055.7, 868.9 cm^{-1}. **Specific rotation** $[\alpha]_D^{24}$= -31.4 (c = 2.2 in CH_2Cl_2).

(4*R*,5*R*)-4-((4,5-dimethoxy-2-nitrophenethoxy)methyl)-2-methyl-5-phenyl-4,5-dihydrooxazole (2-30)

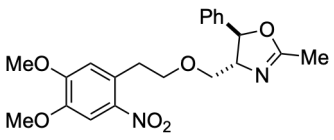

A slight modification to the general procedure was made as this substrate was not run on a 1 mmol scale, although the stoichiometry, concentrations and experimental operations remained the same. The general procedure was followed using 1,2-dimethoxy-4-nitro-5-vinylbenzene (53 mg, 0.25 mmol, 1 equiv), ((4*R*,5*R*)-2-methyl-5-phenyl-4,5-dihydrooxazol-4-yl)methanol[2] (58 mg, 0.3 mmol, 1.2 equiv), P_4-*t*-Bu (0.8 M in hexane, 31 µL, 0.025 mmol, 0.1 equiv) and PhMe (0.25 mL). The reaction solution was stirred at 50 °C for 24 h. The product was isolated by flash column chromatography (ethyl acetate:hexane = 1:1) as a yellow oil (38 mg, 0.09 mmol, 38% yield). **^{1}H**

NMR (400 MHz, $CDCl_3$) δ 7.60 (s, 1H), 7.30 – 7.36 (m, 3H), 7.21 – 7.23 (m, 2H), 6.77 (s, 1H), 5.21 (d, J = 6.8 Hz, 1H), 4.05 – 4.10 (m, 1H), 3.93 (s, 3H), 3.86 (s, 3H), 3.78 – 3.82 (m, 2H), 3.67 (dd, J = 9.7, 4.4 Hz, 1H), 3.55 (dd, J = 9.7, 6.2 Hz, 1H), 3.23 (m, 2H), 2.07 (d, J = 1.2 Hz, 3H). **^{13}C NMR** (101 MHz, $CDCl_3$) δ 165.5, 152.9, 147.5, 141.5, 140.9, 129.6, 128.8, 128.3, 125.6, 114.5, 108.2, 83.8, 74.6, 72.6, 71.1, 56.4, 56.4, 34.3, 14.2. **HRMS [DART]** $[M+H]^+$ calcd. for $[C_{21}H_{25}N_2O_6]^+$ 401.1707, 401.1735 found. **IR** (neat): 2926.7, 2873.3, 1672.3, 1520.8, 1496.5, 1267.4, 1218.3, 1063.7 cm^{-1}. **Specific rotation** $[\alpha]_D^{24}$= +160.9 (c = 1.1 in CH_2Cl_2).

A1.5.2 Improved Selectivity for O-selective Aminoalcohol Addition Reaction.

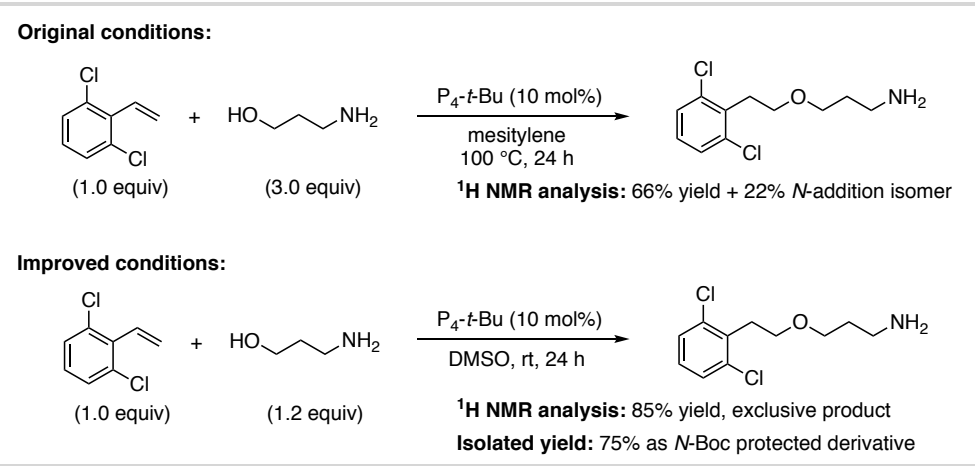

Figure A1-24. Comparison of original conditions to improved conditions.

Improved protocol: the general procedure from Section A1.5.1. was followed using 2,6-dichlorostyrene (173 mg, 1 mmol, 1 equiv), 3-aminopropanol (92 µL, 1.2 mmol, 1.2 equiv) and P_4-*t*-Bu (0.8 M in hexane, 125 µL, 0.1 mmol, 0.1 equiv) with DMSO (1 mL) as solvent. The reaction was stirred at rt for 24 h. The yield and selectivity were determined by ^{1}H NMR analysis of the crude reaction mixture using benzyl ether (95 µL, 0.5 mmol, 0.5 equiv) as an internal standard (85% yield of *O*-addition product, no *N*-addition product observed). A description of this

analysis and full characterization details are provided in reference 1. The *O*-addition product was isolated as the *N*-Boc protected amine, described below.

***tert*-butyl (3-(2,6-dichlorophenethoxy)propyl)carbamate**

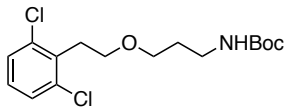

Water (15 mL) was added to the above crude reaction solution and the mixture was extracted using EtOAc (2 x 15 mL). The combined organic phase was dried (anhydrous Na_2SO_4) and concentrated *in vacuo*. The resulting crude material was dissolved in dichloromethane (2 mL), then triethylamine (0.28 mL, 2.0 mmol, 2.0 equiv) and di-*tert*-butyl dicarbonate (0.46 mL, 2.0 mmol, 2.0 equiv) were sequentially added at 0 °C using an ice bath. The reaction mixture was allowed to warm to rt and stirred overnight. The reaction solution was concentrated and the product was isolated by flash column chromatography (ethyl acetate:hexane = 1:8) as a colorless oil (260 mg, 0.75 mmol, 75% yield). The spectroscopic data matches our previous report.[Error! Bookmark not defined.]

A1.5.3 P_4-t-Bu-Catalyzed Alcohol Addition to Mildly-Activated Styrenes.

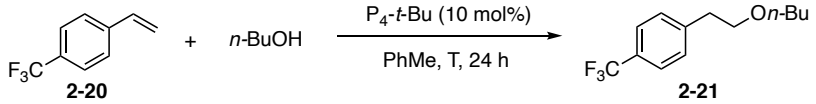

2-20			**2-21**
1 equiv	3 equiv	80 °C	49% yield
3 equiv	1 equiv	23 °C	61% yield
5 equiv	1 equiv	23 °C	76% yield

Figure A1-25. Effects of reactant stoichiometry on product yield.

General procedure for reactions with excess 4-(trifluoromethyl)styrene (2-20). In a nitrogen-filled glovebox, 4-(trifluoromethyl)styrene, *n*-butanol (0.1 mmol of the limiting reagent, 17.2 mg 4-(trifluoromethyl)styrene or 9.2 µL *n*-butanol) and toluene (0.2 mL) were added to an oven-dried 4 mL reaction vial (Thermo Scientific B7990-2) containing a magnetic stir bar. P_4-*t*-Bu (0.8 M in hexane, 12.5 µL, 0.01 mmol, 0.1 equiv) was then added to the reaction solution. The reaction vial was capped (Thermo Scientific C4015-1A with 10/50 septa), removed from the glovebox, and

placed in a preheated aluminum heating block at the indicated temperature. After stirring for 24 h, the reaction vial was cooled to rt. To the reaction mixture was added dibenzyl ether (19.0 μL, 0.1 mmol, 1.0 equiv). An aliquot (approximately 50 μL) of the reaction solution was directly transferred to an NMR tube with $CDCl_3$ (0.6 mL). The yield was determined by comparison of product signal integration to internal standard integration in the ^{1}HNMR spectrum of the crude reaction mixture.

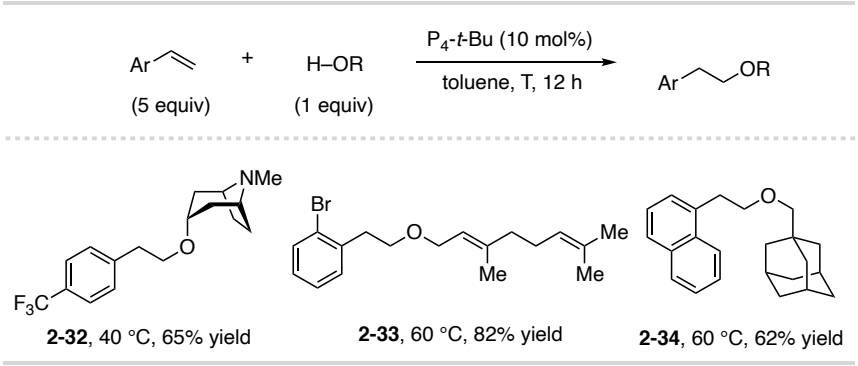

Figure A1-26. Alcohol addition reactions to mildly-activated styrenes.

General Procedure: In a nitrogen-filled glovebox, aryl alkene (5.0 mmol, 5.0 equiv), alcohol (1.0 mmol, 1.0 equiv) and toluene were added to an oven-dried 4 mL reaction vial (Thermo Scientific B7990-2) containing a magnetic stir bar. P_4-*t*-Bu (0.8 M in hexanes, 125 μL, 0.1 mmol, 0.1 equiv) was then added to the reaction solution. The reaction vial was capped (Thermo Scientific C4015-1A with 10/50 septa), removed from the glovebox, and placed in a preheated aluminum reaction block at the indicated temperature. After stirring for 12 h, the reaction solution was cooled to rt. The reaction mixture was directly loaded for flash column chromatography using the given eluent conditions.

8-methyl-3-(4-(trifluoromethyl)phenethoxy)-8-azabicyclo[3.2.1]octane (2-32)

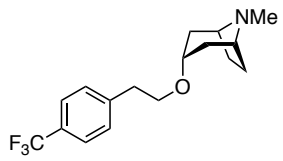

The general procedure was followed using 4-(trifluoromethyl)styrene (860.8 mg, 5 mmol, 5 equiv), tropine (141.2 mg, 1 mmol, 1 equiv), toluene (1.3 mL, 0.75 M) and P_4-*t*-Bu (0.8 M in hexane, 125 µL, 0.1 mmol, 0.1 equiv). The reaction solution was stirred for 12 h at 40 °C. The product was isolated by flash column chromatography (10% MeOH/1% NH_4OH/DCM) to yield the title product as a colorless oil (first run: 211 mg, 0.67 mmol, 67% yield; second run: 191 mg, 6.1 mmol, 61% yield; 65 % average yield). **^{1}H NMR** (400 MHz, $CDCl_3$) δ 7.50 (d, J = 7.8 Hz, 2H), 7.31 (d, J = 7.8 Hz, 2H), 3.53 (t, J = 6.4 Hz, 2H), 3.43 (t, J = 5.2 Hz, 1H), 3.02 (dq, J = 5.6, 3.0 Hz, 2H), 2.86 (t, J = 6.4 Hz, 2H), 2.24 (s, 3H), 1.95 (dt, J = 14.7, 4.4 Hz, 2H), 1.84 – 1.69 (m, 6H). **^{13}C NMR** (101 MHz, $CDCl_3$) δ 144.0 (m), 129.4, 128.4 (q, J = 32.5 Hz), 125.0 (q, J = 3.9 Hz), 124.4 (q, J = 271.6 Hz), 72.2, 69.1, 60.4, 40.5, 36.7, 35.9, 25.4. **^{19}F NMR** (376 MHz, $CDCl_3$) δ -62.29. **HRMS [DART]** $[M+H]^+$ calcd. for $[C_{17}H_{23}F_3NO]^+$ 314.1726, 314.1758 found. **IR** (neat): 2926.5, 2868.6, 1322.4, 1111.4, 1065.4, 827.6 cm^{-1}.

(*E*)-1-bromo-2-(2-((3,7-dimethylocta-2,6-dien-1-yl)oxy)ethyl)benzene (2-33)

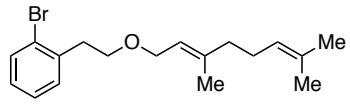

The general procedure was followed using 2-bromostyrene (915.3 mg, 5 mmol, 5 equiv), geraniol (154.3 mg, 1 mmol, 1 equiv), toluene (2 mL, 0.5 M), and P_4-*t*-Bu (0.8 M in hexane, 125 µL, 0.1 mmol, 0.1 equiv). The reaction solution was stirred for 12 h at 60 °C. The product was isolated by flash column chromatography (100% hexanes to 2.5% ethyl acetate/hexanes) to yield the title product as a yellow oil (277 mg, 0.82 mmol, 82% yield). **^{1}H NMR** (400 MHz, $CDCl_3$) δ 7.53 (dd, J = 8.0 Hz, 1.3 Hz, 1H), 7.21 – 7.31 (m, 2H), 7.07 (td, J = 7.3, 1.9 Hz, 1H), 5.36 (tq, J = 6.7, 1.3 Hz, 1H), 5.10 (m, 1H), 4.03 (d, J = 6.6 Hz, 2H), 3.66 (t, J = 7.3 Hz, 2H), 3.06 (t, J = 7.3 Hz, 2H), 2.08 – 1.90 (m, 4H), 1.62 – 1.52 (m,

6H), 1.61 (s, 3H). **^{13}C NMR** (101 MHz, $CDCl_3$) δ 140.2, 138.4, 132.8, 131.7, 131.2, 128.0, 127.5, 124.8, 124.1, 120.9, 69.2, 67.4, 39.7, 36.7, 26.5, 25.8, 17.8, 16.6. **GCMS** (EI) M^+ calcd. for $[C_{18}H_{25}BrO]^+$ 336.1, 336.1 found. **IR** (neat): 2965.4, 2923.5, 2854.3, 1098.8, 1078.6, 747.7 cm^{-1}.

1-((2-(naphthalen-1-yl)ethoxy)methyl)adamantane (2-34)

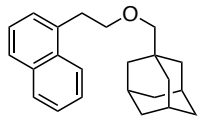

The general procedure was followed using 1-vinylnaphthlene (771.1 mg, 5 mmol, 5 equiv), 1-hydroxymethyladamantane (166.3 mg, 1 mmol, 1 equiv), toluene (1.3 mL, 0.75 M) and P_4-*t*-Bu (0.8 M in hexane, 125 µL, 0.1 mmol, 0.1 equiv). The reaction solution was stirred for 12 h at 60 °C. The product was isolated by flash column chromatography (100% hexanes to 10% ethyl acetate/hexanes) to yield the title product as a colorless oil (198 mg, 0.62 mmol, 62% yield). **^{1}H NMR** (400 MHz, $CDCl_3$) δ 7.98 (d, J = 8.5 Hz, 1H), 7.71 (dd, J = 8.0, 1.6 Hz, 1H), 7.60 (dd, J = 7.7, 1.9 Hz, 1H), 7.44 – 7.19 (m, 4H), 3.61 (t, J = 7.3 Hz, 2H), 3.24 (t, J = 7.3 Hz, 2H), 2.91 (s, 2H), 1.84 (m, 3H), 1.65 – 1.46 (m, 6H), 1.41 (d, J = 3.2 Hz, 6H). **^{13}C NMR** (101 MHz, $CDCl_3$) δ 135.5, 133.9, 132.4, 128.8, 127.0, 126.9, 125.9, 125.6, 125.5, 124.1, 82.2, 72.1, 39.8, 37.4, 34.2, 33.4, 28.4. **HRMS [DART] [**$M+H]^+$ calcd. for $[C_{23}H_{29}O]^+$ 321.2213, 321.2211 found. **IR** (neat): 2896.6, 2844.8, 1094.3 cm^{-1}.

A1.5.4 P_4-t-Bu-Catalyzed Alkenol Cyclization Reactions.

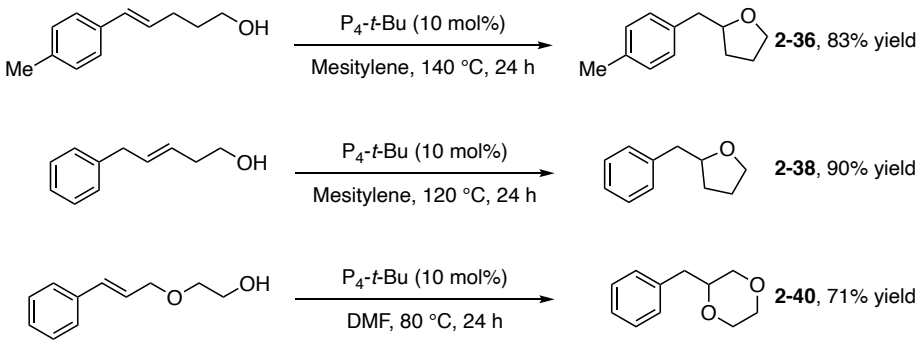

Figure A1-27. Base-catalyzed alkenol cyclization reactions.

General Procedure: In a nitrogen-filled glovebox, alkenol (1.0 mmol) and solvent were added to an oven-dried 4 mL reaction vial (Thermo Scientific B7990-2) containing a magnetic stir bar. P_4-*t*-Bu (0.8 M in hexanes, 125 µL, 0.1 mmol, 0.1 equiv) was then added to the reaction solution. The reaction vial was capped (Thermo Scientific C4015-1A with 10/50 septa), removed from the glovebox, and placed in a preheated aluminum reaction block at the indicated temperature. After stirring for 24 h, the reaction solution was cooled to rt. The reaction mixture was directly loaded for flash column chromatography using the given eluent conditions.

2-(4-methylbenzyl)tetrahydrofuran (2-36)

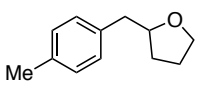

The general procedure was followed using (*E*)-5-(p-tolyl)pent-4-en-1-ol[2] (176.3 mg, 1 mmol, 1 equiv), mesitylene (2 mL, 0.5 M) and P_4-*t*-Bu (0.8 M in hexane, 125 µL, 0.1 mmol, 0.1 equiv). The reaction solution was stirred at 140 °C for 24 h. The product was isolated by flash column chromatography (100% hexanes to 2% ethyl acetate/hexanes) to yield the title product as a yellow oil (145.8 mg, 0.83 mmol, 83% yield). The spectroscopic data matches a previous literature report.[5] **^{1}H NMR** (400 MHz, $CDCl_3$) δ 7.18 – 7.09 (m, 4H), 4.10 – 4.03 (m, 1H), 3.95 – 3.90 (m, 1H), 3.81 – 3.71 (m, 1H), 2.92 (dd, *J* = 13.6, 6.5 Hz, 1H), 2.74 (dd, *J* = 13.6, 6.5 Hz, 1H), 2.35 (s, 3H), 2.00 – 1.77 (m, 3H), 1.64 – 1.45 (m, 1H). **^{13}C NMR** (101 MHz, $CDCl_3$) *δ* 136.0, 135.7, 129.2, 129.1, 80.3, 68.0, 41.6, 31.0, 25.7, 21.1.

2-benzyltetrahydrofuran (2-38)

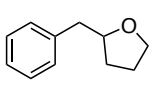

The general procedure was followed using (*E*)-5-phenylpent-3-en-1-ol[**Error! Bookmark not defined.**] (162.3 mg, 1 mmol, 1 equiv), mesitylene (2 mL, 0.5 M) and P_4-*t*-Bu (0.8 M in hexane, 125 µL, 0.1 mmol, 0.1 equiv). The reaction solution was stirred at 120 °C for 24 h.

The product was isolated by flash column chromatography (100% hexanes to 2% ethyl acetate/hexanes) to yield the title product as a colorless oil (145.8 mg, 0.90 mmol, 90% yield). The spectroscopic data matches a previous literature report.[3] **^{1}H NMR** (400 MHz, $CDCl_3$) δ 7.24 – 7.17 (m, 2H), 7.17 – 7.07 (m, 3H), 3.98 (m, 1H), 3.81 (m, 1H), 3.65 (m, 1H), 2.84 (dd, J = 13.6, 6.4 Hz, 1H), 2.66 (dd, J = 13.6, 6.4 Hz, 1H), 1.89 – 1.67 (m, 3H), 1.55 – 1.40 (m, 1H). **^{13}C NMR** (101 MHz, $CDCl_3$) δ 139.1, 129.3, 128.4, 126.2, 80.1, 68.0, 42.0, 31.1, 25.7.

2-benzyl-1,4-dioxane (2-40)

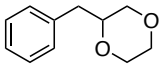

The general procedure was varied by using an oven dried 8 mL reaction vial (Thermo Scientific B7999-3 with septum cap Thermo Scientific B7995-15) using 2-(cinnamyloxy)ethan-1-ol[7] (178.3 mg, 1 mmol, 1 equiv), *N*,*N*-dimethylformamide (DMF, 4 mL, 0.25 M) and P_4-*t*-Bu (0.8 M in hexane, 125 µL, 0.1 mmol, 0.1 equiv). The reaction solution was stirred at 80 °C for 24 h. The reaction solution was cooled to rt, water (8 mL) was added and the mixture was extracted with ethyl acetate (3 x 25 mL). The combined organic extracts were washed with brine (50 mL), dried over Na_2SO_4, and concentrated under reduced pressure. Flash column chromatography (100% hexanes to 10% ethyl acetate/hexanes) yielded the title product as a pale-yellow oil (126.8 mg, 0.71 mmol, 71% yield). The spectroscopic data matches a previous literature report.[4] **^{1}H NMR** (400 MHz, $CDCl_3$) δ 7.22 – 7.17 (m, 2H), 7.15 – 7.06 (m, 3H), 3.75 – 3.44 (m, 6H), 3.23 (dd, J = 11.5, 9.9 Hz, 1H), 2.70 (dd, J = 14.0, 7.1 Hz, 1H), 2.52 (dd, J = 14.0, 6.3 Hz, 1H). **^{13}C NMR** (101 MHz, $CDCl_3$) δ 137.4, 129.2, 128.4, 126.5, 76.1, 71.0, 66.9, 66.5, 38.5. **Note:** reactions of this substrate performed in nonpolar aromatic solvents at elevated temperatures (>100 °C) results in isomerization to (*E*)-2-((3-phenylprop-1-en-1-yl)oxy)ethan-1-ol with reduced cyclization yields.

A1.5.5 P_4-t-Bu-Catalyzed Alcohol Addition to a β-Substituted Acrylamide.

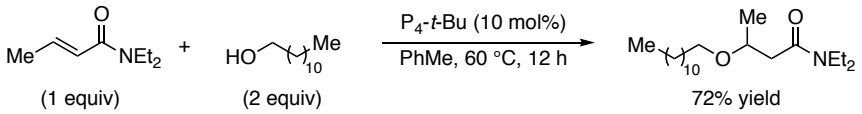

3-(dodecyloxy)-*N*,*N*-diethylbutanamide (2-42)

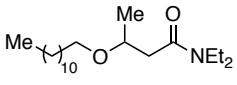

In a nitrogen-filled glovebox, (*E*)-*N*,*N*-diethylbut-2-enamide[9] (157.2 mg, 1.0 mmol, 1.0 equiv), 1-dodecanol (372.7 mg, 2.0 mmol, 2.0 equiv) and toluene (1.0 mL) were added to an oven-dried 4 mL reaction vial (Thermo Scientific B7990-2) containing a magnetic stir bar. P_4-*t*-Bu (0.8 M in hexane, 125 µL, 0.1 mmol, 0.1 equiv) was then added to the reaction solution. The reaction vial was capped (Thermo Scientific C4015-1A with 10/50 septa), removed from the glovebox, and placed in a preheated aluminum reaction block at 60 °C. After stirring for 12 h, the reaction solution was cooled to rt. The reaction mixture was directly loaded for flash column chromatography (100% hexanes to 20% ethyl acetate/hexanes) to yield the title product as a colorless oil (240.9 mg, 0.72 mmol, 72% yield). **^{1}H NMR** (400 MHz, $CDCl_3$) δ 3.96 (sextet, J = 6.2 Hz, 1H), 3.56 – 3.22 (m, 6H), 2.66 (dd, J = 14.5, 6.9 Hz, 1H), 2.21 (dd, J = 14.5, 6.1 Hz, 1H), 1.46 (pentet, J = 6.7 Hz, 2H), 1.26 – 1.20 (m, 18H), 1.15 (d, J = 6.1 Hz, 3H), 1.12 (t, J = 7.1 Hz, 3H), 1.05 (t, J = 7.1 Hz, 3H), 0.86 (t, J = 6.8 Hz, 3H). **^{13}C NMR** (101 MHz, $CDCl_3$) δ 170.4, 73.3, 69.2, 42.2, 40.6, 40.3, 32.0, 30.2, 29.7, 29.7, 29.7, 29.5, 29.4, 26.2, 22.7, 20.3, 14.5, 14.1, 13.1. **HRMS [DART]** $[M+H]^+$ calcd. for $[C_{20}H_{42}NO_2]^+$ 328.3210, 328.3237 found. **IR** (neat): 2961.3, 2923.7, 2853.4, 1637.8, 1459.8, 1132.3, 1097.3 cm^{-1}.

A1.6 Superbase Precatalyst Activation and Recovery

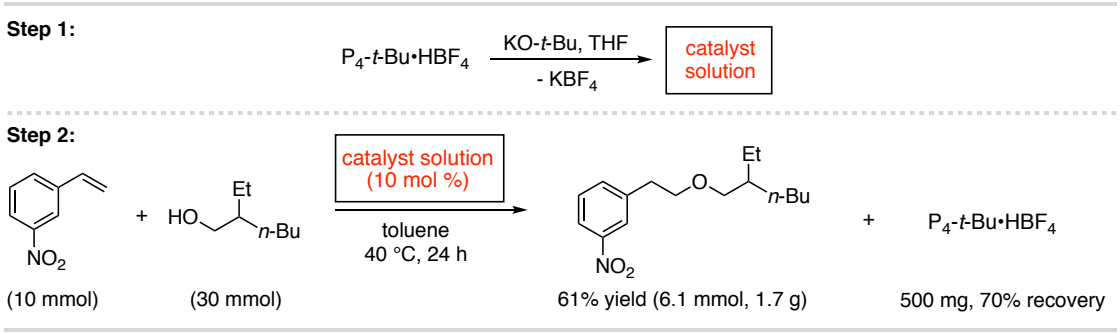

Figure A1-28. Superbase precatalyst activation and recovery for an alcohol addition reaction.

Procedure for Step 1: In a nitrogen-filled glovebox, to an oven-dried 4 mL reaction vial (Thermo Scientific B7990-2) containing a solution of potassium *tert*-butoxide (112 mg, 1.0 mmol) in THF (1.25 mL) was added P_4-*t*-Bu·HBF_4[5] (721 mg, 1.0 mmol) and the mixture was stirred for 2 min. The precipitate was removed by passing the mixture through a short cotton plug (~ 1 cm) in a glass pipette. The filtrate was directly used as the catalyst solution in **Step 2**.

Procedure for Step 2: In an oven-dried 25 mL round-bottom flask containing a magnetic stir bar, 3-nitrostyrene (1.49 g, 10 mmol, 1.0 equiv) and 2-ethyl-1-hexanol (3.91 g, 30 mmol, 3.0 equiv) were dissolved in toluene (10 mL). To the solution was added the P_4-*t*-Bu catalyst solution from **Step 1** (1.0 mmol, 0.1 equiv assumed as calculated from original quantity of P_4-*t*-Bu·HBF_4 used). The flask was sealed with a rubber septum, removed from the glovebox and inserted into an oil bath preheated to 70 °C. The reaction mixture was stirred for 24 h. The reaction mixture was cooled to rt and 1M HCl (10 mL) was added. The mixture was extracted with diethyl ether (3 x 15 mL). To the aqueous phase was slowly added saturated aqueous $NaBF_4$ (approximately 10 mL) until a white solid began to precipitate. After 25 min, the precipitate was collected by filtration and dried under vacuum (500 mg, 0.69 mmol, 69% recovery of P_4-*t*-Bu·HBF_4 as confirmed by ^1H and ^{31}P NMR spectroscopy).[Error! Bookmark not defined.] The combined organic phase was dried over anhydrous Na_2SO_4, filtered and concentrated to a crude oil. The product was isolated by flash column chromatography (dichloromethane:hexane = 30:70, then ethyl acetate:hexane = 1:10) as a brown

oil (1.7 g, 6.1 mmol, 61% yield). **^{1}H NMR** (400 MHz, $CDCl_3$) δ 8.12 (t, J = 2.0 Hz, 1H), 8.05 – 8.09 (m, 1H), 7.57 (d, J = 7.6 Hz, 1H), 7.44 (t, J = 7.9 Hz, 1H), 3.65 (t, J = 6.4 Hz, 2H), 3.30 (d, J = 5.9 Hz, 2H), 2.97 (t, J = 6.4 Hz, 2H), 1.42 – 1.51 (m, 1H), 1.40 – 1.15 (m, 9H), 0.90 – 0.78 (m, 6H). The spectroscopic data matches our previous report.**Error! Bookmark not defined.**

Note on precatalyst generality: the above procedure was applied to three other substrate combinations to demonstrate its generality. Thus, use of the precatalyst procedure to access hydroetherification products **3**, **7** and **19** (from Schemes 6 and 8) resulted in identical yields as using P_4-*t*-Bu directly. As a control, we found that use of KO-*t*-Bu as the base in the absence of the P_4-*t*-Bu·HBF_4 precatalyst did not produce any product.

A1.7 Starting Material Preparation and Characterization

General overview: 1-Bromo-3-vinylbenzene, 1-(trifluoromethyl-4-vinylbenzene and 1-vinylnaphthylene were purchased from Combi-Blocks and used as received. 1,3-dichloro-2-vinylbenzene[11], 2-chloro-3-vinylpyridine[12], 1-nitro-3-vinylbenzene[13], 1-(trifluoromethoxy)-2-vinylbenzene[14], 1-chloro-4-(trifluoromethyl)-2-vinylbenzene[15], 2-chloro-1-(trifluoromethyl)-3-vinylbenzene[16], 4-methyl-2-nitro-1-vinylbenzene[17], 1,2-dimethoxy-4-nitro-5-vinylbenzene[18], 2-(4-vinylphenyl)pyridine[19], 1-iodo-4-vinylbenzene[20], (trifluoromethyl)(4-vinylphenyl)sulfane[21], (2-methoxyethyl)benzene[22], 1-(2-methoxyethyl)-4-(trifluoromethyl)benzene[22],1-methoxy-4-(2-methoxyethyl)benzene[22], and 1-(2-butoxyethyl)-4-methoxybenzene[23] were prepared according to the general procedures below unless otherwise noted. Characterization of the listed compounds matched reported literature data.

A1.7.1 Preparation of Styrene Compounds.

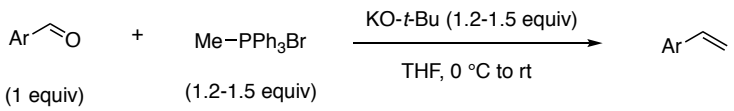

General procedure for styrene preparation: Methyltriphenylphosphonium bromide (1.2-1.5 eq) was added to an oven-dried round bottom flask containing a magnetic stir bar. Anhydrous THF (20 mL per 1 g of aldehyde) was added and the mixture was stirred and cooled to 0 °C using an ice bath. KO-*t*-Bu (1.2-1.5 eq) was slowly added, leading to a yellow-colored solution. The reaction mixture was stirred for 15 min at 0 °C and then the appropriate aldehyde (1 equiv) was added slowly via syringe. The mixture was stirred at 0 °C until the aldehyde was consumed as indicated by TLC analysis (approximately 15 to 30 min). The reaction solution was quenched with H_2O (equal volume to THF used) and extracted with ethyl acetate (3 x reaction volume). The organic layer was dried over Na_2SO_4 and concentrated *in vacuo.* Silica gel chromatography was used to purify all substrates using the indicated eluent conditions.

4-nitro-4'-vinyl-1,1'-biphenyl

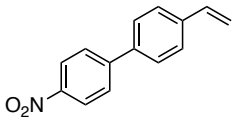

The title compound was prepared according to the above general procedure from 4'-nitro-[1,1'-biphenyl]-4-carbaldehyde (5.91 g, 26 mmol, 1 equiv), methyltriphenylphosphonium bromide (12.07 g, 33.8 mmol, 1.3 eq), KO-*t*-Bu (3.79 g, 33.8 mmol, 1.3 equiv), and THF (100 mL). Purification by silica gel chromatography (50% DCM/hexanes) yielded the product as a light-yellow powder (4.86 g, 21.6 mmol, 83% yield). **^{1}H NMR** (400 MHz, $CDCl_3$) δ 8.29 (d, J = 8.8 Hz, 2H), 7.74 (d, J = 8.8 Hz, 2H), 7.60 (d, J = 8.4 Hz, 2H), 7.53 (d, J = 8.4 Hz, 2H), 6.77 (dd, J = 17.6, 10.9 Hz, 1H), 5.85 (d, J = 17.6 Hz, 1H), 5.35 (d, J = 10.9 Hz, 1H). **^{13}C NMR** (101 MHz, $CDCl_3$) δ 147.2, 147.2, 138.4, 138.1, 136.1, 127.7, 127.1, 124.3, 115.3. **GCMS (EI)** M^+ calcd. for $[C_{14}H_{11}NO_2]^+$ 225.1, 225.1 found. **IR** (neat): 2926.3, 2873.7, 1672.0, 1518.3, 1496.3, 1438.1, 1331.8, 12167.6, 1218.3 cm^{-1}. **Melting point** = 153 – 155 °C.

2-chloro-1,4-difluoro-3-vinylbenzene

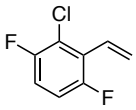

The title compound was prepared according to the above general procedure from methyltriphenylphosphonium bromide (4.30 g, 12 mmol, 1.2 equiv), KO-*t*-Bu (1.35 g, 12 mmol, 1.2 equiv), and 2-chloro-3,6-difluorobenzaldehyde (1.76 g, 10 mmol, 1.0 equiv). Flash column chromatography with hexanes yielded the title product as a colorless liquid (1.20 g, 6.87 mmol, 69% yield). **^{1}H NMR** (400 MHz, $CDCl_3$) δ 7.06 – 6.90 (m, 2H), 6.79 (dd, *J* = 17.9, 11.9 Hz, 1H), 6.02 (dt, *J* = 17.9, 1.4 Hz, 1H), 5.71 (dt, *J* = 11.9, 1.8 Hz, 1H). **^{13}C NMR** (101 MHz, $CDCl_3$) δ 157.2 (dd, *J* = 248.1, 2.0 Hz), 155.0 (dd, *J* = 243.5, 2.8 Hz), 127.1 (dd, *J* = 2.9, 1.5 Hz), 125.8 (d, *J* = 16.1 Hz), 123.5 (d, *J* = 11.8 Hz), 121.4 (dd, *J* = 19.4, 6.4 Hz), 115.0(dd, *J* = 8.9, 2.3 Hz), 114.7 (dd, *J* = 8.9, 4.2 Hz). **^{19}F NMR** (376 MHz, $CDCl_3$) δ -117.45 (d, *J* = 15.2 Hz), -118.02 (d, *J* = 15.2 Hz). **LRMS** $[M+H]^+$ calcd. for $[C_8H_6ClF_2]^+$ 175.0, found 175.0. **IR** (neat, cm^{-1}) 3100.3, 1851.7, 1473.0, 1383.6, 1231.9, 966.3, 933.6, 861.3, 808.1.

***N*-methyl-*N*-phenyl-2-vinylbenzamide**

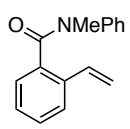

The title compound was prepared from 2-iodobenzoic acid. To an oven-dried round bottom flask containing a stir bar and 2-iodobenzoic acid (2 g, 8.0 mmol, 1 equiv) was added thionyl chloride (10 mL) and the mixture heated at 75 °C for 20 h. The reaction solution was allowed to cool to rt and then was concentrated under reduced pressure. To the crude mixture was added dichloromethane (25 mL) and the solution was cooled to 0 °C using an ice bath. Triethylamine (1.84 mL, 1.33 g, 13.2 mmol, 1.7 equiv) and *N*-methylaniline (1.42 mL, 1.47 g, 13.7 mmol, 1.7 equiv) were added dropwise. The reaction solution was stirred at rt for 12 h. The reaction mixture was concentrated under reduced pressure and flash chromatography (ethyl acetate/hexanes

= 1:2.5) yielded 2-iodo-*N*-methyl-*N*-phenylbenzamide as a yellow liquid (2.70 g, 8 mmol, >99% yield).[24]

Next, in a nitrogen-filled glovebox, 2-iodo-*N*-methyl-*N*-phenylbenzamide (from above step, 2.0 g, 5.9 mmol, 1 equiv), potassium trifluoro(vinyl)borate (0.99 g, 7.38 mmol, 1.25 equiv), palladium(II) chloride (20.9 mg, 0.12 mmol, 2 mol%), triphenylphosphine (103.5 mg, 0.35 mmol, 6 mol%), cesium carbonate (5.77 g, 17.7 mmol, 3 equiv), and THF/H_2O 9:1 solvent mixture (12 mL) were added to an oven-dried round bottom flask with magnetic stir bar. The round bottom flask was removed from the glovebox and connected to a reflux condenser capped with a rubber septum. The connected condenser and round bottom flask were evacuated and backfilled with nitrogen three times. A nitrogen-filled balloon was attached and the reaction solution was stirred at 85 °C for 24 h. The reaction solution was cooled to rt, water (20 mL) was added, and the solution was washed three times with ethyl acetate (20 mL), the combined organic layers were washed with brine and dried over sodium sulfate. The organic layer was concentrated and silica gel column chromatography (ethyl acetate/hexanes = 1:3) yielded product as a brown oil (1.05 g, 4.4 mmol, 75% yield). **^{1}H NMR** (400 MHz, $CDCl_3$) δ 7.55 – 6.95 (m, 9H), 6.90 (dd, J = 17.5, 11.0 Hz, 1H), 5.68 (d, J = 17.5 Hz, 1H), 5.34 (d, J = 11.0 Hz, 1H), 3.50 (s, 3H). **^{13}C NMR** (101 MHz, $CDCl_3$) (101 MHz, $CDCl_3$) δ 170.8, 135.8, 134.3, 129.8, 129.3, 129.0, 128.9, 127.8, 127.8, 127.1, 127.1, 126.9, 126.8, 126.6, 125.3, 116.3, 37.4 (**note**: significant broadening observed in ^{13}C NMR spectrum due to amide rotamers). **HRMS [DART]** $[M+H]^+$ calcd. for $[C_{16}H_{16}NO]^+$ 238.1226, 238.1257 found. **IR** (neat): 3061.3, 2933.0, 1640.4, 1493.6, 1364.3, 1112.2 cm^{-1}.

A1.7.2 Preparation of ether compounds.

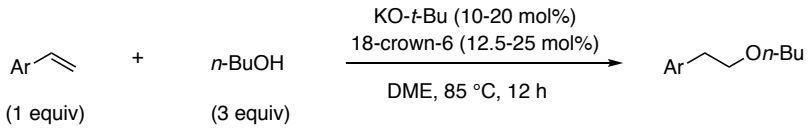

Preparation of β-phenethyl ethers from aryl alkenes general procedure: Aryl alkene (1 equiv) was added to an oven-dried round bottom flask containing a magnetic stir bar. 18-Crown-6 (12.5 – 25 mol%), KO-*t*-Bu (10 - 20 mol%), *n*-butanol (3 equiv) and 1,2-dimethoxyethane (1-1.5 M with respect to alkene) were added to the flask (solid reagents were added to first, followed by solvent, then liquid reagents). The reaction solution was refluxed at 85 °C for 12 h. The reaction mixture was then cooled to rt and neutralized with H_2O, extracted with ethyl acetate (3 x reaction volume) and dried over Na_2SO_4. The combined organic layer was concentrated *in vacuo* and purified via silica gel chromatography.

2-(2-butoxyethyl)-1,3-dichlorobenzene

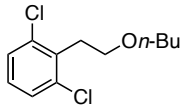

The title compound was prepared according to the above general procedure using 1,3-dichloro-2-vinylbenzene (1.00 g, 5.8 mmol, 1 equiv), *n*-butanol (1.59 mL, 17.3 mmol, 3 equiv), KO-*t*-Bu (64.9 mg, 0.58 mmol, 10 mol%), 18-crown-6 (229.7 mg, 0.87 mmol, 15 mol%), and DME (5.8 mL). Purification by silica gel chromatography (hexanes then 10% diethyl ether/hexanes) yielded the product as a colorless oil (1.02 g, 4.23 mmol, 73% yield). **^{1}H NMR** (400 MHz, $CDCl_3$) δ 7.19 (d, J = 7.9 Hz, 2H), 7.00 (t, J = 8.0 Hz, 1H), 3.51 (d, J = 7.0 Hz, 2H), 3.40 (t, J = 6.6 Hz, 2H), 3.18(t, J = 7.0, 2H), 1.57 – 1.43 (m, 2H), 1.30 (sextet, J = 7.6 Hz, 2H), 0.84 (t, J = 7.4 Hz, 3H). **^{13}C NMR** (101 MHz, $CDCl_3$) δ 136.0, 134.7, 128.3, 128.1, 70.9, 68.2, 32.0, 31.8, 19.4, 14.1. **HRMS [DART]** $[M+H]^+$ calcd. for $[C_{12}H_{17}Cl_2O]^+$ 247.0651. 247.0652 found. **IR** (neat): 2957.2, 2932.7, 2862.9, 1561.66, 1434.9, 1105.8, 773.7 cm^{-1}.

2-(4-(2-butoxyethyl)phenyl)pyridine

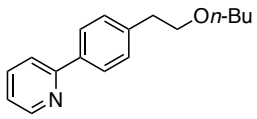

The title compound was prepared according to the above general procedure using 2-(4-vinylphenyl)pyridine (3.81 g, 21 mmol, 1 equiv), *n*-butanol (5.76

mL, 63 mmol, 3 equiv), 18-crown-6 (0.83 g, 3.15 mmol, 15 mol%), KO-*t*-Bu (0.215 g, 2.63 mmol, 12.5 mol%), and DME (20 mL). Purification by silica gel chromatography (100% DCM, then 25% ethyl acetate/hexanes) yielded the product as a colorless oil (510 mg, 2 mmol, 10% yield). **^{1}H NMR** (400 MHz, $CDCl_3$) δ 8.67 (dt, J = 4.8, 1.4 Hz, 1H), 7.96 – 7.88 (m, 2H), 7.74 – 7.65 (m, 2H), 7.37 – 7.29 (m, 2H), 7.20 – 7.14 (m, 1H), 3.65 (t, J = 7.2 Hz, 2H), 3.44 (t, J = 6.6 Hz, 2H), 2.93 (t, J = 7.2 Hz, 2H), 1.52 – 1.59 (m, 2H), 1.43 – 1.30 (m, 2H), 0.91 (t, J = 7.4 Hz, 3H). **^{13}C NMR** (101 MHz, $CDCl_3$) δ 157.4, 149.7, 140.2, 137.4, 136.7, 129.4, 126.9, 121.9, 120.3, 71.6, 70.9, 36.2, 31.9, 19.4, 14.0. **HRMS [DART]** $[M+H]^+$ calcd. for $[C_{17}H_{22}NO]^+$ 256.1696. 256.1724 found. **IR** (neat): 2955.91, 2931.1, 2861.2, 1586.7, 1465.7, 1105.4 cm^{-1}.

1-(2-butoxyethyl)-4-iodobenzene

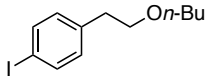

The title compound was prepared according to the above general procedure from 1-iodo-4-vinylbenzene (2.07 g, 9 mmol, 1 equiv), *n*-butanol (2.00 g, 27 mmol, 3 equiv), 18-crown-6 (0.357 g, 1.35 mmol, 15 mol%), KO-*t*-Bu (0.126 g, 1.125 mmol, 12.5 mol%), and DME (9 mL). Purification by silica gel chromatography (hexanes then 2% ethyl acetate/hexanes) yielded the product as a yellow liquid (303 mg, 1.0 mmol, 11% yield). **^{1}H NMR** (400 MHz, $CDCl_3$) δ 7.60 (d, J = 8.2 Hz, 2H), 6.98 (d, J = 8.2 Hz, 2H), 3.59 (t, J = 7.0 Hz, 2H), 3.42 (t, J = 6.6 Hz, 2H), 2.81 (t, J = 7.0 Hz, 2H), 1.60 – 1.48 (m, 2H), 1.41 – 1.33 (m, 2H), 0.90 (t, J = 7.4 Hz, 3H). **^{13}C NMR** (101 MHz, $CDCl_3$) δ 139.1, 137.5, 131.2, 91.4, 71.4, 71.0, 36.0, 31.9, 19.5, 14.1. **GCMS (EI)** M^+ calcd. for $[C_{12}H_{17}IO]^+$ 304.0, 304.1 found. **IR** (neat): 2955.3, 2929.9, 2860.2, 1484.3, 1107.1, 800.4 cm^{-1}.

1-bromo-3-(2-butoxyethyl)benzene

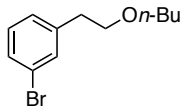

The title compound was prepared according to the above general procedure from 3-bromostyrene (1.464 g, 8 mmol, 1 equiv), *n*-butanol (1.78 g, 24 mmol, 3 equiv), KO-*t*-Bu (0.18 g, 1.6 mmol, 20 mol%), 18-crown-6 (0.48 g, 1.8 mmol, 22.5 mol%), and DME (5.3 mL). Purification by silica gel chromatography (hexanes then 10% ethyl acetate/hexanes) yielded the product as a colorless liquid (0.288 g, 1.12 mmol, 14% yield). **^{1}H NMR** (400 MHz, $CDCl_3$) δ 7.37 – 7.40 (m, 1H), 7.31 – 7.36 (m, 1H), 7.19 – 7.10 (m, 2H), 3.61 (t, J = 7.0 Hz, 2H), 3.43 (t, J = 6.6 Hz, 2H), 2.85 (t, J = 7.0 Hz, 2H), 1.59 – 1.49 (m, 2H), 1.31 – 1.40 (m, 2H), 0.91 (t, J = 7.4 Hz, 3H). **^{13}C NMR** (101 MHz, $CDCl_3$) δ 141.8, 132.1, 129.9, 129.4, 127.7, 122.5, 71.4, 71.0, 36.1, 31.9, 19.5, 14.0. **LCMS** $[M+H]^+$ calcd. for $[C_{12}H_{18}BrO]^+$ 257.1, 257.1 found. **IR** (neat): 2956.4, 2931.2, 2861.3, 1567.2, 1473.2, 1108.5, 776.6, 692.4 cm^{-1}.

(4-(2-butoxyethyl)phenyl)(trifluoromethyl)sulfane

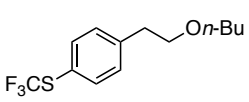

The title compound was prepared according to the above general procedure from (trifluoromethyl)(4-vinylphenyl)sulfane (1.634 g, 8 mmol, 1 equiv), *n*-butanol (4.90 g, 24 mmol, 3 equiv), KO-*t*-Bu (0.112 g, 1.2 mmol, 12.5 mol%), 18-crown-6 (0.317 g, 1.2 mmol, 15 mol%), and DME (5 mL). Purification by silica gel chromatography (hexanes then 5% ethyl acetate/hexanes) yielded the product as a yellow liquid (0.50 g, 1.8 mmol, 22% yield). **^{1}H NMR** (400 MHz, $CDCl_3$) δ 7.57 (d, J = 8.2 Hz, 2H), 7.29 (d, J = 8.2 Hz, 2H), 3.64 (t, J = 6.9 Hz, 2H), 3.44 (t, J = 6.6 Hz, 2H), 2.92 (t, J = 6.9 Hz, 2H), 1.61 – 1.50 (m, 2H), 1.42 – 1.28 (m, 2H), 0.91 (t, J = 7.4 Hz, 3H). **^{13}C NMR** (101 MHz, $CDCl_3$) δ 142.9, 136.5, 130.2, 129.7 (q, J = 304.9 Hz), 121.8 (q, J = 2.0 Hz), 71.2, 71.0, 36.2, 31.9, 19.5, 14.0. **^{19}F NMR** (376 MHz, $CDCl_3$) δ -43.0. **HRMS [DART]** $[M+H]^+$ calcd. for $[C_{13}H_{18}F_3OS]^+$ 279.1025, 279.1662 found. **IR** (neat): 2958.9, 2934.0, 2863.9, 1492.6, 1362.4, 1152.8, 1108.0, 1085.0 cm^{-1}.

1-(2-butoxyethyl)-4-(trifluoromethyl)benzene

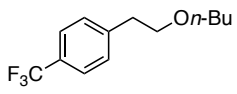

The title compound was prepared according to the above general procedure from 1-(trifluoromethyl)-4-vinylbenzene (3.96 g, 23 mmol, 1 equiv), *n*-butanol (5.1 g, 69 mmol, 3 equiv), KO-*t*-Bu (0.258 g, 2.3 mmol, 10 mol%), 18-crown-6 (0.912 g, 3.45 mmol, 15 mol%), and DME (23 mL). Purification by silica gel chromatography (hexanes then 10% ethyl acetate/hexanes) yielded the product as a colorless liquid (1.5 g, 6.1 mmol, 26% yield). **^{1}H NMR** (400 MHz, $CDCl_3$) δ 7.54 (d, J = 7.8 Hz, 2H), 7.34 (d, J = 7.8 Hz, 2H), 3.64 (t, J = 6.9 Hz, 2H), 3.43 (t, J = 6.6 Hz, 2H), 2.93 (t, J = 6.9 Hz, 2H), 1.60 – 1.49 (m, 2H), 1.41 – 1.23 (m, 2H), 0.90 (t, J = 7.4 Hz, 3H). The spectroscopic data matches our previous report.**Error! Bookmark not defined.**

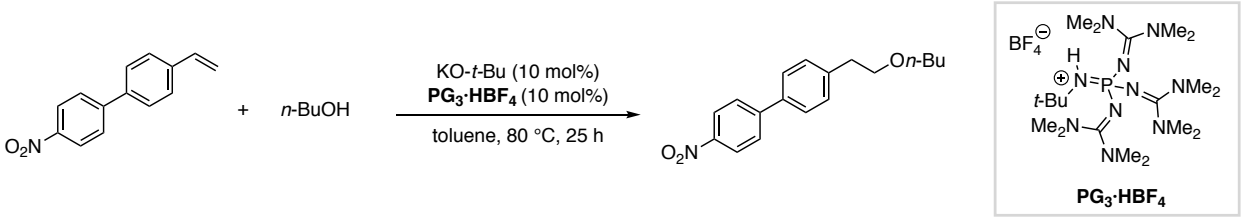

4-(2-butoxyethyl)-4'-nitro-1,1'-biphenyl

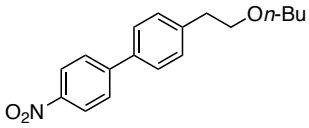

The title compound was prepared according to the following procedure: KO-*t*-Bu (0.247 g, 2.2 mmol, 10 mol%), guanidine, *N*",*N*"",*N*"""-(butylphosphinimylidyne)tris[*N,N,N',N'*-tetramethyl-, tetrafluoroborate[25] ($PG_3 \cdot HBF_4$, 1.17 g, 2.2 mmol, 10 mol%), and were added to an oven-dried round bottom flask containing a magnetic stir bar and sealed with a rubber septum. A needle connected to a nitrogen/vacuum manifold was inserted through the septum; the flask was put under vacuum and refilled with nitrogen three times before inserting a nitrogen filled balloon. THF (17.6 mL) was added by syringe and the resulting mixture was stirred for 24 h at rt. A toluene (88 mL) solution containing 4-nitro-4'-vinyl-1,1'-

biphenyl (4.96 g, 22 mmol, 1 equiv) and *n*-butanol (4.89 g, 66 mmol, 3 equiv) was then added. The reaction mixture was heated to 80 °C in a silicon oil bath and stirred for 24 h. The reaction mixture was then cooled to rt and added to a separatory funnel containing H_2O (200 mL). The mixture was extracted with ethyl acetate (3 x 150 mL) and the organic extracts were dried with anhydrous Na_2SO_4 and concentrated *in vacuo*. Purification by silica gel chromatography (50% DCM/hexanes) yielded the product as a yellow liquid (0.253 g, 0.85 mmol, 4% yield). **^{1}H NMR** (400 MHz, $CDCl_3$) δ 8.28 (d, J = 8.8 Hz, 2H), 7.72 (d, J = 8.8 Hz, 2H), 7.56 (d, J = 8.1 Hz, 2H), 7.36 (d, J = 8.1 Hz, 2H), 3.67 (t, J = 7.0 Hz, 2H), 3.46 (t, J = 6.6 Hz, 2H), 2.95 (t, J = 7.0 Hz, 2H), 1.57 – 1.50 (m, 2H), 1.44 – 1.30 (m, 2H), 0.92 (t, J = 7.4 Hz, 3H). **^{13}C NMR** (101 MHz, $CDCl_3$) δ 147.7, 147.1, 140.6, 136.7, 129.9, 127.7, 127.4, 124.2, 71.5, 71.0, 36.2, 31.9, 19.5, 14.1. **HRMS [DART]** $[M+H]^+$ calcd. for $[C_{18}H_{22}NO_3]^+$ 300.1594, 300.1626 found. **IR** (neat): 2956.3, 2933.8, 2864.5, 2850.2, 1597.0, 1515.8, 1340.5, 1106.6, 820.0 cm^{-1}.

1-(2-butoxyethyl)-3-nitrobenzene

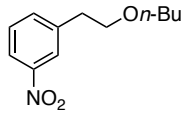

The title compound was prepared according to the same procedure as 4-(2-butoxyethyl)-4'-nitro-1,1'-biphenyl from 3-nitrostyrene (1.342 g, 7 mmol, 1 equiv), *n*-butanol (2.00 g, 27 mmol, 3 equiv), guanidine, *N″,N‴″,N⁗″*-(butylphosphinimylidyne) tris[*N,N,N′,N′*-tetramethyl-, tetrafluoroborate ($PG_3 \cdot HBF_4$,[Error! Bookmark not defined.] 0.48 g, 0.9 mmol, 13 mol%), KO-*t*-Bu (0.1 g, 0.9 mmol, 13 mol%), THF (2.2 mL), and toluene (9 mL). Purification by silica gel chromatography (50% DCM/hexanes) yielded the product as a yellow liquid (0.179 g, 0.80 mmol, 11% yield). **^{1}H NMR** (400 MHz, $CDCl_3$) δ 8.08 – 8.12 (m, 1H), 8.02 – 8.07 (m, 1H), 7.56 (m, 1H), 7.43 (t, J = 7.9 Hz, 1H), 3.65 (t, J = 6.6 Hz, 2H), 3.41 (t, J = 6.6 Hz, 2H), 2.96 (t, J = 6.5 Hz, 2H), 1.48 – 1.56 (m, 2H), 1.27 – 1.37 (m, 2H), 0.87 (t, J = 7.4 Hz, 3H). **^{13}C NMR**

(101 MHz, $CDCl_3$) δ 148.3, 141.7, 135.4, 129.1, 123.8, 121.4, 71.0, 70.7, 36.0, 31.8, 19.4, 13.9. **GCMS (EI)** M^+ calcd. for $[C_{12}H_{17}NO_3]^+$ 223.1, 223.1 found. **IR** (neat): 2957.4, 2931.7, 2863.9, 1525.6, 1348.3, 1108.2 cm^{-1}.

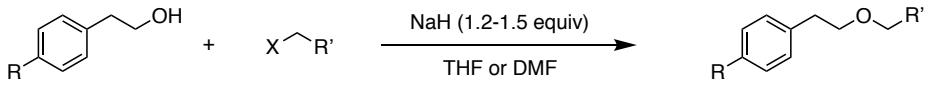

R = CF_3, H, OMe; R'= H, $CH_2CH_2CH_3$

Preparation of β-phenethyl ethers from β-phenethyl alcohol: β-phenethyl alcohol (1 equiv) was added to an oven-dried round bottom flask containing a stir bar. Anhydrous solvent (about 10 mL per g of β-phenethyl ether, THF or DMF) was added and the solution was cooled to 0 °C in an ice bath. Sodium hydride (1.2 to 1.5 equiv) was slowly added and the resulting mixture was stirred for 10 min. ***Warning: caution should be taken using NaH in DMF as heated mixtures can be explosive.***[26] Haloalkane (iodomethane or 1-bromobutane, 2.5 equiv) was then added slowly via syringe and the mixture was allowed to warm to rt and stirred overnight. The reaction solution was quenched with H_2O, extracted with ethyl acetate (3 x reaction volume) and dried over Na_2SO_4. The combined organic layer was concentrated *in vacuo* and purified via silica gel chromatography. The following compounds were prepared via the above method; 1-(2-methoxyethyl)-4-(trifluoromethyl)benzene[Error! Bookmark not defined.], (2-methoxyethyl)benzene[Error! Bookmark not defined.], 1-methoxy-4-(2-methoxyethyl)benzene[Error! Bookmark not defined.], and (2-butoxyethyl)benzene[Error! Bookmark not defined.]; the spectroscopic data matches previous literature reports. 1-(2-butoxyethyl)-4-methoxybenzene was prepared via the above method and is characterized below.

1-(2-butoxyethyl)-4-methoxybenzene

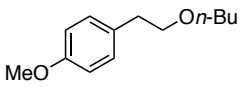

The title compound was prepared according to the above procedure using 2-(4-methoxyphenyl)ethan-1-ol (3.0 g, 18 mmol, 1 equiv), 1-bromobutane (6.1

g, 45 mmol, 2.5 equiv), NaH (0.91 g, 27 mmol, 1.5 equiv), and DMF (50 mL). Purification by silica gel chromatography (hexanes then 10% ethyl acetate/hexanes) yielded the product as a colorless liquid (2.05 g, 9.8 mmol, 51% yield). **^{1}H NMR** (400 MHz, $CDCl_3$) δ 7.19 – 7.10 (m, 2H), 6.88 – 6.79 (m, 2H), 3.79 (s, 3H), 3.59 (t, J = 7.3 Hz, 2H), 3.44 (t, J = 6.7 Hz, 2H), 2.83 (t, J = 7.3 Hz, 2H), 1.63 – 1.50 (m, 2H), 1.43 – 1.30 (m, 2H), 0.92 (t, J = 7.4 Hz, 3H). **^{13}C NMR** (101 MHz, $CDCl_3$) δ 158.1, 131.3, 129.9, 113.9, 72.2, 70.9, 55.3, 35.6, 32.0, 19.5, 14.0. **HRMS [DART]** [M+H]$^{+}$ calcd. for $[C_{13}H_{21}O_2]^{+}$ 209.1536, 209.1546 found. **IR** (neat): 2932.5, 2865.5, 2833.6, 1511.8, 1243.4, 1111.1, 1034.7 cm^{-1}.

A1.9 References

[1] Chaosheng, L.; Bandar, J. S. Superbase-Catalyzed anti-Markovnikov Alcohol Addition Reactions to Aryl Alkenes. *J. Am. Chem. Soc.* **2018**, *140*, 3547–3550.

[2] Valkonen, A.; Sievänen, E.; Ikonen, S.; Lukashev, N. V.; Donez, P. A.; Averin, A. D.; Lahtinen, M.; Kolehmainen, E. Novel Lithocholaphanes: Syntheses, NMR, MS, and Molecular Modeling Studies. *J. Mol. Struct*. **2007**, *846*, 65–73.

[3] Meyers, A. I.; Knaus, G.; Kamata, K.; Ford, M. E. Asymmetric synthesis of R and S □-alkylalkanoic acids from metalation and alkylation of chiral 2-oxazolines. *J. Am. Chem. Soc*. **1976**, *98*, 567–576.

[4] Burnt, A. J.; Bailey, C. D.; Cons, B. D.; Edwards, S. J. Elsworth, J. D.; Pheko, T.; Willis, C. L. Bicyclic Oxygen Heterocycles from γ,δ-Unsaturated Alcohols: Synthetic Targets Inspired by Blepharocalyxin D. *Angew. Chem. Int. Ed*. **2012**, *51*, 3901–3904.

[5] Senda, Y.; Kanto, H.; Itoh, H. Controlling factors determining the regiochemistry of intramolecular alkoxymercuration. *J. Chem. Soc., Perkin Trans. 2* **1997**, 1143–1146.

[6] Sahoo, B.; Hopkinson, M. N.; Glorius, F. Combining Gold and Photoredox Catalysis: Visible Light-Mediated Oxy- and Aminoarylation of Alkenes. *J. Am. Chem. Soc*. **2013**, *135*, 5505–5508.

[7] Li, G.-Y.; Che, C.-M. Highly Selective Intra- and Intermolecular Coupling Reactions of Diazo Compounds to Form cis-Alkenes Using a Ruthenium Porphyrin Catalyst. *Org. Lett*. **2004**, *6*, 1621–1623.

[8] Pedroli, C.; Ravelli, D.; Protti, S.; Albini, A.; Fagnoni, M. Singlet vs Triplet Reactivity of Photogenerated α,n-Didehydrotoluenes. *J. Org. Chem*. **2017**, *82*, 6592–6603.

[9] Kim, Y.; Chang, S. Borane-Catalyzed Reductive α-Silylation of Conjugated Esters and Amides Leaving Carbonyl Groups Intact. *Angew. Chem. Int. Ed*. **2016**, *55*, 218–222.

[10] Schwesinger, R.; Schlemper, H. Peralkylated Polyaminophosphazenes— Extremely Strong, Neutral Nitrogen Bases. *Angew. Chem., Int. Ed*. **1987**, *26*, 1167–1169.

[11] Smith, C. R.; Rajanbabu, T. V. Low pressure vinylation of aryl and vinyl halides via Heck–Mizoroki reactions using ethylene. *Tetrahedron* **2010**, *66*, 1102–1110.

[12] Lafaye, K.; Nicolas, L.; Guérinot, A.; Reymond, S.; Cossy, J. Lewis Basicity Modulation of N-Heterocycles: A Key for Successful Cross-Metathesis. *Org. Lett*. **2014**, *16*, 4972–4975.

[13] Lebel, H.; Davi, M.; Díez-González, S.; Nolan, S. P. Copper−Carbene Complexes as Catalysts in the Synthesis of Functionalized Styrenes and Aliphatic Alkenes. *J. Org. Chem*. **2007**, *72*, 144–149.

[14] Wang, C. H.; White, A. R.; Schwartz, S. N.; Alluri, S.; Cattabiani, T. M.; Zhang, L. K.; C han, T. M.; Buevich, A. V.; Ganguly, A. K. Novel synthesis and functionalization of o rtho–ortho disubstituted biphenyls and a highly condensed novel heterocycle using radical cyclization reaction. *Tetrahedron* **2012***, 68*, 9750–9762

[15] Gülak, S.; Gieshoff, T. N.; von Wangelin, A. J. Olefin-Assisted Iron-Catalyzed Alkylation of Aryl Chlorides. *Adv. Synth. Catal.* **2013**, *355*, 2197–2202.

[16] Puleo, T. R.; Strong, A. J.; Bandar, J. S. Catalytic α-Selective Deuteration of Styrene Derivatives. *J. Am. Chem. Soc*. **2019**, *141*, 1467–1472.

[17] Yang, L.; Shi, L.; Xing, Q.; Huang, K.-W.; Xia, C.; Li, F. Enabling CO Insertion into o-Nitrostyrenes beyond Reduction for Selective Access to Indolin-2-one and Dihydroquinolin-2-one Derivatives. *ACS Catal.* **2018**, *8*, 10340–10348.

[18] Huleatt, P. B.; Lau, J.; Chua, S.; Tan, Y. L.; Duong, H. A.; Chai, C. L. L. Concise, efficient and practical assembly of bromo-5,6-dimethoxyindole building blocks. *Tetrahedron Lett*. **2011**, *52*, 1339–1342.

[19] Mizuno, H.; Takaya, J.; Iwasawa, N. Rhodium(I)-Catalyzed Direct Carboxylation of Arenes with CO2 via Chelation-Assisted C−H Bond Activation. *J. Am. Chem. Soc*. **2011**, *133*, 1251–1253.

[20] Tang, M.; Han, S.; Huang, S.; Huang, S.; Xie, L.-G. Carbosulfenylation of Alkenes with Organozinc Reagents and Dimethyl(methylthio)sulfonium Trifluoromethanesulfonate. *Org. Lett*. **2020**, *22*, 9729–9734.

[21] Shao, X.; Wang, X.; Yang, T.; Lu, L.; Shen, Q. An Electrophilic Hypervalent Iodine Reagent for Trifluoromethylthiolation. *Angew. Chem. Int. Ed*. **2013***, 52*, 3457–3460.

[22] Fleury-Brégeot, N.; Presset, M.; Beaumard, F.; Colombel, V.; Oehlrich, D.; Rombouts, F.; Molander, G. A. Suzuki–Miyaura Cross-Coupling of Potassium Alkoxyethyltrifluoroborates: Access to Aryl/Heteroarylethyloxy Motifs. *J. Org. Chem*. **2012**, *77*, 10399–10408.

[23] Sakai, N.; Moriya, T.; Konakahara, T. An Efficient One-Pot Synthesis of Unsymmetrical Ethers: A Directly Reductive Deoxygenation of Esters Using an InBr3/Et3SiH Catalytic System. *J. Org. Chem*. **2007**, *72*, 5920–5922.

[24] Zhang, G., Zhao, X., Yan, Y. and Ding, C. Direct Arylation under Catalysis of an Oxime-Derived Palladacycle: Search for a Phosphane-Free Method. *Eur. J. Org. Chem*. **2012**, 2012, 669–672.

[25] Kolomeitsev, A. A.; Koppel, I. A.; Rodima, T.; Barten, J.; Lork, E.; Röschenthaler, G.-V.; Kaljurand, I.; Kütt, A.; Koppel, I.; Mäemets, V. Leito, I. Guanidinophosphazenes: Design, Synthesis, and Basicity in THF and in the Gas Phase. *J. Am. Chem. Soc*. **2005**, *127*, 17656–17666.

[26] Yang, Q.; Sheng, M.; Henkelis, J. J.; Tu, S.; Wiensch, E.; Zhang, H.; Zhang, Y.; Tucker, C.; Ejeh, D E. Explosion Hazards of Sodium Hydride in Dimethyl Sulfoxide, N,N-Dimethylformamide, and N,N-Dimethylacetamide. *Org. Process Res. Dev*. **2019**, *23*, 2210–2217.

A1.10 Copies of NMR Spectra

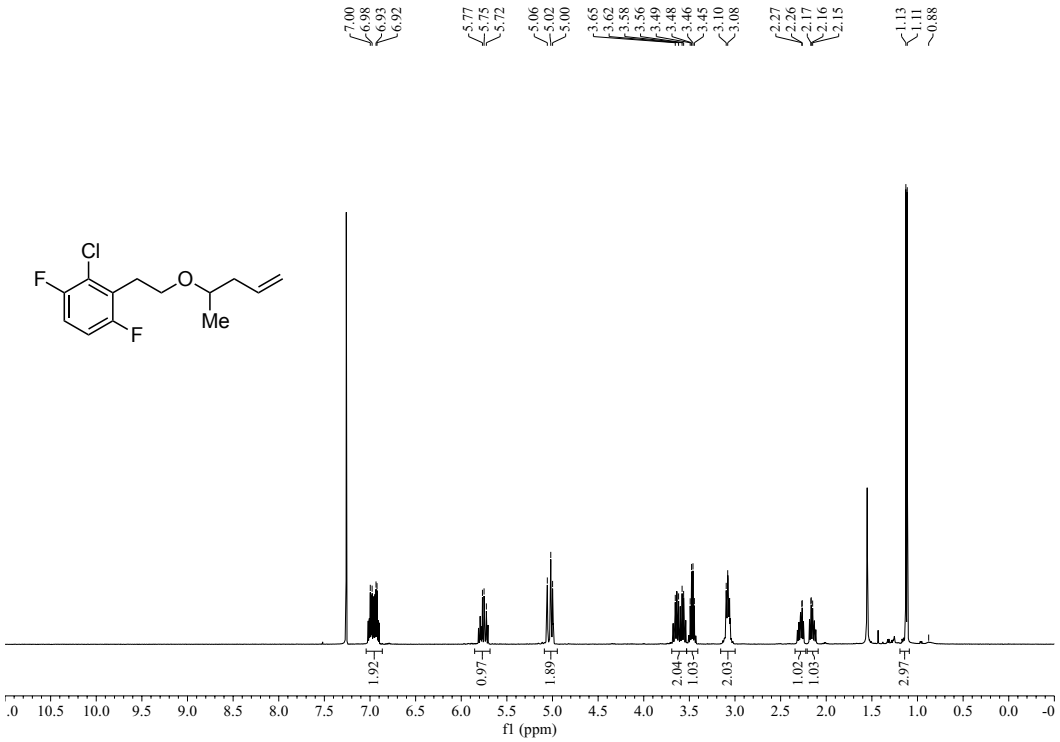

^{1}H NMR spectrum of (**2-46**) (400 MHz, $CDCl_3$)

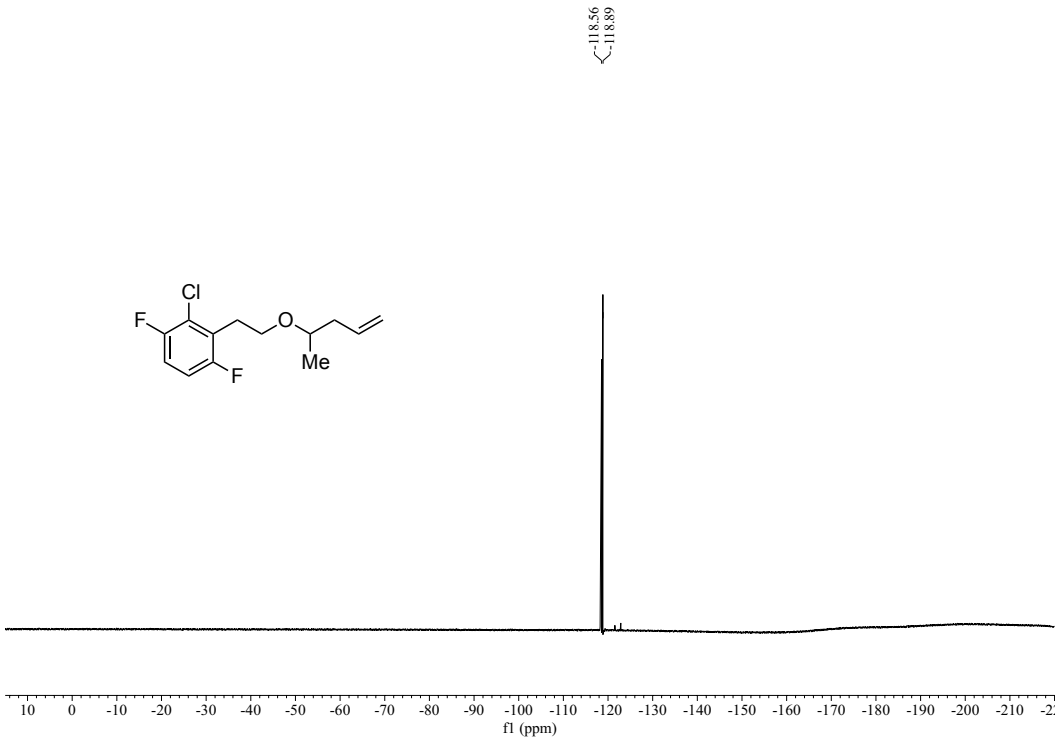

^{19}F NMR spectrum of (**2-46**) (376 MHz, $CDCl_3$)

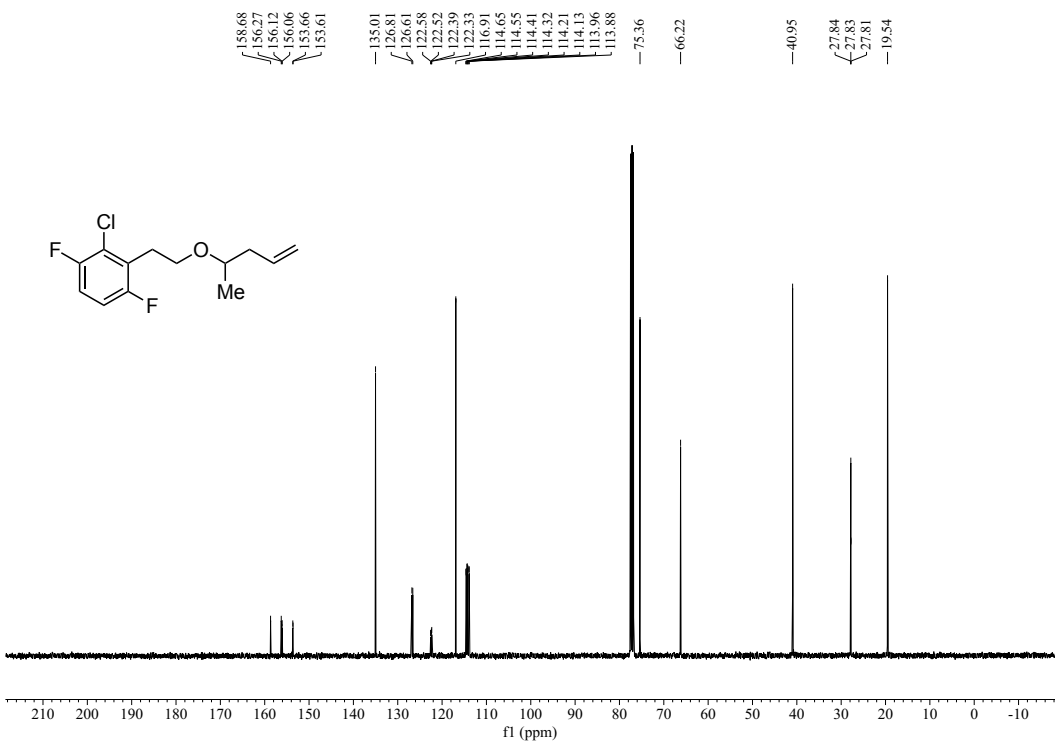

^{13}C NMR spectrum of (**2-46**) (101 MHz, $CDCl_3$)

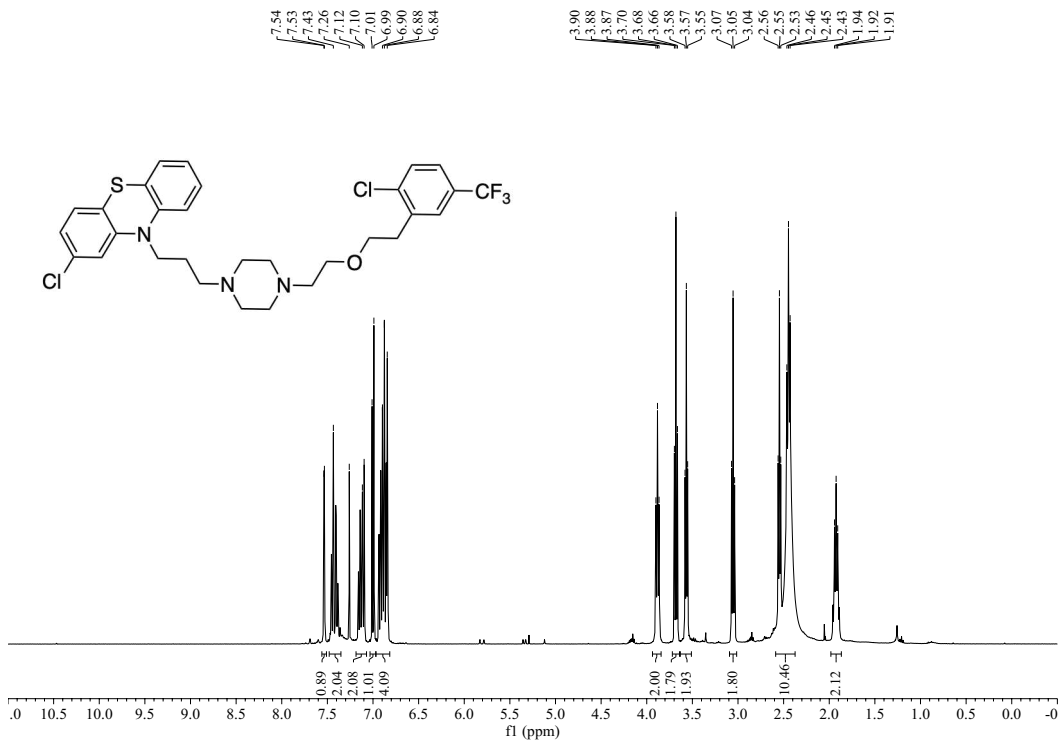

^{1}H NMR spectrum of (**2-23**) (400 MHz, $CDCl_3$)

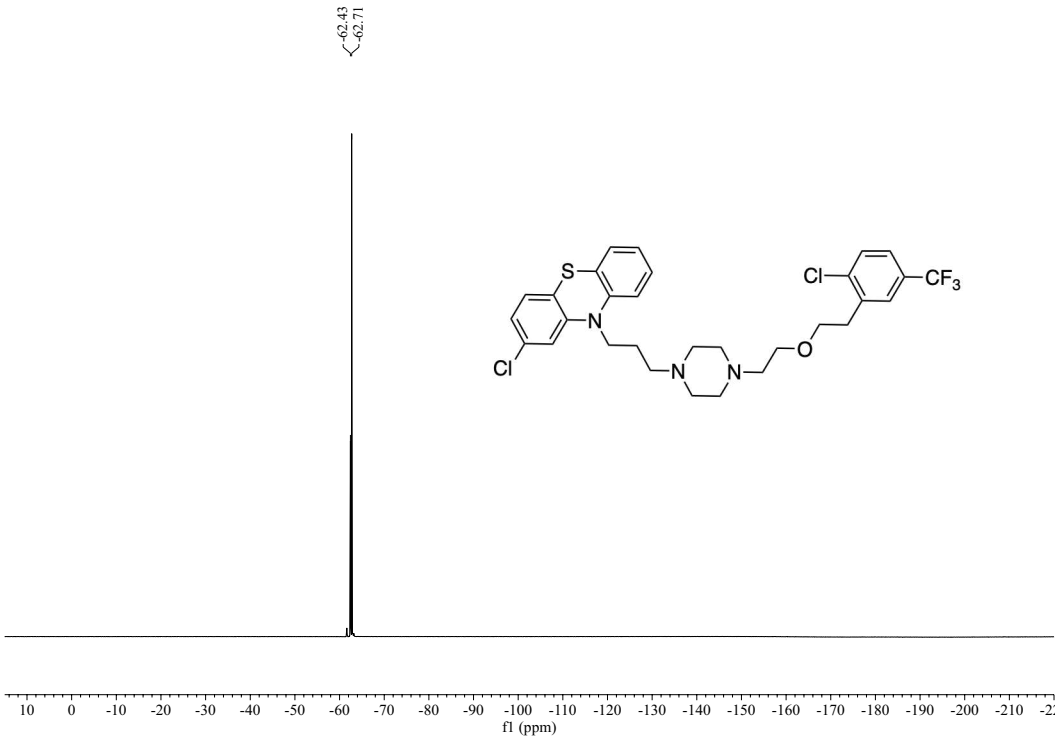

^{19}F NMR spectrum of (**2-23**) (376 MHz, $CDCl_3$)

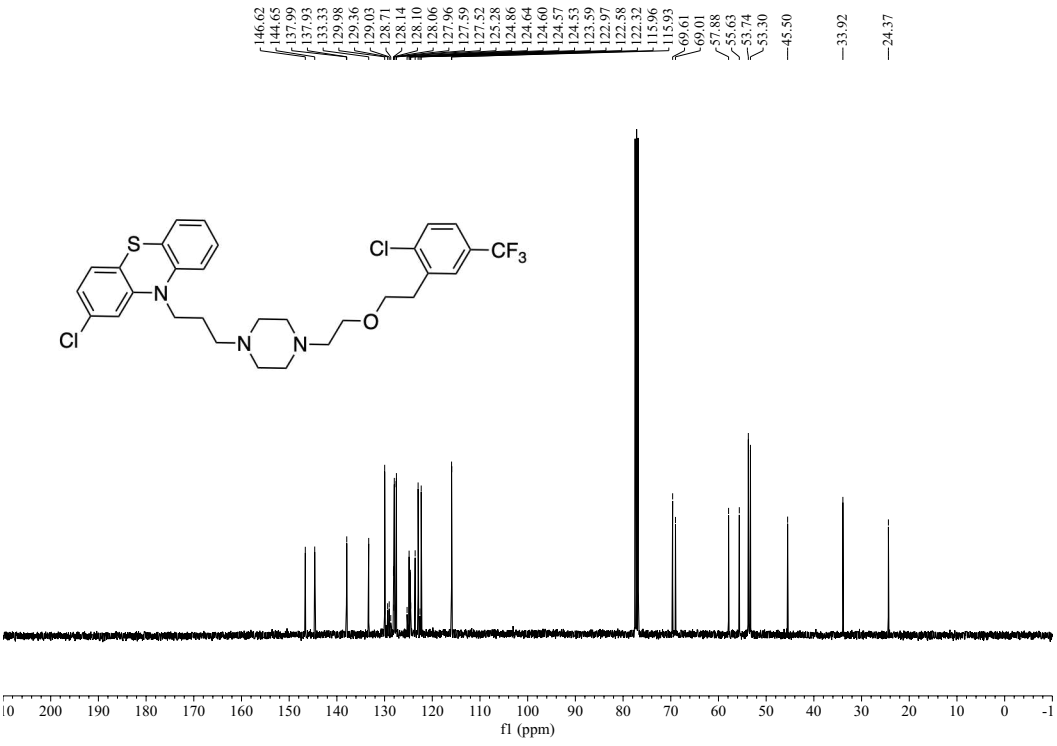

^{13}C NMR spectrum of (**2-23**) (101 MHz, $CDCl_3$)

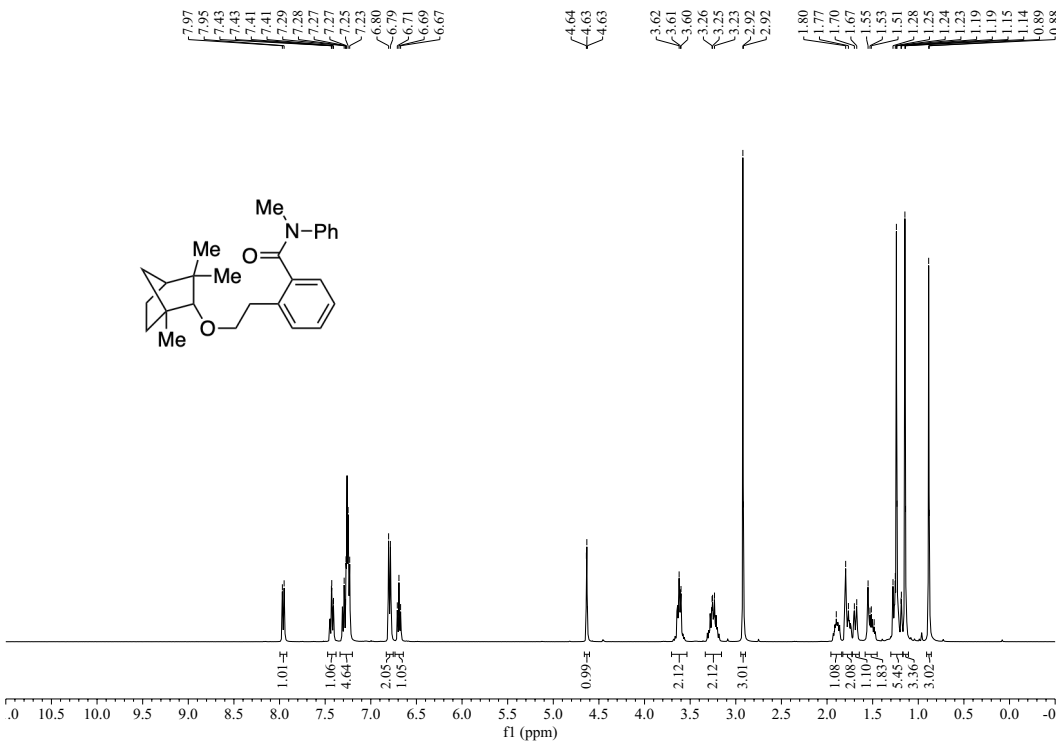

^{1}H NMR spectrum of (**2-25**) (400 MHz, $CDCl_3$)

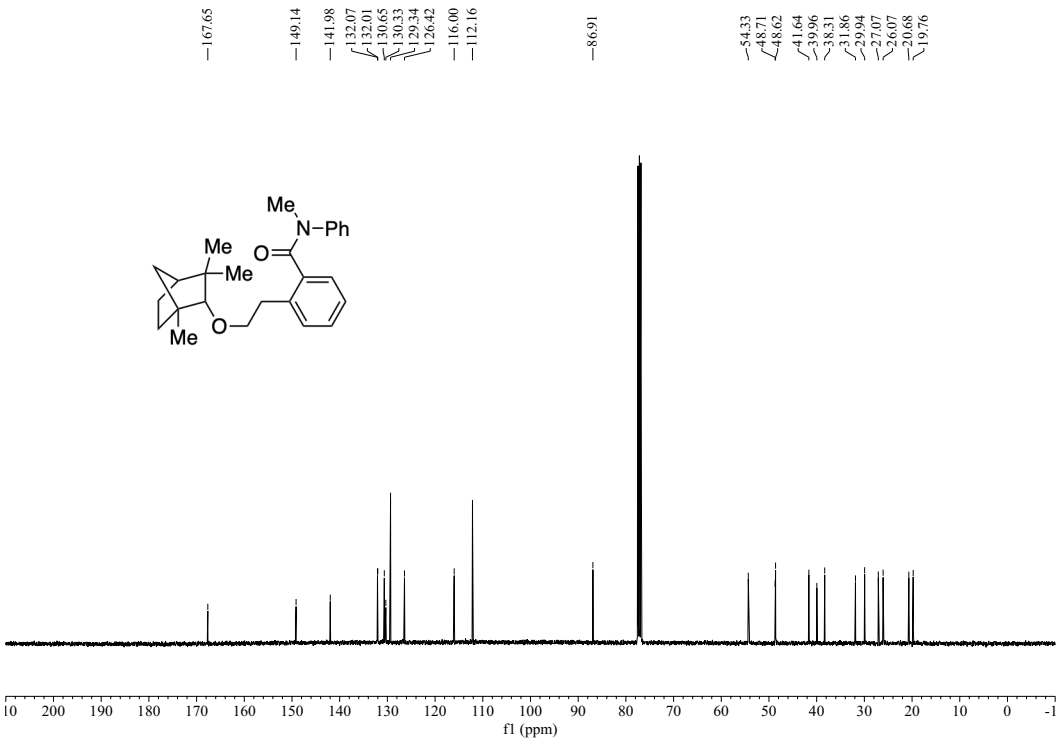

^{13}C NMR spectrum of (**2-25**) (101 MHz, $CDCl_3$)

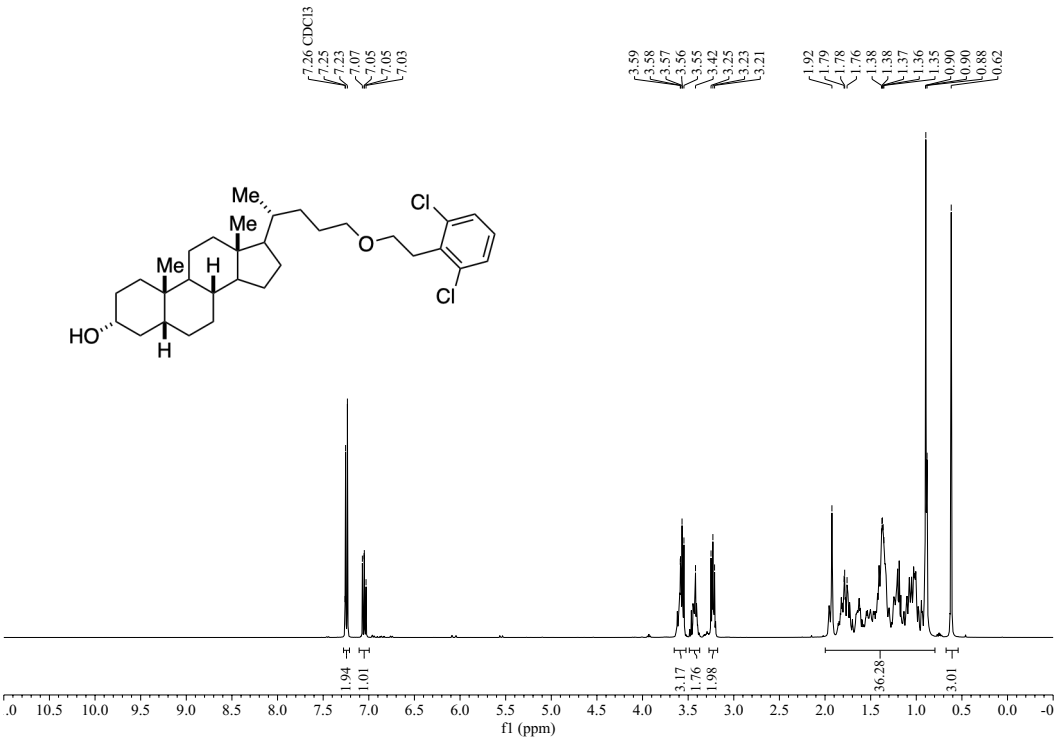

^{1}H NMR spectrum of (**2-24**) (400 MHz, $CDCl_3$)

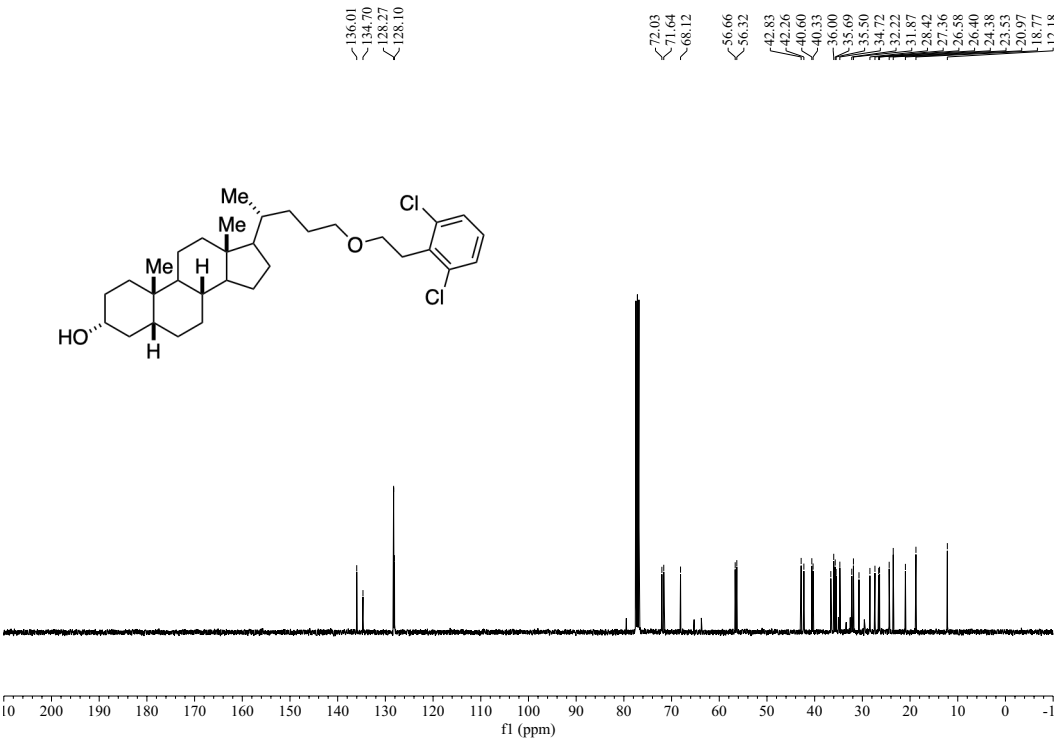

^{13}C NMR spectrum of (**2-24**) (101 MHz, $CDCl_3$)

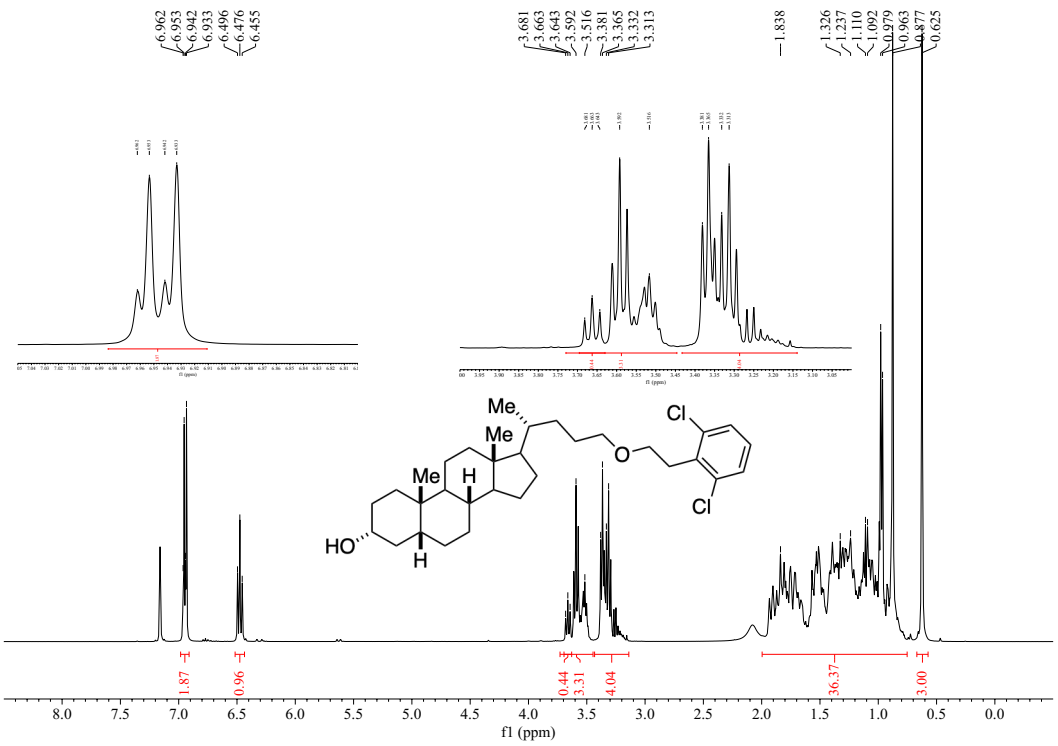

^{1}H NMR spectrum of (**2-24**) (400 MHz, C_6D_6)

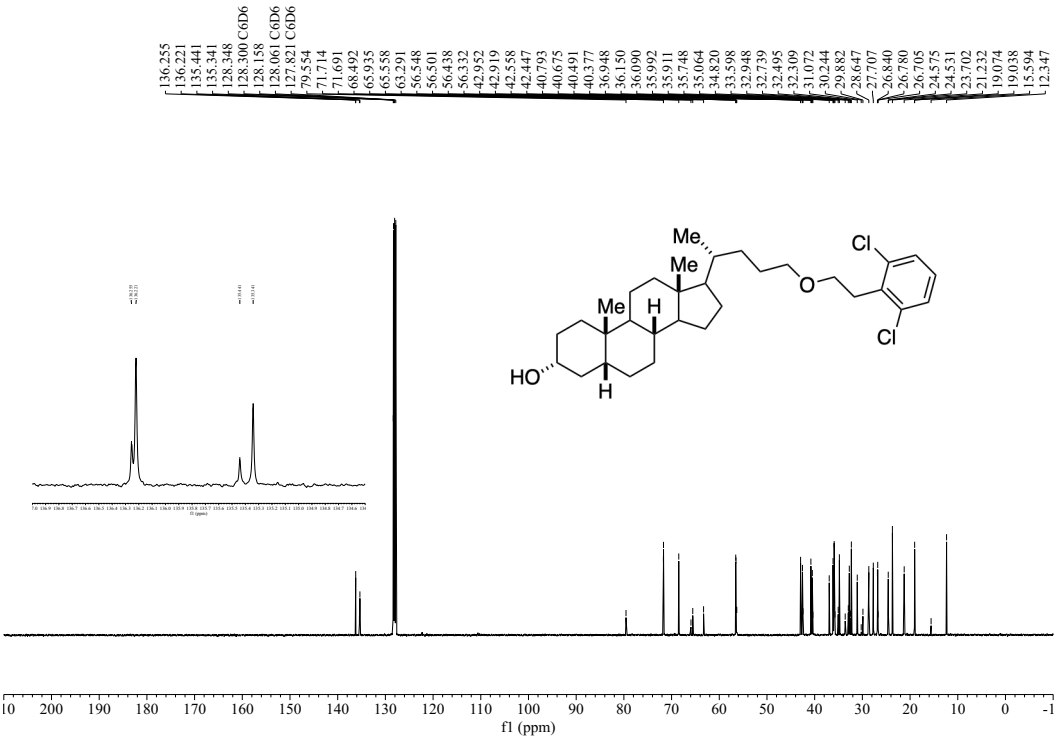

^{13}C NMR spectrum of (**2-24**) (101 MHz, C_6D_6)

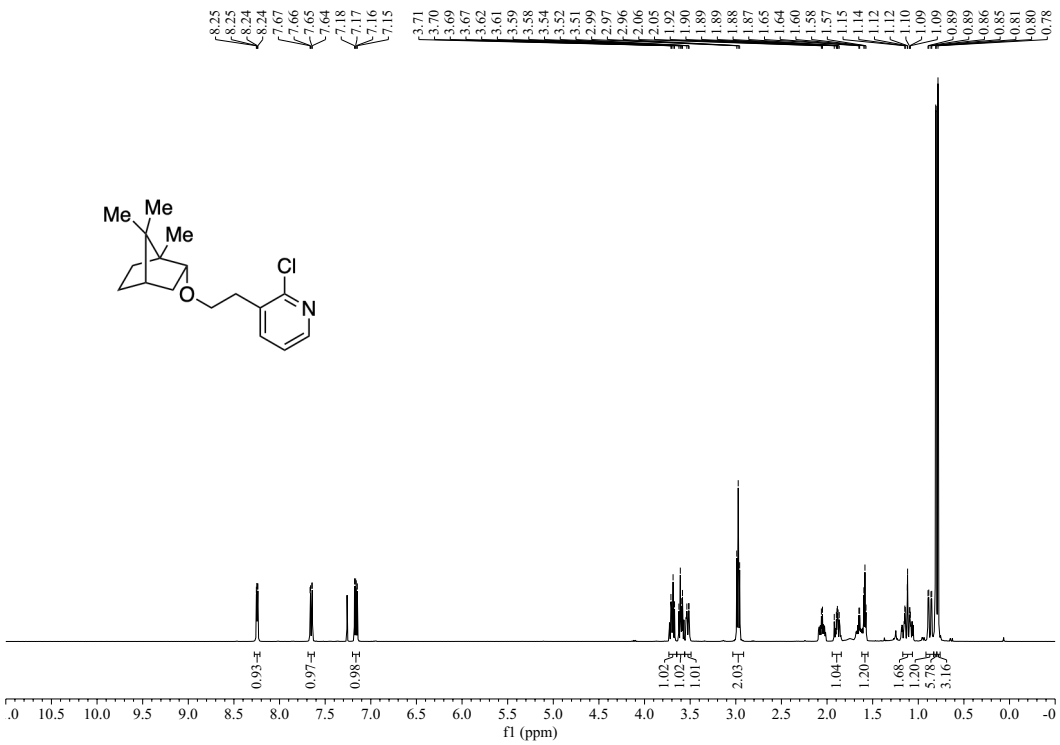

^{1}H NMR spectrum of (**2-46**) (400 MHz, $CDCl_3$)

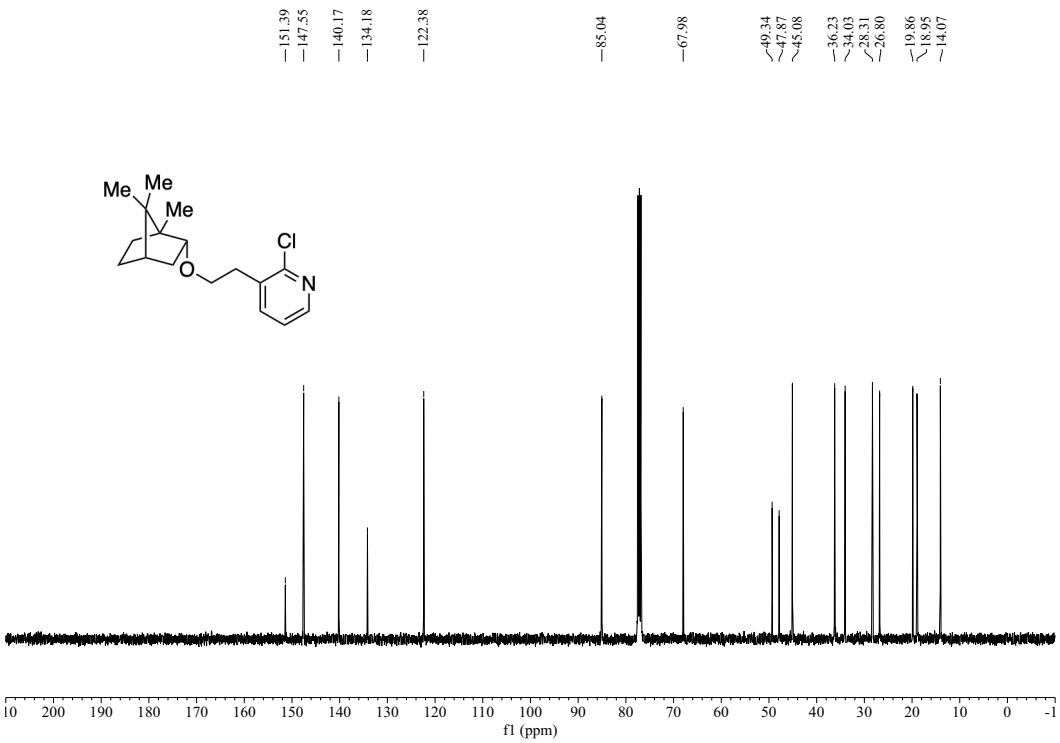

^{13}C NMR spectrum of (**2-46**) (101 MHz, $CDCl_3$)

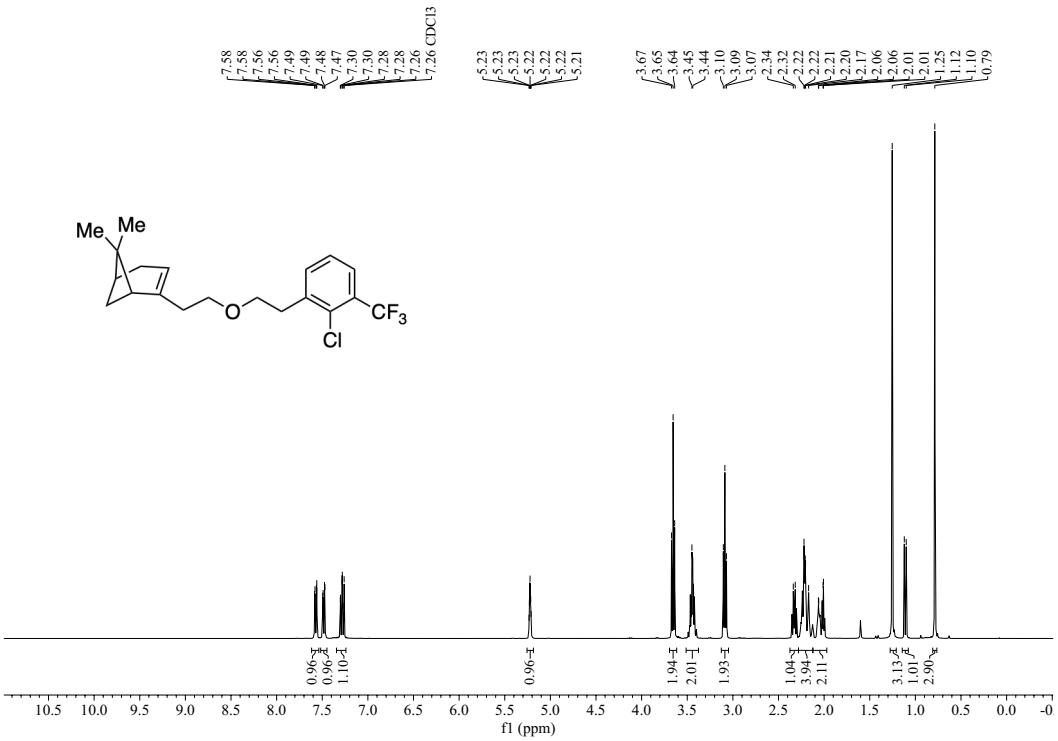

^{1}H NMR spectrum of (**2-28**) (400 MHz, $CDCl_3$)

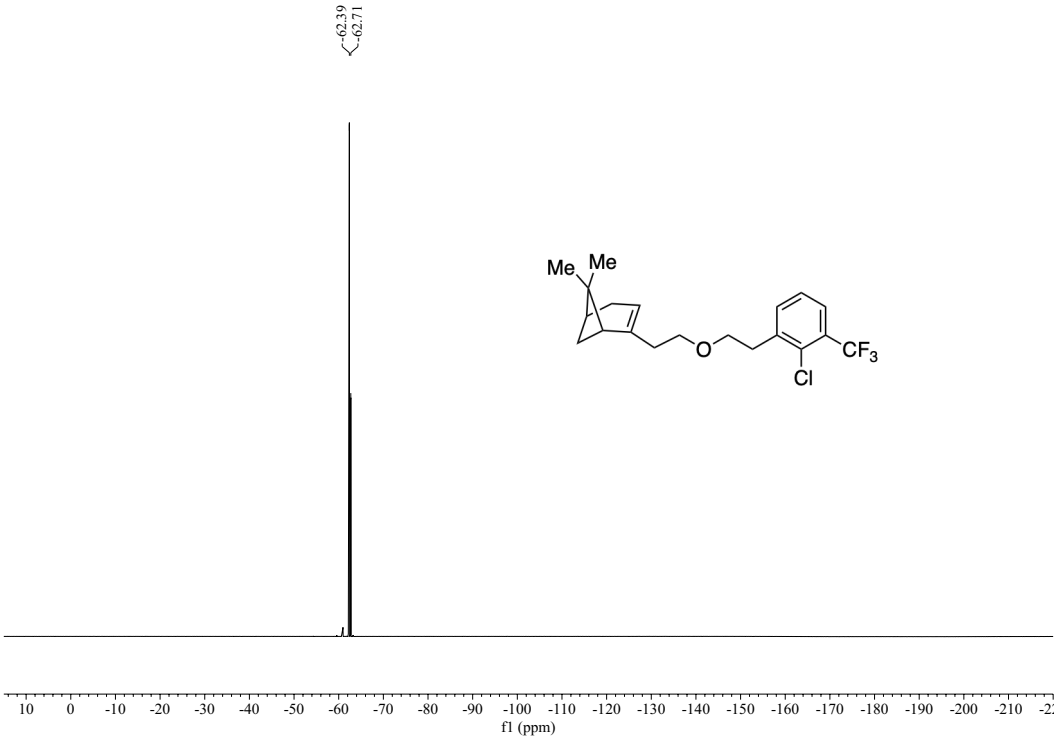

^{19}F NMR spectrum of (**2-28**) (376 MHz, $CDCl_3$)

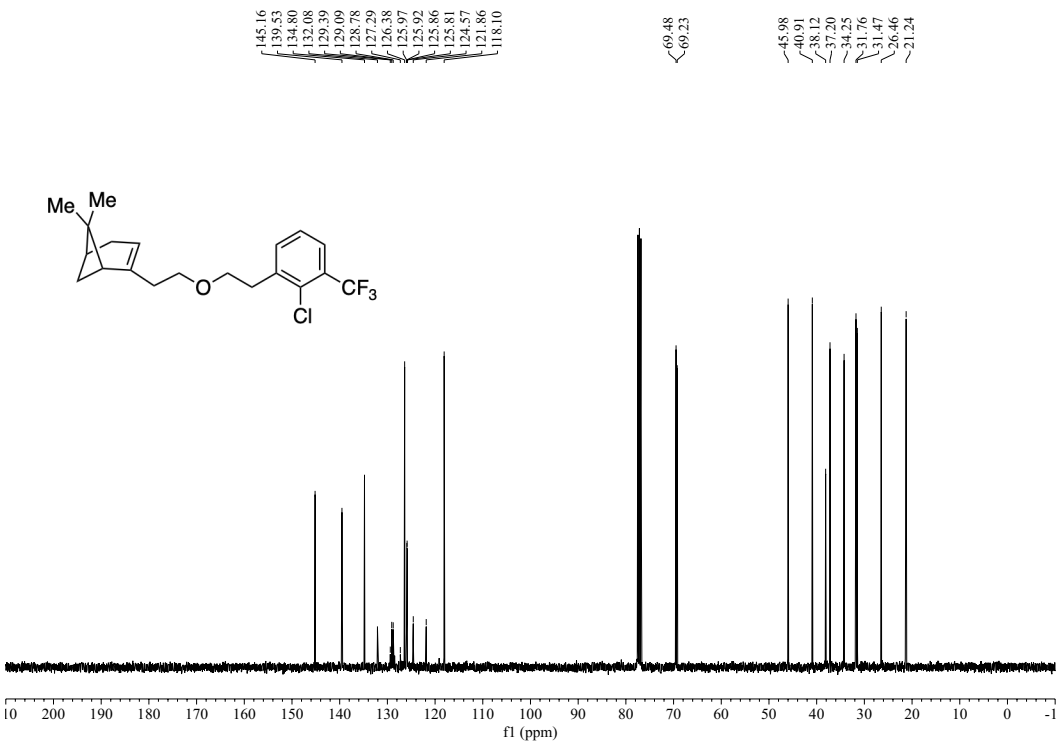

^{13}C NMR spectrum of (**2-28**) (101 MHz, $CDCl_3$)

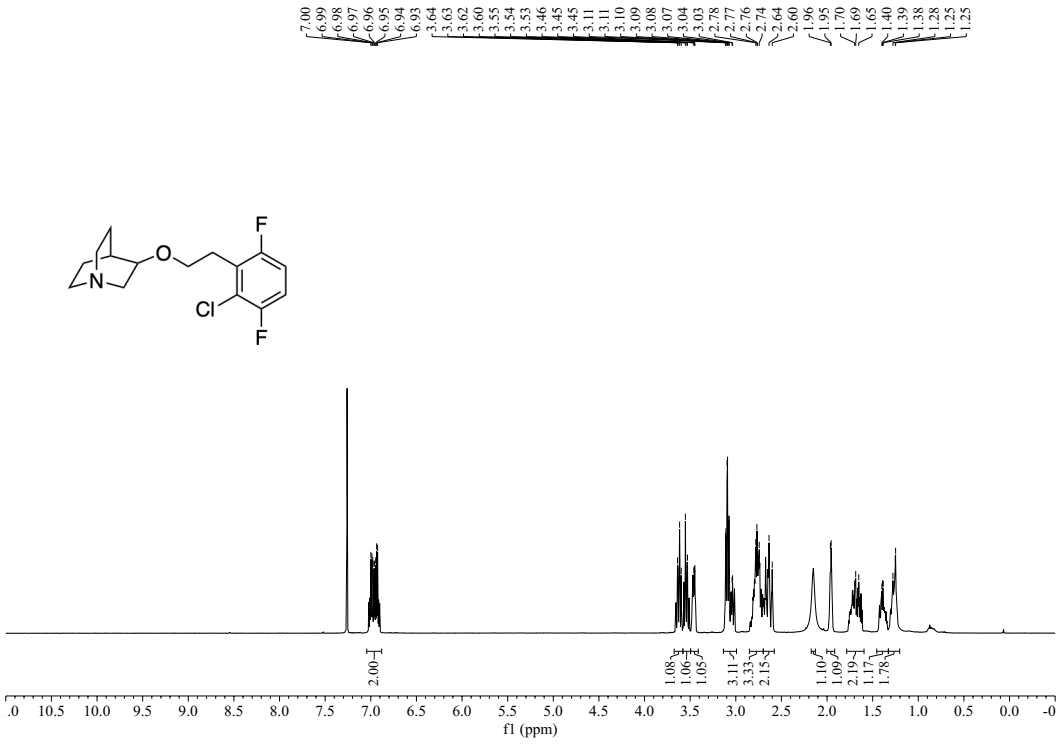

^{1}H NMR spectrum of (**2-27**) (400 MHz, $CDCl_3$)

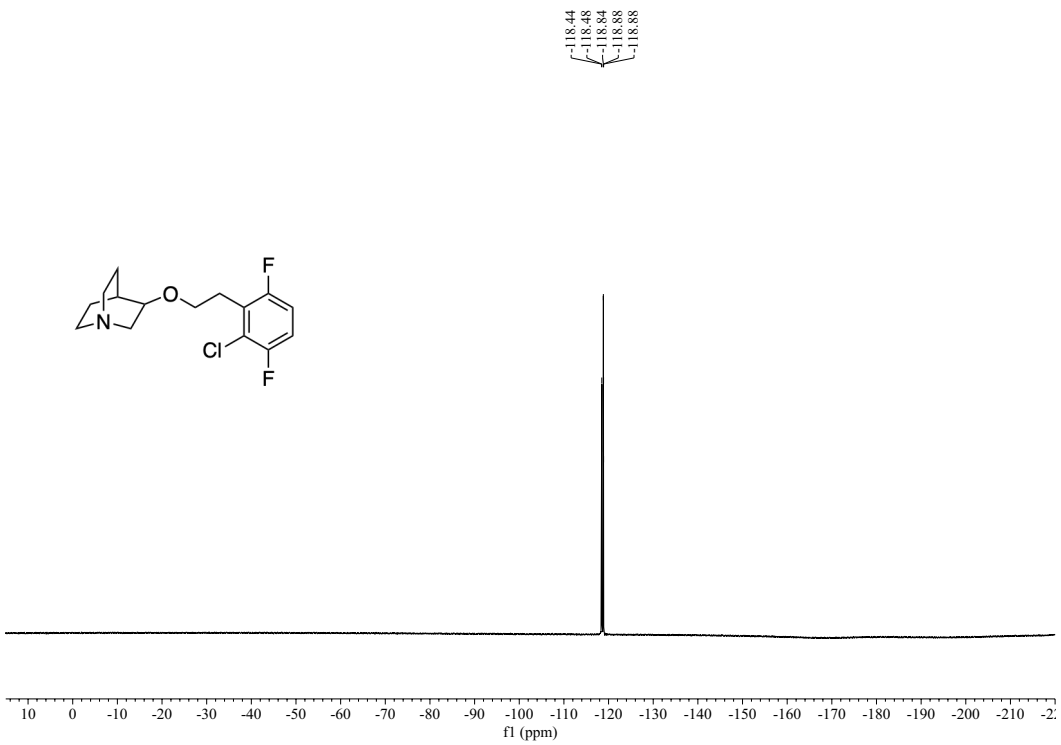

^{19}F NMR spectrum of (**2-27**) (376 MHz, $CDCl_3$)

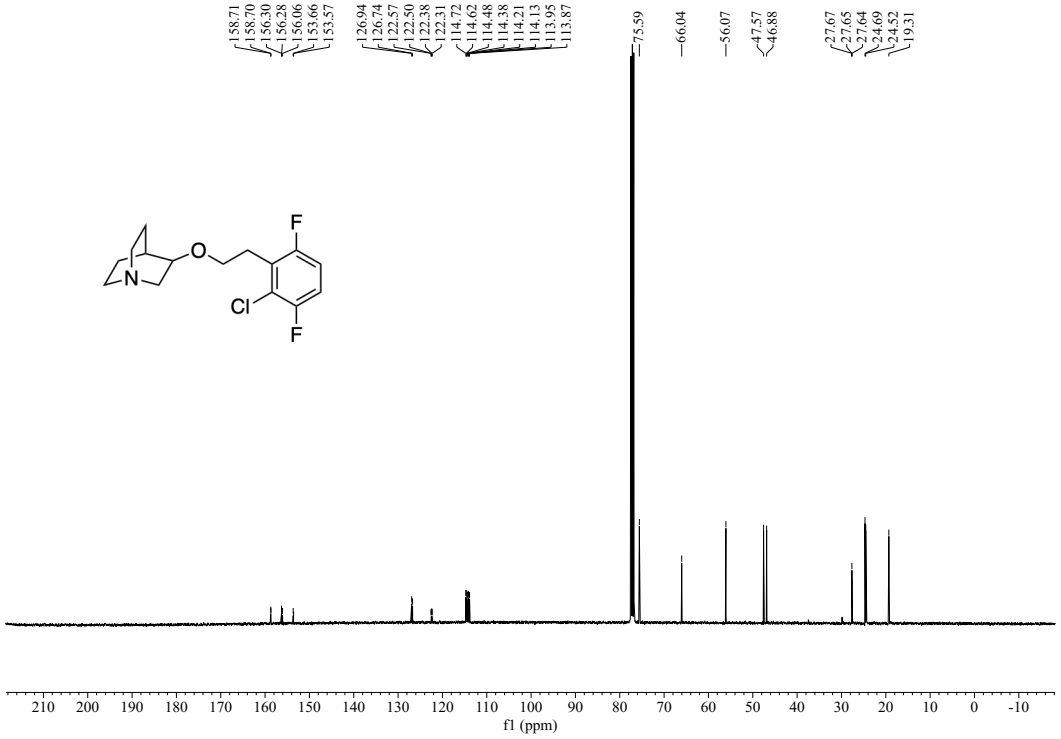

^{13}C NMR spectrum of (**2-27**) (101 MHz, $CDCl_3$)

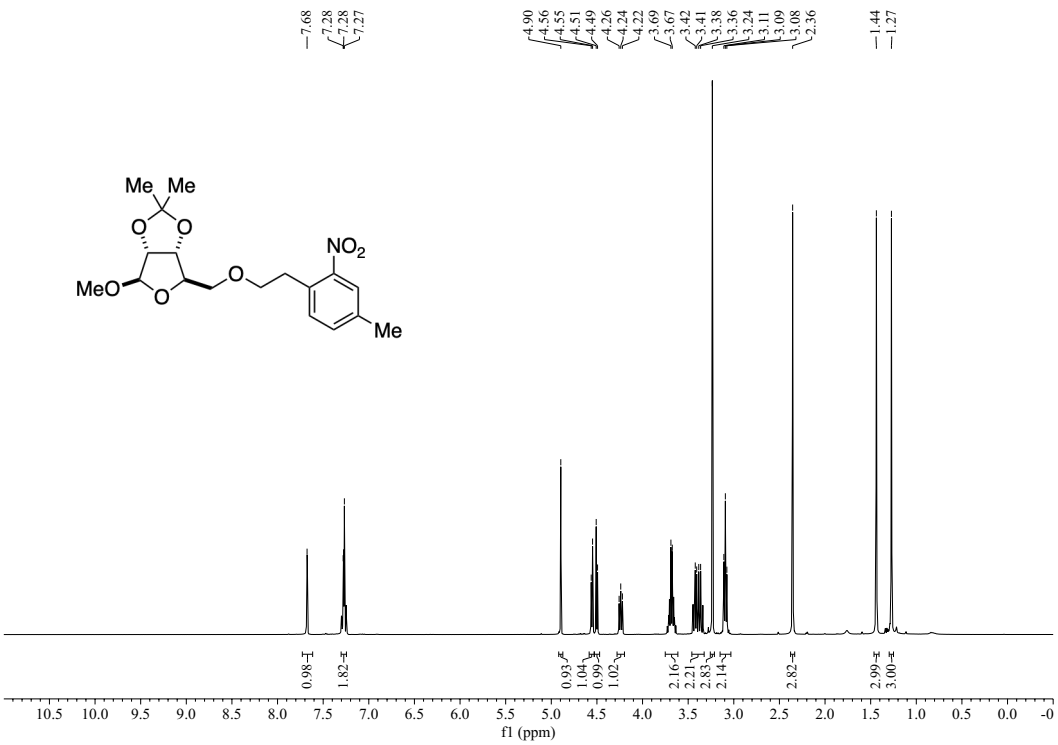

^{1}H NMR spectrum of (**2-29**) (400 MHz, $CDCl_3$)

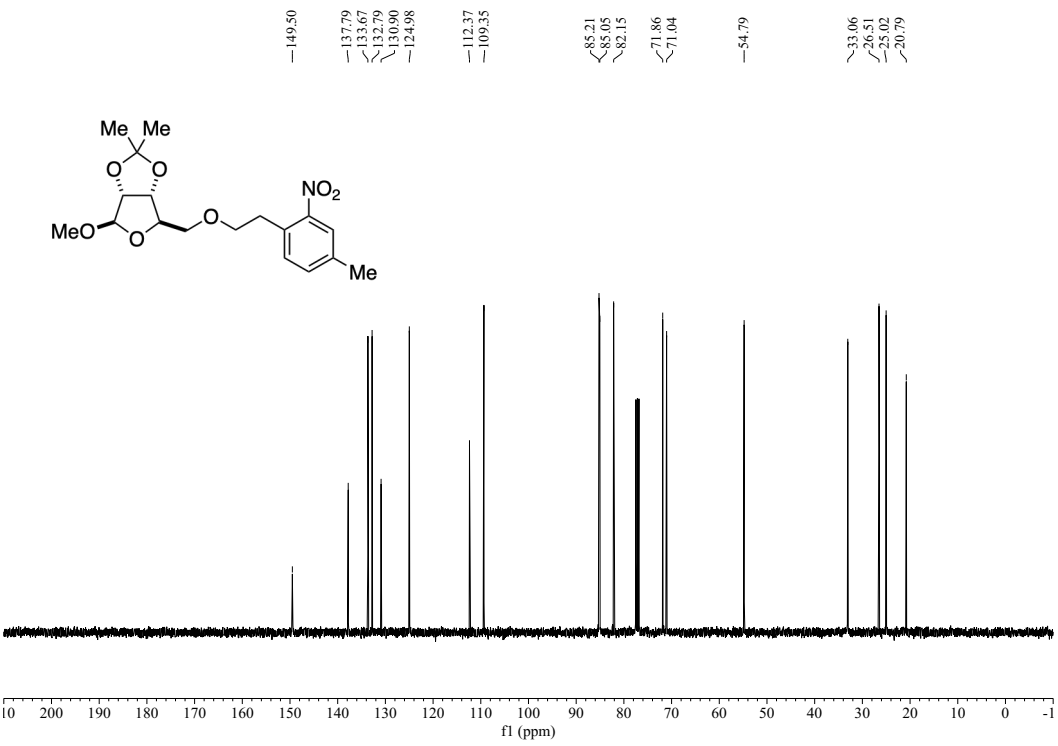

^{13}C NMR spectrum of (**2-29**) (101 MHz, $CDCl_3$)

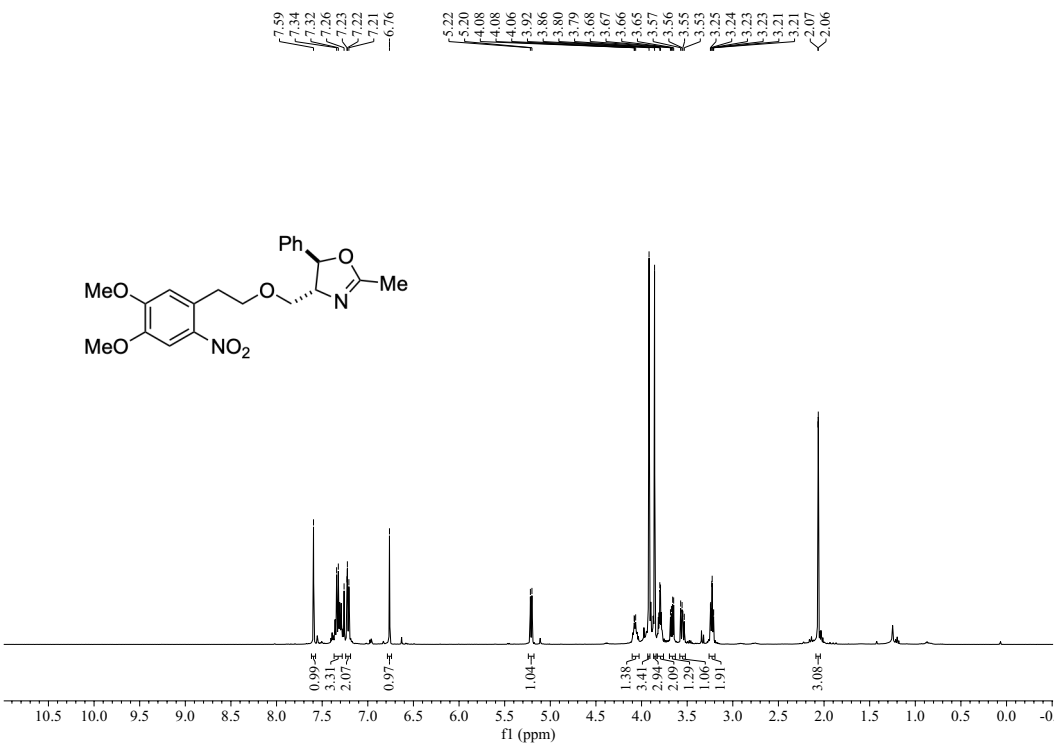

^{1}H NMR spectrum of (**2-30**) (400 MHz, $CDCl_3$)

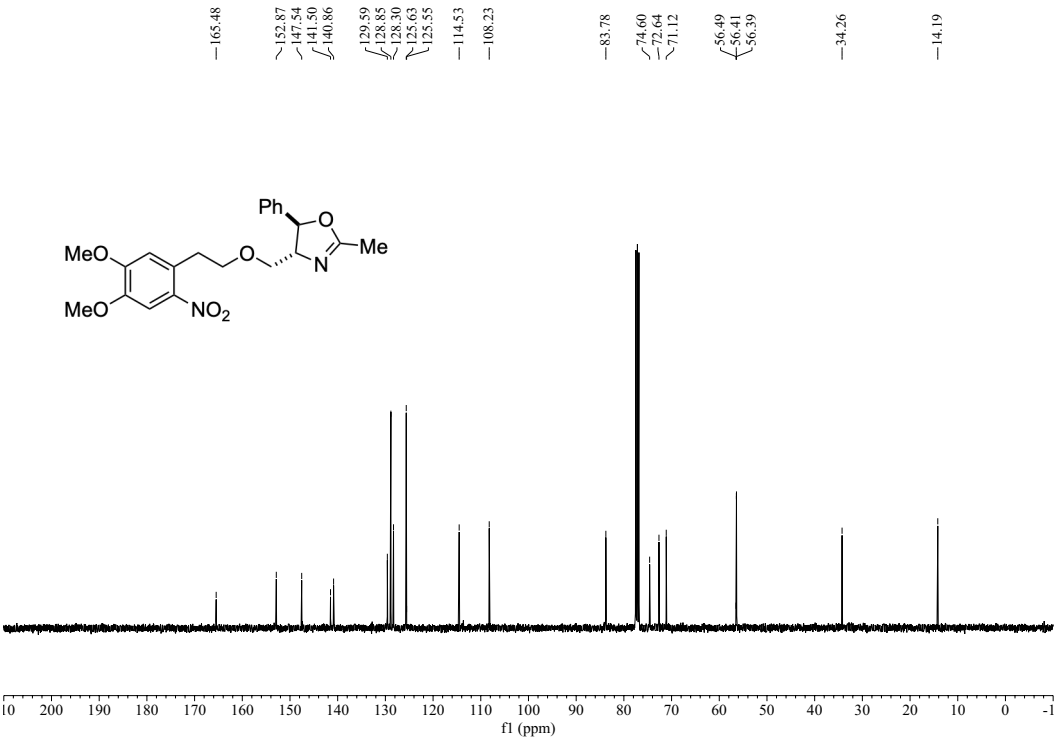

^{13}C NMR spectrum of (**2-30**) (101 MHz, $CDCl_3$)

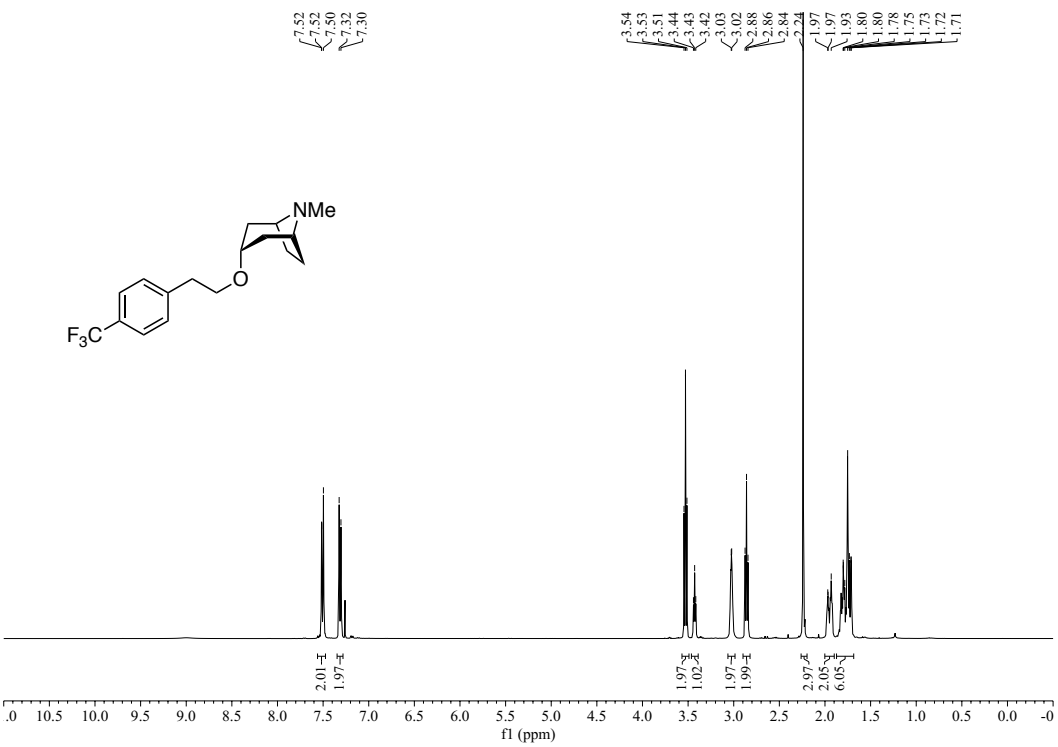

^{1}H NMR spectrum of (**2-32**) (400 MHz, $CDCl_3$)

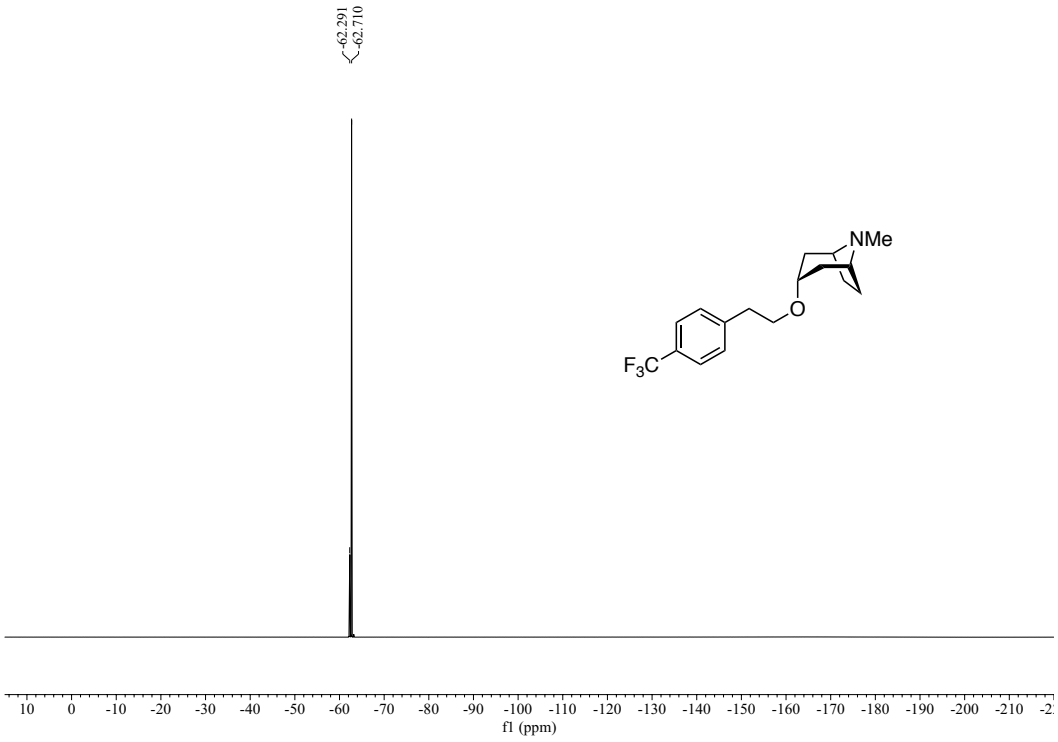

^{19}F NMR spectrum of (**2-32**) (376 MHz, $CDCl_3$)

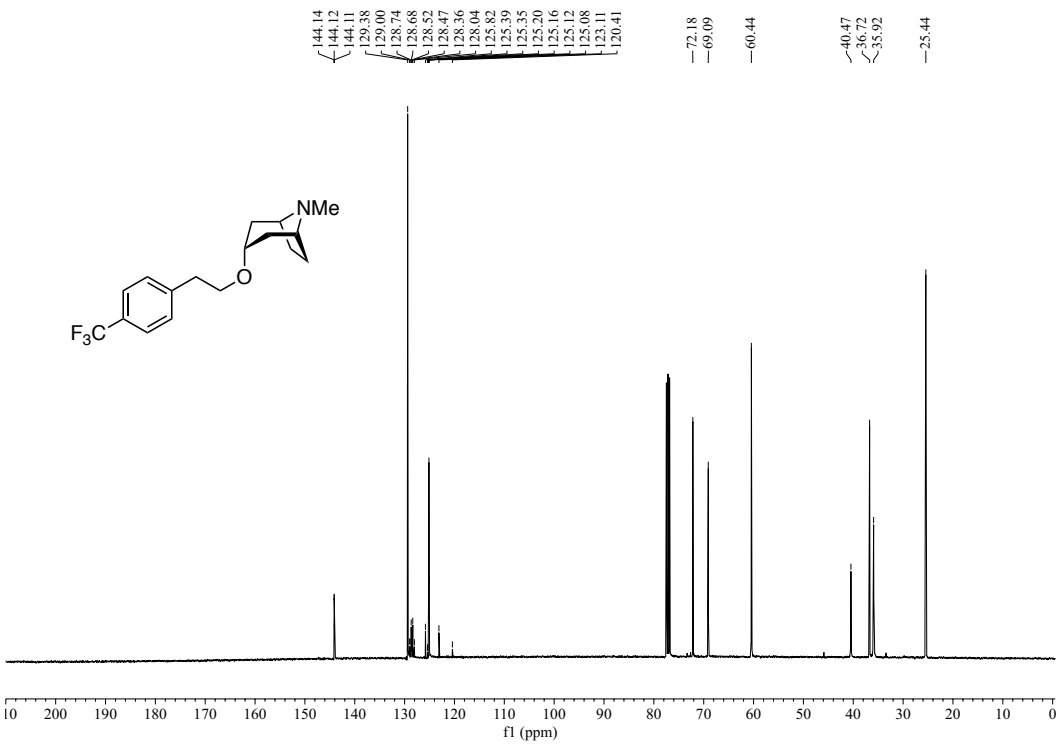

^{13}C NMR spectrum of (**2-32**) (101 MHz, $CDCl_3$)

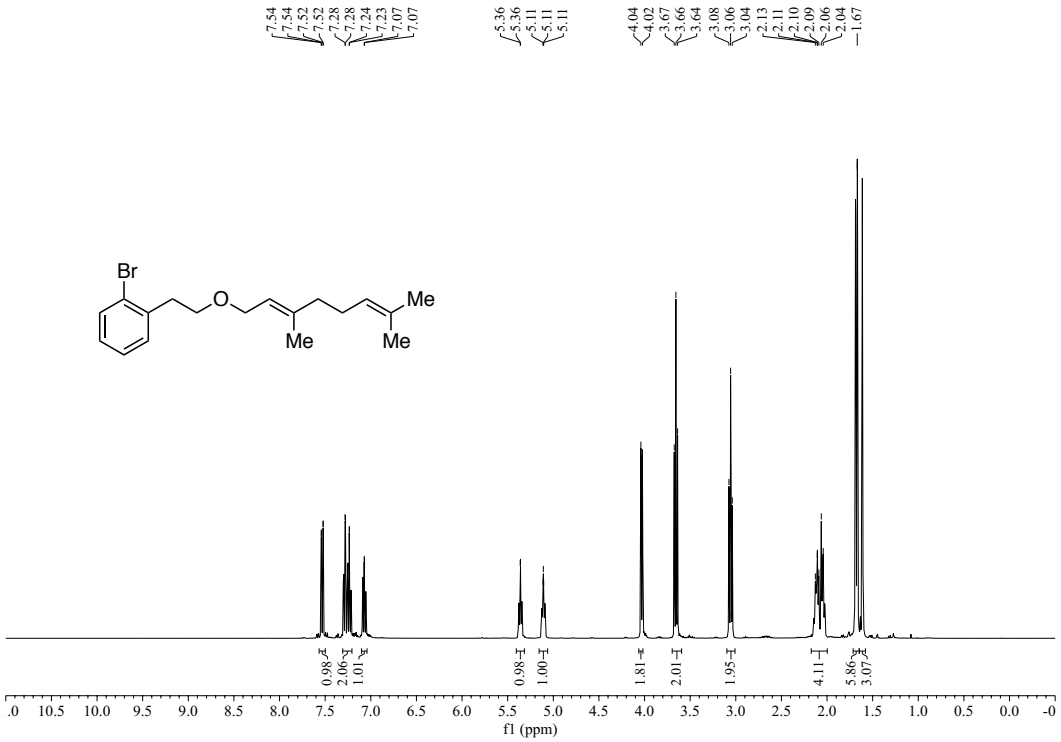

^{1}H NMR spectrum of (**2-33**) (400 MHz, $CDCl_3$)

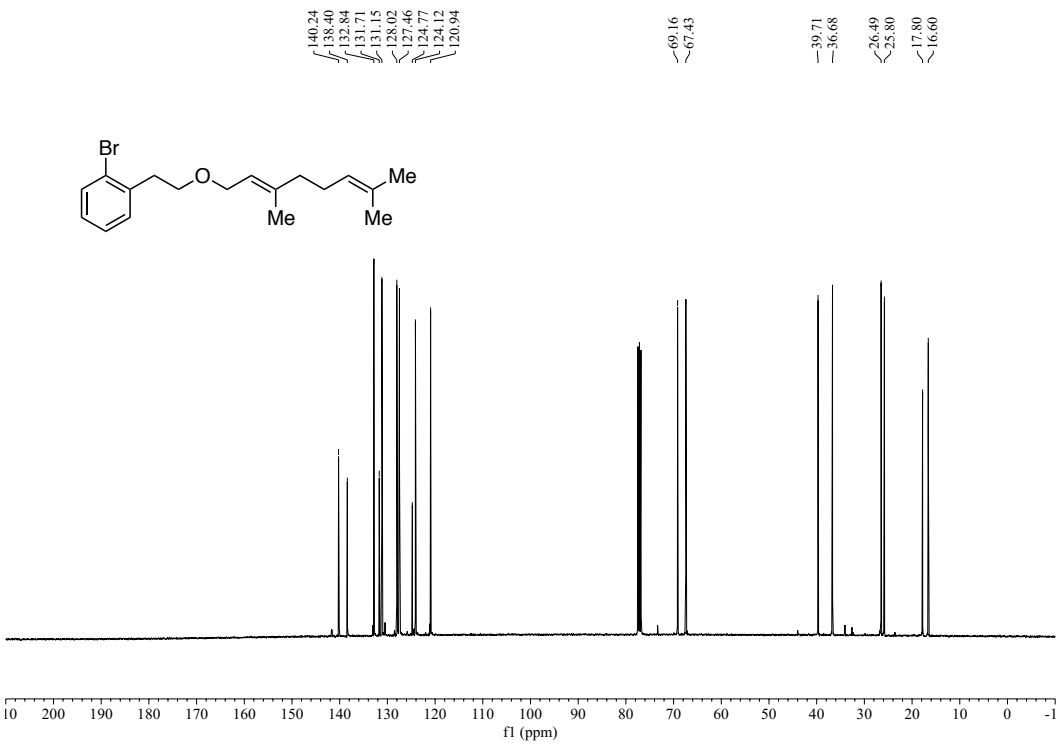

^{13}C NMR spectrum of (**2-33**) (101 MHz, $CDCl_3$)

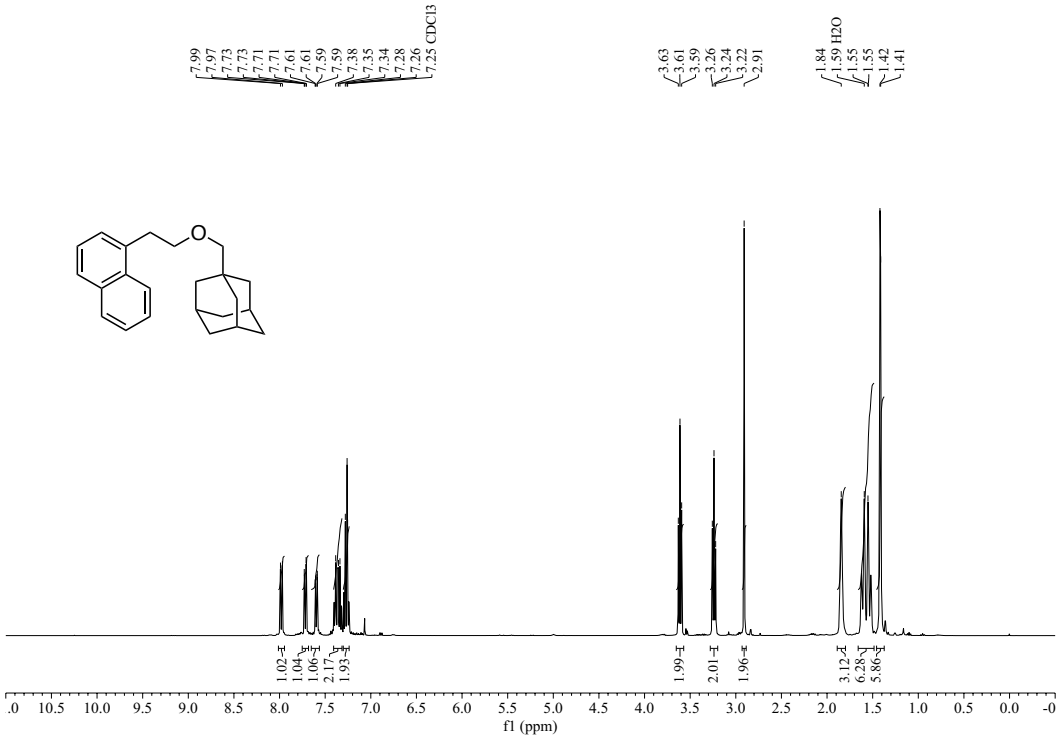

^{1}H NMR spectrum of (**2-34**) (400 MHz, $CDCl_3$)

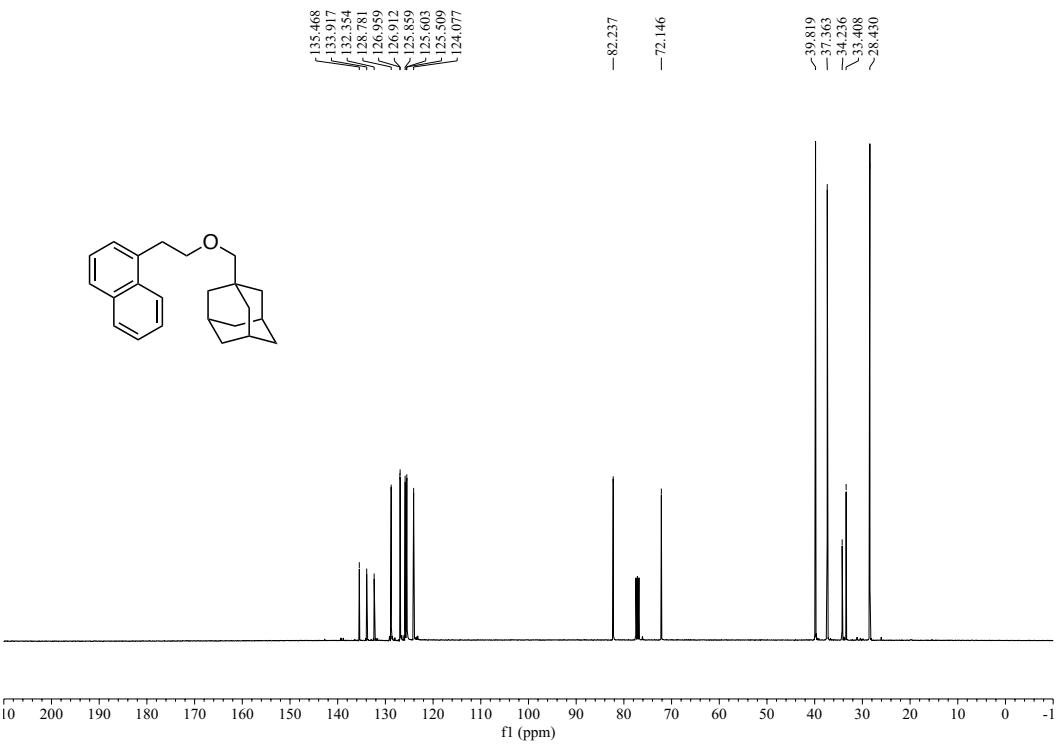

^{13}C NMR spectrum of (**2-34**) (101 MHz, $CDCl_3$)

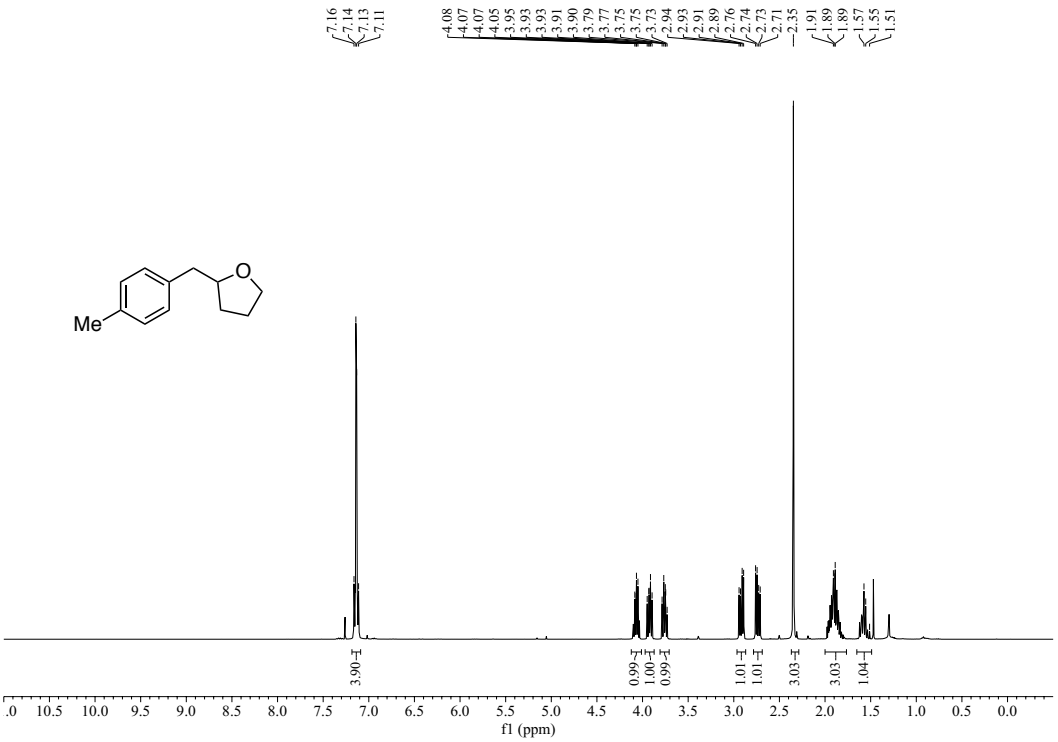

^{1}H NMR spectrum of (**2-36**) (400 MHz, $CDCl_3$)

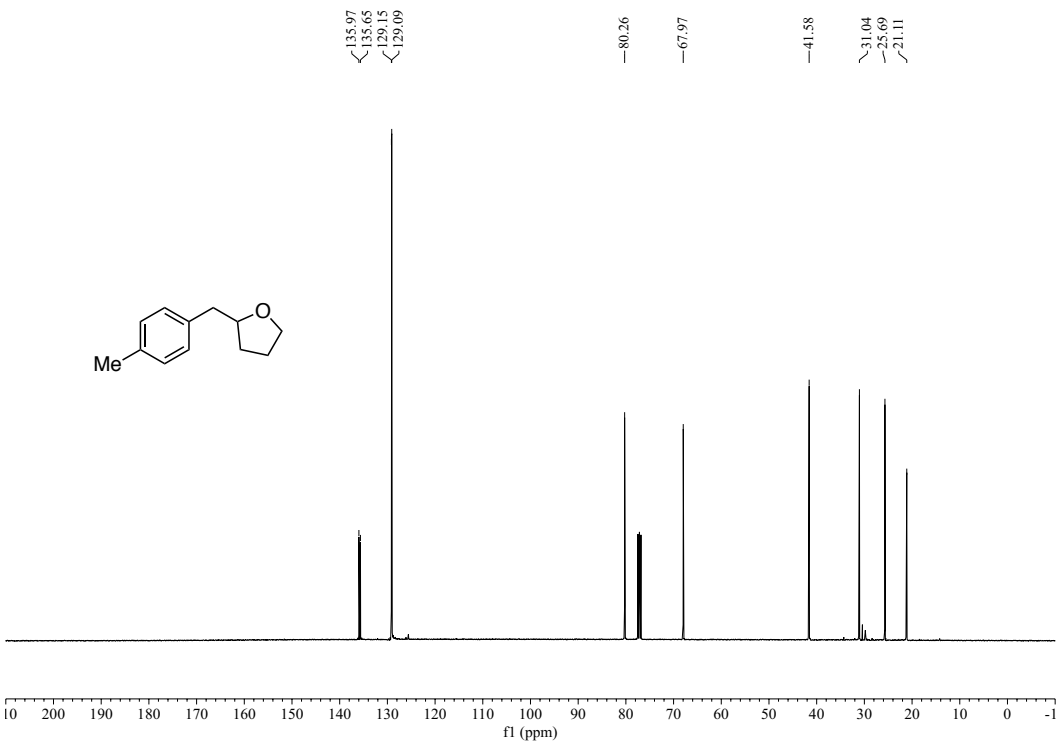

^{13}C NMR spectrum of (**2-36**) (101 MHz, $CDCl_3$)

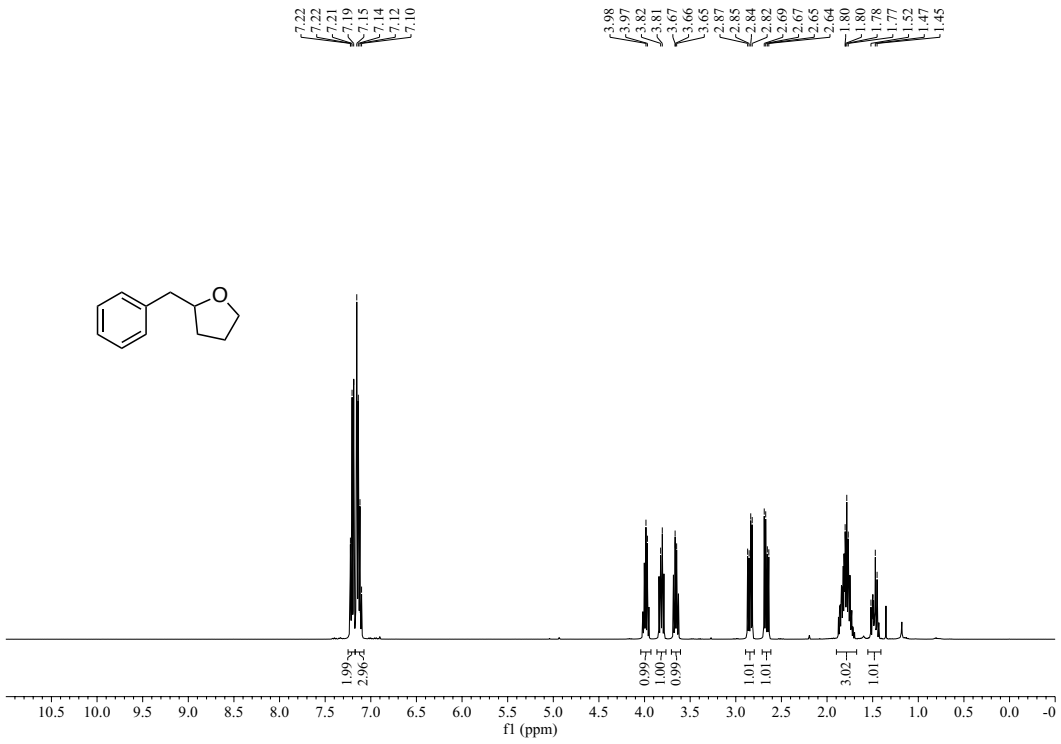

^{1}H NMR spectrum of (**2-38**) (400 MHz, $CDCl_3$)

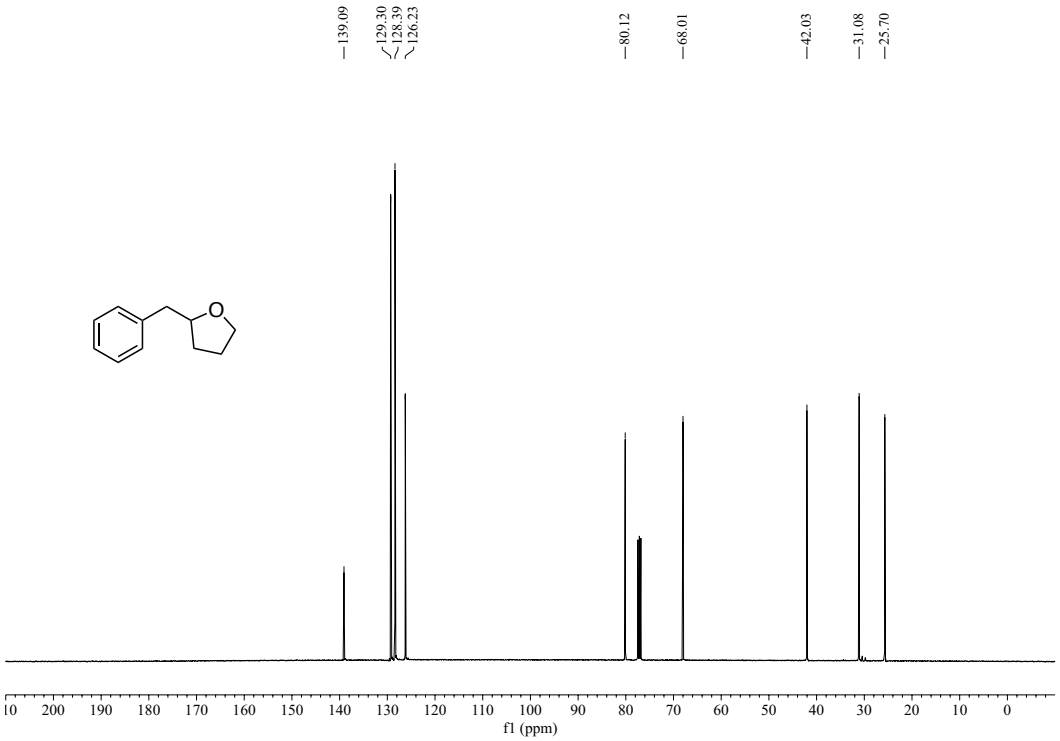

^{13}C NMR spectrum of (**2-38**) (101 MHz, $CDCl_3$)

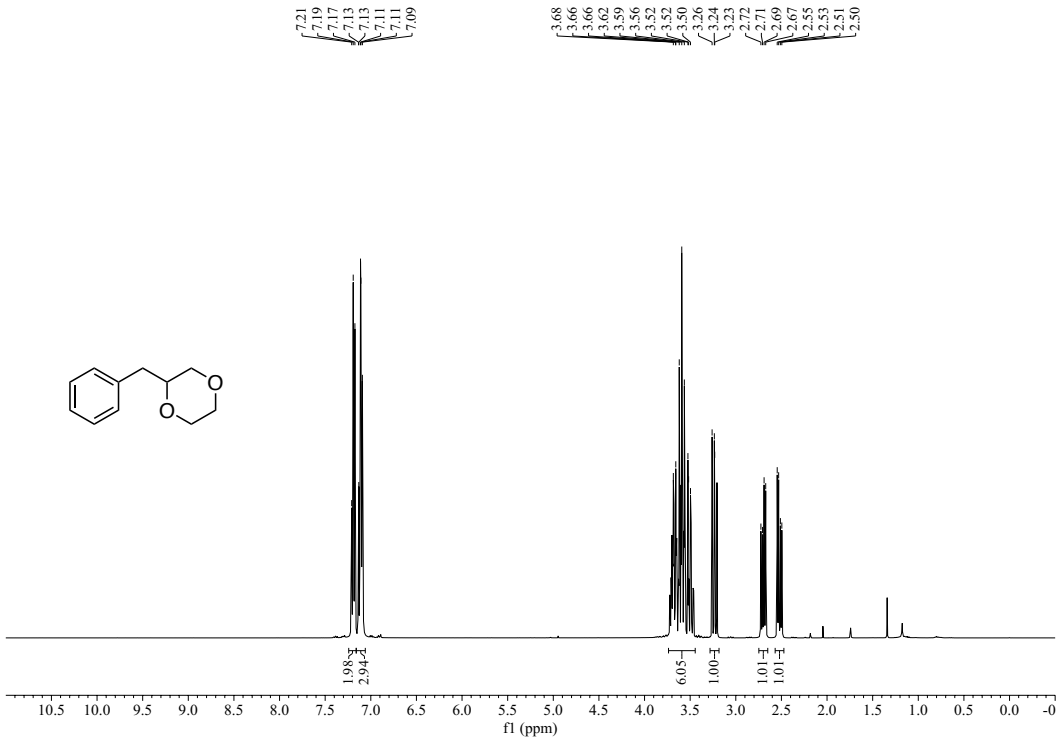

^{1}H NMR spectrum of (**2-40**) (400 MHz, $CDCl_3$)

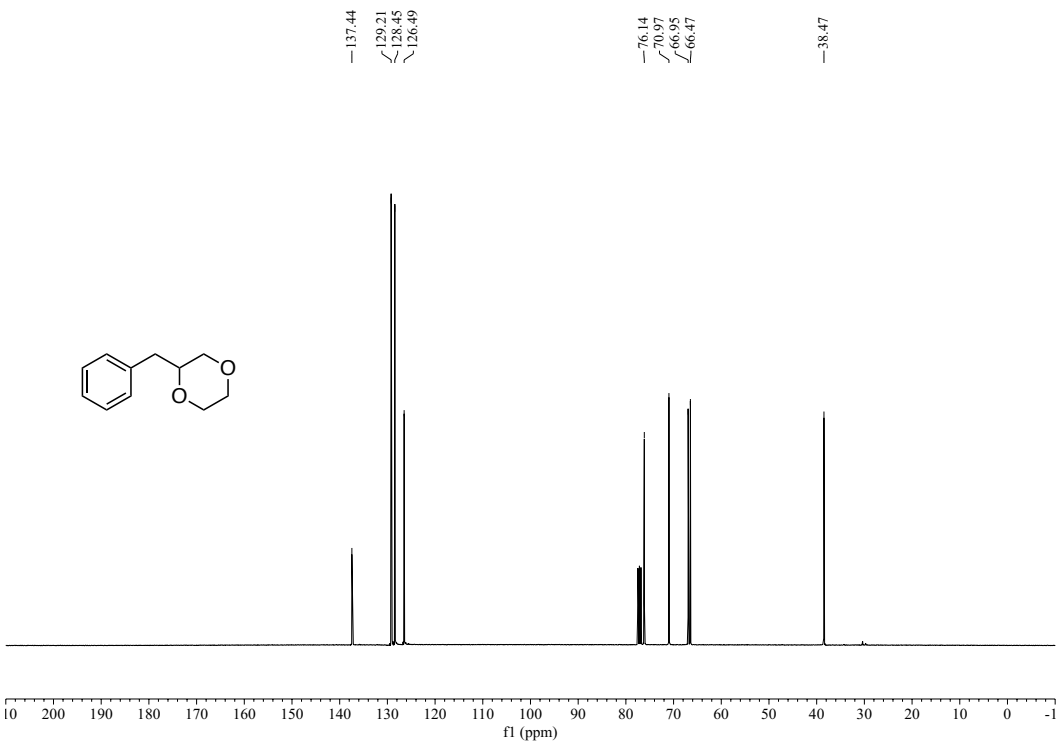

^{13}C NMR spectrum of (**2-40**) (101 MHz, $CDCl_3$)

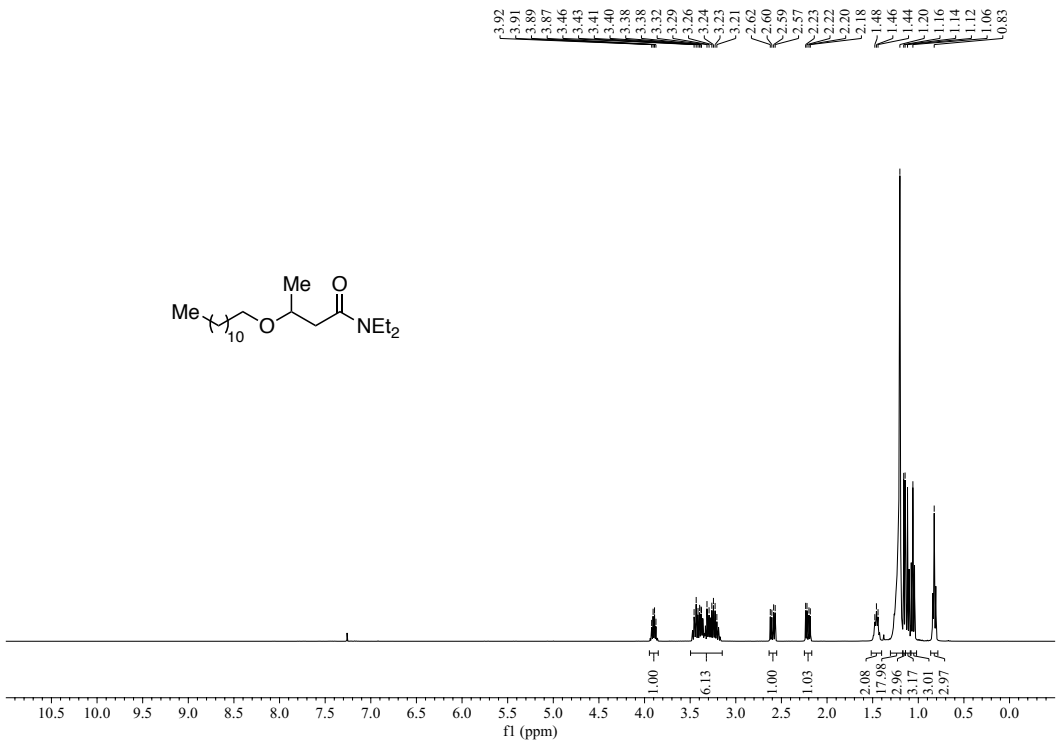

^{1}H NMR spectrum of (**2-42**) (400 MHz, $CDCl_3$)

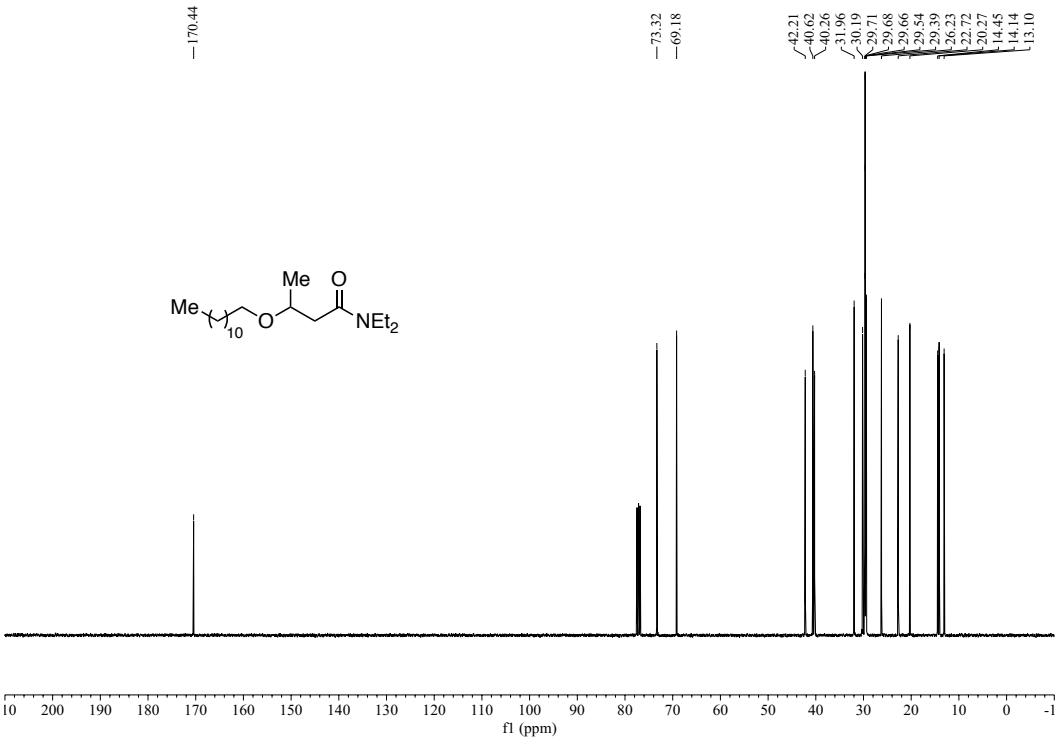

^{13}C NMR spectrum of (**2-42**) (101 MHz, $CDCl_3$)

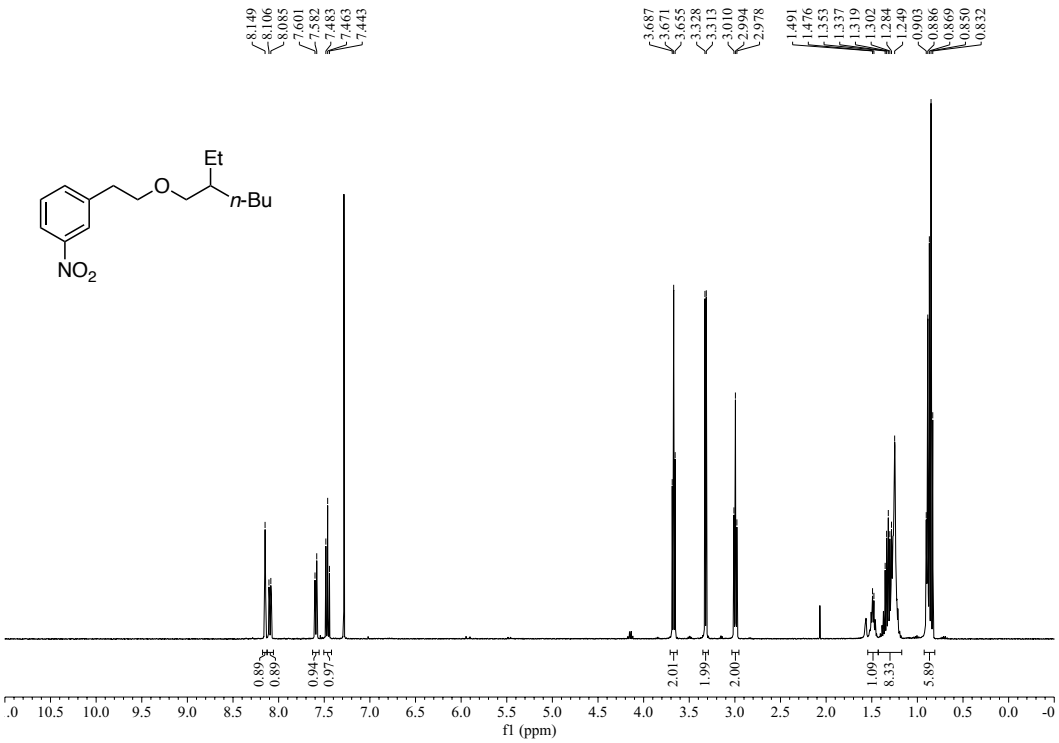

^{1}H NMR spectrum of (**2-47**) (400 MHz, $CDCl_3$)

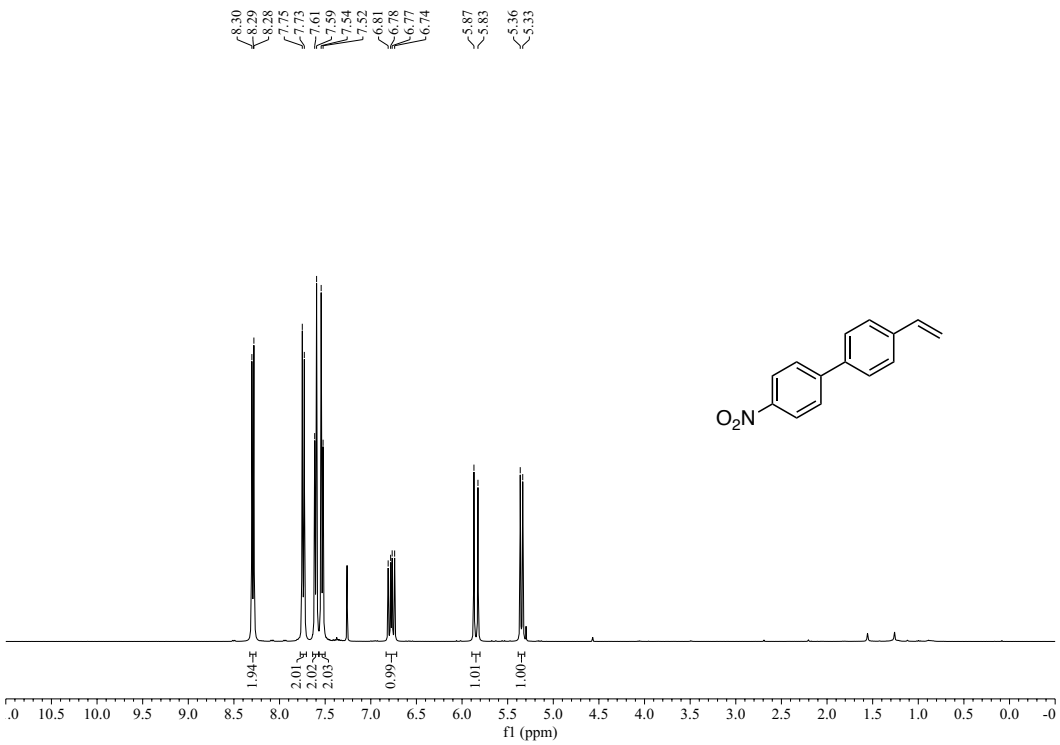

^{1}H NMR spectrum of **4-nitro-4'-vinyl-1,1'-biphenyl** (400 MHz, $CDCl_3$)

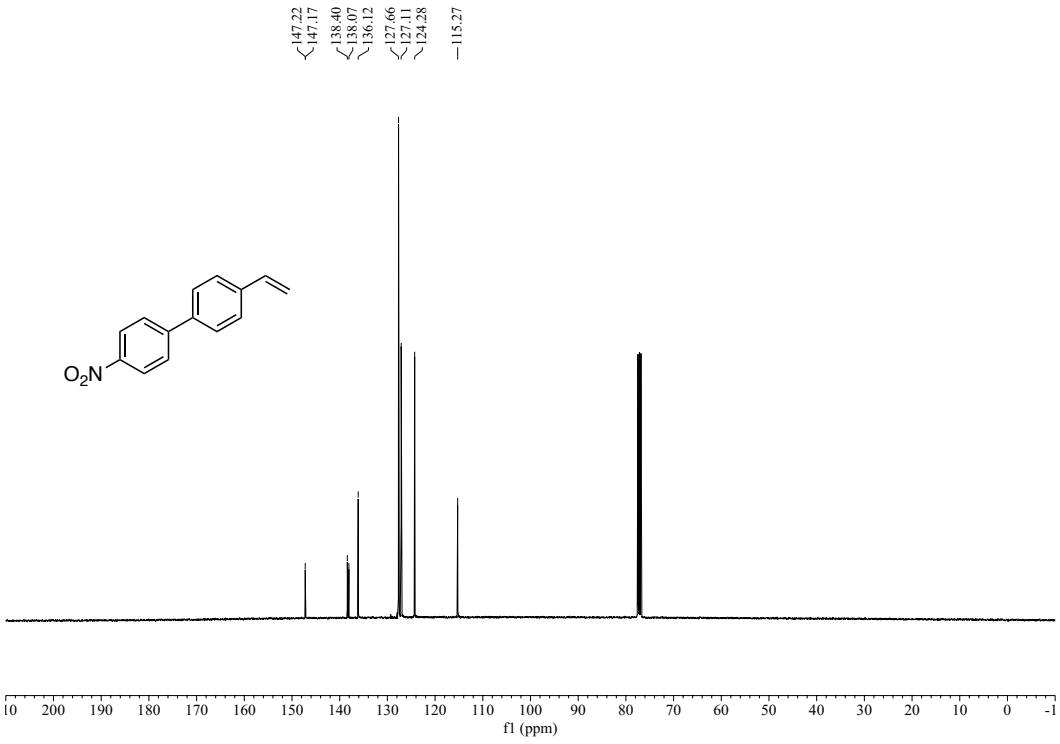

^{13}C NMR spectrum of **4-nitro-4'-vinyl-1,1'-biphenyl** (101 MHz, $CDCl_3$)

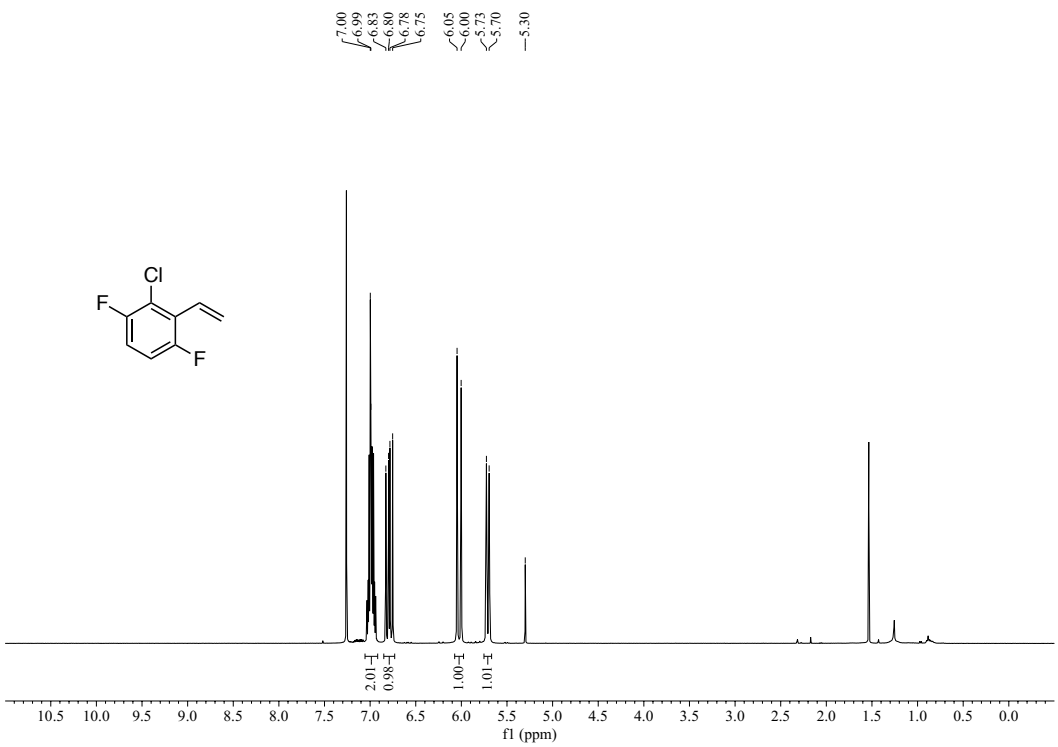

^{1}H NMR spectrum of **2-chloro-1,4-difluoro-3-vinylbenzene** (400 MHz, $CDCl_3$)

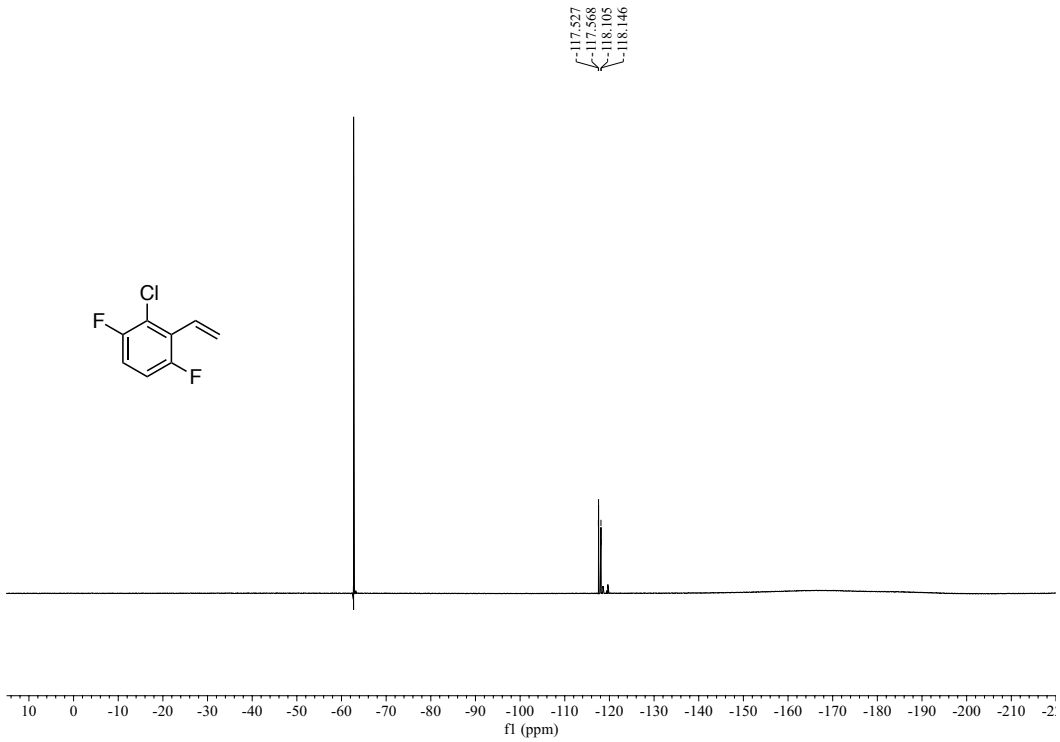

^{19}F NMR spectrum of **2-chloro-1,4-difluoro-3-vinylbenzene** (376 MHz, $CDCl_3$)

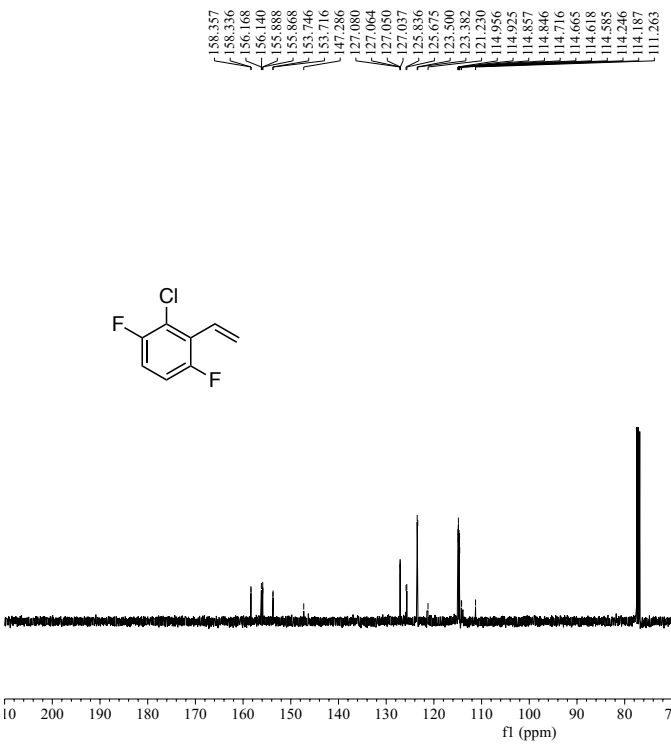

^{13}C NMR spectrum of **2-chloro-1,4-difluoro-3-vinylbenzene** (101 MHz, $CDCl_3$)

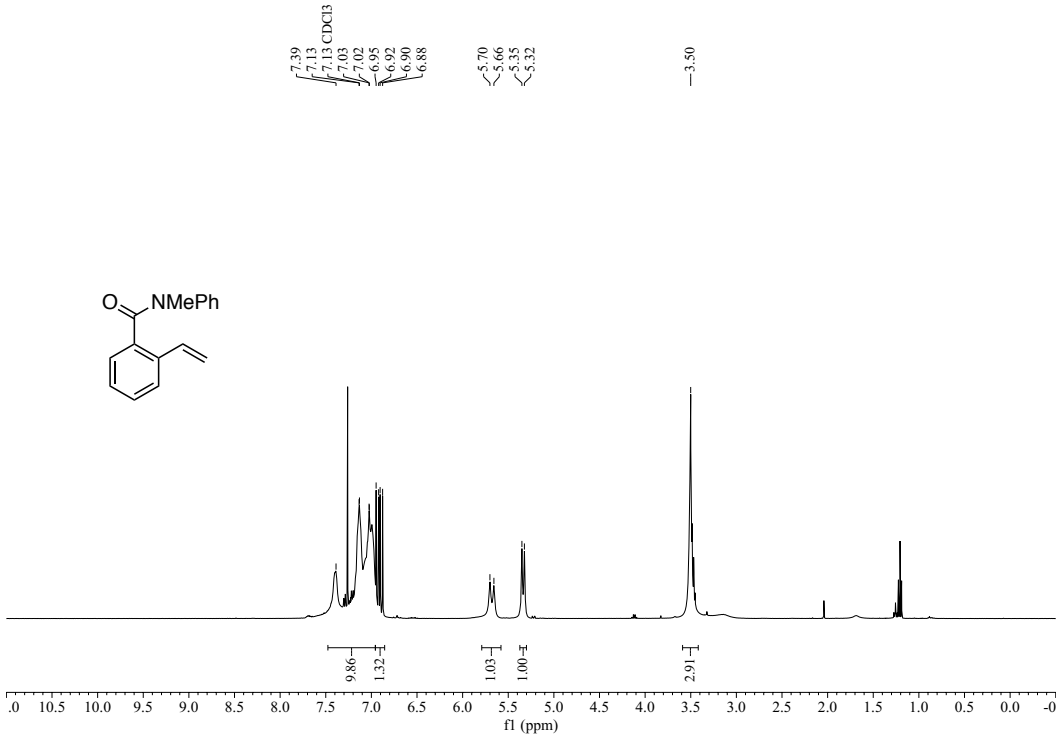

^{1}H NMR spectrum of ***N*-methyl-*N*-phenyl-2-vinylbenzamide** (400 MHz, $CDCl_3$)

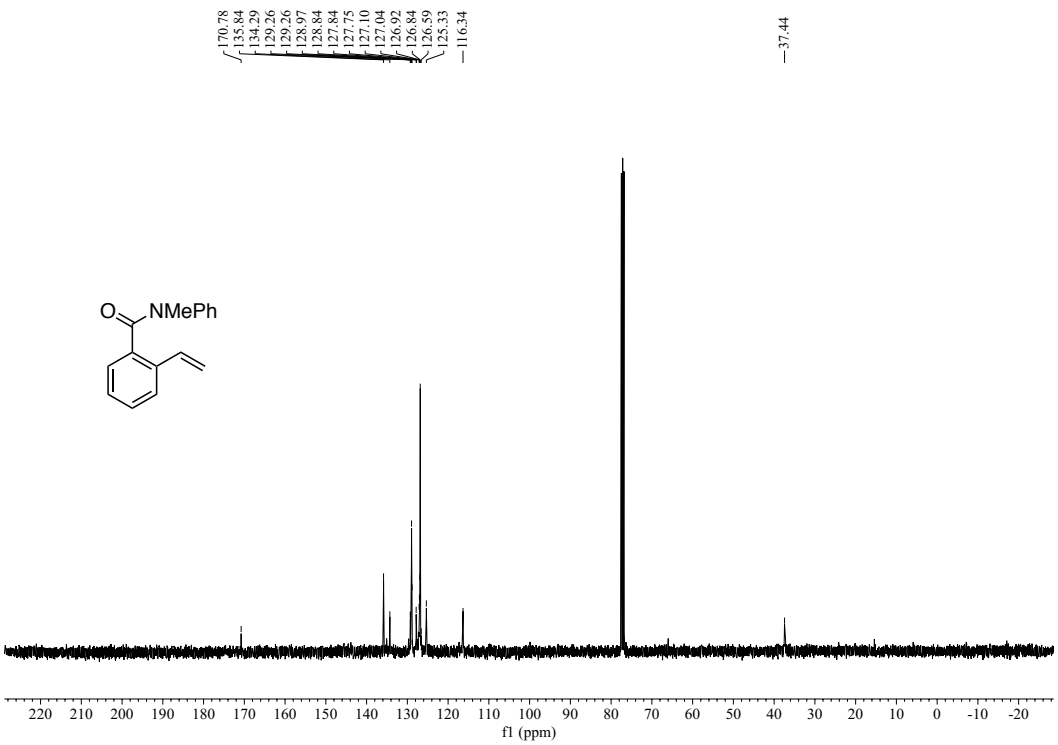

^{13}C NMR spectrum of ***N*-methyl-*N*-phenyl-2-vinylbenzamide** (101 MHz, $CDCl_3$)

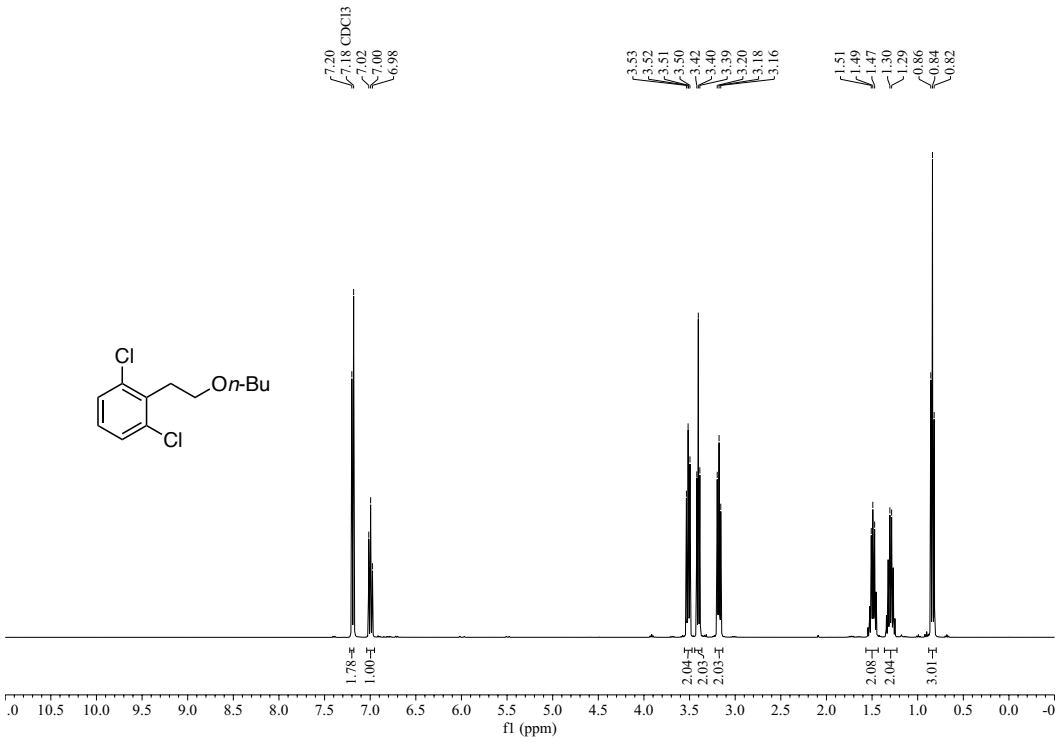

^{1}H NMR spectrum of **2-(2-butoxyethyl)-1,3-dichlorobenzene** (400 MHz, $CDCl_3$)

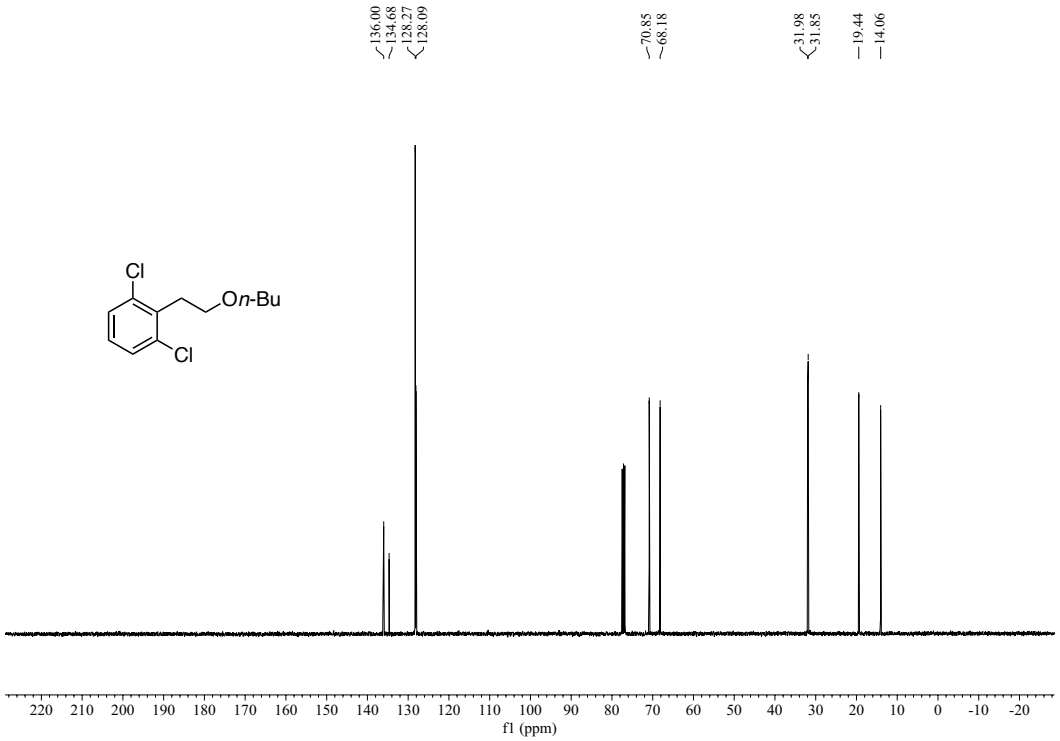

^{13}C NMR spectrum of **2-(2-butoxyethyl)-1,3-dichlorobenzene** (101 MHz, $CDCl_3$)

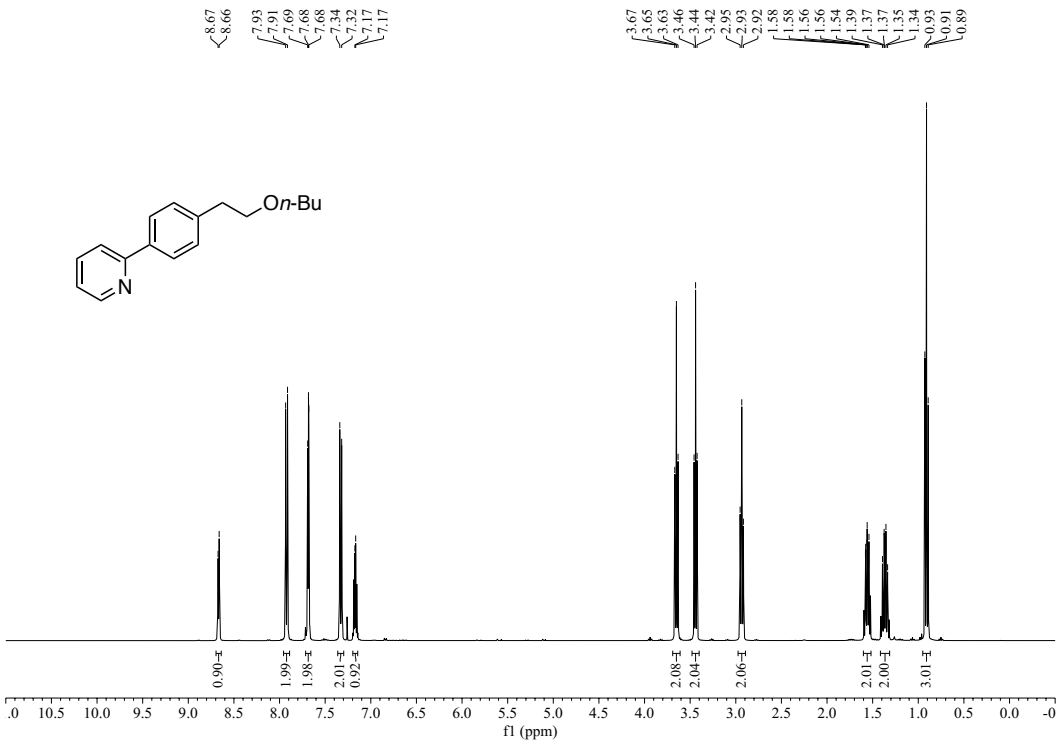

^{1}H NMR spectrum of **2-(4-(2-butoxyethyl)phenyl)pyridine** (400 MHz, $CDCl_3$)

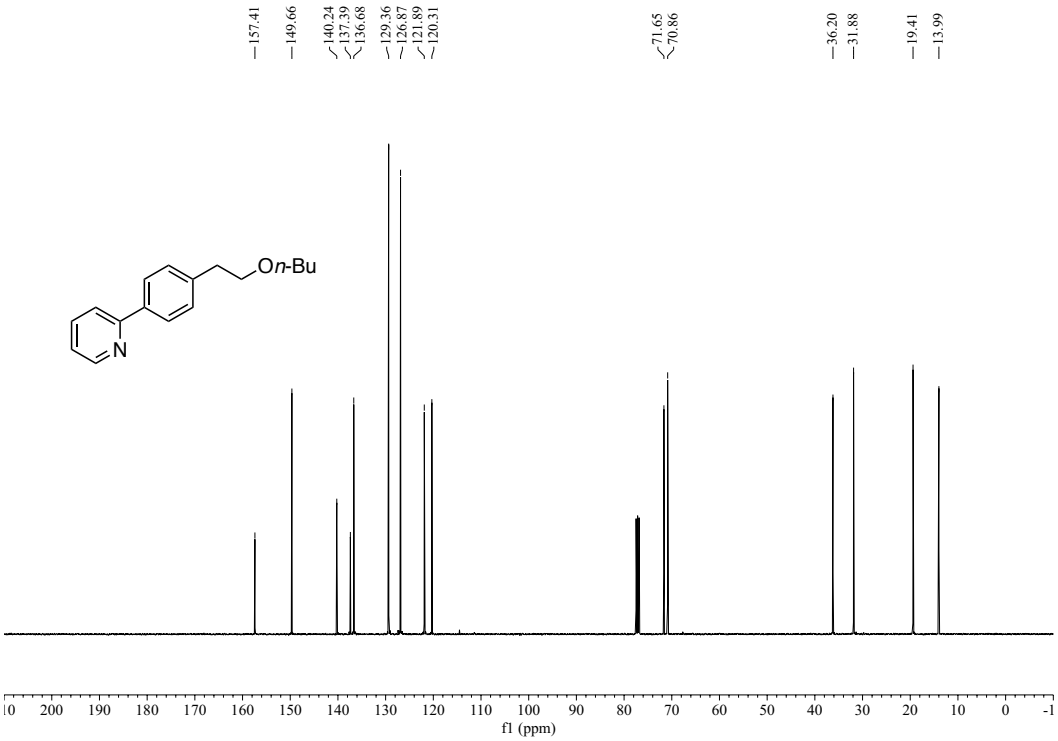

^{13}C NMR spectrum of **2-(4-(2-butoxyethyl)phenyl)pyridine** (101 MHz, $CDCl_3$)

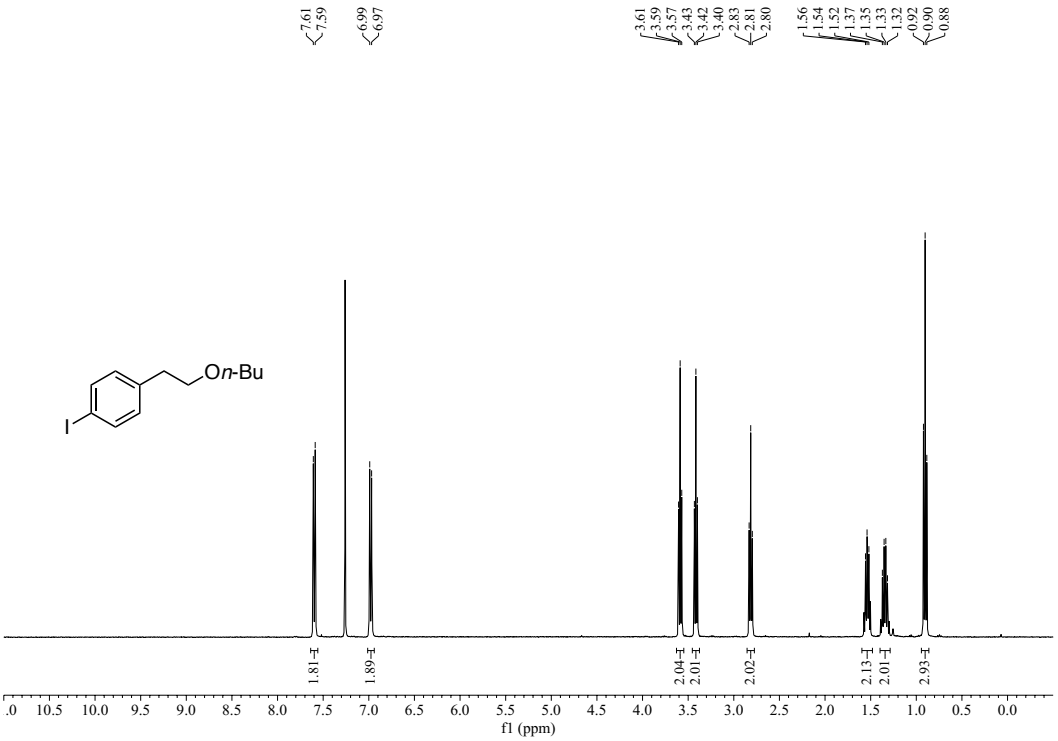

^{1}H NMR spectrum of **1-(2-butoxyethyl)-4-iodobenzene** (400 MHz, $CDCl_3$)

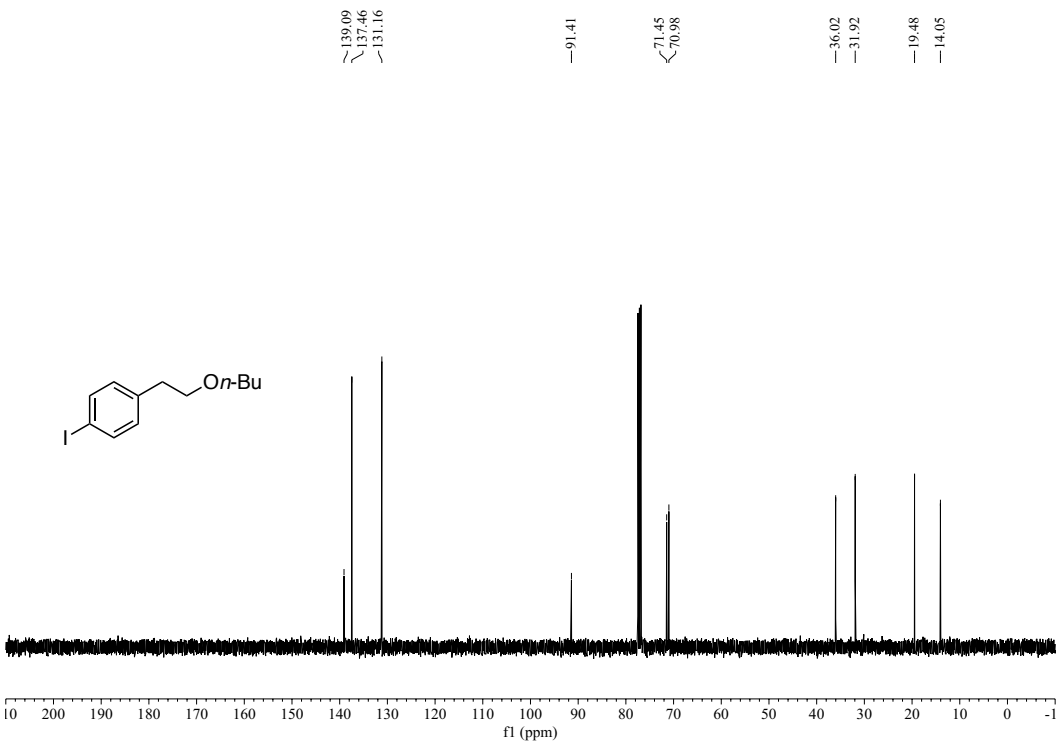

^{13}C NMR spectrum of **1-(2-butoxyethyl)-4-iodobenzene** (101 MHz, $CDCl_3$)

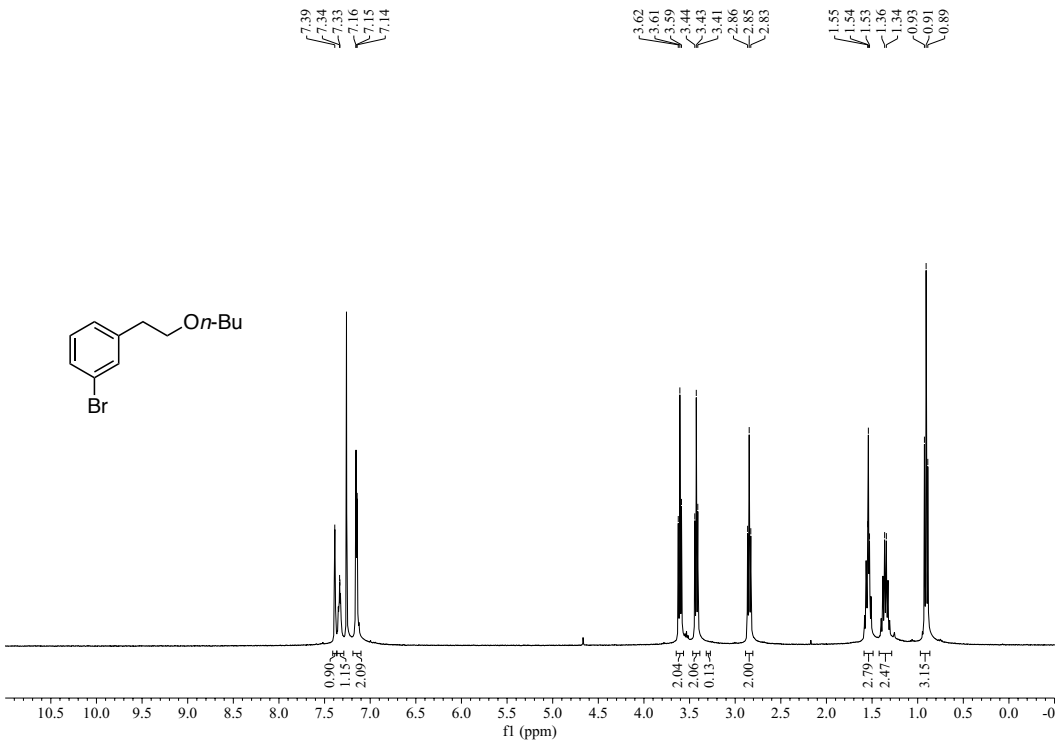

^{1}H NMR spectrum of **1-bromo-3-(2-butoxyethyl)benzene** (400 MHz, $CDCl_3$)

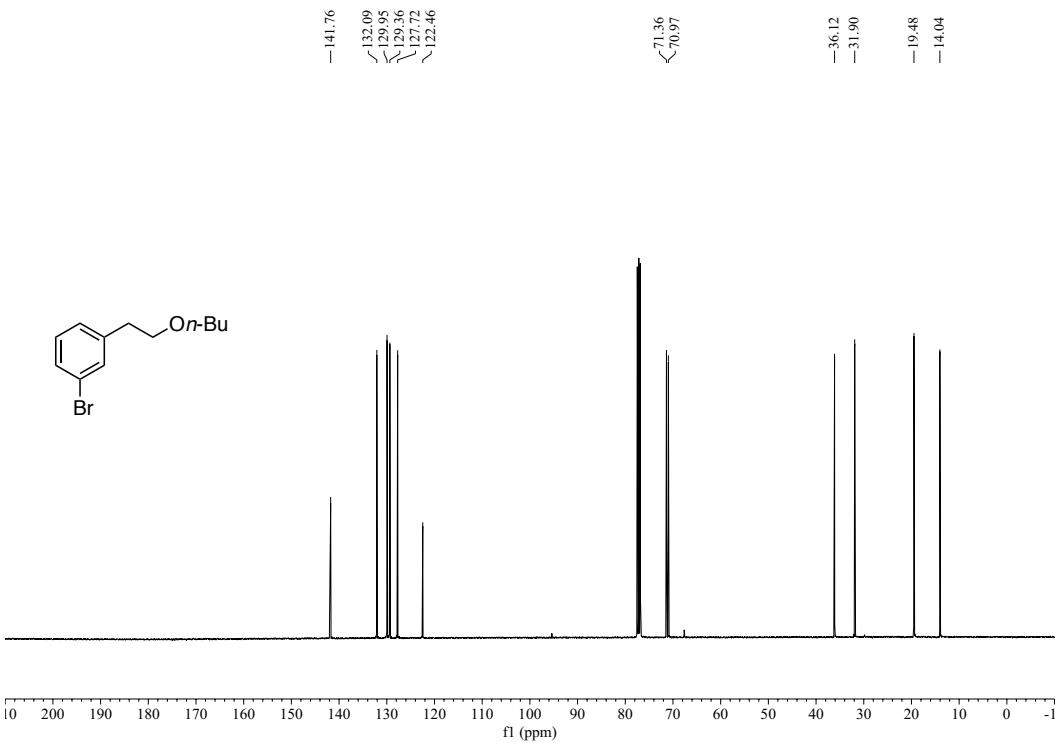

^{13}C NMR spectrum of **1-bromo-3-(2-butoxyethyl)benzene** (101 MHz, $CDCl_3$)

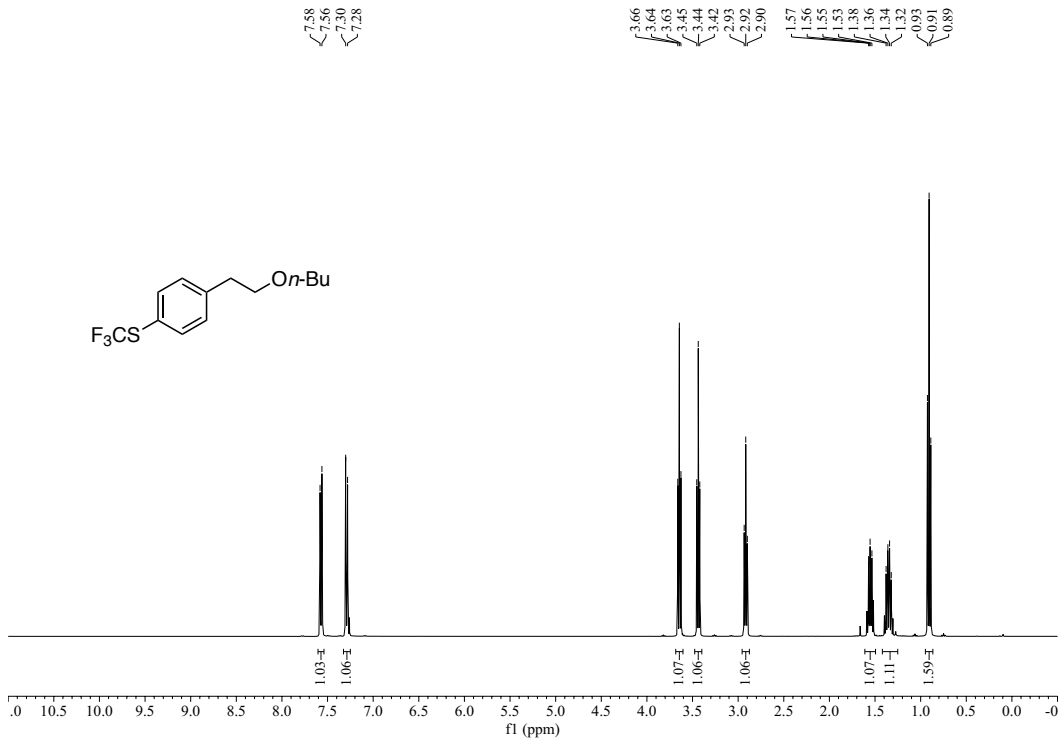

^{1}H NMR spectrum of **(4-(2-butoxyethyl)phenyl)(trifluoromethyl)sulfane** (400 MHz, $CDCl_3$)

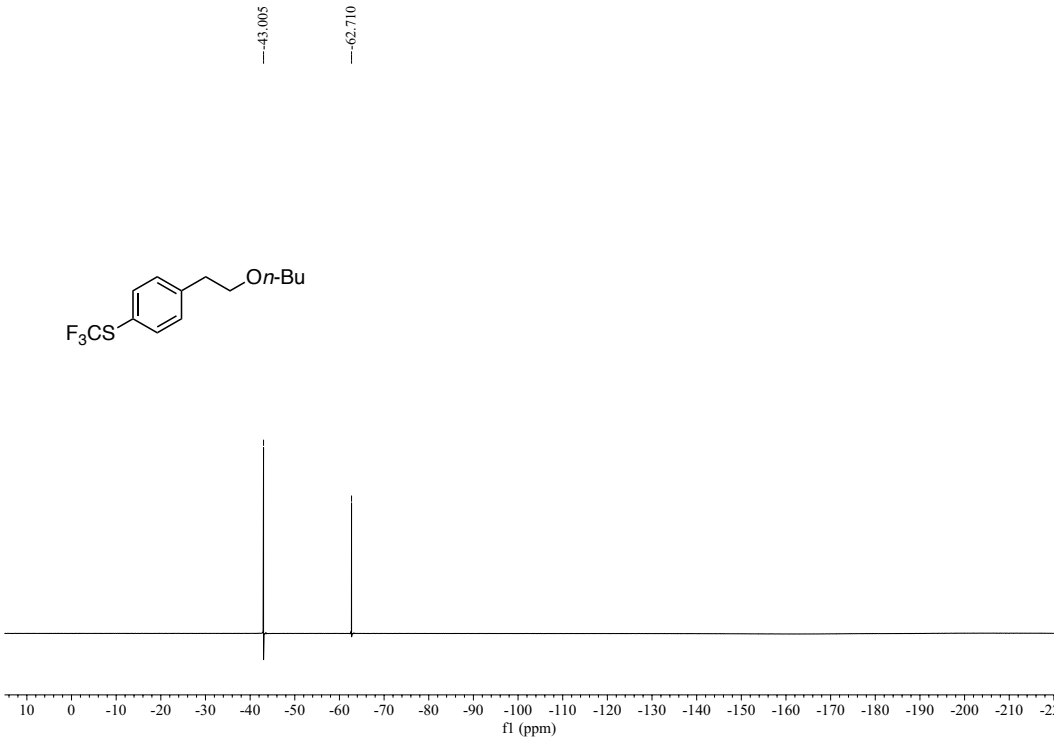

^{19}F NMR spectrum of **(4-(2-butoxyethyl)phenyl)(trifluoromethyl)sulfane** (376 MHz, $CDCl_3$)

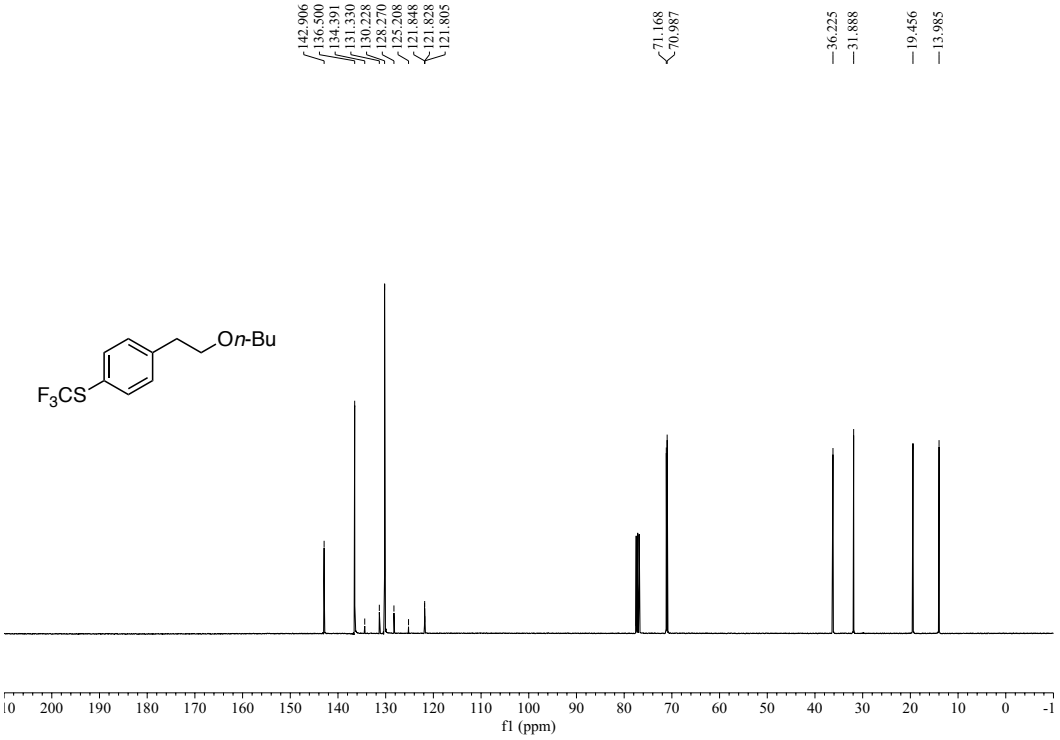

^{13}C NMR spectrum of **(4-(2-butoxyethyl)phenyl)(trifluoromethyl)sulfane** (101 MHz, $CDCl_3$)

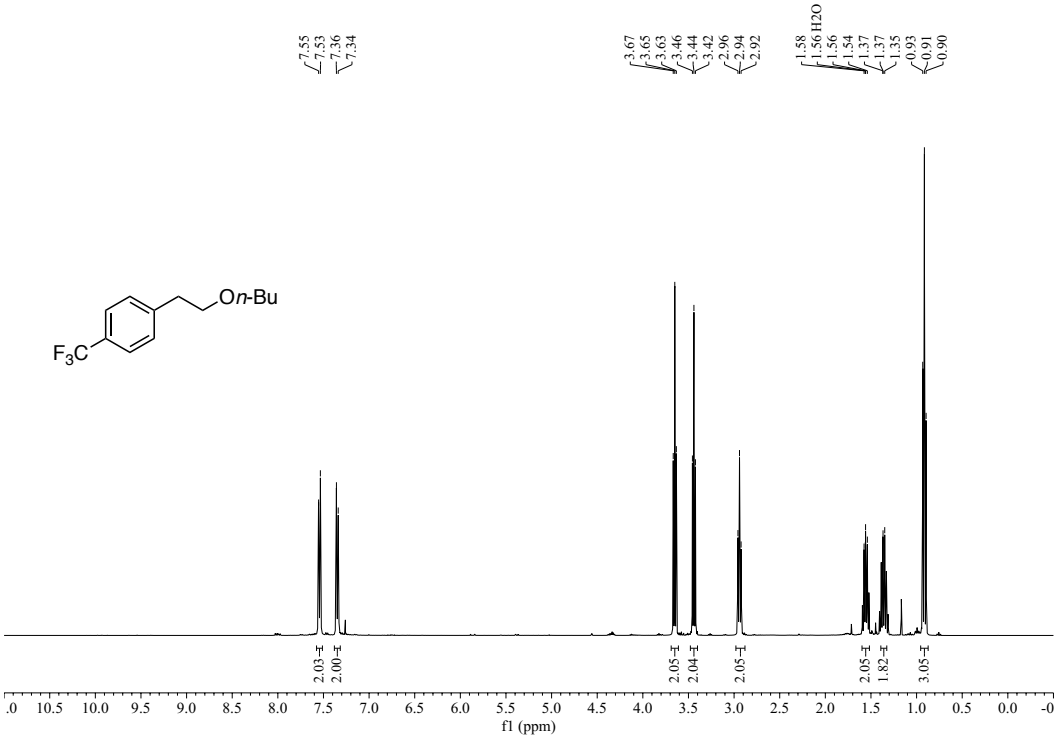

^{1}H NMR spectrum of **1-(2-butoxyethyl)-4-(trifluoromethyl)benzene** (400 MHz, $CDCl_3$)

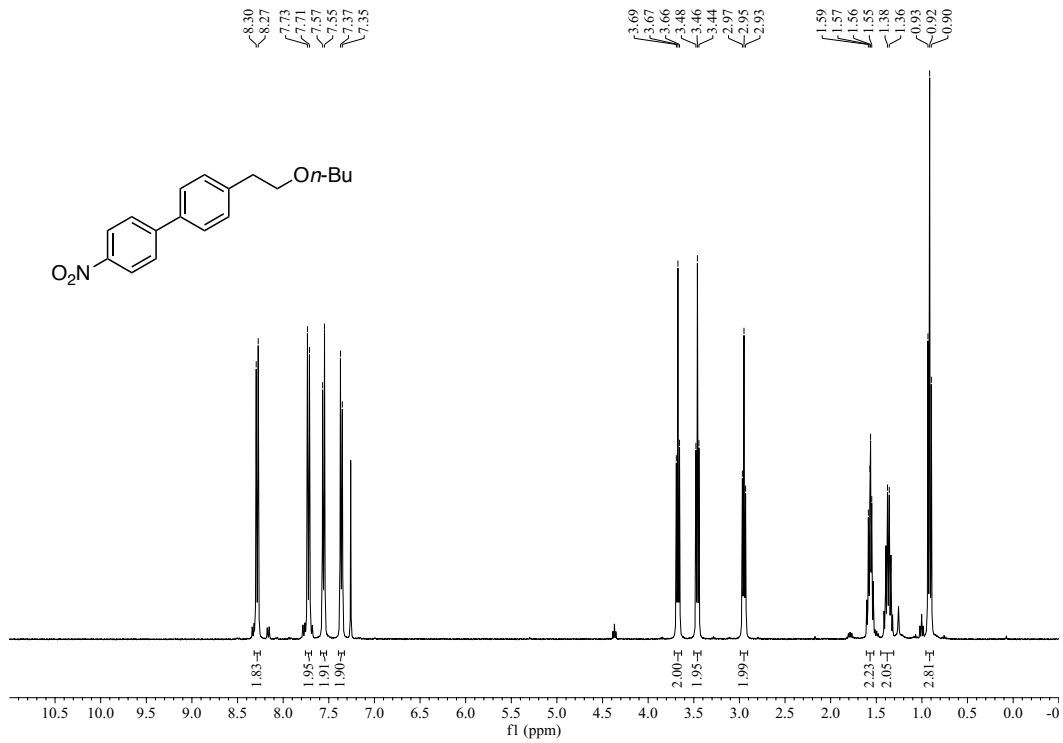

^{1}H NMR spectrum of **4-(2-butoxyethyl)-4'-nitro-1,1'-biphenyl** (400 MHz, $CDCl_3$)

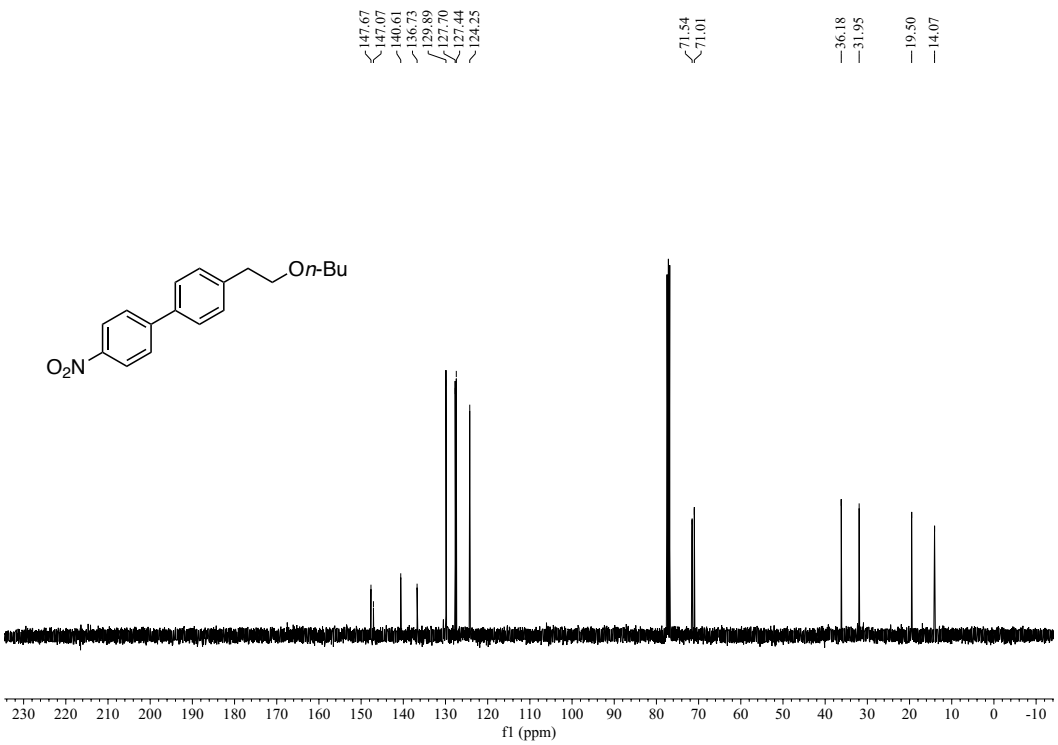

^{13}C NMR spectrum of **4-(2-butoxyethyl)-4'-nitro-1,1'-biphenyl** (101 MHz, $CDCl_3$)

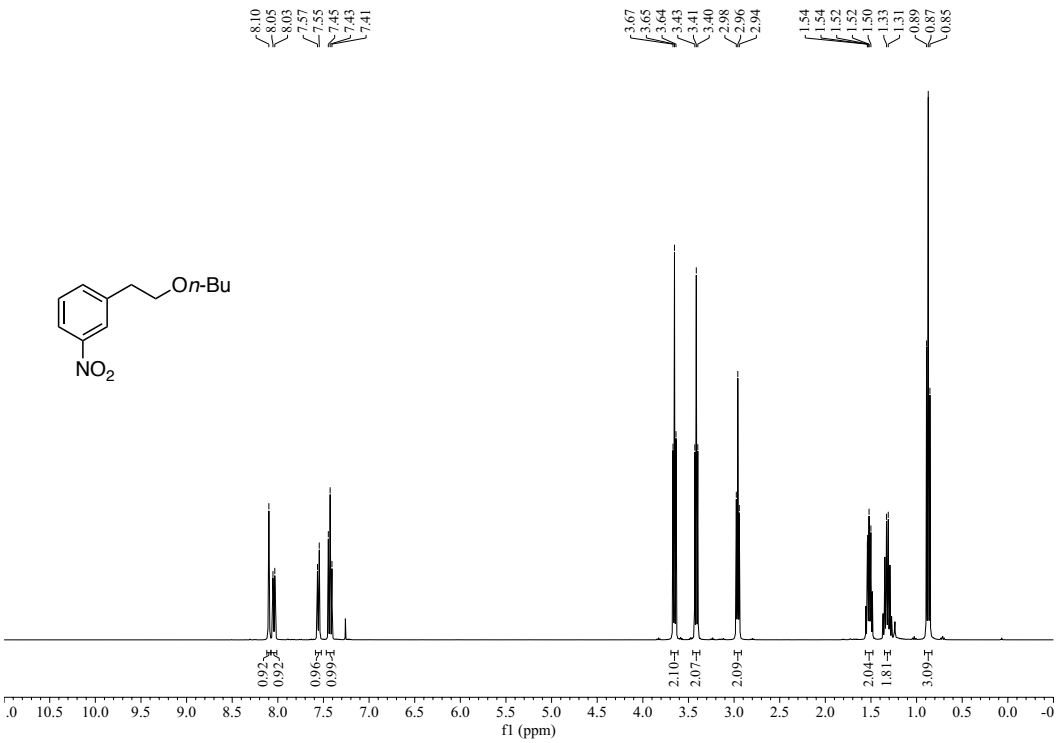

^{1}H NMR spectrum of **1-(2-butoxyethyl)-3-nitrobenzene** (400 MHz, $CDCl_3$)

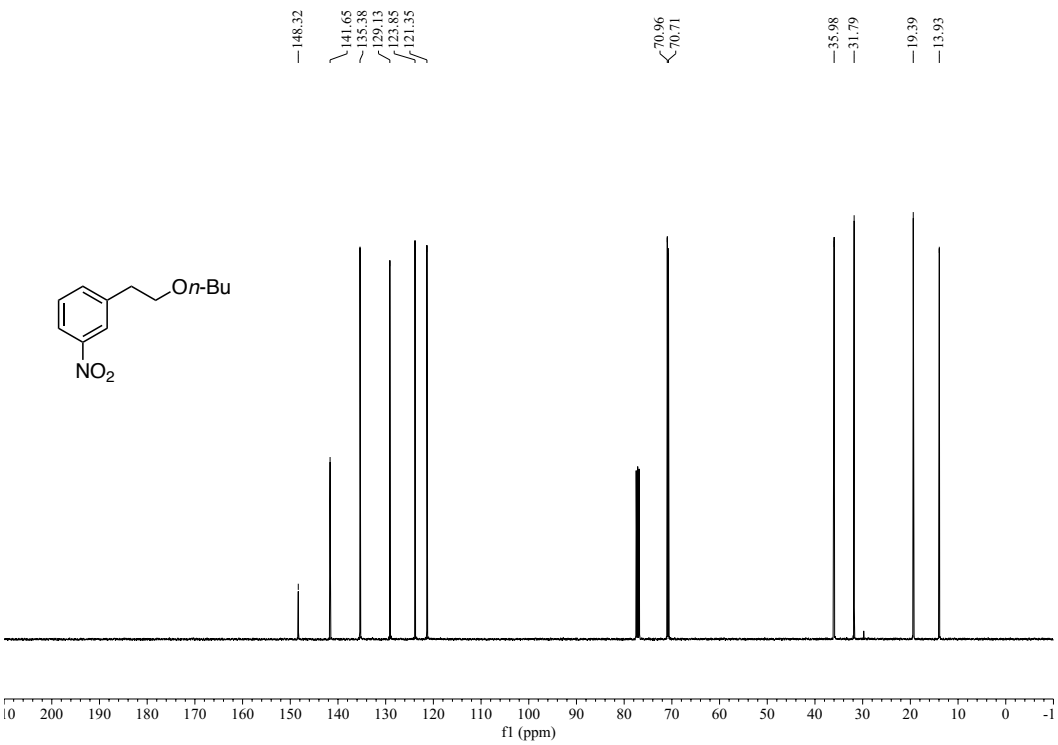

^{13}C NMR spectrum of **1-(2-butoxyethyl)-3-nitrobenzene** (101 MHz, $CDCl_3$)

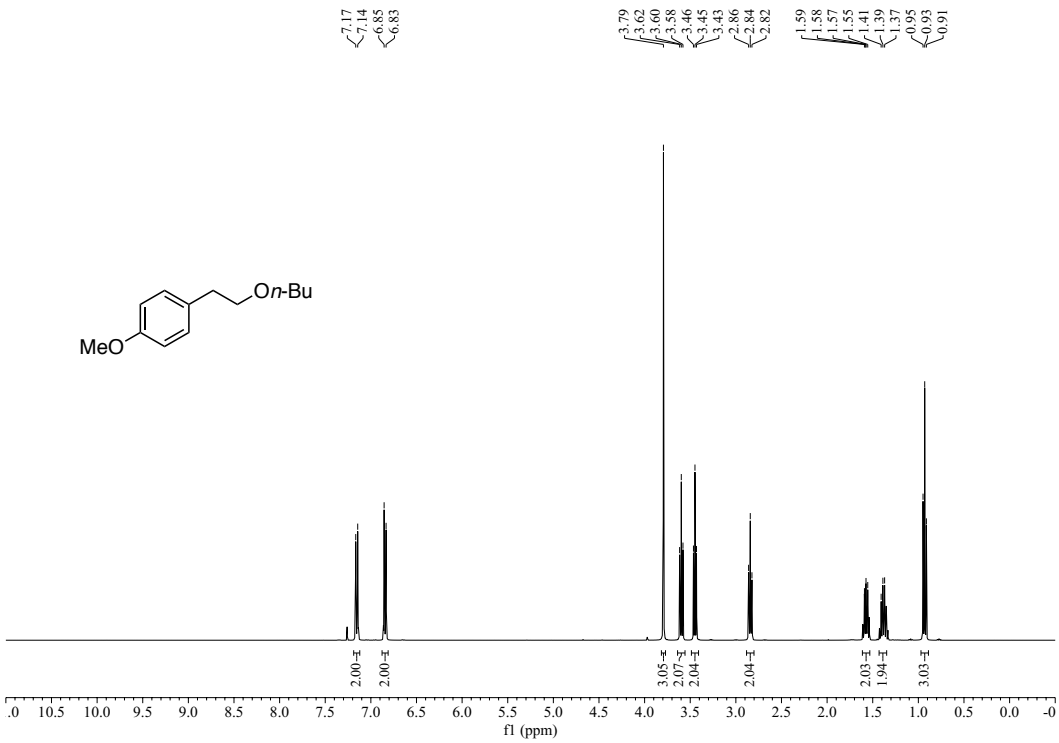

^{1}H NMR spectrum of **1-(2-butoxyethyl)-4-methoxybenzene** (400 MHz, $CDCl_3$)

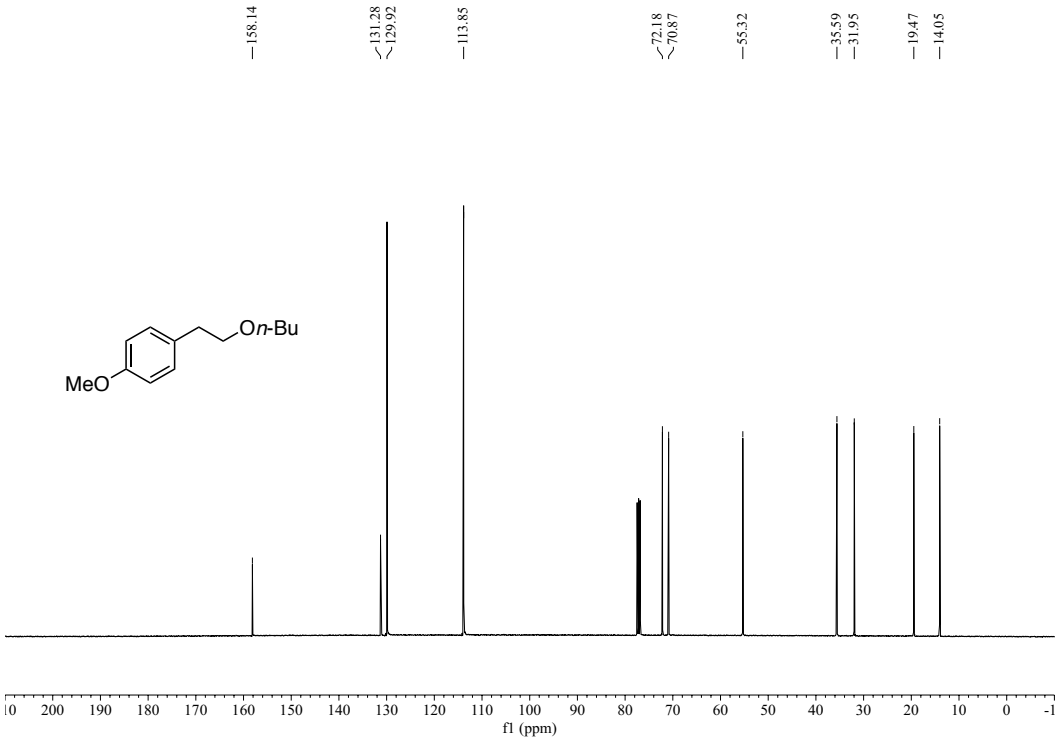

^{13}C NMR spectrum of **1-(2-butoxyethyl)-4-methoxybenzene** (101 MHz, $CDCl_3$)

APPENDIX TWO

A BASE-CATALYZED APPROACH FOR THE ANTI-MARKOVNIKOV HYDRATION OF STYRENE DERIVATIVES: EXPERIMENTAL

A2.1 General Information

This appendix is adapted from "A base-catalyzed approach for the anti- Markovnikov hydration of styrene derivatives" *Chem. Sci*., **2022**, *13*, 11427-11432. The intent of this information is to provide experimental details as they relate to my contributions to this work. Refer to the above publication and the corresponding supporting information for complete experimental details.

General Reagent Information: 1-*tert*-Butyl-4,4,4-tris(dimethylamino)-2,2-bis[tris(dimethylamino)-phosphoranylidenamino]-2λ^5,4λ^5-catenadi(phosphazene) (P_4-*t*-Bu, as a 0.8 M solution in hexanes) was purchased from Millipore Sigma (Product #79421) and stored in the freezer of a nitrogen-filled glovebox. Approximately 2 mL of the P_4-*t*-Bu solution was removed from the freezer on a weekly basis and stored at room temperature (rt) in the nitrogen-filled glovebox for routine use. Potassium *tert*-butoxide (KO-*t*-Bu) was purchased from Acros Organics (Product #27317) and stored in a nitrogen-filled glovebox. 1,4,7,10,13,16-Hexaoxacyclooctadecane (18-crown-6) was purchased from Chem-Impex (Catalog #03901) and stored in a nitrogen-filled glovebox. 1-Cyclopropylethanol was purchased from TCI (Catalog #C0984) and used as purchased. Borane tetrahydrofuran complex solution (catalog #176192), 9-borabicyclo[3.3.1]nonane solution (catalog #151076) and anhydrous 1,2-dimethoxyethane

(catalog #259527) were purchased from Millipore Sigma and used as received. Tetrahydrofuran, dichloromethane, and toluene were deoxygenated and dried by passage over packed columns of neutral alumina and copper (II) oxide under positive pressure of nitrogen. All other solvents and reagents were purchased from Millipore Sigma, Combi-Blocks, TCI, Acros Organics, Matrix, or Alfa-Aesar and used as received unless otherwise noted. Flash Chromatography was performed on 40-63 μm silica gel (SiliaFlash® F60 from Silicycle).

General Analytical Information: All reported new compounds were characterized by ^{1}H, ^{13}C and ^{19}F NMR spectroscopy, FTIR spectroscopy and mass spectrometry. Melting point analysis was conducted if the compound was solid. ^{1}H NMR, ^{13}C NMR, and ^{19}F NMR spectra were obtained on a Bruker Advanced NEO or Varian Inova 400 spectrometer. ^{1}H NMR data is reported as follows: chemical shift (δ ppm), multiplicity (s = singlet, d = doublet, t = triplet, q = quartet, dd = doublet of doublets, td = triplet of doublets, dq, doublet of quartets, m = multiplet), coupling constant (Hz), and integration.^{13}C NMR data is reported as follows: chemical shift (δ ppm), multiplicity (if applicable, q = quartet, d = doublet, dd = doublet of doublets). All ^{1}H NMR signals are reported as chemical shifts (δ ppm) relative to residual $CHCl_3$, at 7.26 ppm. All ^{13}C NMR signals are reported as chemical shifts (δ ppm) relative to $CDCl_3$ at 77.23 ppm. α,α,α-Trifluorotoluene (δ -62.61 ppm) internal standard was added to all ^{19}F NMR samples. High resolution mass spectra (HRMS) were recorded on an Agilent 6224 TOF LC-MS (ESI) provided by Colorado State University Central Instrumentation Facility. GC-MS data was recorded on an Agilent 7890B GC/5977A MSD system. Low resolution mass spectra (LRMS) were recorded on an Agilent 6130 Quadrupole LC-MS. Elemental analysis was performed by Atlantic Microlab, Inc., Norcross, GA. IR spectra were recorded using a Thermo Scientific Nicolet iS-50 FTIR Spectrometer and reported as frequency of absorption (cm^{-1}). Melting point analyses were

conducted using a Mel-Temp capillary melting point apparatus. Thin-layer chromatography analysis was performed on silica gel 60Å F_{254} plates (250 μm, SiliaPlate from Silicycle, #TLG-R10014B-323) and interpreted using UV light (254 nm), I_2 or $KMnO_4$ stain.

Note on nomenclature: The names provided for the structures below were obtained from ChemDraw Professional 16.0.

A2.2 General Procedure for Preparation of Vinyl Arenes

Vinyl arene preparation: The majority of vinyl arenes were prepared according to known procedures and are known compounds: 2-chloro-3-vinylpyridine[1], 4-chloro-2-(trifluoromethyl)styrene[2], 3-chloro-2-vinylpyridine[3], 4-methyl-2-nitrostyrene[4], 3-nitrostyrene[5], 2,6-dichlorostyrene[6], 2-chloro-3-(trifluoromethyl)styrene[7], 4-vinylbenzophenone[8], 2-bromo-5-(trifluoromethyl)styrene[9], 1-bromo-2-vinylnaphthalene[10], 2-vinylquinoline[11], 3-bromo-4-vinylpyridine[12], and 2-bromo-6-vinylpyridine[13]. New vinyl arene substrates were prepared according to Methods A and B below and characterization is provided in Section A2.8.

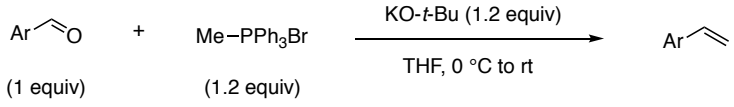

Method A: An oven-dried round bottom flask was charged with a magnetic stir bar and methyltriphenylphosphonium bromide (1.2 equiv). Anhydrous THF (20 mL per 1 g of aldehyde) was then added and the mixture was cooled to 0 °C in an ice bath with stirring. KO-*t*-Bu (1.2 equiv) was slowly added to the mixture resulting in a yellow-colored slurry. After the reaction mixture was stirred for 30 min at 0 °C, the aldehyde (1 equiv) was added dropwise into the mixture and the solution was then allowed to warm to rt for 4 h. At the completion of the reaction as indicated by TLC analysis, water (equal volume to THF used) was added to the reaction mixture and the resulting mixture was transferred to a separatory funnel. The mixture was extracted with

EtOAc (3 x reaction volume), and the resulting organic solution was washed with brine (1 x reaction volume) and dried over Na_2SO_4. The solvent was removed *in vacuo* and the resulting residue was purified by silica gel chromatography using the given eluent conditions to provide the vinyl arene.

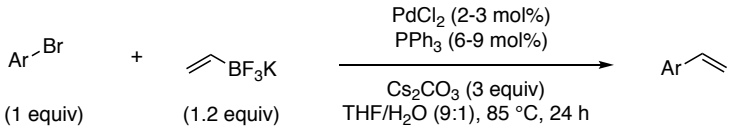

Method B: A flame-dried round bottom flask was charged with a magnetic stir bar, palladium(II) chloride (2-3 mol%), triphenylphosphine (6-9 mol%), aryl bromide (1 equiv), potassium vinyltrifluoroborate (1.2 equiv), and cesium carbonate (3 equiv) in a nitrogen-filled glovebox. The flask was removed from the glovebox, equipped with a reflux condenser with a rubber septum and evacuated and backfilled with nitrogen three times and left under positive pressure with a nitrogen balloon after the third cycle. A mixture of THF/H_2O (9/1) was then added via syringe. The reaction mixture was stirred for 24 h at 85 °C and then allowed to cool to rt. The reaction mixture was added to a separatory funnel, extracted with EtOAc (3 x reaction volume), and the organic solution was washed with brine (1 x reaction volume) and dried over anhydrous Na_2SO_4. After evaporation of the solvent *in vacuo*, the resulting residue was purified by silica gel chromatography using the given eluent conditions to provide the vinyl arene.

A2.3 General Procedure for Screening of Alcohol

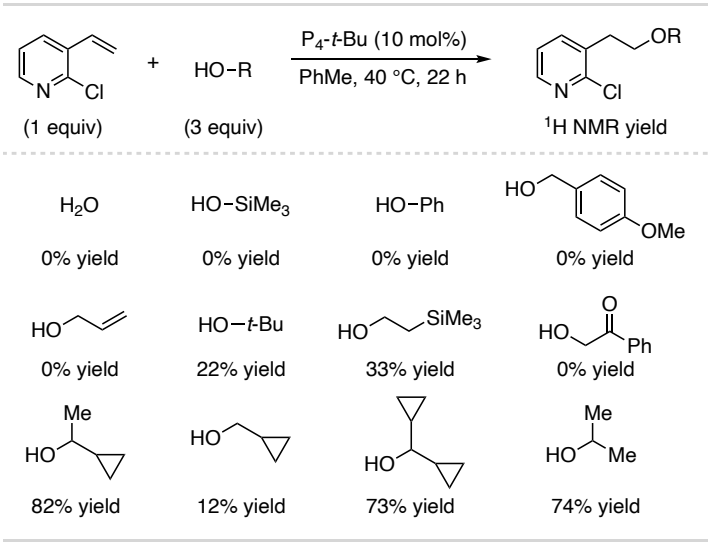

Figure A2-1. Alcohol addition yields for various potential protected water equivalents.

General procedure for screening of alcohol: In a nitrogen-filled glovebox, 2-chloro-3-vinylpyridine (27.9 mg, 0.2 mmol, 1.0 equiv), alcohol (0.6 mmol, 3.0 equiv) and toluene (0.2 mL) were added to an oven-dried 1-dram reaction vial (Thermo Scientific B7990-2) containing a magnetic stir bar. A commercial 0.8 M solution of P_4-*t*-Bu in hexanes (25 μL, 0.02 mmol, 0.1 equiv) was then added to the reaction solution. The reaction vial was capped (Thermo Scientific C4015-1A with 10/50 septa), removed from the glovebox, and placed in a preheated aluminum reaction heating block (Chemglass CG-1991-04) with stirring at 40 °C for 22 h. The reaction mixture was then allowed to cool to rt before dibenzyl ether (9.5 μL, 0.05 mmol) was added and an aliquot (approximately 50 μL) of the reaction solution was directly transferred to an NMR tube with $CDCl_3$ (0.6 mL). The reaction conversion was determined by ^{1}H NMR spectroscopy by comparison of the product integration to the dibenzyl ether internal standard. The results are tabulated above in Figure A2-1.

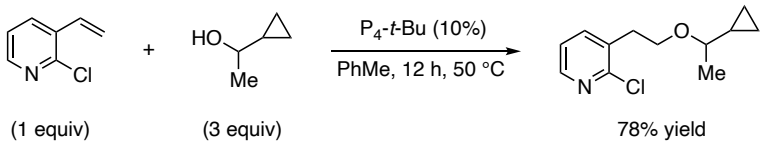

Independent preparation of ether 2: In a nitrogen filled glovebox, 2-chloro-3-vinylpyridine (139.6 mg, 1 mmol, 1 equiv), 1-cyclopropylethanol (**2-48**) (293 μL, 3 mmol, 3 equiv), P_4-*t*-Bu (125 μL of a 0.8 M solution in hexanes, 0.1 mmol, 0.1 equiv) and PhMe (0.50 mL) were added to an oven-dried 2-dram reaction vial (Thermo Scientific B7999-3) with a magnetic stir bar. The vial was capped (Thermo Scientific B7995-15 with 10/90 septa), removed from the glovebox and placed in a preheated oil bath at 50 °C. The reaction mixture was stirred for 12 h. Direct subjection of the crude reaction material to silica gel flash chromatography (5% ethyl acetate/hexanes to 20% ethyl acetate/hexanes) yielded product as a colorless oil (176.1 mg, 0.78 mmol, 78% yield). **^{1}H NMR** (400 MHz, $CDCl_3$) δ 8.23 (d, *J* = 4.7 Hz, 1H), 7.63 (d, *J* = 7.5 Hz, 1H), 7.16 (dd, *J* = 7.5, 4.7 Hz, 1H), 3.86 – 3.76 (m, 1H), 3.71 – 3.61 (m, 1H), 2.97 (t, *J* = 6.6 Hz, 2H), 2.73 (p, *J* = 6.4 Hz, 1H), 1.17 (dd, *J* = 6.3, 1.2 Hz, 3H), 0.84 – 0.70 (m, 1H), 0.51 (m, 1H), 0.40 (m, 1H), 0.27 (m, 1H), 0.02 (m, 1H). **^{13}C NMR** (101 MHz, $CDCl_3$) δ 151.5, 147.6, 139.9, 133.9, 122.6, 80.3, 66.6, 34.1, 20.4, 16.6, 4.6, 1.1. **HRMS** (DART) $[M+H]^+$ calcd. for $[C_{12}H_{17}NOCl]^+$, 226.0993 found, 226.1017. **IR** (neat, cm^{-1}) 3078.2, 2970.4, 2859.8, 1562.7, 1407.7, 1102.3, 1078.7, 795.1, 747.8.

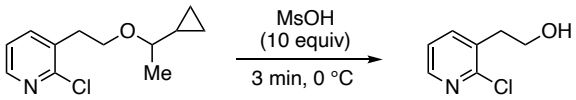

Independent procedure for the deprotection of ether: To an oven-dried 2-dram vial (Thermo Scientific B7999-3) containing a magnetic stir bar was added 2-chloro-3-(2-(1-cyclopropylethoxy)ethyl)pyridine (225.6 mg, 1 mmol, 1 equiv) and PhMe (1 mL). The vial was capped (Thermo Scientific B7995-15 with 10/90 septa), and the reaction solution was cooled to 0 °C in an ice bath and methanesulfonic acid (0.65 mL, 10 mmol, 10 equiv) was then added dropwise. The reaction mixture was stirred at 0 °C for 3 min. The biphasic mixture was then

neutralized with saturated aqueous Na_2CO_3 (2 mL) and extracted with ethyl acetate (3 x 2 mL). The combined organic solution was washed with brine (5 mL), dried over Na_2SO_4, concentrated *in vacuo*, and purified via silica gel column chromatography (40% ethyl acetate/hexanes) to give 2-(2-chloropyridin-3-yl)ethan-1-ol (138 mg, 0.87 mmol, 87% yield). See Section A2.8 for characterization data.

A2.4 Optimization and General Procedure for Hydration of Vinyl Arenes using P_4-*t*-Bu

Initial reaction condition optimization discussion: The initial conditions for P_4-*t*-Bu-catalyzed hydration and water surrogate screening were chosen based on our previous work in which PhMe was observed to provide the highest equilibrium ether yield.[14,15] Consistent with our prior work, Table A2-1 below shows the addition of 1-cyclopropylethanol (**2-48**) to be most favored in PhMe at 2 M concentration of the alkene. The "**General procedure for screening of alcohol**" from Section A2.3 above was followed to prepare Table A2-1. Other solvents are also effective but do not provide as high of equilibrium yields. Thus, PhMe was used in the General Procedure for the superbase conditions and for the comparison of **2-48** to other potential water surrogates shown in Table A2-1.

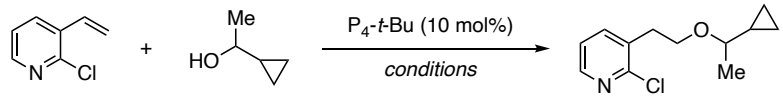

(1 equiv) **2-48** (3 equiv) ^{1}H NMR addition yield

Table A2-1: Initial conditions examined for P_4-*t*-Bu-catalyzed addition of **2-48** to **styrene**.

Solvent	Concentration of styrene	Temperature (°C)	^{1}H NMR yield (%)
PhMe	1 M	50	39
PhMe	2 M	50	71
PhMe	2 M	rt	25
PhMe	2 M	40	82
PhMe	2 M	60	62
PhMe	2 M	70	38
DME	2 M	50	55
Dioxane	2 M	50	49
THF	2 M	50	49

DMSO	2 M	50	33
n-Bu_2O	2 M	50	59
DMF	2 M	50	35
MeCN	2 M	50	44

Alcohol stoichiometry discussion: Excess alcohol (3 equiv of **2-48**) is typically used to provide high equilibrium addition yields. We have previously shown superbase-catalyzed alcohol addition to aryl alkenes can be efficient using 1.2 equiv of alcohol at lower reaction temperatures.[15] For this method using alcohol **2-48**, we typically obtained higher ether yields using 3 equiv of **2-48** at higher reaction temperatures. This is demonstrated in Table S3 with representative examples. However, this information does indicate that synthetically useful yields can be obtained using near stoichiometric amounts of **2-48** and styrene substrate.

Alcohol stoichiometry variation general procedure: In a nitrogen-filled glovebox, vinyl arene (0.1 mmol, 1.0 equiv), 1-cyclopropylethanol (11.7 µL, 0.12 mmol, 1.2 equiv) and PhMe (0.05 mL) were added to an oven-dried 1-dram reaction vial (Thermo Scientific B7990-2). A commercial 0.8 M solution of P_4-*t*-Bu in hexanes (12.5 µL, 0.01 mmol, 0.1 equiv) was then added to the reaction solution. The reaction vial was capped (Thermo Scientific C4015-1A with 10/50 septa), removed from the glovebox, and placed into a preheated aluminum reaction heating block (Chemglass CG-1991-04) and stirred for 24 h. The reaction solution was then allowed to cool to rt before dibenzyl ether (19.0 µL, 0.1 mmol, 1.0 equiv) was added and an aliquot (approximately 50 µL) of the reaction solution was directly transferred to an NMR tube with $CDCl_3$ (0.6 mL). The reaction yield was determined by ^1H NMR spectroscopy by comparison of the product integration to the dibenzyl ether internal standard. The results are tabulated in figure A2-2 below.

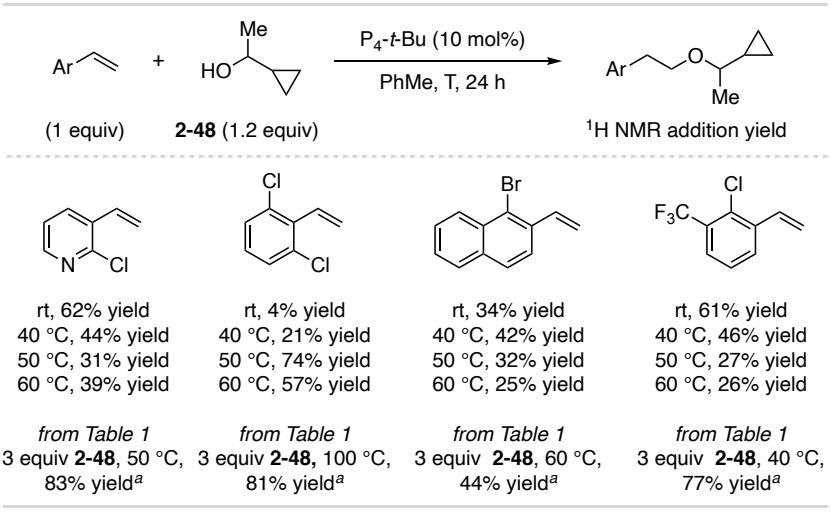

Figure A2-2: Yield comparison using 1.2 equiv of **2-48** at various temperatures to using 3 equiv of **2-48**.

Description of condition optimization on small scale for each styrene: We found that for each substrate examined, the optimal alcohol addition yield was temperature and concentration dependent as the reaction is under equilibrium control. Thus, for each substrate, we first obtained ^{1}H NMR yields of the reaction at a variety of temperatures (5 to 10 °C intervals) at 1 M in toluene. The reaction was then run at the highest yielding temperature at concentrations of 0.5 M and 2 M. Once optimal conditions were determined, the reaction was repeated on a 1.0 mmol scale and an isolated yield was obtained.

General procedure for condition optimization on small scale: In a nitrogen-filled glovebox, vinyl arene (0.15 mmol, 1.0 equiv), 1-cyclopropylethanol (44 μL, 0.45 mmol, 3.0 equiv) and toluene (0.15 mL) were added to an oven-dried 1-dram reaction vial (Thermo Scientific B7990-2) containing a magnetic stir bar. A commercial 0.8 M solution of P$_4$-*t*-Bu in hexanes (18.8 μL, 0.015 mmol, 0.1 equiv) was then added to the reaction solution. The reaction vial was capped (Thermo Scientific C4015-1A with 10/50 septa), removed from the glovebox, and placed in a preheated aluminum reaction heating block (Chemglass CG-1991-04) for 12 h. The reaction mixture was allowed to cool to rt before dibenzyl ether (14.3 μL, 0.075 mmol, 0.5 equiv) was added and an

aliquot (approximately 50 μL) of the reaction solution was directly transferred to an NMR tube with $CDCl_3$ (0.6 mL). The alcohol addition yield was determined by ^1H NMR spectroscopy by comparison of the addition product integration to the dibenzyl ether internal standard.

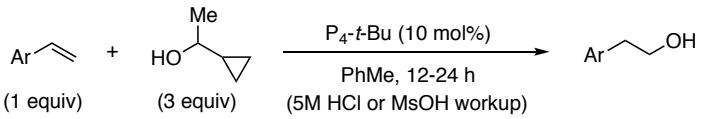

General procedure C for isolated hydration yields: In a nitrogen-filled glovebox, vinyl arene (1.0 mmol, 1.0 equiv), 1-cyclopropylethanol (293 μL, 3.0 mmol, 3.0 equiv) and toluene (amount indicated for each substrate) were added to a flame-dried 25 mL round bottom flask containing a magnetic stir bar. A commercial 0.8 M solution of P_4-*t*-Bu in hexanes (125 μL, 0.1 mmol, 0.1 equiv) was then added to the reaction solution. The reaction flask was sealed with a rubber septum, removed from the glovebox, and placed in an oil bath preheated to the indicated temperature. After 12-24 h (time indicated for each substrate), the flask was removed from the oil bath and inserted into a 0 °C ice bath. Methanesulfonic acid (667 μL, 10.3 mmol, 10.3 equiv) was then added dropwise and the resulting solution was stirred for the indicated time. For certain heterocyclic substrates, 5M aqueous HCl (4.0 mL, 20 mmol, 20 equiv) was used in place of methanesulfonic acid, with stirring at rt for 1 h. For both deprotection methods, the biphasic mixture was then neutralized with saturated aqueous Na_2CO_3 (amount equal to the total reaction volume) and extracted with ethyl acetate (3 x reaction volume). The combined organic layer was washed with brine (1 x reaction volume), concentrated *in vacuo* and the product was purified *via* silica gel column chromatography using the given eluent conditions.

A2.4 Optimization and General Procedure for Inorganic Base-Catalyzed Hydration of Vinyl Arenes

Inorganic base discussion: In our prior work, we investigated many inorganic bases, additives and solvents for the catalytic addition of *n*-butanol to 4-(trifluoromethyl)styrene as a model reaction.[14,15] This led to the discovery of KO-*t*-Bu with 18-crown-6 additive as an effective inorganic base system for styrene hydroetherification in 1,2-dimethoxyethane (DME), with lower yields obtained in nonpolar aromatic solvents. Shown below in Table S4, we examined similar inorganic catalyst mixtures in a variety of solvents and conditions for the addition of 1-cyclopropylethanol to 2-chloro-3-vinylpyridine. Moderate addition yields (50-60%) were obtained in a variety of solvents, although none outperformed the previously optimized conditions or the superbase conditions. In general, the trends in Table A2-4 are consistent with our prior studies, and more information regarding inorganic bases, additives, solvents and concentration effects can be found in our prior reports.[14,15] Therefore, KO-*t*-Bu with 18-crown-6 in DME was used as the standard inorganic catalyst system, with additional temperature optimization conducted for each substrate.

General procedure for optimization: In a nitrogen filled glovebox, inorganic base (0.1 equiv, 0.01 mmol), 18-crown-6 (2.9 mg, 0.011 mmol, 0.11 equiv), solvent (amount indicated as molarity of alkene in solvent), 1-cyclopropylethanol (0.3 to 0.5 mmol, 3.0 to 5.0 equiv) and 2-chloro-3-vinylpyridine (14.0 mg, 0.1 mmol, 1.0 equiv) were added to an oven-dried 1-dram reaction vial (Thermo Scientific B7990-2) containing a magnetic stir bar. The reaction vial was capped (Thermo Scientific C4015-1A with 10/50 septa) and placed in a preheated aluminum reaction heating block (Chemglass CG-1991-04) and stirred for 24 h. The reaction solution was allowed to cool to rt before dibenzyl ether (19.0 μL, 0.1 mmol, 1.0 equiv) was added and an aliquot (approximately 50 μL) of the reaction solution was directly transferred to an NMR tube with $CDCl_3$ (0.6 mL). The

alcohol addition yield was determined by ^{1}H NMR spectroscopy by comparison of the product integration to the dibenzyl ether internal standard. The results are tabulated in Table A2-2 below.

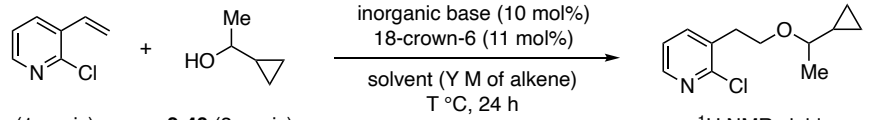

(1 equiv) **2-48** (3 equiv) ^{1}H NMR yield

Table A2-2. Condition and solvent effects for inorganic base-catalyzed addition of 1-cyclopropylethanol (**2-48**) to 2-chloro-3-vinylpyridine.

Entry	Base	Solvent (Y M)	Temp (°C)	2-48 (X equiv)	Yield %
1	KO-*t*-Bu	DME (2 M)	50 °C	3	60
2	KO-*t*-Bu, no 18-crown-6	DME (2 M)	50 °C	3	0
3	KOH	DME (2 M)	50 °C	3	51
4	CsOH•H_2O	DME (2 M)	50 °C	3	47
5	CsF+LiO-*t*-Bu	DME (2 M)	50 °C	3	54
6	KH	DME (2 M)	50 °C	3	0
7	KO-*t*-Bu	MeCN (2 M)	50 °C	3	56
8	KO-*t*-Bu	PhCN (2 M)	50 °C	3	59
9	KO-*t*-Bu	THF (2 M)	50 °C	3	53
10	KO-*t*-Bu	PhMe (2 M)	50 °C	3	54
11	KO-*t*-Bu	DME (0.5 M)	50 °C	3	44
12	KO-*t*-Bu	DME (1 M)	50 °C	3	19
13	KO-*t*-Bu	DME (1.5 M)	50 °C	3	56
14	KO-*t*-Bu	DME (2 M)	50 °C	4	62
15	KO-*t*-Bu	DME (2 M)	50 °C	5	67
16	KO-*t*-Bu	DME (2 M)	40 °C	3	56
17	KO-*t*-Bu	DME (2 M)	40 °C	4	63
18	KO-*t*-Bu	DME (2 M)	40 °C	5	70

General procedure for inorganic condition optimization on small scale for each styrene: We found that for each substrate examined, the optimal addition yield was obtained at a specific temperature since the reaction is under equilibrium control. Thus, for each substrate, we first obtained ^{1}H NMR yields of the reaction at a variety of temperatures (5 °C intervals) at 2M concentration in 1,2-dimethoxyethane (DME). Once an optimal temperature was determined, the reaction was repeated on a 1.0 mmol scale and an isolated yield was obtained.

In the open air, KO-*t*-Bu (2.2 mg, 0.02 mmol, 0.1 equiv), 18-crown-6 (5.8 mg, 0.022 mmol, 0.11 equiv), 1,2-dimethoxyethane (0.1 mL), 1-cyclopropylethanol (58.7 µL ,0.6 mmol, 3.0 equiv) and vinyl arene (0.2 mmol, 1.0 equiv) were added to an oven-dried 1-dram reaction vial (Thermo Scientific B7990-2) containing a magnetic stir bar. The reaction vial was capped (Thermo Scientific C4015-1A with 10/50 septa) and placed in a preheated aluminum reaction heating block (Chemglass CG-1991-04) for 16 h. The reaction solution was allowed to cool to rt before dibenzyl ether (9.5 µL, 0.05 mmol, 0.25 equiv) was added and an aliquot (approximately 50 µL) of the reaction solution was directly transferred to an NMR tube with $CDCl_3$ (0.6 mL). The alcohol addition yield was determined by ^1H NMR spectroscopy by comparison of the product integration to the dibenzyl ether internal standard.

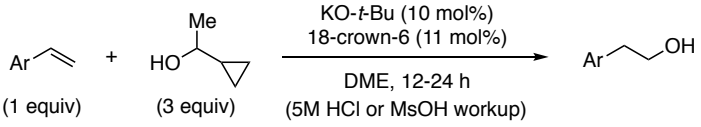

General procedure D for isolated yields: In the open air, KO-*t*-Bu (11.2 mg, 0.10 mmol, 0.1 equiv), 18-crown-6 (29.1 mg, 0.11 mmol, 0.11 equiv), 1,2-dimethoxyethane (0.5 mL), 1-cyclopropylethanol (293 µL, 3.0 mmol, 3.0 equiv) and vinyl arene (1.0 mmol, 1.0 equiv) were added in successive order to a flame-dried 25 mL round bottom flask containing a magnetic stir bar. The flask was capped with a rubber septum, a nitrogen-filled balloon was inserted and the flask was placed in a preheated oil bath at the indicated temperature with stirring. After the indicated time, the flask was removed from the oil bath and inserted into a 0 °C ice bath. To the reaction solution was then added methanesulfonic acid (667 µL, 10.3 mmol, 10.3 equiv) dropwise and the resulting mixture was stirred for the indicated time. For certain heterocyclic substrates, 5M aqueous HCl (4.0 mL, 20 mmol, 20 equiv) was used in place of methanesulfonic acid, with stirring at rt for 1 h. For both deprotection methods, the biphasic mixture was then neutralized with

saturated aqueous sodium carbonate (amount equal to the total reaction volume) and extracted with ethyl acetate (3 x reaction volume). The combined organic layer was washed with brine (1 x reaction volume), concentrated *in vacuo* and the product was purified *via* silica gel column chromatography using the given eluent conditions.

A2.6 Alcohol Addition Yield Comparisons Using Inorganic Base and Superbase Conditions

Purpose and discussion: Base-catalyzed addition yields of 1-cyclopropylethanol to vinyl arenes were compared using the organic superbase P_4-*t*-Bu and the inorganic base conditions KO-*t*-Bu with 18-crown-6. The reaction temperatures are not always the same between the superbase and inorganic conditions; semi-optimized temperatures were obtained from small scale optimizations described in the general procedures above (generally, optimal temperatures for the two conditions were within 10 °C of each other). These comparisons are summarized in Figure A2-3 and show that P_4-*t*-Bu is a more general catalyst, typically giving higher addition yields, although the inorganic system also provides synthetically useful yields for many substrates. This information is provided to help users select proper bases for their intended applications or substrate of interest.

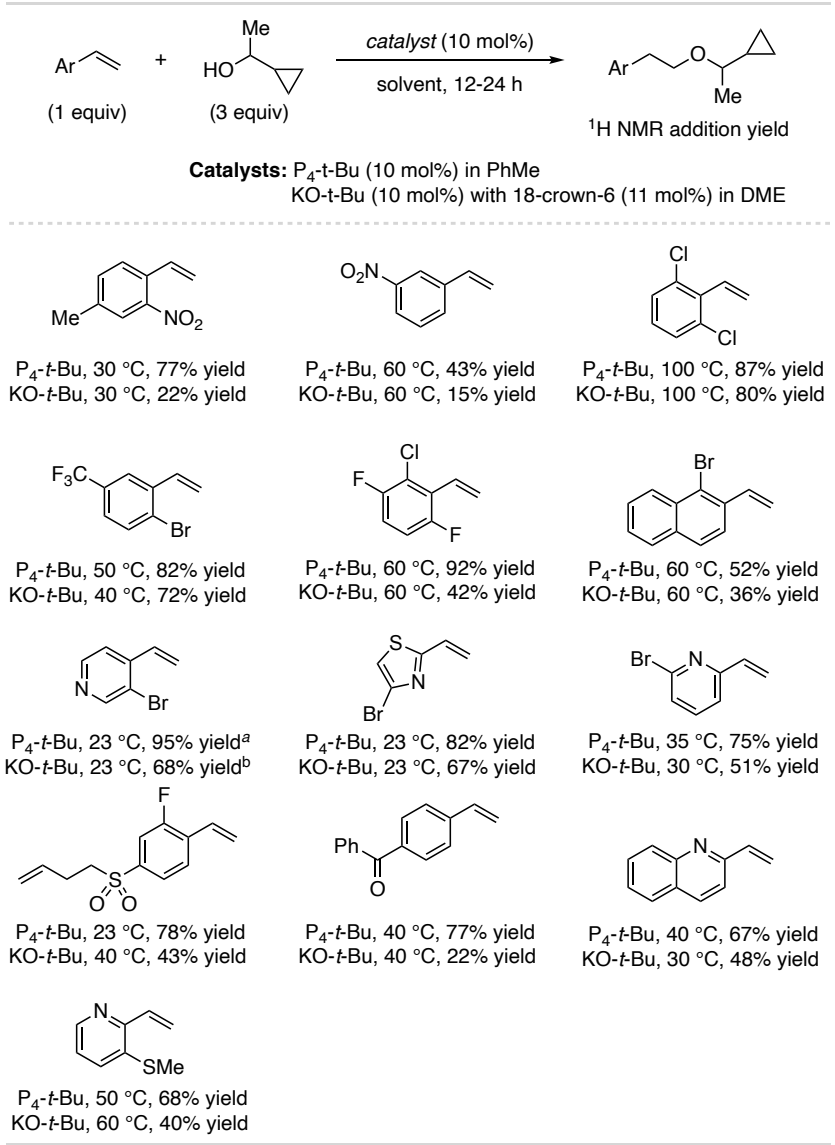

Figure A2-3. Comparison of ^{1}H NMR alcohol addition yields using superbase and inorganic base conditions. [a] 6 h reaction time; [b] 10 min reaction time; mass balance decreased significantly over longer times.

General procedure for P$_4$-*t*-Bu as catalyst: In a nitrogen-filled glovebox, vinyl arene (0.2 mmol, 1.0 equiv), 1-cyclopropylethanol (58.7 μL, 0.6 mmol, 3.0 equiv) and PhMe (0.2 mL) were added to an oven-dried 1-dram reaction vial (Thermo Scientific B7990-2). A commercial 0.8 M solution of P$_4$-*t*-Bu in hexanes (25 μL, 0.02 mmol, 0.1 equiv) was then added to the reaction solution. The reaction vial was capped (Thermo Scientific C4015-1A with 10/50 septa), removed from the glovebox, and placed into a preheated aluminum reaction heating block (Chemglass CG-1991-04)

and stirred for 12-24 h (time as indicated in product characterization section for products from Table 1 and Scheme 2). The reaction solution was then allowed to cool to rt before dibenzyl ether (9.5 μL, 0.05 mmol, 0.25 equiv) was added and an aliquot (approximately 50 μL) of the reaction solution was directly transferred to an NMR tube with $CDCl_3$ (0.6 mL). The reaction yield was determined by ^1H NMR spectroscopy by comparison of the product integration to the dibenzyl ether internal standard.

General procedure for KO-*t*-Bu/18-crown-6 as catalyst: On the bench top, KO-*t*-Bu (0.02 mmol, 0.1 equiv), 18-crown-6 (0.022 mmol, 0.11 equiv), 1,2-dimethoxyethane (0.2 mL), 1-cyclopropylethanol (58.7 μL, 0.6 mmol, 3.0 equiv) and vinyl arene (0.2 mmol, 1.0 equiv) were added to an oven-dried 1-dram reaction vial (Thermo Scientific B7990-2). The reaction vial was capped (Thermo Scientific C4015-1A with 10/50 septa), and placed in a preheated aluminum reaction heating block (Chemglass CG-1991-04) and stirred for 12-24 h. The reaction solution was allowed to cool to rt before dibenzyl ether (9.5 μL, 0.05 mmol, 0.25 equiv) was added and an aliquot (approximately 50 μL) of the reaction solution was directly transferred to an NMR tube with $CDCl_3$ (0.6 mL). The reaction yield was determined by ^1H NMR spectroscopy by comparison of the product integration to the dibenzyl ether internal standard. **Note:** The general procedure used for inorganic conditions does not require the use of a strict inert atmosphere and thus these reactions were setup open to air. As a control, three substrates from Table A2-5 (4-methyl-2-nitrostyrene, 1-bromo-2-vinylnaphthalene and 2,6-dichlorostyrene; 4-(trifluoromethyl)styrene was also tested) were repeated using the general procedure above under a nitrogen atmosphere. These reactions led to near identical yields (± 2-3%) to those provided in Table A2-5.

A2.7 Discussion of Styrene Scope Limitations

Discussion: The base-catalyzed reversible addition of alcohols to styrenes provides the highest equilibrium yields for electron-deficient and heteroaryl derivatives.[14,15] To clarify the limitations of this protocol, Table A2-6 shows examples of mildly activated, unactivated and 1,1-disubstituted aryl-substituted alkenes varying the stoichiometry of alkene and 1-cyclopropylethanol.

Procedure: In a nitrogen-filled glovebox, the alkene (0.1 mmol, 1.0 equiv or 0.5 mmol, 5.0 equiv), 1-cyclopropylethanol (29.3 µL, 0.3 mmol, 3.0 equiv; 48.9 µL, 0.5 mmol, 5.0 equiv; 9.8 µL, 0.1 mmol, 1.0 equiv; 11.7 µL, 0.12 mmol, 1.2 equiv) and PhMe (0.05 mL) were added to an oven-dried 1-dram reaction vial (Thermo Scientific B7990-2). A commercial 0.8 M solution of P_4-*t*-Bu in hexanes (12.5 µL, 0.01 mmol, 0.1 equiv) was then added to the reaction solution. The reaction vial was capped (Thermo Scientific C4015-1A with 10/50 septa), removed from the glovebox, and placed into a preheated aluminum reaction heating block (Chemglass CG-1991-04) and stirred for 24 h. The reaction solution was then allowed to cool to rt before dibenzyl ether (19.0 µL, 0.1 mmol, 1.0 equiv) was added and an aliquot (approximately 50 µL) of the reaction solution was directly transferred to an NMR tube with $CDCl_3$ (0.6 mL). The reaction yield was determined by ^{1}H NMR spectroscopy by comparison of the product integration to the dibenzyl ether internal standard.

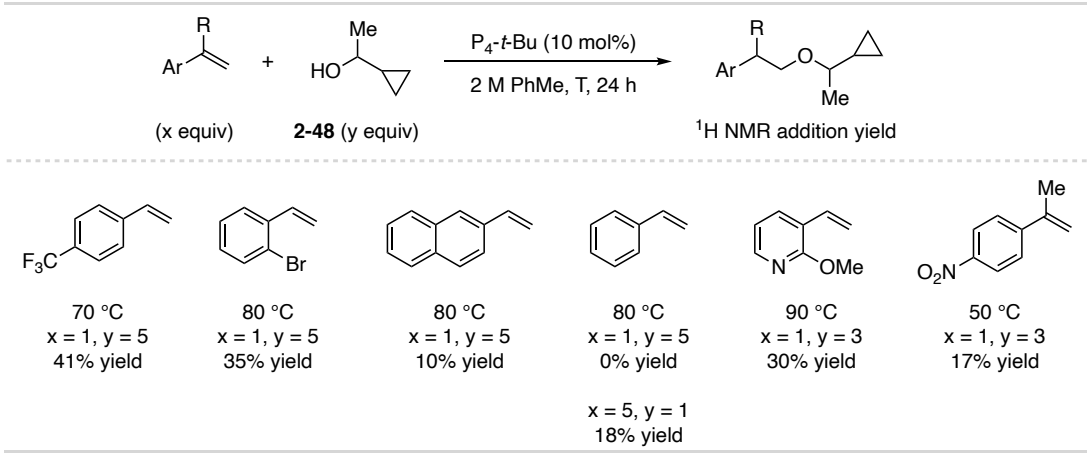

Figure A2-4: Aryl alkene scope limitations, including electron-neutral to electron-rich aryl alkenes, and 1,1-disubstituted variants that provide low equilibrium ether yields.

A2.8 Synthesis and Characterization Data for Vinyl Arenes

2-Fluoro-4-(methylsulfonyl)styrene

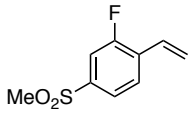

General Procedure B was followed with triphenylphosphine (94 mg, 0.36 mmol, 0.06 equiv), palladium(II) chloride (21 mg, 0.1 mmol, 0.02 equiv), cesium carbonate (5.87 g, 18 mmol, 3 equiv), potassium vinyltrifluoroborate, and 1-bromo-2-fluoro-4-(methylsulfonyl)benzene (1.52 g, 6.0 mmol, 1.0 equiv). Flash column chromatography (10% ethyl acetate/hexanes) yielded the title product as a yellow liquid (865 mg, 4.32 mmol, 72% yield). **^{1}H NMR** (400 MHz, $CDCl_3$) δ 7.74 – 7.55 (m, 3H), 6.90 (dd, *J* = 17.7, 11.3 Hz, 1H), 5.99 (dd, *J* = 17.7, 0.7 Hz, 1H), 5.59 (dd, *J* = 11.3, 0.8 Hz, 1H), 3.06 (s, 3H). **^{13}C NMR** (101 MHz, $CDCl_3$) δ 159.6 (d, J = 255.5 Hz), 140.7 (d, *J* = 6.9 Hz), 130.9 (d, *J* = 12.2 Hz), 128.2 (d, *J* = 3.8 Hz), 128.1 (d, *J* = 3.7 Hz), 123.1 (d, *J* = 3.8 Hz), 120.6 (d, *J* = 4.8 Hz), 115.3 (d, *J* = 25.7 Hz), 44.6. **^{19}F NMR** (376 MHz, CDCl3) δ -114.42. **HRMS** (DART) $[M+NH_4]^+$ calcd. for $[C_9H_{13}FNO_2S]^+$ 218.0646, found 218.0655. **IR** (neat, cm^{-1}) 3076.8, 3015.3, 2925.7, 1629.0, 1483.5, 1403.5, 1403.5, 1295.2, 1226.1, 1141.0, 991.3, 760.9, 529.4.

2-Chloro-3,6-difluorostyrene

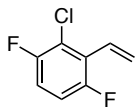

General Procedure A was followed with methyltriphenylphosphonium bromide (4.30 g, 12 mmol, 1.2 equiv), KO-*t*-Bu (1.35 g, 12 mmol, 1.2 equiv), and 2-chloro-3,6-difluorobenzaldehyde (1.76 g, 10 mmol, 1.0 equiv). Flash column chromatography with hexanes yielded the title product as a colorless liquid (1.20 g, 6.87 mmol, 69% yield). **^{1}H NMR** (400 MHz, $CDCl_3$) δ 7.06 – 6.90 (m, 2H), 6.79 (dd, *J* = 18.0, 12.0 Hz, 1H), 6.02 (dt, *J* = 18.0, 1.4 Hz, 1H), 5.71 (dt, *J* = 11.9, 1.8 Hz, 1H). **^{13}C NMR** (101 MHz, $CDCl_3$) δ 157.1 (dd, *J* = 249.1, 1.9 Hz), 155.0 (dd, *J* = 244.5, 2.8 Hz), 127.1 (dd, *J* = 2.9, 1.5 Hz), 125.8 (d, *J* = 16.2 Hz), 123.5 (d, *J* = 11.8 Hz),

121.4 (dd, J = 19.4, 6.4 Hz), 115.0 (dd, J = 8.9, 2.3 Hz), 114.7 (dd, J = 8.9, 4.2 Hz). **^{19}F NMR** (376 MHz, $CDCl_3$) δ -117.45 (d, J = 15.2 Hz), -118.02 (d, J = 15.2 Hz). **LRMS** $[M+H]^+$ calcd. for $[C_8H_6ClF_2]^+$ 175.0, found 175.0. **IR** (neat, cm^{-1}) 3100.3, 1851.7, 1473.0, 1383.6, 1231.9, 966.3, 933.6, 861.3, 808.1.

4-Bromo-2-vinylthiazole

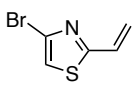

A slightly modified variant of General Procedure A was followed for this substrate. An oven-dried round bottom flask was charged with a magnetic stir bar and methyltriphenylphosphonium bromide (3.29 g, 9.6 mmol, 1.2 equiv), capped with a rubber septum, evacuated and backfilled with nitrogen three times and left under positive pressure with a nitrogen filled balloon. Anhydrous THF (30 mL) was added and the mixture was cooled to 0 °C in an ice bath with stirring. *n*-Butyllithium (5.50 mL of 1.6M solution in hexanes, 8.8 mmol, 1.1 equiv) was added dropwise with a nitrogen flushed syringe. Procedure A was then followed with 4-bromothiazole-2-carbaldehyde (1.54 g, 8.0 mmol, 1.0 equiv). Flash column chromatography (5% ethyl acetate/hexanes) yielded the title product as a yellow liquid (624 mg, 3.28 mmol, 41% yield). **^{1}H NMR** (400 MHz, $CDCl_3$) δ 7.13 (s, 1H), 6.86 (dd, J = 17.5, 10.9 Hz, 1H), 6.08 (d, J = 17.5 Hz, 1H), 5.58 (d, J = 10.9 Hz, 1H). **^{13}C NMR** (101 MHz, $CDCl_3$) δ 167.9, 129.8, 125.9, 121.1, 116.4. **HRMS** (DART) $[M+H]^+$ calcd. for $[C_5H_5BrNS]^+$ 189.9321, found 189.9330. **IR** (neat, cm^{-1}) 3120.2, 1621.6, 1468.6, 1278.4, 1224.8, 1081.2, 974.5, 886.4, 832.3, 698.1.

4-(2-Vinylpyrimidin-5-yl)thiomorpholine

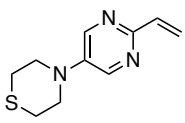

General Procedure A was followed with methyltriphenylphosphonium bromide (428.7 mg, 1.2 mmol, 1.2 equiv), KO-*t*-Bu (134.7mg, 1.2 mmol, 1.2 equiv), 5-

thiomorpholinopyrimidine-2-carbaldehyde (209 mg, 1.0 mmol, 1.0 equiv, synthesis described below). Flash column chromatography (40% ethyl acetate/hexanes) yielded the title product as a clear liquid (100 mg, 0.48 mmol, 48% yield). **^{1}H NMR** (400 MHz, $CDCl_3$) δ 8.31 (s, 2H), 6.81 (dd, *J* = 17.4, 10.7 Hz, 1H), 6.39 (dd, *J* = 17.4, 1.7 Hz, 1H), 5.56 (dd, *J* = 10.7, 1.7 Hz, 1H), 3.76 – 3.47 (m, 4H), 2.88 – 2.35 (m, 4H). **^{13}C NMR** (101 MHz, $CDCl_3$) δ 144.9, 144.6, 142.3, 135.8, 120.8, 50.7, 26.4. **HRMS** (DART) $[M+H]^+$ calcd. for $[C_{10}H_{14}N_3S]^+$ 208.0903, found 208.0904. **IR** (neat, cm^{-1}) 2953.9, 2913.7, 1653.1, 1538.7, 1455.4, 1402.4, 1301.7, 1224.7, 1199.3, 997.0, 924.3, 817.2.

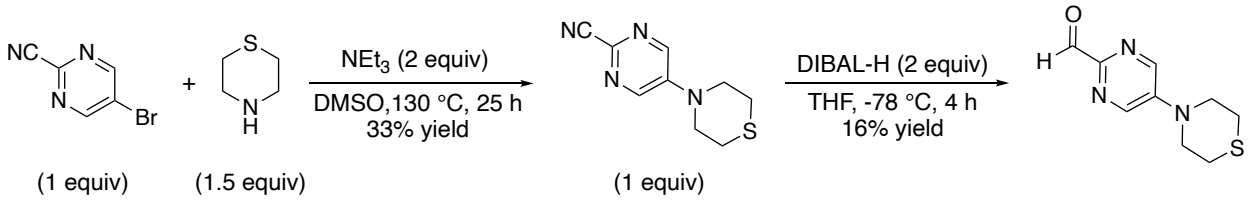

5-Thiomorpholinopyrimidine-2-carbaldehyde preparation: 5-bromopyrimidine-2-carbonitrile (4.60 g, 25 mmol, 1 equiv) was added to an oven-dried 100 mL round bottom flask containing a magnetic stir bar. The flask was sealed with a rubber septum and evacuated and backfilled with nitrogen three times and left under a positive pressure of nitrogen. DMSO (25 mL) was added *via* a nitrogen flushed syringe. Thiomorpholine (3.77 mL, 37.5 mmol, 1.5 equiv) and triethylamine (6.79 mL, 50 mmol, 2 equiv) were then added *via* nitrogen flushed syringes. The reaction flask was placed in a preheated oil bath at 130 °C and stirred for 25 h. The reaction mixture was cooled to room temperature and water (25 mL) was added. The resulting mixture was added to a separatory funnel, extracted with EtOAc (3 x reaction volume), and the organic solution was washed with brine (50 mL) and dried over Na_2SO_4. After evaporation of the solvent *in vacuo*, the resulting residue was purified by silica gel chromatography (10% ethyl acetate/1% triethylamine/hexanes to 40% ethyl acetate/1% triethylamine/hexanes) to yield 5-

thiomorpholinopyrimidine-2-carbonitrile as a brownish orange solid (1.695 g, 8.2 mmol, 33% yield). **^{1}H NMR** (400 MHz, $CDCl_3$) δ 8.29 (s, 2H), 3.86 – 3.79 (m, 4H), 2.78 – 2.71 (m, 4H). **^{13}C NMR** (101 MHz, $CDCl_3$) δ 143.7, 142.4, 133.0, 116.7, 49.2, 26.0.

5-Thiomorpholinopyrimidine-2-carbonitrile (1.25 g, 6.10 mmol, 1 equiv) was added to an oven-dried 100 mL round bottom flask containing a magnetic stirbar. The flask was sealed with a rubber septum and evacuated and backfilled with nitrogen three times and left under a positive pressure of nitrogen. THF (25 mL) was added *via* a nitrogen flushed syringe and the solution was cooled to -78 °C. DIBAL-H (1M solution in hexane, 12.2 mL, 12.2 mmol, 2 equiv) was added dropwise *via* a nitrogen flushed syringe. The reaction solution was allowed to warm to room temperature and stirred for 4 h. HCl (1 M aqueous solution, 15 mL) was added dropwise open to ambient air. A saturated solution of Rochelle's salt (50 mL) was added and stirred for 12 h. The solution was then filtered over a bed of celite. The resulting solution was added to a separatory funnel, extracted with EtOAc (3 x 75 mL), and the organic solution was washed with brine (1 x 100 mL) and dried over Na_2SO_4. After evaporation of the solvent *in vacuo*, the resulting residue was purified by silica gel chromatography (20% ethyl acetate/1% triethylamine/hexanes to 75% ethyl acetate/1% triethylamine/hexanes) to yield 5-thiomorpholinopyrimidine-2-carbaldehyde as a yellow solid (218.6 mg, 1.0 mmol, 16% yield). **^{1}H NMR** (400 MHz, $CDCl_3$) δ 9.94 (s, 1H), 8.43 (s, 2H), 3.94 – 3.79 (m, 4H), 2.84 – 2.68 (m, 4H). **^{13}C NMR** (101 MHz, $CDCl_3$) δ 190.0, 150.5, 143.5, 142.1, 49.4, 26.1.

3-(methylthio)-2-vinylpyridine

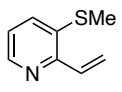

A slightly modified variant of General Procedure A was followed for this substrate. An oven-dried round bottom flask was charged with a magnetic stir bar and methyltriphenylphosphonium bromide (6.157 g, 17.24 mmol, 1.5 equiv), capped with a rubber

septum, evacuated and backfilled with nitrogen three times and left under positive pressure with a nitrogen filled balloon. Anhydrous THF (72 mL) was then added, and the mixture was cooled to 0 °C in an ice bath with stirring. *n*-Butyllithium (10.77 mL of 1.6M solution in hexanes, 17.24 mmol, 1.5 equiv) was added dropwise with a nitrogen flushed syringe. Procedure A was then followed with 3-(methylthio)picolinaldehyde (1.76 g, 11.49 mmol, 1.0 equiv, synthesis described below). Flash column chromatography (5% ethyl acetate/hexanes to 15% ethyl acetate/hexanes) yielded the title product as a brown oil (128.4 mg, 0.8 mmol, 7% yield). **^{1}H NMR** (400 MHz, $CDCl_3$) δ 8.28 (d, *J* = 4.6 Hz, 1H), 7.40 (d, *J* = 8.0 Hz, 1H), 7.20 (dd, *J* = 16.9 Hz, 10.7 Hz, 1H), 7.10 (dd, *J* = 8.0, 4.6 Hz, 1H), 6.36 (dd, *J* = 10.8, 1.3 Hz 1H), 5.51 (dd, *J* = 10.8, 1.3 Hz, 1H), 2.41 (s, 3H). **^{13}C NMR** (101 MHz, $CDCl_3$) δ 153.0, 146.1, 134.7, 133.4, 132.8, 122.9, 120.2, 16.1. **HRMS** (DART) $[M+H]^+$ calcd. for $[C_8H_{10}NS]^+$, 152.0528 found, 152.0539. **IR** (neat, cm^{-1}) 3035.4, 2920.2, 1550.9, 1547.6, 1440.2, 1421.6, 1384.0, 1139.1, 1053.0, 982.2, 931.6, 785.1.

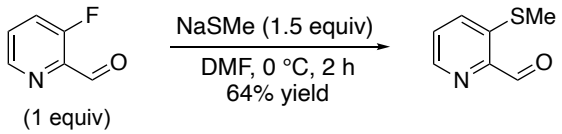

3-(methylthio)picolinaldehyde preparation: 3-Fluoropicolinaldehyde (2.5 g, 20.0 mmol, 1.0 equiv) was added to an oven-dried 250 mL round bottom flask with magnetic stir bar. DMF (100 mL) was added, and the solution was cooled to 0 °C with stirring. Sodium thiomethoxide (2.1 g, 30 mmol, 1.5 equiv) was slowly added. The reaction solution was stirred at 0 °C for 2 h. A saturated solution of ammonium chloride (50 mL) was then added. The resulting solution was transferred to a separatory funnel, extracted with EtOAc (3 x 50 mL), and the organic solution was washed with brine (1 x 100 mL) and dried over Na_2SO_4. After evaporation of the solvent *in vacuo*, the resulting residue was purified by silica gel chromatography (10% ethyl acetate/hexanes to 20% ethyl acetate/hexanes) to yield 3-(methylthio)picolinaldehyde as a brown oil (1.76 g, 12.5 mmol, 64%

yield). **^{1}H NMR** (400 MHz, $CDCl_3$) δ 10.15 (s, 1H), 8.51 (dd, *J* = 4.5, 1.4 Hz, 1H), 7.67 (d, *J* = 8.3 Hz, 1H), 7.43 (dd, *J* = 8.3, 4.5 Hz, 1H), 2.45 (s, 3H).

4-(But-3-en-1-ylsulfonyl)-2-fluoro-1-vinylbenzene

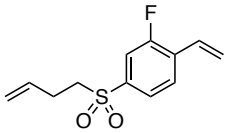

General Procedure B was followed with triphenylphosphine (50.5 mg, 0.19 mmol, 0.09 equiv), palladium(II) chloride (11.4 mg, 0.06 mmol, 0.03 equiv), cesium carbonate (2.09 g, 6.42 mmol, 3.0 equiv), potassium vinyltrifluoroborate (344.0 mg, 2.57 mmol, 1.2 equiv), and 1-bromo-4-(but-3-en-1-ylsulfonyl)-2-fluorobenzene (626.0 mg, 2.14 mmol, 1.0 equiv, synthesis described below). Flash column chromatography (10% ethyl acetate/hexanes) yielded the title product as a light-yellow oil (340 mg, 1.41 mmol, 66% yield). **^{1}H NMR** (400 MHz, $CDCl_3$) δ 7.74 – 7.62 (m, 2H), 7.60 (dd, *J* = 9.7, 1.6 Hz, 1H), 6.90 (dd, *J* = 17.7, 11.2 Hz, 1H), 5.99 (dd, *J* = 17.7, 0.7 Hz, 1H), 5.79 – 5.66 (m, 1H), 5.59 (dd, *J* = 11.2, 0.7 Hz, 1H), 5.08 (dq, *J* = 8.2, 1.4 Hz, 1H), 5.05 (t, *J* = 1.5 Hz, 1H), 3.26 – 3.00 (m, 2H), 2.56 – 2.39 (m, 2H). **^{13}C NMR** (101 MHz, $CDCl_3$) δ 159.9 (d, *J* = 255.4 Hz), 139.3 (d, *J* = 6.8 Hz), 133.7, 131.2 (d, *J* = 12.4 Hz), 128.3 (d, *J* = 3.7 Hz), 128.2 (d, *J* = 3.8 Hz), 124.1 (d, *J* = 3.8 Hz), 120.7 (d, *J* = 4.8 Hz), 117.6, 116.2 (d, *J* = 25.4 Hz), 55.6, 27.1. **^{19}F NMR** (376 MHz, $CDCl_3$) δ -114.52. **HRMS** (DART) $[M+H]^+$ calcd. for $[C_{12}H_{14}FO_2S]^+$ 241.0693, found 241.0680. **IR** (neat, cm^{-1}) 3081.4, 2983.1, 2922.9, 1642.4, 1629.7, 1567.0, 1486.8, 1407.1, 1310.2, 1270.7, 1226.9, 1183.7, 1141.7, 1114.9, 1072.9, 991.0, 920.7, 784.1.

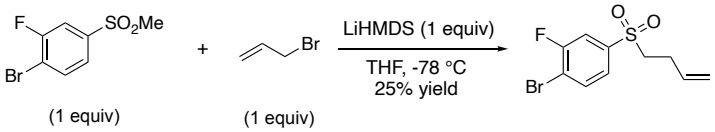

1-Bromo-4-(but-3-en-1-ylsulfonyl)-2-fluorobenzene preparation: 1-Bromo-2-fluoro-4-(methylsulfonyl)benzene (2.53 g, 10 mmol, 1 equiv) was added to an oven-dried 100 mL round bottom flask containing a magnetic stirbar. The flask was sealed with a rubber septum and

evacuated and backfilled with nitrogen three times and left under a positive pressure of nitrogen. THF (40 mL) was added *via* a nitrogen flushed syringe. The reaction mixture was cooled to -78 °C. LiHMDS (0.9 – 1.1 M solution in hexane, 10 mL, 10 mmol, 1 equiv) was added dropwise *via* a nitrogen flushed syringe and the reaction mixture was stirred at -78 °C for 30 min. 3-Bromoprop-1-ene (0.87 mL, 10 mmol, 1 equiv) was then added dropwise *via* a nitrogen flushed syringe. The reaction mixture was stirred for 15 min at -78 °C, then allowed to warm to room temperature and stirred for 40 min. The reaction mixture was quenched with saturated NH_4Cl solution (1 x 50 mL). The resulting mixture was transferred to a separatory funnel, extracted with EtOAc (3 x 50 mL), and the organic solution was washed with brine (1 x 100 mL) and dried over Na_2SO_4. After evaporation of the solvent *in vacuo*, the resulting residue was purified by silica gel chromatography (5% ethyl acetate/hexanes to 15% ethyl acetate/hexanes) to yield the title compound as a brown oil (0.724 g, 2.5 mmol, 25% yield). **^{1}H NMR** (400 MHz, $CDCl_3$) δ 7.79 (m, 1H), 7.66 (d, *J* = 7.4, Hz, 1H), 7.59 (d, *J* = 8.3, Hz, 1H), 5.78 - 5.65 (m, 1H), 5.14 – 5.03 (m, 2H), 3.22 – 3.13 (m, 2H), 2.52 – 2.42 (m, 2H). **^{13}C NMR** (101 MHz, $CDCl_3$) δ 159.3 (d, J = 253.9 Hz), 140.3 (d, J = 5.5 Hz), 135.1, 133.5, 125.0 (d, J = 4.2 Hz), 117.8, 116.6 (d, J = 25 Hz), 116.5 (d, J = 21.0 Hz), 55.6, 27.0.

A2.9 Synthesis and Characterization Data for Hydration Products

2-(4-Chloro-2-(trifluoromethyl)phenyl)ethan-1-ol (2-62)

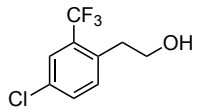

General Procedure C was followed using 4-chloro-2-(trifluoromethyl)styrene (207 mg, 1.0 mmol, 1.0 equiv), 1-cyclopropylethanol (293 µL, 3.0 mmol, 3.0 equiv), P_4-*t*-Bu (0.8M, 125 µL, 0.1 mmol, 0.1 equiv) and toluene (667 µL) as the solvent at 40 °C for 12 h. Methanesulfonic acid (667 µL, 10.3 mmol, 10.3 equiv) was used in the deprotection step and flash column chromatography (20% ethyl acetate/hexanes) yielded the title product as a yellow oil (135 mg, 0.60 mmol, 60% yield). **^{1}H NMR** (400 MHz, $CDCl_3$) δ 7.62 (d, *J* = 2.3 Hz, 1H), 7.44

(dd, J = 8.3, 2.3 Hz, 1H), 7.35 (d, J = 8.3 Hz, 1H), 3.85 (q, J = 6.4 Hz, 2H), 3.02 (t, J = 6.7 Hz, 2H), 1.44 (s, 1H). **^{13}C NMR** (101 MHz, $CDCl_3$) δ 135.9 (q, J = 1.3 Hz), 133.5, 132.7, 131.9, 130.6 (q, J = 30.5 Hz), 126.6 (q, J = 5.9 Hz), 123.9 (q, J = 274.2 Hz), 63.1, 35.5 (q, J = 2.0 Hz). **^{19}F NMR** (376 MHz, $CDCl_3$) δ -65.45. **LRMS** $[M+H]^+$ calcd. for $[C_9H_9ClF_3O]^+$ 225.0, found 225.0. **IR** (neat, cm^{-1}) 3322.2, 2917.2, 2848.9, 1486.6, 1410.4, 1304.8, 1118.9, 1054.1, 828.3, 697.9, 535.0.

For this substrate, General Procedure D was also followed using 4-chloro-2-(trifluoromethyl)styrene (207 mg, 1.0 mmol, 1.0 equiv), 1-cyclopropylethanol (293 µL, 3.0 mmol, 3.0 equiv), KO-*t*-Bu (11.2 mg, 0.1 equiv), 18-crown-6 (29.1 mg, 0.11 equiv) and 1,2-dimethoxyethane (0.5 mL) as the solvent at 60 °C for 24 h. Methanesulfonic acid (667 µL, 10.3 mmol, 10.3 equiv) was used in the deprotection step and flash column chromatography (20% ethyl acetate/hexanes) yielded the title product as a yellow oil (110 mg, 0.49 mmol, 49% yield).

2-(2-Chloropyridin-3-yl)ethan-1-ol (2-61)

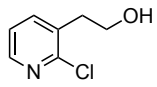

General Procedure C was followed using 2-chloro-3-vinylpyridine (139 mg, 1.0 mmol, 1.0 equiv), 1-cyclopropylethanol (293 µL, 3.0 mmol, 3.0 equiv), P_4-*t*-Bu (0.8M, 125 µL, 0.1 mmol, 0.1 equiv) and toluene (500 µL) as the solvent at 50 °C for 12 h. Methanesulfonic acid (667 µL, 10.3 mmol, 10.3 equiv) was used in the deprotection step and flash column chromatography (40% ethyl acetate/hexanes) yielded the title product as a colorless oil (160 mg, 0.83 mmol, 83% yield). **^{1}H NMR** (400 MHz, $CDCl_3$) δ 8.25 (dd, J = 4.8, 1.9 Hz, 1H), 7.62 (dd, J = 7.5, 1.9 Hz, 1H), 7.17 (dd, J = 7.5, 4.8 Hz, 1H), 3.92 (t, J = 6.5 Hz, 2H), 2.98 (t, J = 6.5 Hz, 2H), 1.65 (s, 1H). **^{13}C NMR** (101 MHz, $CDCl_3$) δ 151.5, 147.7, 140.2, 133.4, 122.7, 61.1, 36.5. **HRMS** (DART) $[M+H]^+$ calcd. for $[C_7H_9ClNO]^+$ 158.0367, found 158.0370. **IR** (neat, cm^{-1}) 3330.9, 2935.8, 2877.6, 1564.6, 1407.3, 1078.3, 1047.7, 795.7, 746.5, 680.3.

For this substrate, General Procedure D was also followed using 2-chloro-3-vinylpyridine (139 mg, 1.0 mmol, 1.0 equiv), 1-cyclopropylethanol (484 μL, 5.0 mmol, 5.0 equiv), KO-*t*-Bu (11.2 mg, 0.1 equiv), 18-crown-6 (29.1 mg, 0.11 equiv) and 1,2-dimethoxyethane (0.5 mL) as the solvent at 40 °C for 24 h. Methanesulfonic acid (667 μL, 10.3 mmol, 10.3 equiv) was used in the deprotection step and flash column chromatography (40% ethyl acetate/hexanes) yielded the title product as a colorless oil (96 mg, 0.61 mmol, 61% yield).

2-(2-Fluoro-4-(methylsulfonyl)phenyl)ethan-1-ol (2-64)

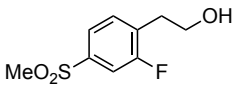

General Procedure C was followed using 2-fluoro-4-(methylsulfonyl)-1-vinylbenzene (200 mg, 1.0 mmol, 1.0 equiv), 1-cyclopropylethanol (488 μL, 5.0 mmol, 5.0 equiv), P_4-*t*-Bu (0.8M, 125 μL, 0.1 mmol, 0.1 equiv) and toluene (500 μL) as the solvent at rt for 12 h. Methanesulfonic acid (667 μL, 10.3 mmol, 10.3 equiv) was used in the deprotection step and flash column chromatography (70% ethyl acetate/hexanes) yielded the title product as a white solid (139 mg, 0.64 mmol, 64% yield). **Melting point**: 72-73 °C. **^{1}H NMR** (400 MHz, $CDCl_3$) δ 7.67 (dd, *J* = 8.0, 1.9 Hz, 1H), 7.62 (dd, *J* = 8.9, 1.9 Hz, 1H), 7.49 (t, *J* = 7.4 Hz, 1H), 3.91 (q, *J* = 6.1 Hz, 2H), 3.05 (s, 3H), 2.99 (td, *J* = 6.4, 1.3 Hz, 2H), 1.60 (t, *J* = 5.5 Hz, 1H). **^{13}C NMR** (101 MHz, $CDCl_3$) δ 161.1 (d, *J* = 251.3 Hz), 140.4 (d, *J* = 6.6 Hz), 133.0 (d, *J* = 16.0 Hz), 132.8 (d, *J* = 5.0 Hz), 123.2 (d, *J* = 3.9 Hz), 114.8 (d, *J* = 26.0 Hz), 61.8, 44.6, 32.6 (d, *J* = 1.6 Hz). **^{19}F NMR** (376 MHz, $CDCl_3$) δ -113.98. **HRMS** (DART) $[M+NH_4]^+$ calcd. for $[C_9H_{15}FNO_3S]^+$ 236.0751, found 236.0752. **IR** (neat, cm^{-1}) 3520.6, 3381.7, 3012.7, 2930.0, 1406.7, 1299.6, 1229.3, 1139.2, 1054.7, 969.8, 764.1, 607.7.

For this substrate, General Procedure D was also followed using 2-fluoro-4-(methylsulfonyl)-1-vinylbenzene (200 mg, 1.0 mmol, 1.0 equiv), 1-cyclopropylethanol (488 μL, 5.0 mmol, 5.0 equiv), KO-*t*-Bu (11.2 mg, 0.10 mmol, 0.1 equiv), 18-crown-6 (29.1 mg, 0.11 mmol, 0.11 equiv) and 1,2-

dimethoxyethane (0.5 mL) as the solvent at rt for 24 h. Methanesulfonic acid (667 μL, 10.3 mmol, 10.3 equiv) was used in the deprotection step and flash column chromatography (70% ethyl acetate/hexanes) yielded the title product as a white solid (133 mg, 0.61 mmol, 61% yield).

2-(3-Chloropyridin-2-yl)ethan-1-ol (2-63)

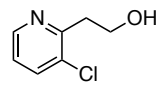

General Procedure C was followed using 3-chloro-2-vinylpyridine (140 mg, 1.0 mmol, 1.0 equiv), 1-cyclopropylethanol (293 μL, 3.0 mmol, 3.0 equiv), P_4-*t*-Bu (0.8M, 125 μL, 0.1 mmol, 0.1 equiv) and toluene (667 μL) as the solvent at 40 °C for 12 h. Methanesulfonic acid (533 μL, 8.2 mmol, 8.2 equiv) was used in the deprotection step and flash column chromatography (40% ethyl acetate/hexanes) yielded the title product as a colorless oil (102 mg, 0.65 mmol, 65% yield). **^{1}H NMR** (400 MHz, $CDCl_3$) δ 8.39 (dd, *J* = 4.7, 1.5 Hz, 1H), 7.66 (dd, *J* = 8.1, 1.5 Hz, 1H), 7.13 (dd, *J* = 8.1, 4.7 Hz, 1H), 4.13 – 3.92 (m, 3H), 3.13 (t, *J* = 5.2 Hz, 2H). **^{13}C NMR** (101 MHz, $CDCl_3$) δ 158.0, 146.8, 137.2, 131.7, 122.7, 60.6, 36.1. **HRMS** (DART) $[M+H]^+$ calcd. for $[C_7H_9ClNO]^+$ 158.0367, found 158.0370. **IR** (neat, cm^{-1}) 3326.4, 3059.5, 2933.5, 2877.0, 1575.9, 1426.3, 1045.2, 794.4.

For this substrate, General Procedure D was also followed using 3-chloro-2-vinylpyridine (140 mg, 1.0 mmol, 1.0 equiv), 1-cyclopropylethanol (293 μL, 3.0 mmol, 3.0 equiv), KO-*t*-Bu (11.2 mg, 0.10 mmol, 0.1 equiv), 18-crown-6 (29.1 mg, 0.11 mmol, 0.11 equiv) and 1,2-dimethoxyethane (0.5 mL) as the solvent at 40 °C for 20 h. Methanesulfonic acid (667μL, 10.3 mmol, 10.3 equiv) was used in the deprotection step and flash column chromatography (40% ethyl acetate/hexanes) yielded the title product as a colorless oil (80 mg, 0.51 mmol, 51% yield).

2-(4-Methyl-2-nitrophenyl)ethan-1-ol (2-49)

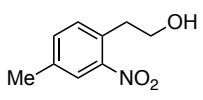

General Procedure C was followed using 4-methyl-2-nitrostyrene (163 mg, 1.0 mmol, 1.0 equiv), 1-cyclopropylethanol (293 μL, 3.0 mmol, 3.0 equiv), P_4-*t*-Bu (0.8M, 125 μL, 0.1 mmol, 0.1 equiv) and toluene (1.0 mL) as the solvent at 30 °C for 12 h. Methanesulfonic acid (667 μL, 10.3 mmol, 10.3 equiv) was used in the deprotection step and flash column chromatography (25% to 40% ethyl acetate/hexanes) yielded the title product as an amorphous brown solid (115 mg, 0.64 mmol, 64% yield). **^{1}H NMR** (400 MHz, $CDCl_3$) δ 7.69 (s, 1H), 7.31 (d, *J* = 7.9 Hz, 1H), 7.27 – 7.19 (m, 1H), 3.87 (t, *J* = 6.4 Hz, 2H), 3.07 (t, *J* = 6.4 Hz, 2H), 2.36 (s, 3H), 1.73 (s, 1H). **^{13}C NMR** (101 MHz, $CDCl_3$) δ 149.8, 138.2, 134.0, 132.8, 130.8, 125.3, 63.0, 36.0, 20.9. **LRMS** $[M+H]^+$ calcd. for $[C_9H_{12}NO_3]^+$ 182.1, found 182.1. **IR** (neat, cm^{-1}) 3226.5, 2923.7, 2879.9, 1523.6, 1345.7, 1046.9, 831.9, 678.6.

2-(3-Nitrophenyl)ethan-1-ol (2-50)

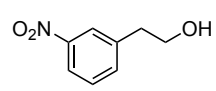

General Procedure C was followed using 3-nitrostyrene (149 mg, 1.0 mmol, 1.0 equiv), 1-cyclopropylethanol (293 μL, 3.0 mmol, 3.0 equiv), P_4-*t*-Bu (0.8M, 125 μL, 0.1 mmol, 0.1 equiv) and toluene (1.0 mL) as the solvent at 60 °C for 12 h. Methanesulfonic acid (667 μL, 10.3 mmol, 10.3 equiv) was used in the deprotection step and flash column chromatography (25% ethyl acetate/hexanes) yielded the title product as an orange solid (81.0 mg, 0.48 mmol, 48% yield). **Melting point**: 47-48 °C. **^{1}H NMR** (400 MHz, $CDCl_3$) δ 8.14 – 8.05 (m, 2H), 7.58 (d, *J* = 7.6 Hz, 1H), 7.48 (t, *J* = 7.8 Hz, 1H), 3.93 (q, *J* = 6.0 Hz, 2H), 2.98 (t, *J* = 6.4 Hz, 2H), 1.58 (t, *J* = 5.0 Hz, 1H). **^{13}C NMR** (101 MHz, $CDCl_3$) δ 148.6, 141.1, 135.6, 129.5, 124.0, 121.8, 63.1, 38.8. **HRMS** (DART) $[M+NH_4]^+$ calcd. for $[C_8H_{13}N_2O_3]^+$ 185.0921, found 185.0924. **IR** (neat, cm^{-1}) 3307.0, 3090.0, 2931.7, 2870.9, 1522.5, 1342.4, 1083.9, 1056.2, 883.1, 735.4. The characterization data is consistent with reported literature values.[16]

2-(2,6-Dichlorophenyl)ethan-1-ol (2-51)

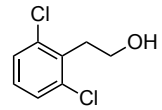

General Procedure C was followed using 2,6-dichlorostyrene (173 mg, 1.0 mmol, 1.0 equiv),1-cyclopropylethanol (293 µL, 3.0 mmol, 3.0 equiv), P_4-*t*-Bu (0.8M, 125 µL, 0.1 mmol, 0.1 equiv) and toluene (1.0 mL) as the solvent at 100 °C for 12 h. Methanesulfonic acid (667 µL, 10.3 mmol, 10.3 equiv) was used in the deprotection step and flash column chromatography (40% dichloromethane/hexanes to 20% ethyl acetate/hexanes) yielded the title product as a white solid (154 mg, 0.81 mmol, 81% yield). **Melting point**: 69-70 °C. **^{1}H NMR** (400 MHz, $CDCl_3$) δ 7.30 (d, *J* = 8.0 Hz, 2H), 7.10 (t, *J* = 8.0 Hz, 1H), 3.88 (q, *J* = 6.8 Hz, 2H), 3.27 (t, *J* = 7.2 Hz, 2H), 1.45 (s, 1H). **^{13}C NMR** (101 MHz, $CDCl_3$) δ 136.1, 134.5, 128.5, 128.4, 61.2, 34.8. The characterization data is consistent with reported literature values.[17]

2-(2-Chloro-3-(trifluoromethyl)phenyl)ethan-1-ol (2-52)

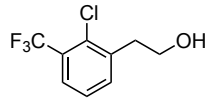

General Procedure C was followed using 2-chloro-3-(trifluoromethyl)styrene (207 mg, 1.0 mmol, 1.0 equiv), 1-cyclopropylethanol (293 µL, 3.0 mmol, 3.0 equiv), P_4-*t*-Bu (0.8M, 125 µL, 0.1 mmol, 0.1 equiv) and toluene (1.0 mL) as the solvent at 40 °C for 12 h. Methanesulfonic acid (667 µL, 10.3 mmol, 10.3 equiv) was used in the deprotection step and flash column chromatography (20% ethyl acetate/hexanes) yielded the title product as colorless liquid (173 mg, 0.77 mmol, 77% yield). **^{1}H NMR** (400 MHz, $CDCl_3$) δ 7.61 (dd, *J* = 7.8, 1.7 Hz, 1H), 7.50 (d, *J* = 7.8 Hz, 1H), 7.32 (td, *J* = 7.8, 0.9 Hz, 1H), 3.93 (t, *J* = 6.6 Hz, 2H), 3.11 (t, *J* = 6.6 Hz, 2H), 1.44 (s, 1H). **^{13}C NMR** (101 MHz, $CDCl_3$) δ 139.0, 134.9, 132.3, 129.3 (q, *J* = 30.7 Hz), 126.6, 126.3 (q, *J* = 5.5 Hz), 123.2 (q, *J* = 273.2 Hz), 61.8, 37.1. **^{19}F NMR** (376 MHz, $CDCl_3$) δ -62.89. **LRMS** $[M+H]^+$ calcd. for $[C_9H_9ClF_3O]^+$ 225.0, found 225.0. **IR** (neat, cm^{-1}) 3326.1, 2939.6, 2885.0, 1586.2, 1434.1, 1314.7, 1129.1, 1045.7, 797.8, 732.7, 699.0.

2-(2-Chloro-3,6-difluorophenyl)ethan-1-ol (2-53)

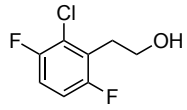

General Procedure C was followed using 2-chloro-3,6-difluorostyrene (175 mg, 1.0 mmol, 1.0 equiv),1-cyclopropylethanol (293 μL, 3.0 mmol, 3.0 equiv), P_4-*t*-Bu (0.8M, 125 μL, 0.1 mmol, 0.1 equiv) and toluene (1.0 mL) as the solvent at 65 °C for 12 h. Methanesulfonic acid (667 μL, 10.3 mmol, 10.3 equiv) was used in the deprotection step and flash column chromatography (75% dichloromethane/hexanes) yielded the title product as a colorless oil (160 mg, 0.83 mmol, 83% yield). **^{1}H NMR** (400 MHz, $CDCl_3$) δ 7.09 – 6.81 (m, 2H), 3.85 (t, *J* = 6.9 Hz, 2H), 3.09 (td, *J* = 6.9, 2.3 Hz, 2H), 1.80 (s, 3H). **^{13}C NMR** (101 MHz, $CDCl_3$) δ 157.5 (dd, *J* = 258.2, 2.5 Hz), 155.1 (dd, *J* = 258.8, 2.5 Hz),126.4 (d, *J* = 20.7 Hz), 122.5 (dd, *J* = 19.2, 6.7 Hz), 114.8 (dd, *J* = 23.9, 9.5 Hz), 114.3 (dd, *J* = 25.7, 7.8 Hz), 61.3, 30.3 (t, *J* = 1.6 Hz). **^{19}F NMR** (376 MHz, $CDCl_3$) δ -118.04 (d, *J* = 16.0 Hz), -118.71 (d, *J* = 16.0 Hz). **EA** Calc for $C_8H_7ClF_2O$: C, 49.89; H, 3.66; Found: C, 50.00; H, 3.62. **IR** (neat, cm^{-1}) 3319.5, 2944.4, 2885.6, 1472.7, 1231.0, 1039.5, 866.0, 808.2, 746.5, 726.5.

(4-(2-Hydroxyethyl)phenyl)(phenyl)methanone (2-54)

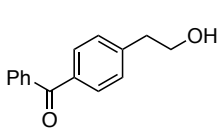

General Procedure C was followed using phenyl(4-vinylphenyl)methanone (208.3 mg, 1.0 mmol, 1.0 equiv), 1-cyclopropylethanol (488 μL, 5.0 mmol, 5.0 equiv), P_4-*t*-Bu (0.8M, 125 μL, 0.1 mmol, 0.1 equiv) and toluene (500 μL) as the solvent at 40 °C for 24 h. Methanesulfonic acid (667 μL, 10.3 mmol, 10.3 equiv) was used in the deprotection step and flash column chromatography (10% ethyl acetate/hexanes) yielded the title product as a light yellow oil (110 mg, 0.49 mmol, 49% yield). **^{1}H NMR** (400 MHz, $CDCl_3$) δ 7.78 (td, *J* = 8.1, 1.4 Hz, 4H), 7.59 (t, *J* = 7.1 Hz, 1H), 7.48 (m, 2H), 7.35 (d, *J* = 7.9 Hz, 2H), 3.93 (td, *J* = 6.5, 1.6 Hz, 2H), 2.96 (t, *J* = 6.5 Hz, 2H), 1.74 (s, 1H). **^{13}C NMR** (101 MHz, $CDCl_3$) δ 196.7, 144.0, 137.9,

136.1, 132.5, 130.7, 130.2, 129.2, 128.5, 63.5, 39.4. **HRMS** (DART) $[M+H]^+$ calcd. for $[C_{15}H_{15}O_2]^+$ 227.1067, found 227.1066. **IR** (neat, cm^{-1}) 3397.3, 3057.8, 2935.3, 2873.6, 1651.9, 1604.8, 1446.2, 1412.3, 1316.0, 1276.7, 1174.9, 1043.6, 938.0, 923.2, 698.8.

2-(2-Bromo-5-(trifluoromethyl)phenyl)ethan-1-ol (2-55)

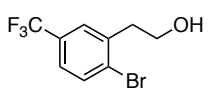

General Procedure C was followed using 2-bromo-5-(trifluoromethyl)styrene (251 mg, 1.0 mmol, 1.0 equiv), 1-cyclopropylethanol (293 µL, 3.0 mmol, 3.0 equiv), P_4-*t*-Bu (0.8M, 125 µL, 0.1 mmol, 0.1 equiv) and toluene (667 µL) as the solvent at 50 °C for 12 h. Methanesulfonic acid (667 µL, 10.3 mmol, 10.3 equiv) was used in the deprotection step and flash column chromatography (70% dichloromethane/hexanes) yielded the title product as a yellow oil (122 mg, 0.75 mmol, 75% yield). **^{1}H NMR** (400 MHz, $CDCl_3$) δ 7.68 (dd, *J* = 8.3, 0.9 Hz, 1H), 7.54 (d, *J* = 2.2 Hz, 1H), 7.33 (dd, *J* = 8.3, 2.2 Hz, 1H), 3.91 (td, *J* = 6.6, 5.6 Hz, 2H), 3.07 (t, *J* = 6.6 Hz, 2H), 1.43 (t, *J* = 5.6 Hz, 1H). **^{13}C NMR** (101 MHz, $CDCl_3$) δ 139.3, 133.6, 130.1 (q, *J* = 33.0 Hz), 128.7, 128.1 (q, *J* = 3.6 Hz), 125.0 (q, *J* = 3.7 Hz), 124.0 (q, *J* = 272.2 Hz), 61.8, 39.4. **^{19}F NMR** (376 MHz, $CDCl_3$) δ -62.69. **LRMS** $[M+H]^+$ calcd. for $[C_9H_9BrF_3O]^+$ 269.0, found 269.1. **IR** (neat, cm^{-1}) 3319.2, 2937.6, 2883.8, 1604.5, 1322.5, 1165.4, 1120.8, 1080.8, 1036.0, 823.2, 725.2.

2-(1-Bromonaphthalen-2-yl)ethan-1-ol (2-56)

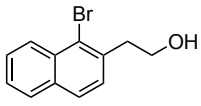

General Procedure C was followed using 1-bromo-2-vinylnaphthalene (206 mg, 0.88 mmol, 1.0 equiv), 1-cyclopropylethanol (258 µL, 2.64 mmol, 3.0 equiv), P_4-*t*-Bu (0.8M, 111 µL, 0.09 mmol, 0.1 equiv) and toluene (880 µL) as the solvent at 60 °C for 12 h. Methanesulfonic acid (587 µL, 9.1 mmol, 10.3 equiv) was used in the deprotection step and flash column chromatography (20% to 40% ethyl acetate/hexanes) yielded the title

product as a white solid (97 mg, 0.39 mmol, 44% yield). **Melting point**: 68-70 °C. **^{1}H NMR** (400 MHz, $CDCl_3$) δ 8.32 (d, *J* = 8.5 Hz, 1H), 7.81 (d, *J* = 8.1 Hz, 1H), 7.77 (d, *J* = 8.3 Hz, 1H), 7.59 (t, *J* = 7.6 Hz, 1H), 7.50 (m, 1H), 7.40 (d, *J* = 8.3 Hz, 1H), 3.99 (q, *J* = 6.5 Hz, 2H), 3.29 (t, *J* = 6.7 Hz, 2H), 1.42 (t, *J* = 5.8 Hz, 1H). **^{13}C NMR** (101 MHz, $CDCl_3$) δ 136.3, 133.6, 132.8, 128.8, 128.2, 127.8, 127.6, 127.5, 126.3, 124.5, 62.5, 40.7. **HRMS** (DART) $[M+NH_4]^+$ calcd. for $[C_{12}H_{15}BrNO]^+$ 268.0332, found 268.0330. **IR** (neat, cm^{-1}) 3230.2, 2958.9, 2925.6, 2875.4, 1556.7, 1500.4, 1444.9, 1371.0, 1332.5, 1253.0, 1046.1, 970.7, 811.7, 749.4, 736.5.

2-(Quinolin-2-yl)ethan-1-ol (2-57)

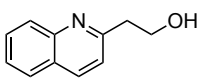

General Procedure C was followed using 2-vinylquinoline (155 mg, 1.0 mmol, 1.0 equiv), 1-cyclopropylethanol (293 µL, 3.0 mmol, 3.0 equiv), P_4-*t*-Bu (0.8M, 125 µL, 0.1 mmol, 0.1 equiv) and toluene (1 mL) as the solvent at 40 °C for 12 h. Aqueous 5M HCl (4.0 mL, 20 mmol, 20 equiv) was used in the deprotection step and flash column chromatography (100% ethyl acetate) yielded the title product as a white solid (108 mg, 0.62 mmol, 62% yield). **Melting point**: 101-102 °C. **^{1}H NMR** (400 MHz, $CDCl_3$) δ 8.06 (d, *J* = 8.4 Hz, 1H), 7.99 (d, *J* = 8.4 Hz, 1H), 7.76 (d, *J* = 8.0 Hz, 1H), 7.67 (ddd, *J* = 8.4, 6.8, 1.5 Hz, 1H), 7.48 (t, *J* = 7.7 Hz, 1H), 7.25 (d, *J* = 8.2 Hz, 1H), 4.79 (s, 1H), 4.13 (t, *J* = 5.4 Hz, 2H), 3.18 (t, *J* = 5.4 Hz, 2H). **^{13}C NMR** (101 MHz, $CDCl_3$) δ 161.6, 147.5, 136.7, 129.8, 128.9, 127.7, 127.0, 126.2, 122.0, 61.6, 39.5. **HRMS** (DART) $[M+H]^+$ calcd. for $[C_{11}H_{12}NO]^+$ 174.0913, found 174.0931. **IR** (neat, cm^{-1}) 3126.7, 2953.8, 2923.6, 2840.7, 1600.7, 1505.1, 1430.5, 1334.5, 1244.7, 1052.0, 818.2, 764.4.

2-(3-Bromopyridin-4-yl)ethan-1-ol (2-58)

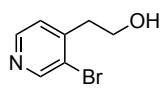

General Procedure C was followed using 3-bromo-4-vinylpyridine (184 mg, 1.0 mmol, 1.0 equiv), 1-cyclopropylethanol (259 μL, 3.0 mmol, 3.0 equiv), P_4-*t*-Bu (0.8M, 125 μL, 0.1 mmol, 0.1 equiv) and toluene (500 μL) as the solvent at rt for 1 h. Aqueous 5M HCl (4.0 mL, 20 mmol, 20 equiv) was used in the deprotection step and flash column chromatography (80% ethyl acetate/hexanes) yielded the title product as a white solid (152 mg, 0.75 mmol, 75% yield). **Melting point**: 48-49 °C. **^{1}H NMR** (400 MHz, $CDCl_3$) δ 8.61 (s, 1H), 8.35 (d, *J* = 4.9 Hz, 1H), 7.23 (d, *J* = 4.9 Hz, 1H), 3.92 (t, *J* = 6.4 Hz, 2H), 2.99 (t, *J* = 6.4 Hz, 2H), 2.49 (s, 1H). **^{13}C NMR** (101 MHz, $CDCl_3$) δ 151.9, 148.0, 147.7, 126.3, 123.5, 60.9, 38.7. **HRMS** (DART) $[M+H]^+$ calcd. for $[C_7H_9BrNO]^+$ 201.9862, found 201.9863. **IR** (neat, cm^{-1}) 3216.9, 3019.4, 2955.7, 2934.5, 2871.2, 1587.7, 1400.2, 1365.2, 1306.4, 1055.9, 1038.5, 694.3, 609.9.

2-(6-Bromopyridin-2-yl)ethan-1-ol (2-59)

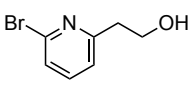

General Procedure C was followed using 2-bromo-6-vinylpyridine (184 mg, 1.0 mmol, 1.0 equiv), 1-cyclopropylethanol (293 μL, 3.0 mmol, 3.0 equiv), P_4-*t*-Bu (0.8M, 125 μL, 0.1 mmol, 0.1 equiv) and toluene (667 μL) as the solvent at 35 °C for 12 h. Aqueous 5M HCl (4.0 mL, 20 mmol, 20 equiv) was used in the deprotection step and flash column chromatography (50% ethyl acetate/hexanes) yielded the title product as a yellow oil (122 mg, 0.60 mmol, 60% yield). **^{1}H NMR** (400 MHz, $CDCl_3$) *δ* 7.46 (t, *J* = 7.7 Hz, 1H), 7.33 (d, *J* = 7.9 Hz, 1H), 7.12 (d, *J* = 7.5 Hz, 1H), 3.99-4.00 (m, 2H), 2.97-3.00 (m, 3H). **^{13}C NMR** (101 MHz, $CDCl_3$) δ 161.8, 141.5, 139.0, 126.0, 122.6, 61.6, 39.6. **HRMS** (DART) $[M+H]^+$ calcd. for $[C_7H_9BrNO]^+$ 201.9862, found 201.9866. **IR** (neat, cm^{-1}) 3313.2, 2930.8, 2875.8, 1582.5, 1552.2, 1436.5, 1403.7, 1122.0, 1044.4, 781.9, 678.8.

2-(4-Bromothiazol-2-yl)ethan-1-ol (2-60)

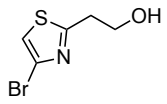

General Procedure C was followed using 4-bromo-2-vinylthiazole (190 mg, 1.0 mmol, 1.0 equiv), 1-cyclopropylethanol (391 μL, 4.0 mmol, 4.0 equiv), P_4-*t*-Bu (0.8M, 63 μL, 0.05 mmol, 0.05 equiv) and toluene (500 μL) as the solvent at rt for 12 h. Methanesulfonic acid (667 μL, 10.3 mmol, 10.3 equiv) was used in the deprotection step and flash column chromatography (40% ethyl acetate/hexanes) yielded the title product as a yellow oil (153 mg, 0.74 mmol, 74% yield). **^{1}H NMR** (400 MHz, $CDCl_3$) δ 7.12 (s, 1H), 4.02 (t, *J* = 5.7 Hz, 2H), 3.22 (t, *J* = 5.7 Hz, 2H), 2.68 (s, 1H). **^{13}C NMR** (101 MHz, $CDCl_3$) δ 169.8, 124.4, 116.6, 61.2, 36.3. **HRMS** (DART) $[M+H]^+$ calcd. for $[C_5H_7BrNOS]^+$ 207.9426, found 207.9435. **IR** (neat, cm^{-1}) 3331.2, 3120.3, 2923.0, 2878.3, 1478.7, 1255.4, 1133.1, 1083.7, 1048.6, 830.9, 729.4.

2-(3-(Methylthio)pyridin-2-yl)ethan-1-ol (2-68)

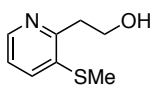

General Procedure C was followed using 3-(methylthio)-2-vinylpyridine (75.6 mg, 0.5 mmol, 1.0 equiv), 1-cyclopropylethanol (145 μL, 1.5 mmol, 3.0 equiv), P_4-*t*-Bu (0.8M, 62.5 μL, 0.05 mmol, 0.1 equiv) and toluene (250 μL) as the solvent at 50 °C for 24 h. Methanesulfonic acid (332 μL, 5.15 mmol, 10.3 equiv) was used in the deprotection step and flash column chromatography (5% methanol/dichloromethane) yielded the title product as a white solid (53.0 mg, 0.31 mmol, 63% yield). **Melting point**: 58-59 °C. **^{1}H NMR** (400 MHz, $CDCl_3$) δ 8.26 (dd, *J* = 4.9, 1.5 Hz, 1H), 7.47 (dd, *J* = 8.0, 1.5 Hz, 1H), 7.20 – 7.12 (m, 1H), 4.38 (s, 1H), 4.08 (t, *J*= 5.4 Hz, 2H), 3.02 (t, *J* = 5.4 Hz, 2H), 2.45 (s, 3H). **^{13}C NMR** (101 MHz, $CDCl_3$) δ 157.6, 144.1, 134.9, 132.6, 122.1, 60.7, 35.8, 15.2. **HRMS** (DART) $[M+H]^+$ calcd. for $[C_8H_{12}NOS]^+$ 170.0634, found 170.0653. **IR** (neat, cm^{-1}) 3243.7, 3053.0, 2959.1, 2920.1, 2867.3, 1568.5, 1442.5, 1416.0, 1370.0, 1048.2, 1015.6, 783.0, 756.3, 693.3, 671.4.

2-(5-Thiomorpholinopyrimidin-2-yl)ethan-1-ol (2-69)

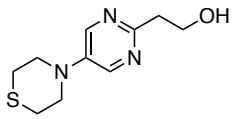

General Procedure C was followed using 4-(2-vinylpyrimidin-5-yl)thiomorpholine (41.4 mg, 0.2 mmol, 1.0 equiv), 1-cyclopropylethanol (58 µL, 0.6 mmol, 3.0 equiv), P_4-*t*-Bu (0.8M, 25 µL, 0.02 mmol, 0.1 equiv) and toluene (100 µL) as the solvent at 50 °C for 24 h. Methanesulfonic acid (130 µL, 2.06 mmol, 10.3 equiv) was used in the deprotection step and flash column chromatography (1% to 5% methanol/dichloromethane) yielded the title product as a light yellow oil (18.0 mg, 0.080 mmol, 40% yield). **^{1}H NMR** (400 MHz, $CDCl_3$) δ 8.30 (s, 2H), 4.04 (m, 2H), 3.63 – 3.55 (m, 4H), 3.15 (t, *J* = 5.5 Hz, 2H), 2.83 – 2.70 (m, 4H). **^{13}C NMR** (101 MHz, $CDCl_3$) δ 159.8, 144.9, 142.7, 61.0, 50.9, 39.3, 26.5. **HRMS** (DART) $[M+H]^+$ calcd. for $[C_{10}H_{16}N_3OS]^+$ 226.1009, found 226.1022. **IR** (neat, cm^{-1}) 3337.7, 2920.8, 1683.8, 1458.0, 1031.8, 981.6, 954.1, 667.9.

2-(4-(But-3-en-1-ylsulfonyl)-2-fluorophenyl)ethan-1-ol (2-70)

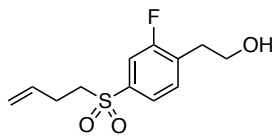

General Procedure C was followed using 4-(but-3-en-1-ylsulfonyl)-2-fluoro-1-vinylbenzene (96.1 mg, 0.4 mmol, 1.0 equiv), 1-cyclopropylethanol (194 µL, 2.0 mmol, 5.0 equiv), P_4-*t*-Bu (0.8M, 50 µL, 0.04 mmol, 0.1 equiv) and toluene (200 µL) as the solvent at rt for 24 h. Methanesulfonic acid (267 µL, 4.12 mmol, 10.3 equiv) was used in the deprotection step and flash column chromatography (50% ethyl acetate/hexanes) yielded the title product as a colorless oil (74 mg, 0.286 mmol, 72% yield). **^{1}H NMR** (400 MHz, $CDCl_3$) δ 7.65 (dt, *J* = 7.9, 2.1 Hz, 1H), 7.59 (dt, *J* = 8.9, 2.1 Hz, 1H), 7.50 (t, *J* = 7.4 Hz, 1H), 5.80 – 5.65 (m, 1H), 5.11 – 5.05 (m, 1H), 5.05 (m, 1H), 3.93 (td, *J* = 6.4, 2.4 Hz, 2H), 3.21 – 3.10 (m, 2H), 3.00 (tt, *J* = 6.4, 1.6 Hz, 2H), 2.56 – 2.42 (m, 2H), 1.52 (s, 1H). **^{13}C NMR** (101 MHz, $CDCl_3$) δ 161.1 (d, *J* = 251.3 Hz), 139.1 (d, *J* = 6.6

Hz), 133.7, 133.0 (d, J = 16.1 Hz), 132.7 (d, J = 4.9 Hz), 124.0 (d, J = 3.8 Hz), 117.5, 115.6 (d, J = 25.7 Hz), 61.9, 55.5, 32.6 (d, J = 1.6 Hz), 27.0. **^{19}F NMR** (377 MHz, $CDCl_3$) δ -114.06. **LRMS** $[M+H]^+$ calcd. for $[C_{12}H_{16}FO_3S]^+$ 259.1, found 259.1. **IR** (neat, cm^{-1}) 3503.5, 3072.8, 2931.1, 1642.6, 1576.8, 1489.1, 1407.1, 1304.0, 1271.3, 1227.7, 1136.7, 1117.4, 1071.4, 1046.2, 912.0, 784.9.

2-(3-Bromopyridin-4-yl)ethan-1-ol (2-58)

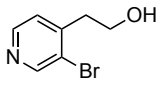

General Procedure C was followed using an oven-dried 100 mL round bottom flask and 3-bromo-4-vinylpyridine (**22**, 1.84 g, 10.0 mmol, 1.0 equiv), 1-cyclopropylethanol (2.9 mL, 30.0 mmol, 3.0 equiv), P_4-*t*-Bu (0.8M, 625 μL, 0.5 mmol, 0.05 equiv) and toluene (10 mL) as the solvent at rt for 9 h. The reaction solution was then cooled to 0 °C in an ice bath and aqueous 4M HCl (40.0 mL, 160 mmol, 16 equiv) was added dropwise with vigorous stirring. The biphasic mixture was allowed to warm to rt and stirred for 1 h before being quenched with saturated aqueous Na_2CO_3 (100 mL), extracted with ethyl acetate (3 x 100 mL), washed with brine (200 mL), and concentrated *in vacuo*. Purification of the resulting residue via flash column chromatography (80% ethyl acetate/hexanes) yielded the title product as a white solid (1.42 g, 7.03 mmol, 70% yield).

A2.10 Intramolecular C–O Coupling Reactions for Dihydrobenzofuran Synthesis

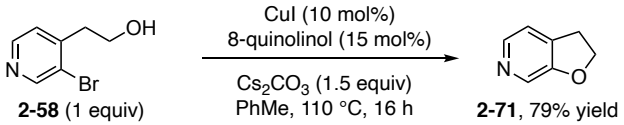

2,3-Dihydrofuro[2,3-*c*]pyridine (2-71)

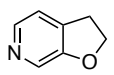

In a nitrogen-filled glovebox, to an oven-dried 2-dram reaction vial (Thermo Scientific B7999-3) containing a magnetic stir bar was added copper(I) iodide (7.6 mg, 0.04 mmol, 0.1 equiv), 8-quinolinol (8.7 mg, 0.06 mmol, 0.15 equiv), cesium carbonate (195.5 mg, 0.6 mmol, 1.5 equiv), PhMe (0.4 mL), and 2-(3-bromopyridin-4-yl)ethan-1-ol (80.8 mg, 0.4 mmol, 1.0 equiv) in successive order. The reaction vial was capped (Thermo Scientific B7995-15 with 10/90 septa), removed from the glovebox, and inserted into a preheated silicon oil bath at 110 °C. After stirring for 16 h, the reaction mixture was cooled to rt, water was added (3 mL), and the mixture was extracted with Et_2O (3 x 3 mL). The combined organic layer was washed with brine (10 mL) and concentrated *in vacuo*. Purification of the resulting residue *via* flash column chromatography (33% diethyl ether/hexanes) yielded the desired product as colorless oil (38.0 mg, 0.314 mmol, 79% yield). **^{1}H NMR** (400 MHz, $CDCl_3$) δ 8.15 (s, 1H), 8.12 (d, *J* = 4.7 Hz, 1H), 7.15 (dd, *J* = 4.7, 1.0 Hz, 1H), 4.58 (t, *J* = 8.8 Hz, 2H), 3.22 (td, *J* = 8.8, 1.1 Hz, 2H). **^{13}C NMR** (101 MHz, $CDCl_3$) δ 157.5, 142.2, 136.3, 131.8, 120.3, 71.2, 29.6. The spectroscopic data is consistent with literature data.[19]

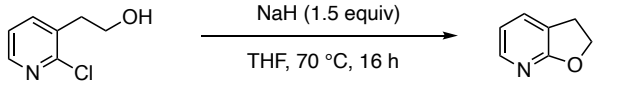

2-61 (1 equiv) **2-72**, 88% yield

2,3-Dihydrofuro[2,3-*b*]pyridine (2-72)

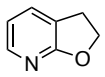

In a nitrogen-filled glovebox, to an oven-dried 2-dram vial (Thermo Scientific B7999-3) containing a magnetic stir bar was added 2-(2-chloropyridin-3-yl)ethan-1-ol (47.3 mg, 0.3 mmol, 1.0 equiv) and THF (0.6 mL). NaH (60% dispersion in mineral oil, 18 mg, 0.45 mmol, 1.5 equiv) was then added slowly to the mixture at rt in the glovebox. The reaction vial was capped (Thermo Scientific B7995-15 with 10/90 septa), removed from the glovebox, and inserted into a preheated silicon oil bath at 70 °C. After stirring for 16 h, the reaction mixture was cooled

to rt and quenched with water (2 mL), extracted with Et_2O (3 x 3 mL), washed with brine (10 mL), and concentrated *in vacuo*. Purification of the resulting residue *via* flash column chromatography with (75% diethyl ether/hexanes) yielded the desired product as colorless oil (32.0 mg, 0.264 mmol, 88% yield). **^{1}H NMR** (400 MHz, $CDCl_3$) δ 7.95 (m, 1H), 7.44 (dq, *J* = 7.2, 1.4 Hz, 1H), 6.74 (dd, *J* = 7.1, 5.2 Hz, 1H), 4.58 (t, *J* = 8.7 Hz, 2H), 3.22 (tt, *J* = 8.6, 1.2 Hz, 2H). **^{13}C NMR** (101 MHz, $CDCl_3$) δ 168.8, 146.7, 133.7, 119.7, 116.6, 69.0, 28.2. The spectroscopic data is consistent with literature data.[20]

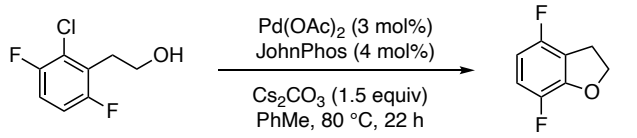

2-53 (1 equiv) **2-73**, 71% yield

4,7-Difluoro-2,3-dihydrobenzofuran (2-73)

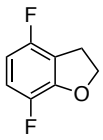

In a nitrogen-filled glovebox, to an oven-dried 2-dram vial (Thermo Scientific B7999-3) containing a magnetic stir bar was added palladium(II) acetate (2.0 mg, 0.009 mmol, 0.03 equiv), (2-biphenyl)di-*tert*-butylphosphine (JohnPhos, 3.6 mg, 0.012 mmol, 0.04 equiv), cesium carbonate (147 mg, 0.45 mmol, 1.5 equiv), PhMe (0.3 mL), and 2-(2-chloro-3,6-difluorophenyl)ethan-1-ol (57.8 mg, 0.3 mmol, 1.0 equiv) in successive order. The reaction vial was capped (Thermo Scientific B7995-15 with 10/90 septa), removed from the glovebox, and inserted into a preheated silicon oil bath at 80 °C. After stirring for 22 h, the reaction mixture was cooled to rt and quenched with water (2 mL), extracted with Et_2O (3 x 3 mL), washed with brine (10 mL), and concentrated *in vacuo*. Purification of the resulting residue *via* flash column chromatography (100% hexanes) yielded the desired product as colorless oil (33.0 mg, 0.211 mmol, 71% yield). **^{1}H NMR** (400 MHz, $CDCl_3$) δ 6.89 – 6.81, (m, 1H), 6.47 (ddd, *J* = 9.1, 7.8, 3.0 Hz, 1H), 4.72 (t, *J* = 8.7 Hz, 2H), 3.29 (tt, *J* = 8.7, 1.0 Hz, 2H). **^{13}C NMR** (101 MHz, $CDCl_3$) δ 155.3 (dd, *J* = 242.7, 2.2 Hz), 148.4 (dd, *J* = 12.4, 8.7 Hz), 144.3 (dd, *J* = 240.4, 3.2 Hz), 116.6

(dd, J = 23.8, 3.0 Hz), 116.3 (dd, J = 19.7, 9.0 Hz), 107.4 (dd, J = 23.5, 6.1 Hz), 73.5, 27.6 (m). **^{19}F NMR** (377 MHz, $CDCl_3$) δ -122.43 (d, J = 20.5 Hz), -144.44 (d, J = 19.7 Hz). **IR** (neat, cm^{-1}) 2923.4, 2852.4, 1640.8, 1499.0, 1458.9, 1234.3, 1198.6, 1041.4, 994.0, 792.8. **GCMS** $[M]^+$ calc for $[C_8H_6F_2O]^+$ 156.0, found 156.

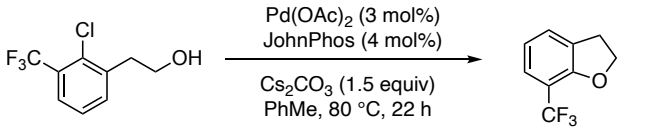

2-52 (1 equiv) **2-74**, 62% yield

7-(Trifluoromethyl)-2,3-dihydrobenzofuran (2-74)

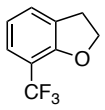

In a nitrogen-filled glovebox, to an oven-dried 2-dram vial (Thermo Scientific B7999-3) containing a magnetic stir bar was added palladium(II) acetate (2.0 mg, 0.009 mmol, 0.03 equiv), (2-biphenyl)di-*tert*-butylphosphine (JohnPhos, 3.6 mg, 0.012 mmol, 0.04 equiv), cesium carbonate (147 mg, 0.45 mmol, 1.5 equiv), PhMe (0.3 mL), and 2-(2-chloro-3-(trifluoromethyl)phenyl)ethan-1-ol (67.4 mg, 0.3 mmol, 1.0 equiv) in successive order. The reaction vial was capped (Thermo Scientific B7995-15 with 10/90 septa), removed from the glovebox, and inserted into a preheated silicon oil bath at 80 °C. After stirring for 22 h, the reaction mixture was cooled to rt and quenched with water (2 mL), extracted with Et_2O (3 x 3 mL), washed with brine (10 mL), and concentrated *in vacuo*. Purification of the resulting residue *via* flash column chromatography (100% hexanes) yielded the desired product as colorless oil (35.0 mg, 0.186 mmol, 62% yield). **^{1}H NMR** (400 MHz, $CDCl_3$) δ 7.34 (m, 2H), 6.96 – 6.82 (m, 1H), 4.71 (t, J = 8.8 Hz, 2H), 3.25 (t, J = 8.8 Hz, 2H). **^{13}C NMR** (101 MHz, $CDCl_3$) δ 157.6 (q, J = 2.0 Hz), 129.4, 128.6, 125.0 (q, J = 4.5 Hz), 123.8 (q, J = 271.5 Hz), 120.3, 112.9, 72.6, 29.4. **^{19}F NMR** (377 MHz, $CDCl_3$) δ -61.83. **IR** (neat, cm^{-1}) 2923.4, 2849.9, 1621.3, 1606.0, 1482.5, 1460.8, 1444.1, 1345.7, 1315.2, 1221.9, 1124.3, 1058.6, 986.7, 780.8. **LRMS** $[M-H]^-$ calc for $[C_9H_6F_3O]^-$ 187.0, found 187.1.

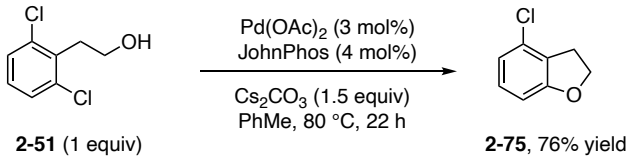

2-51 (1 equiv) **2-75**, 76% yield

4-Chloro-2,3-dihydrobenzofuran (2-75)

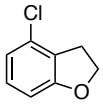

In a nitrogen-filled glovebox, to an oven-dried 2-dram vial (Thermo Scientific B7999-3) containing a magnetic stir bar was added palladium(II) acetate (3.4 mg, 0.015 mmol, 0.03 equiv), (2-biphenyl)di-*tert*-butylphosphine (JohnPhos, 6.0 mg, 0.02 mmol, 0.04 equiv), cesium carbonate (244 mg, 0.75 mmol, 1.5 equiv), PhMe (0.5 mL), and 2-(2,6-dichlorophenyl)ethan-1-ol (95.5 mg, 0.5 mmol, 1.0 equiv) in successive order. The reaction vial was capped (Thermo Scientific B7995-15 with 10/90 septa), removed from the glovebox, and inserted into a preheated silicon oil bath at 80 °C. After stirring for 22 h, the reaction mixture was cooled to rt and quenched with water (2 mL), extracted with Et_2O (3 x 3 mL), washed with brine (10 mL), and concentrated *in vacuo*. Purification of the resulting residue *via* flash column chromatography (100% hexanes) yielded the desired product as colorless oil (59.0 mg, 0.382 mmol, 76% yield). **^{1}H NMR** (400 MHz, $CDCl_3$) δ 7.04 (tt, J = 8.0, 0.8 Hz, 1H), 6.83 (dd, J = 8.0, 0.8 Hz, 1H), 6.67 (dd, J = 8.0, 0.8 Hz, 1H), 4.61 (t, J = 8.8 Hz, 2H), 3.25 (t, J = 8.8 Hz, 2H). **^{13}C NMR** (101 MHz, $CDCl_3$) δ 161.2, 130.9, 129.4, 126.2, 120.7, 107.9, 71.3, 29.6. **IR** (neat, cm^{-1}) 2972.8, 2898.0, 1606.5, 1588.2, 1478.2, 1467.4, 1450.8, 1437.1, 1236.9, 1156.1, 1139.8, 981.3, 944.6, 905.4, 761.2. **GCMS** $[M]^+$ calc for $[C_8H_7ClO]^+$ 154.0, found 154.

A2.11 Hydroboration/Oxidation Comparison of Vinyl Arene Substrates

Discussion. The purpose of these experiments was to compare a base-catalyzed styrene hydration approach to traditional hydroboration/oxidation protocols. Two common boranes (BH_3·THF and 9-BBN) were first employed for three control styrene substrates. Thus, styrene, 4-fluorostyrene

and 4-*tert*-butylstyrene underwent high yielding hydroboration/oxidation using the general procedure described below. Next, several vinyl arenes from Table 2 were examined using the same general procedure and the results are provided in Table S7. The general experimental procedure is provided below with an example spectrum to illustrate how ^{1}H NMR yields were used to determine product distribution.

General procedure. Vinyl arene (0.2 mmol, 1.0 equiv) was added to an oven-dried 2-dram reaction vial (Thermo Scientific B7999-3) with a magnetic stir bar. The vial was capped (Thermo Scientific B7995-15 with 10/90 septa) and evacuated and filled with nitrogen three times. Anhydrous THF (0.4 mL) was added and the reaction solution was cooled to 0 °C using an ice bath. Borane solution, BH_3·THF (1.0 M solution in THF, 0.4 mL, 2.0 equiv) or 9-BBN (0.5 M solution in THF, 0.8 mL, 2.0 equiv) was then added dropwise. The reaction mixture was allowed to warm to rt or 80 °C and stirred for 14 h. After cooling the reaction mixture to 0 °C in an ice bath, MeOH (0.4 mL), aqueous NaOH (2 M, 0.95 mL, 9.5 equiv), and 30% H_2O_2 (0.14 mL, 6.0 equiv) were added successively to the reaction mixture. The reaction mixture was stirred for 4 h at rt and then dibenzyl ether (19.0 μL, 0.1 mmol, 0.5 equiv) was added as an internal standard. The reaction mixture was extracted with EtOAc (3 x 3 mL) and the organic layer was concentrated *in vacuo*. $CDCl_3$ (approximately 0.6 mL) was added to the concentrate, homogenized and transferred to an NMR tube. The product yield and distribution were determined by ^{1}H NMR spectroscopy by comparison of the product integration to the dibenzyl ether internal standard. The results are summarized in Table A2-3 below.

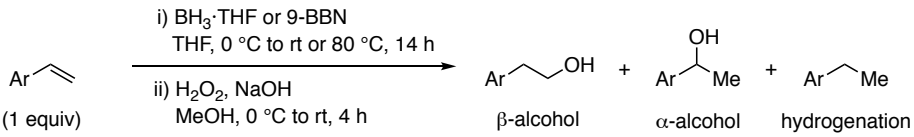

Table A2-3. Comparison of multiple hydroboration/oxidation methods for the formal anti-Markovnikov hydration of various vinyl arenes (β = *liner alcohol,* α = *branch alcohol*).

	BH_3·THF	**9-BBN**

vinyl arene	0 °C to rt	0 °C to 80 °C	0 °C to rt	0 °C to 80 °C
	^{1}H NMR yield (%)		^{1}H NMR yield (%)	
styrene	85	75	100	100
4-fluorostyrene	71	63	77	77
4-*tert*-butylstyrene	79	83	96	97
2,6-dichlorostyrene	15 (β), 34 (α)	-	15 (β)	63 (β), 11 (α)
4-methyl-2-nitrostyrene	39	28	15	18
3-bromo-4-vinylpyridine	no alcohol, hydrogenation	-	no alcohol, hydrogenation	-

Example NMR spectra interpretation for hydroboration/oxidation of 4-methyl-2-nitrostyrene. Provided below is an example ^{1}H NMR spectrum of the crude reaction mixture for the hydroboration/oxidation of 4-methyl-2-nitrostyrene using BH_3·THF (0 °C to rt). Integration of dibenzyl ether chemical shifts compared to alcohol methylene chemical shifts were used to determine ^{1}H NMR yields. Yields for other reaction conditions and styrenes were determined analogously.

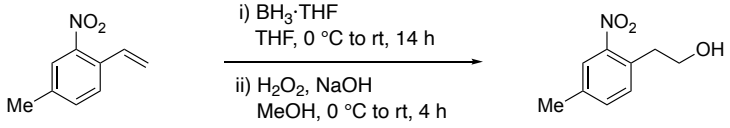

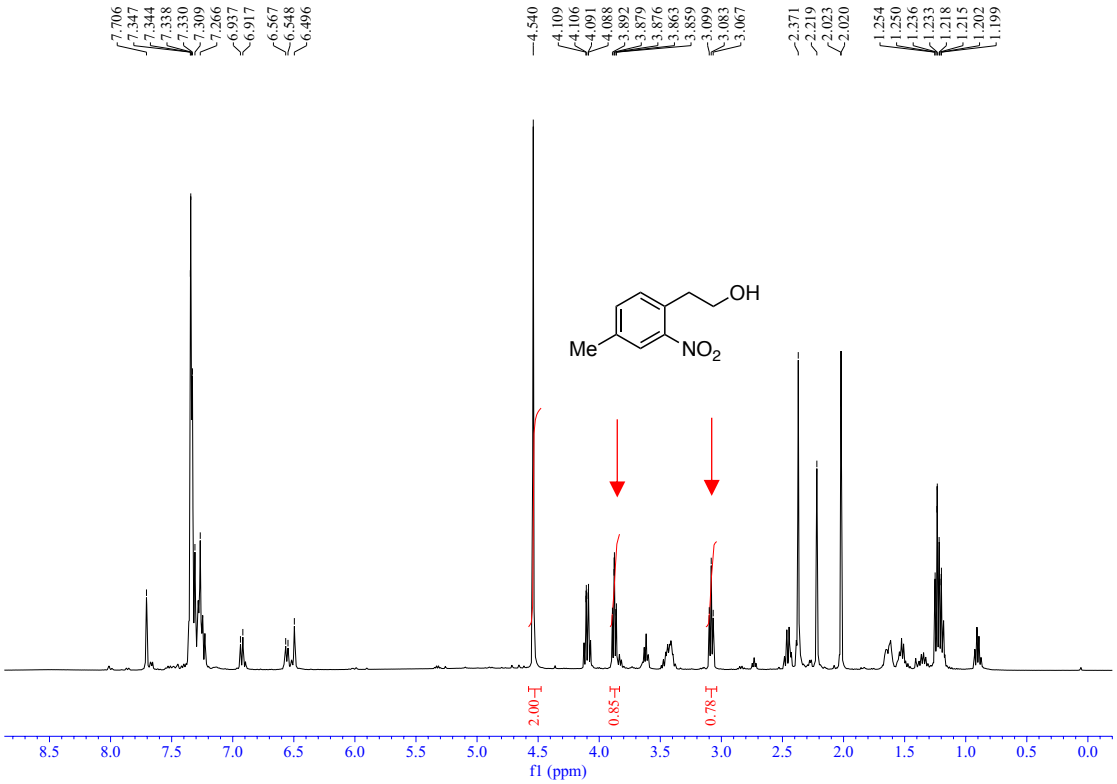

Figure A2-5. Example NMR spectrum for the hydroboration/oxidation of 4-methyl 2-nitrostyrene. A 39% yield is indicated by the integration of the product triplet at 3.08 ppm.

A2.12 References

[1] K. Lafaye, L. Nicolas, A. Guérinot, S. Reymond, J. Cossy. *Org. Lett*. **2014**, *16*, 4972 – 4975.

[2] E. T. McBee, R. A. Sanford, *J. Am. Chem. Soc*. **1950**, *72*, 4053 – 4055.

[3] A. A. Friedman, J. Panteleev, J. Tsoung, V. Huynh, M. Lautens. *Angew. Chem. Int. Ed*. **2013**, *52*, 9755 – 9758.

[4] L. Yang, L. Shi, Q. Xing, K.-W. Huang, C. Xia, F. Li. *ACS Catal*. **2018**, *8*, 10340 – 10348.

[5] H. Lebel, M. Davi, S. Díez-González, S. P. Nolan. *J. Org. Chem*. **2007**, *72*, 144 – 149.

[6] C. R. Smith, T. V. RajanBabu. *Tetrahedron* **2010**, *66*, 1102 – 1110.

[7] T. R. Puleo, A. J. Strong, J. S. Bandar. *J. Am. Chem. Soc*. **2019**, *141*, 1467 – 1472.

[8] C.-T. Yang, J. Han, J. Liu, Y. Li, F. Zhang, H.-Z. Yu, S. Hu, X. Wang. *Chem. Eur. J*. **2018**, *24*, 10324 – 10328.

[9] R. Van Hoveln, B. M. Hudson, H. B. Wedler, D. M. Bates, G. Le Gros, D. J. Tantillo, J. M. Schomaker. *J. Am. Chem. Soc*. **2015**, *137*, 5346 – 5354.

[10] Y. Yang, S. L. Buchwald. *Angew. Chem. Int. Ed*. **2014**, *53*, 8677 – 8681.

[11] M. A. Fakhfakh, X. Franck, A. Fournet, R. Hocquemiller, B. Figadère. *Tetrahedron Lett*. **2001**, *42*, 3847 – 3850.

[12] S. He, P. Li, X. Dai, H. Liu, Z. Lai, D. Xiao, C. C. McComas, C. Du, Y. Liu, J. Yin, Q. Dang, N. Zorn, X. Peng, R. P. Nargund, A. Palani. *Tetrahedron Lett*. **2017**, *58,* 1373 – 1375.

[13] M. Zhang, J. Xie, C. Zhu. *Nat Commun* **2018**, *9*, 3517.

[14] C. Luo, J. S. Bandar, *J. Am. Chem. Soc*. **2018**, *140*, 3547 – 3550.

[15] C. Luo, J. V. Alegra-Requena, S. J. Sujansky, S. P. Pajk, L. C. Gallegos, R. S. Paton, J. S. Bandar, *J. Am. Chem. Soc*. **2022**, *144*, 9586 – 9596.

[16] B. P. Fors, S. L. Buchwald. *J. Am. Chem. Soc*. **2009**, *131*, 12898 – 12899.

[17] B. Plouvier, G. N. Beatch, G. L. Jung, A. Zolotoy, T. Sheng, L. Clohs, T. D. Barrett, D. Fedida, W. Q. Wang, J. J. Zhu, Y. Liu, S. Abraham, L. Lynn, Y. Dong, R. A. Wall, M. J. A. Walker. *J. Med. Chem*. **2007**, *50*, 2818 – 2841.

[18] A. S. Norgren, S. Zhang, P. I. Arvidsson. *Org. Lett.* **2006**, *8*, 4533 – 4536.

[19] D. A. De Bie, A. Ostrowicz, G. Geurtsen, H. C. van der Plas. *Tetrahedron*, **1988**, 44, 2977 – 2983

[20] A. E. Frissen, A. T. M. Marcelis, H. C. van der Plas. *Tetrahedron Lett*. **1987**, *28*, 1589 – 1592.

A2.13 Copies of NMR Spectra

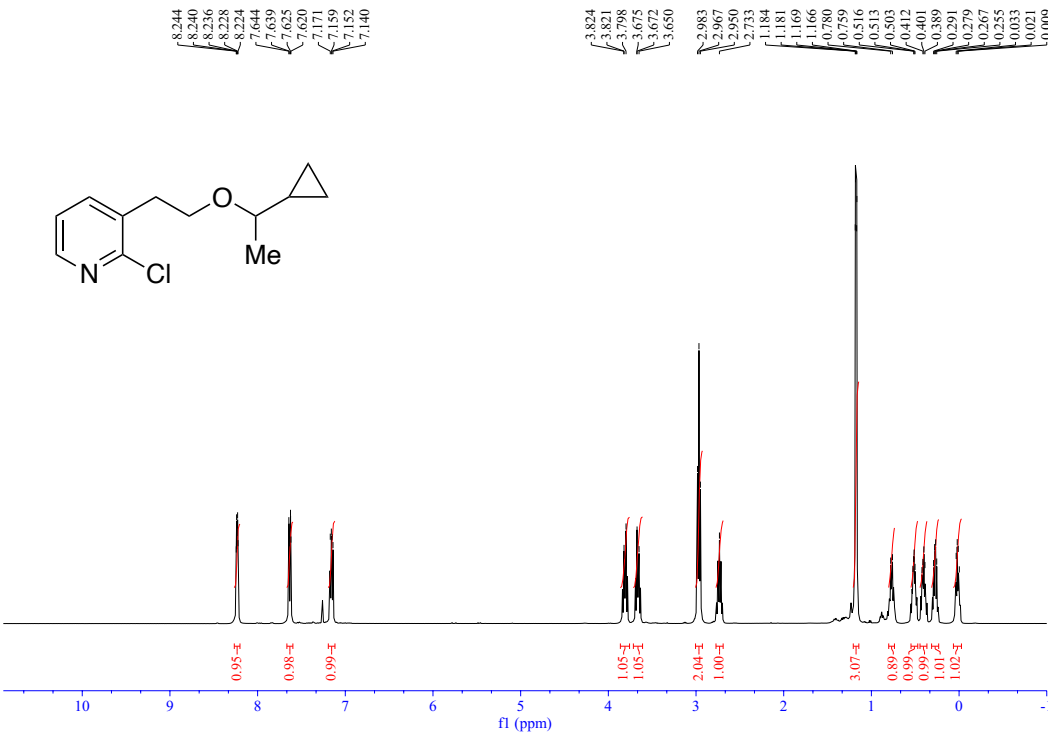

^{1}H NMR spectrum (400 MHz, $CDCl_3$)

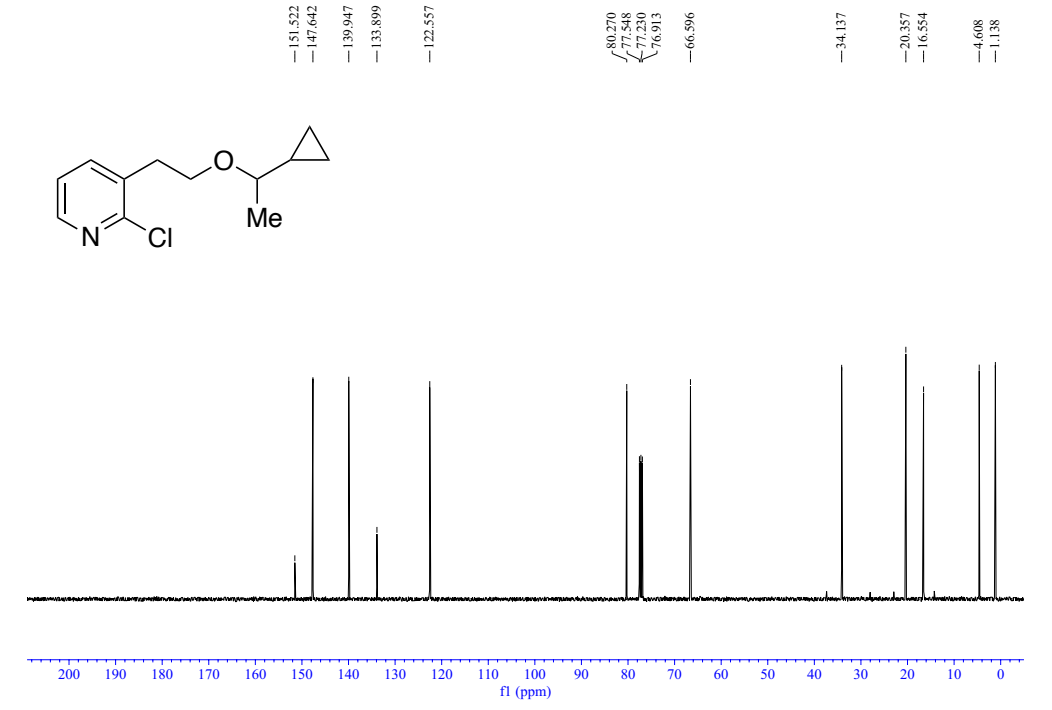

^{13}C NMR spectrum (101 MHz, $CDCl_3$)

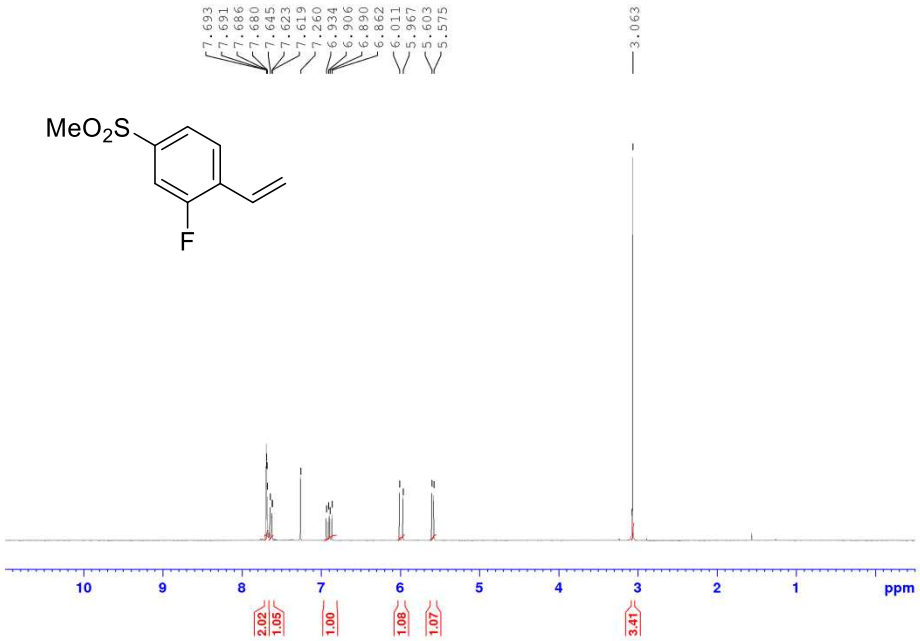

^{1}H NMR spectrum of 2-fluoro-4-(methylsulfonyl)styrene (400 MHz, $CDCl_3$)

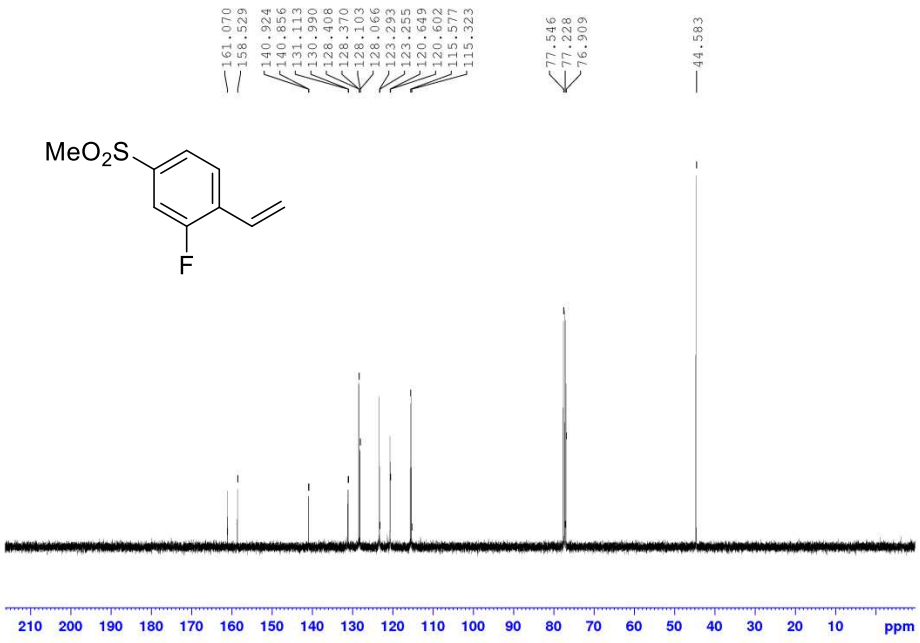

^{13}C NMR spectrum of 2-fluoro-4-(methylsulfonyl)styrene (101 MHz, $CDCl_3$)

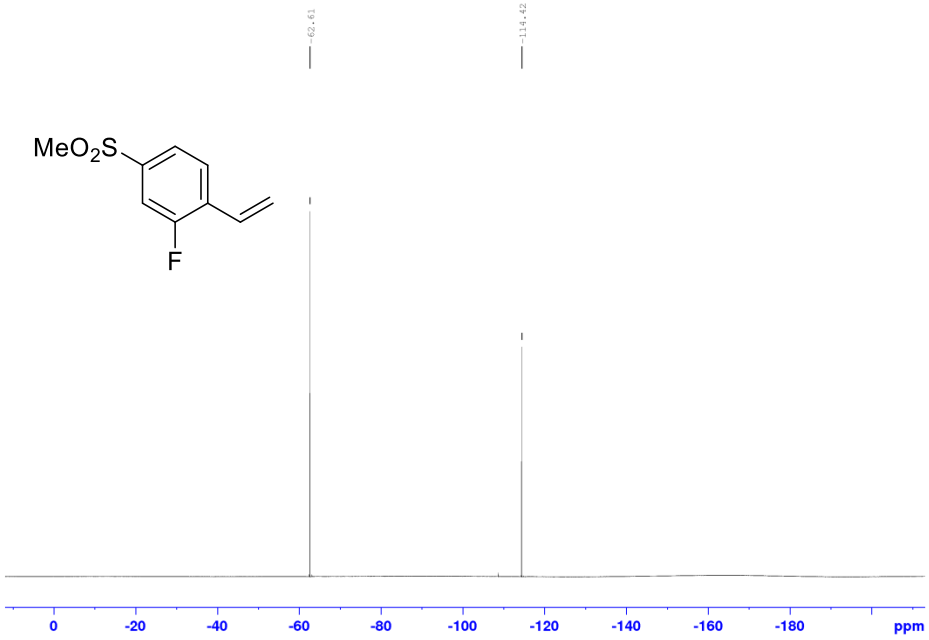

^{19}F NMR spectrum of 2-fluoro-4-(methylsulfonyl)styrene (377 MHz, $CDCl_3$, $PhCF_3$ internal standard set at -62.61 ppm)

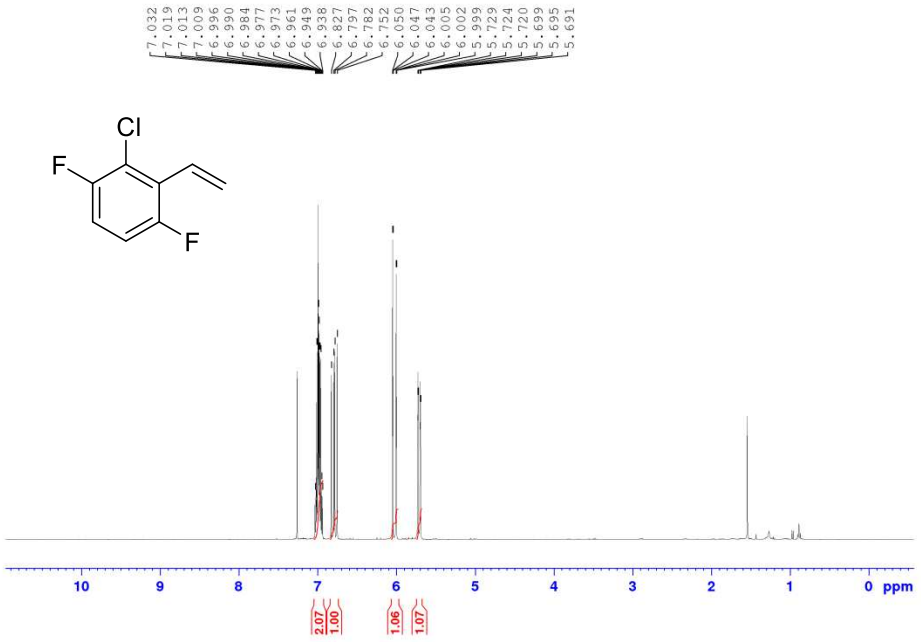

^{1}H NMR spectrum of 2-chloro-3,6-difluorostyrene (400 MHz, $CDCl_3$)

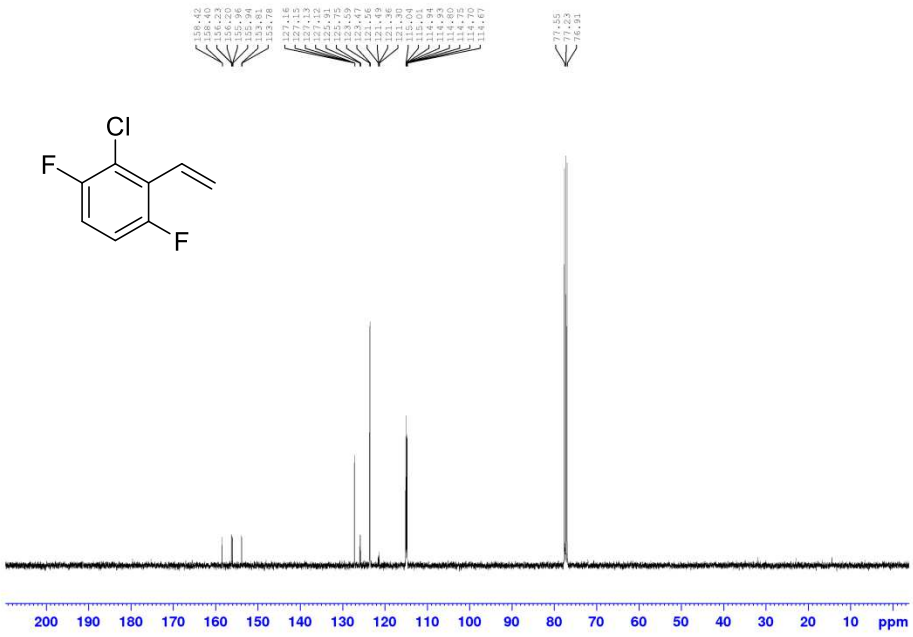

^{13}C NMR spectrum of 2-chloro-3,6-difluorostyrene (101 MHz, $CDCl_3$)

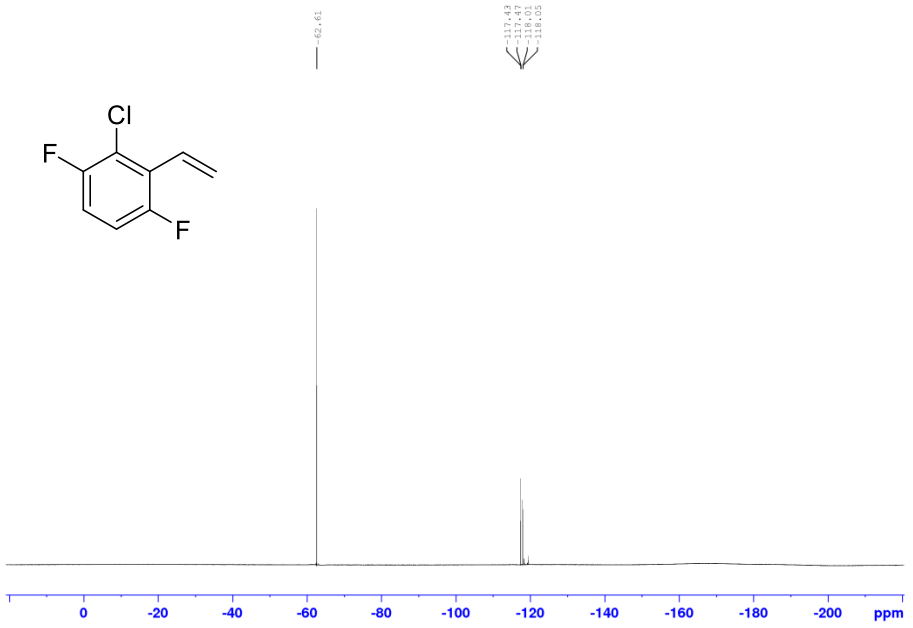

^{19}F NMR spectrum of 2-chloro-3,6-difluorostyrene (377 MHz, $CDCl_3$, $PhCF_3$ internal standard set at -62.61 ppm)

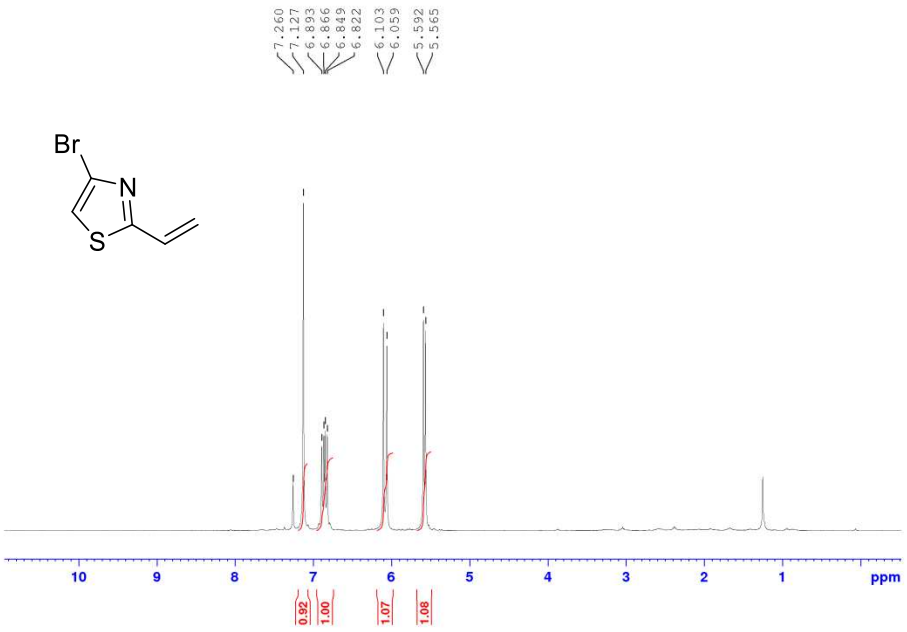

^{1}H NMR spectrum of 4-bromo-2-vinylthiazole (400 MHz, $CDCl_3$)

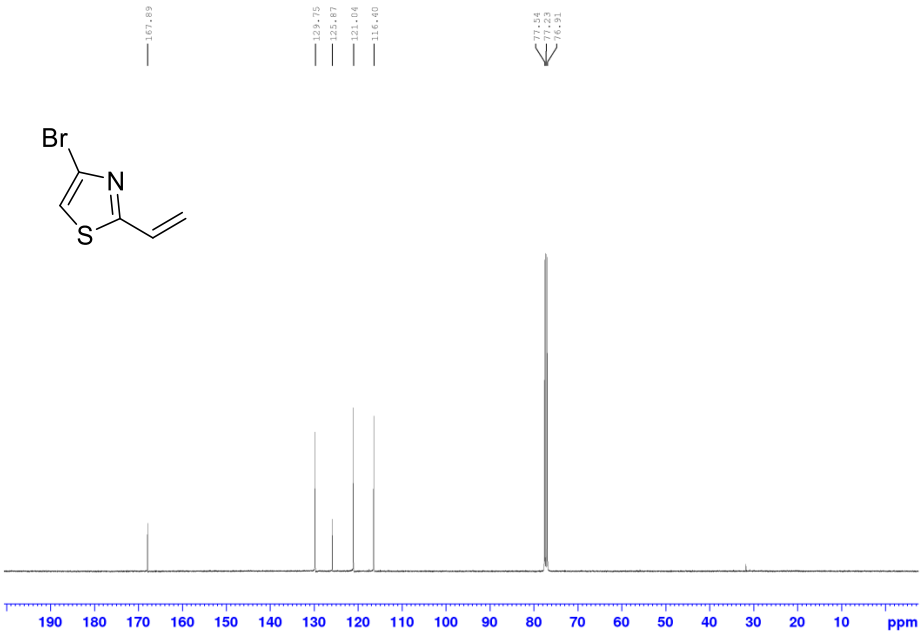

^{13}C NMR spectrum of 4-bromo-2-vinylthiazole (101 MHz, $CDCl_3$)

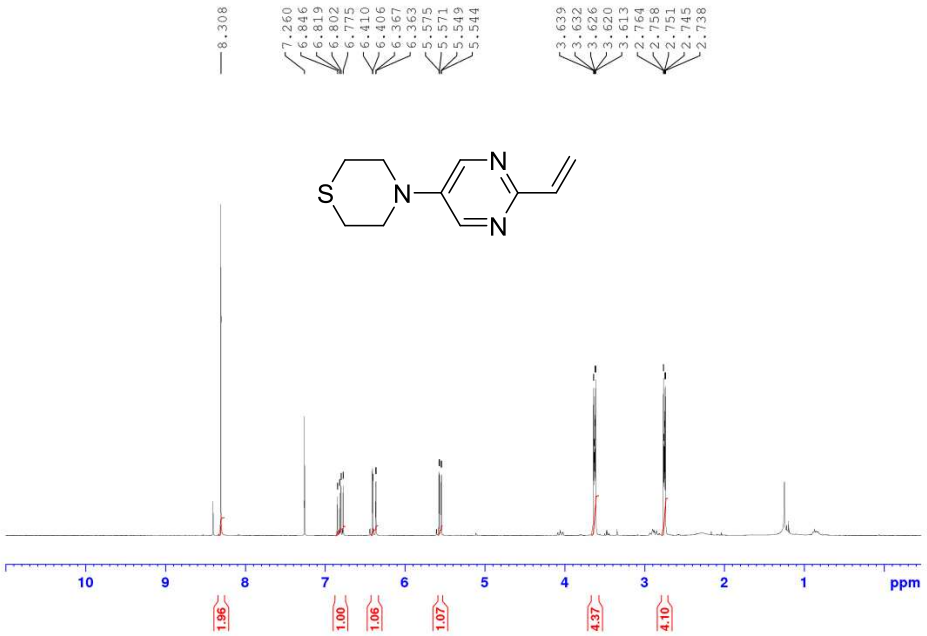

^{1}H NMR spectrum of 4-(2-vinylpyrimidin-5-yl)thiomorpholine (400 MHz, $CDCl_3$)

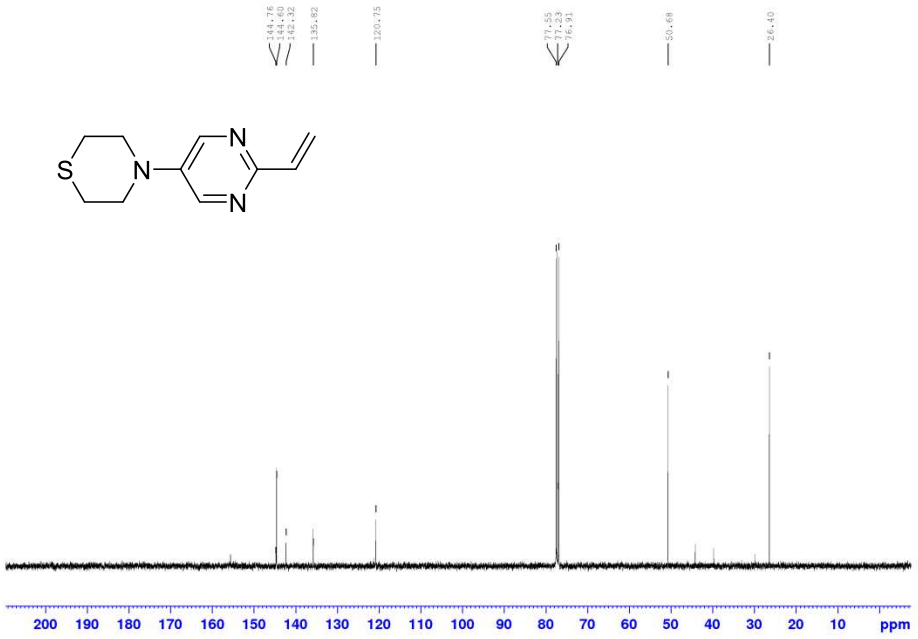

^{13}C NMR spectrum of 4-(2-vinylpyrimidin-5-yl)thiomorpholine (101 MHz, $CDCl_3$)

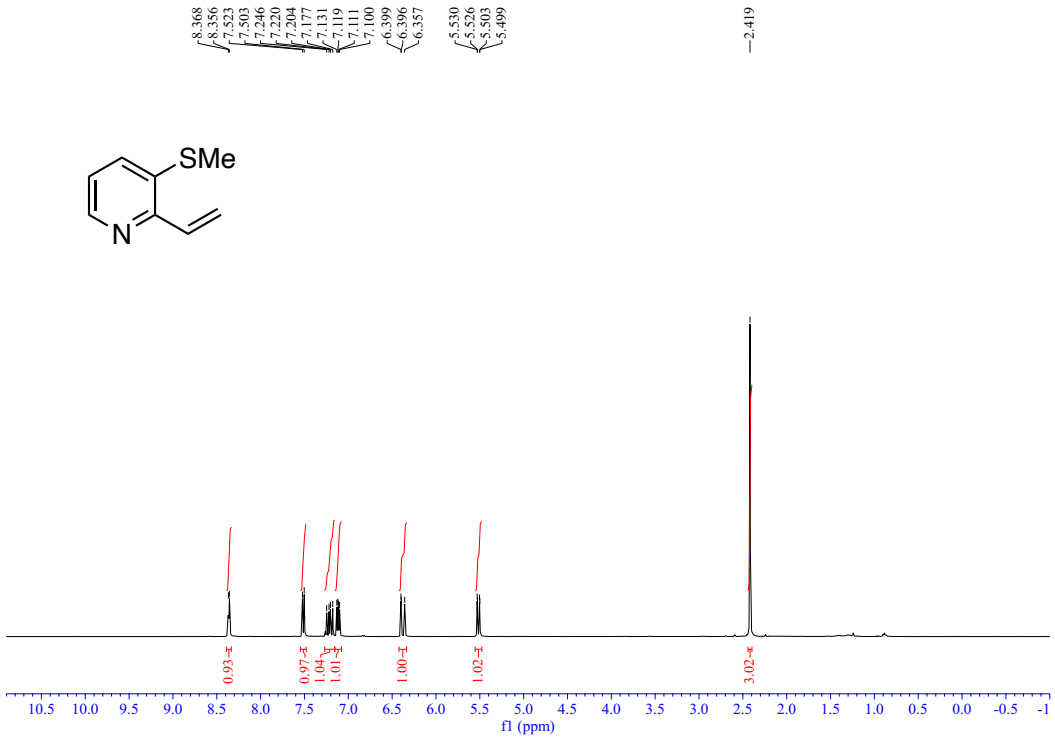

^{1}H NMR spectrum of 3-(methylthio)-2-vinylpyridine (400 MHz, $CDCl_3$)

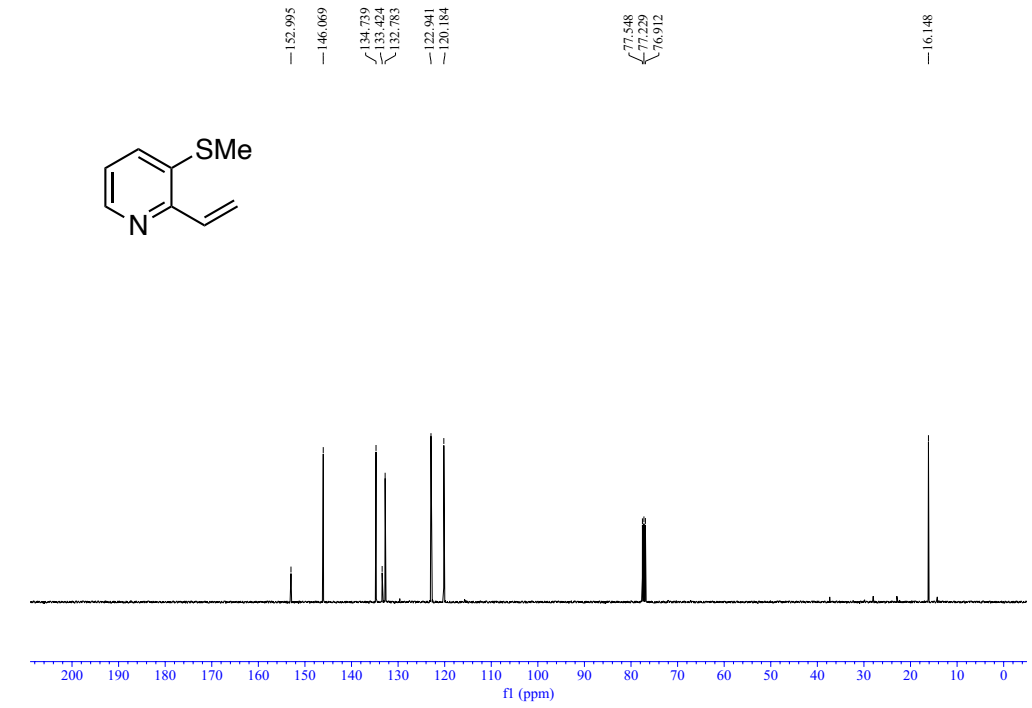

^{13}C NMR spectrum of 3-(methylthio)-2-vinylpyridine (101 MHz, $CDCl_3$)

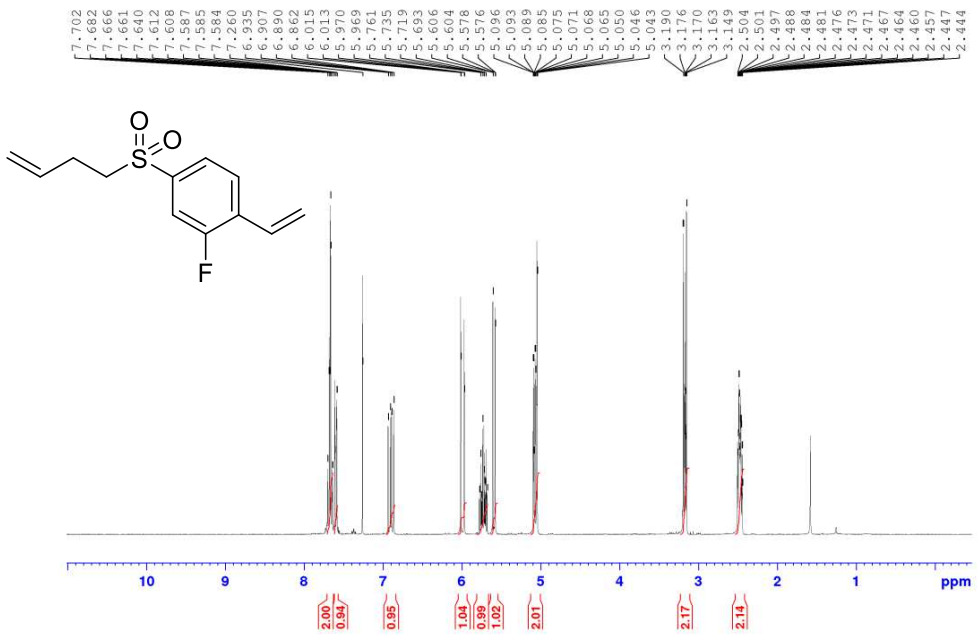

^{1}H NMR spectrum of 4-(but-3-en-1-ylsulfonyl)-2-fluoro-1-vinylbenzene (400 MHz, $CDCl_3$)

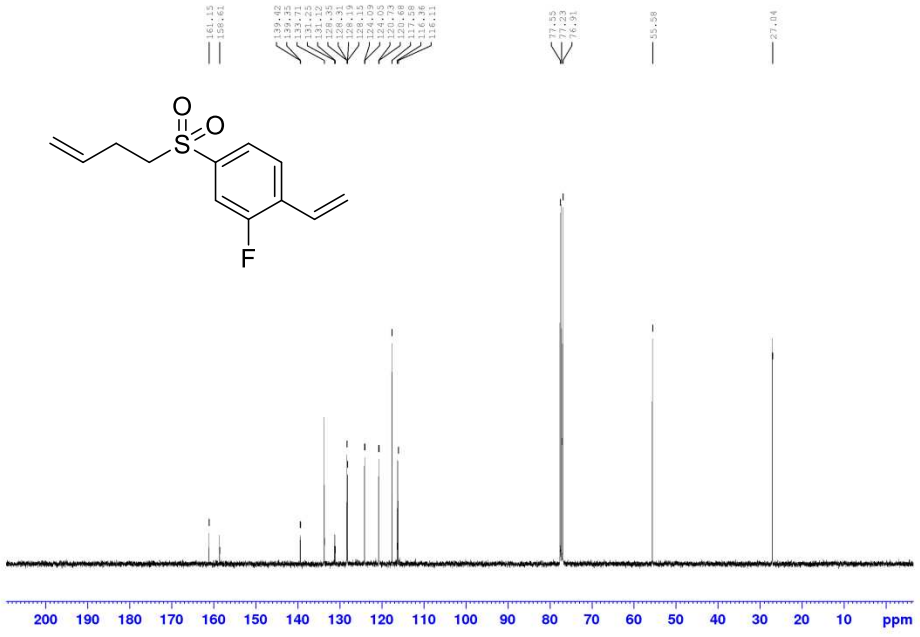

^{13}C NMR spectrum of 4-(but-3-en-1-ylsulfonyl)-2-fluoro-1-vinylbenzene (101 MHz, $CDCl_3$)

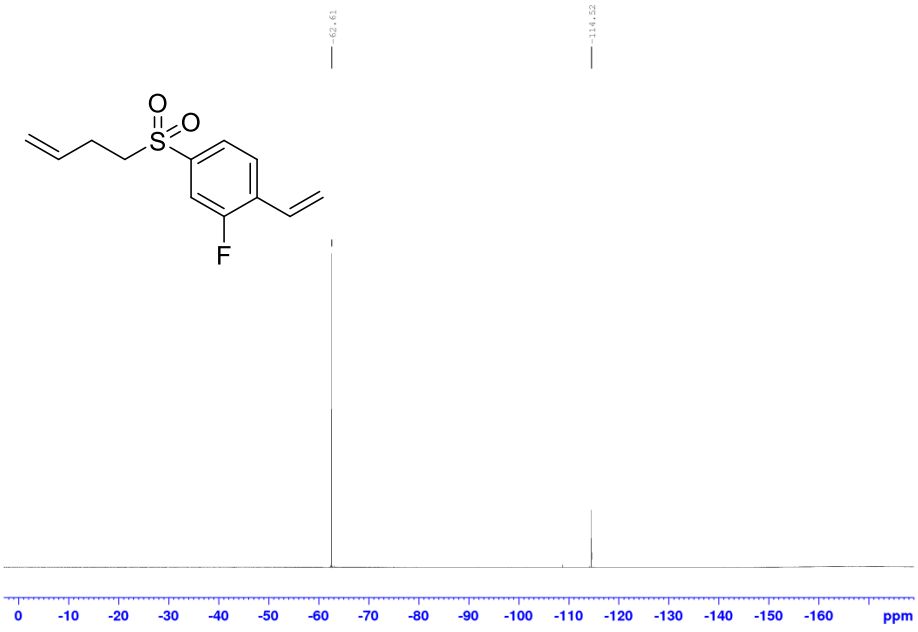

^{19}F NMR spectrum of 4-(but-3-en-1-ylsulfonyl)-2-fluoro-1-vinylbenzene (377 MHz, $CDCl_3$, $PhCF_3$ internal standard set at -62.61 ppm)

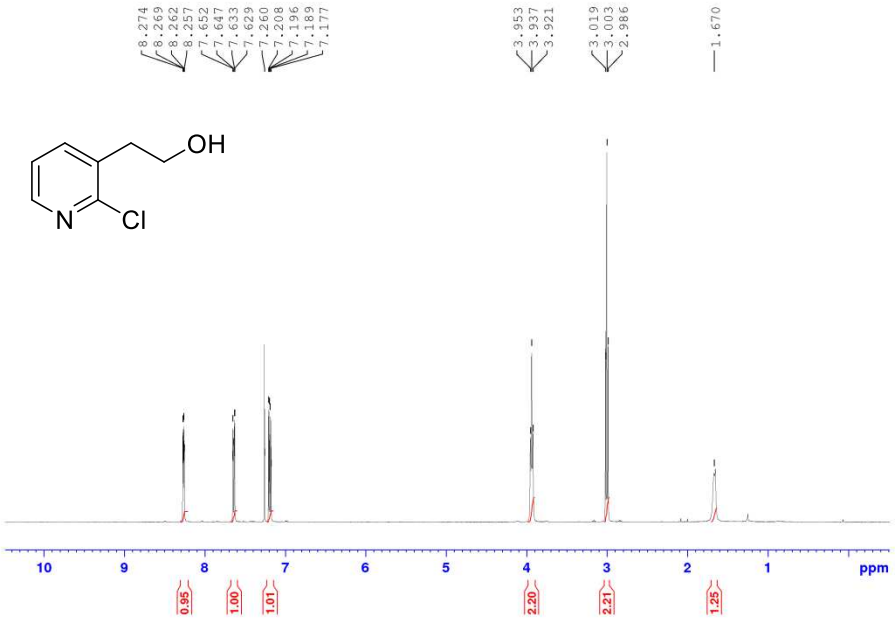

^{1}H NMR spectrum of **2-61** (400 MHz, $CDCl_3$)

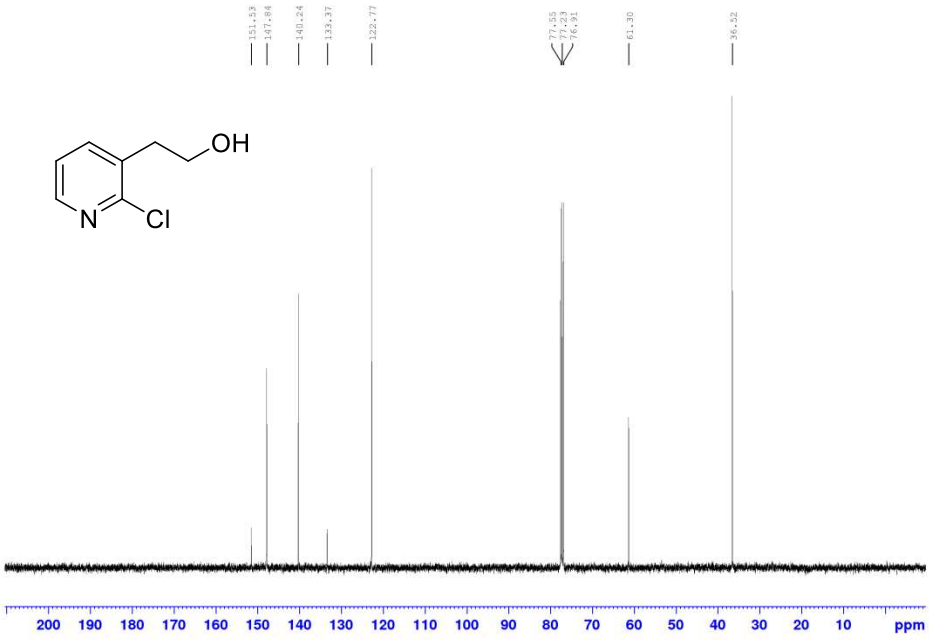

^{13}C NMR spectrum of **2-61** (101 MHz, $CDCl_3$)

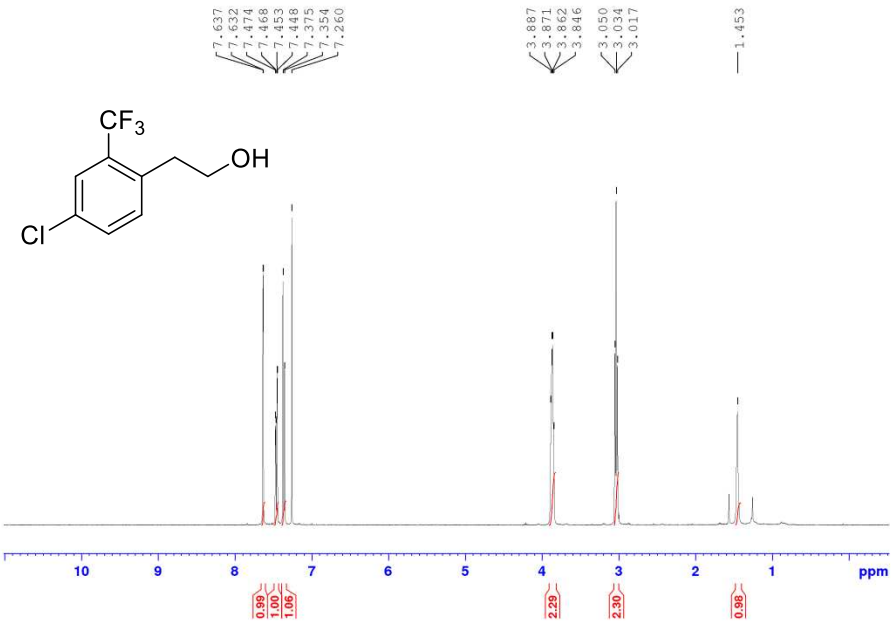

^{1}H NMR spectrum of **2-62** (400 MHz, $CDCl_3$)

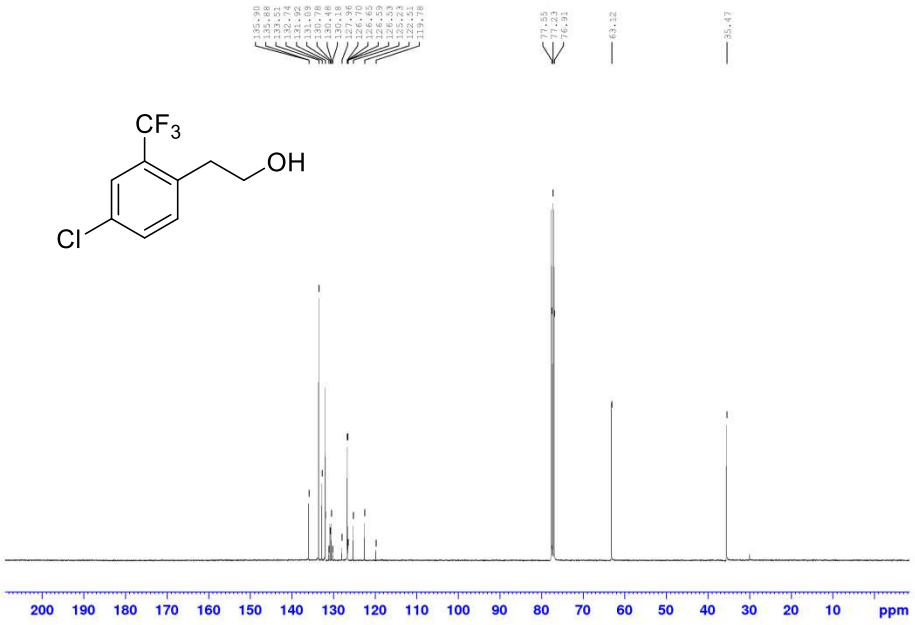

^{13}C NMR spectrum of **2-62** (101 MHz, $CDCl_3$)

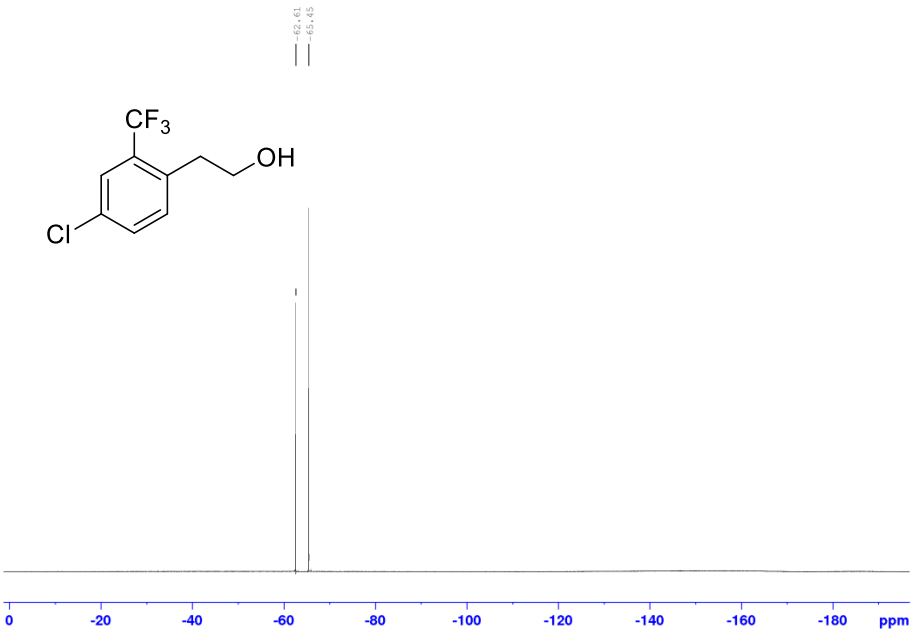

^{19}F NMR spectrum of **2-62** (377 MHz, $CDCl_3$, $PhCF_3$ internal standard set at -62.61 ppm)

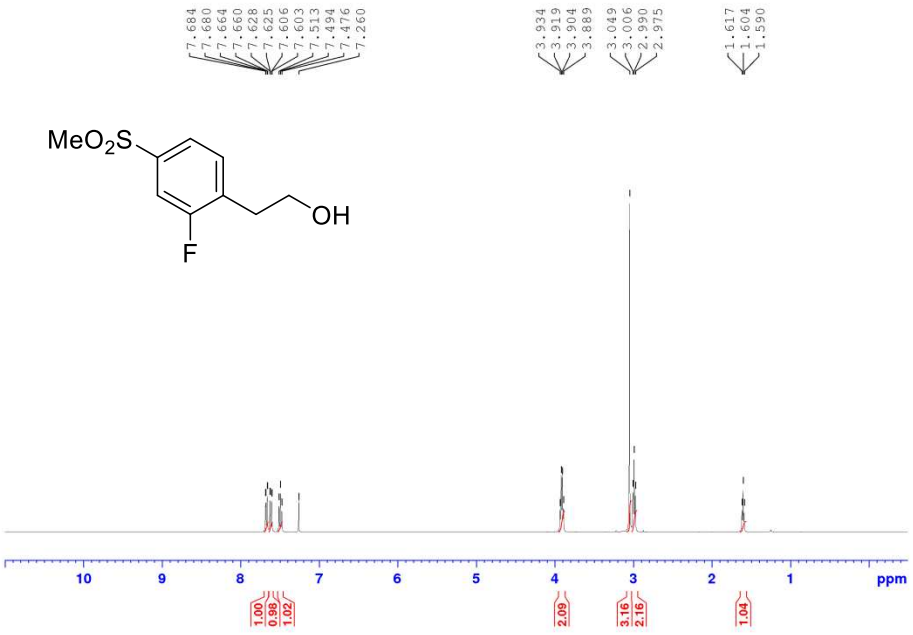

^{1}H NMR spectrum of **2-64** (400 MHz, $CDCl_3$)

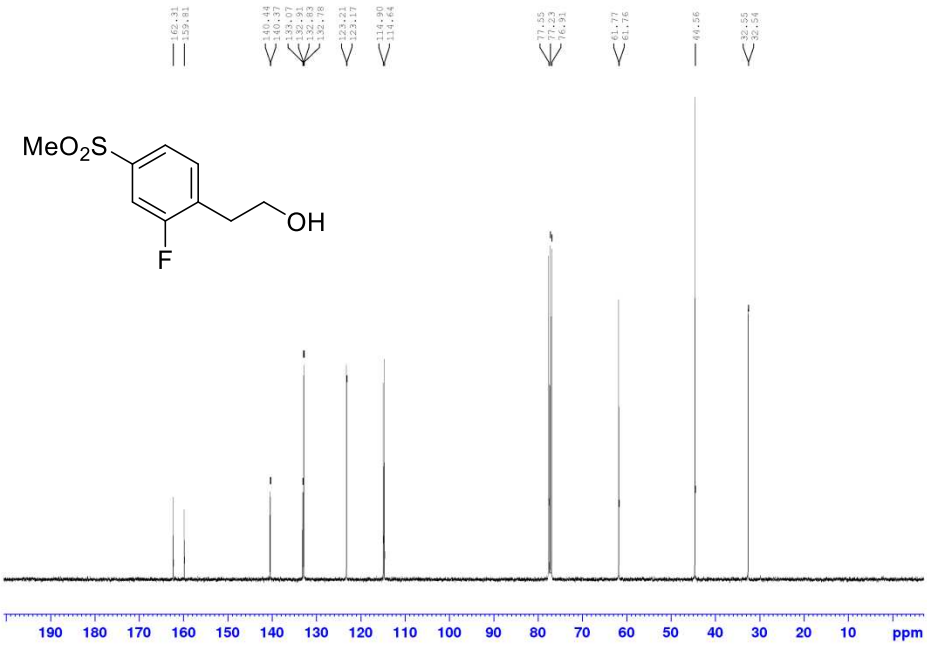

^{13}C NMR spectrum of **2-64** (101 MHz, $CDCl_3$)

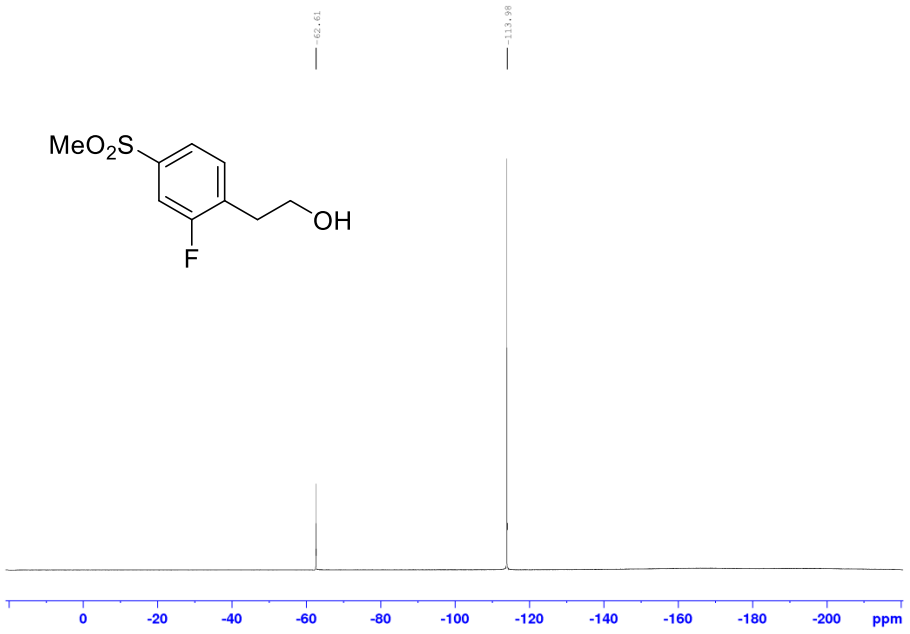

^{19}F NMR spectrum of **2-64** (377 MHz, $CDCl_3$, $PhCF_3$ internal standard set at -62.61 ppm)

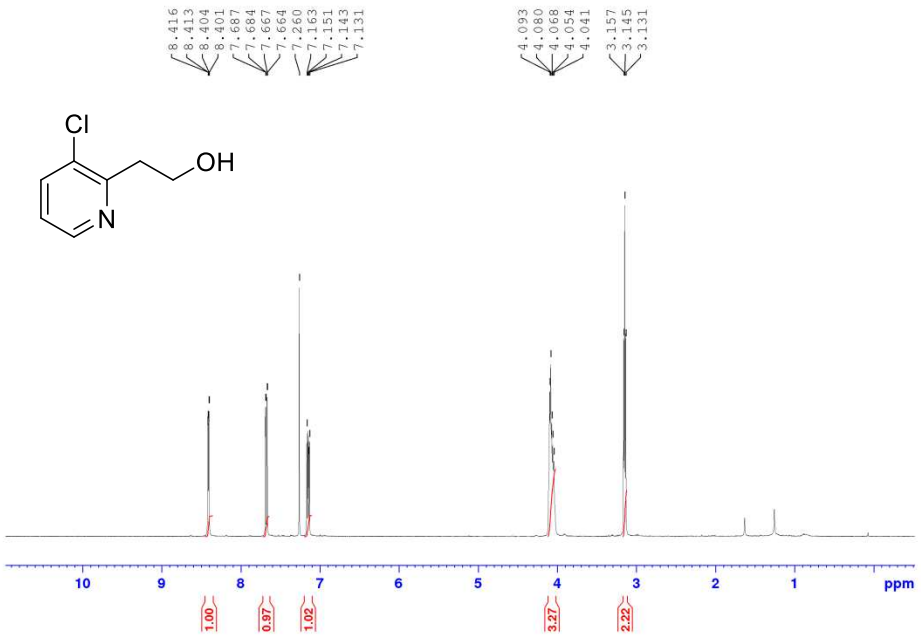

^{1}H NMR spectrum of **2-63** (400 MHz, $CDCl_3$)

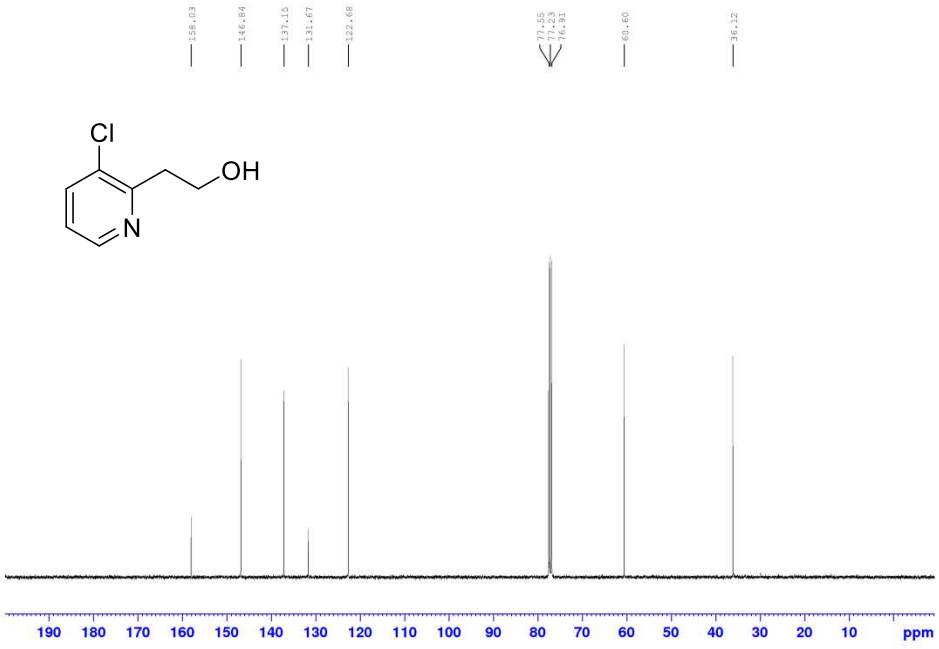

^{13}C NMR spectrum of **2-63** (101 MHz, $CDCl_3$)

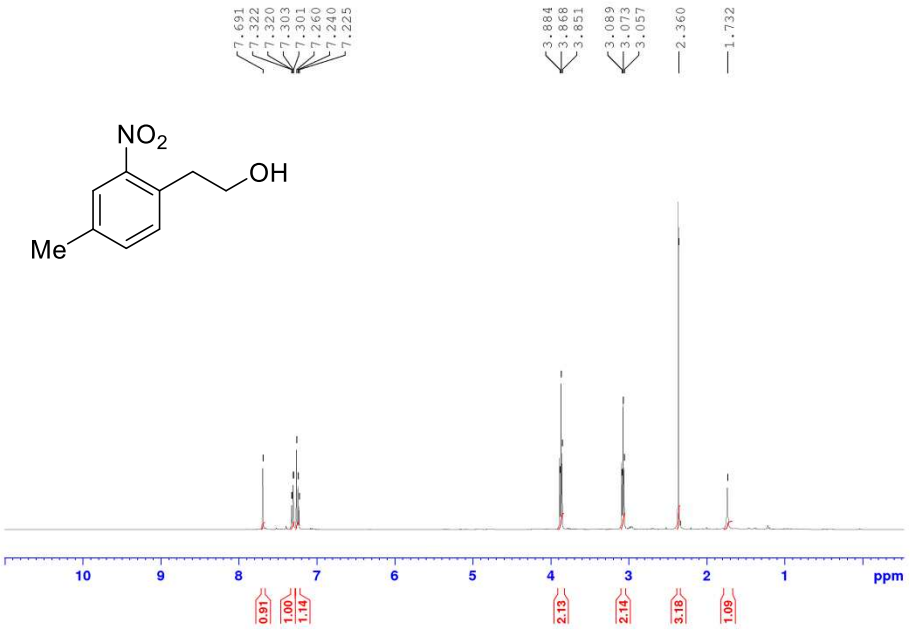

^{1}H NMR spectrum of **2-49** (400 MHz, $CDCl_3$)

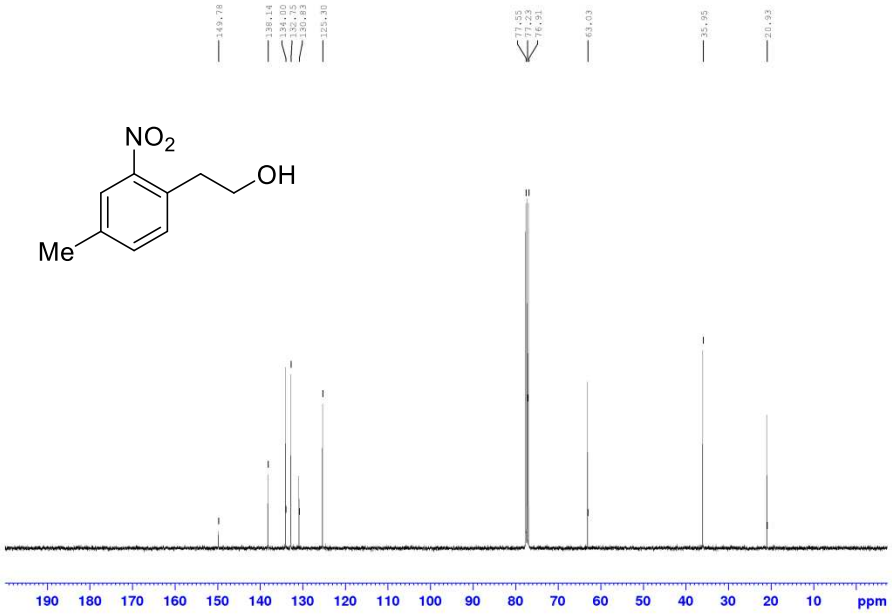

^{13}C NMR spectrum of **2-49** (101 MHz, $CDCl_3$)

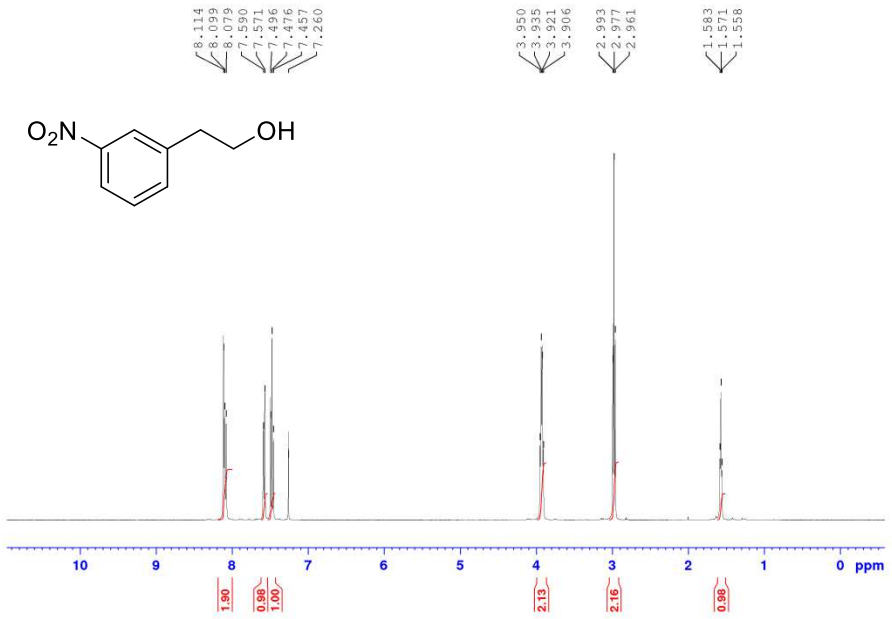

^{1}H NMR spectrum of **2-50** (400 MHz, $CDCl_3$)

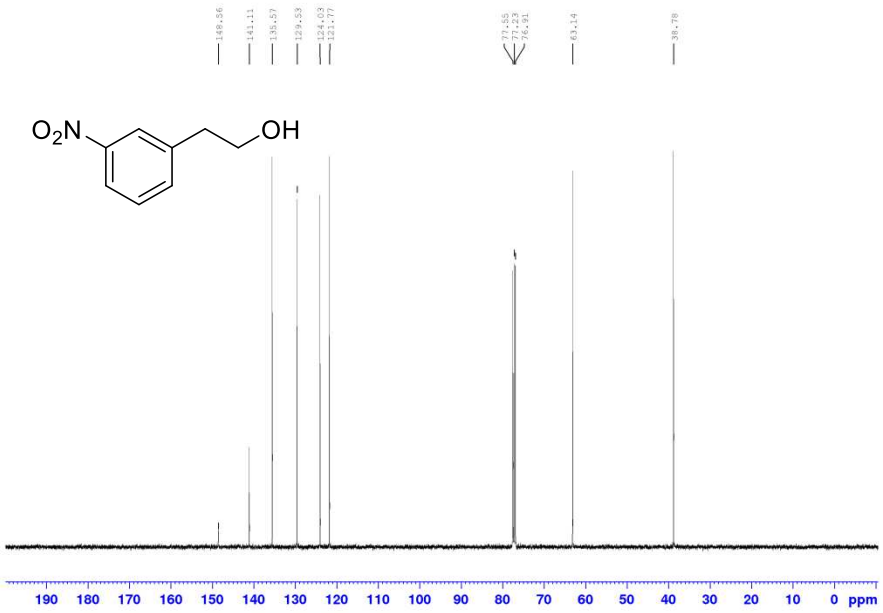

^{13}C NMR spectrum of **2-50** (101 MHz, $CDCl_3$)

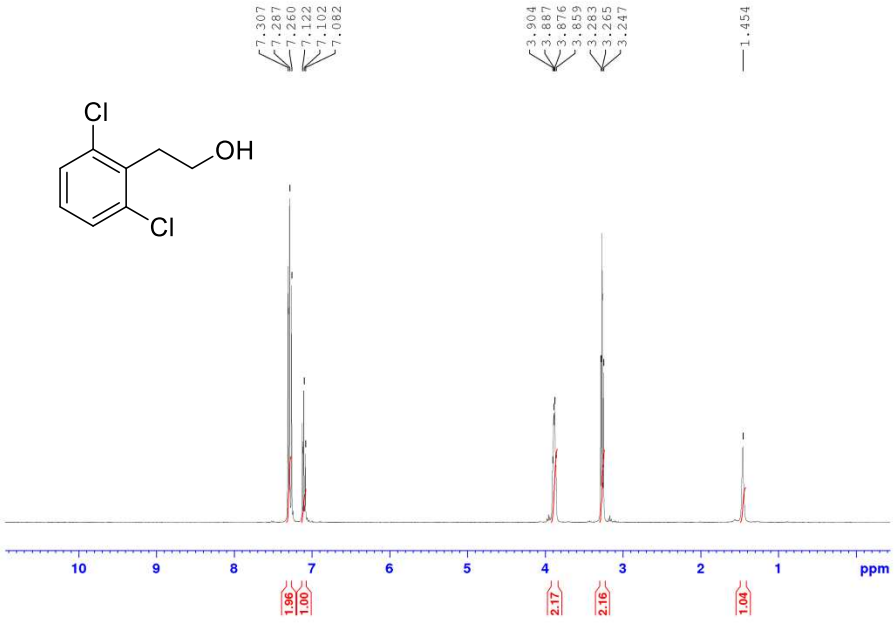

^{1}H NMR spectrum of **2-51** (400 MHz, $CDCl_3$)

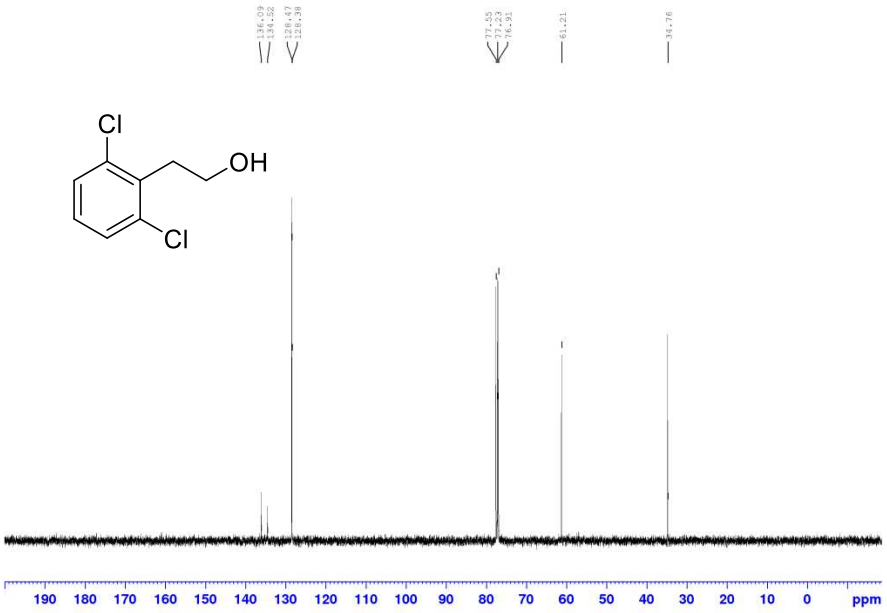

^{13}C NMR spectrum of **2-51** (101 MHz, $CDCl_3$)

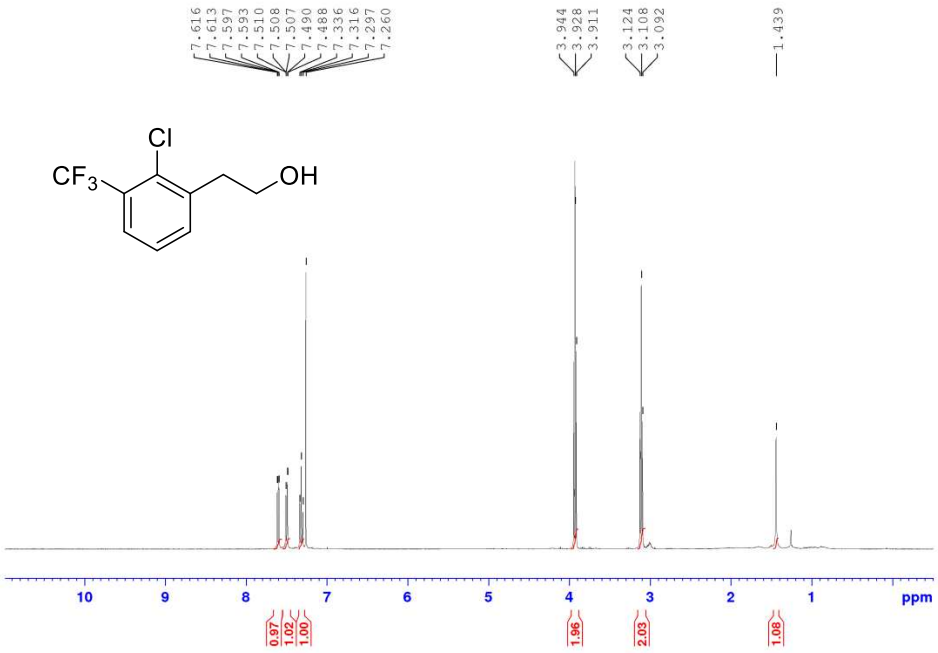

^{1}H NMR spectrum of **2-52** (400 MHz, $CDCl_3$)

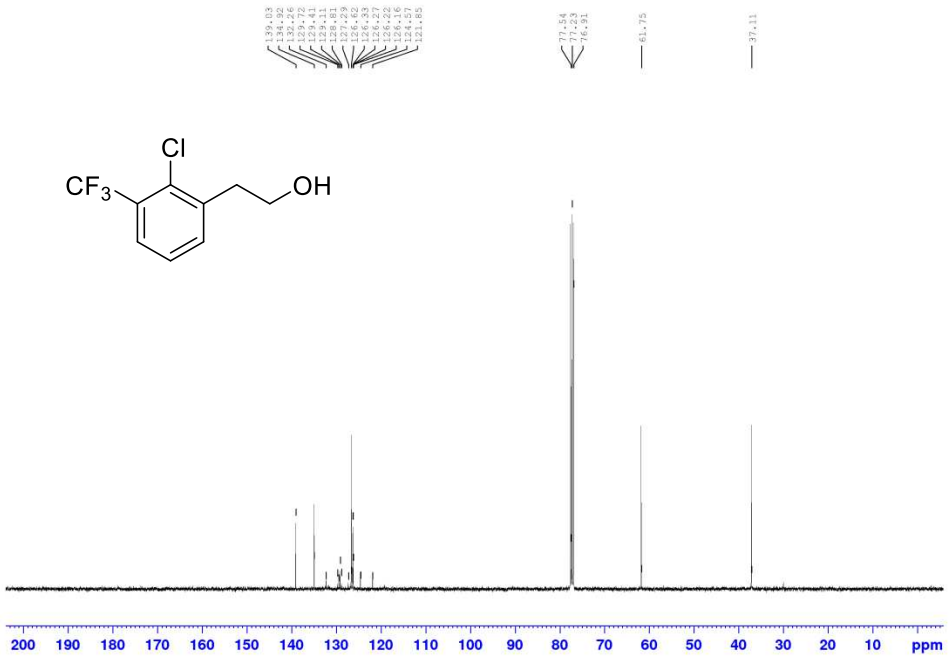

^{13}C NMR spectrum of **2-52** (101 MHz, $CDCl_3$)

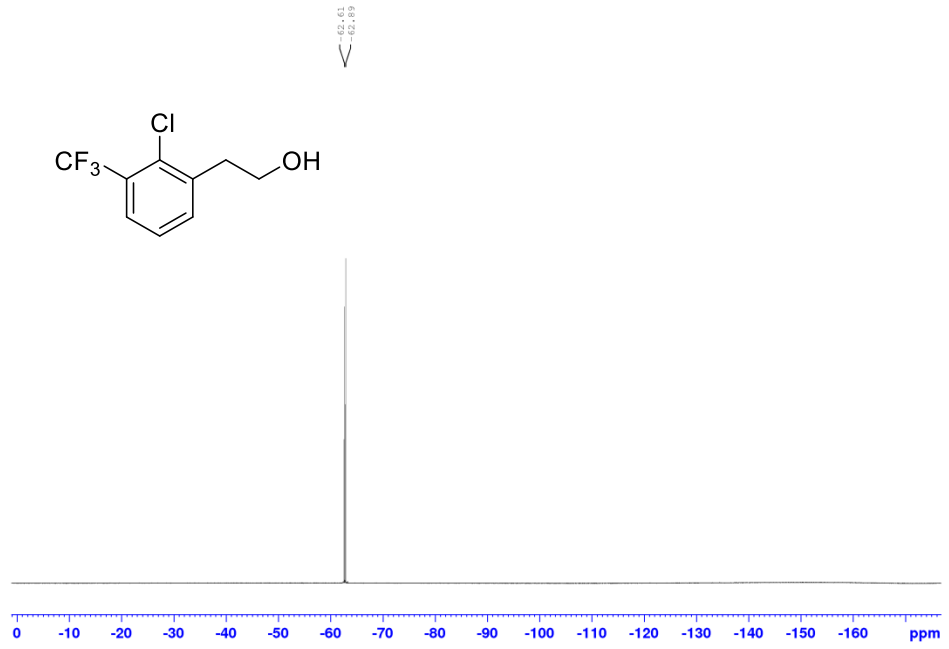

^{19}F NMR spectrum of **2-52** (377 MHz, $CDCl_3$, $PhCF_3$ internal standard set at -62.61 ppm)

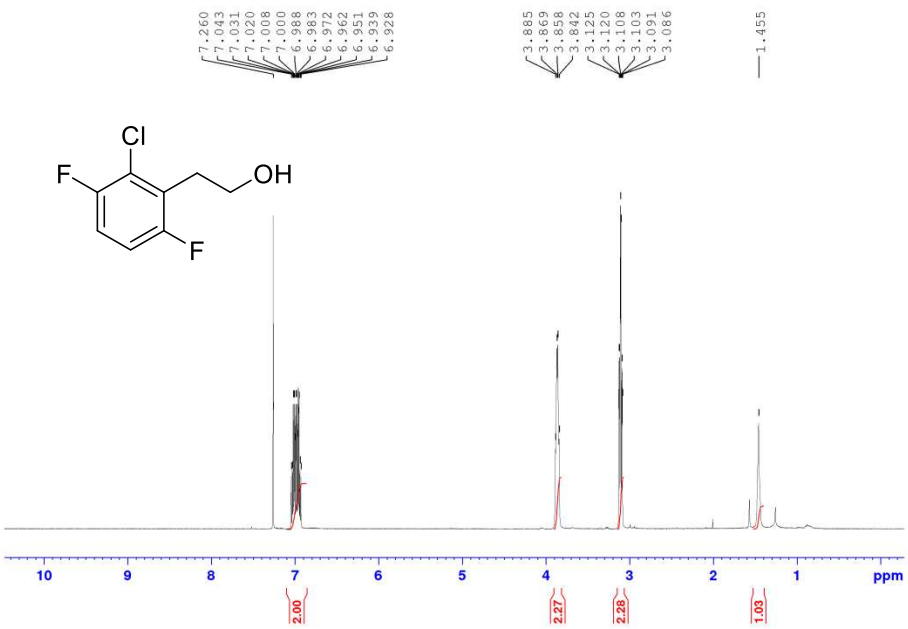

^{1}H NMR spectrum of **2-53** (400 MHz, $CDCl_3$)

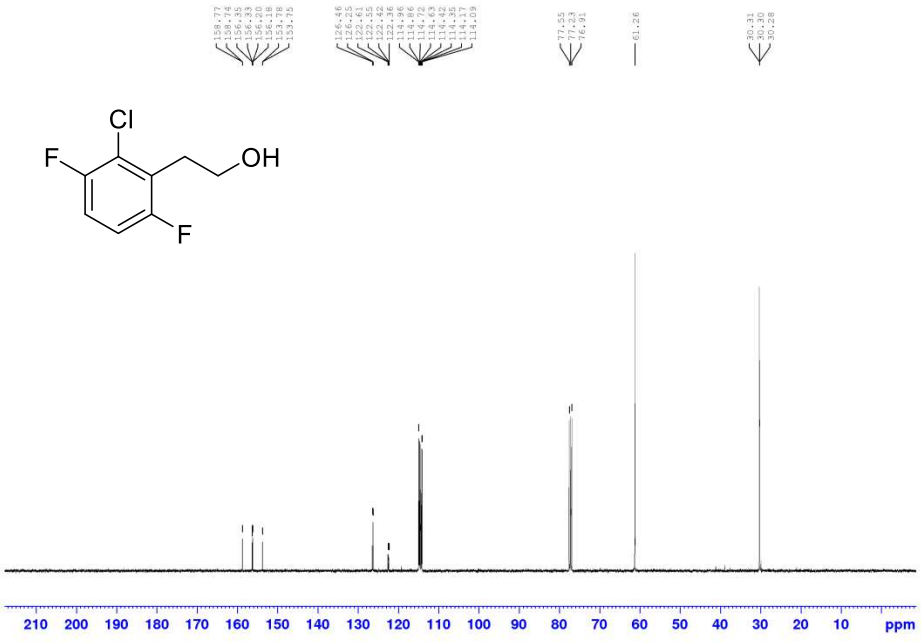

^{13}C NMR spectrum of **2-53** (101 MHz, $CDCl_3$)

^{19}F NMR spectrum of **2-53** (377 MHz, $CDCl_3$, $PhCF_3$ internal standard set at -62.61 ppm)

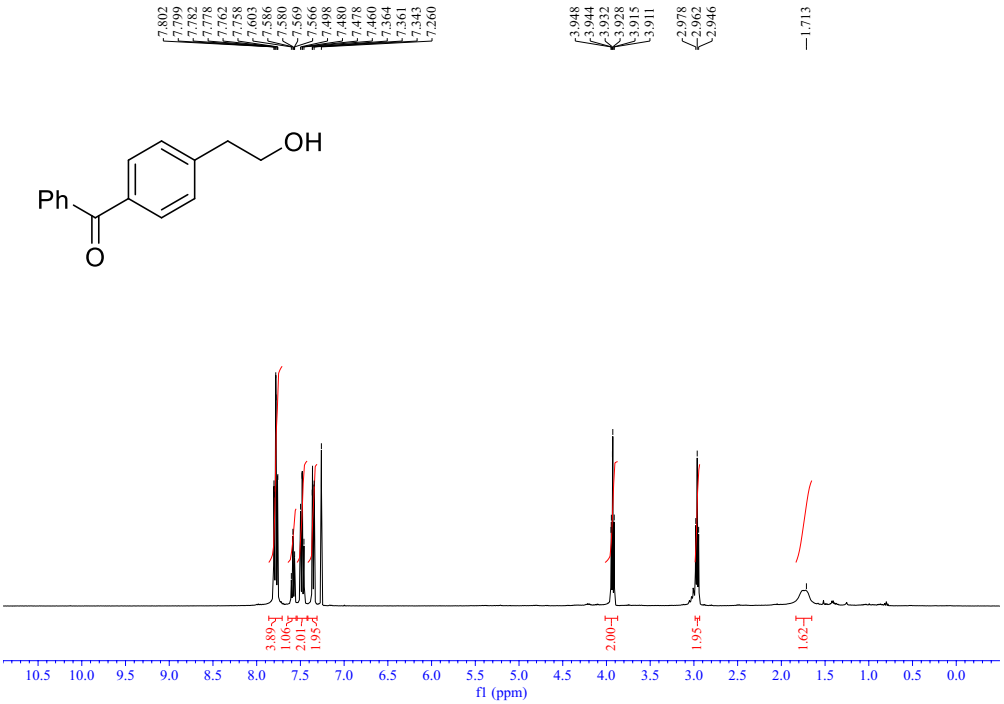

^{1}H NMR spectrum of **2-54** (400 MHz, $CDCl_3$)

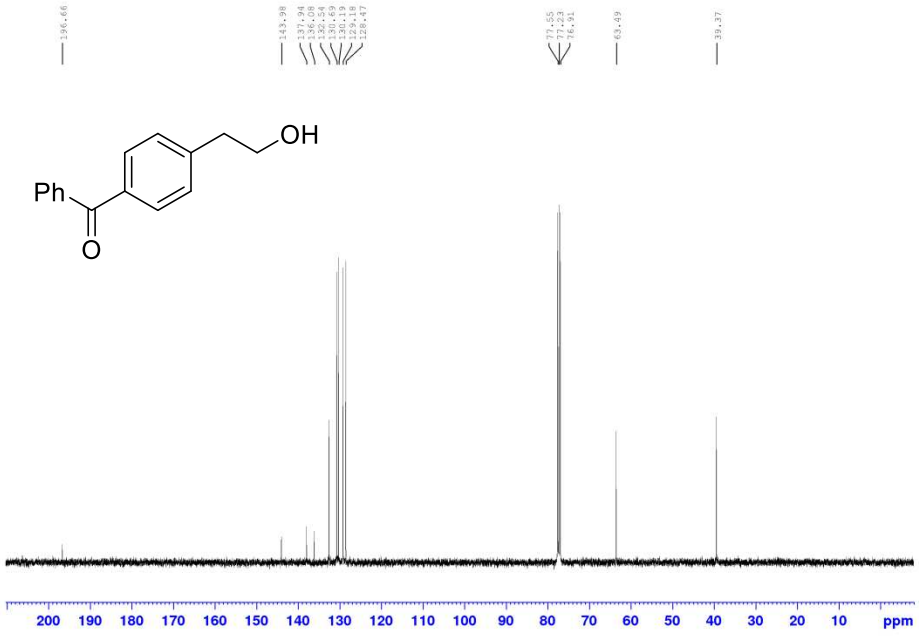

^{13}C NMR spectrum of **2-54** (101 MHz, $CDCl_3$)

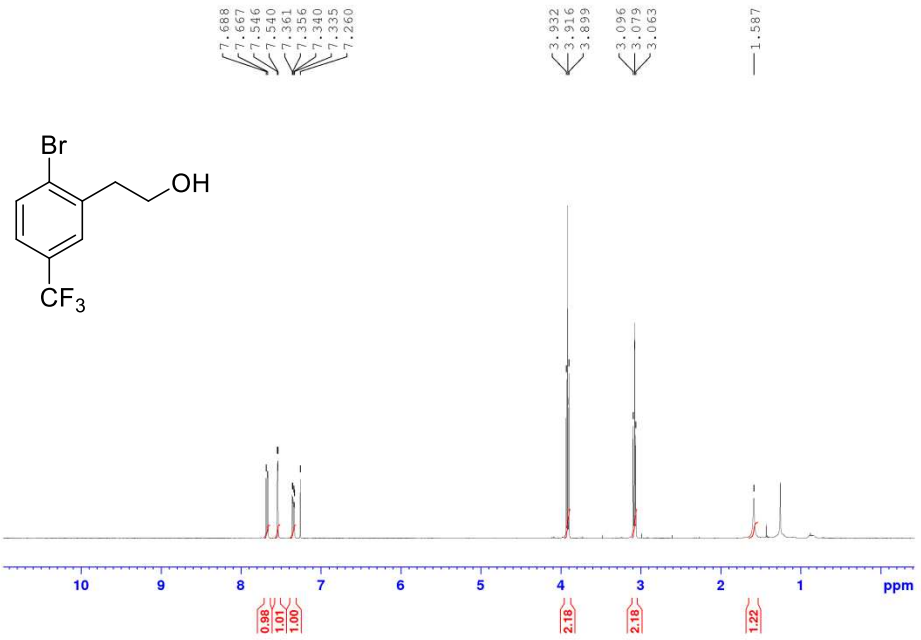

^{1}H NMR spectrum of **2-55** (400 MHz, $CDCl_3$)

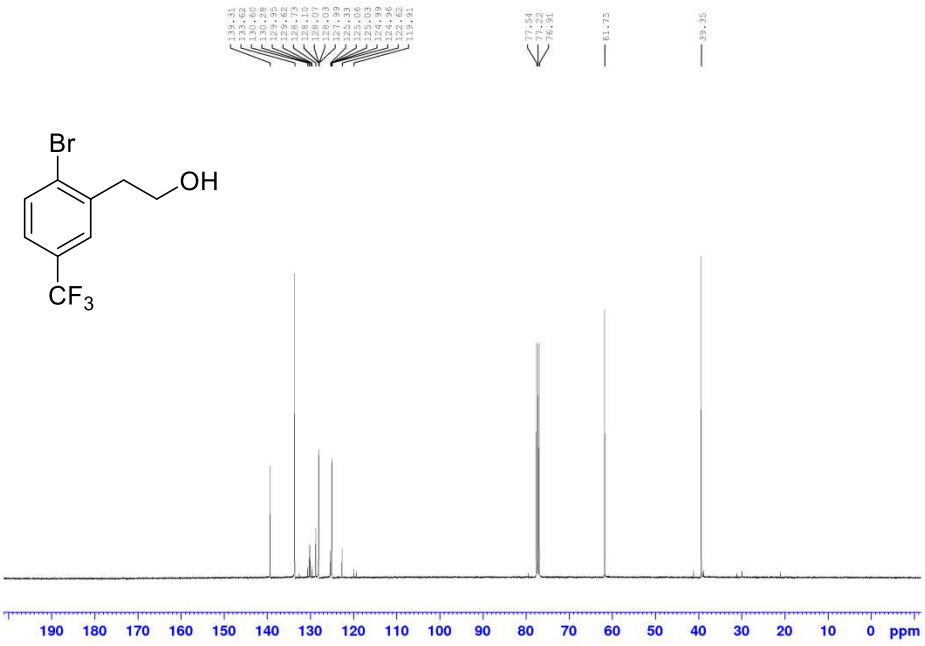

^{13}C NMR spectrum of **2-55** (101 MHz, $CDCl_3$)

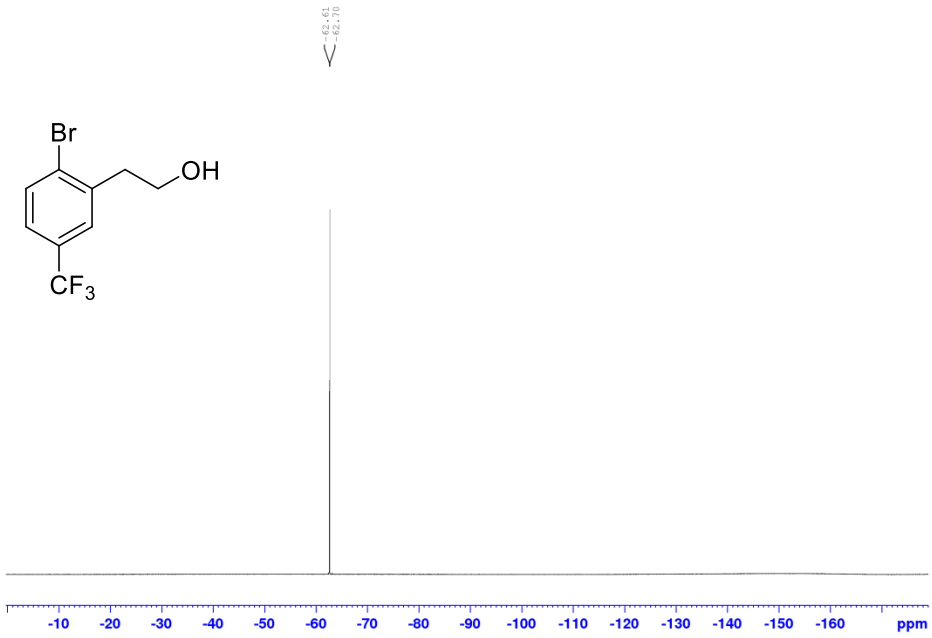

^{19}F NMR spectrum of **2-55** (377 MHz, $CDCl_3$, $PhCF_3$ internal standard set at -62.61 ppm)

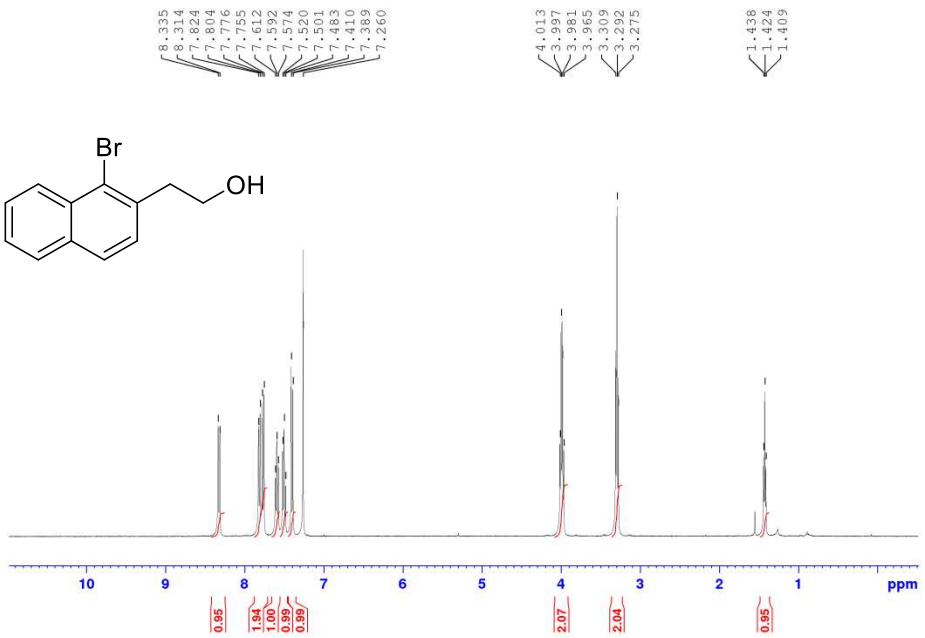

^{1}H NMR spectrum of **2-56** (400 MHz, $CDCl_3$)

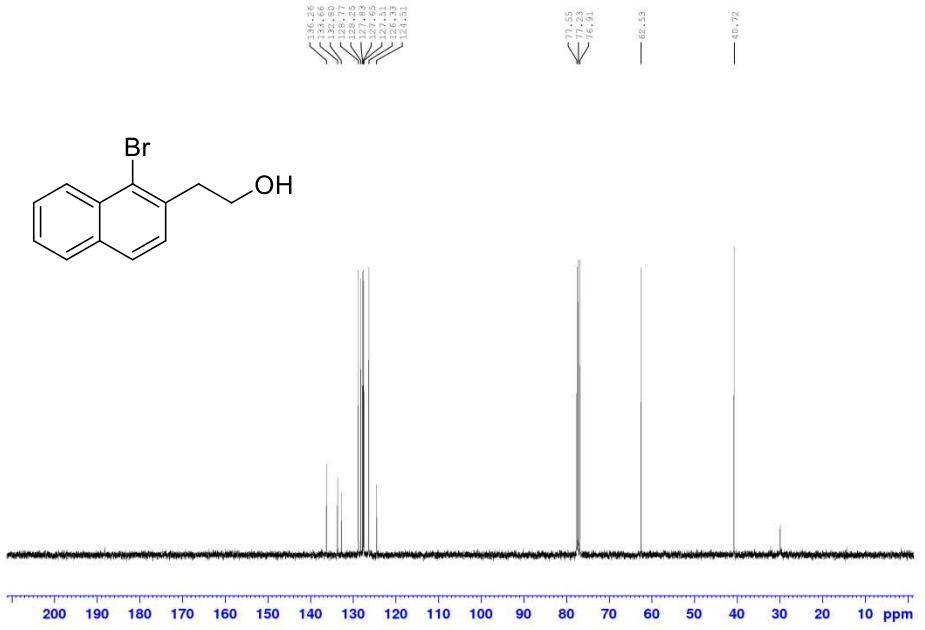

^{13}C NMR spectrum of **2-56** (101 MHz, $CDCl_3$)

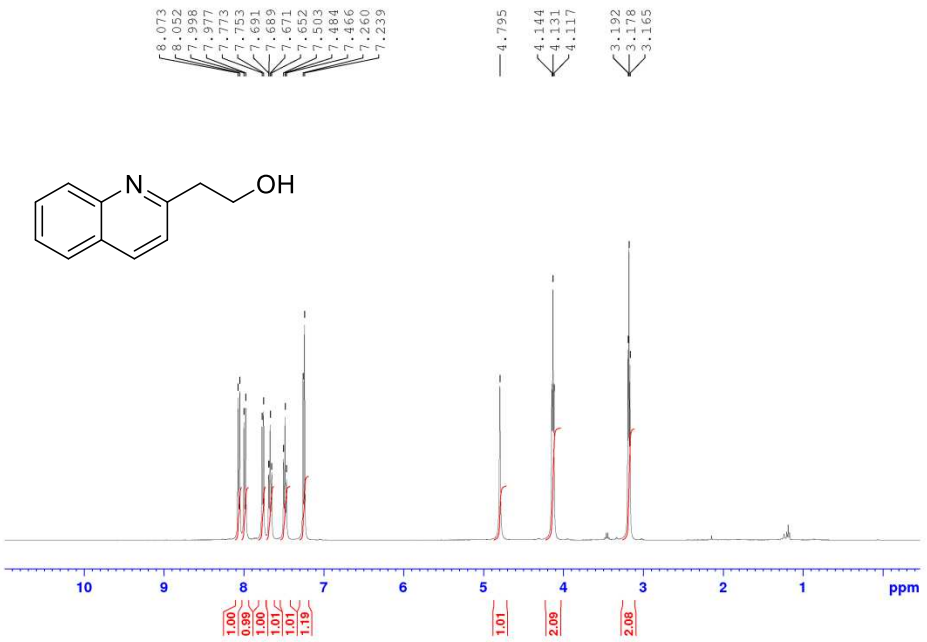

^{1}H NMR spectrum of **2-57** (400 MHz, $CDCl_3$)

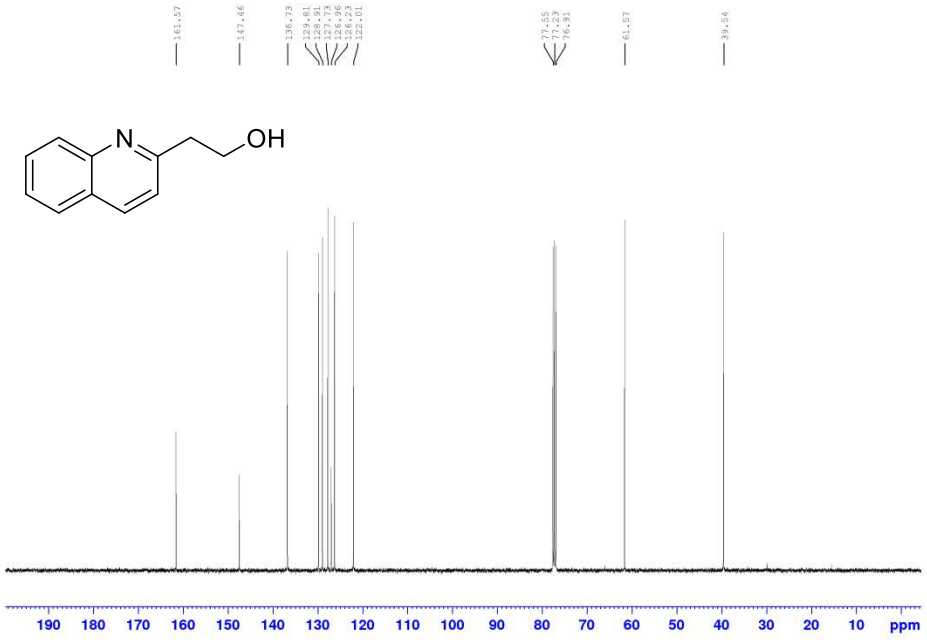

^{13}C NMR spectrum of **2-57** (101 MHz, $CDCl_3$)

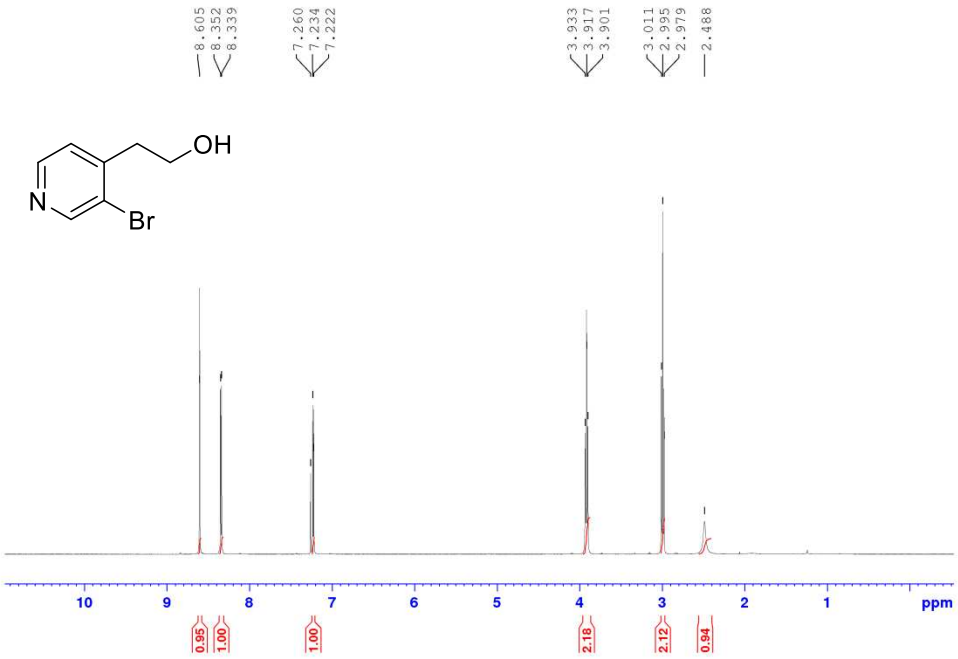

^{1}H NMR spectrum of **2-58** (400 MHz, $CDCl_3$)

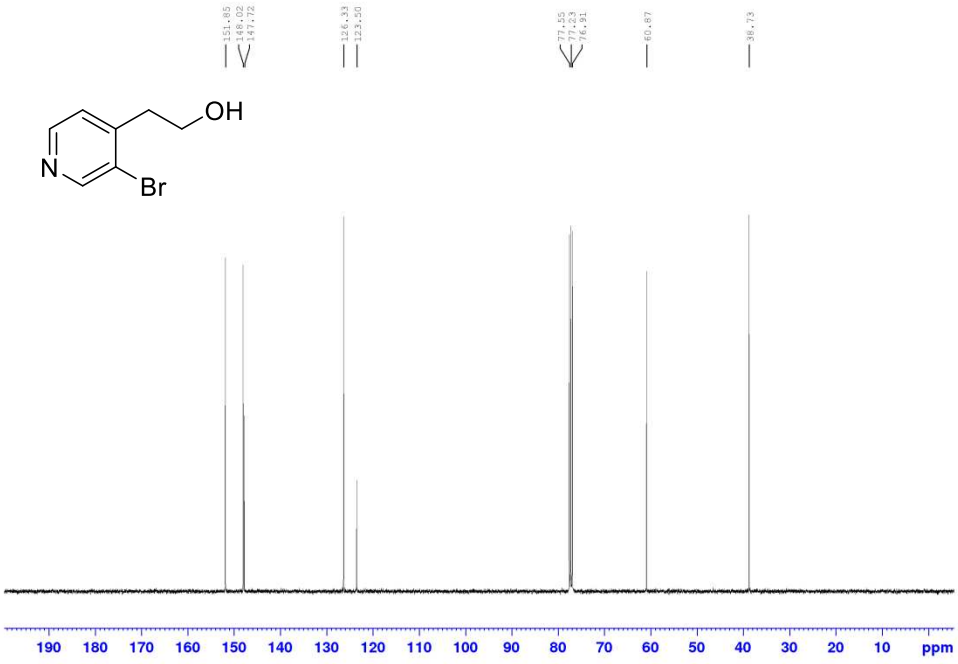

^{13}C NMR spectrum of **2-58** (101 MHz, $CDCl_3$)

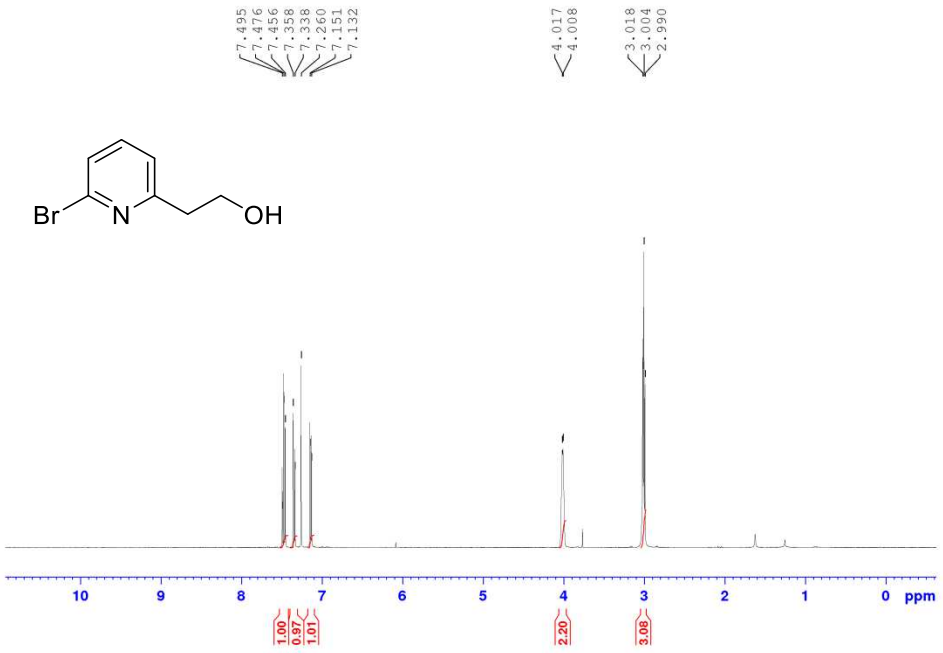

^{1}H NMR spectrum of **2-59** (400 MHz, $CDCl_3$)

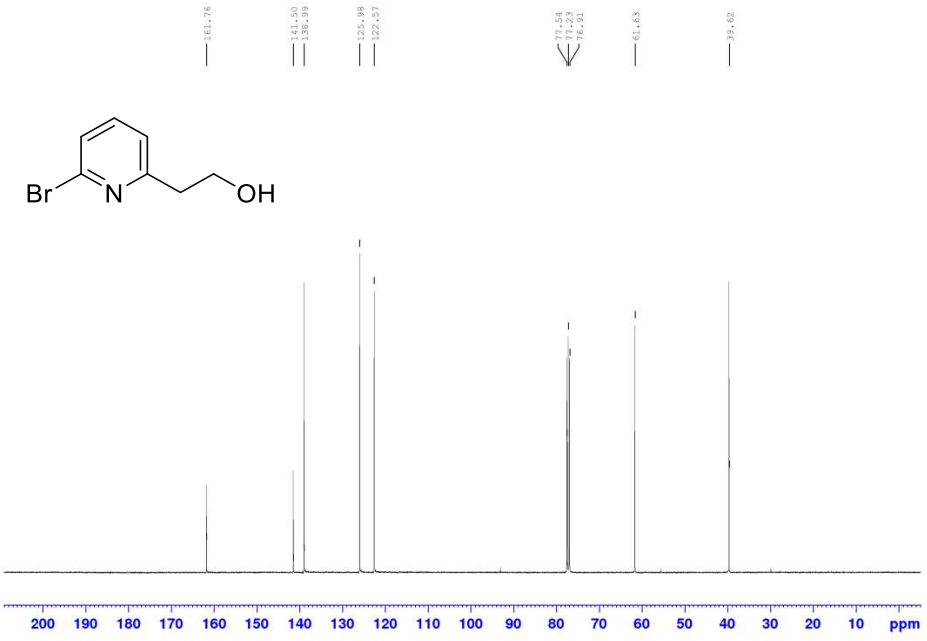

^{13}C NMR spectrum of **2-59** (101 MHz, $CDCl_3$)

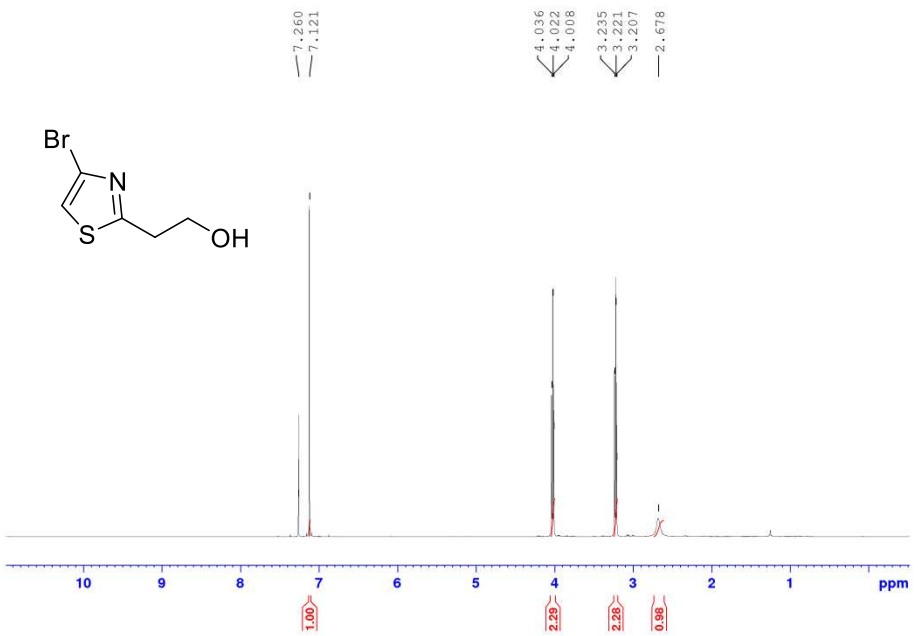

^{1}H NMR spectrum of **2-60** (400 MHz, $CDCl_3$)

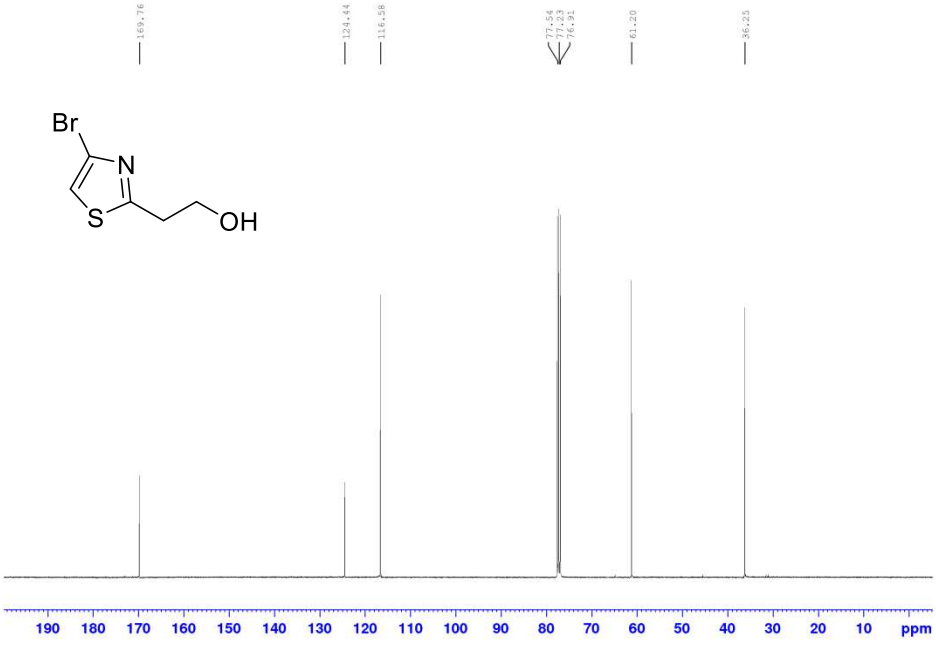

^{13}C NMR spectrum of **2-60** (101 MHz, $CDCl_3$)

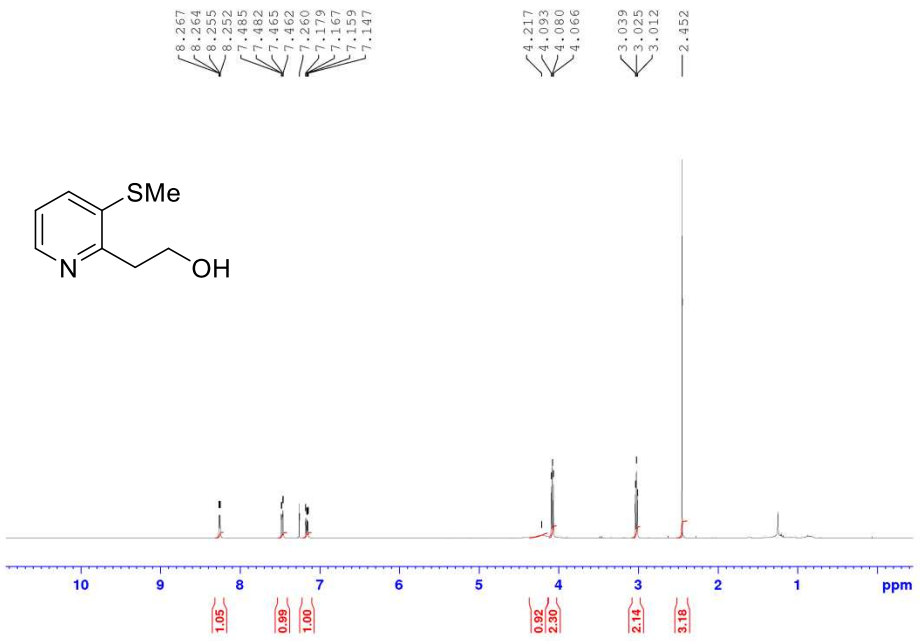

^{1}H NMR spectrum of **2-68** (400 MHz, $CDCl_3$)

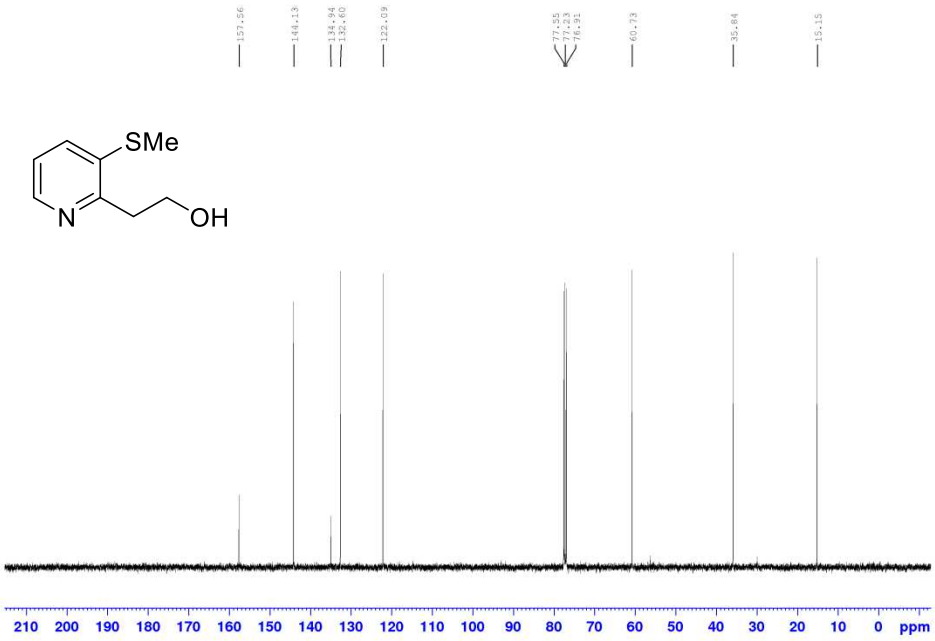

^{13}C NMR spectrum of **2-68** (101 MHz, $CDCl_3$)

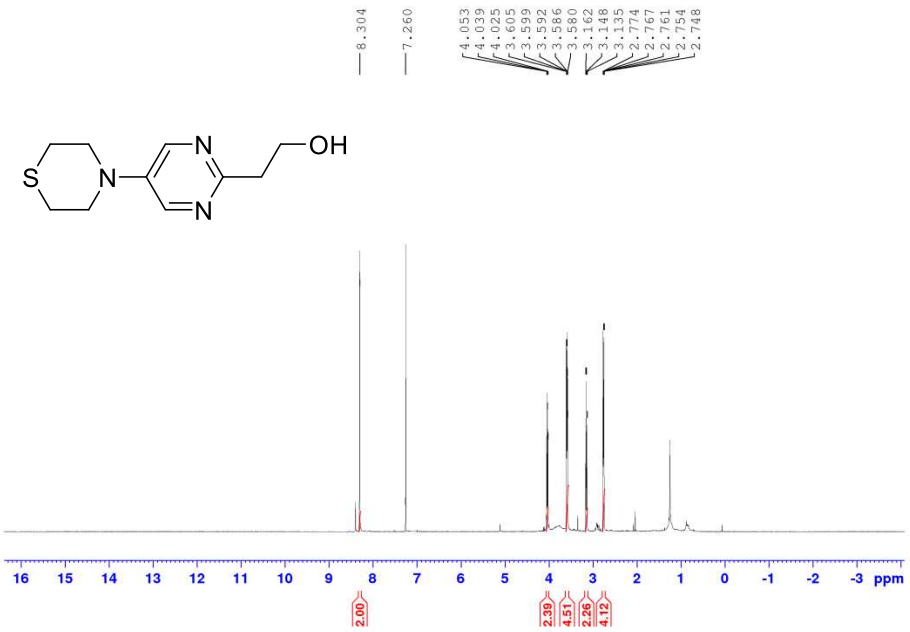

^{1}H NMR spectrum of **2-69** (400 MHz, $CDCl_3$)

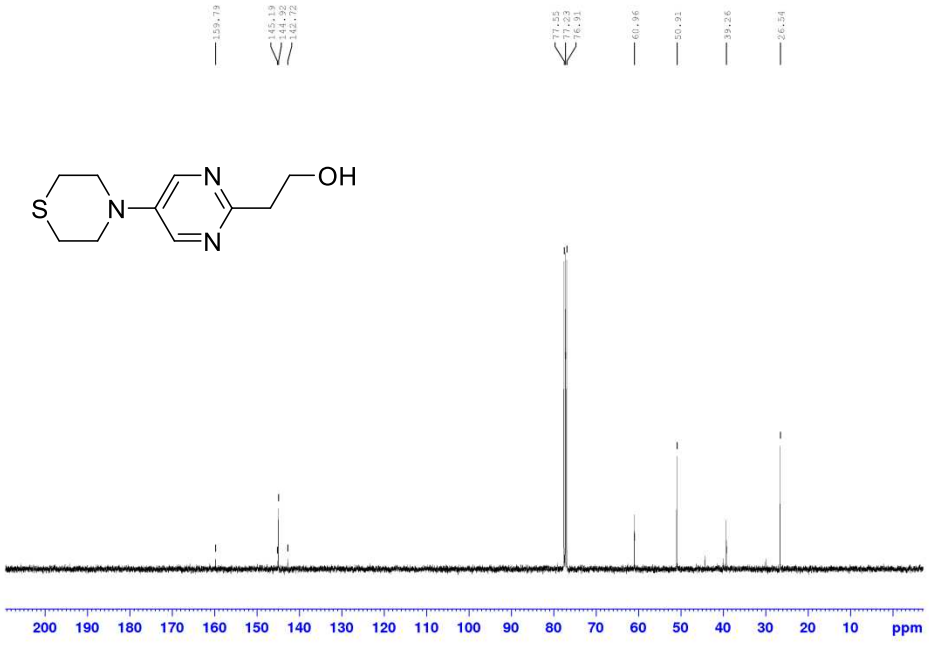

^{13}C NMR spectrum of **2-69** (101 MHz, $CDCl_3$)

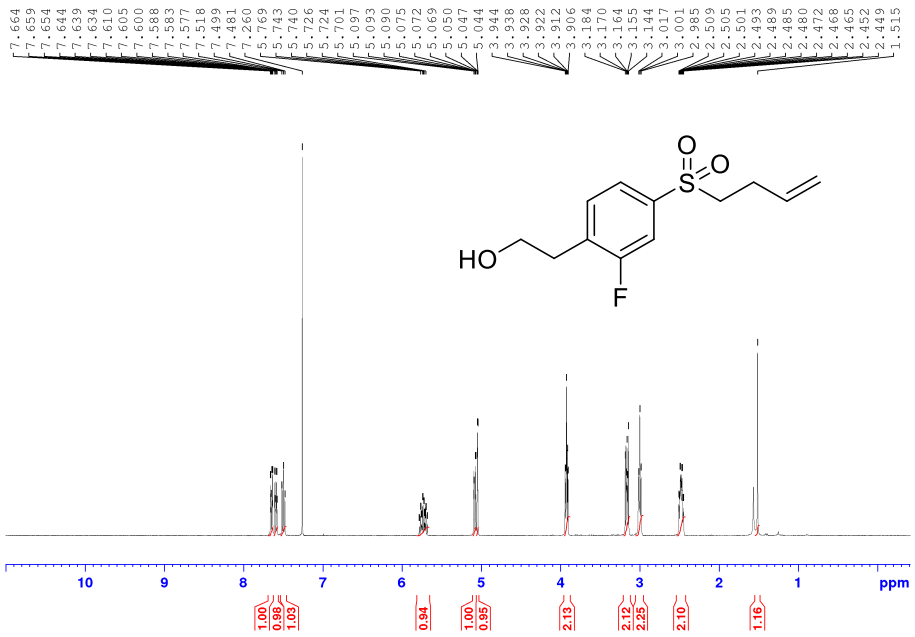

^{1}H NMR spectrum of **2-70** (400 MHz, $CDCl_3$)

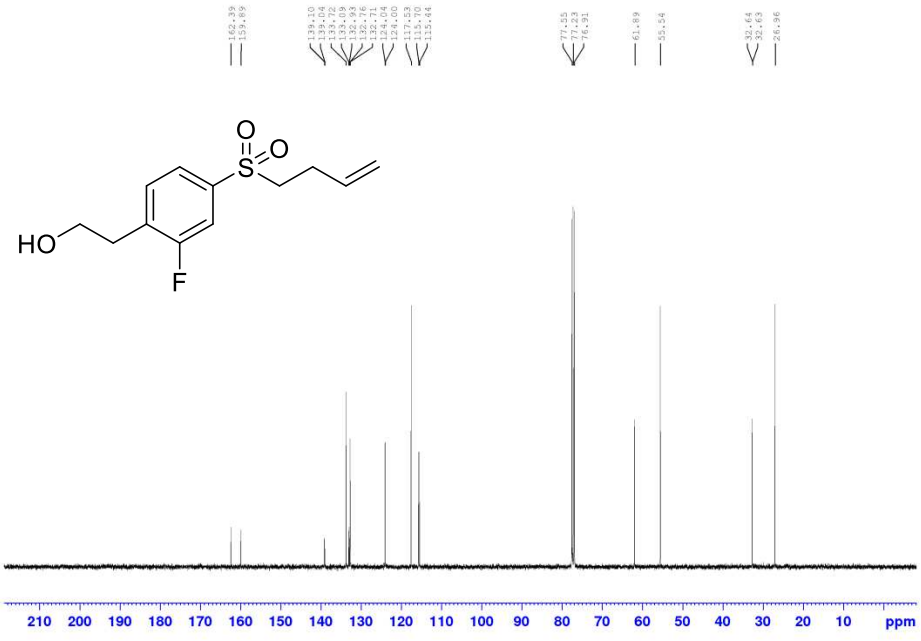

^{13}C NMR spectrum of **2-70** (101 MHz, $CDCl_3$)

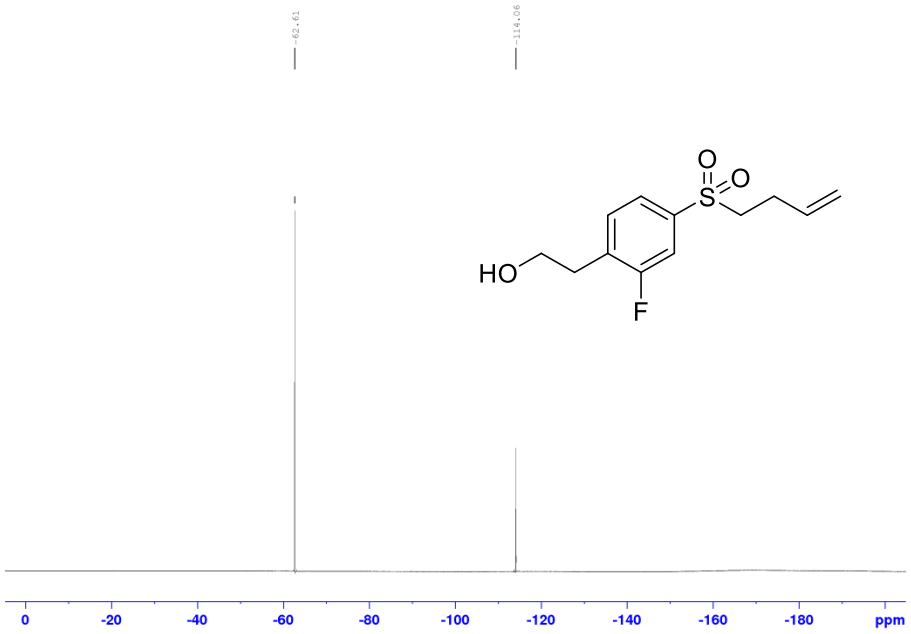

^{19}F NMR spectrum of **2-70** (377 MHz, $CDCl_3$, $PhCF_3$ internal standard set at -62.61 ppm)

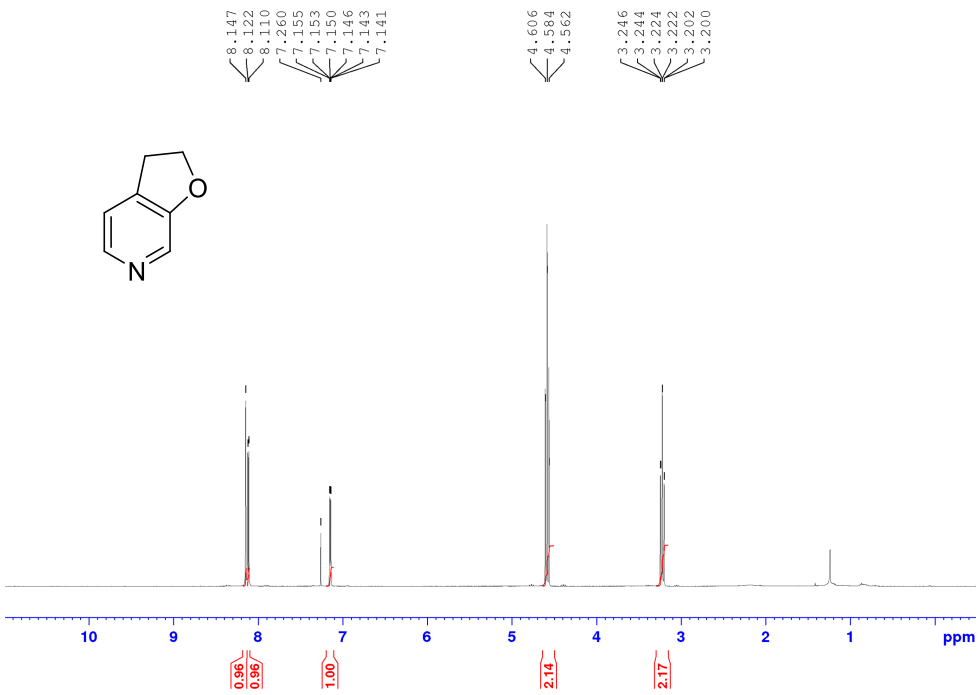

^{1}H NMR spectrum of **2-71** (400 MHz, $CDCl_3$)

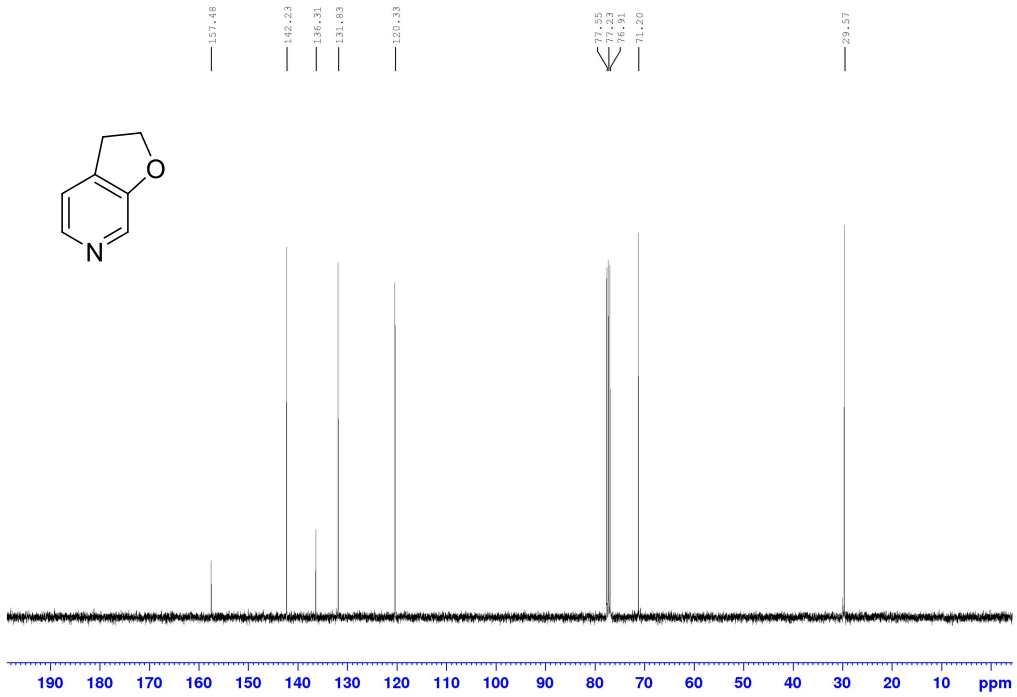

^{13}C NMR spectrum of **2-71** (101 MHz, $CDCl_3$)

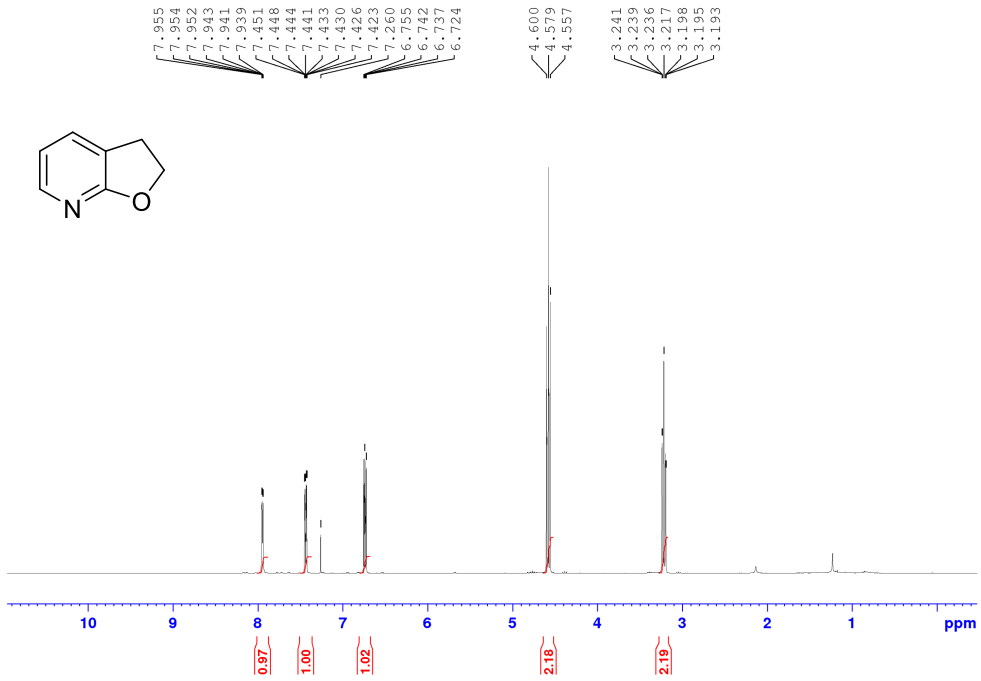

^{1}H NMR spectrum of **2-72** (400 MHz, $CDCl_3$)

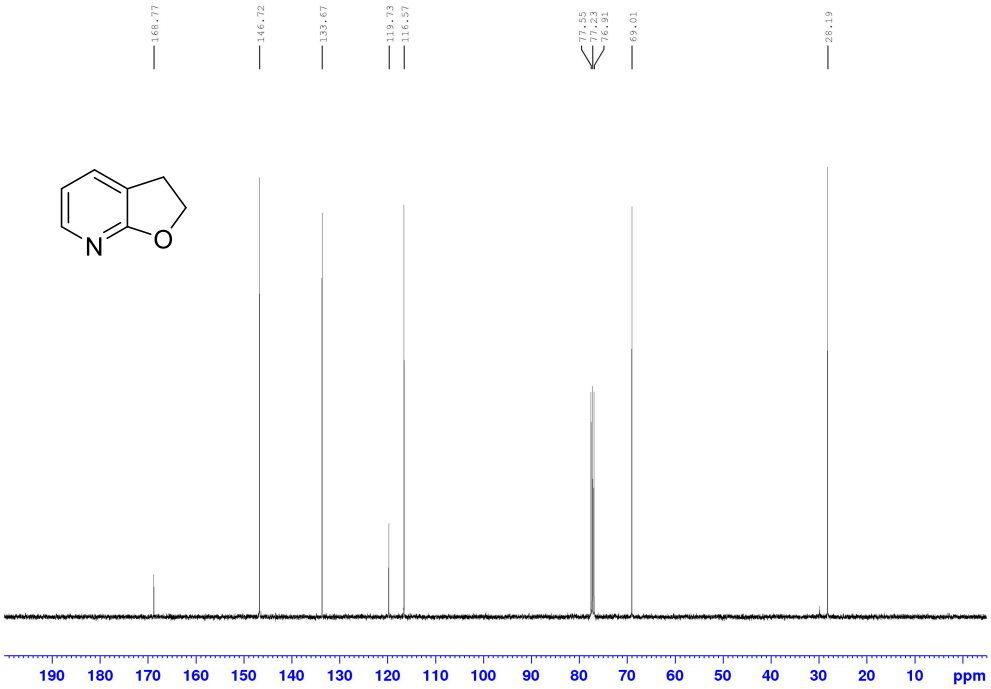

^{13}C NMR spectrum of **2-72** (101 MHz, $CDCl_3$)

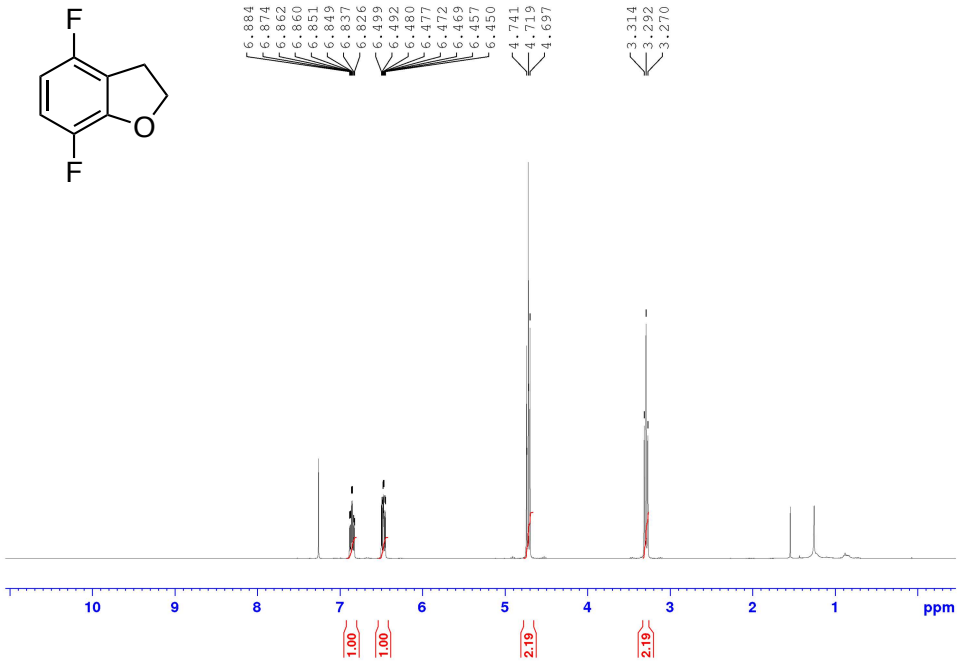

^{1}H NMR spectrum of **2-73** (400 MHz, $CDCl_3$)

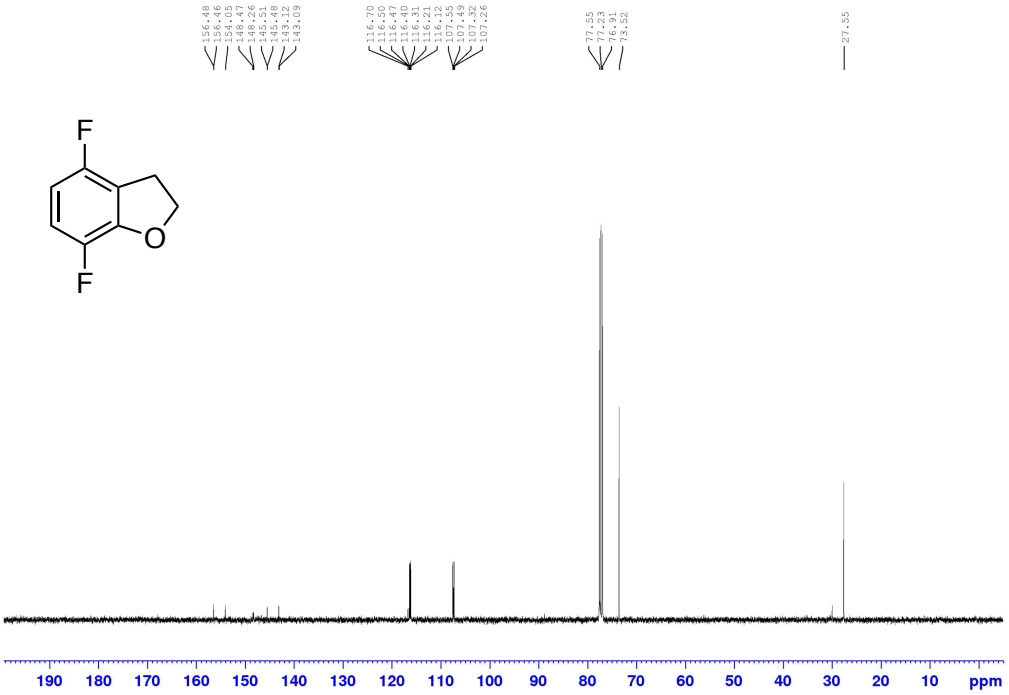

^{13}C NMR spectrum of **2-73** (101 MHz, $CDCl_3$)

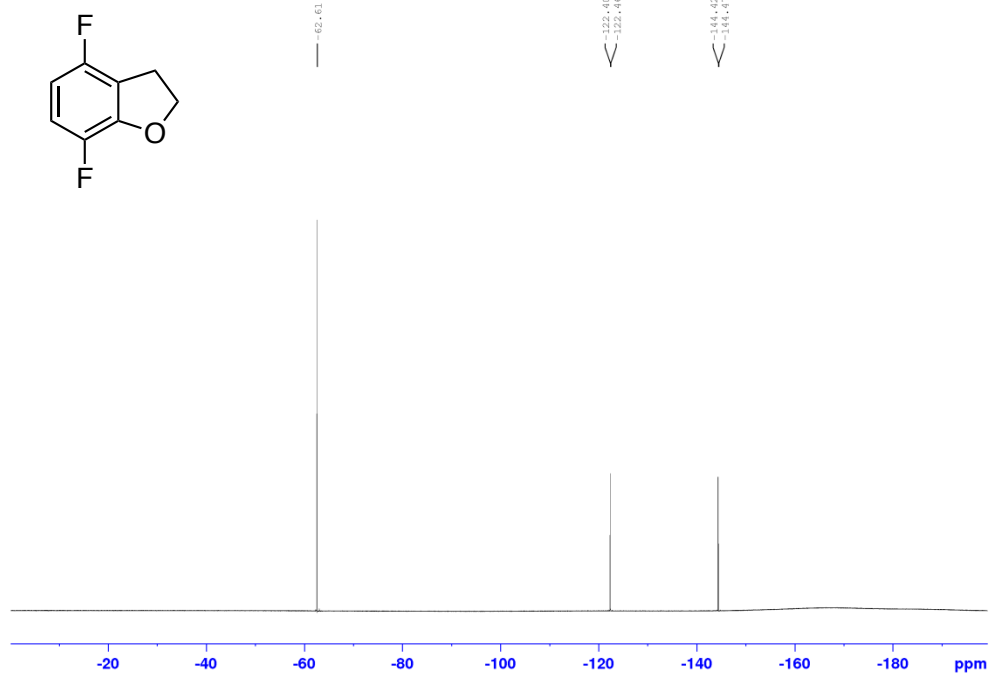

^{19}F NMR spectrum of **2-73** (377 MHz, $CDCl_3$, $PhCF_3$ internal standard set at -62.61 ppm)

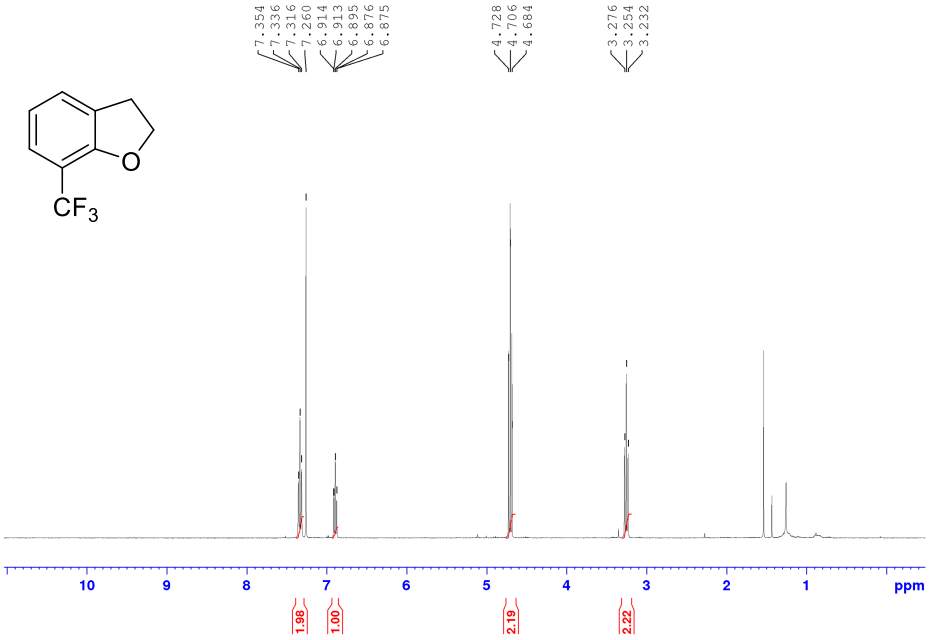

^{1}H NMR spectrum of **2-74** (400 MHz, $CDCl_3$)

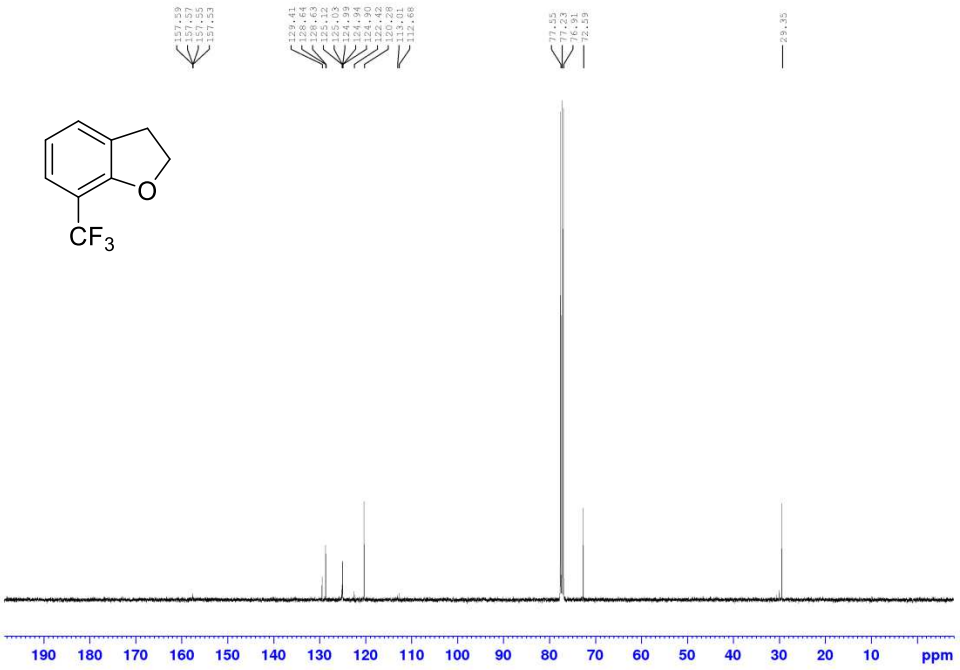

^{13}C NMR spectrum of **2-74** (101 MHz, $CDCl_3$)

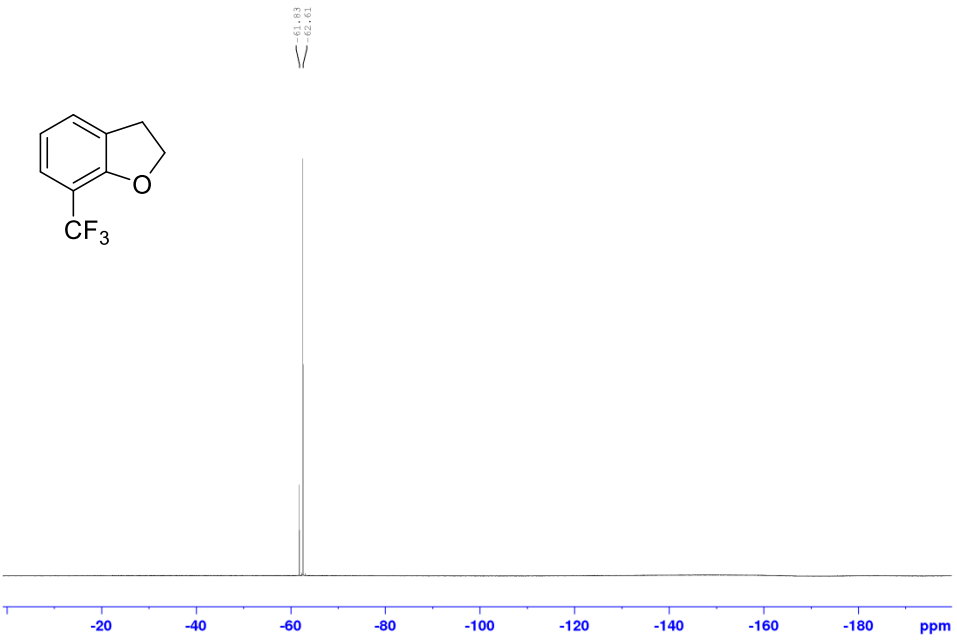

^{19}F NMR spectrum of **2-74** (377 MHz, $CDCl_3$, $PhCF_3$ internal standard set at -62.61 ppm)

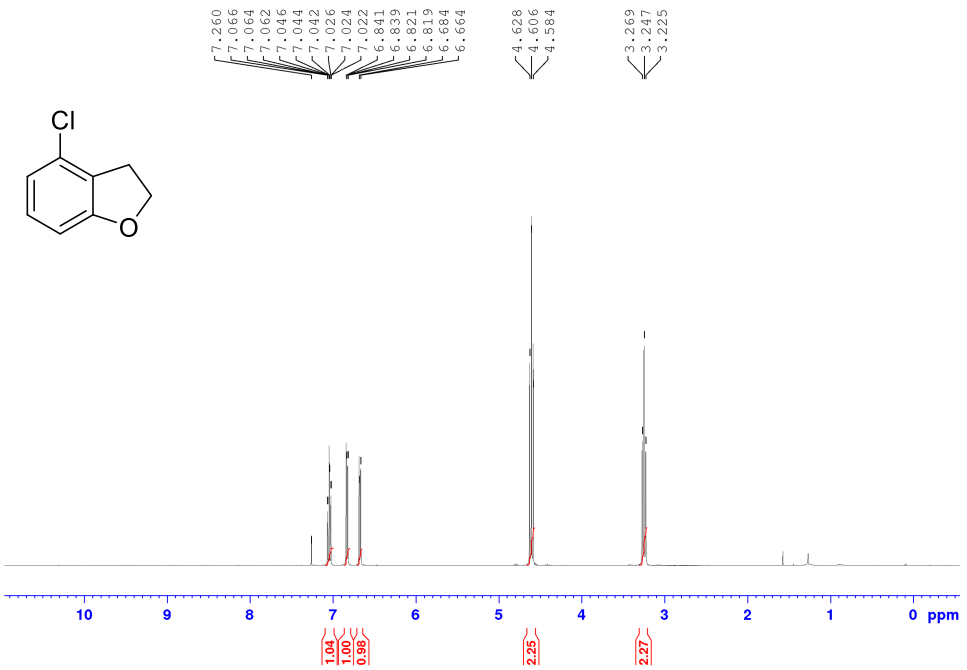

^{1}H NMR spectrum of **2-75** (400 MHz, $CDCl_3$)

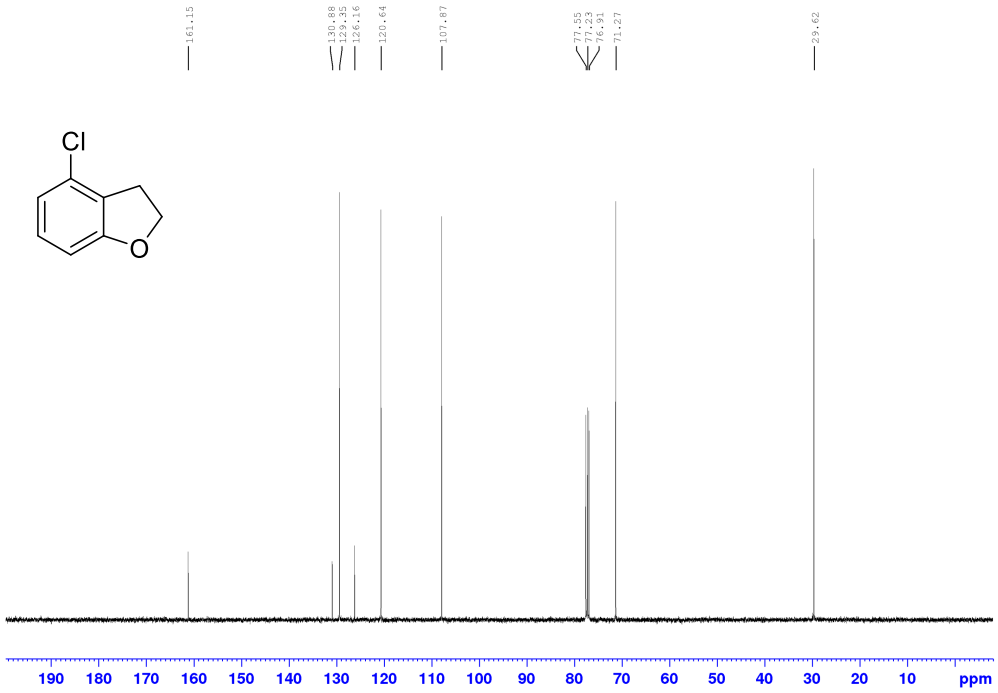

^{13}C NMR spectrum of **2-75** (101 MHz, $CDCl_3$)

APPENDIX THREE

CONTROLLABLE GENERATION OF ORGANIC SUPERBASES FROM PRECATALYST SALTS: EXPERIMENTAL

A3.1 General Information

This appendix is adapted from a manuscript in preparation, Controllable Generation of Organic Superbases from Precatalyst Salt. It is intended to provide experimental details and supporting information for the material discussed in Chapter 3. This Appendix contains data collected by Garrett and his contributions are outlined as needed throughout.

General Reagent Information: tert-Butylimino-tri(pyrrolidino)phosphorane and 1-*tert*-Butyl-2,2,4,4,4-pentakis(dimethylamino)-2λ^5,4 λ^5-catenadi(phosphazene) were purchased from Millipore Sigma (product #XX and XX respectively) and were stored in a -30 °C freezer inside a nitrogen-filled glovebox. Before use, the superbases were allowed to warm to room temperature and homogenize if any solid was evident. Tetrahydrofuran and toluene were deoxygenated and dried by passage over packed columns of neutral alumina and copper (II) oxide under positive pressure of nitrogen. Potassium tert-butoxide (KO-t-Bu) from Chem-Impex (product number #27317) was used as purchased and stored inside a nitrogen-filled glovebox. Methyltriphenylphosphonium bromide was purchased from CombiBlocks (product #QA-8732) and used as received. The following solvents were purchased anhydrous from Millipore Sigma and used as received: dimethyl sulfoxide (#276855), N,N-dimethylformamide (#227056), N-methyl-2-pyrrolidone (#328634), benzonitrile (#294098), 1,4-dioxane (#296309), 1,2-dimethoxyethane (#259527), All other reagents were purchased from Millipore Sigma, Combi-

Blocks, TCI, Acros Organics, Matrix, or Alfa Aesar and used as received unless otherwise noted. Flash Chromatography was performed on 40-63 μm silica gel (SiliaFlash® F60 from Silicycle).

General Analytical Information: All new compounds were characterized by ^{1}H, ^{13}C, ^{19}F and ^{31}P (as appropriate) NMR spectroscopy, FTIR spectroscopy, mass spectrometry, melting point analysis (if solid) and specific rotation analysis (if chiral). ^{1}H NMR, ^{13}C NMR, ^{19}F NMR, and ^{31}P NMR spectra were obtained on a Bruker Advanced NEO or Varian Inova 400 MHz spectrometer. Gel permeation chromatography (GPC) was used to analyze number (M_n) and weight (M_w) average molecular weights and dispersity index of polymers. ^{1}H NMR data is reported as follows: chemical shift (δ ppm), multiplicity (s = singlet, d = doublet, t = triplet, q = quartet, dd = doublet of doublets, td = triplet of doublets, m = multiplet), coupling constant (Hz), and integration. ^{13}C NMR data is reported as follows: chemical shift (δ ppm), multiplicity (if applicable, q = quartet, T = 1:1:1 multiplicity). ^{31}P NMR data is reported as follows: chemical shift (δ ppm), multiplicity (if applicable, q = quartet, T = 1:1:1 multiplicity). All ^{1}H NMR signals are reported as chemical shifts (δ ppm) relative to residual $CHCl_3$ at 7.26 ppm and ^{13}C NMR signals are reported as chemical shifts (δ ppm) relative to $CDCl_3$ at 77.16 ppm. Thin-layer chromatography analysis was performed on silica gel 60Å F254 plates (250 μm, SiliaPlate from Silicycle, #TLGR10014B-323) and interpreted using UV light (254 nm) or $KMnO_4$ stain. **Note on nomenclature**: The names provided for the structures below were obtained from ChemDraw Professional 16.0.

A3.2 P_1-*t*-Bu and P_2-*t*-Bu Superbase Salt Syntheses

A3.2.1 Identification of a crystalline carboxylate salt for P_1-*t*-Bu

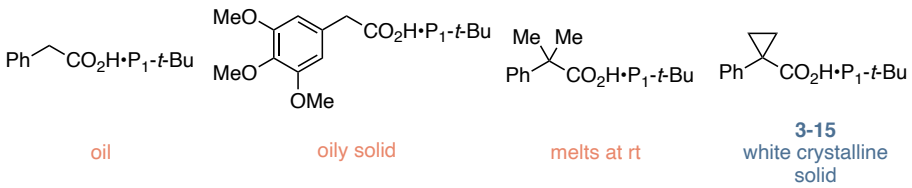

Figure A3-1: P_1-*t*-Bu•carboxylate salts prepared to identify a solid salt.

We investigated a series of carboxylic acids that would form a solid, shelf stable salt with the protonated superbase. We conducted our investigation with a series of phenylacetic acids (Figure A3-1), as they have good potential to form crystalline salts. Pleasingly, we were able to find that 1-phenyl-1-cyclopropanecarboxylic acid formed a stable salt with P_1-*t*-Bu.

General Procedure: An oven-dried 1 dram vial (ThermoFisher, C4015-1) was charged with a magnetic stir bar, carboxylic acid (0.25 mmol, 1 equiv). In a nitrogen filled glovebox diethyl ether (0.5 mL, 0.5 M) and P_1-*t*-Bu (78.1 mg, 0.25 mmol, 1 equiv) were added to the vial. The vial was capped with a PTFE lined cap (ThermoFisher, C4015-1A), and removed from the glovebox and stirred for 2 h at 25 °C. The solutions were concentrated *in vacuo*, then placed under high vacuum for drying. The physical state of each salt was then evaluated visually and with agitation using a spatula.

A3.2.2 Synthesis of P_1-*t*-Bu Salt 3-15 from freebase

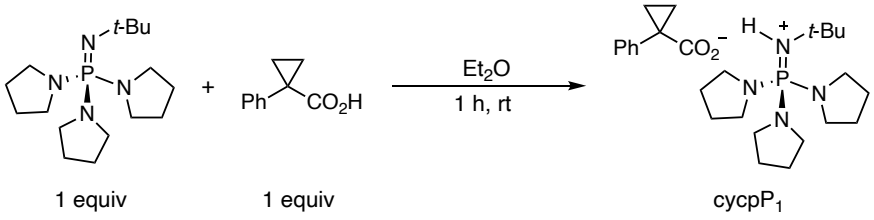

General Procedure: An oven-dried 250 mL round bottom flask was charged with a magnetic stir bar, 1-phenyl-1-cyclopropanecarboxylic acid (811.0 mg, 5 mmol, 1 equiv) and diethyl ether (10 mL, 0.5 M). In a nitrogen filled glovebox an oven-dried 20 mL scintillation vial (ThermoFisher, 03-341-25D) was charged with P_1-*t*-Bu (1.562 g, 5 mmol, 1 equiv) and diluted with dry diethyl ether (10 mL). The vial was capped and removed from the glovebox. The vial containing P_1-*t*-Bu, protected from air by diethyl ether, was uncapped and added slowly to the stirring solution of 1-

Phenyl-1-cyclopropanecarboxylic acid. The reaction solution was stirred for 1 hour at room temperature. The reaction solution was concentrated and the resulting crystalline solid was washed with cold diethyl ether, dried in vacuo, and collected as a white powder (2.01 g, 4.24 mmol, 85 % yield). **^{1}H NMR** (400 MHz, $CDCl_3$) δ 7.84 (d, J = 10.2 Hz, 1H), 7.33 (d, J = 7.5 Hz, 2H), 7.10 (t, J = 7.5 Hz, 2H), 7.03 – 6.94 (m, 1H), 3.17 – 3.08 (m, 12H), 1.83 – 1.71 (m, 12H), 1.36 (q, J = 3.2 Hz, 2H), 1.23 (s, 8H), 0.74 (q, J = 3.2 Hz, 2H).; **^{31}P NMR** (162 MHz, $CDCl_3$) δ 22.5 (s); **^{13}C NMR** (101 MHz, $CDCl_3$) δ 177.23, 146.13, 130.42, 127.07, 124.60, 51.97 (d, J = 2.0 Hz), 47.37 (d, J = 5.1 Hz), 31.70, 31.31 (d, J = 4.9 Hz), 26.04 (d, J = 8.0 Hz), 14.11.; **IR (neat):** 2962.90, 2861.66, 2812.18, 1585.40, 1442.74, 1343.22, 1198.60, 1065.3, 984.39, 740.71 cm^{-1}; **HRMS (DART)** $[M+H]^+$ calcd. for $[C_{12}H_{34}N_7P]^+$ = 313.2516, found 313.2533

A3.2.3 Synthesis of salt 3-13 from simple starting materials

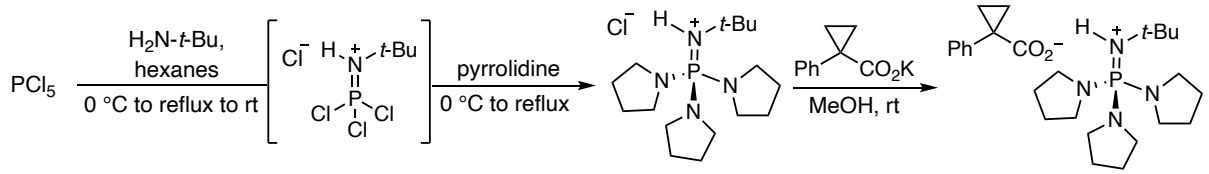

tert-Butyliminotri(pyrrolidino)phosphorane • hydrogen chloride (1-2): Phosphorus pentachloride and *tert*-butylphosphorimidoyl trichloride are air and moisture sensitive, care was taken to exclude ambient air and moisture for the following procedure. In a nitrogen filled glovebox an oven-dried 1000 mL round bottom flask was charged with a magnetic stir bar and PCl_5 (15.62 g, 75 mmol, 1 equiv). The flask was capped with a rubber septum, removed from the glovebox and connected to a nitrogen flushed reflux condenser with a positive pressure of nitrogen. Hexanes (250 mL, 0.2 M) was added *via* a nitrogen flushed syringe. The solution was cooled to 0 °C in an ice bath with stirring and *tert*-butylamine (24.43 mL, 232.5 mmol, 3.1 equiv) was added dropwise *via* a nitrogen flushed syringe. The reaction solution was stirred for 30 min at 0 °C. The solution was warmed to room temperature, placed in an oil bath and refluxed at 70 °C for 2 h. The reaction was removed from the oil bath, cooled to room temperature, and then cooled to 0 °C in

an ice bath. Pyrrolidine (43.12 mL, 525.0 mmol, 7 equiv) was added *via* a nitrogen flushed syringe and stirred for 30 min at 0 °C. The solution was warmed to room temperature, placed in an oil bath and refluxed at 70 °C for 2 h. The reaction was removed from the oil bath and cooled to room temperature. Water (400 mL) was added and the solution was transferred to a separatory funnel, then washed with ethyl acetate (2x 200 mL). The aqueous layer was then extracted with dichloromethane (3x 150 mL). The combined dichloromethane layers were washed with brine (150 mL), dried over Na_2SO_4, then concentrated *in vacuo* to yield. **^{1}H NMR** (400 MHz, $CDCl_3$) δ 6.51 (d, J = 9.5 Hz, 1H), 3.28 – 3.19 (m, 12H), 1.88 – 1.79 (m, 12H), 1.31 (s, 9H); **^{31}P NMR** (162 MHz, $CDCl_3$) δ 22.3 (s); **^{13}C NMR** (101 MHz, $CDCl_3$) δ 52.48 (d, J = 2.0 Hz), 47.68 (d, J = 5.1 Hz), 31.49 (d, J = 4.6 Hz), 26.11 (d, J = 8.1 Hz). **Anion metathesis with P_1-*t*-Bu•HCl and potassium 1-phenyl-1-cyclopropanecarboxylate to form salt 3-15**: An oven-dried 250 mL round bottom flask was charged with a magnetic stir bar, all P_1-*t*-Bu•HCl crude from above, and MeOH (100 mL). Potassium 1-phenyl-1-cyclopropanecarboxylate (18.78 g, 93.75 mmol, 1.25 equiv) was added. The solution was stirred at room temperature for 2 h. The methanol was then removed *in vacuo*. Ethyl acetate was then used to filter the pale yellow solid with vacuum filtration. The ethyl acetate solution was then concentrated and dried *in vacuo*. The yellow oil solidified under vacuum drying. The solid was then recrystallized from a minimal amount of hot ethyl acetate with hexanes layered on top to yield salt **3-15** (21.66 g, 45.64 mmol, 61% yield) as a colorless crystals. **^{1}H NMR** (400 MHz, $CDCl_3$) δ 7.84 (d, J = 10.2 Hz, 1H), 7.33 (d, J = 7.5 Hz, 2H), 7.10 (t, J = 7.5 Hz, 2H), 7.03 – 6.94 (m, 1H), 3.17 – 3.08 (m, 12H), 1.83 – 1.71 (m, 12H), 1.36 (q, J = 3.2 Hz, 2H), 1.23 (s, 8H), 0.74 (q, J = 3.2 Hz, 2H).

The above procedure was adapted from previous phosphazene superbase synthesis.[1,2]

Potassium 1-phenyl-1-cyclopropanecarboxylate preparation (3-26): An oven-dried 500 mL 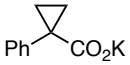 round bottom flask was charged with a magnetic stir bar, 1-phenyl-1-cyclopropanecarboxylic acid (51.78 g, 319.25 mmol, 1.0 equiv) and MeOH (200 mL). An oven-dried 250 mL Erlenmeyer flask was charged with KOH (85%) (20.60 g, 319.25 mmol, 1.0 equiv) and solubilized with a minimal amount to MeOH (about 50 mL). The KOH/MeOH solution was added dropwise to the stirring acid/MeOH solution. The round bottom flask was capped with a rubber septum and the combined solution was stirred for 1 h at room temperature. The MeOH was removed *in vacuo*, PhMe (150 mL) was added and removed *in vacuo* three times. The white solid was filtered and washed with ethyl acetate. The solid was collected and dried *in vacuo*. **^{1}H NMR** (400 MHz, *d6*-DMSO) δ 7.21 (d, J = 8.1 Hz, 1H), 7.14 (t, J = 7.4 Hz, 1H), 7.03 (t, J = 7.1 Hz, 1H), 1.12 (m, 1H), 0.59 (m, 1H).; **^{13}C NMR** (101 MHz, *d6*-DMSO) δ 13C NMR (101 MHz, DMSO) δ 175.4, 146.6, 130.6, 127.4, 124.9, 31.7, 13.9.; **HRMS (DART)** $[M+NH_4]^+$ calcd. for $[C_{10}H_{13}NO_2]^+$ = 180.1019, found 180.1027

A3.2.4 Identification of a crystalline carboxylate salt for P$_2$-*t*-Bu

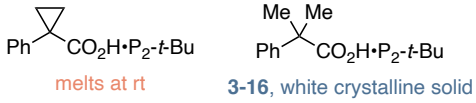

Here, we investigated carboxylate structures beginning 1-phenyl-1-cyclopropanecarboxylic acid, which forms a crystalline solid salt with P$_1$-*t*-Bu. Unfortunately, a solid salt does not form between 1-phenyl-1-cyclopropanecarboxylic acid and P$_2$-*t*-Bu, but with a slight modification to the carboxylate structure, we found that 2-methyl-1-phenylpropanecarboxylic acid forms a solid salt with P$_2$-*t*-Bu.

A3.2.5 Synthesis of P$_2$-*t*-Bu Salt 3-16 from freebase

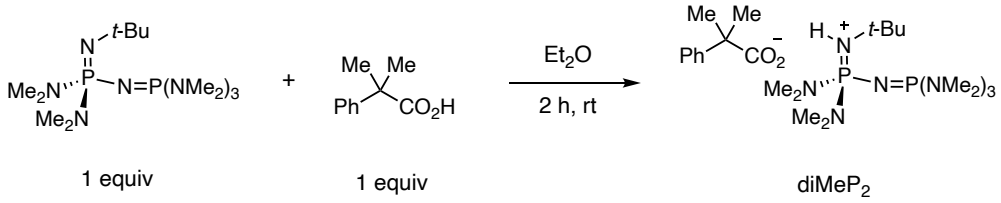

General Procedure: An oven-dried 250 mL round bottom flask was charged with a magnetic stir bar, 2-methyl-2-phenylpropionic acid (1.64 g, 10 mmol, 1 equiv) and diethyl ether (50 mL, 0.2 M). In a nitrogen filled glovebox an oven-dried 20 mL scintillation vial (ThermoFisher, 03-341-25D) was charged with P_2-*t*-Bu (5 mL of a 2 M THF solution, 10 mmol, 1 equiv) and diluted with diethyl ether (10 mL). The vial was capped and removed from the glovebox. The vial containing the P_2-*t*-Bu dissolved in diethyl ether was uncapped and added slowly to the stirring solution of 2-methyl-2-phenylpropionic acid. The reaction solution was stirred for 2 hours at room temperature as a homogeneous, colorless solution. The reaction mixture was concentrated, and the resulting crystalline solid was washed with 10 mL of cold diethyl ether, dried *in vacuo*, and collected as a white powder (4.92 g, 9.3 mmol, 93% yield). **^{1}H NMR** (400 MHz, $CDCl_3$) δ 7.56 (d, J = 7.7 Hz, 2H), 7.17 (t, J = 7.7 Hz, 2H), 7.02 (t, J = 7.7 Hz, 2H), 2.67-2.37 (m, 30H), 1.56 (s, 6H), 1.25 (s, 9H); **^{31}P NMR** (162 MHz, $CDCl_3$) δ 16.2 (d, J = 67.4 Hz, 1P), 12.2 (d, J = 67.4 Hz, 1P); **^{13}C NMR** (101 MHz, $CDCl_3$) δ 180.0, 150.9, 127.2, 126.6, 124.2, 48.2, 37.1 (dd, J = 16.2, 5.4 Hz), 31.2 (dd, J = 4.8, 2.7 Hz), 28.5

A3.2.6 Storage of Superbases and Precatalyst Salts

This section outlines general descriptions of how we stored and used the commercial freebases and superbase salts throughout the course of our studies. See Section A3.8 for a more detailed discussion of the air stability of the freebases and superbase salts over time and in more humid environments.

Commercial Superbases Stored in Glovebox: The commercial P_1-*t*-Bu and P_2-*t*-Bu superbases were purchased from MilliporeSigma, brought into a nitrogen filled glovebox and stored in a freezer at -30 °C. Prior to use in reactions, the bases were removed from the freezer and allowed to warm to room temperature and homogenized if necessary.

Commercial Superbases Stored in Air: For P_1-*t*-Bu, a sample of the base was transferred from the commercial bottle into a 20 mL scintillation vial (ThermoFisher, 03-341-25D) and brought out of the nitrogen filled glovebox. For P_2-*t*-Bu, a sample of the base as a 2.0 M solution in THF was transferred from the commercial bottle into a 20 mL sample vial and brought out of the nitrogen filled glovebox. The THF was removed *in vacuo*, resulting in the pure crystalline P_2-*t*-Bu. For both bases, the vials were stored on the benchtop uncapped to observe their behavior open to air.

Superbase Carboxylate Salts Stored in Air: For a given superbase carboxylate salt, a sample of the freshly synthesized material was added to a 20 mL scintillation vial (ThermoFisher, 03-341-25D). The vial was stored capped on the benchtop to be utilized in reactions by weighing it open to air. Additionally, the vial was opened two times per week and the salt was mixed with a metal spatula to mimic more frequent use and then stored back on the benchtop capped.

Superbase Carboxylate Salts Stored in a Benchtop Desiccator: For a given superbase carboxylate salt, a sample of the freshly synthesized material was added to a 20 mL scintillation vial (ThermoFisher, 03-341-25D). The vial was stored capped inside a benchtop desiccator to be used in reactions by weighing it open to air. Additionally, the vial was removed from the desiccator and opened two times per week and the salt was mixed with a metal spatula to mimic more frequent use and then stored back in the benchtop desiccator capped.

Superbase Carboxylate Salts Stored in a Freezer: For a given superbase carboxylate salt, a sample of the freshly synthesized material was added to a 20 mL scintillation vial (ThermoFisher,

03-341-25D). The vial was stored capped inside a freezer at -30 °C to be used in reactions by weighing it open to air. This storage method was used most frequently to ensure the stability of the superbase salt over time and thus did not require any additional mixing of the salt to mimic heavier use. As a note, the superbase carboxylate salt was allowed to warm to room temperature before being used in reactions.

A3.3 Superbase Salt 3-15 Activation

A variety of epoxide additives and conditions were tested with cycpP_1. The following sections show different epoxides and a range of conditions with activation profiles showing the varied rate of superbase release.

A3.3.1 General Activation Procedure and Analysis for P_1-*t*-Bu Activation Studies

General activation procedure: Activation studies were carried out under nitrogen and in deuterated solvents. An oven-dried 1 dram vial (ThermoFisher, C4015-1) was charged with a magnetic stir bar and salt **3-15** (23.7 mg, 0.05 mmol, 1 equiv). The vial was brought into a nitrogen filled glovebox where deuterated solvent (0.1 mL, 0.5 M) and epoxide additive (0.1 mmol, 2 equiv) were added. The reaction was capped with a PTFE lined cap (ThermoFisher, C4015-1A), removed from the glovebox, and placed in a preheated aluminum reaction block and stirred for the indicated time. The vial was then taken into a nitrogen filled glovebox where the solution was diluted with deuterated solvent (0.4 mL, total of 0.5 mL), transferred to an NMR tube, which was then capped and sealed with parafilm wax. ^{1}HNMR and ^{31}PNMR spectroscopy were used to assess each reaction and determine the percentage of free base produced.

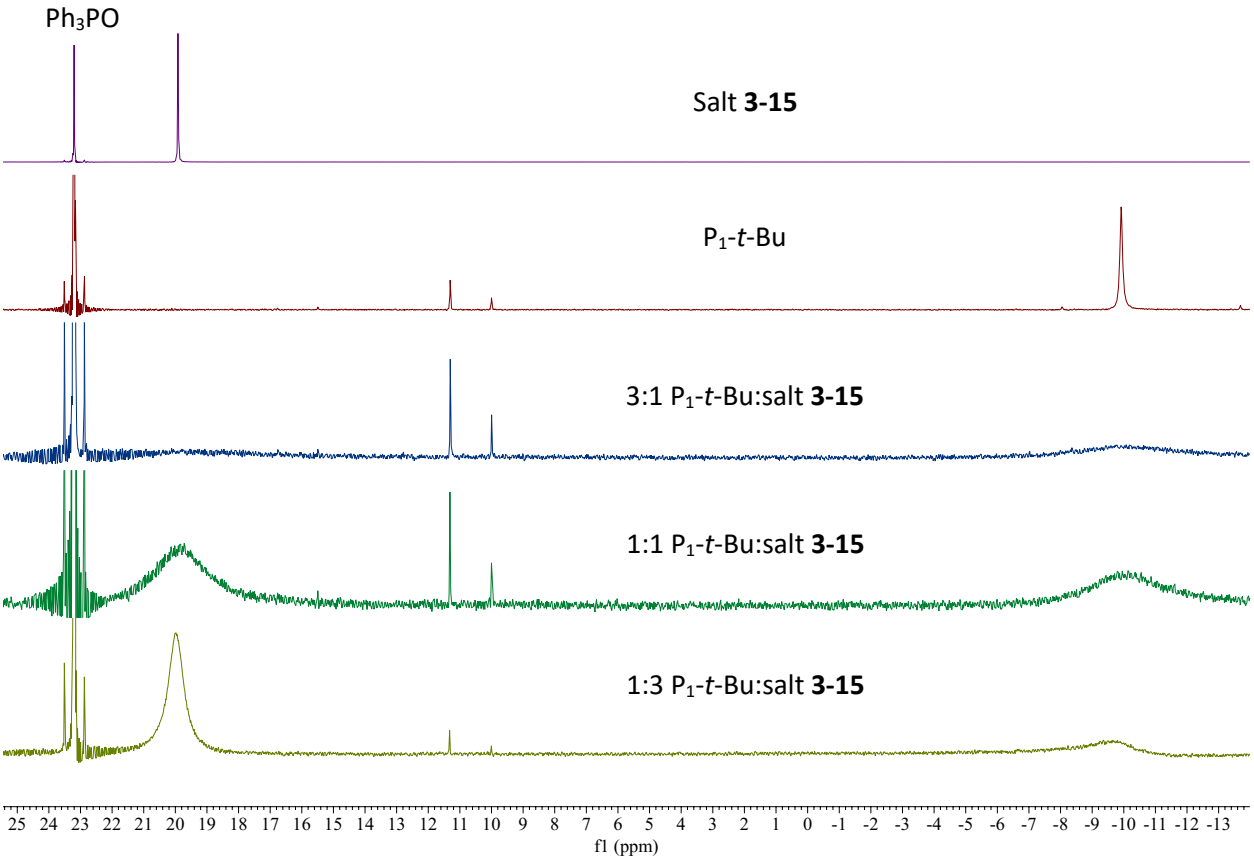

Figure A3-2: ^{31}P NMR spectra of P$_1$-*t*-Bu and salt **3-15** in various ratios without activation byproduct present. Signals at approximately 10 to 12 ppm correspond to decomposed P$_1$-*t*-Bu and phosphoramide.

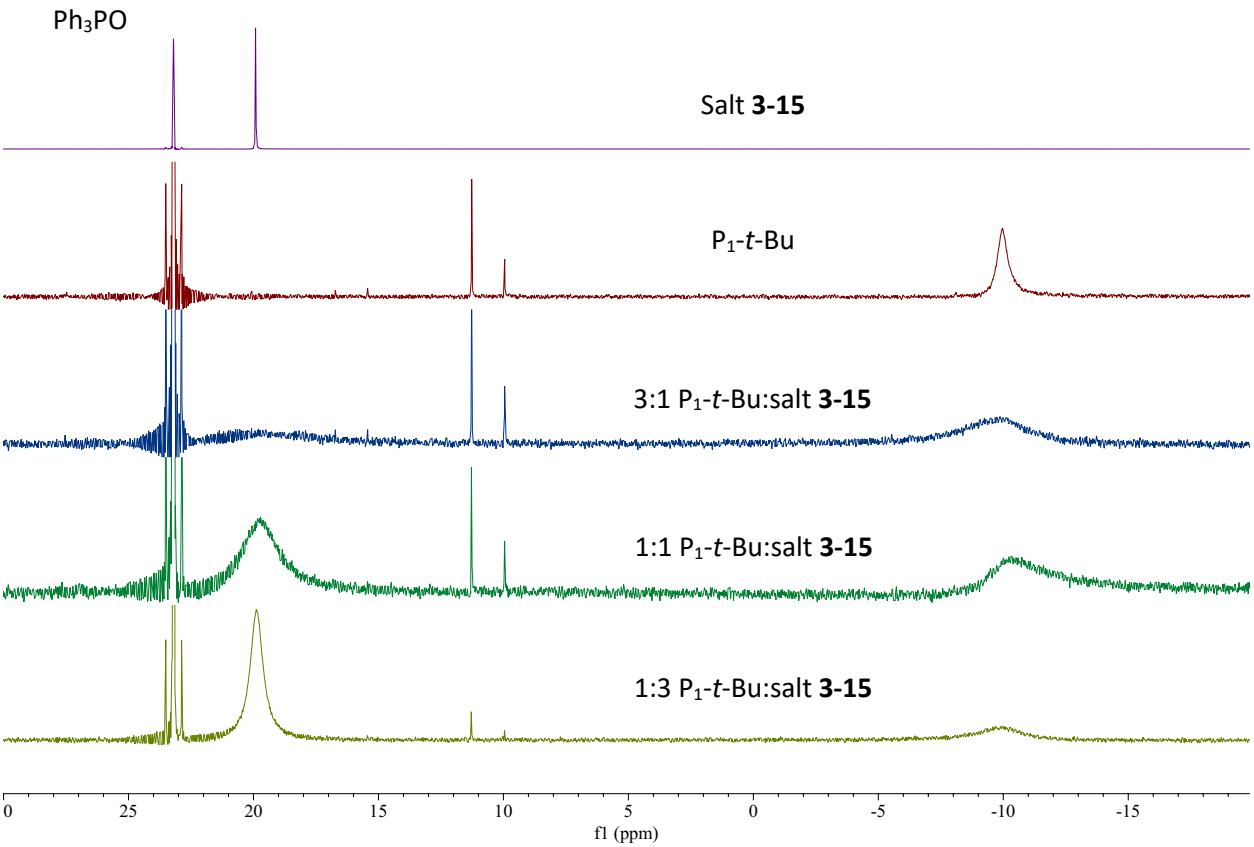

Figure A3-3: ^{31}P NMR spectra of P_1-*t*-Bu and salt **3-15** in various ratios with 1 equiv activation byproduct present. Signals at approximately 10 to 12 ppm correspond to decomposed P_1-*t*-Bu and phosphoramide.

Note on ^{31}P NMR analysis of P_1-*t*-Bu: The proton exchange is slow enough to observe separate signals for two phosphorus environments as opposed to a single, averaged signal. The activation byproduct leads to more defined and resolved signals in ^{31}P NMR spectra, Figure A3-2 vs. Figure A3-3 above. The signal at 20 ppm corresponds to the protonated base and the peak at -10 ppm corresponds to the free base. By comparing the ratio of the areas of the two signals, we are able to evaluate the percentage of the free base produced as a result of the activation reaction (Figure A3-4). In all cases the amount of free base as determined by ^{31}P NMR analysis was in close agreement, within 5%, with the amount of byproduct as determined by ^{1}H NMR analysis. An example is provided below in Figures A3-4 and A3-5.

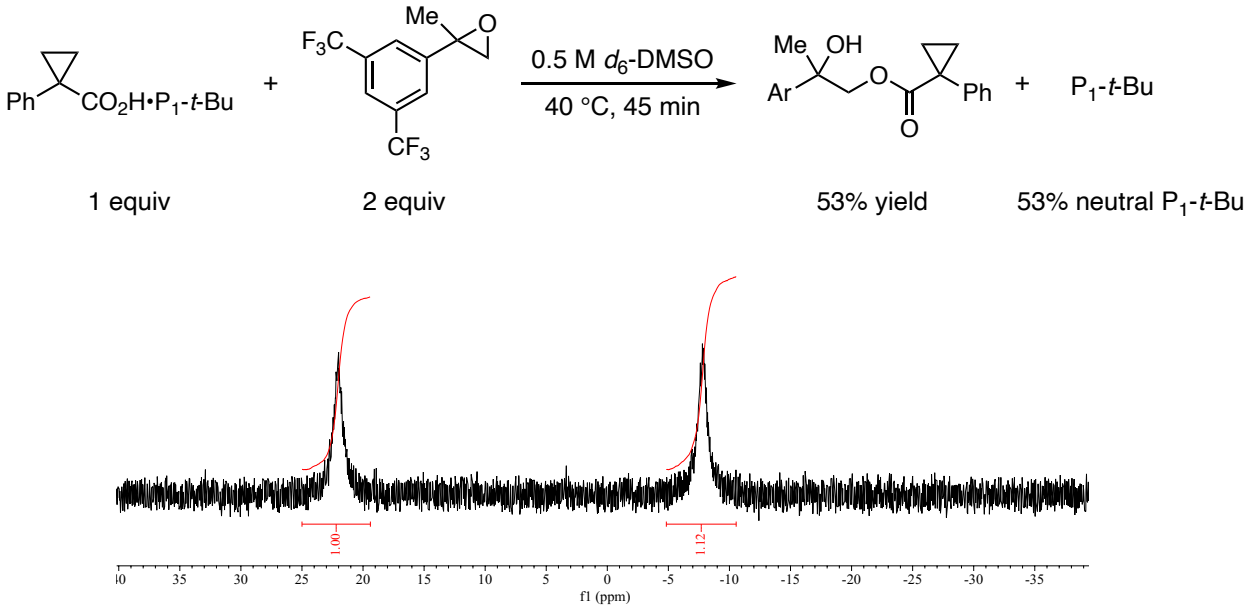

Figure A3-4: Example ^{31}P NMR spectrum from above activation profile overlay with epoxide **3-23** at 45 minutes, 53% free base.

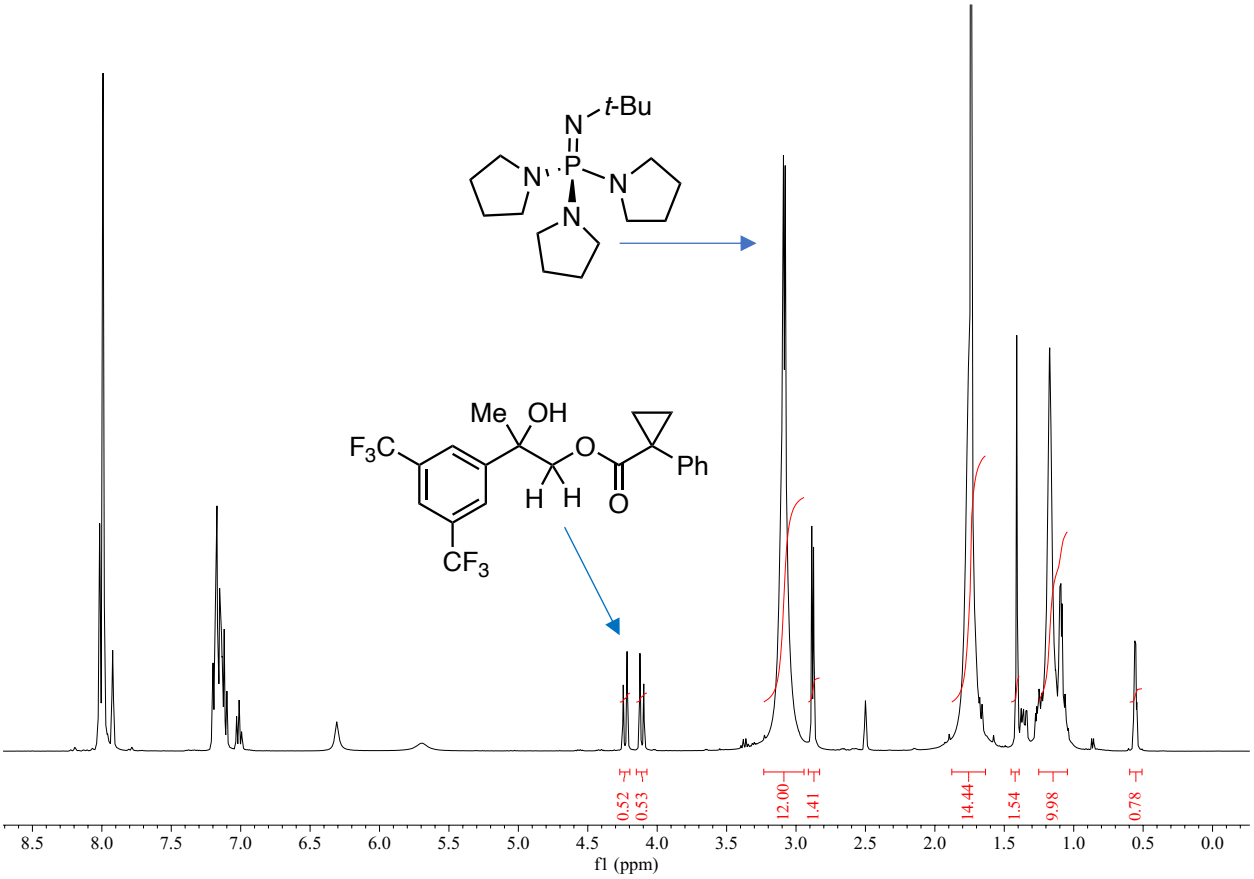

Figure A3-5: Example ^{1}H NMR spectrum from above activation profile overlay with epoxide **3-23** at 45 minutes, 53% free base. Integrations are calculated with respect to methylene protons of P_1-*t*-Bu.

b. Activation studies under various conditions

Epoxide controlled base release: The general activation procedure was followed using epoxides **3-23 – 3-25** and **3-19**. Each time point was setup as an individual reaction and stopped at the indicated time *via* dilution with d_6-DMSO in a nitrogen filled glovebox. Percentage of free base was determined with ^{31}PNMR by the area ratio of phosphorous signals.

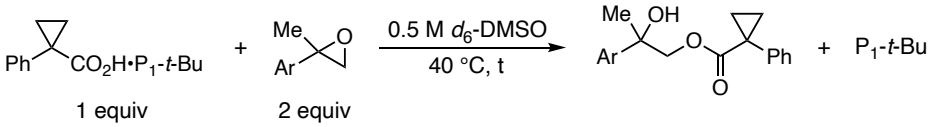

Table A3-1: Amount of free base generated over time by epoxides **3-23**, **3-24**, **3-25**, and **3-19**.

Entry	Time (min)	% Free base			
		3-23	**3-24**	**3-25**	**3-19**
1	0	0	0	0	0
2	5	17	7	0	0
3	15	31	13	2.5	0
4	45	53	28	5	0
5	90	70	40	10	3
6	240	93	69	30	10

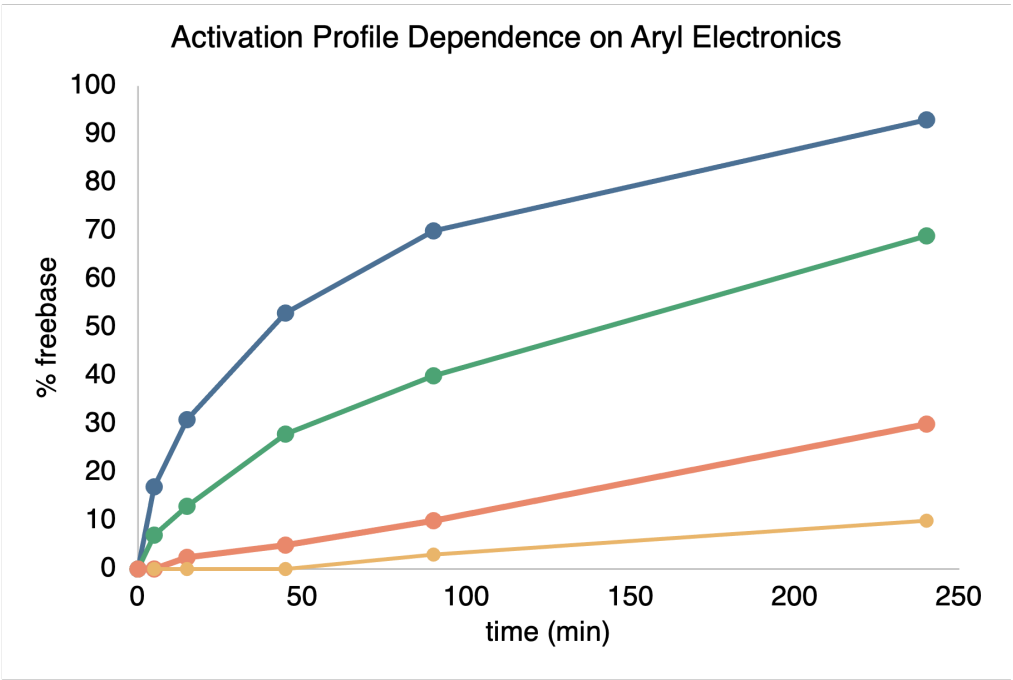

Figure A3-6: Activation curves for epoxides **3-23**, **3-24**, **3-25**, and **3-19**.

Solvent dependent base release: The general activation procedure was followed using epoxide **3-23**. Each time point was setup as an individual reaction and stopped at the indicated time *via* dilution with deuterated solvent (d_6-DMSO, CD_3CN, d_8-THF, d_8-PhMe) in a nitrogen filled glovebox. Percentage of free base was determined with ^{31}PNMR by the area ratio of phosphorous signals.

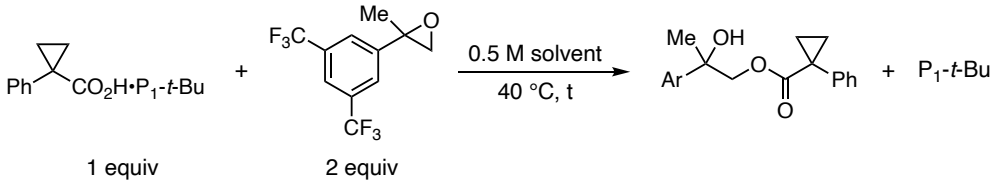

Table A3-2: Amount of free base generated over time in d_6-DMSO, d_3-MeCN, d_8-THF, and d_8-PhMe.

Entry	Time (min)	% Free base			
		d_6-DMSO	CD_3CN	d_8-THF	d_8-PhMe
1	0	0	0	0	0
2	5	17	10	24	24
3	15	31	15	39	32
4	45	53	25	60	44

5	90	70	50	76	54
6	240	93	55	93	73

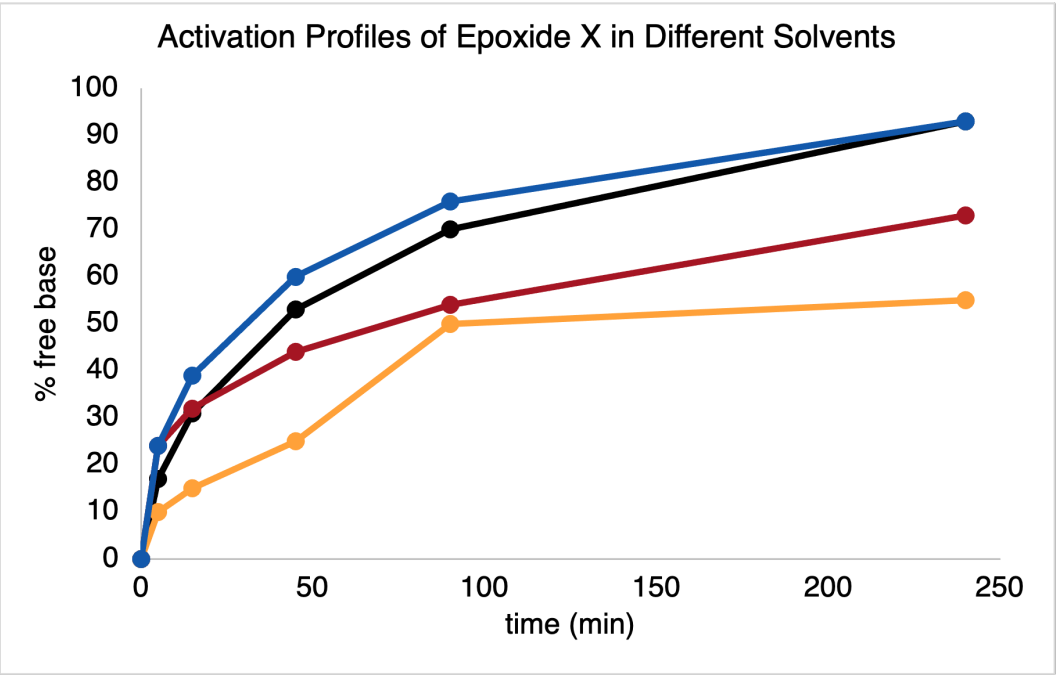

Figure A3-7: Activation curves in d_6-DMSO, d_3-MeCN, d_8-THF, and d_8-PhMe.

Temperature dependent base release: The general activation procedure was followed using epoxide **3-23**. Each time point was setup as an individual reaction and stopped at the indicated time *via* dilution with d_6-DMSO in a nitrogen filled glovebox. Percentage of free base was determined with ^{31}PNMR by the area ratio of phosphorous signals.

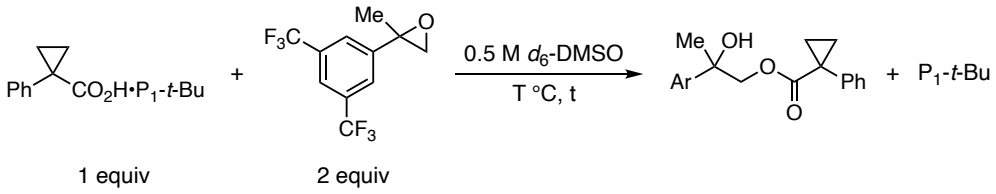

Table A3-3: Amount of free base generated over time at 25, 40, 60, and 80 °C.

Entry	**Time**	**% Free base**			
	(min)	**25 °C**	**40 °C**	**60 °C**	**80 °C**
1	0	0	0	0	0
2	5	11	17	60	99

3	15	17	31	85	99
4	45	29	53	99	99
5	90	40	70	99	99
6	240	64	93	99	99

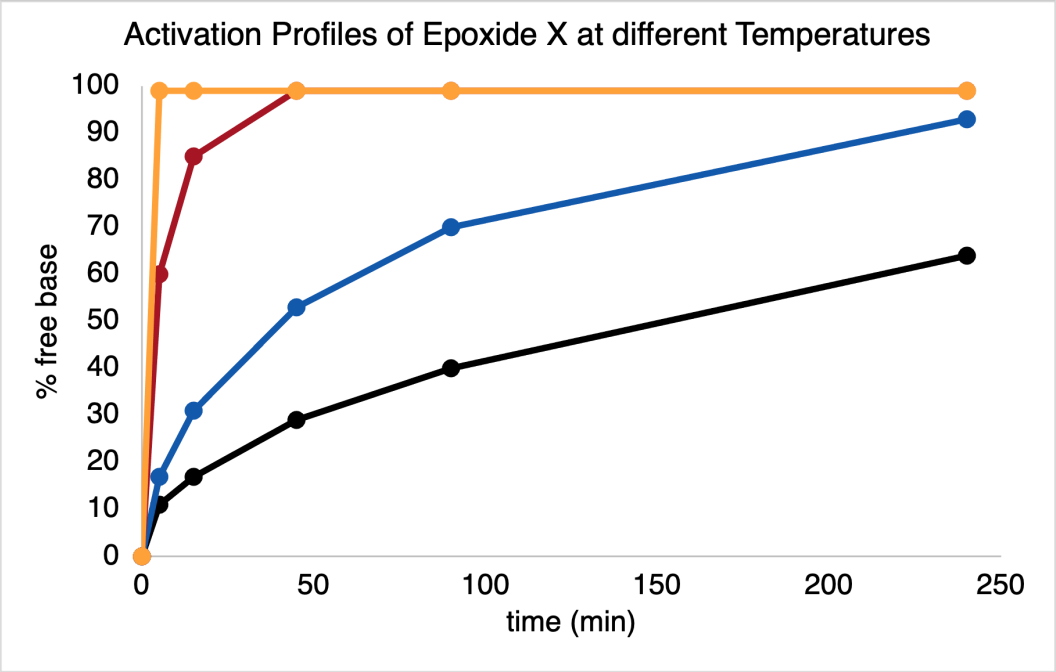

Figure A3-8: Activation curves at 25, 40, 60, and 80 °C.

A3.4 P_1-*t*-Bu Salt System Reaction Applications

A3.4.1 Catalytic Michael-type and Aldol-type Addition Reactions

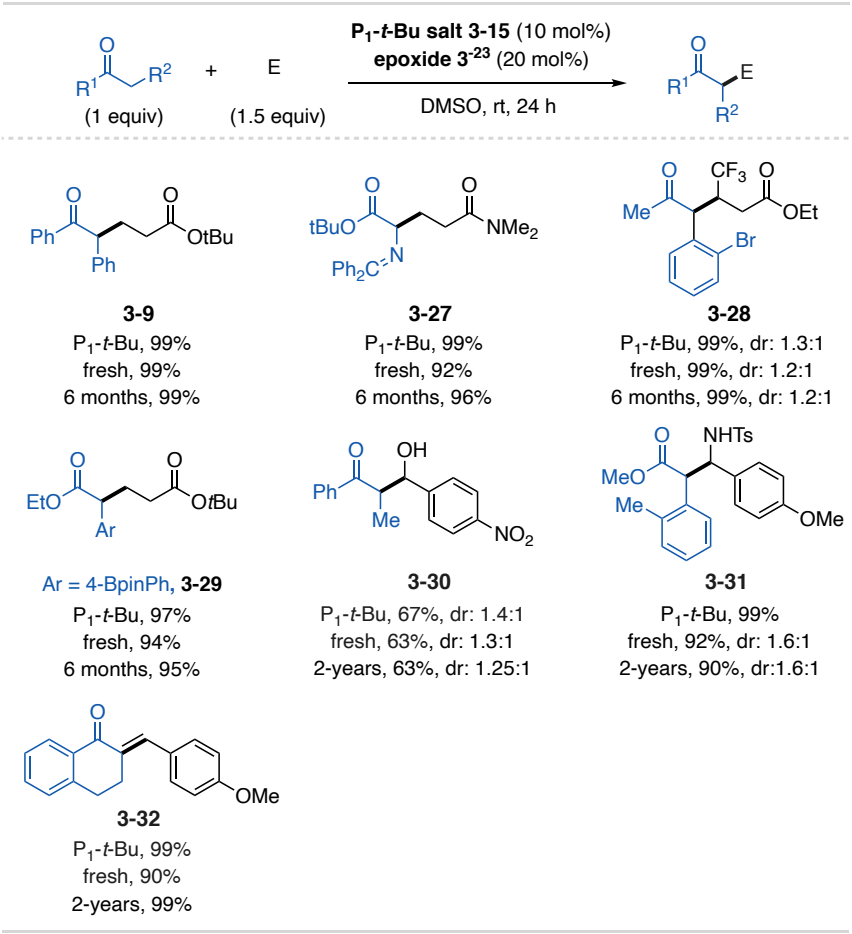

Figure A3-9: Example substrates of addition reactions using salt **3-15** and epoxide **3-23**. General procedure B followed for P_1-*t*-Bu free base yields.

Note: The salt **3-15** reaction was run using salts stored in a series of environments as discussed in Section A3.2. The results are shown in Figure A3-9.

General Procedure Using a Schlenk Line (A): An oven-dried 1 dram vial (ThermoFisher, C4015-1) was charged with a magnetic stir bar and salt **3-15** (47.5 mg, 0.1 mmol, 10 mol%). For solid pronucleophiles and Michael acceptors, the pronucleophile (1.0 mmol, 1 equiv) and Michael acceptor (1.5 mmol, 1.5 equiv) were added to the vial. The vial was sealed with a PTFE lined screw cap (ThermoFisher, C4015-A) and evacuated then flushed with nitrogen three times on a Schlenk manifold. DMSO (2 mL, 0.5M) and epoxide **3-23** (54.0 mg, 0.2 mmol, 20 mol%) was added to the vial *via* nitrogen-flushed syringe. For liquid pronucleophiles and Michael acceptors,

the pronucleophile (1.0 mmol, 1 equiv) and Michael acceptor (1.5 mmol, 1.5 equiv) were added to the vial *via* a nitrogen flushed syringe. The reaction vial was left under a positive pressure of nitrogen and placed into a preheated aluminum reaction block at 25 °C and stirred for 24 h. Dibromomethane (35.1 mL, 0.5 mmol, 0.5 equiv) internal standard was added to the reaction solution, a 50 μL aliquot was taken and added to an NMR tube, then diluted with $CDCl_3$. ^1H NMR spectroscopy was used to determine the yield of the crude reaction.

General Procedure Using a Nitrogen Filled Glovebox (B): An oven-dried 1 dram vial (ThermoFisher, C4015-1) was charged with a magnetic stir bar, salt **3-15** (47.5 mg, 0.1 mmol, 10 mol%) For solid pronucleophiles and Michael acceptors, the pronucleophile (1.0 mmol, 1 equiv) and Michael acceptor (1.5 mmol, 1.5 equiv) were added to the vial. The vial was brought into a nitrogen filled glovebox and DMSO (2 mL, 0.5M) and epoxide **3-23** (54.0 mg, 0.2 mmol, 20 mol%) was added to the vial. For liquid pronucleophiles and Michael acceptors, pronucleophile (1.0 mmol, 1 equiv) and Michael acceptor (1.5 mmol, 1.5 equiv) were added to the vial *via* syringe. The vial was sealed with a PTFE lined screw cap (ThermoFisher, C4015-A), removed from the glovebox, and placed into a preheated aluminum reaction block at 25 °C and stirred for 24 h. Dibromomethane (1.0 mmol, 70 μL, 1.0 equiv) internal standard was added to the reaction solution, a 50 μL aliquot was taken and added to an NMR tube, then diluted with $CDCl_3$. The product was purified *via* silica gel chromatography.

Reaction and Characterization Data

Substrate Characterization: The substrates were subjected to flash column chromatography to yield purified products. The purification conditions and characterization data are given below.

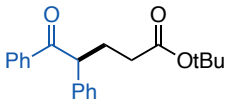

***tert*-butyl 5-oxo-4,5-diphenylpentanoate (3-9).** General procedure A was followed using deoxybenzoin (196.2 mg, 1.0 mmol, 1.0 equiv), *tert*-butyl acrylate (219.7 µL, 1.5 mmol, 1.5 equiv), salt **3-15** (47.5 mg, 0.1 mmol, 10 mol%), and epoxide **3-23** (54.0 mg, 0.2 mmol, 20 mol%) in 2 mL of DMSO. ^{1}HNMR was used to determine the yield (>99% yield). The product was purified *via* silica gel chromatography using 100% hexanes to 6% EtOAc/hexanes to afford **3-9** as a white solid. **^{1}H NMR** (400 MHz, $CDCl_3$) δ 7.95 (d, J = 8.3 Hz, 1H), 7.47 (t, J = 7.2 Hz, 1H), 7.38 (t, J = 7.6 Hz, 2H), 7.29 (d, J = 4.4 Hz, 4H), 7.24 – 7.18 (m, 2H), 4.68 (t, J = 7.2 Hz, 1H), 2.48 – 2.35 (m, 1H), 2.21 (t, J = 6.9 Hz, 2H), 2.18 – 2.07 (m, 1H), 1.43 (s, 9H). Characterization data matches previous reports.[3]

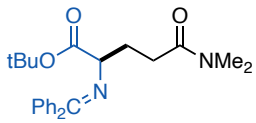

***tert*-butyl 5-(dimethylamino)-2-((diphenylmethylene)amino)-5-oxopentanoate (3-27).** General procedure A was followed using *tert*-butyl 2-((diphenylmethylene)amino)acetate (295.4 mg, 1.0 mmol, 1.0 equiv), *N,N*-dimethylacrylamide (154.9 µL, 1.5 mmol, 1.5 equiv), salt **3-15** (47.5 mg, 0.1 mmol, 10 mol%), and epoxide **3-23** (54.0 mg, 0.2 mmol, 20 mol%) in 2 mL of DMSO. ^{1}HNMR was used to determine the yield (96% yield). The product was purified *via* silica gel chromatography using 50% EtOAc/hexanes to afford **3-27** as a white solid. **^{1}H NMR** (400 MHz, $CDCl_3$) δ z7.64 (dd, J = 7.3, 1.8 Hz, 2H), 7.47 – 7.40 (m, 3H), 7.37 (d, J = 7.1 Hz, 1H), 7.32 (t, J = 7.4 Hz, 3H), 7.16 (dd, J = 6.6, 2.9 Hz, 2H), 4.01 (t, J = 6.0 Hz, 1H), 3.00 (s, 3H), 2.90 (s, 3H), 2.50 – 2.27 (m, 2H), 2.21 (s, 2H), 1.43 (s, 9H). Characterization data matches previous reports.[4]

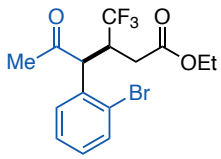

ethyl 4-(2-bromophenyl)-5-oxo-3-(trifluoromethyl)hexanoate (3-28). General procedure A was followed using 1-(2-bromophenyl)propan-2-one (213.1 mg, 1.0 mmol, 1.0 equiv), ethyl 4,4,4-trifluorobutanoate (224.2 µL, 1.5 mmol, 1.5 equiv), salt **3-15** (47.5 mg, 0.1 mmol, 10 mol%), and epoxide **3-23** (54.0 mg, 0.2 mmol, 20 mol%) in 2 mL of DMSO. ^{1}HNMR was used to determine the yield (>99% yield, 1.2:1 dr). The product was purified *via* silica gel chromatography using 5% EtOAc to 25% EtOAc/hexanes to afford **3-28** as a pale yellow oil. **^{1}H NMR** (400 MHz, $CDCl_3$) δ 7.66 (d, J = 7.8 Hz, 1H), 7.37 – 7.12 (m, 9H), 4.91 (d, J = 9.4 Hz, 1H), 4.74 (d, J = 10.6 Hz, 1H), 4.17 (q, J = 7.1 Hz, 2H), 4.10 – 3.81 (m, 3H), 3.62 – 3.46 (m, 1H), 2.80 (dd, J = 16.6, 7.0 Hz, 1H), 2.62 (dd, J = 16.6, 3.9 Hz, 1H), 2.43 (dd, J = 16.7, 6.7 Hz, 1H), 2.16 (s, 3H), 2.13 (s, 2H), 2.06 (dd, J = 16.7, 6.0 Hz, 1H), 1.28 (t, J = 7.1 Hz, 3H), 1.13 (t, J = 7.1 Hz, 3H); **^{13}C NMR** (101 MHz, $CDCl_3$) δ 13C NMR (101 MHz, CDCl3) δ 204.5, 203.7, 170.7, 170.4, 134.5, 133.9, 133.8, 133.1, 130.5, 130.3, 130.1, 129.8, 129.6, 128.7, 128.5, 128.3, 128.1, 126.8, 125.9, 125.9, 61.2, 61.1, 55.0, 54.5, 42.2, 41.9, 41.0, 40.8, 32.0, 32.0, 31.5, 31.5, 31.4, 31.4, 30.2, 30.0, 17.0, 14.2, 14.1.

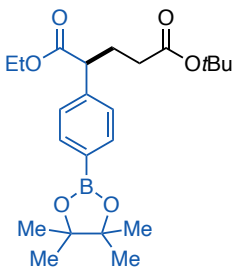

5-(tert-butyl) 1-ethyl 2-(4-(4,4,5,5-tetramethyl-1,3,2-dioxaborolan-2-yl)phenyl)pentanedioate (3-29). General procedure A was followed using ethyl 2-(4-(4,4,5,5-tetramethyl-1,3,2-dioxaborolan-2-yl)phenyl)acetate (290.2 mg, 1.0 mmol, 1.0 equiv), *tert*-butyl acrylate (219.7 µL, 1.5 mmol, 1.5 equiv), salt **3-15** (47.5 mg, 0.1 mmol, 10 mol%), and epoxide **3-23** (54.0 mg, 0.2 mmol, 20 mol%) in 2 mL of DMSO. ^{1}HNMR was used to determine the yield (>99 XX% yield). The product was purified *via* silica gel chromatography using 5%MeOH/DCM with dried silica gel to afford **3-29** as a colorless oil. About 10% protodeboronation occurred during purification. **^{1}H NMR** (400 MHz,

$CDCl_3$) δ 7.76 (d, J = 7.5 Hz, 2H), 7.29 (d, J = 7.7 Hz, 2H), 4.20 – 4.01 (m, 2H), 3.66 – 3.54 (m, 1H), 2.38 – 2.23 (m, 1H), 2.20 – 2.11 (m, 1H), 2.13 – 1.96 (m, 1H), 1.42 (s, 7H), 1.33 (s, 10H), 1.18 (t, J = 7.1 Hz, 2H).; **^{13}C NMR** (101 MHz, $CDCl_3$) δ 13C NMR (101 MHz, CDCl3) δ 173.4, 172.3, 141.8, 135.3, 135.2, 128.8, 127.5, 83.9, 80.5, 61.0, 61.0, 50.9, 41.8, 33.2, 28.6, 28.2, 25.0, 14.2.

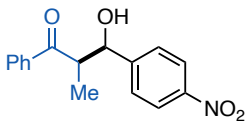

3-hydroxy-2-methyl-3-(4-nitrophenyl)-1-phenylpropan-1-one (3-30). General procedure A was followed using propiophenone (130.0 µL, 1.0 mmol, 1.0 equiv), 4-nitrobenzaldehyde (227.0 mg, 1.5 mmol, 1.5 equiv), salt **3-15** (47.5 mg, 0.1 mmol, 10 mol%), and epoxide **3-23** (81.0 mg, 0.3 mmol, 30 mol%) in 4 mL of DMSO. ^{1}H NMR was used to determine the yield (61% yield). An authentic sample of this product was prepared *via* the general procedure B. The product was purified *via* silica gel chromatography using 20% EtOAc in hexanes to afford **3-30** as a yellow oil (173.4 mg, 0.61 mmol, 61% yield). Prepared and isolated by Garrett.

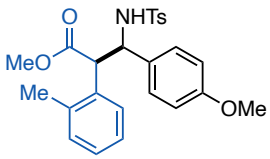

Methyl 3-((4-methylphenyl)sulfonamido)-3-(4-nitrophenyl)-2-(o-tolyl)propanoate (3-31). General procedure A was followed using methyl 2-(*o*-tolyl)acetate (160.0 mg, 1.0 mmol, 1.0 equiv), (Z)-*N*-(4-methoxybenzylidene)-4-methylbenzenesulfonamide (430.0 mg, 1.5 mmol, 1.5 equiv), salt **3-15** (47.5 mg, 0.1 mmol, 10 mol%), and epoxide **3-23** (54.0 mg, 0.2 mmol, 20 mol%) in 4 mL of DMSO. ^{1}HNMR was used to determine the yield (94% yield). An authentic sample of this product was prepared *via* the general procedure B. The product was purified *via* silica gel chromatography

using 20% EtOAc in hexanes to afford **3-31** as a white solid (363.5 mg, 0.80 mmol, 80% yield). Prepared and isolated by Garrett.

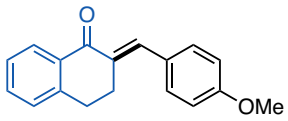

2-(4-methoxybenzylidene)-3,4-dihydronaphthalen-1(2H)-one (3-32). General procedure A was followed using 3,4-dihydronaphthalen-1(2*H*)-one (130.0 µL, 1.0 mmol, 1.0 equiv), (Z)-*N*-(4-methoxybenzylidene)-4-methylbenzenesulfonamide (430.0 mg, 1.5 mmol, 1.5 equiv), salt **3-15** (47.5 mg, 0.1 mmol, 10 mol%), and epoxide **3-23** (54 mg, 0.2 mmol, 20 mol%) in 4 mL of DMSO. ^{1}HNMR was used to determine the yield (94% yield). An authentic sample of this product was prepared *via* the general procedure B. The product was purified *via* silica gel chromatography using 10% EtOAc in hexanes to afford **3-32** as a yellow solid (248.5 mg, 0.94 mmol, 94% yield). Prepared and isolated by Garrett.

Control Reactions: A series of control reactions were investigated by altering and/or excluding certain components of the reaction. This is intended to probe any background or side reactions taking place. They also ensure that the reaction is being catalyzed by the P_1-*t*-Bu produced from the activation of the precatalyst system. The results of these control reactions are compiled below in Table SX. General procedure B was followed for each entry.

General Procedure Used for Control Reactions (C): In a nitrogen filled glovebox an oven-dried 1 dram vial (ThermoFisher, C4015-1) was charged with a magnetic stir bar, basic "catalyst" (0.01 mmol, 10 mol% (unless excluded)), pronucleophile (0.1 mmol, 1 equiv), DMSO (0.2 mL, 0.5 M), epoxide **3-23** (5.4 mg, 0.2 mmol, 20 mol% (unless excluded)) and Michael acceptor (0.15 mmol,

1.5 equiv,) in successive order. The vial was capped with a PTFE-lined cap (ThermoFisher, C4015-1A), removed from the glovebox and placed into a preheated aluminum reaction block at 25 °C and stirred for 24 h. Dibromomethane (0.1 mmol, 7 μL, 1 equiv) internal standard was added to the reaction solution, a 50 μL aliquot was taken and added to an NMR tube, then diluted with $CDCl_3$. ^{1}HNMR spectroscopy was used to determine the yield of product.

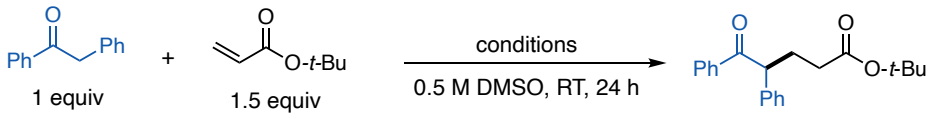

Table A3-4: Control reactions for the Michael addition between deoxybenzoin and tert-Butylacrylate with various basic catalyst. Result indicate P_1-*t*-Bu is the active catalyst and is only generated with salt **3-15** and epoxide **3-23** are in solution.

Entry	Conditions	Results
1	10% salt **3-15** + 20% Epoxide **3-23**	>99%
2	5% salt **3-15** + 10% Epoxide **3-23**	6%
3	2.5% salt **3-15** + 5% Epoxide **3-23**	trace
4	1% salt **3-15** + 2% Epoxide **3-23**	0%
5	10% P_1-*t*-Bu	>99%
6	10% salt **3-15**	0%
7	20% Epoxide **3-23**	0%
8	10% **3-26**	0%
9	10% **3-26** + 20% Epoxide **3-23**	0%
10	10% Bu_4NOAc + 20% Epoxide **3-23**	0%
11	10% Bu_4NOAc	10%
12	No Base	0%

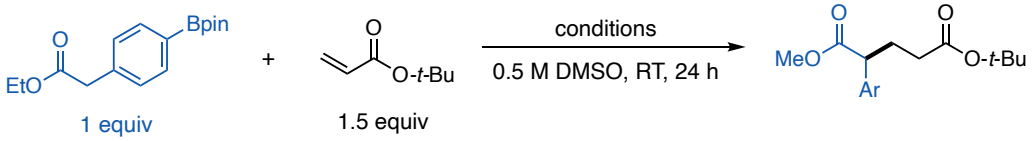

Table A3-5: Control reactions for the Michael addition between ethyl 2-(4-(4,4,5,5-tetramethyl-1,3,2-dioxaborolan-2-yl)phenyl)acetate and *tert*-Butylacrylate with various basic catalyst. Result indicate P_1-*t*-Bu is the active catalyst and is only generated with salt **3-15** and epoxide **3-23** are in solution.

Entry	Conditions	Results
1	10% salt **3-15** + 20% Epoxide **3-23**	>99%

2	5% salt **3-15** + 10% Epoxide **3-23**	58%
3	2.5% salt **3-15** + 5% Epoxide **3-23**	0%
4	1% salt **3-15** + 2% Epoxide **3-23**	0%
5	10% P_1-*t*-Bu	>99%
6	10% salt **3-15**	0%
7	20% Epoxide **3-23**	0%
8	10% **3-26**	0%
9	10% **3-26** + 20% Epoxide **3-23**	93%
10	10% Bu_4NOAc + 20% Epoxide **3-23**	0%
11	10% Bu_4NOAc	0%
12	No Base	0%

A3.4.2 Catalytic Ester Amidation Reaction

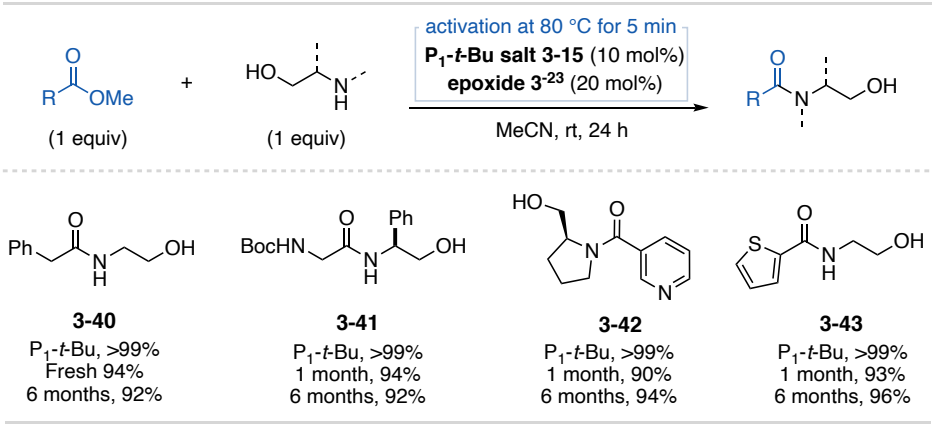

Figure A3-10: Example substrates of ester amidation using salt **3-15** and epoxide salt **3-23**. General procedure D followed for P_1-*t*-Bu free base yields.

Note: The salt **3-15** reaction was run using salts stored in a series of environments as discussed in Section A3-2. The results are shown in Figure A3-10.

General Procedure Using a Schlenk Line (D): a pre-activation procedure was required for amidation reactions. An oven-dried 1 dram vial (ThermoFisher, C4015-1) was charged with a magnetic stir bar and cycpP_1 (47.5 mg, 0.1 mmol, 10 mol%). The vial was capped with a PTFE-lined cap (ThermoFisher, C4015-1A) and evacuated then back filled with nitrogen three times. The reaction solution was left under positive pressure of nitrogen. DMSO (0.2 mL, 0.5 M in salt

3-15) and epoxide **3-23** (54.0 mg, 0.2 mmol, 20 mol%) were added *via* nitrogen flushed syringe. The pre-activation solution was placed in a preheated aluminum reaction block at 80 °C for 5 minutes.

Reagent solution: another oven-dried 1 dram vial (ThermoFisher, C4015-1) was charged with a magnetic stir bar and capped (ThermoFisher, C4015-1A) and evacuated then back filled with nitrogen three times. Ester (1 mmol, 1 equiv), MeCN (0.8 mL, 1 M with total reaction volume) and aminoalcohol (1 mmol, 1 equiv) were added *via* nitrogen flushed syringe. The pre-activation solution was cooled to room temperature and the reagent solution was transferred to the pre-activation solution *via* nitrogen flushed syringe. The combined reaction solution was placed into an aluminum reaction block at room temperature with stirring. The reaction solution was stirred for 24 h. Dibromomethane (35.1mL, 0.5 mmol, 0.5 equiv) internal standard was added to the reaction solution, a 50 µL aliquot was taken and added to an NMR tube, then diluted with CDCl3. ^{1}HNMR spectroscopy was used to determine the yield of the crude reaction. The crude reaction material was subjected to flash chromatography to obtain purified product.

Reaction and Characterization Data

Substrate Characterization: The substrates were subjected to flash column chromatography to yield purified products. The purification conditions and characterization data are given below.

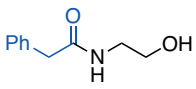

N-(2-hydroxyethyl)-2-phenylacetamide (3-40). General procedure D was followed using salt **3-15** (47.5 mg, 0.1 mmol, 10 mol%), and epoxide **3-23** (54.0 mg, 0.2 mmol, 20 mol%), DMSO (0.2 mL), methyl phenylacetate (140.8 µL, 1.0 mmol, 1.0 equiv), 2-aminoethan-1-ol (60.4 µL, 1.0 mmol, 1.0 equiv), and MeCN (0.8 mL). ^{1}HNMR was used to determine the yield (93% yield). An authentic sample of this product was prepared *via* the general

procedure B. The product was purified *via* silica gel chromatography using 100% DCM to 6% MeOH/DCM to afford **3-40** as a white solid. **^{1}H NMR** (400 MHz, $CDCl_3$) δ 7.34 (t, J = 7.6 Hz, 2H), 7.30 – 7.24 (m, 3H), 6.10 (s, 1H), 3.63 (t, J = 5.0 Hz, 2H), 3.56 (s, 2H), 3.34 (q, J = 5.3 Hz, 2H), 2.97 (s, 1H). Characterization data matches previous reports.[5]

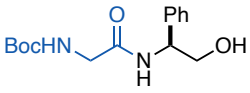

tert-butyl (S)-(2-((2-hydroxy-1-phenylethyl)amino)-2-oxoethyl)carbamate (3-41). General procedure D was followed using salt **3-15** (47.5 mg, 0.1 mmol, 10 mol%), and epoxide **3-23** (54.0 mg, 0.2 mmol, 20 mol%), DMSO (0.2 mL), methyl (*tert*-butoxycarbonyl)glycinate (189.2 mg, 1.0 mmol, 1.0 equiv), (S)-2-amino-2-phenylethan-1-ol (151.7 mg, 1.0 mmol, 1.0 equiv), and MeCN (0.8 mL). ^{1}HNMR was used to determine the yield (94% yield). An authentic sample of this product was prepared *via* the general procedure B. The product was purified *via* silica gel chromatography using 100% DCM to 6% MeOH/DCM to afford **3-41** as a white solid. **^{1}H NMR** (400 MHz, $CDCl_3$) δ 7.37 – 7.25 (m, 5H), 7.11 (d, J = 7.8 Hz, 1H), 5.44 (s, 1H), 5.07 (td, J = 6.9, 4.1 Hz, 1H), 3.89 – 3.75 (m, 4H), 3.20 (s, 1H), 1.43 (s, 9H). Characterization data matches previous reports. [5]

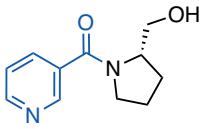

(S)-(2-(hydroxymethyl)pyrrolidin-1-yl)(pyridin-3-yl)methanone (3-42). General procedure D was followed using salt **3-15** (47.5 mg, 0.1 mmol, 10 mol%), and epoxide **3-23** (54.0 mg, 0.2 mmol, 20 mol%), DMSO (0.2 mL), methyl nicotinate (137.1 mg, 1.0 mmol, 1.0 equiv), (R)-pyrrolidin-2-ylmethanol (98.7 µL, 1.0 mmol, 1.0 equiv), and MeCN (0.8 mL). ^{1}HNMR was used to determine the yield (90% yield). An authentic sample of this product was prepared *via* the general procedure B. The product was purified *via* silica gel chromatography using 100% DCM to 6% MeOH/DCM to afford **3-42**as a colorless oil (XX g, XX

mmol, XX% yield). **^{1}H NMR** (400 MHz, $CDCl_3$) δ 8.76 (s, 1H), 8.66 (d, J = 4.9 Hz, 1H), 7.84 (d, J = 7.9 Hz, 1H), 7.35 (dd, J = 7.9, 4.9 Hz, 1H), 4.56 (s, 1H), 4.46 – 4.34 (m, 1H), 3.82 (dd, J = 11.5, J = 3.0, 1H), 3.74 (dd, J = 11.5, J = 7.0 Hz, 1H), 3.56 – 3.46 (m, 2H), 2.22 – 2.11 (m, 1H), 1.98 – 1.87 (m, 1H), 1.89 – 1.64 (m, 2H). Characterization data matches previous reports. [5]

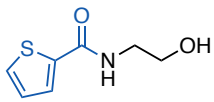

N-(2-hydroxyethyl)thiophene-2-carboxamide (3-43). General procedure D was followed using salt **3-15** (47.5 mg, 0.1 mmol, 10 mol%), and epoxide **3-23** (54.0 mg, 0.2 mmol, 20 mol%), DMSO (0.2 mL), ethyl thiophene-2-carboxylate (134.4 µL, 1.0 mmol, 1.0 equiv), 2-aminoethan-1-ol (60.4 µL, 1.0 mmol, 1.0 equiv), and MeCN (0.8 mL). ^{1}HNMR was used to determine the yield (93% yield). An authentic sample of this product was prepared *via* the general procedure B. The product was purified *via* silica gel chromatography using 100% DCM to 5% MeOH/DCM to afford **3-43** as a white solid. **^{1}H NMR** (400 MHz, $CDCl_3$) δ 7.54 (d, J = 3.7 Hz, 1H), 7.42 (d, J = 4.9 Hz, 1H), 7.13 (t, J = 5.7 Hz, 1H), 7.00 (t, J = 4.4 Hz, 1H), 3.75 (t, J = 5.1 Hz, 2H), 3.63 (s, 1H), 3.54 (q, J = 5.3 Hz, 2H). Characterization data matches previous reports. [5]

Control Reactions: A series of control reactions were investigated by altering and/or excluding certain components of the reaction. This is intended to probe any background or side reactions taking place. They also ensure that the reaction is being catalyzed by the P_1-*t*-Bu produced from the activation of the precatalyst system. The results of these control reactions are compiled below in Table A3-6. General procedure B was followed for each entry.

General Procedure Used for control reactions (E): Since a pre-activation procedure was required for amidation reactions with the salt **3-15** precatalyst, a pre-activation procedure was used for control reactions that employed epoxide **3-23**. If epoxide was excluded from the control

reaction all reagents were added sequentially inside a nitrogen filled glovebox. Pre-activation procedure: in a nitrogen filled glovebox an oven-dried 1 dram vial (ThermoFisher, C4015-1) was charged with a magnetic stir bar, basic "catalyst" (0.05 mmol, 1 equiv to epoxide **3-23**), DMSO (0.1 mL, 0.5 M in basic "catalyst") and epoxide **3-23** (0.1 mmol, 2 equiv to basic "catalyst"). The vial was capped with a PTFE-lined cap (ThermoFisher, C4015-1A), removed from the glovebox and placed in a preheated aluminum reaction block at 80 °C for 5 minutes. Reagent solution: in a nitrogen filled glovebox another oven-dried 1 dram vial (ThermoFisher, C4015-1) was charged with a magnetic stir bar, if epoxide was excluded: basic "catalyst" (0.01 mmol, 10 mol%), ester (0.1 mmol, 1 equiv), MeCN (0.1 mL, 1 M) and aminoalcohol (0.1 mmol, 1 equiv). The vial was capped (ThermoFisher, C4015-1A), removed from the glovebox, connected to a positive pressure of nitrogen. After 5 minutes the pre-activation solution was cooled to room temperature. The pre-activated solution (20 µL, 0.01 mmol, 10 mol% basic "catalyst") was transferred *via* a nitrogen flushed syringe to the reagent solution. Combined reaction solution was stirred for 24 h in a preheated aluminum reaction block at 25 °C. Dibromomethane (1 equiv, 0.1 mmol 7 µL) internal standard was added to the reaction solution, a 50 µL aliquot was taken and added to an NMR tube, then diluted with CDCl3. ^{1}HNMR spectroscopy was used to determine the yield of product.

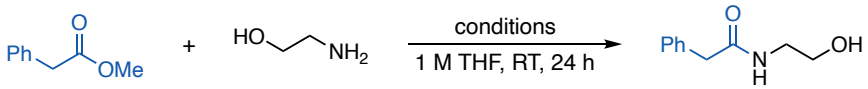

Table A3-6: Control reactions for the ester amidation reaction between methyl phenylacetate and 2-aminoethan-1-ol various basic catalyst. Result indicate P_1-*t*-Bu is the active catalyst and is only generated with salt **3-15** and epoxide **3-23** are in solution.

Entry	Conditions	Results
1	10% salt **3-15** + 20% Epoxide **3-23**	>94%
2	5% salt **3-15** + 10% Epoxide **3-23**	trace
3	2.5% salt **3-15** + 5% Epoxide **3-23**	trace
4	10% P_1-*t*-Bu	>99%
5	10% salt **3-15**	trace
6	20% Epoxide **3-23**	0%

7	10% **3-26**	0%
8	10% **3-26** + 20% Epoxide **3-23**	trace
9	10% Bu_4NOAc + 20% Epoxide **3-23**	8%
10	10% Bu_4NOAc	0%
11	No Base	trace

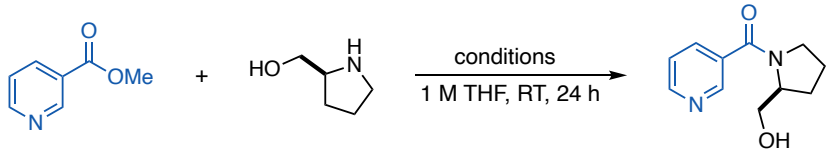

Table A3-7: Control reactions for the ester amidation reaction between methyl nicotinate and (R)-pyrrolidin-2-ylmethanol with various basic catalyst. Result indicate P_1-*t*-Bu is the active catalyst and is only generated with salt **3-15** and epoxide **3-23** are in solution.

Entry	Conditions	Results
1	10% salt **3-15** + 20% Epoxide **3-23**	>99%
2	5% salt **3-15** + 10% Epoxide **3-23**	82%
3	2.5% salt **3-15** + 5% Epoxide **3-23**	68%
4	10% P_1-*t*-Bu	>99%
5	10% salt **3-15**	46%
6	20% Epoxide **3-23**	0%
7	10% **3-26**	0%
8	10% **3-26** + 20% Epoxide **3-23**	37%
9	10% Bu_4NOAc + 20% Epoxide **3-23**	33%
10	10% Bu_4NOAc	0%
11	No Base	21%

A3.4.3 Stoichiometric Deoxyfluorination

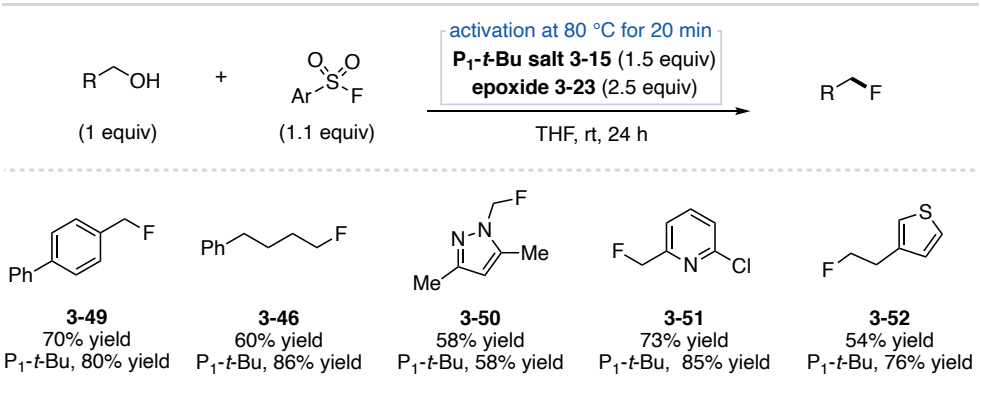

Figure A3-11: Example substrates of ester amidation using salt **3-15** and epoxide **3-23**. General procedure F followed for P_1-*t*-Bu free base yields.

Note: The salt **3-15** reaction was run using salts stored in a series of environments as discussed in Section A3-2. The results are shown in Figure A3-11.

General Procedure Using a Schlenk Line (F): A pre-activation procedure was required for deoxyfluorination reactions. An oven-dried 1 dram vial (ThermoFisher, C4015-1) was charged with a magnetic stir bar and cycpP_1 (178.0 mg, 0.375 mmol, 1.5 equiv). The vial was capped with a PTFE-lined cap (ThermoFisher, C4015-1A) and evacuated then back filled with nitrogen three times. The reaction solution was left under positive pressure of nitrogen. THF (0.4 mL, 0.94 M in cycpP_1) and epoxide **3-23** (168.83 mg, 0.625 mmol, 2.5 equiv) were added *via* nitrogen flushed syringe. The pre-activation solution was placed in a preheated aluminum reaction block at 80 °C for 20 minutes with stirring. **Reagent solution:** another oven-dried 1 dram vial (ThermoFisher, C4015-1) was charged with sulfonyl fluoride (62.7 mg, 0.275 mmol, 1.1 equiv). The vial was capped with a PTFE-lined cap (ThermoFisher, C4015-1A) and evacuated then back filled with nitrogen three times. The reaction solution was left under positive pressure of nitrogen. THF (.25 mL, 1.0 M) and alcohol (1 equiv, 0.25 mmol) were added *via* nitrogen flushed syringe. The pre-activation solution was cooled to room temperature and the reagent solution was transferred to the pre-activation solution *via* nitrogen flushed syringe. The combined reaction solution was placed into an aluminum reaction block at 25 °C with stirring. The reaction solution was stirred for 24 h. Dibromomethane (17.5 mL, 0.205 mmol, 1.0 equiv) internal standard was added to the reaction solution, a 50 µL aliquot was taken and added to an NMR tube, then diluted with $CDCl_3$. ^{1}HNMR spectroscopy was used to determine the yield of the crude reaction. The crude reaction material was subjected to flash chromatography to yield purified product.

Reaction and Characterization Data

Substrate Characterization: The substrates were subjected to flash column chromatography to yield purified products. The purification conditions and characterization data are given below.

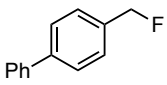

4-(fluoromethyl)-1,1'-biphenyl (3-49). General procedure F was followed using salt **3-15** (178.0 mg, 1.5 mmol, 1.5 equiv) epoxide **3-23** (168.8 mg, 0.625 mmol, 2.5 equiv), THF (0.4 mL), [1,1'-biphenyl]-4-ylmethanol (38.2 mL, 1.0 mmol, 1.0 equiv), 4-(trifluoromethyl)benzenesulfonyl fluoride (62.7 mg, 0.275 mmol, 1.1 equiv), and THF (0.25 mL). ^{1}HNMR was used to determine the yield (70% yield). The product was purified *via* silica gel chromatography using 1%EtOAc /hexanes to afford **3-49** as a white solid. **^{1}H NMR** (400 MHz, $CDCl_3$) δ 7.62 (dd, J = 10.6, 7.8 Hz, 4H), 7.50 – 7.42 (m, 4H), 7.42 – 7.33 (m, 1H), 5.50 (s, 1H), 5.38 (s, 1H). Characterization data matches previous reports. [6]

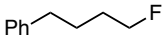

(4-fluorobutyl)benzene (3-46). General procedure F was followed using salt **3-15** (178.0 mg, 1.5 mmol, 1.5 equiv) epoxide **3-23** (168.8 mg, 0.625 mmol, 2.5 equiv), THF (0.4 mL), 4-phenylbutan-1-ol (38.2 mL, 1.0 mmol, 1.0 equiv), 4-(trifluoromethyl)benzenesulfonyl fluoride (62.7 mg, 0.275 mmol, 1.1 equiv), and THF (0.25 mL). ^{1}HNMR was used to determine the yield (60% yield). The product was purified *via* preparatory thin layer chromatography using 1%EtOAc/hexanes to afford **3-46** as a colorless oil. **^{1}H NMR** (400 MHz, $CDCl_3$) δ 7.25 – 7.15 (m, 2H), 7.15 – 7.06 (m, 3H), 4.48 – 4.39 (m, 1H), 4.32 (t, J = 5.7 Hz, 1H), 2.59 (t, J = 7.3 Hz, 2H), 1.75 – 1.55 (m, 4H). Characterization data matches previous reports. [6]

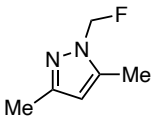

1-(fluoromethyl)-3,5-dimethyl-1H-pyrazole (3-50). General procedure F was followed using cycpP_1 (178.0 mg, 1.5 mmol, 1.5 equiv) epoxide **x** (168.8 mg, 0.625

mmol, 2.5 equiv), THF (0.4 mL), (3,5-dimethyl-1H-pyrazol-1-yl)methanol (31.5 mg, 1.0 mmol, 1.0 equiv), 4-(trifluoromethyl)benzenesulfonyl fluoride (62.7 mg, 0.275 mmol, 1.1 equiv), and THF (0.25 mL). ^{1}HNMR was used to determine the yield (58% yield). The product is not stable to silica gel chromatography. Therefore, the crude material was concentrated *in vacuo* and solvated in 5 mL $CDCl_3$. The solution was rinsied with 10 mL saturated aqueous sodium chloride, the organic layer was dried with sodium sulfate, concentrated to brownish-yellow oil. Workup procedure adapted from Nielsen, M. K.; Ahneman, D. T.; Riera, O.; Doyle, A. G. *J. Am. Chem. Soc*. **2018**, *140*, 5004. Crude material contains P_1-*t*-Bu, byproduct **3-47**, epoxide **3-23**, 4-(trifluoromethyl)benzenesulfonate side products and other minor species. **^{1}H NMR** (400 MHz, $CDCl_3$) (Shown below) δ 5.92 (d, J = 54.4 Hz, 2H), 5.92 (s, 1H), 2.32 (s, 3H), 2.25 – 2.21 (m, 3H, overlapping product). Matches reported crude ^{1}H NMR.[6]

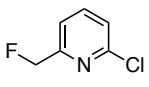

2-chloro-6-(fluoromethyl)pyridine (3-51). General procedure F was followed using salt **3-15** (178.0 mg, 1.5 mmol, 1.5 equiv) epoxide **3-23** (168.8 mg, 0.625 mmol, 2.5 equiv), THF (0.4 mL), (6-chloropyridin-2-yl)methanol (35.9 mg, 1.0 mmol, 1.0 equiv), 4-(trifluoromethyl)benzenesulfonyl fluoride (62.7 mg, 0.275 mmol, 1.1 equiv), and THF (0.25 mL). ^{1}HNMR was used to determine the yield (73% yield). The product could not be separated from the ether dimer side product using normal phase chromatography. The product was prepared *via* deoxyfluorination using DAST.

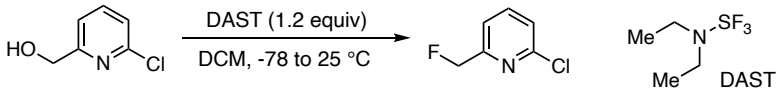

Deoxyfluorination with DAST procedure: an oven-dried 50 mL round bottom flask was charged with a magnetic stir bar, (6-chloropyridin-2-yl)methanol (0.718 g, 5.0 mmol, 1.0 equiv) and DCM

(20 mL). The flask was capped with a rubber septa, connected to a positive pressure of nitrogen and cooled to -78 °C. DAST (0.967 g, 6 mmol, 1.2 equiv) was solubilized in DCM (5 mL). The DAST solution was added dropwise to the reaction flask *via* syringe. The reaction solution was allowed to warm to 25 °C then stirred for 12 h. The reaction solution was transferred to a separatory funnel and water (25mL) was added followed by slow addition of a saturated sodium bicarbonate solution (25 mL). The mixture was extracted with Et_2O (3x 25 mL). The combined organic layers were washed with brine (25 mL), dried over sodium sulfate, filtered and concentrated *in vacuo*. Silica gel column chromatography using 100% hexanes to 5% EtOAc/hexanes yielded product as a colorless oil (XX g, XX mmol, XX% yield). **^{1}H NMR** (400 MHz, $CDCl_3$) δ 7.71 (t, J = 7.8 Hz, 1H), 7.38 (d, J = 7.6 Hz, 1H), 7.27 (d, J = 8.1 Hz, 1H), 5.43 (d, J = 46.6 Hz, 2H). ; **^{13}C NMR** (101 MHz, $CDCl_3$) δ; **IR** (neat): cm^{-1}; **HRMS (DART)** $[M+H]^+$ calcd. for $[C_6H_6ClFN]^+$ = 146.0167, found 146.0173.

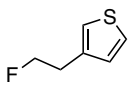

3-(2-fluoroethyl)thiophene (3-52). General procedure F was followed using salt **3-15** (178.0 mg, 1.5 mmol, 1.5 equiv) epoxide **3-23** (168.8 mg, 0.625 mmol, 2.5 equiv), THF (0.4 mL), 2-(thiophen-3-yl)ethan-1-ol (32.1 mg, 1.0 mmol, 1.0 equiv), 4-(trifluoromethyl)benzenesulfonyl fluoride (62.7 mg, 0.275 mmol, 1.1 equiv), and THF (0.25 mL). ^{1}HNMR was used to determine the yield (54% yield). The product was not isolated to volatility.

Control Reactions A series of control reactions were investigated by altering and/or excluding certain components of the reaction. This is intended to probe any background or side reactions taking place. They also ensure that the reaction is being promoted by the P_1-*t*-Bu produced from the activation of the precatalyst system. The results of these control reactions are compiled below in Table A3-8. General procedure B was followed for each entry.

General Procedure Used for control reactions (G): since a pre-activation procedure was required for deoxyfluorination reactions with the cycpP_1 precatalyst, a pre-activation procedure was used for control reactions that employed epoxide **3-23**. If epoxide was excluded from the control reaction all reagents were added sequentially inside a nitrogen filled glovebox. Pre-activation procedure: in a nitrogen filled glovebox an oven-dried 1 dram vial was charged with a magnetic stir bar, basic "reagent" (0.075 mmol, 1.5 equiv), THF (0.125 mL, 0.5 M) and epoxide **3-23** (0.1 mmol, 2 equiv to basic "reagent"). The vial was capped with a PTFE-lined cap (ThermoFisher, C4015-1A), removed from the glovebox and placed in a preheated aluminum reaction block at 80 °C for 20 minutes. After 20 minutes the pre-activation solution was cooled to room temperature and taken into a nitrogen filled glovebox. Alcohol (0.05 mmol, 1 equiv) and sulfonyl fluoride (0.055 mmol, 1.1 equiv) were added, the vial was recapped, removed from the glovebox and placed in an aluminum reaction block at 25 °C with stirring for 24 h. Dibromomethane (1 equiv, 0.1 mmol 7 μL) internal standard was added to the reaction solution, a 50 μL aliquot was taken and added to an NMR tube, then diluted with CDCl3. ^{1}HNMR spectroscopy was used to determine the yield of product.

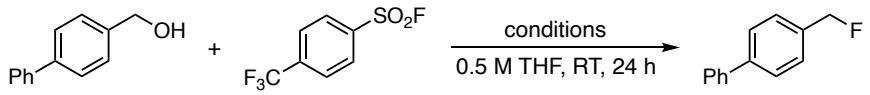

Table A3-8: Control reactions for the deoxyfluorination reaction of [1,1'-biphenyl]-4-ylmethanol with various basic promoters. Result indicate P_1-*t*-Bu is the active promoter and is only generated with salt **3-15** and epoxide **3-23** are in solution.

Entry	Conditions	Results
1	1.5 equiv salt **3-15** + 2.0 equiv epoxide **3-23**	70%
2	1.5 equiv P_1-*t*-Bu	80%
3	1.5 equiv salt **3-15**	0%
4	1.5 equiv Bu_4NOAc + 2.0 equiv Epoxide **3-23**	0%

5	1.5 equiv Bu_4NOAc	0%
6	No Base	0%

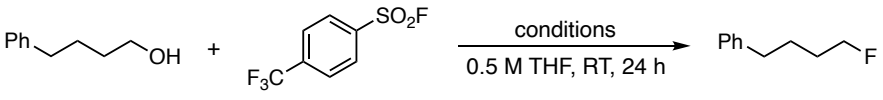

Table A3-9: Control reactions for the deoxyfluorination reaction of 4-phenylbutan-1-ol with various basic promoters. Result indicate P_1-*t*-Bu is the active promoter and is only generated with salt **3-15** and epoxide **3-23** are in solution.

Entry	Conditions	Results
1	1.5 equiv salt **3-15** + 2.0 equiv epoxide **3-23**	60%
2	1.5 equiv P_1-*t*-Bu	86%
3	1.5 equiv salt **3-15**	0%
4	1.5 equiv Bu_4NOAc + 2.0 equiv Epoxide **3-23**	0%
5	1.5 equiv Bu_4NOAc	0%
6	No Base	0%

A3.5 Superbase Salt 3-16 Activation

To note, Garrett preformed most of the work in this section. This section is critical to this project therefore I have included all of his work here.

A3.5.1 Activation Optimization

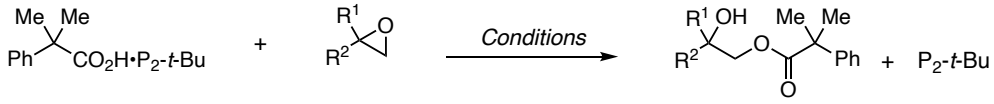

General Activation Procedure: Activation studies were carried out under an atmosphere of nitrogen and in deuterated solvents. An oven-dried 1 dram vial (ThermoFisher, C4015-1) was charged with a magnetic stir bar and salt **3-16** (26.6 mg, 0.05 mmol, 1 equiv) open to air. The vial was brought into a nitrogen filled glovebox where deuterated solvent (0.1 mL, 0.5 M) and epoxide additive (0.1 mmol, 2 equiv) were added successively. The vial was sealed with a PTFE-lined cap (ThermoFisher, C4015-1A), removed from the glovebox, placed in a preheated aluminum reaction block and stirred for the indicated time. The vial was brought into a nitrogen filled glovebox where

the reaction solution was diluted with deuterated solvent (0.4 mL, total of 0.5 mL), transferred to an NMR tube that was capped and sealed with parafilm wax. ^{1}HNMR and ^{31}P NMR spectroscopy were used to assess each reaction and determine the amount of free base produced and yield of the alcohol byproduct according to the process described below.

Process for Evaluating Activation: This section outlines how we estimate the percentage of free P_2-*t*-Bu and the alcohol byproduct as a result of the activation reaction. The amount of free base can be estimated using ^{31}P NMR spectroscopy by evaluating the position of the two phosphorus peaks on the baseline. Completely protonated P_2-*t*-Bu, in the form of precatalyst salt **3-16**, has two doublets at 16.2 and 13.6 ppm, while the free base has two doublets at 14.8 and -6.7 ppm. To gain an understanding of what varying degrees of activation looks like *in situ*, we prepared a series of solutions by mixing commercial P_2-*t*-Bu with diMeP_2 at various ratios on a 0.1 mmol scale. Figure **A3-12** shows 0%, 10%, 25%, 50%, 75%, 90%, and 100% free base mixtures. The ^{31}P NMR spectra of activation studies were compared directly to these spectra to evaluate the percentage of free base generated. The amount of the alcohol byproduct formed in the reaction was determined using ^{1}H NMR spectroscopy. After the completion of the activation reaction, 1 equiv of 1,3,5-trimethoxybenzene internal standard was added to the reaction solution. The percentage of the byproduct was then evaluated relative to the integration of the standard peaks. The amount of freebase was determined using the described estimation method and confirmed by the amount of the byproduct that was formed, which always matches well with the estimated amount of freebase.

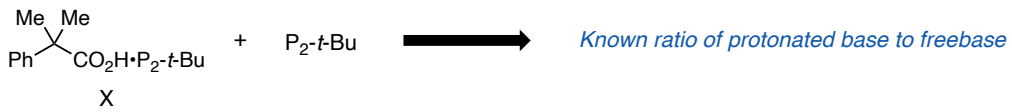

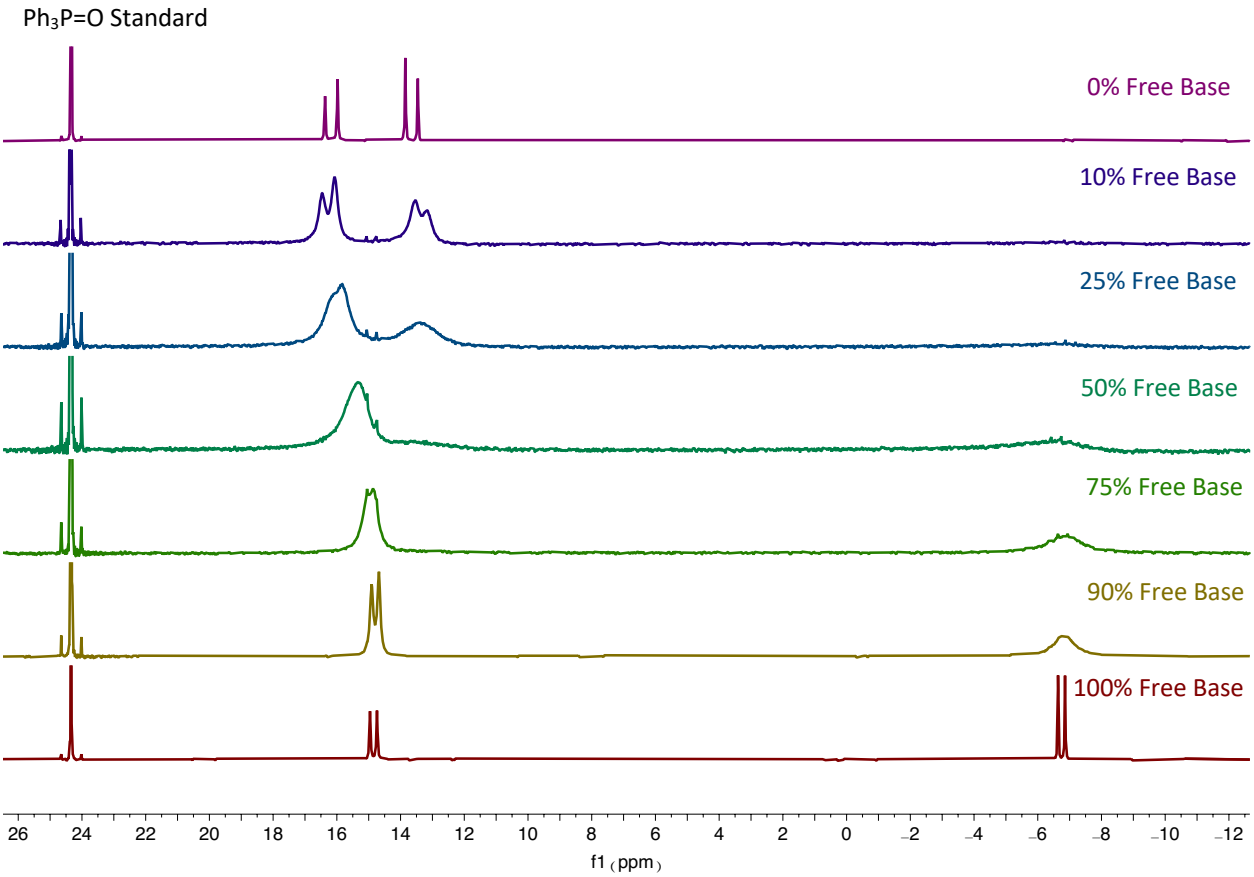

Figure A3-12: Stacked ^{31}P NMR spectra of various percentages of the free base of P_2-*t*-Bu.

Examination of Epoxide Additives: We began our investigation with the general activation procedure and epoxide **3-23**, as this was the most ideal structure for rapid and facile activation of salt **3-15**. The activation studies were run at 80 °C for 24 hours. After testing, we found that epoxide **3-23** only activated diMeP_2 to 40% free base with 49% byproduct formation (Figure A3-15). In an effort to achieve complete formation of free base, we investigated a series of aryl-substituted epoxide structures (Figure A3-15). None produced greater than 50% free base under the same reaction conditions. Figure **A3-13** shows the ^{31}P NMR and 1H NMR spectra for an example activation study using **epoxide 3-19**. Only 40% freebase and 44% byproduct is observed.

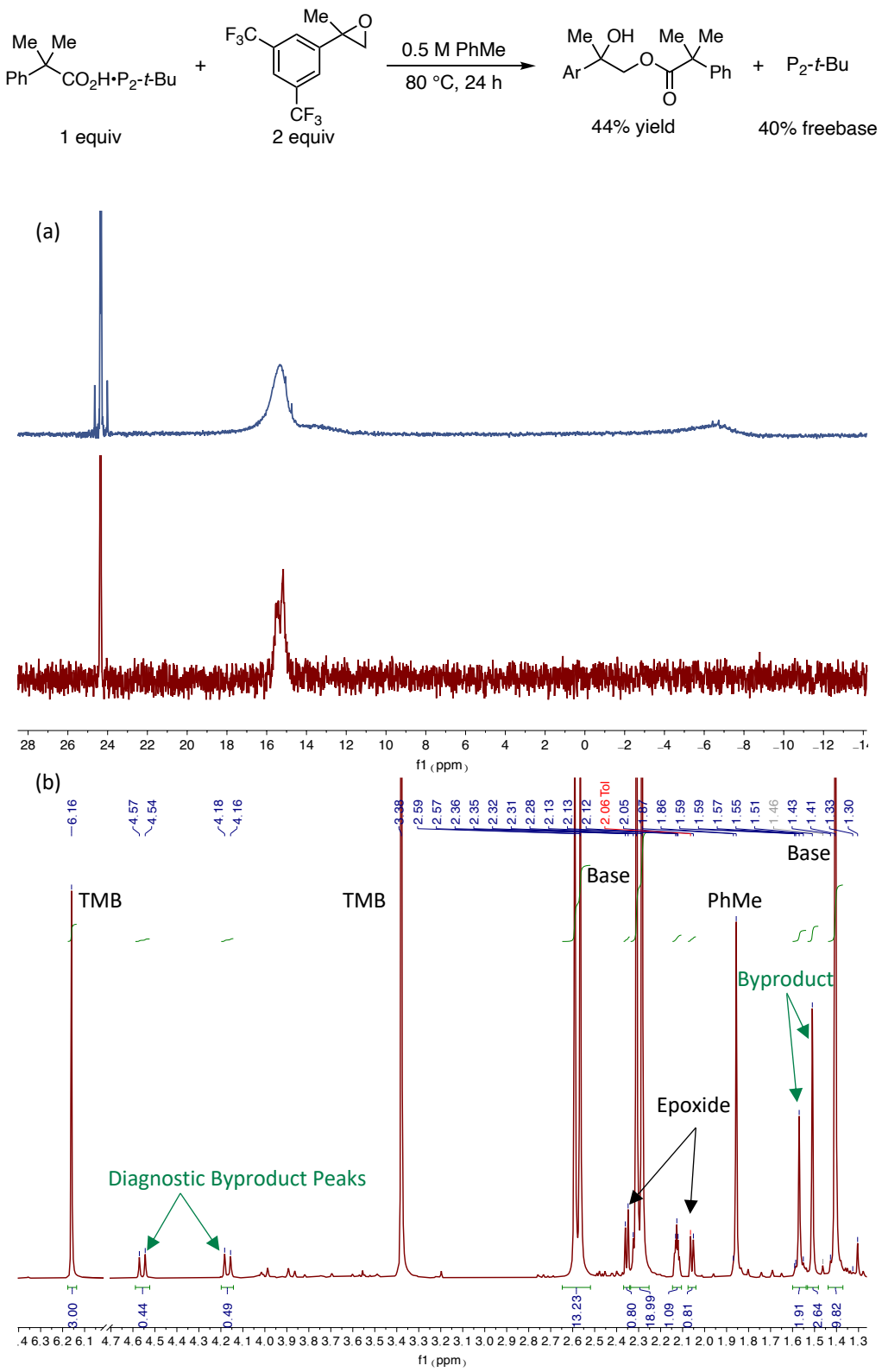

Figure A3-13: (a) ^{31}P NMR spectrum of 50% salt **3-16** mixed with 50% P$_2$-*t*-Bu overlayed with ^{31}P NMR spectrum of epoxide **3-23** activation reaction. [a]Peak at 24 ppm corresponds to

triphenylphosphine oxide standard. (b) ^{1}H NMR spectrum of epoxide **3-23** activation reaction with byproduct peaks labeled and integrated compared to 1,3,5-trimethoxybenzene internal standard.

Through investigating epoxide structures, it became evident that aryl-substituted epoxides were not able to exceed 50% conversion to free base, regardless of their rate of activation. Our hypothesis for this phenomenon is that the activation reaction reaches its equilibrium point at 50% conversion to the free base. To test this, we studied the forward and reverse reactions of the precatalyst activation, utilizing epoxide **3-19** due to its slower rate of activation allowing for more facile data collection. The forward reaction was set up with one equivalent of salt **3-16** and two equivalents of epoxide **3-19** and the reverse was set up with one equivalent of commercial P_2-*t*-Bu, one equivalent of epoxide **3-19**, and one equivalent of byproduct. Each reaction was run in toluene at 40 °C over the course of seven hours with data points collected every fifteen minutes for the first hour and every hour for the following six hours. For each time point, the sample was quenched with $CDCl_3$ and 1,3,5-trimethoxybenzene internal standard was added. The amount of epoxide **3-19** and byproduct in the crude reaction mixture were evaluated *via* ^{1}H NMR spectroscopy. The results show the forward and reverse reactions converge at 50% conversion (Figure **A3-14**), indicating that the activation of salt **3-16** using aryl epoxides is limited by the equilibrium of the reaction.

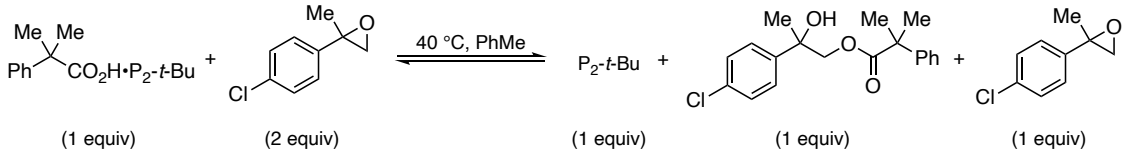

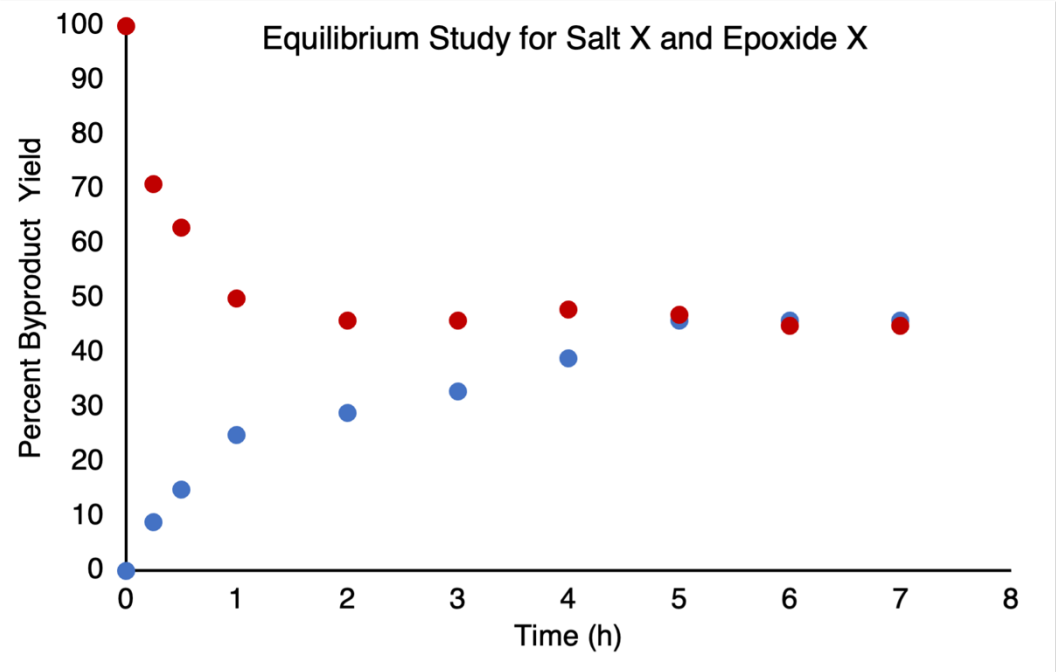

Figure A3-14: Equilibrium study showing forward and reverse activation reaction for epoxide **3-19**.

With an understanding of the equilibrium limitations of the aryl-substituted epoxides, we investigated other epoxide structures, which would increase the energy gap between the starting materials and products, promoting the formation of the byproduct and free P_2-*t*-Bu (Figure A3-15**b**). Garrett investigated all epoxides shown in Figure A3-15a and found that none of the epoxides exceeded 50% activation. The epoxides shown in Figure A3-15b demonstrate moderate activation, up to 70% generation of the free base. Epoxide **3-21** was successful in generating 90% of the free base. Figure A3-15 shows the spectrum of the activation of salt **3-16** using epoxide **3-21** compared with the reference spectrum for 90% conversion to free base. We propose epoxide **x** as the most effective additive for salt **3-16** activation due to added ring strain as a result of the spirocyclic structure.

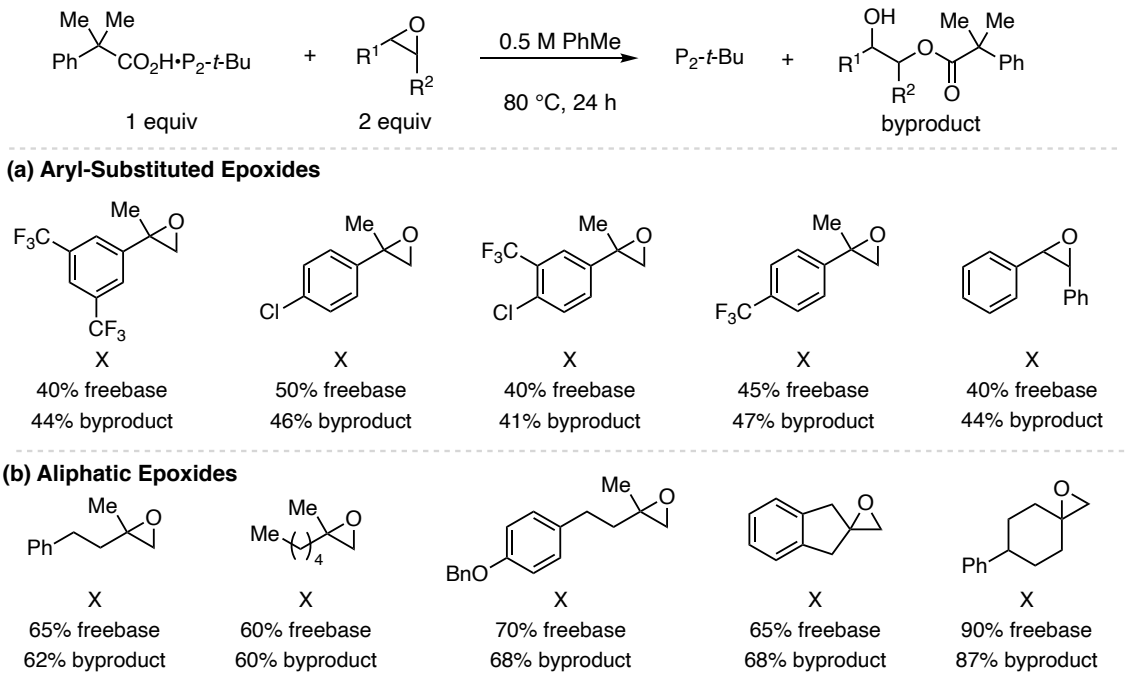

Figure A3-15. (a) Aryl epoxide structures and their activation yields. (b) New epoxide structures and their activation yields. Shown are the percentages of free base and yields of alcohol byproduct(s).

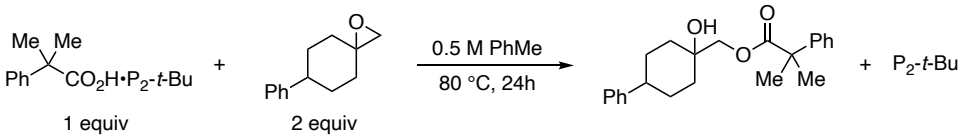

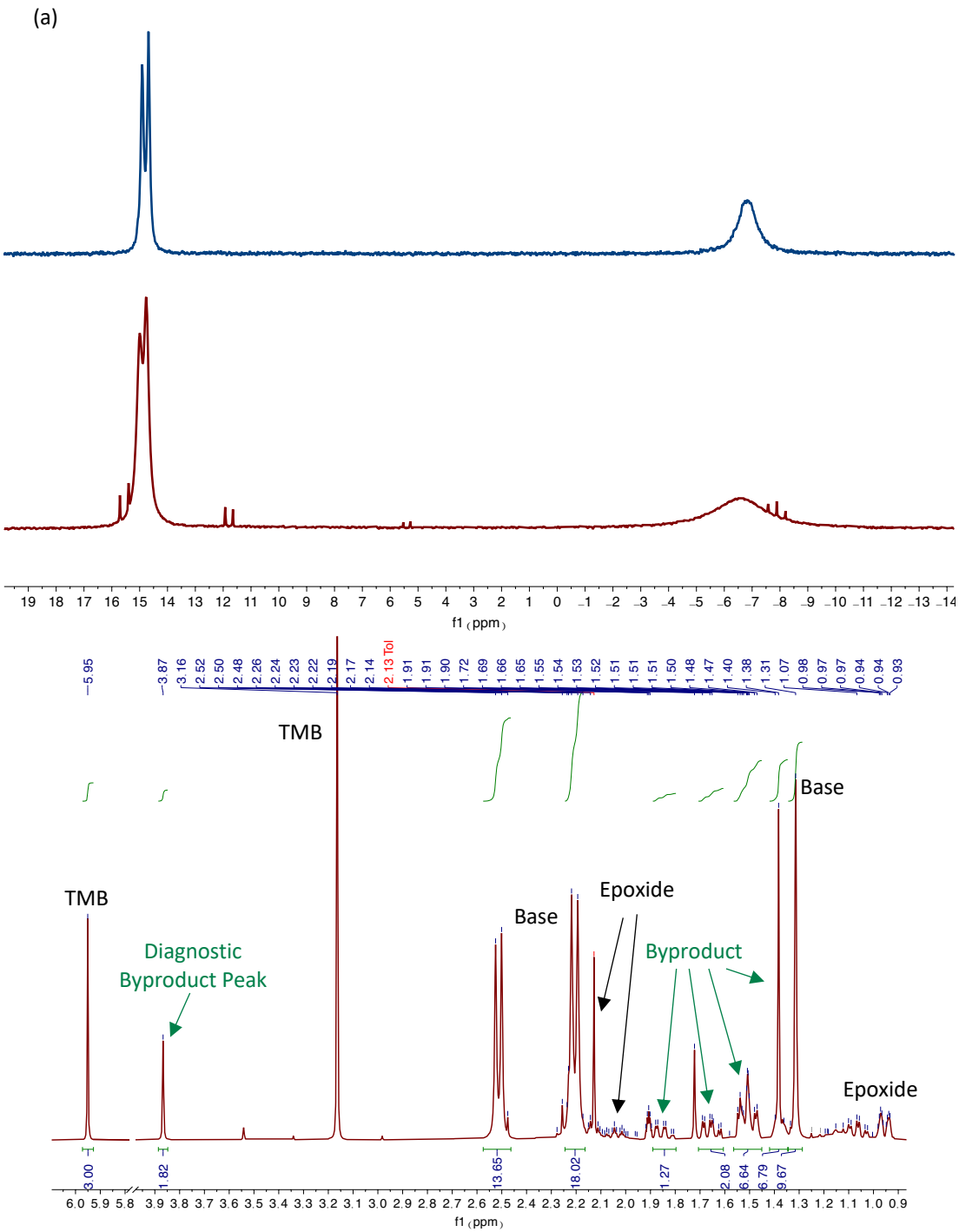

Figure A3-16: (a) ^{31}P NMR spectrum of 10% salt **3-16** mixed with 90% P_2-*t*-Bu overlayed with ^{31}P NMR spectrum of epoxide **3-21** activation reaction. (b) ^{1}H NMR spectrum of epoxide **3-21** activation reaction.

Activation Behavior Under Various Reaction Conditions

This section outlines the effectiveness of epoxide **3-21** at activating salt **3-16** under various reaction conditions (Table A3-10). Entry 1 shows the initial conditions that were used to evaluate the utility of epoxide structures. This shows the behavior of this activation system is in a variety of solvents, temperatures, concentrations, and reaction times.

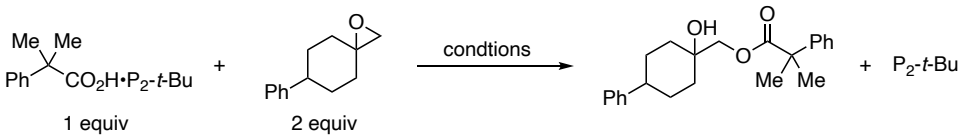

Table A3-10: Data for the activation of salt **3-16** with epoxide **3-21** under various conditions. Entry 1 indicates previously optimized conditions.

Entry	Conditions	Free Base Yield	Byproduct Yield
1	80 °C, 24h, 0.5M in PhMe	90%	80%
2	80 °C, 3h, 0.5M in PhMe	50%	54%
3	80 °C, 24h, 1M in THF	80%	88%
4	80 °C, 3h, 1M in THF	70%	83%
5	40 °C, 24h, 1M in PhMe	45%	52%
6	40 °C, 24h, 1M in THF	55%	62%
7	60 °C, 3h, 1M in THF	70%	70%

A3.6 diMeP$_2$ Salt System Reaction Applications

A3.6.1 Catalytic Oxa/Aza-Michael Addition Reaction

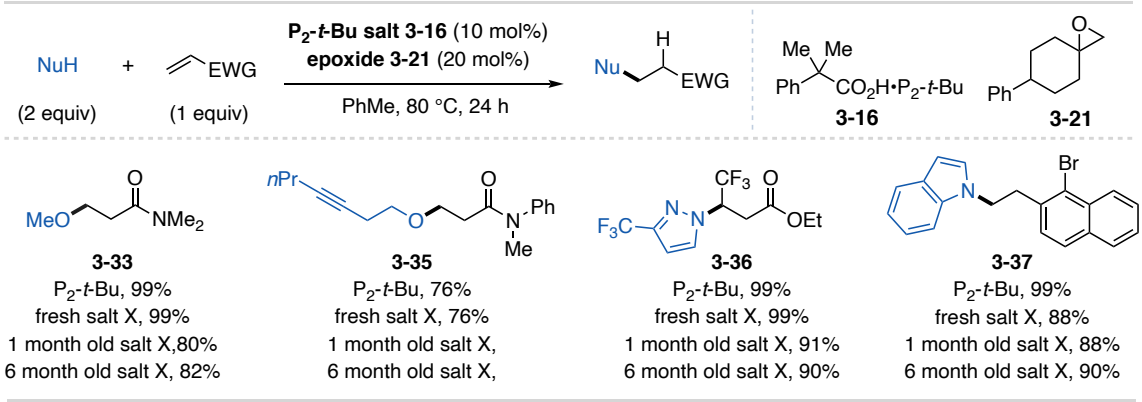

Figure A3-17: Substrate table of oxa/aza-Michael addition reactions run using P$_2$-*t*-Bu catalyst systems stored in various environments. [i]Reaction run in DMSO instead of PhMe.

Note: The salt **3-16** reaction was run using salts stored in a series of environments as discussed in Section A3.2 The results are shown in Figure A3-17.

General Procedure Using a Schlenk Line (A): An oven-dried 1 dram vial (ThermoFisher, C4015-1) was charged with a magnetic stir bar, salt **3-16** (53.2 mg, 0.10 mmol, 10 mol%), and epoxide **3-21** (37.6 mg, 0.20 mmol, 20 mol%). For solid Michael acceptors and pronucleophiles, the Michael acceptor (1.0 mmol, 1.0 equiv) and pronucleophile (2.0 mmol, 2.0 equiv) were added to the vial. The vial was sealed with a PTFE lined screw cap (ThermoFisher, C4015-A) and evacuated then flushed with nitrogen three times on a Schlenk manifold line. Toluene (2.0 mL, 0.5 M) was added to the vial *via* N_2-flushed syringe. For liquid Michael acceptors and pronucleophiles, the Michael acceptor (1.0 mmol, 1.0 equiv) and pronucleophile (2.0 mmol, 2.0 equiv) were added to the vial *via* N_2-flushed syringe. The manifold line was removed from the vial and the cap was wrapped in parafilm and PVC tape. The vial was placed into a preheated aluminum reaction block at 80 °C and stirred for 24 h. The reaction solution was cooled to room temperature and dibromomethane (70 μL, 1.0 mmol, 1.0 equiv) was added to the reaction solution, a 50 μL aliquot was taken and added to an NMR tube, then diluted with $CDCl_3$. ^{1}HNMR spectroscopy was used to determine the yield of the reaction. The crude reaction material was subjected to flash chromatography to yield purified product.

General Procedure Using a Nitrogen Filled Glovebox (B): An oven-dried 1 dram vial (ThermoFisher, C4015-1) was charged with a magnetic stir bar, salt **3-16** (53.2 mg, 0.10 mmol, 10 mol%), and epoxide **3-21** (37.6 mg, 0.20 mmol, 20 mol%). For solid pronucleophiles and Michael acceptors, the pronucleophile (2.0 mmol, 2.0 equiv) and Michael acceptor (1.0 mmol, 1.0 equiv) were added to the vial. The vial was brought into a nitrogen filled glovebox and PhMe (2 mL, 0.5M) was added to the vial. For liquid pronucleophiles and Michael acceptors, pronucleophile

(2.0 mmol, 2.0 equiv) and Michael acceptor (1.0 mmol, 1.0 equiv) were added to the vial *via* syringe. The vial was sealed with a PTFE lined screw cap (ThermoFisher, C4015-A), removed from the glovebox, and placed into a preheated aluminum reaction block at 80 °C and stirred for 24 h. The solution was cooled to room temperature and dibromomethane (1.0 mmol, 70 µL, 1.0 equiv) internal standard was added to the reaction solution, a 50 µL aliquot was taken and added to an NMR tube, then diluted with $CDCl_3$. The product was purified *via* silica gel chromatography.

Reaction and Characterization Data

Substrate Characterization: The substrates were subjected to flash column chromatography to yield purified products. The purification conditions and characterization data are given below. These substrates were prepared and purified by Garrett.

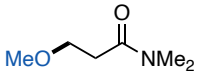

3-Methoxy-*N*,*N*-dimethylpropanamide (3-33). General procedure A was followed using *N*,*N*-dimethylacrylamide (0.099 g, 1.0 mmol, 1.0 equiv), methanol (81 µL, 2.0 mmol, 2.0 equiv), salt **3-16** (53.2 mg, 0.1 mmol, 10 mol%), and epoxide **3-21** (37.6 mg, 0.2 mmol, 20 mol%) in 2 mL of PhMe for 24 h. ^{1}H NMR was used to determine the yield (99% yield). An authentic sample of this product was prepared *via* the general procedure B. The product was purified *via* silica gel chromatography and PMA stain using 10% EtOAc in hexanes to afford **3-33** as a colorless oil (98.1 mg, 0.75 mmol, 75% yield). **^{1}H NMR** (400 MHz, $CDCl_3$) δ 3.69 (t, J = 6.6 Hz, 2H), 3.34 (s, 3H), 3.00 (s, 3H), 2.93 (s, 3H), 2.58 (t, J = 6.6 Hz, 2H); **^{13}C NMR** (101 MHz, $CDCl_3$) δ 170.9, 68.8, 58.9, 37.3, 35.3, 33.6.

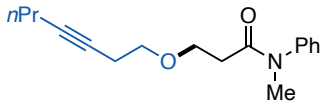

3-(Hept-3-yn-1-yloxy)-*N*-methyl-*N*-phenylpropanamide (3-35). General procedure A was followed using *N*-methyl-*N*-phenylprop-2-enamide (161.0 mg, 1.0 mmol, 1.0 equiv), 3-heptyn-1-ol (0.25 mL, 2.0 mmol, 2.0 equiv), salt **3-**

16 (53.2 mg, 0.1 mmol, 10 mol%), and epoxide **3-21** (37.6 mg, 0.2 mmol, 20 mol%) in 2 mL PhMe for 24 h. ^{1}H NMR was used to determine the yield (74% yield). An authentic sample of this product was prepared *via* the general procedure B. The product was purified *via* silica gel chromatography using 20% EtOAc in hexanes to afford **3-35** as a colorless oil (167.6 mg, 0.61 mmol, 61% yield). **^{1}H NMR** (400 MHz, $CDCl_3$) δ 7.46-7.26 (m, 3H), 7.24-7.17 (m, 2H), 3.71 (t, *J* = 6.8 Hz, 2H), 3.47 (t, *J* = 7.1 Hz, 2H), 3.27 (s, 3H), 2.43-2.33 (m, 4H), 2.10 (tt, *J* = 7.0, 2.4 Hz, 2H), 1.48 (h, *J* = 7.3 Hz, 2H), 0.94 (t, *J* = 7.4 Hz, 3H); **^{13}C NMR** (101 MHz, $CDCl_3$) δ 144.0, 129.8, 127.9, 127.5, 81.2, 76.8, 69.9, 67.2, 37.3, 34.6, 22.4, 20.8, 20.1, 13.5.

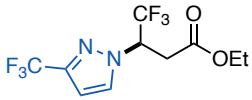

Ethyl-4,4,4-trifluoro-3-(3-(trifluoromethyl)-1*H*-pyrazol-1-yl)-butanoate (3-36). General procedure A was followed using ethyl 4,4,4-trifluorocrotonate (0.13 mL, 1.0 mmol, 1.0 equiv), 3-(trifluoromethyl)pyrazole (0.272 g, 2.0 mmol, 2.0 equiv), salt **3-16** (53.2 mg, 0.1 mmol, 10 mol%), and epoxide **3-21** (37.6 mg, 0.2 mmol, 20 mol%) in 2 mL PhMe for 24 h. ^{1}H NMR was used to determine the yield (99% yield). An authentic sample of this product was prepared *via* the general procedure B. The product was purified *via* silica gel chromatography using 20% EtOAc in hexanes to afford **3-36** as a colorless oil (152.1 mg, 0.50 mmol, 50% yield). **^{1}H NMR** (400 MHz, $CDCl_3$) δ 7.60 (d, *J* = 2.5 Hz, 2H), 6.59 (d, *J* = 2.5 Hz, 2H), 5.25 (dqd, *J* = 10.6, 6.9, 3.6 Hz, 1H), 4.11 (qd, *J* = 7.1, 1.4 Hz, 2H), 3.54 (dd *J* = 17.2, 10.5 Hz, 1H), 3.07 (dd, *J* = 17.2, 3.6 Hz, 1H), 1.18 (t, *J* = 7.1 Hz, 3H); **^{19}F NMR** (376 MHz, $CDCl_3$) δ - 62.4 (s, 3F), -74.8 (s, 3F); **^{13}C NMR** (101 MHz, $CDCl_3$) δ 168.5, 144.1 (q, *J* = 38.8 Hz), 132.8, 124.7, 122.1 (d, *J* = 41.0 Hz), 119.4 (d, *J* = 54.1 Hz), 105.5 (q, *J* = 2.1 Hz), 61.8, 60.0 (q, *J* = 32.4 Hz), 32.7, 14.0.

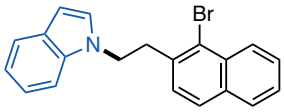

1-(2-(1-bromonaphthalen-2-yl)ethyl)-1*H*-indole (3-37). General procedure A was followed using 1-bromo-2-vinylnaphthalene (0.233g, 1.0 mmol, 1.0 equiv), 1*H*-indole (0.234 g, 2.0 mmol, 2.0 equiv), salt **3-16** (53.2 mg, 0.1 mmol, 10 mol%), and epoxide **3-21** (37.6 mg, 0.2 mmol, 20 mol%) in 2 mL DMSO for 24 h. ^{1}H NMR was used to determine the yield (99% yield). An authentic sample of this product was prepared *via* the general procedure B. The product was purified *via* silica gel chromatography using 5% EtOAc in hexanes with 2% NEt_3 to neutralize the silica to afford **3-37** as a white solid (295.0 mg, 0.84 mmol, 84% yield). **^{1}H NMR** (400 MHz, $CDCl_3$) δ 8.36 (dd, *J* = 8.5, 1.2 Hz, 1H), 7.80 (dd, *J* = 8.1, 1.3 Hz, 1H), 7.70-7.58 (m, 3H), 7.56-7.45 (m, 2H), 7.23 (t, *J* = 7.5 Hz, 1H), 7.13 (t, *J* = 7.4 Hz, 1H), 7.07 (d, *J* = 8.3 Hz, 1H), 6.97 (d, *J* = 3.1 Hz, 1H), 6.46 (dd, *J* = 3.1, 0.9 Hz, 1H), 4.47 (t, *J* = 7.7 Hz, 2H), 3.50 (t, *J* = 7.7 Hz, 2H); **^{13}C NMR** (101 MHz, $CDCl_3$) δ 136.0, 135.8, 131.8 (d, *J* = 1.8 Hz), 126.6, 126.4 (q, *J* = 5.5 Hz), 124.4, 121.6, 120.5, 104.4, 48.7, 36.5.

Control Reactions

This section outlines a series of control reactions to test certain components' roles in the reaction. These were used to support that the P_2-*t*-Bu generated from the salt activation is responsible for catalyzing the reaction and not any other components.

General Procedure Used for control reactions (C): In a nitrogen filled glovebox, an oven-dried 1 dram vial (ThermoFisher, C4015-1) was charged with a magnetic stir bar, basic "catalyst" (0.01 mmol, 10 mol%), pronucleophile (0.2 mmol, 2.0 equiv), PhMe (0.2 mL, 0.5 M), epoxide **3-21** (0.02 mmol, 20 mol% (unless excluded)) and Michael acceptor (0.1 mmol, 1.0 equiv) in successive order. The vial was sealed with a PTFE lined cap (ThermoFisher, C4015-1A), removed from the glovebox, placed in a preheated aluminum reaction block at 80 °C with stirring for 24 h. The

reaction solution was cooled to room temperature and dibromomethane (7 µL, 0.1 mmol, 1.0 equiv) internal standard was added to the reaction solution. A 50 µL aliquot was taken and added to an NMR tube, then diluted with 0.5 mL of $CDCl_3$. ^1H NMR spectroscopy was used to determine the yield of the product.

Table A3-11. Control reactions for methanol addition to *N,N*-dimethylacrylamide.

Entry	Conditions	Results
1	P_2-*t*-Bu freebase	99%
2	10% salt **3-16** + 20% Epoxide **3-21**	99%
3	5% salt **3-16** + 10% Epoxide **3-21**	93%
4	2.5% salt **3-16** + 5% Epoxide **3-21**	33%
5	1% salt **3-16** + 2% Epoxide **3-21**	25%
6	10% salt **3-16** + 20% Epoxide **3-23**	99%
7	10% salt **3-16**	0%
8	20% Epoxide **3-21**	0%
9	10% KO_2CCMe_2Ph +20% Epoxide **3-21**	0%
10	10% KO_2CCMe_2Ph	0%
11	10% Bu_4NOAc + 20% Epoxide **3-21**	0%
12	10% Bu_4NOAc	0%
13	No Base	0%

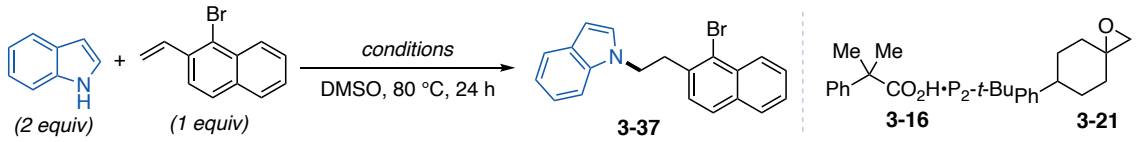

Table A3-12: Control reactions for salt **3-16** catalyzed addition of indole to 1-bromo-2-vinylnaphthalene.

Entry	Conditions	Results
1	P_2-*t*-Bu freebase	99%
2	10% salt **3-16** + 20% Epoxide **3-21**	88%
1	10% salt **3-16**	0%
2	20% Epoxide **3-21**	0%

3	10% KO_2CCMe_2Ph +20% Epoxide **3-21**	0%
4	10% KO_2CCMe_2Ph	0%
5	10% Bu_4NOAc + 20% Epoxide **3-21**	0%
6	10% Bu_4NOAc	0%
7	No Base	0%

A3.6.2 Stoichiometric S_NAr Reactions

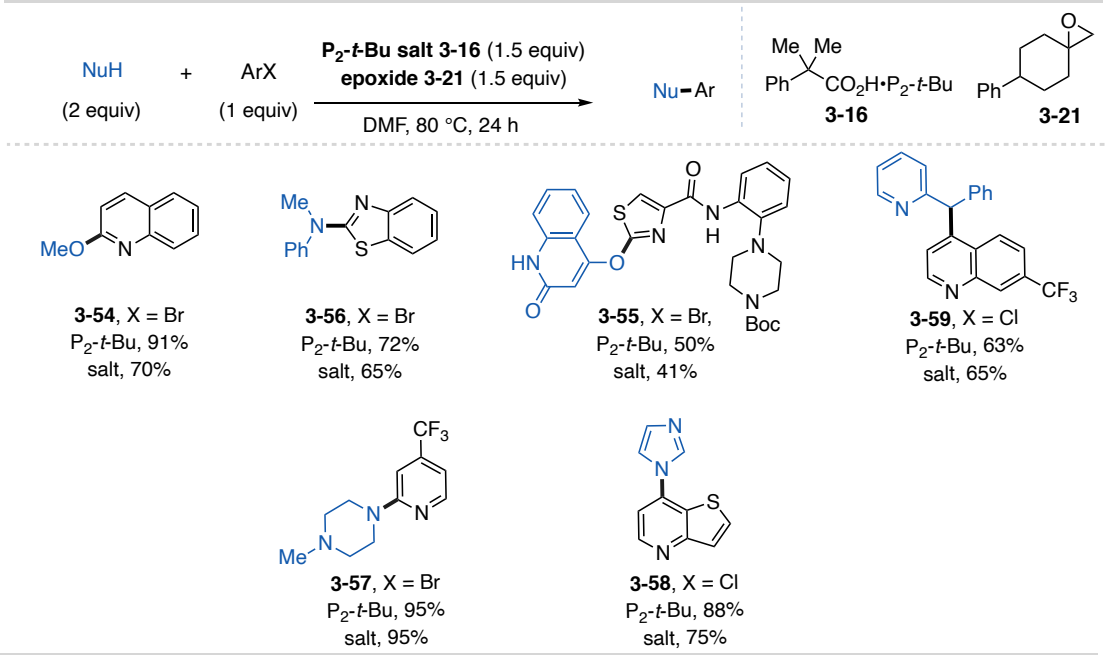

Figure A3-18: Substrate table for S_NAr reactions run using the P_2-*t*-Bu prereagent system compared to P_2-*t*-Bu freebase. Footnotes for substrates.

General Procedure Using P_2-*t*-Bu Freebase in Nitrogen Filled Glovebox (G): An oven-dried 1 dram vial (ThermoFisher, C4015-1) was charged with a magnetic stir bar. For solid electrophiles and pronucleophiles, the electrophile (1.0 mmol, 2.0 equiv) and the pronucleophile (0.5 mmol, 1.0 equiv) were added to the vial. The vial was brought into a nitrogen filled glovebox where solvent (2.0 mL, 0.25M) was added *via* syringe. For liquid electrophiles and pronucleophiles, the electrophile (1.0 mmol, 2.0 equiv) and the pronucleophile (0.5 mmol, 1.0 equiv) were added to the vial. P_2-*t*-Bu (2.0 M solution in THF, 0.375 mL, 0.75 mmol, 1.5 equiv) was added to the vial *via* syringe. The vial was sealed with a PTFE-lined cap (ThermoFisher, C4015-1A) and placed into a

preheated aluminum reaction block at 80 °C and stirred for 24 h. The reaction solution was cooled to room temperature and dibromomethane (35 µL, 0.5 mmol, 1.0 equiv) was added to the reaction solution, a 50 µL aliquot was taken and added to an NMR tube, then diluted with $CDCl_3$. ^{1}HNMR spectroscopy was used to determine the yield of the reaction. The product was purified *via* silica gel chromatography.

General Procedure Using a Schlenk Line (H): An oven-dried 1-dram vial (ThermoFisher, C4015-1) was charged with a magnetic stir bar, salt **3-16** (79.7 mg, 0.15 mmol, 1.5 equiv), and epoxide **3-21** (28.2 mg, 0.15 mmol, 1.5 equiv). The vial was sealed with a PTFE-lined cap (ThermoFisher, C4015-1A) and evacuated then backfilled with nitrogen three times. To the vial, solvent (0.4 mL, 0.25M) was added *via* N_2-flushed syringe and the vial was evacuated then backfilled with nitrogen three times under vigorous stirring. To a separate oven-dried 1 dram vial (ThermoFisher, C4015-1), solid electrophile (0.1 mmol, 1.0 equiv) and solid pronucleophile (0.2 mmol, 2.0 equiv) were added. The vial was sealed with a PTFE-lined cap (ThermoFisher, C4015-1A) and evacuated then backfilled with nitrogen three times. To the vial, DMSO (0.4 mL, 0.25M) liquid electrophile (0.1 mmol, 1.0 equiv) and liquid pronucleophile (0.2 mmol, 2.0 equiv) were added to the vial *via* N_2-flushed syringe and the vial was evacuated then backfilled with nitrogen three times under vigorous stirring. The prereagent solution was transferred to the reagent vial *via* N_2-flushed syringe. The manifold line was removed from the vial and the cap was wrapped in parafilm and PVC tape. The vial was placed in a preheated aluminum reaction block at 80 °C for 24 h with stirring. The reaction solution was cooled to room temperature and dibenzyl ether (19 µL, 0.1 mmol, 1.0 equiv) was added to the reaction solution, a 50 µL aliquot was taken and added to an NMR tube, then diluted with $CDCl_3$. ^{1}HNMR spectroscopy was used to determine the yield of the reaction.

General Procedure Using a Schlenk Line with Preactivation (I): An oven-dried 1-dram vial (ThermoFisher, C4015-1) was charged with a magnetic stir bar, salt **3-16** (79.7 mg, 0.15 mmol, 1.5 equiv), and epoxide **3-21** (28.2 mg, 0.15 mmol, 1.5 equiv). The vial was sealed with a PTFE-lined cap (ThermoFisher, C4015-1A) and evacuated then back filled with nitrogen three times. PhMe (0.2 mL, 0.75 M) was added to the vial *via* N_2-flushed syringe and the vial was evacuated and backfilled with nitrogen three times under vigorous stirring. The manifold line was removed from the vial and the cap was wrapped in parafilm and PVC tape. The vial was placed in a preheated aluminum reaction block at 100 °C for 1 h with stirring. A separate oven-dried 1-dram vial (ThermoFisher, C4015-1) was charged with a magnetic stir bar, solid pronucleophile (0.1 mmol, 1.0 equiv), and solid electrophile (0.2 mmol, 2.0 equiv). The vial was sealed with a PTFE-lined cap (ThermoFisher, C4014-1A) and evacuated and backfilled with nitrogen three times. DMSO (0.2 mL, 0.5 M), liquid electrophile (0.1 mmol, 1.0 eqiuv), liquid pronucleophile (0.2 mmol, 2.0 equiv) was added to the vial *via* N_2-flushed syringe and the vial was evacuated and backfilled with nitrogen three times under vigorous stirring. The vial containing the preactivation solution was removed from the reaction block and placed under a nitrogen atmosphere. The preactivaiton solution was transferred to the starting material solution *via* N_2-flushed syringe. The manifold line was removed from the vial and the cap was wrapped in parafilm and PVC tape. The vial was placed in a preheated aluminum reaction block at 80 °C for 24 h with stirring. The reaction solution was cooled to room temperature and dibenzyl ether (19 µL, 0.1 mmol, 1.0 equiv) was added to the reaction solution, a 50 µL aliquot was taken and added to an NMR tube, then diluted with $CDCl_3$. ^{1}HNMR spectroscopy was used to determine the yield of the reaction.

Reaction and Characterization Data

Substrate Characterization: The substrates were subjected to flash column chromatography to yield purified products. The purification conditions and characterization data are given below. These substrates were prepared and purified by Garrett.

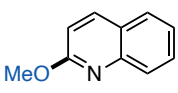

2-Methoxyquinoline (3-54). General procedure H was followed using 2-bromoquinoline (104.1 mg, 0.5 mmol, 1.0 equiv), methanol (60.7 µL, 1.5 mmol, 3.0 equiv), and P_2-*t*-Bu (2.0 M solution in THF, 0.375 mL, 0.75 mmol, 1.5 equiv) in 2 mL DMF for 24 h. ^{1}H NMR was used to determine the yield (70% yield). An authentic sample of this product was prepared *via* the general procedure using G. The product was purified *via* silica gel chromatography using 10% EtOAc in hexanes to afford **3-54** as a yellow oil (68.4 mg, 0.40 mmol, 80% yield). **^{1}H NMR** (400 MHz, $CDCl_3$) δ 7.97 (d, *J* = 9.4 Hz, 1H), 7.87 (dd, *J* = 8.4, 1.5 Hz, 1H), 7.71 (dd, *J* = 8.0, 1.5 Hz, 1H), 7.63 (ddd, *J* = 8.5, 7.0, 1.5 Hz, 1H), 7.38 (ddd, *J* = 8.1, 7.0, 1.2 Hz, 1H), 6.91 (d, *J* = 8.8 Hz, 1H), 4.09 (s, 3H); **^{13}C NMR** (101 MHz, $CDCl_3$) δ 162.4, 146.6, 138.7, 129.5, 127.5, 127.3, 125.1, 124.0, 113.1, 53.4.

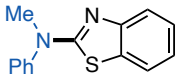

***N*-methyl-*N*-phenylbenzo[d]thiazol-2-amine (3-56).** General procedure H was followed using 2-bromobenzothiazole (107.0 mg, 0.5 mmol, 1.0 equiv), *N*-methylaniline (108.3 µL, 1.0 mmol, 2.0 equiv), and P_2-*t*-Bu (2.0 M solution in THF, 0.375 mL, 0.75 mmol, 1.5 equiv) in 2 mL DMF for 24 h. ^{1}H NMR was used to determine the yield (65% yield). An authentic sample of this product was prepared *via* the general procedure G. The product was purified *via* silica gel chromatography using 5% EtOAc in hexanes to afford **3-56** as a yellow oil (93.2 mg, 0.39 mmol, 78% yield). **^{1}H NMR** (400 MHz, $CDCl_3$) δ 7.62 (d, *J* = 7.5 Hz, 1H),

7.53-7.40 (m, 5H), 7.39-7.27 (m, 2H), 7.07 (t, J = 7.5 Hz, 1H), 3.65 (s, 3H); **^{13}C NMR** (101 MHz, $CDCl_3$) δ 168.3, 152.7, 145.9, 131.2, 130.0, 127.5, 126.0, 125.9, 121.7, 120.5, 119.2, 40.5.

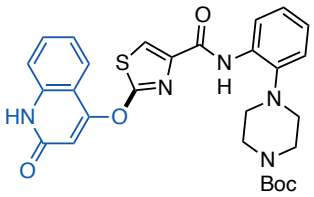

***Tert*-butyl 4-(2-(2-((2-oxo-1,2-dihydroquinolin-4-yl)oxy)thiazole-4-carboxamido)phenyl)piperazine-1-carboxyalte (3-55).** General procedure H was followed on a 0.25 mmol scale using *tert*-butyl 4-(2-(2-bromothiazole-4-carboxamido)phenyl)piperazine-1-carboxylate (116.8 mg, 0.25 mmol, 1.0 equiv), 4-hydroxyquinolin-2(1*H*)-one (80.6 mg, 0.5 mmol, 2.0 equiv), and P_2-*t*-Bu (2.0 M solution in THF, 0.190 mL, 0.375 mmol, 1.5 equiv) in 2 mL DMSO for 24 h. ^{1}H NMR was used to determine the yield (41% yield). An authentic sample of this product was prepared *via* the general procedure G. The product was purified *via* silica gel chromatography using 100% EtOAc to afford **3-55** as a pale-yellow solid (72.9 mg, 0.13 mmol, 51% yield). **^{1}H NMR** (400 MHz, $CDCl_3$) δ 11.31 (s, 1H), 10.02 (s, 1H), 8.53 (d, J = 9.7 Hz, 1H), 8.00 (s, 1H), 7.94 (dd, J = 8.1, 1.4 Hz, 1H), 7.61 (ddd, J = 8.5, 7.3, 1.4 Hz, 1H), 7.41 (d, J = 8.2 Hz, 1H), 7.32 (ddd, J = 8.2, 7.2, 1.0 Hz, 1 H), 7.21 (m, 1H), 7.11 (m, 2H), 6.63 (s, 1H), 3.27 (bs, 4H), 2.77 (t, 4.9 Hz, 4H), 1.44 (s, 9H); **^{13}C NMR** (101 MHz, $CDCl_3$) δ 168.7, 164.1, 161.3, 157.9, 154.4, 145.2, 141.5, 138.7, 132.8, 132.3, 125.6, 124.3, 123.1, 122.6, 120.4, 120.1, 119.8, 116.2, 114.5, 106.3, 79.8, 52.1, 28.4.

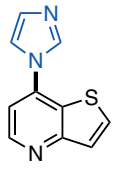

7-(1*H*-Imidazol-1-yl)thieno[3,2-*b*]pyridine (3-58). General procedure I was followed using 7-chlorothieno[3,2-*b*]pyridine (84.8 mg, 0.5 mmol, 1.0 equiv), 1*H*-imidazole (68.1 mg, 1.0 mmol, 2.0 equiv), and P_2-*t*-Bu (2.0 M solution in THF, 0.375 mL, 0.75 mmol, 1.5 equiv) in 2 mL DMF for 24 h. ^{1}H NMR was used to determine the yield (75% yield). An authentic sample of this product was prepared *via* the general procedure G. The product was

purified *via* silica gel chromatography using 5% MeOH in DCM to afford **3-58** as a pale-yellow solid (67.5 mg, 0.34 mmol, 68% yield).**^{1}H NMR** (400 MHz, $CDCl_3$) δ 8.82 (d, *J* = 5.1 MHz, 1H), 8.17 (s, 1H), 7.89 (d, *J* = 5.6 Hz, 1H), 7.71 (d, *J* = 5.5 Hz, 1H), 7.60 (s, 1H), 7.37 (s, 1H), 7.30 (d, *J* = 5.1 Hz, 2H); **^{13}C NMR** (101 Hz, $CDCl_3$) δ 159.1, 148.9, 139.6, 136.1, 131.5, 131.5, 131.3, 126.2, 125.7, 118.2, 111.6.

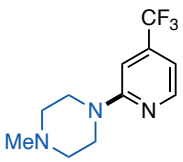

1-Methyl-4-(4-(trifluoromethyl)pyridine-2-yl)piperazine (3-57). General procedure H was followed using 2-chloro-4-(trifluoromethyl)pyridine (61.8 µL, 0.5 mmol, 1.0 equiv), *N*-Methylpiperazine (110.9 µL, 1.0 mmol, 2.0 equiv), and P_2-*t*-Bu (2.0 M solution, 0.375 mL, 0.75 mmol, 1.5 equiv) in 2 mL DMF for 24 h. ^{1}H NMR was used to determine the yield (95% yield). An authentic sample of this product was prepared *via* the general procedure G. The product was purified *via* silica gel chromatography using 5% MeOH in DCM to afford **3-57** as a yellow solid (93.0 mg, 0.38 mmol, 76% yield). **^{1}H NMR** (400 MHz, $CDCl_3$) δ 8.32 (d, *J* = 5.1 Hz, 1H), 6.82 (s, 1H), 6.80 (d, *J* = 5.1 Hz, 1H), 3.65 (t, *J* = 5.1 Hz, 4H), 2.55 (t, *J* = 5.1 Hz, 4H), 2.38 (s, 3H); **^{19}F NMR** (376 MHz, $CDCl_3$) δ -65.1 (s, 3F); **^{13}C NMR** (101 MHz, $CDCl_3$) δ 159.5, 149.2, 139.7 (q, *J* = 99 Hz, 33 Hz), 124.6, 121.9, 108.2, 102.5, 54.7, 46.2, 44.9.

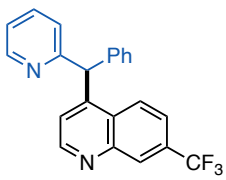

4-(Phenyl(pyridine-2-yl)methyl)-7-(trifluoromethyl)quinoline (3-59). General procedure H was followed using 4-chloro-7-(trifluoromethyl)quinoline (115.8 mg, 0.5 mmol, 1.0 equiv), 2-benzylpyridine (169.2 mg, 1.0 mmol, 2.0 equiv), and P_2-*t*-Bu (2.0 M solution, 0.375 mL, 0.75 mmol, 1.5 equiv) in 2 mL DMF for 24 h. ^{1}H NMR was used to determine the yield (65% yield). An authentic sample

of this product was prepared *via* the general procedure G. The product was purified *via* silica gel chromatography using 40% EtOAc in hexanes to afford **3-59** as a yellow solid (106.8 mg, 0.29 mmol, 58% yield). **^{1}H NMR** (400 MHz, $CDCl_3$) δ 8.91 (d, *J* = 4.5 Hz, 1H), 8.62 (ddd, *J* = 4.9, 1.9, 0.9 Hz, 1H), 8.42 (s, 1H), 8.08 (d, *J* = 8.8 Hz, 1H), 7.63 (qd, *J* = 8.2, 1.8 Hz, 2H), 7.39-7.27 (m, 3H), 7.21 (ddd, *J* = 7.5, 4.9, 1.2 Hz, 1H), 7.18-7.13 (m, 2H), 7.05 (s, 1H), 7.04-7.00 (m, 1H), 6.39 (s, 1H); **^{19}F NMR** (376 MHz, $CDCl_3$) δ -62.7 (s, 3F); **^{13}C NMR** (101 MHz, $CDCl_3$) δ 161.2, 151.6, 150.1, 148.8, 147.7, 140.3, 136.9, 130.8 (q, *J* = 32.9 Hz), 129.4, 129.0, 128.1 (q, *J* = 4.4 Hz), 127.4, 125.6, 125.2, 124.0, 123.5, 122.5, 122.3 (q, *J* = 3.1 Hz), 122.1, 55.5.

Stoichiometric S_NAr Control Reactions

This section outlines a series of control reactions to test certain components' roles in the reaction. These were used to confirm that the P_2-*t*-Bu generated from the salt activation is responsible for promoting the reaction and not any other components.

General Procedure Used for Control Reactions (J): In a nitrogen filled glovebox, an oven-dried 1 dram vial (ThermoFisher, C4015-1) was charged with a magnetic stir bar, pronucleophile (0.10 mmol, 2.0 equiv), electrophile (0.05 mmol, 1.0 equiv), basic reagent (0.075 mmol, 1.5 equiv), epoxide (0.075 mmol, 1.5 equiv), and solvent (0.2 mL, 0.25 M) in successive order. The vial was sealed with a PTFE lined cap (ThermoFisher, C4015-1A), removed from the glovebox, and placed in a preheated aluminum reaction block at 80 °C with stirring for 24 h. The reaction solution was cooled to room temperature and dibenzyl ether (9.5 μL, 0.05 mmol, 1.0 equiv) internal standard was added to the reaction solution. A 50 μL aliquot was taken and added to an NMR tube, then diluted with 0.5 mL of $CDCl_3$. ^{1}H NMR spectroscopy was used to determine the yield of the product.

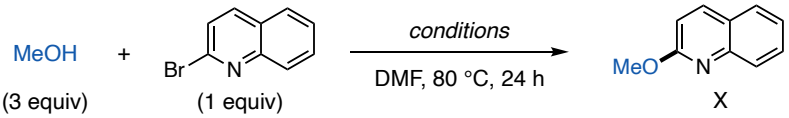

Table A3-13: Control reactions for the salt **3-16** promoted S_NAr between MeOH and 2-bromoquinoline.

Entry	Conditions	% Conversion
1	1.5 equiv P_2-*t*-Bu freebase	91%
2	1.5 equiv salt **3-16** + 1.5 equiv epoxide **3-21**	70%
3	1.5 equiv salt **3-16**	12%
4	1.5 equiv KO_2CCMe_2Ph	9%
5	1.5 equiv KO_2CCMe_2Ph + 1.5 equiv Epoxide **3-21**	17%
6	1.5 equiv Bu_4NOAc	5%
7	1.5 equiv Bu_4NOAc + 1.5 equiv Epoxide **3-21**	9%
8	1.5 equiv Epoxide **X**	0%
9	No Base	0%

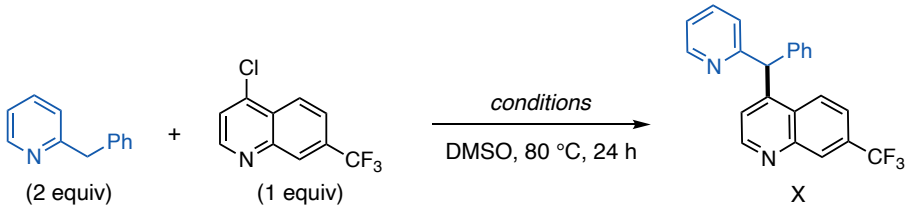

Table A3-14: Control reactions for the salt **3-16** promoted SnAr between 4-chloro-7 (trifluoromethyl) quinoline and 2-benzylpyridine.

Entry	Conditions	% Yield
1	1.5 equiv P_2-*t*-Bu freebase	63%
2	1.5 equiv salt **3-16** + 1.5 equiv epoxide **3-21**	65%
3	1.5 equiv salt **3-16**	0%
4	1.5 equiv KO_2CCMe_2Ph	0%
5	1.5 equiv KO_2CCMe_2Ph + 1.5 equiv Epoxide **3-21**	0%
6	1.5 equiv Bu_4NOAc	0%
7	1.5 equiv Bu_4NOAc + 1.5 equiv Epoxide **3-21**	0%
8	1.5 equiv Epoxide **X**	0%
9	No Base	0%

A3.7 Buchwald-Hartwig Amination

A3.7.1 General Substrate Scope

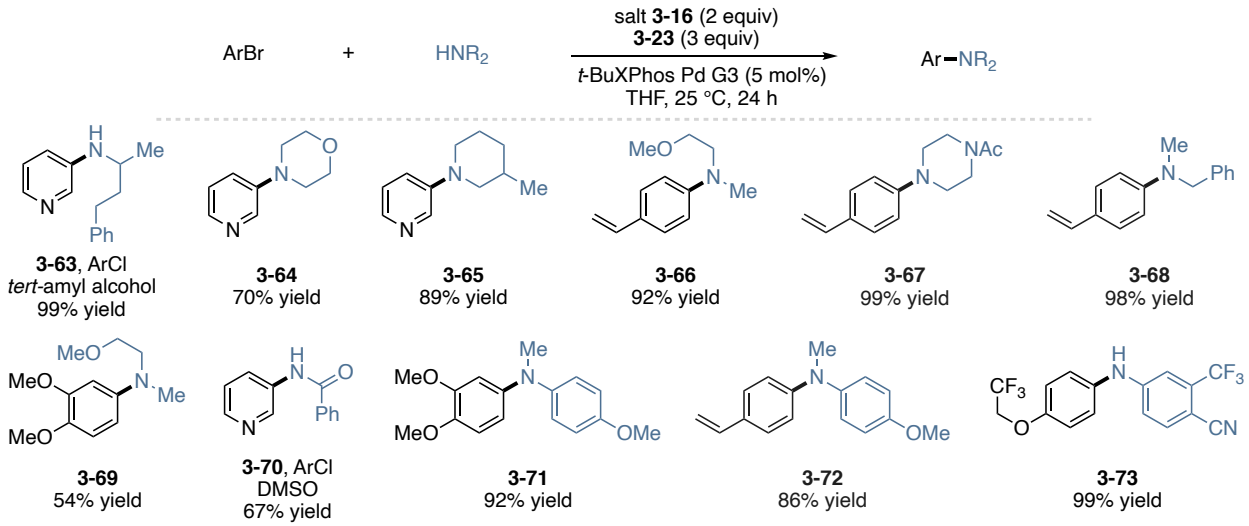

Figure A3-19: Example substrates of Pd-catalysis using salt **3-16** and epoxide **3-23** as the stoichiometric base promotor.

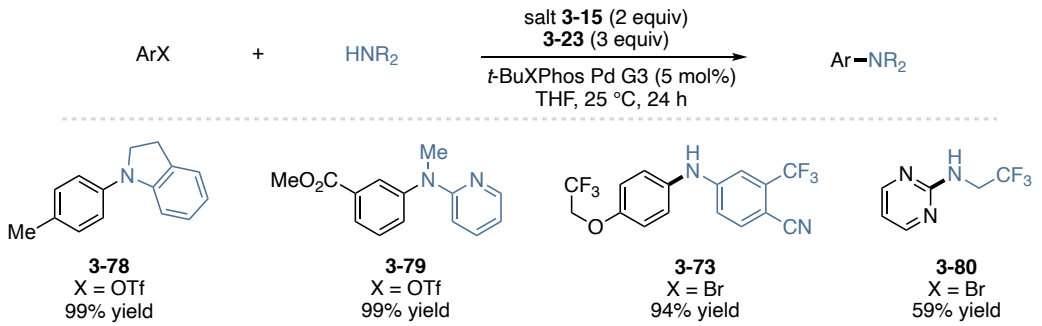

Figure A3-20: Example substrates of Pd-catalysis using salt **3-15** and epoxide **3-23** as the stoichiometric base promotor.

General Procedure Using a Schlenk Line (A): An oven-dried 1-dram vial (ThermoFisher, C4015-1) was charged with a magnetic stir bar, salt **3-16** (XXmg, 0.2 mmol, 2 equiv) or salt **3-15** (XXmg, 0.2 mmol, 2 equiv) and Pd precatalyst (0.005 mmol, 5 mol%). The vial was sealed with a PTFE-lined cap (ThermoFisher, C4015-1A), connected to a Schlenk line manifold, and evacuated then backfilled with nitrogen three times. To the vial, solvent (0.5 mL, 0.2 M) was added *via* N_2-flushed syringe. Aryl halide (0.1 mmol, 1.0 equiv), nucleophile (0.15 mmol, 1.5 equiv), then epoxide **3-23** (0.3 mmol, 3 equiv) were added *via* N_2-flushed syringes. Aryl halide and/or nucleophile were charged to the vial prior to capping and N_2 flushing if they were solids at room

temperature. The reaction vial was then disconnected from the Schlenk line, sealed with parafilm wax, and placed in a preheated aluminum reaction block at 25 °C with magnetic stirring for 24 h. Dibromomethane (7 µL, 0.1 mmol, 1.0 equiv) was added to the reaction solution, a 50 µL aliquot was taken and added to an NMR tube, then diluted with $CDCl_3$. ^{1}HNMR spectroscopy was used to determine the yield of the reaction.

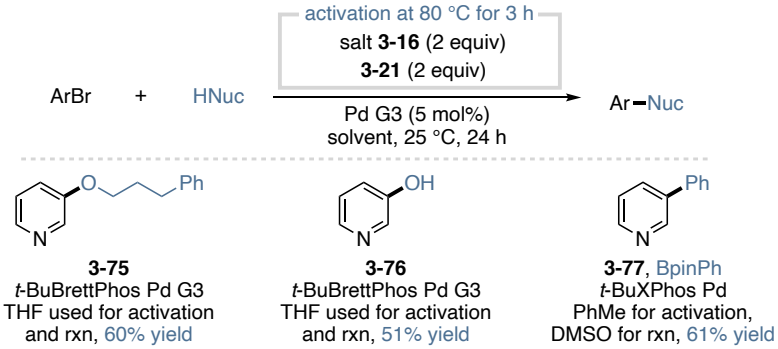

Figure A3-21: Example substrates of Pd-catalysis using salt **3-16** and epoxide **3-21** as the stoichiometric base promotor and a pre-activation procedure.

General Procedure Using a Schlenk Line with Preactivation (B): *Preactivation*. An oven-dried 1-dram vial (ThermoFisher, C4015-1) was charged with a magnetic stir bar, salt **3-16** (XXmg, 0.2 mmol, 2 equiv) and epoxide **3-21** (0.2 mmol, 2.0 equiv). The vial was sealed with a PTFE-lined cap (ThermoFisher, C4015-1A), connected to Schlenk line, and evacuated then backfilled with nitrogen three times. Solvent (0.2 mL, 0.5 M) was added *via* N_2-flushed syringe. The preactivation vial was then disconnected from the Schlenk line, sealed with parafilm wax and electrical tape, and placed in a preheated aluminum reaction block at 80 °C with magnetic stirring for 3 h.

Reagent solution preparation. An oven-dried 1-dram vial (ThermoFisher, C4015-1) was charged with Pd precatalyst (0.005 mmol, 5 mol%). The vial was sealed with a PTFE-lined cap (ThermoFisher, C4015-1A), connected to Schlenk line, and evacuated then backfilled with nitrogen three times. Solvent (0.3 mL) was added *via* N_2-flushed syringe. Aryl halide (0.1 mmol, 1.0 equiv) and nucleophile (0.15 mmol, 1.5 equiv) were added *via* N_2-flushed syringe and the

solution was mixed thoroughly. If the nucleophile was a solid at room temperature it was added prior to capping and N_2-flushing.

Reagent solution addition. The preactivation vial was removed from heat, cooled to room temperature, then connected to a positive pressure of N_2. The reagent solution was then transferred to the preactivation vial *via* N_2-flushed syringe. The combined solution was removed from the positive pressure of N_2, sealed with parafilm wax, and placed in a preheated aluminum reaction block at 25 °C with magnetic stirring for 24 h. Dibromomethane (7 µL, 0.1 mmol, 1.0 equiv) was added to the reaction solution, a 50 µL aliquot was taken and added to an NMR tube, then diluted with $CDCl_3$. ^{1}HNMR spectroscopy was used to determine the yield of the reaction.

Reaction and Characterization Data

Substrate Characterization: The substrates were subjected to flash column chromatography to yield purified products. The purification conditions and characterization data are given below.

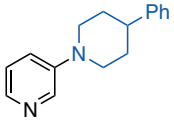

3-(4-phenylpiperidin-1-yl)pyridine. General procedure A was followed using salt **3-16** (106.3 mg, 0.2 mmol, 2.0 equiv), *t*BuXPhos Pd G3 (4.0 mg, 0.005 mmol, 5 mol%), epoxide **3-23** (81.0 mg, 0.3 mmol, 3.0 equiv), 3-bromopyridine (9.6 µL, 0.1 mmol, 1.0 equiv), 4-phenylpiperidine (24.2 mg, 0.15 mmol, 1.5 equiv), and THF (0.5 mL, 0.2 M). ^{1}HNMR was used to determine the yield (96% yield). Silica gel column chromatography with 100% DCM to 5% MeOH/DCM was used to obtain pure product. **^{1}H NMR** (400 MHz, $CDCl_3$) δ 8.42 (d, J = 2.9 Hz, 1H), 8.15 (d, J = 4.5 Hz, 1H), 7.38 (t, J = 7.5 Hz, 2H), 7.33 – 7.18 (m, 4H), 3.88 (dt, J = 11.9, 2.8 Hz, 2H), 2.93 (td, J = 12.2, 2.9 Hz, 2H), 2.73 (ddt, J = 11.9, 7.8, 4.0 Hz, 1H), 2.08 – 1.87 (m, 4H). Characterization data matches previous reports.[7,8]

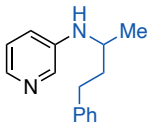

N-(4-phenylbutan-2-yl)pyridin-3-amine. General procedure A was followed using salt **3-16** (106.3 mg, 0.2 mmol, 2.0 equiv), *t*BuXPhos Pd G3 (4.0 mg, 0.005 mmol, 5 mol%), epoxide **3-23** (81.0 mg, 0.3 mmol, 3.0 equiv), 3-chloropyridine (9.5 µL, 0.1 mmol, 1.0 equiv), 4-phenylbutan-2-amine (24.3 µL, 0.15 mmol, 1.5 equiv), and *tert*-amyl alcohol (0.5 mL, 0.2 M). ^{1}HNMR was used to determine the yield (> 99% yield). Silica gel column chromatography with 1%NEt_3/DCM to 8% MeOH/1%NEt_3/DCM was used to obtain pure product. **^{1}H NMR** (400 MHz, $CDCl_3$) δ 8.00 (d, J = 2.9 Hz, 1H), 7.96 (d, J = 4.7 Hz, 1H), 7.33 (t, J = 7.4 Hz, 2H), 7.22 (t, J = 7.4 Hz, 2H), 7.08 (dd, J = 8.3, 4.6 Hz, 1H), 6.83 – 6.76 (m, 1H), 3.52 (dd, J = 12.2, 6.0 Hz, 2H), 2.77 (t, J = 7.8 Hz, 2H), 2.00 – 1.78 (m, 2H), 1.32 – 1.24 (m, 4H). Characterization data matches previous reports.[8]

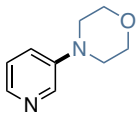

4-(pyridin-3-yl)morpholine. General procedure A was followed using salt **3-16** (106.3 mg, 0.2 mmol, 2.0 equiv), *t*BuXPhos Pd G3 (4.0 mg, 0.005 mmol, 5 mol%), epoxide **3-23** (81.0 mg, 0.3 mmol, 3.0 equiv), 3-bromopyridine (9.6 µL, 0.1 mmol, 1.0 equiv), morpholine (13.1 mg, 0.15 mmol, 1.5 equiv), and THF (0.5 mL, 0.2 M). ^{1}HNMR was used to determine the yield (96% yield). The product was not isolated.

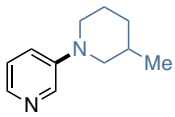

3-(3-methylpiperidin-1-yl)pyridine. General procedure A was followed using salt **3-16** (106.3 mg, 0.2 mmol, 2.0 equiv), *t*BuXPhos Pd G3 (4.0 mg, 0.005 mmol, 5 mol%), epoxide **3-23** (81.0 mg, 0.3 mmol, 3.0 equiv), 3-bromopyridine (9.6 µL, 0.1 mmol, 1.0 equiv), 3-methylpiperidine (14.9 mg, 0.15 mmol, 1.5 equiv), and THF (0.5 mL, 0.2 M). ^{1}HNMR was used to determine the yield (96% yield). The product was not isolated.

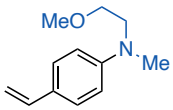

N-(2-methoxyethyl)-N-methyl-4-vinylaniline. General procedure A was followed using salt **3-16** (106.2 mg, 0.2 mmol, 2.0 equiv), *t*BuXPhos Pd G3 (4.0 mg, 0.005 mmol, 5 mol%), epoxide **3-23** (81.0 mg, 0.3 mmol, 3.0 equiv), 4-bromostyrene (13.1 µL, 0.1 mmol, 1.0 equiv), 2-methoxy-*N*-methylethan-1-amine (16.3 µL, 0.15 mmol, 1.5 equiv), and THF (0.5 mL, 0.2 M). ^{1}HNMR was used to determine the yield (92% yield). Silica gel column chromatography with 100% hexanes to 20% EtOAc/hexanes was used to obtain pure product **^{1}H NMR** (400 MHz, $CDCl_3$) δ 7.31 (d, J = 8.6 Hz, 2H), 6.75 – 6.59 (m, 3H), 5.55 (dd, J = 17.6, 1.2 Hz, 1H), 5.03 (d, J = 11.0 Hz, 1H), 3.55 (dt, J = 9.2, 4.6 Hz, 4H), 3.37 (s, 3H), 3.01 (s, 3H).; **^{13}C NMR** (101 MHz, $CDCl_3$) δ 149.1, 136.7, 127.4, 126.1, 112.1, 109.3, 70.3, 59.2, 52.5, 39.1

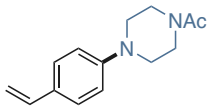

1-(4-(4-vinylphenyl)piperazin-1-yl)ethan-1-one. General procedure A was followed using salt **3-16** (106.2 mg, 0.2 mmol, 2.0 equiv), *t*BuXPhos Pd G3 (4.0 mg, 0.005 mmol, 5 mol%), epoxide **3-23** (81.0 mg, 0.3 mmol, 3.0 equiv), 4-bromostyrene (13.1 µL, 0.1 mmol, 1.0 equiv), 1-(piperazin-1-yl)ethan-1-one (19.2 mg, 0.15 mmol, 1.5 equiv), and THF (0.5 mL, 0.2 M). ^{1}HNMR was used to determine the yield (92% yield). The product was not isolated.

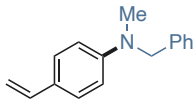

N-benzyl-N-methyl-4-vinylaniline. General procedure A was followed using salt **3-16** (106.2 mg, 0.2 mmol, 2.0 equiv), *t*BuXPhos Pd G3 (4.0 mg, 0.005 mmol, 5 mol%), epoxide **3-23** (81.0 mg, 0.3 mmol, 3.0 equiv), 4-bromostyrene (13.1 µL, 0.1 mmol, 1.0 equiv), *N*-methylbenzylamine (18.2 mg, 0.15 mmol, 1.5 equiv), and THF (0.5 mL, 0.2 M). ^{1}HNMR was used to determine the yield (92% yield). The product was not isolated.

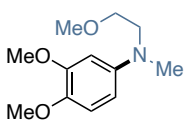

3,4-dimethoxy-N-(2-methoxyethyl)-N-methylaniline. General procedure A was followed using salt **3-16** (106.2 mg, 0.2 mmol, 2.0 equiv), *t*BuXPhos Pd G3 (4.0 mg, 0.005 mmol, 5 mol%), epoxide **3-23** (81.0 mg, 0.3 mmol, 3.0 equiv), 4-bromo-1,2-dimethoxybenzene (14.4 µL, 0.1 mmol, 1.0 equiv), 2-methoxy-*N*-methylethan-1-amine (16.3 µL, 0.15 mmol, 1.5 equiv), and THF (0.5 mL, 0.2 M). ^{1}HNMR was used to determine the yield (92% yield). The product was not isolated.

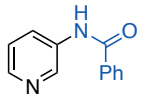

N-(pyridin-3-yl)benzamide. General procedure A was followed using salt **3-16** (106.3 mg, 0.2 mmol, 2.0 equiv), *t*BuBrettPhos Pd G3 (4.3 mg, 0.005 mmol, 5 mol%), epoxide **3-23** (81.0 mg, 0.3 mmol, 3.0 equiv), 3-bromopyridine (mg, 0.1 mmol, 1.0 equiv), benzamide (18.2 mg, 0.15 mmol, 1.5 equiv), and DMSO (0.5 mL, 0.2 M). ^{1}HNMR was used to determine the yield (67% yield). Silica gel column chromatography with 100%hexanes to 75% EtOAc/hexanes was used to obtain pure product. **^{1}H NMR** (400 MHz, $CDCl_3$) δ 8.66 (d, J = 2.6 Hz, 1H), 8.54 (s, 1H), 8.31 (d, J = 4.6 Hz, 1H), 8.27 (d, J = 8.3 Hz, 1H), 7.87 (d, J = 7.3 Hz, 2H), 7.54 (t, J = 7.4 Hz, 1H), 7.45 (t, J = 7.6 Hz, 2H), 7.28 (dd, J = 8.4, 4.7 Hz, 1H). Characterization data matches previous reports.[8]

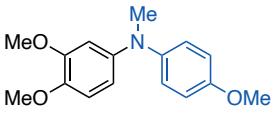

3,4-dimethoxy-N-(4-methoxyphenyl)-N-methylaniline. General procedure A was followed using salt **3-16** (106.3 mg, 0.2 mmol, 2.0 equiv), *t*BuXPhos Pd G3 (4.0 mg, 0.005 mmol, 5 mol%), epoxide **3-23** (81.0 mg, 0.3 mmol, 3.0 equiv), 4-bromo-1,2-dimethoxybenzene (14.4 µL, 0.1 mmol, 1.0 equiv), 4-methoxy-*N*-methylaniline (20.6 mg, 0.15 mmol, 1.5 equiv), and THF (0.5 mL, 0.2 M). ^{1}HNMR was used to determine the yield (92% yield). Preparatory thin layer chromatography with 40%EtOAc/hexanes was used to

obtain pure product. **^{1}H NMR** (400 MHz, $CDCl_3$) δ 6.95 (d, J = 8.9 Hz, 2H), 6.84 (d, J = 9.0 Hz, 2H), 6.79 (d, J = 8.5 Hz, 2H), 6.56 – 6.45 (m, 2H), 3.85 (s, 3H), 3.79 (s, 4H), 3.77 (s, 4H), 3.23 (s, 3H).; **^{13}C NMR** (101 MHz, $CDCl_3$) δ 154.8, 149.6, 144.3, 143.9, 143.6, 122.3, 114.7, 112.3, 111.4, 105.1, 56.5, 55.9, 55.7, 41.2.

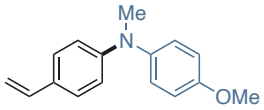

4-methoxy-N-methyl-N-(4-vinylphenyl)aniline. General procedure A was followed using salt **3-16** (106.2 mg, 0.2 mmol, 2.0 equiv), *t*BuXPhos Pd G3 (4.0 mg, 0.005 mmol, 5 mol%), epoxide **3-23** (81.0 mg, 0.3 mmol, 3.0 equiv), 4-bromostyrene (13.1 µL, 0.1 mmol, 1.0 equiv), 4-methoxy-*N*-methylaniline (20.6 mg, 0.15 mmol, 1.5 equiv), and THF (0.5 mL, 0.2 M). ^{1}HNMR was used to determine the yield (92% yield). The product was not isolated.

4-((4-(2,2,2-trifluoroethoxy)phenyl)amino)-2-(trifluoromethyl)benzonitrile. General procedure A was followed using salt **3-16** (106.2 mg, 0.2 mmol, 2.0 equiv), *t*BuXPhos Pd G3 (4.0 mg, 0.005 mmol, 5 mol%), epoxide **3-23** (81.0 mg, 0.3 mmol, 3.0 equiv), 1-bromo-4-(2,2,2-trifluoroethoxy)benzene (25.5 mg, 0.1 mmol, 1.0 equiv), 4-amino-2-(trifluoromethyl)benzonitrile (27.9 mg, 0.15 mmol, 1.5 equiv), and THF (0.5 mL, 0.2 M). ^{1}HNMR was used to determine the yield (92% yield). Silica gel column chromatography with 100% hexanes to 40% EtOAc/hexanes was used to obtain pure product. **^{1}H NMR** (400 MHz, $CDCl_3$) δ 7.57 (dd, J = 8.6, 0.8 Hz, 1H), 7.21 – 7.12 (m, 2H), 7.10 (d, J = 2.4 Hz, 1H), 7.04 – 6.91 (m, 3H), 6.25 (s, 1H), 4.37 (q, J = 8.1 Hz, 2H).

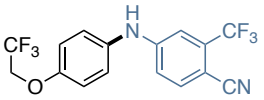

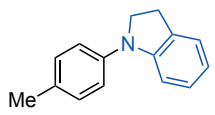

1-(*p*-tolyl)indoline. General procedure A was followed with slight modifications, salt **3-15** (94.9 mg, 0.2 mmol, 2.0equiv), *t*BuXPhos Pd G3 (4.0 mg, 0.005 mmol, 5 mol%), epoxide **3-23** (81.0 mg, 0.3 mmol, 3.0 equiv), *p*-tolyl trifluoromethanesulfonate (17.9 µL, 0.1 mmol, 1.0 equiv), indoline (16.8 µL, 0.15 mmol, 1.5 equiv), and THF (0.5 mL, 0.2 M). ^{1}HNMR was used to determine the yield (>99% yield). Preparatory thin layer chromatography with 10%EtOAc/hexanes was used to obtain pure product.**^{1}H NMR** (400 MHz, $CDCl_3$) δ 7.17 (s, 5H), 7.08 (d, J = 4.2 Hz, 2H), 6.79 – 6.71 (m, 1H), 3.94 (t, J = 8.4 Hz, 2H), 3.14 (t, J = 8.4 Hz, 2H), 2.36 (s, 3H). Characterization data matches previous reports.[10]

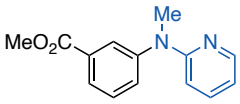

methyl 3-(methyl(pyridin-2-yl)amino)benzoate. General procedure A was followed with slight modifications, salt **3-15** (94.9 mg, 0.2 mmol, 2.0equiv), *t*BuXPhos Pd G3 (4.0 mg, 0.005 mmol, 5 mol%), epoxide **3-23** (81.0 mg, 0.3 mmol, 3.0 equiv), methyl 3-(((trifluoromethyl)sulfonyl)oxy)benzoate (28.4 mg, 0.1 mmol, 1.0 equiv), N-methylpyridin-2-amine (12.3 µL, 0.15 mmol, 1.5 equiv), and THF (0.5 mL, 0.2 M). ^{1}HNMR was used to determine the yield (95% yield). 50% EtOAc/hexanes was used to obtain pure product. **^{1}H NMR** (400 MHz, $CDCl_3$) δ 8.27 – 8.21 (m, 1H), 7.94 (s, 1H), 7.89 – 7.80 (m, 1H), 7.49 – 7.42 (m, 2H), 7.38 – 7.32 (m, 1H), 6.66 (dd, J = 7.2, 5.0 Hz, 1H), 6.57 (dd, J = 8.7, 1.1 Hz, 1H), 3.91 (s, 3H), 3.49 (s, 3H). Characterization data matches previous reports.[10]

4-((4-(2,2,2-trifluoroethoxy)phenyl)amino)-2-(trifluoromethyl)benzonitrile. General

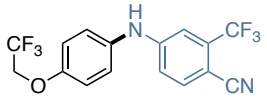

procedure A was followed using salt **3-15** (106.2 mg, 0.2 mmol, 2.0 equiv), *t*BuXPhos Pd G3 (4.0 mg, 0.005 mmol, 5 mol%), epoxide **3-23** (81.0 mg, 0.3 mmol, 3.0 equiv), 1-bromo-4-(2,2,2-trifluoroethoxy)benzene (25.5 mg, 0.1 mmol, 1.0 equiv), 4-amino-2-

(trifluoromethyl)benzonitrile (27.9 mg, 0.15 mmol, 1.5 equiv), and THF (0.5 mL, 0.2 M). ^{1}HNMR was used to determine the yield (94% yield).

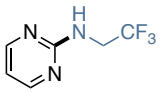

***N*-(2,2,2-trifluoroethyl)pyrimidin-2-amine.** General procedure A was followed using salt **3-15** (106.2 mg, 0.2 mmol, 2.0 equiv), *t*BuXPhos Pd G3 (4.0 mg, 0.005 mmol, 5 mol%), epoxide **3-23** (81.0 mg, 0.3 mmol, 3.0 equiv), 2-bromopyrimidine (16.0 mg, 0.1 mmol, 1.0 equiv), 2,2,2-trifluoroethan-1-amine (14.9 mg, 0.15 mmol, 1.5 equiv), and THF (0.5 mL, 0.2 M). ^{1}HNMR was used to determine the yield (59% yield). The product was not isolated. Characterization data matches previous reports.[11]

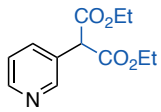

diethyl 2-(pyridin-3-yl)malonate. General procedure A was followed using salt **3-16** (106.3 mg, 0.2 mmol, 2.0 equiv), *t*BuBrettPhos Pd G3 (4.3 mg, 0.005 mmol, 5 mol%), epoxide **3-23** (81.0 mg, 0.3 mmol, 3.0 equiv), 3-chloropyridine (9.5 µL, 0.1 mmol, 1.0 equiv), diethyl malonate (22.5 µL, 0.15 mmol, 1.5 equiv), and *tert*-amyl alcohol (0.5 mL, 0.2 M). ^{1}HNMR was used to determine the yield (61% yield). Silica gel column chromatography with 100% hexanes to 40% EtOAc/hexanes was used to obtain pure product. **^{1}H NMR** (400 MHz, $CDCl_3$) δ 8.56 (dd, J = 3.7, 2.1 Hz, 2H), 7.83 (dd, J = 8.1, 2.2 Hz, 1H), 7.30 (dd, J = 8.0, 4.8 Hz, 1H), 4.61 (s, 1H), 4.26 – 4.15 (m, 4H), 1.25 (t, J = 7.1 Hz, 6H). Characterization data matches previous reports.[8]

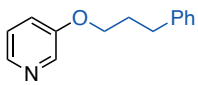

3-(3-phenylpropoxy)pyridine. General procedure B was followed using salt **3-16** (106.3 mg, 0.2 mmol, 2.0 equiv), epoxide **3-21** (37.7 mg, 0.2 mmol, 2.0 equiv), THF (0.2 mL), *t*BuBrettPhos Pd G3 (4.3 mg, 0.005 mmol, 5 mol%), 3-bromopyridine (9.6

µL, 0.1 mmol, 1.0 equiv), 3-phenylpropan-1-ol (20.4 µL, 0.15 mmol, 1.5 equiv), and THF (0.3 mL, 0.2 M total volume). ^{1}HNMR was used to determine the yield (60% yield). Silica gel column chromatography with 100% hexanes to 40% EtOAc/hexanes was used to obtain pure product **^{1}H NMR** (400 MHz, $CDCl_3$) δ 8.32 (d, J = 2.6 Hz, 1H), 8.21 (d, J = 4.4 Hz, 1H), 7.30 (t, J = 7.5 Hz, 2H), 7.24 – 7.13 (m, 5H), 4.00 (t, J = 6.2 Hz, 2H), 2.82 (t, J = 7.6 Hz, 2H), 2.13 (p, J = 6.6 Hz, 3H). Characterization data matches previous reports.[8]

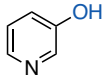

pyridin-3-ol. General procedure B was followed using salt **3-16** (106.3 mg, 0.2 mmol, 2.0 equiv), epoxide **3-21** (37.7 mg, 0.2 mmol, 2.0 equiv), THF (0.2 mL), *t*BuBrettPhos Pd G3 (4.3 mg, 0.005 mmol, 5 mol%), 3-bromopyridine (9.6 mg, 0.1 mmol, 1.0 equiv), water (2.7 µL, 0.15 mmol, 1.5 equiv), and THF (0.3 mL, 0.2 M total volume). ^{1}HNMR was used to determine the yield (51% yield). Product was not isolated. Characterization data matches previous reports.[8]

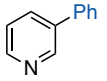

3-phenylpyridine. General procedure B was followed using salt **3-16** (106.3 mg, 0.2 mmol, 2.0 equiv), epoxide **3-21** (37.7 mg, 0.2 mmol, 2.0 equiv), PhMe (0.2 mL), *t*BuXPhos Pd G3 (4.0 mg, 0.005 mmol, 5 mol%), 3-bromopyridine (9.6 mg, 0.1 mmol, 1.0 equiv), 4,4,5,5-tetramethyl-2-phenyl-1,3,2-dioxaborolane (30.6 mg, 0.15 mmol, 1.5 equiv), water (3.6 µL, 0.2 mmol, 2.0 equiv), and DMSO (0.3 mL, 0.2 M total volume). ^{1}HNMR was used to determine the yield (61% yield). Product was not isolated. Characterization data matches previous reports.[8]

A3.7.2 Control Experiments with prereagent use in Pd-catalysis

This section outlines a series of control reactions to test certain components' roles in the reaction. These were used to assess what was responsible for acting as the base-promoter in the reaction and to see if any background processes could be promoting reactivity.

General Procedure for Control Reactions (C): In a nitrogen filled glovebox, an oven-dried 1-dram vial (ThermoFisher, C4015-1) was charged with a magnetic stir bar, basic promoter (0.2 mmol, 2 equiv), epoxide **3-23** (if applicable) (0.3 mmol, 3 equiv), *t*BuXPhos Pd G3 (XX mg, 0.005 mmol, 5 mol%), 3-bromopyridine (mg, 0.1 mmol, 1.0 equiv), 4-phenylpipiridine (mg, 0.15 mmol, 1.5 equiv), THF (0.5 mL, 0.2 M). The vial was sealed with a PTFE-lined cap (ThermoFisher, C4015-1A) and removed from the glovebox. The reaction vial was then placed in a preheated aluminum reaction block at 25 °C with magnetic stirring for 24 h. Dibromomethane (7 µL, 0.1 mmol, 1.0 equiv) was added to the reaction solution, a 50 µL aliquot was taken and added to an NMR tube, then diluted with $CDCl_3$. ^{1}HNMR spectroscopy was used to determine the yield of the reaction.

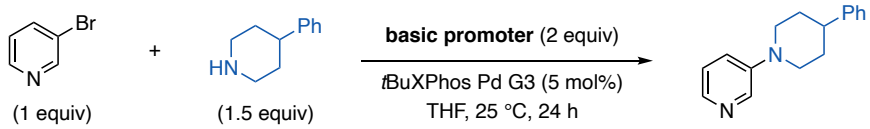

Table A3-15: Control reactions for the Pd-catalyzed C-N coupling reaction of 3-bromopyridine and 4-phenylpiperidine with various basic promoters. Result indicate P_2-*t*-Bu is the active promoter and is only generated with salt **3-16** and epoxide **3-23** are in solution. * General procedure B was followed.

Entry	Conditions	Results
1	2.0 equiv salt **3-16** + 3.0 equiv epoxide **3-23**	93%
2	2.0 equiv salt **3-16** + 2.0 equiv epoxide **3-21***	83%
3	2.0 equiv salt **3-16** + 2.0 equiv epoxide **3-21**	trace
4	2.0 equiv P_2-*t*-Bu	61%
5	2.0 equiv P_2-Et	83%
6	2.0 equiv salt **3-16**	0%
7	3.0 equiv epoxide **3-23**	0%
8	2.0 equiv epoxide **3-21**	0%
9	2.0 equiv $KO_2CCMe2Ph$ + 3.0 equiv epoxide **3-23**	0%
10	2.0 equiv KO_2CCMe_2Ph	0%
11	2.0 equiv Bu_4NOAc + 3.0 equiv epoxide **3-23**	0%
12	2.0 equiv Bu_4NOAc	0%
13	No Base	0%

A3.7.3 Larger scale product isolation and salt 3-16 recovery and regeneration

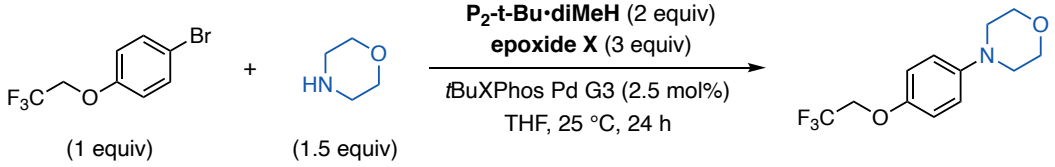

(1 equiv) (1.5 equiv)

isolated product yield: 96%
recovered and regenerated P_2-*t*-Bu•diMeH: 71%

Procedure: An oven-dried 25 mL round bottom flask was charged with a magnetic stir bar, *t*BuXPhos Pd G3 (19.9 mg, 0.025 mmol, 2.5 mol%), salt **3-16** (1.063 g, 2.0 mmol, 2.0 equiv), and 1-bromo-4-(2,2,2-trifluoroethoxy)benzene (255.0 mg, 1.0 mmol, 1.0 equiv). The flask was sealed with a rubber septum (Chemglass, CG-3022-06) and connected to a Schlenk line manifold and evacuated then backfilled with nitrogen three times. To the flask, THF (5.0 mL, 0.2 M), morpholine (131.2 µL, 1.5 mmol, 1.5 equiv), and epoxide **3-23** (810.4 mg, 3.0 mmol, 3.0 equiv) was added *via* N_2-flushed syringe. The reaction flask was disconnected from the manifold, then placed in a preheated oil bath at 25 °C with stirring. The reaction solution was stirred for 24 h. After 24 h, THF was removed *in vacuo* then the crude material was transferred to a separatory funnel using 10 mL of diethyl ether. The diethyl ether solution was extracted with 5 mL of 0.25 M aqueous HCl 3x and once with 5 mL water. The combined aqueous layers were added to a round bottom flask with a magnetic stir bar and activated carbon then stirred for 12 h at room temperature. The aqueous solution was filtered through a bed of celite then concentrated *in vacu.* HP_2-*t*-BuCl (686.8 mg, 1.70 mmol, 85% recovery) was collected then added to a 25 mL round bottom flask with a 10 mL MeOH and a magnetic stir bar. Potassium 2-methyl-2-phenylpropanoate (404.4 mg, 2.0 mmol, 1.2 equiv) was added and stirred for 12 h. Then the MeOH was removed *in vacu* and the crude salt mixture was suspended in ethyl acetate and filtered through a fine fritted funnel. The ethyl acetate solution was concentrated *in vacu* and dried under vacuum. The pale yellow oil was placed in a -30 °C freezer overnight to crystallize. The diMeP_2 crystals were collected *via* vacuum

filtration with a fine fritted funnel and cold diethyl ether. The crystallization and filtration process was repeated to yield white powdery crystals of diMeP$_2$ (542.7 mg, 1.02 mmol, 51% regeneration). The organic layer was washed with brine, 5 mL, and dried over Na_2SO_4, the concentrated *in vacuo*. The material was purified by column chromatography (100% hexanes to 20% ethyl acetate). The pure product **4-(4-(2,2,2-trifluoroethoxy)phenyl)morpholine** was collected as a pale-orange solid (250.0 mg, 96% isolated yield). **^{1}H NMR** (400 MHz, $CDCl_3$) δ 6.92 – 6.87 (m, 4H), 4.30 (q, J = 8.2 Hz, 2H), 3.90 – 3.79 (m, 4H), 3.15 – 3.01 (m, 4H). Characterization data matches previous reports.[11]

A3.7.4 Reaction profiles controlled by the base system

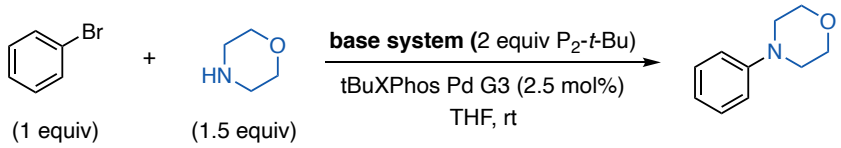

Procedure: In a nitrogen filled glovebox, an oven-dried 1-dram vial (ThermoFisher, C4015-1) was charged with a magnetic stir bar, *t*BuXPhos Pd G3 (4.0 mg, 0.005 mmol, 5 mol%), 1,3,5-trimethoxybenzene (16.8 mg, 0.1 mmol, 1.0 equiv) (an internal NMR standard), THF (0.5 mL, 0.2 M), bromobenzene (16.8 mg, 0.1 mmol, 1.0 equiv), morpholine (13.1 µL, 0.15 mmol, 1.5 equiv), then P$_2$-*t*-Bu (2.0 M THF solution) (50 µL, 0.2 mmol, 2 equiv) or salt **3-16** (106.2 mg, 0.2 mmol, 2.0 equiv) and epoxide (0.3 mmol, 3 equiv). The vial was capped with a PTFE-lined cap (ThermoFisher, C4015-1A) and homogenized. Immediately after, a 50 µL aliquot was taken and added to an NMR tube, then diluted with $CDCl_3$ as time point 0 min. The reaction vial was then placed on a magnetic stir plate at room temperature. Aliquots, 50 µL, were taken at various time points, each aliquot was added to an NMR tube, then diluted with $CDCl_3$. ^{1}HNMR spectroscopy

was used to determine the amount of product at each time point. The amount of product versus time is graphed below.

Table A3-16: ^{1}H NMR yields over time with epoxides **3-23**, **3-24**, and **3-25**. Salt **3-16** + **3-25** reaches 86% yield after 24 h.

Entry	Time (min)	Base system (% yield)			
		P_2-*t*-Bu	Salt **3-16** + **2-23**	Salt **3-16** + **3-24**	Salt **3-16** + **3-25**
1	0	11	0	0	0
2	5	41	22	6	2
3	10	64	49	16	2
4	15	94	71	25	3
5	20	100	85	37	6
6	40	-	-	62	11
7	60	100	100	80	20
8	120	-	-	100	39

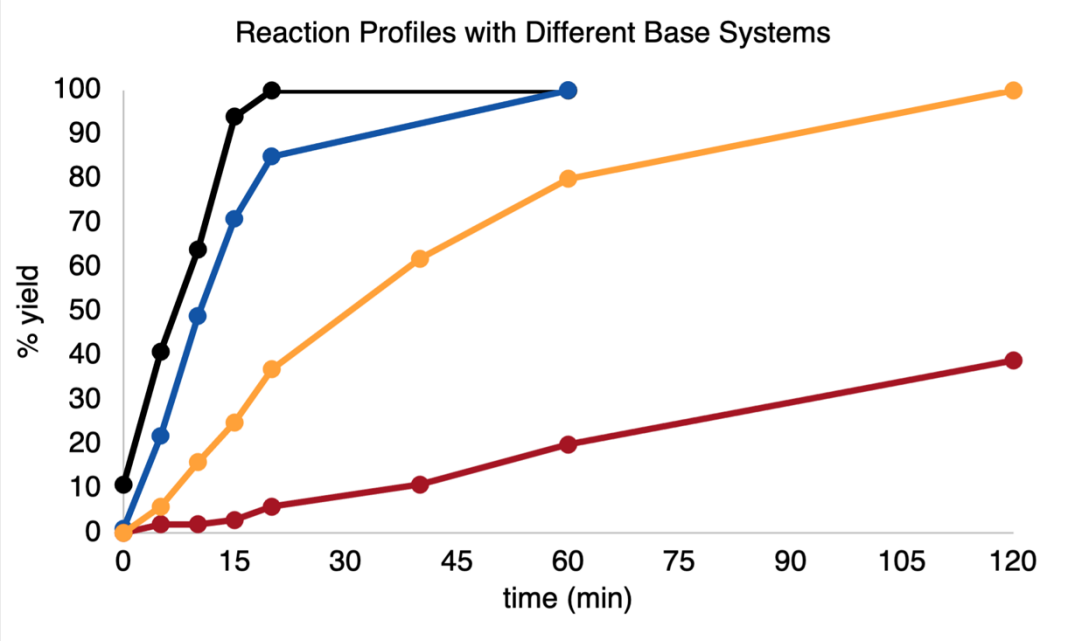

Figure A3-22: reaction profiles with epoxides **3-23**, **3-24**, and **3-25**. Salt **3-16** + **3-25** reaches 86% yield after 24 h.

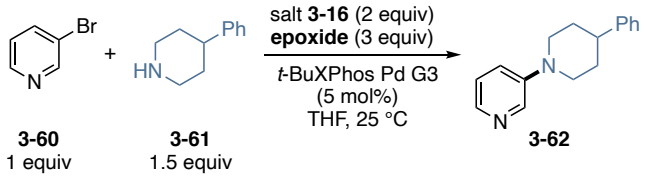

Procedure: In a nitrogen filled glovebox, an oven-dried 1-dram vial (ThermoFisher, C4015-1) was charged with a magnetic stir bar, *t*BuXPhos Pd G3 (4.0 mg, 0.005 mmol, 5 mol%), 1,3,5-trimethoxybenzene (16.8 mg, 0.1 mmol, 1.0 equiv) (an internal NMR standard), THF (0.5 mL, 0.2 M), 3-bromopyridine (9.6 µL, 0.1 mmol, 1.0 equiv), 4-phenylpiperidine (24.2 mg, 0.15 mmol, 1.5 equiv), then P_2-*t*-Bu (2.0 M THF solution) (50 µL, 0.2 mmol, 2 equiv) or salt **3-16** (106.2mg, 0.2 mmol, 2.0 equiv) and epoxide (0.3 mmol, 3 equiv). The vial was capped with a PTFE-lined cap (ThermoFisher, C4015-1A) and homogenized. Immediately after, a 50 µL aliquot was taken and added to an NMR tube, then diluted with $CDCl_3$ as time point 0 min. The reaction vial was then placed on a magnetic stir plate at room temperature. Aliquots, 50 µL, were taken at various time points, each aliquot was added to an NMR tube, then diluted with $CDCl_3$. ^{1}HNMR spectroscopy was used to determine the amount of product at each time point. The amount of product versus time is graphed below.

Table A3-17: ^{1}H NMR yields over time with epoxides **3-23**, **3-24**, and **3-25**. Salt **3-16** + **3-25** reaches 60% yield after 8 h.

Entry	Time (min)	Base system (% yield)			
		P_2-*t*-Bu	Salt **3-16** + **2-23**	Salt **3-16** + **3-24**	Salt **3-16** + **3-25**
1	0		12	0	0
2	2		60	-	-
3	5		64	0	0
4	7		71	-	-
5	10		82	3	0
6	15		95	9	0
7	20		-	14	2
8	40		-	38	-
9	60		-	57	-

10	100	-	76	40
11	150	-	80	
12	200	-	79	54

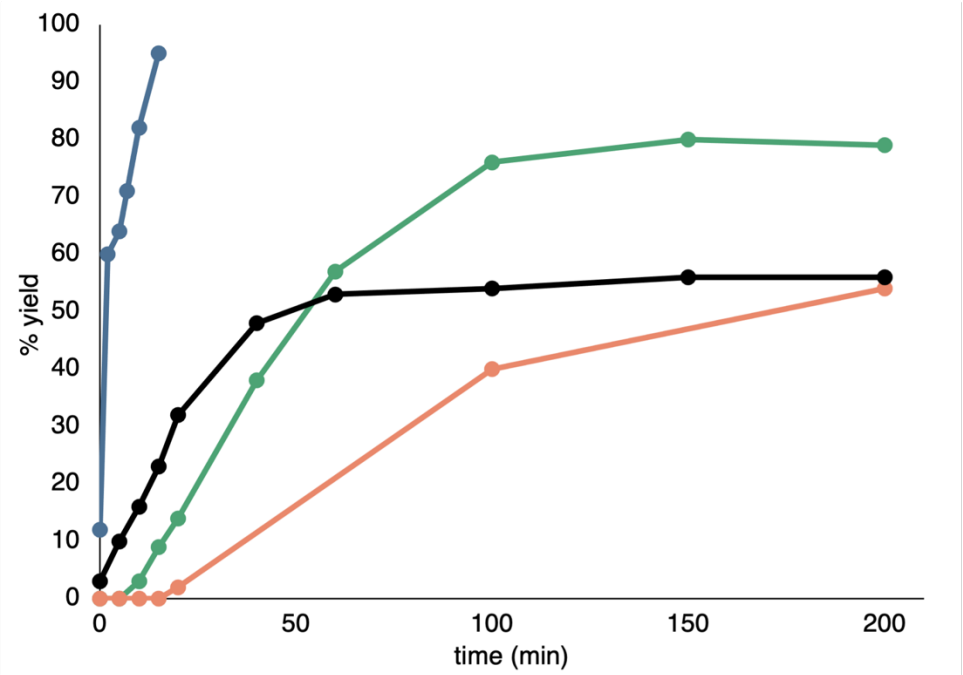

Figure A3-23: reaction profiles with epoxides **3-23**, **3-24**, and **3-25**. Salt **3-16** + **3-25** reaches 60% yield after 8 h.

A3.7.5 Base-sensitive substrate coupling enabled by epoxide-controlled base release

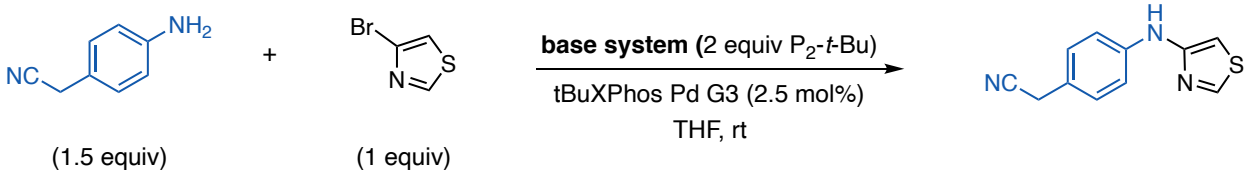

2-(4-(thiazol-4-ylamino)phenyl)acetonitrile

1) General procedure A was followed using salt **3-16** (106.2 mg, 0.2 mmol, 2.0 equiv), *t*BuXPhos Pd G3 (4.0 mg, 0.005 mmol, 5 mol%), epoxide **3-25** (81.0 mg, 0.3 mmol, 3.0 equiv) or epoxide **x** (60.7 mg, 0.3 mmol, 3.0 equiv), 4-bromothiazole (8.9 µL, 0.1 mmol, 1.0 equiv), 2-(4-aminophenyl)acetonitrile (19.8 mg, 0.15 mmol, 1.5 equiv), and THF (0.5 mL, 0.2 M). ^{1}HNMR was used to determine the yield (see table below). Preparatory thin layer chromatography with 100% DCM was used to obtain pure product. **^{1}H NMR** (400 MHz, $CDCl_3$) δ 8.64 (s, 1H), 7.25 (d,

J = 9.3 Hz, 2H), 7.14 (d, J = 8.4 Hz, 2H), 6.68 (s, 1H), 6.51 (s, 1H), 3.70 (s, 2H). Characterization data matches previous reports.[12]

2) General procedure C was followed using **3-16** (106.2 mg, 0.2 mmol, 2.0 equiv) and epoxides **3-23** and **3-24** (0.3 mmol, 3.0 equiv) or P_2-t-Bu (2.0 M THF solution) (50 µL, 0.2 mmol, 2 equiv) in place of the diMeP_2 and epoxide, *t*BuXPhos Pd G3 (4.0 mg, 0.005 mmol, 5 mol%), 4-bromothiazole (8.9 µL, 0.1 mmol, 1.0 equiv), 2-(4-aminophenyl)acetonitrile (19.8 mg, 0.15 mmol, 1.5 equiv), and THF (0.5 mL, 0.2 M). ^{1}HNMR was used to determine the yield (see table below).

Table A3-18: Yields for the Pd-catalyzed coupling reaction of XXX and XXX with various base systems.

Entry	P_2-*t*-Bu source	Epoxide	Procedure	Product yield (%)
1	commercial P_2-*t*-Bu	-	2	9%
2	diMeP_2	X	2	11%
3	diMeP_2	X	2	24%
4	diMeP_2	X	1	99%

A3.8 Long-Term Stability of Superbase Carboxylate Salts

This section outlines the experiments and studies performed to test the long-term stability of the carboxylate salts.

Stability of P_1-*t*-Bu exposed to air

A sample of P_1-*t*-Bu was placed in a 1 dram vial and removed from the glovebox. The vial was then capped under ambient air. The vial was uncapped and agitated daily. ^{1}H NMR and ^{31}P NMR spectra were taken at the start, and at one and two weeks of this treatment. The spectra are shown below.

P_1-*t*-Bu, fresh

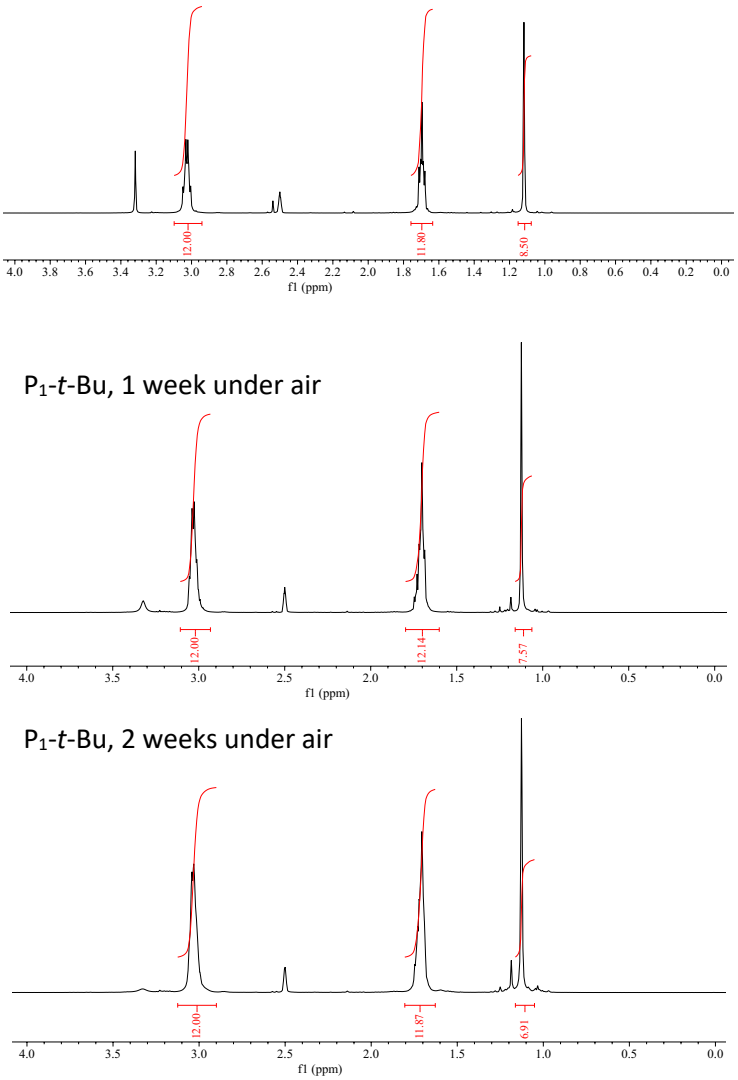

Figure A3-24: ^{1}H NMR spectra of P_1-*t*-Bu; top shows fresh base directly from commercial bottle; middle shows P_1-*t*-Bu exposed to ambient air for 1 week, *t*-Bu signal integration decreases; bottom shows P_1-*t*-Bu exposed to ambient air for 2 weeks, *t*-Bu signal integration decreases more. P_1-*t*-Bu decomposes when exposed to air. Spectra taken in d_6-DMSO.

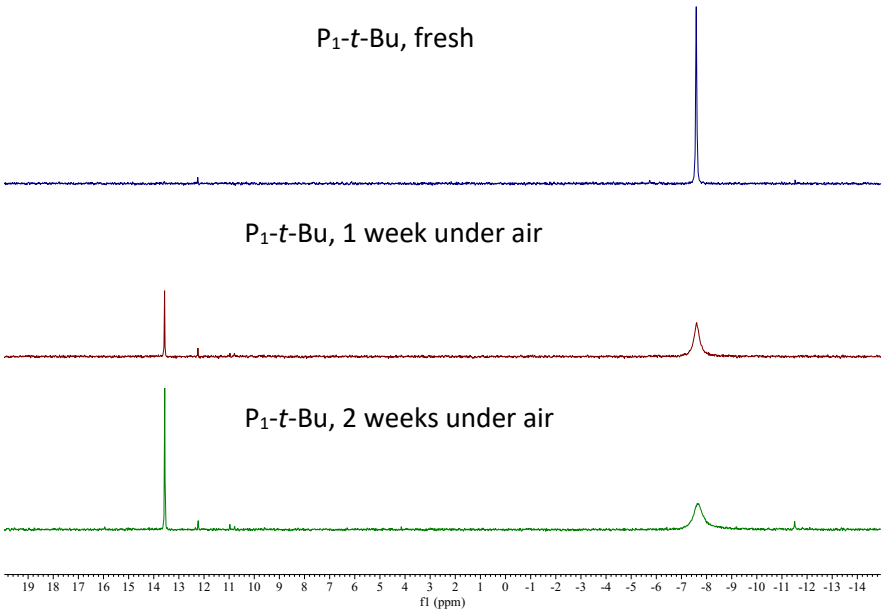

Figure A3-25: ^{31}P NMR spectra of P_1-*t*-Bu; top shows fresh base directly from commercial bottle; middle shows P_1-*t*-Bu exposed to ambient air for 1 week, phosphoramide formed; bottom shows P_1-*t*-Bu exposed to ambient air for 2 weeks, more phosphoramide formed. P_1-*t*-Bu decomposes when exposed to air. Spectra taken in d_6-DMSO.

Observation of Moisture Sensitivity with Superbase Carboxylate Salts

During our studies, the superbase carboxylate salts have been stable over long periods of time in a benchtop desiccator. However, upon exposure to high humidity (greater than 60%) the salts are observed to be hygroscopic and absorb moisture, evident by the collection of droplets on the weigh paper and eventually turned to wet semi-solids. To test the fidelity of the superbase carboxylate salts in humid environments, we purchased humidity control packets that can maintain 72% (Boveda 72% RH size 8) and 84% (Boveda 84% RH size 8) humidity and placed them in a glass chamber sealed with high-vacuum grease (Dow Corning High-Vacuum Grease, Thermo Scientific, 044224KT) and kept on the benchtop (see images below). To test how long a salt can last in the humid environment, it was placed into the humidity chamber on a piece of weigh paper completely open to the atmosphere. Every five minutes, the chamber was opened, and the salt was mixed around with a metal spatula to mimic use in the humid environment.

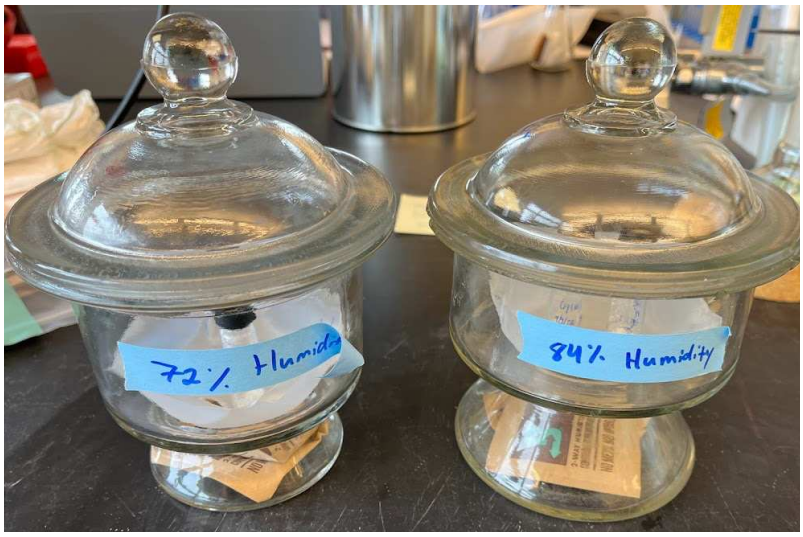

Solutions to Moisture Sensitivity of Superbase Carboxylate Salts

To address this limitation, we have identified two solutions that allow for the use of superbase carboxylate salts in more humid environments. First, we developed a restoration process that allows for the facile removal of the absorbed water to re-obtain the crystalline solid through a simple procedure described below. For the second solution, simple changes in the carboxylate structure led to superbase salts that are far less hygroscopic and last for longer periods of time in the humid chamber. Ultimately, we recommend storage of the superbase salts in a benchtop desiccator or freezer to ensure their long-term stability.

Addressing Moisture Sensitivity of Precatalyst Salts

For the P_1-*t*-Bu and P_2-*t*-Bu precatalyst salts stored on the benchtop and in air, we observed over time the accumulation of water by the formation of droplets in the vial and *via* ^{1}HNMR spectroscopy. In a more humid environment, mimicked by a sealed container with a controlled humidity of 72%, the precatalyst salts absorbed a significant amount of water and turned into wet solids, no longer characteristic free-flowing powders. The following procedure details how to regenerate the crystalline superbase salts after they absorb water. In each case, the recovered superbase salts can be utilized in reactions with no decrease in yield.

Regeneration of crystalline solid superbase salts. To the vial containing the water absorbed carboxylate salt, PhMe was added, then concentrated using a rotary evaporator (3x). The vial was next attached to a Schlenk line and was put under vacuum for 12 h, resulting in the dry, crystalline powder. The regenerated crystalline superbase salts were stored in a benchtop desiccator for further use.

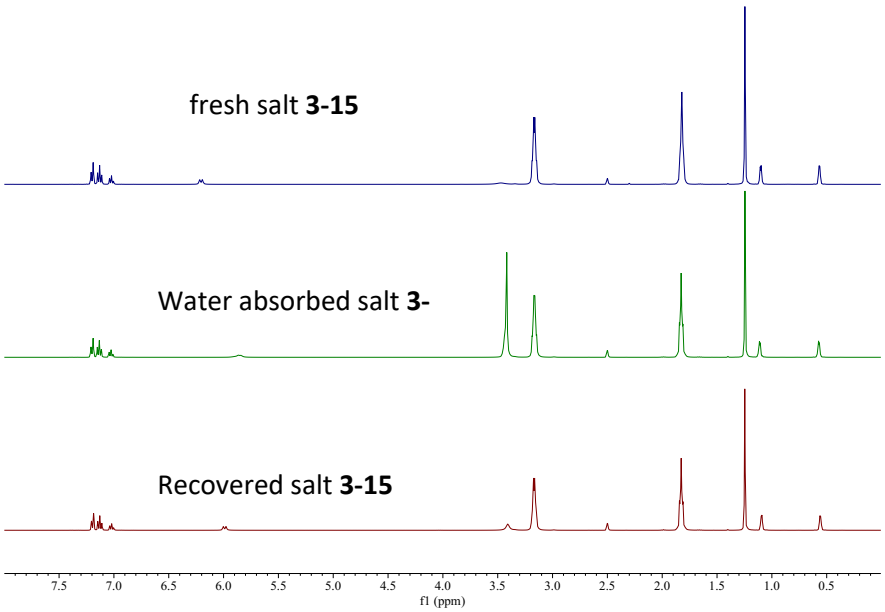

Figure A3-26. ^{1}H NMR spectra taken in d_6-DMSO for fresh superbase salt **3-15**, water absorbed superbase salt **3-15**, and recovered salt **3-15** *via* azeotrope with PhMe. No change was observed in the ^{31}P NMR spectra for the about samples. Very little water present in fresh salt **3-15**, a large amount of water in wet salt **3-15**, and very little water in regenerated salt **3-15**.

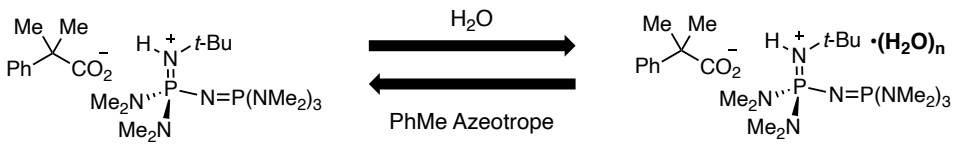

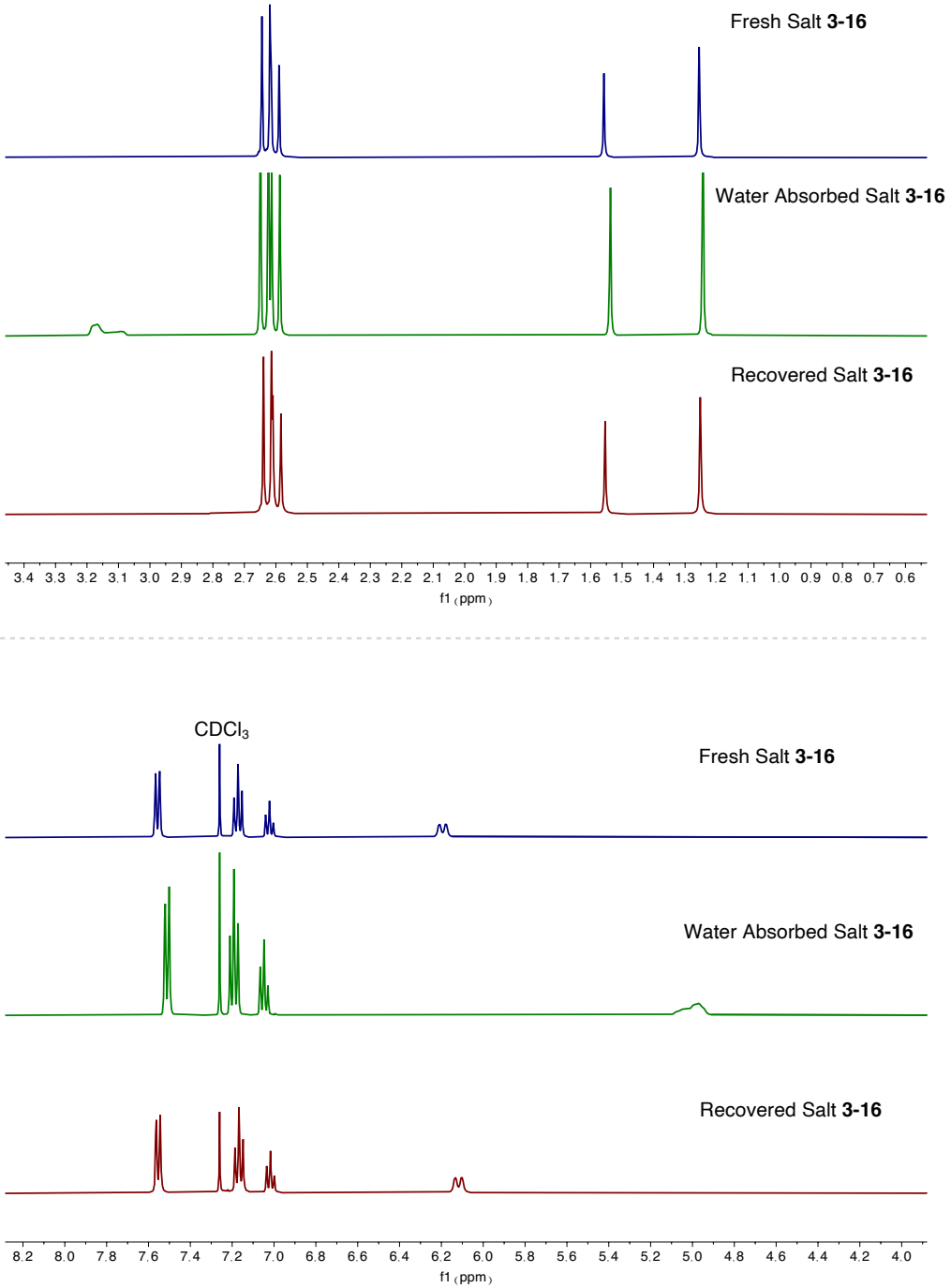

Figure A3-27. [1]HNMR spectra for fresh superbase salt **3-16**, water absorbed superbase salt **3-16**, and recovered salt **3-16** *via* azeotrope with PhMe.

Synthesis of less hygroscopic superbase carboxylate salts. Garrett prepared superbase salts with alternate carboxylate anions were synthesized from the commercial superbase and a carboxylic acid following the general procedure below using either diethyl ether or ethyl acetate as the

reaction solvent. For P_1-*t*-Bu, salt **3-17** was found to be stable to high humidity for six hours while salt **3-15** was only stable for fifteen minutes. For P_2-*t*-Bu, salt **3-18** was found to be stable to high humidity for 24 hours and salt **3-16** was only stable for twenty minutes.

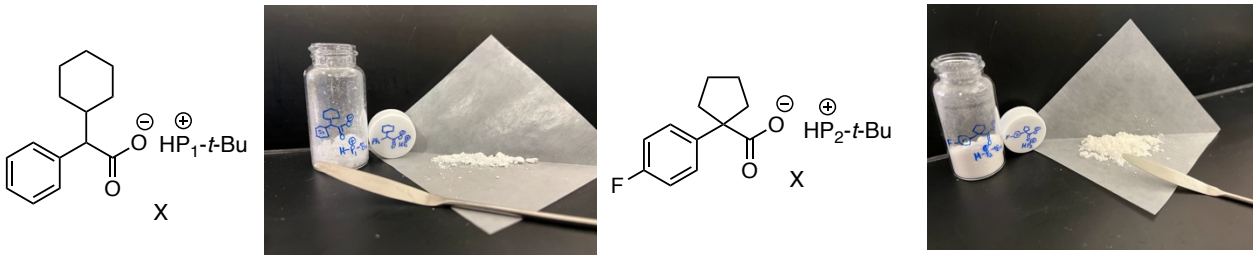

Figure A3-28. Structures and images of new precatalyst salts with improved moisture stability.

A3.9 References

[1] Schwesinger, R; Schlemper, H.; Hasenfratz, C.; Willaredt, J.; Dambacher, T.; Breu- era, T.; Ottaway, C; Fletschingera, M.; Boele, J.; Fritz, H.; Putzas, D.; Rotter, H. W.; Bordwell, F. G.; Satish, A. V.; Ji, D.-Z.; Peters, E.-M.; Peters, K.; von Schnering, H. V.; Wakz, L. Extremely Strong, Uncharged Auxiliary Bases; Monomeric and Polymer-Supperted Polyaminophosphazenes (P_2-P_5). *Liebigs Ann*. **1996**, 1055-1081.

[2] Weitkamp, R. F.; Neumann, B.; Stammler, H.-G.; Hoge, B. Generation and Applications of the Hydroxide Trihydrate Anion, $[OH(OH)_3]^-$, Stabilized by a Weakly Coordinating Cation *Angew. Chem. Int. Ed*. **2019**, *58*, 14633 –14638.

[3] Chu, X.-Q.; Meng, H.; Zi, Y.; Xu, X.-P.; Ji, S.-J. Metal-Free Oxidative Radical Addition of Carbonyl Compounds to a,a-Diaryl Allylic Alcohols: Synthesis of Highly FunctionalizedKetones *Chem. Eur. J*. **2014**, *20*, 17198 – 17206.

[4] Gururaja, G. N.; Herchl, R.; Pichler, A.; Gratzer, K.; Waser, A. Application Scope and Limitations of TADDOL-Derived Chiral Ammonium Salt Phase-Transfer Catalysts *Molecules* **2013**, *18*, 4357-4372.

[5] Caldwell, N.; Jamieson, C.; Simpson, I.; Tuttle, T. Organobase-Catalyzed Amidation of Esters with Amino Alcohols *Org. Lett*. **2013**, *15*, 2506-2509.

[6] Nielsen, M. K.; Ahneman, D. T.; Riera, O.; Doyle, A. G. *J. Am. Chem. Soc*. **2018**, *140*, 5004.

[7] Santanilla, A. B.; Regalado, E. L.; Pereira, T.; Shevlin, M.; Bateman, K.; Campeau, L.-C.; Schneeweis, J.; Berritt, S.; Shi, Z.-C.; Nantermet, P.; Liu, Y.; Helmy, R.; Welch, C. J.; Vachal, P.; Davies, I. W.; Cernak, T.; Dreher, S. D. Nanomole-scale high-throughput chemistry for the synthesis of complex molecules *Science* **2015**, *347,* 49 - 53.

[8] Santanilla, A. B.; Christensen, M.; Campeau, L.-C.; Davies, I. W.; Dreher, S. D. P_2Et Phosphazene: A Mild, Functional Group Tolerant Base for Soluble, Room Temperature Pd-Catalyzed C−N, C−O, and C−C Cross- Coupling Reactions *Org. Lett*. **2015**, *17*, 3370−3373.

[9] Dennis, J. M.; White, N. A.; Liu, R. Y.; Buchwald, S. L. Pd-Catalyzed C−N Coupling Reactions Facilitated by Organic Bases: Mechanistic Investigation Leads to Enhanced Reactivity in the Arylation of Weakly Binding Amines *ACS Catal*. **2019**, *9*, 3822−3830.

[10] Dennis, J. M.; White, N. A.; Liu, R. Y.; Buchwald, S. L. Breaking the Base Barrier: An Electron-Deficient Palladium Catalyst Enables the Use of a Common Soluble Base in C−N Coupling *J. Am. Chem. Soc*. **2018**, *140*, 4721–4725.

[11] Szpera, R.; Isenegger, P. G.; Ghosez, M.; Straathof, N. J. W.; Cookson, R.; Blakemore, D. C.; Richardson, P.; Gouverneur, V. Synthesis of Fluorinated Alkyl Aryl Ethers by Palladium-Catalyzed C–O Cross-Coupling *Org. Lett*. **2020**, *22*, 6573–6577.

[12] Reichert, E. C.; Feng, K.; Sather, A. C.; Buchwald, S. L. Pd-Catalyzed Amination of Base-Sensitive Five-Membered Heteroaryl Halides with Aliphatic Amines *J. Am. Chem. Soc.* **2023**, *145*, 3323-3329.

LIST OF ABREVIATIONS

DBU	1,8-diazabicyclo[5.4.0]undec-7-ene
BTMG	1,8-diazabicyclo[5.4.0]undec-7-ene
TBD	1,5,7-triazabicyclo[4.4.0]dec-5-ene
MTBD	7-Methyl-1,5,7-triazabicyclo[4.4.0]dec-5-ene
P_1-*t*-Bu	tert-butylimino-tri(pyrrolidino)phosphorane
P_2-*t*-Bu	1-tert-Butyl-2,2,4,4,4-pentakis(dimethylamino)-2λ5,4λ5-catenadi(phosphazene)
P_4-*t*-Bu	1-tert-Butyl-4,4,4-tris(dimethylamino)-2,2-bis[tris(dimethylamino)-phosphoranylidenamino]-2λ5,4λ5-catenadi(phosphazene)
PG_3	2,2',2''-((tert-butylimino)-λ5-phosphanetriyl)tris(1,1,3,3-tetramethylguanidine)
MeCN	acetonitrile
DMSO	dimethyl sulfoxide
PhMe	toluene
HMPA	hexamethylphosphoramide
DME	1,2-dimethoxyethane
n-Bu_2O	dibutyl ether
DCM	dichloromethane
EtOAc	ethyl acetate
Et_2O	ethyl ether
DMF	dimethylformamide
THF	tetrahydrofuran
MeOH	methanol

EtOH	ethanol
i-PrOH	2-propanol
n-BuOH	1-butanol
18-crown-6	1,4,7,10,13,16-Hexaoxacyclooctadecane
9-BBN	9-methoxy-9-borabicyclo[3.3.1]nonane
E	electrophile
HNuc	pronucleophile
L.A.	Lewis acid
L.B.	Lewis base
K_{eq}	equilibrium constant
ΔG	change in Gibbs free energy
ΔH	change in enthalpy
ΔS	change in entropy
T	temperature
h	hour
min	minutes
equiv	equivalents
PCET	proton coupled electron transfer
EWG	electron-withdrawing group
OTBS	*tert*-butyldimethylsilyl ether
H-bonding	hydrogen-bonding
S_NAr	nucleophilic aromatic substitution
SB	superbase

NMR	nuclear magnetic resonance
GC	gas chromatography
ArX	aryl halide or aryl pseudohalide